UNCLASSIFIED

DEPARTMENT OF DEFENSE
UNITED STATES OF AMERICA

AD NUMBER

AD 128 783

CLASSIFICATION CHANGES

TO **UNCLASSIFIED**

FROM **CONFIDENTIAL**

AUTHORITY

OASD; Oct 9, 1975.

19990302146

THIS PAGE IS UNCLASSIFIED

UNCLASSIFIED

AD NUMBER

AD-128 783

NEW LIMITATION CHANGE

TO

DISTRIBUTION STATEMENT - A

Approved for public release;
distribution is unlimited.

LIMITATION CODE: 1

FROM

No Previously Assigned,DoD Distr Scty Cntrl St'mt

AUTHORITY

OASD; Oct 9, 1975.

THIS PAGE IS UNCLASSIFIED

[redacted]

AD 128783

Armed Services Technical Information Agency

Reproduced by

DOCUMENT SERVICE CENTER

KNOTT BUILDING, DAYTON, 2, OHIO

This document is the property of the United States Government. It is furnished for the duration of the contract and shall be returned when no longer required, or upon recall by ASTIA to the following address: **Armed Services Technical Information Agency, Document Service Center, Knott Building, Dayton 2, Ohio.**

NOTICE: WHEN GOVERNMENT OR OTHER DRAWINGS, SPECIFICATIONS OR OTHER DATA ARE USED FOR ANY PURPOSE OTHER THAN IN CONNECTION WITH A DEFINITELY RELATED GOVERNMENT PROCUREMENT OPERATION, THE U. S. GOVERNMENT THEREBY INCURS NO RESPONSIBILITY, NOR ANY OBLIGATION WHATSOEVER; AND THE FACT THAT THE GOVERNMENT MAY HAVE FORMULATED, FURNISHED, OR IN ANY WAY SUPPLIED THE SAID DRAWINGS, SPECIFICATIONS, OR OTHER DATA IS NOT TO BE REGARDED BY IMPLICATION OR OTHERWISE AS IN ANY MANNER LICENSING THE HOLDER OR ANY OTHER PERSON OR CORPORATION, OR CONVEYING ANY RIGHTS OR PERMISSION TO MANUFACTURE, USE OR SELL ANY PATENTED INVENTION THAT MAY IN ANY WAY BE RELATED THERETO.

[redacted]

REPRODUCTION QUALITY NOTICE

This document is the best quality available. The copy furnished to DTIC contained pages that may have the following quality problems:

- Pages smaller or larger than normal.
- Pages with background color or light colored printing.
- Pages with small type or poor printing; and or
- Pages with continuous tone material or color photographs.

Due to various output media available these conditions may or may not cause poor legibility in the microfiche or hardcopy output you receive.

☐ If this block is checked, the copy furnished to DTIC contained pages with color printing, that when reproduced in Black and White, may change detail of the original copy.

NOTICE: THIS DOCUMENT CONTAINS INFORMATION AFFECTING THE NATIONAL DEFENSE OF THE UNITED STATES WITHIN THE MEANING OF THE ESPIONAGE LAWS, TITLE 18, U.S.C., SECTIONS 793 and 794. THE TRANSMISSION OR THE REVELATION OF ITS CONTENTS IN ANY MANNER TO AN UNAUTHORIZED PERSON IS PROHIBITED BY LAW.

[redacted]

PREPRINTS
VOLUME - 1

PFL 212/13

AD No. 128783

ASTIA FILE COPY

LIQUID PROPELLANTS SYMPOSIUM

(U)

27 - 28 MARCH 195

SPECIAL HANDLING REQUIRED
NOT RELEASABLE TO FOREIGN NATIONALS
The information contained in this document
will not be disclosed to foreign nationals
or their representatives.

Sponsored by the
TECHNICAL ADVISORY PANEL ON FUELS AND LUBRICANTS

OASD RESEARCH AND DEVELOPMENT

WASHINGTON 25, D.C.

[redacted]

MAY 3 1957

57AA 20013

[redacted]

Preprints
Volume - 1

PFL 212/13

LIQUID PROPELLANTS SYMPOSIUM (U)

27-28 March 1957

THIS DOCUMENT CONTAINS INFORMATION AFFECTING THE NATIONAL DEFENSE OF THE UNITED STATES WITHIN THE MEANING OF THE ESPIONAGE LAWS, TITLE 8, U.S.C., SECTIONS 793 AND 794. THE TRANSMISSION OR THE REVELATION OF ITS CONTENTS IN ANY MANNER TO AN UNAUTHORIZED PERSON IS PROHIBITED BY LAW.

SPECIAL HANDLING REQUIRED
NOT RELEASABLE TO FOREIGN NATIONALS
The information contained in this document will not be disclosed to foreign nationals or their representatives.

Sponsored by
Technical Advisory Panel on Fuels and Lubricants
OFFICE OF THE ASSISTANT SECRETARY OF DEFENSE
RESEARCH AND DEVELOPMENT

[redacted]

FOREWORD

This Liquid Propellants Symposium was organized by the Technical Advisory Panel on Fuels and Lubricants, of the Office of the Assistant Secretary of Defense, Research and Development, as part of a continuing effort to promote the interchange of ideas. Papers to be presented or read by title are being distributed in advance of the symposium to stimulate discussion (Volume 1, papers to be presented; Volume 2, papers to be read by title only).

Authors have been asked to limit their reviews to ten minutes. An equal time has been allotted for prepared discussions of most papers, after which general discussion will follow.

A stenotype record will be made of unprepared discussion, and the discussers will be given an opportunity to edit their remarks before the proceedings are published. Papers received too late for advance distribution will also be included in the proceedings.

CONTENTS

Page

Foreword. iii

SURVEY OF RESEARCH ON FREE RADICALS AS PROPELLANTS 1
Lt Colonel Paul G. Atkinson
Air Force Office of Scientific Research

THE EFFECT OF PROPELLANT ENERGY AND MASS DISTRIBUTION ON ROCKET PROPULSION EFFICIENCY. 18
Howard S. Seifert
Ramo-Wooldridge Corporation

AN EVALUATION OF LIQUID OZONE-OXYGEN MIXTURES AS ROCKET OXIDIZERS 29
J. P. Layton, I. Glassman, D. Garvin
James Forrestal Research Center, Princeton University
(TEXT NOT YET AVAILABLE)

HYDROGEN PEROXIDE PROPELLANTS 30
Andrew J. Kubica and John H. Keefe
Becco Chemical Division of Food Machinery & Chemical Corp.

PERFORMANCE OF PERCHLORYL FLUORIDE. 65
E. A. Mickle, K. Berman, E. S. C. Gantz
General Electric Company

HIGH TEMPERATURE RESEARCH AT TEMPLE 76
A. V. Grosse, C. S. Stokes, W. L. Doyle
The Research Institute of Temple University
(ABSTRACT ONLY)

TOXIC HAZARDS OF LIQUID PROPELLANTS 78
Keith H. Jacobson
Army Chemical Center

HEAT TRANSFER PROPERTIES OF ANHYDROUS AMMONIA 85
T. F. Reinhardt, R. L. Potter, F. M. Moore
Bell Aircraft Corporation

PETROLEUM DERIVABLE NITROGEN COMPOUNDS AS LIQUID ROCKET FUELS . . 98
J. E. Mahan, H. M. Fox, H. W. Bost, O. E. Larsen, R. C. Doss
Phillips Petroleum Company

THEORETICAL AND EXPERIMENTAL EVALUATION OF SEVERAL AMINE FUELS, WITH FUMING NITRIC ACID. 115
J. S. Gordon
Wright Air Development Center

Page

DESENSITIZATION OF LIQUID MONOPROPELLANTS TO ADIABATIC AIR COMPRESSION IMPACT BY THE ADDITION OF ETHYLENE OXIDE. 136
C. W. Tait and W. A. Cuddy
Wyandotte Chemicals Corporation

EFFECT OF HYDROCARBON FUEL COMPOSITION ON ROCKET PERFORMANCE. . . . 150
Jacob Silverman and Robert J. Thompson
Rocketdyne, A Division of North American Aviation, Inc.

THE PERFORMANCE OF UNSYM-DIMETHYLHYDRAZINE-RED NITRIC ACID IN A MOTOR AT VARYING THRUST LEVELS. 192
N. J. Sippel, D. H. Couch, Stanley Singer
US Naval Ordnance Test Station

THE TANGENTIAL MODE OF COMBUSTION INSTABILITY 208
R. S. Pickford and H. B. Ellis
Aerojet-General Corporation

FACTORS WHICH INFLUENCE THE SUITABILITY OF LIQUID PROPELLANTS AS ROCKET MOTOR REGENERATIVE COOLANTS 260
D. R. Bartz
Jet Propulsion Laboratory, California Institute of Technology

FACTORS INFLUENCING THE MONOPROPELLANT SPECIFIC IMPULSE OF ACETYLENIC COMPOUNDS. 284
Lloyd E. Line, Jr.
Experiment Incorporated

EFFECT OF HYPERGOLICITY OF THE PROPELLANTS ON THE OPERATION OF A LARGE MISSILE ROCKET 299
R. F. Tangren
Aerojet-General Corporation

SOME PROPELLANT PROPERTIES THAT INFLUENCE THE DESIGN OF ROCKET PROPULSION SYSTEMS 305
K. N. Watts
Rocketdyne, A Division of North American Aviation, Inc.

A NON-COKING ETHYLENE OXIDE REACTOR 335
Loren C. Smith
Wyandotte Chemicals Corporation

HIGH ENERGY FUELS IN AIR BREATHING ENGINES. 349
E. A. DeZubay and S. M. King
Curtiss Wright Corporation

Page

COMPARISON OF LOX/KEROSENE, LOX/HYDRAZINE, AND LF_2/HYDRAZINE MISSILE SYSTEMS FOR LONG RANGE MISSIONS. 357
Johann G. Tschinkel
Army Ballistic Missile Agency
(TEXT NOT YET AVAILABLE)

STUDIES WITH TWO-STAGE ROCKET ENGINES. 358
Anthony Briglio, Jr.
Jet Propulsion Laboratory, California Institute of Technology

SURVEY OF RESEARCH ON FREE RADICALS AS PROPELLANTS

Lt Colonel Paul G. Atkinson
AF Office of Scientific Research
Washington, D. C.

Introduction

The Armed Services became interested in the application of free radicals as possible ultra energy propellants some years ago. The performance looks promising, and investigation of the means of producing, identifying, concentrating, stabilizing, and reacting, free radicals has led to a wide program of exploratory research to ascertain the feasibility of free radicals as ultra energy propellants.

Free radicals or free atoms can be defined as chemical species of neutral charge, with an unpaired electron in the outer ring. For example, dissociated molecules are free atoms or radicals. The atom or radical with the single electron seeks to pair this electron with that of another atom or radical, and this affinity explains the reactivity of free radicals. Related chemical species of higher energy level are excited atoms or molecules, in which an energy addition has rearranged the electrons which seek to return to their natural state. Ionization is a higher energy state in which the electron has been removed, thus imparting an electrical charge.

There are probably as many free radicals as there are stable chemical compounds; but as one might expect, only a few of the most reactive free radicals are of interest as propellants. Unless otherwise indicated, "free radicals" should be taken to include free atoms as well.

Performance

As a point of reference, let us first examine the performance parameters which reduce free radical propellants to the same common denominator as conventional propellants.

The best index of rocket propellant performance is the specific impulse, I_{sp} or the pound seconds of impulse which one pound of propellant will yield.

In pound seconds per pound, I_{sp} is equal to the exhaust velocity divided by the acceleration of gravity. The exhaust velocity is given by:

Figure 1

$$v = \sqrt{\frac{2gK}{K-1} \; \frac{R\,T_c}{\bar{M}} \left[1 - \left(\frac{P_2}{P_1}\right)^{K-1/K}\right]}$$

where K = ratio of the specific heats

R = universal gas constant

g = acceleration of gravity

$\frac{P_2}{P_1}$ = pressure ratio of expansion

T_c = combustion temperature

$\bar{M}$ = average molecular weight of exhaust gases

The predominating factors in this equation are the temperature of combustion and the average molecular weight of the exhaust gases. So we can state our performance equation the form

$$v \text{ or } I_{sp} = f\left(\sqrt{\frac{T_c}{\bar{M}}}\right)$$

To maximize performance, then, we seek a high chamber temperature and a low average molecular weight. With conventional propellants, this chamber temperature is generated by the combustion of a fuel and a oxidizer. In an atomic rocket, the heat from a reactor would be transferred to a working fluid. With the free radical propellants postulated, the "combustion" temperature is generated from the bond dissociation energy or heat liberated by the recombination of unstable free atoms or radicals of the working fluid or contained in the working fluid as a slurry. The average molecular weight of the exhaust gases has the same significance in any case. The lighter the better.

Let's look at a number of conventional propellants in the light of these two criteria - the temperature of combustion and the average molecular weight of exhaust, and see how they compare with free radical possibilities. (See Figure 2)

In this slide, the temperature of combustion is plotted for a number of conventional propellants with their specific impulse on the horizontal scale. The workhorse propellants [1, 2] in general have combustion temperatures in the 5000 - 5500°F range. Some of the exotic propellants run higher, depending on the mixture ratio. Free radical species [3, 4] at various "mixture ratios" with molecular hydrogen calculate out to higher temperatures, reaching 8540°F with 100% atomic hydrogen. The effect of dissociation is to put a ceiling on the maximum temperature that we can achieve. A dissociation equilibrium can be calculated [5] at a given temperature

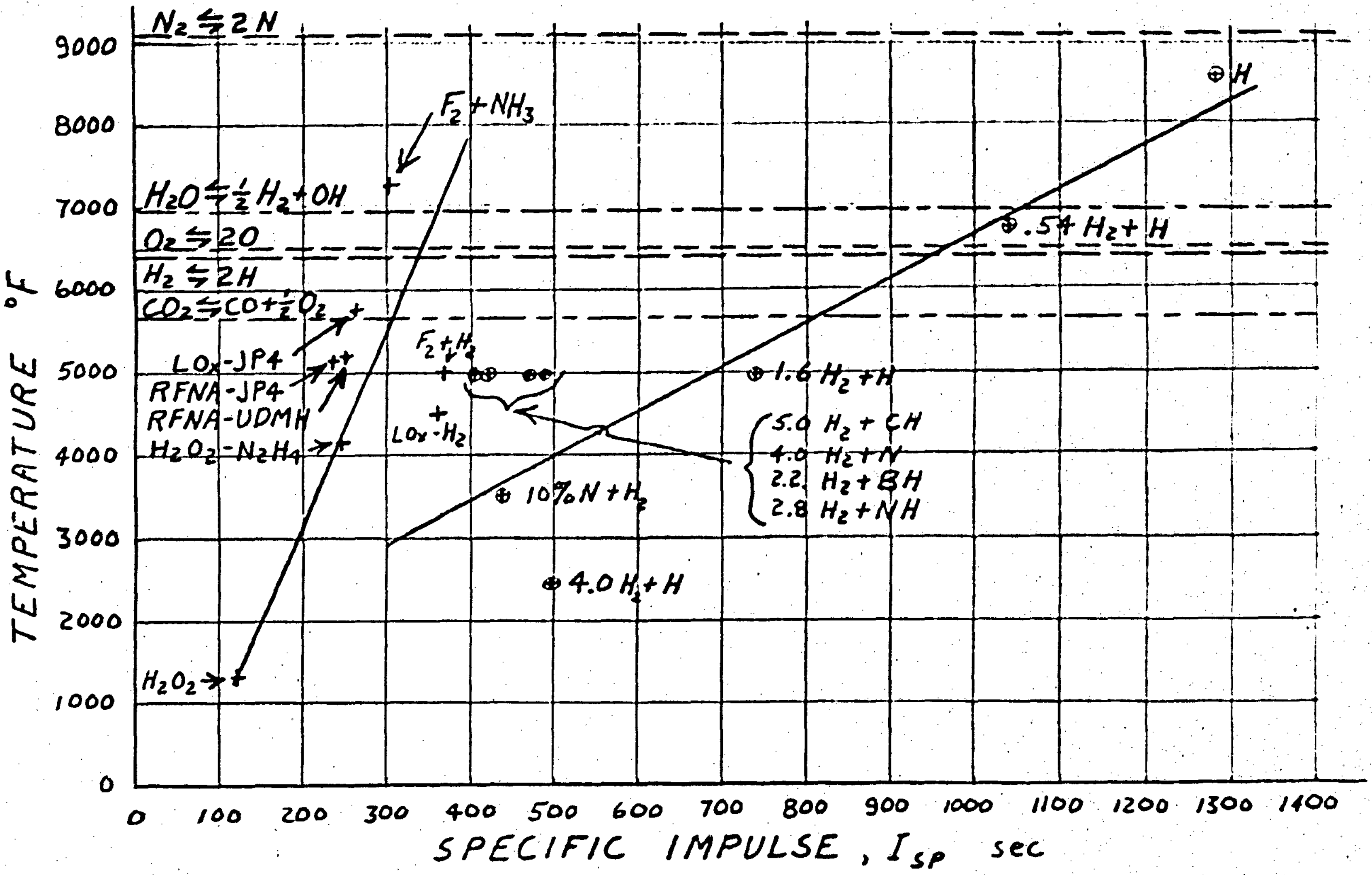

PROPELLANT PERFORMANCE vs T_c

Figure 2

PROPELLANT PERFORMANCE vs $\bar{M}$

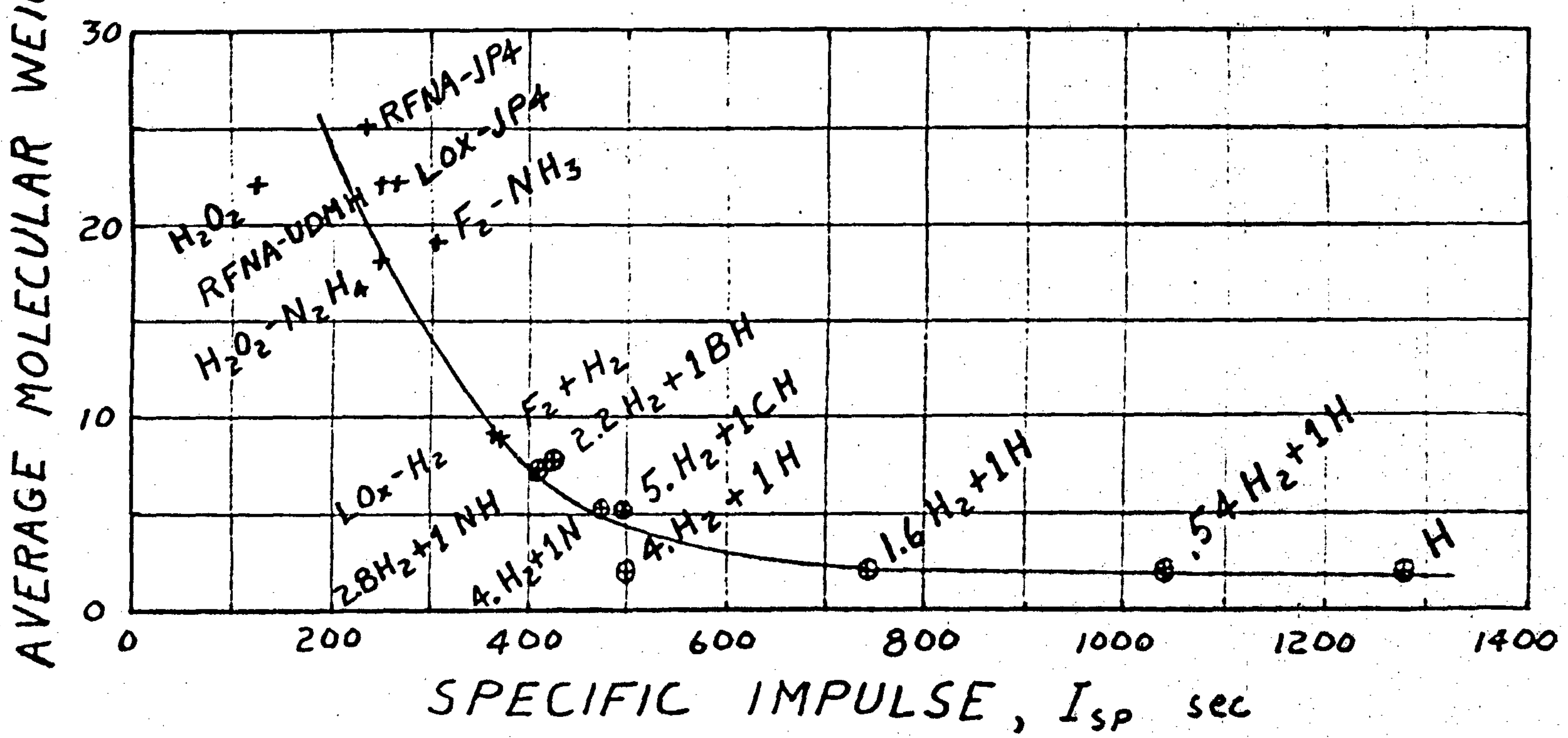

Figure 3

and pressure. The horizontal lines are the temperatures at which the exhaust products are dissociated ten per cent at thirty atmospheres. Dissociation absorbs energy and limits the chamber temperature. On the other hand, dissociation increases the specific volume of exhaust gases and decreases the average molecular weight. While this is beneficial, the temperature effect predominates, and dissociation limits the specific impulse.

Free radicals, then, offer a possible means of producing extremely high temperatures. Let's examine the other performance criterion, that of the average molecular weight of exhaust products. (See Figure 3).

Various conventional propellants [1, 2] containing carbon, oxygen, nitrogen, and hydrogen fall into the region 20 to 25. The exotic combinations are less than 20, and depending on mixture ratio may be as low as 9. Free radical species in slurries of molecular hydrogen are consistently smaller, and for atomic hydrogen alone, $\bar{M}$ would be 2 or less depending upon dissociation. The low average molecular weight is the other attractive feature of free atoms and radicals, and largely accounts for the high specific impulse.

Some sample performance calculations [3, 4, 6] are summarized in Figure 4 for free radical systems.

Theoretical Performance of Some Free Radical Systems

Species	Pc Psia	Isp sec	T_c °F	°K	Source
4.0 mol H_2 to 1 mol H	300	498	2420	1600	Aerojet
2.8 mol H_2 to 1 mol NH	300	410	4940	3000	Aerojet
5.0 mol H_2 to 1 mol CH	300	492	4940	3000	Aerojet
1.6 mol H_2 to 1 mol H	300	740	4940	3000	Aerojet
2.2 mol H_2 to 1 mol BH	300	420	4940	3000	Aerojet
4.0 mol H_2 to 1 mol N	300	472	4940	3000	Aerojet
.54 mol H_2 to 1 mol H	300	1040	6740	4000	Aerojet
H alone	300	1280	8540	5000	WADC
Various radicals → NH_3	300	487 → 836			Aerojet
1 mol NH_3 + various radicals → $2NH_3$	300	324 → 572			Aerojet
Various radicals → N_2H_4	300	334 → 765			Aerojet
1 mol N_2H_4 + various radicals → $2N_2H_4$	300	266 → 555			Aerojet
O alone	600	314	8935	5225	RMI
OH alone	600	289	6137	3666	RMI
CH_3 alone	600	328	4032	2238	RMI
10% N in mixture with H_2	300	440	3500	2200	WADC
20% N in mixture with H_2	300	490	4940	3000	WADC

Figure 4

The free radicals of interest, then, are restricted to a number of the simpler, lighter, and more reactive species - H, N, NH, BH, CH, O, and OH. While there is no question that the most fashionable of these is atomic hydrogen, this little rascal is also the most elusive. Others may prove more amenable to stabilization, and anything over 300 seconds specific impulse is attractive for rocket application.

Research in Free Radicals

Well over two thousand reports applicable to atomic and free radical research dating from 1873 to 1954 are referenced in E. W. R. Steacie's[7] two monumental volumes on the subject. R. A. Marcus[8] has summarized studies presented at the New York Academy of Sciences March 1956. Olson, Pellam, Broida, and Carr[9] in June 1956 surveyed the state of the research underway, pertinent to free radicals as propellants. The AeroJet General Corporation[3] published in July 1956 their final report of their first two years of research and performance calculations on ultra energy fuels for rocket propulsion. The Aeronautical Research Laboratory of WADC[4] made performance calculations and estimated the current prospects in November 1956. The purpose of this paper is to survey the present exploratory research effort pertinent to free radicals as propellants, and to discuss what appear to be the key problems and areas.

The areas can be listed as follows:
(1) Production and concentration
(2) Detection, identification, estimation, and study
(3) Stabilization and storage
(4) Reaction

Production and Concentration

At the present state of the science, generation of free radicals would probably be a better term than production. There are several means of producing free radicals, and all require an input of energy equal to the strength of the bond holding the atoms or radicals together in a stable molecule. Free atoms and radicals can be produced by thermal, chemical, photochemical, electrical, and nuclear processes.

As discussed above, the degree of dissociation of molecules which form free radicals can be calculated for many gases as a function of temperature and pressure. Heated filaments were first used by Langmuir over 40 years ago to produce atomic hydrogen, and have since been widely used by many investigators[7]. Shock pyrolysis, that is the use of shock wave techniques, has been used and is a means of producing free radicals in large concentration. Solar and electrical furnaces are also a means of obtaining high temperatures for inducing molecular dissociation. Efforts by

Nichols[10] at University of Michigan and Gross[11] at Fairchild Engine Division to produce a standing detonation wave, if successful, may offer a method of producing free radicals by thermal means at high concentration in a continous flow device.

Free radicals are produced as intermediates in many chemical reactions. In fact the existence of free radicals was postulated to explain the mechanism of reactions even before there were means to detect free radicals. Although chemical systems are usually complex, production of free radicals by chemical means should not be overlooked.

Electromagnetic radiation in the visible and ultraviolet, absorbed by molecular species, can produce free radicals directly. In wavelengths where these species are transparent to radiation, free radicals can be produced thru photosensitization - the addition of another substance which does absorb energy, and which transfers it to the specie to be dissociated. Flash photolysis of gases can produce free radicals in high concentration.

Free radicals can be produced electrically by passing a molecular specie thru a corona, glow, spark, arc, or electrodeless discharge. Through collisions with electrons or thermal effects a wide variety of ions, atoms, and radicals are produced.

X and gamma radiation absorbed by molecular species produces ions, electrons, and excited molecules, which lead to the formation of free radicals by subsequent collisions. Alpha, beta, neutron or proton bombardment can also produce free radicals. Fission products may be used to produce free radicals with a high efficiency of conversion of nuclear energy directly to chemical energy.

Production of all the free atoms and radicals of interest has been achieved on a laboratory scale by various techniques outlined above. The main problems in production at the present time are to increase the yield or concentration, and to isolate the free radicals of interest from the other hash that is present.

Work on production and concentration of free radicals is being pursued at many places by many means.[12-15] Shock pyrolysis work is underway by Davidson at California Institute of Technology, Green and Hornig at Brown University, and Kistiakowsky at Harvard.

Chemical means are employed by Wertz at University of Minnesota, Norberg at Washington University, Kuentzel of Wyandotte at the National Bureau of Standards, and Fontana of California Research Corporation at NBS. Pimental at University of California is studying free radicals emanating from a combustion flame.

Photolysis techniques are being used by Moe at Aerojet, Anderson at University of Maryland, Prosen at the National Bureau of Standards, Norberg at Washington University, and Pimental at University of California. Flash photolysis is being used by Cross at University of Washington, Livingston at University of Minnesota, Marcus at Brooklyn Polytechnic Institute, Davidson at CIT, and Matheson at Argonne.

Electrical discharge techniques are employed by:-

Cross at University of Washington
Moe at Aerojet
Mann at NBS
Linnett at Oxford
Klein of Olin Mathieson at NBS
Anderson at University of Maryland
Rice at Catholic University.

Lichtin at Boston University is working with a corona discharge, Harteck at Rensselaer and Lichtin also with a glow discharge. Giguere at Laval University and Foner at the Applied Physics Laboratory of Johns Hopkins are using an electrodeless discharge. Hoerl at NBS is producing free radicals by electron bombardment.

Cabrera at University of Virginia is using X ray techniques. Gamma radiation is used by:-

Wertz at Minnesota
Moe at Aerojet
Carr at Phillips Petroleum Company
Florin at NBS
Livingston at Oak Ridge
Matheson at Argonne
Alger at the Naval Radiological Defense Laboratory.

Harteck at Rensselaer has achieved substantial yields with the recoil energy of UO_2 fission fragments in influencing CO_2 equilibrium at ambient temperatures. Bretton at Yale is investigating reactive radicals in irradiated compounds, Currie of Penn State University is studying reactions of energetic tritium atoms, and Marcus at Brooklyn Poly production of radicals by bombardment of species with a molecular beam. Donn of Wayne University at the NBS will study the chemistry of free radicals under conditions simulating comets and interstellar matter.

Carr at Phillips Petroleum Company is investigating concentration by physical means, Golden of Brandeis at NBS by fractionation, and Wall at NBS by electromagnetic separation. Shock photolysis and shock pyrolysis can be expected to yield free radicals in quite high instantaneous concentrations. Concentration is related closely to the ability to stabilize an accumulation, and depends on the means of production employed.

Detection, Identification, Estimation, and Study

The second area with which we are concerned in utilizing free radicals as propellants is in detection, identification of species, estimation of concentration, and study of their properties. There are several means at our disposal, but the problems are difficult at best.

Conventional methods and techniques of chemistry such as analysis of reaction products, the effect of additives which inhibit, catalyze, fix, or react in some way; and use of isotopes can give clues to the presence, type, and amount of species, as well as additional information on chemical properties.

Measurement of the physical properties such as diffusion rate, thermal conductivity, pressure, density, electrical conductivity; and use of calorimetry and mass spectrometry are valuable and accurate means for determination of species. With knowledge of the specie they are tools for further study of free radicals. Techniques of solid state science and low temperature physics can also be adapted to study of free radicals.

Optical spectroscopy is a tool for detection, identification and study of some species but has definite limitations in certain areas. Infrared emission spectroscopy requires fairly high concentration because of instrumental difficulties; IR absorption can detect concentrations which are somewhat less. Both are deficient in time response and sensitivity. In the gas phase infra red can be useful, but in the solid phase the bands shift for many reasons. Visible and ultraviolet are somewhat more sensitive and accurate than infra red, but there are regions in the spectrum in which many radicals of interest are transparent, and the bands shift at lower temperatures.

The fact that free radical species are paramagnetic has led to the more recent technique of paramagnetic resonance absorption. Free radicals located in a cavity subjected to an oscillating magnetic field at microwave frequencies get excited and betray their presence and specie at certain resonant frequencies. Paramagnetic resonance is a very sensitive means in the liquid and solid states, and over the whole temperature range of 0° absolute to the melting point of the cavity envelope. It is effective also with gaseous free atoms, but somewhat more difficult with gaseous free radicals. Studies of the hyperfine structure yield detailed information on properties of free radicals and atoms. This probably reads something like "A Child's Guide to Spectroscopy", however spectroscopy can get extremely specialized and intricate to say the least. Free radical research frequently requires the application of all types.

Progress has been made on detection, identification, estimation, and study of free radicals. The means for gaining additional information and refining laboratory techniques are available. A future problem area will be to evolve a practical means of determining bulk concentration of free radicals for field use in event they are ever stabilized in sufficient concentration to bother with. Specific impulse as shown in performance calculations is extremely sensitive to the free radical content, and ballistic missile range is roughly proportional to the square of the specific impulse.

Work on optical spectroscopic techniques for detection and identification is being pursued by a large number of investigators. Giguere at Laval University, Davidson at CIT, Herzfeld and Pilon at NBS are working with the visible spectrum. In the ultra violet spectrum are Giguere at Laval, Cross at University of Washington, Pimental at University of California, Carr at Phillips Petroleum, Davidson at CIT, Pilon at NBS and Tanaka at AF Cambridge Research Center. Working with infra red are Giguere at Laval, Cross at University of Washington, Pimental at University of California, Carr at Phillips Petroleum, Moe at Aerojet General, Hornig at Brown University, Davidson at CIT and Harvey of Laval University at NBS.

Work with microwave spectroscopy is being pursued by an even larger number of investigators. Employing paramagnetic resonance absorption are:-

Norberg - Washington University
Wertz - University of Minnesota
Fraenkel - Columbia
Anderson - University of Maryland
Pake - Stanford
Pimental - University of California
Carr - Phillips Petroleum
Moe - Aerojet
Mann - National Bureau of Standards
Gordy - Duke
Herzfeld - National Bureau of Standards
Foner - Applied Physics Laboratory, Johns Hopkins
Griffing - Catholic University
Mulliken - University of Chicago
Mattarese - Naval Research Laboratory
Ambler - National Bureau of Standards
Davidson - California Institute of Technology
Broida - National Bureau of Standards
Livingston - Oak Ridge
Matheson - Argonne
Alger - Naval Radiological Defense Laboratory.

Hyperfine splitting has been reported by Norberg at Washington University, Fraenkel at Columbia, Foner at APL, Anderson at University of Maryland, and Livingston at Oak Ridge. Wertz at University of Minnesota is working with nuclear resonance.

Specific studies of the properties of free radicals and free atoms by various means is being pursued by:-

Anderson - University of Maryland
Cross - University of Washington
Mann - National Bureau of Standards
Hornig - Brown University
Griffing - Catholic University
Slater - Massachusetts Institute of Technology
Giaque - University of California
Long - University of Chicago
Hoerl, Furukawa, and Brown - National Bureau of Standards
Rice - Catholic University
Livingston - Oak Ridge

Mauer at NBS is using X ray diffraction, and Klein of Olin Mathieson at NBS, field emission microscopy.

Means to estimate concentration of free radicals are being explored by Fraenkel at Columbia, Bretton at Yale, Mann at NBS, and Boyd at NBS. Moe at Aerojet, Carr at Phillips Petroleum, and Furukawa at NBS are using calorimetry to estimate concentration. Kistiakowsky at Harvard and Dibeler at NBS are using mass spectrometry.

Stabilization and Storage

The most challenging problem of all in the utilization of free radicals for ultra energy propellants is that of stabilization and storage. Steacie writes in effect that free radicals are not inherently unstable; they are just highly reactive. This is not just a hyperfine splitting of filaments.

Stabilization is really a misnomer. Furthermore, everybody knows that a stable is a building where horses are lodged and fed. On the other hand, we are trying to lodge free radicals, so stabilization of free radicals may not be such a misnomer afterall. As long as everyone understands the context of stabilization, lets consider the reaction rate.

The basic equation of chemical kinetics governing free radical reactions is the Arrhenius expression in which the rate is a function of temperature, activation energy, collision factor, and the steric or probability factor. Considerable treatment of these factors and means of stabilization which they suggest are given by Steacie,[7] Aerojet,[3] WADC,[4] and others.

The problem is difficult because free radicals require little or no activation energy to recombine. Lowering the temperature will certainly slow recombination. Immobilizing the radicals or locking them up in a solid inert matrix keeps them from colliding and recombining. When they do collide their probability of recombining is close to one. A possible means of tampering with the probability would be to separate the radicals whose electron has a left hand spin from those radicals whose electron has a right hand spin at the time they are produced, and of keeping the spins aligned by a magnetic field. There is also a catalytic wall effect to contend with. The energy of recombination is so great that a three body collision is believed necessary to absorb all the energy that is liberated. Evidence points to the fact that the wall is a convenient third body because it just happens to be there, and it gets scorched for its trouble.

Most of the free radicals of interest have been produced at high temperatures and stabilized in gram quantities by freezing in an inert matrix at extremely low temperatures before they can recombine. The concentrations stabilized however have not exceeded much more than one percent to date. Present indications are that to stabilize in this manner, the ratio of inert matrix to active species must exceed a ratio of one hundred to one. Recall that free radical propellants begin to show interesting performance at ten percent concentration. Nuclear, X, ultra violet, and visible irradiation of parent molecular substances at low temperatures are promising means of producing and stabilizing free radicals in situ. A large charge of energy is required both to disrupt the molecular bond and to wallop the fragments into different cages in the lattice where they cannot recombine.

Broida [16] reported his own work in low temperature stabilization and summarized other pertinent experimental work in March 1956. More recent progress in production, identification, and stabilization of free radicals was reported by many investigators [17] at the symposium at Laval University, September 1956.

Stabilization of free radicals in amorphous structure, viscous liquids, and on large surfaces bears investigation. Synthesis of radical producing chemical compounds is a possible means of storage. Inhibition of free radicals by chemical means would be perhaps the ideal way to do it. Unfortunately the free radical "inhibitors" of conventional chemical chain reactions merely react with the free radical intermediates, taking them out of circulation before they propagate more free radicals. That mechanism is no help. Some materials are catalytic, some are inert, but no materials known at this time are "anti-catalytic" to free radical recombination. That possibility seems as remote as anti-matter.

As an engineer, a last observation screams at me, and that is the futility of reaction rate calculations that are based on experimental or assumed values of activation energies, steric factors, and collision factors which may be off by a factor up to 10^3. If the minimum objective of this program is to increase the concentration of radicals stabilized by one magnitude, it would seem necessary to obtain basic information accurate to better than three magnitudes. More accurate data might indicate a shift in emphasis in the approaches toward influencing the reaction rate. Further study of the determinant factors seems necessary.

To summarize stabilization, I think everyone agrees that putting radicals in stables is a tough job.

Work on stabilization in the low temperature regimes is underway by:-

Giguere - Laval
Pake - Stanford,
Pimentel - University of California
Carr - Phillips Petroleum
Foner - Applied Physics Laboratory of Johns Hopkins
Anderson - University of Maryland
Cabrera - University of Virginia
Davidson - California Institute of Technology
Giaque - University of California
Long - University of Chicago
Mauer, Wall, Hoerl, and Broida - National Bureau of Standards
Ruehrwein - Monsanto at National Bureau of Standards
Rice - Catholic University
Livingston - Oak Ridge
Matheson - Argonne

Working to trap free radicals in a crystalline matrix, predominantly at low temperature, are:-

Giguere - Laval
Fraenkel - Columbia
Pimentel - University of California
Foner - Applied Physics Laboratory of Johns Hopkins
Davidson - California Institute of Technology
Anderson - University of Maryland
Mauer, Boyd, Florin, Hoerl, and Prosen - National Bureau of Standards
Livingston - Oak Ridge
Matheson - Argonne

Norberg of Washington University and Carr of Phillips Petroleum are investigating trapping of free radicals in viscuous liquids, and on large surfaces.

Pellam at CalTech and Broida of NBS are collaborating on stabilization of free radicals by alignment of electron spins.

Giguere at Laval is studying the influence of the physical parameters on stabilization. Giguere and Harteck of Rensselaer are studying non-catalytic materials.

Collins at MIT is doing cryogenics research on large scale preparation of liquid helium and other efforts are being made on techniques for handling.

Reaction

Reaction is closely related to stabilization in that controlling the reaction is the key to both. If free radicals are ever stabilized experimentally in sufficient concentration, the means of stabilization would suggest ways of controlling the subsequent reaction. In any event, inducing free radicals to combine is not a problem. To estimate the concentration of radicals present by calorimetry, it is necessary only to warm the contents slightly to produce recombination which is evidenced by heat evolution. At least one instance[17] has been reported in which warming produced a violent explosion. It is well to realize that a container of the free-radical propellants postulated would have all the elements of a super-high explosive. A knowledge of recombination rates is certainly essential, as well as other data on chemical and physical properties.

Catalysis offers promise as a means of controlling recombination. Harteck at Rensselaer has found that gold will catalyze the recombination of gaseous O and that aluminum is inert insofar as recombination of O is concerned. He demonstrated a heat evolution (and hence thrust) in a crude "airbreathing" engine in the laboratory. In connection with Zellikoff's studies at the AF Cambridge Research Center, it was demonstrated that there is energy available in the upper atmosphere that can be liberated by a suitable catalyst. An Aerobee rocket at 60 miles altitude discharged nitric oxide which catalyzed the recombination of atomic oxygen in the upper atmosphere, producing a visible glow in the sky.

An approach for studying free radical propellant systems at this time has been suggested [13]. If a model propellant with unreacted chemicals of extremely low activation energy contained in a solid matrix could be prepared, this would be analogous to the kinetics and handling anticipated with the free radical propellants postulated. Some work along this line would give us a feel for the problems of free radical propellants.

It is premature at this time to judge the feasibility of free radical propellants on the basis of their compatibility with current engine hardware concepts. According to Aerojet calculations with hydrogen, at temperatures above 3000°K, performance decreases as chamber pressure increases because of suppression dissociation. It is therefore desirable in high temperature regimes with free radical propellants to operate at as low a chamber pressure as feasible and still maintain a 20/1 pressure ratio. Conventional combustion parameters such as combustion time delay, deflagration, detonation, chamber characteristic length have a radically - changed significance. Would wall effects reverse the familiar temperature profile across a chamber? Every start and shutdown with a free radical propellant would be fuel rich. What happens when a hot combustible gas like hydrogen is belched out at 25000 feet per second into an oxidizing atmosphere? Would this be a flame thrower of gigantic proportions with an invisible flame? Would this necessitate an afterburner or imply a ducted rocket? How large a specific impulse would that give us? A fresh engineering design approach will have to be evolved and tailored around the characteristics of the free radical propellant, if any, that is ultimately evolved.

Recombination reaction rates are being studied by the following investigators:

Harteck - Rensselaer Polytechnic Institute
Norberg - Washington University
Cross - University of Washington
Livingston - University of Minnesota
Anderson - University of Maryland
Pake - Stanford University
Lichtin - Boston University
Boudart - Princeton University
Carr - Phillips Petroleum
Marcus - Brooklyn Polytechnic Institute
Davidson - California Institute of Technology
Hornig - Brown University
Rice - Catholic University
Livingston - Oak Ridge National Laboratory
Herzfeld - National Bureau of Standards
Golden of Brandeis - National Bureau of Standards
Pilon - National Bureau of Standards
Minkoff of Imperial College - National Bureau of Standards
Hoerl - National Bureau of Standards
Furukawa - National Bureau of Standards
Dibeler - National Bureau of Standards
Florin - National Bureau of Standards
Kuentzel of Wyandotte - National Bureau of Standards
Fontana of California Research Corporation - National Bureau of Standards

Reaction of free radicals with other species is being investigated by:

Giguere - Laval University
Zelicoff - AF Cambridge Research Center
Lichtin - Boston University
Linnett - Oxford University
Davidson - California Institute of Technology
Rabinowich - Washington University
Szwarc - New York State Forestry
Florin - National Bureau of Standards
Ruehrwein of Monsanto - National Bureau of Standards
Klein of Olin Mathieson - National Bureau of Standards

Reaction under conditions simulating interstellar matter is being investigated by Donn of Wayne University at NBS. Prosen at NBS is studying reactions induced by ultra violet radiation. Reaction products are being studied by Giguere at Laval University and Lichtin at Boston University.

Catalysis is being investigated by Harteck at Rensselaer, Zelicoff at AF Cambridge Research Center, Giguere at Laval and Boudart at Princeton.

Summary and Conclusions

In this survey of US Government sponsored research on free radicals, the existing programs of the Air Force Office of Scientific Research, Cambridge Research Center, Wright Air Development Center, the Office of Naval Research, Office of Ordnance Research, National Bureau of Standards, Atomic Energy Commission, and the National Science Foundation were reported on. Additional studies are being initiated.

I am aware of considerable additional research underway in Canada, but I was unable to include it in this paper. Knowledge of any other work pertinent to free radical propellants would be of definite interest to the Department of Defense. My sincere apologies if I missed any research projects in this survey.

To date, the only investigators who have trapped and stored active free radicals successfully in large concentrations at ambient temperature are from the Federal Bureau of Investigation.

A great deal of basic research remains to be done. While the technological feasibility of this effort cannot yet be judged, I am reasonably optimistic for several reasons:

1. The progress which has been made in recent years.
2. The caliber of the scientists engaged in this work and their dedication to the effort.
3. The increased emphasis on research by the government and the industry.

As is characteristic of exploratory research, the new knowledge being generated may reveal that free radical propellants as now conceived are not feasible. However, the insight which is being gained into chemical and physical mechanisms will more than pay for itself in industrial and military applications. Basic knowledge is like money. It can be applied to many things. In that sense we can't miss.

Bibliography

1. Rocket Engine Propellants, Rocketdyne, North American Aviation Inc. April 1956
2. Pocket Data for Rocket Engines, Bell Aircraft Corporation, 1953
3. Research on Ultra-Energy Fuels for Rocket Propulsion, Report No. 1149 (Final) AFOSR-TR-56-346 dated 31 July 1956, Aerojet General Corporation, Azusa, California
4. Memorandum on Free Radicals as Fuels by K. Sheller, H. C. Thacker, and J. A. Bierlein, Chemistry Branch, Aeronautical Research Laboratory, Wright Air Development Center. Preliminary draft, November 1956
5. B. Lewis and G. von Elbe, "Combustion, Flames, and Explosion of Gases", Cambridge U. Press, London, 1938
6. Free Radical Data, unpublished, Reaction Motors Incorporated, Denville, N. J.
7. Atomic and Free Radical Reactions, EWR Steacie, 2nd Edition, Reinhold, New York, 1954
8. Some Recent Developments in the Study of Unstable Species, R. A. Marcus, Brooklyn Polytechnic Institute, 1956
9. Report of Task Group on Free Radical Research (to Department of Defense) dated 25 June 1956, CONFIDENTIAL, W. T. Olson, H. P. Broida, D. E. Carr, J. R. Pellam
10. AFOSR Contract AF 18(600)-1199
11. AFOSR Contract AF 49(638)-15
12. Memorandum-The Air Force and Atomic Energy Commission Free Radical Program (in preparation) Lt. Col. Paul Atkinson, Air Force Member, Steering Committee on Free Radical Feasibility Study
13. Memorandum-Navy and National Science Foundation research related to Free Radical Feasibility Study, 7 December 1956, CONFIDENTIAL, Ralph Roberts, Navy Member, Steering Committee on Free Radical Feasibility Study
14. Report of Office of Ordnance Research, 11 December 1956 - Dr. Glockler, Army Member, Steering Committee on Free Radical Feasibility Study
15. Free Radical Research Program, National Bureau of Standards, 11 December 1956, Dr. H. P. Broida
16. H. P. Broida "Stabilization of Free Radicals at Low Temperatures" June 1956
17. Symposium Abstracts, "Free Radicals: Recent Progress in their Production, Isolation, and Identification", Laval University 10 and 11 September 1956, Sponsored by Physical Chemistry Division, Chemical Institute of Canada

UNCLASSIFIED

THE EFFECT OF PROPELLANT ENERGY AND MASS DISTRIBUTION ON ROCKET PROPULSION EFFICIENCY

Howard S. Seifert
Ramo-Wooldridge Corporation
Los Angeles, California

I ABSTRACT

a. The effect of varying the exhaust gas velocity of a rocket so that the exhaust gases possess little or no kinetic energy in an earth observers' frame of reference is examined. Under certain boundary conditions an improvement in terminal velocity of 10 to 20% is obtained relative to a rocket with fixed exhaust velocity.

b. Given a fixed budget of energy per unit payload mass, the optimum mass of working fluid into which to distribute this energy (for maximum burnout speed) is calculated as a function of gravitational field strength.

II INTRODUCTION

A considerable fraction of the propellant energy of a rocket is dissipated in the exhaust, which even if expanded with 100% thermodynamic efficiency, trails along after or away from the rocket at high speed, carrying energy which would preferably have been retained in the payload. The conventional chemical propellant must be ejected at constant speed with respect to the rocket, a relatively inefficient process. Recent general interest in the use of nuclear energy for rocket propulsion suggests the possibility that the exhaust velocity of a rocket may become a controlled variable rather than a constant as it has been so far. This paper will calculate the relative performance of rockets with tapered-velocity and fixed-velocity exhaust under certain boundary constraints, and show that improvement in payload velocity can be obtained. An additional calculation will be made to show certain optimum circumstances under which a constant but arbitrarily adjustable exhaust velocity may be used.

UNCLASSIFIED

III STATEMENT OF THE PROBLEMS

Two problems will be examined:

a. Given two rockets with identical mass ratios, mass flow rates, and propellant masses, what will be the ratio of their burn-out velocities if they consume amounts of energy which are equal, but distributed in the first one in such a way as to cause the exhaust trail to have zero (or small) velocity relative to ground, and in the second in the usual manner with a fixed velocity relative to the rocket? Presumably the first distribution should be more efficient, since more of the propellant energy goes into the payload.

b. Suppose we are given a fixed amount of energy which may be distributed uniformly into any desired fraction ζ of the mass of a rocket in order to propel the remaining fraction $1 - \zeta$. What is the value of ζ which will result in the highest terminal velocity of the residue? The possibility of optimum ζ is intuitively evident, since with fixed energy, if ζ is too low, not much momentum will result per unit energy expended, while if ζ is too high the consequent low exhaust velocity will reduce performance.

In both the above problems it has been assumed that any arbitrary amount of energy may be associated with a unit mass; in other words, temperature is not a limiting factor. This is not true at present, but there is no a priori reason to believe that the containment of high temperature matter is an unsolvable problem.

IV THE TAPERED EXHAUST VELOCITY PROGRAM

The equation of motion of a rocket moving vertically, and possessing at t = 0 an initial exhaust velocity c_o which increases by the same amount that the vehicle speed increases, is

$$(M_o - \dot{m}t)(a + g) = \dot{m}\left[\int_0^t a\,dt + c_o\right] \tag{1}$$

Where M_o = initial total mass
$\dot{m}$ = mass flow rate
a = upward acceleration relative to ground
g = constant gravitational field acceleration
c_o = initial (constant) exhaust velocity

This may be reduced by differentiation to

$$\frac{da}{2a + g} = \frac{dt}{t_o - t} \tag{2}$$

Where $t_o = M_o/\dot{m}$.

If the initial acceleration is $a_o (= \frac{c_o \dot{m}}{M_o} - g)$ then (2) may be integrated twice to give

$$v' = (c_o - \frac{gt_o}{2})(\frac{t}{t_o - t}) - \frac{gt}{2} \qquad (3)$$

Where v' is the vehicle velocity upward. At burnout, $t = t_b = \zeta M_o/\dot{m} = \zeta t_o$, where

$$\zeta = \frac{R - 1}{R} = \frac{M_p}{M_o + M_p} = \text{loading fraction}$$

$$R = \frac{1}{1 - \zeta} = \frac{M_o + M_p}{M_o} = \text{mass ratio}$$

The velocity at burnout ($t = t_b$) follows from (3)

$$v'_b = c_o(R - 1) - \frac{gt_b}{2}(R + 1) \qquad (4)$$

Let us define a gravity loss parameter $\gamma_b = gt_b/c$, which is essentially the decrease in missile speed at burnout caused by the gravitational deceleration measured in multiples of an exhaust velocity c. This exhaust velocity c is that of an equal energy rocket of constant exhaust velocity. It will presently be related to c_o. Using γ_b in (4), we arrive at

$$v'_b = c_o(R-1)(1 - \frac{\gamma_b}{2} \cdot \frac{R + 1}{R - 1} \cdot \frac{c}{c_o}) \qquad (5)$$

The velocity reached by a conventional rocket with the same R and burning time t_b is

$$v_b = c\ln R - gt_b = c\left[\ln R - \gamma_b\right] \qquad (6)$$

We may then express the ratio of the burnout velocities of the tapered c vs constant c vehicles as

$$\frac{v'_b}{v_b} = \frac{c_o(R-1)(1 - \frac{\gamma_b}{2} \cdot \frac{R+1}{R-1} \cdot \frac{c}{c_o})}{c(\ln R - \gamma_b)}$$

$$\frac{v'_b}{v_b} = \left(\frac{(R-1)}{\ln R - \gamma_b}\right)\left(\frac{c_o}{c} - \frac{\gamma_b}{2} \cdot \frac{R+1}{R-1}\right) \qquad (7)$$

The two rockets must expend equal energies, as well as have the same values of M_o, $\dot{m}$, R, and t_b; c_o and c are therefore related. The energy equivalence may be expressed as

$$\frac{1}{2} m_p c^2 = \frac{1}{2} \int \left[v' + c_o\right]^2 \dot{m} dt \qquad (8)$$

Where c = exhaust velocity of constant-c rocket
m_p = total propellant mass of either rocket
$\dot{m}$ = constant mass flow rate of either rocket
v' = instantaneous velocity of tapered-c rocket

Substituting (3) in (8) and simplifying, after extensive algebra, results in

$$\frac{c_o}{c} = \frac{\gamma_b}{2} + \sqrt{\frac{1 - \gamma_b^2/12}{R}} \qquad (9)$$

We may now eliminate c_o/c from (7) by the use of (9) and have the comparison v'_b/v_b in terms of the two fundamental parameters R and γ_b.

$$\frac{v'_b}{v_b} = \frac{1}{\ln R - \gamma_b}\left(\frac{R-1}{R^{(.5)}} \cdot \sqrt{1 - \gamma_b^2/12} - \gamma_b\right) \qquad (10)$$

A typical value of $\gamma_b = gt_b/c$ is .25. In efficient rockets, it is seldom that $\gamma_b > 1$. Therefore we may neglect $\gamma_b^2/12$ relative to unity and simplify (10) to:

$$\frac{v'_b}{v_b} \overset{o}{=} \frac{(R-1)/R^{(.5)} - \gamma_b}{\ln R - \gamma_b} \qquad (11)$$

Values of v'_b/v_b are shown in Table I, and plotted in Figure 1, indicating the effect of the tapered exhaust velocity on v'_b/v_b. It can be seen that in field-free space ($\gamma_o = 0$) at R = 5, an 11% improvement in relative terminal velocity can be obtained. In the presence of gravitational fields, the ratio is increased, although both velocities decrease, of course, in absolute magnitude.

V MAXIMUM TEMPERATURE OF TAPERED EXHAUST

If the exhaust stream is produced by thermal expansion, the temperature of the gas reservoir will be proportional to the square of the exhaust velocity relative to the rocket. The maximum temperature will be reached at burnout in the tapered-c case. The ratio of maximum temperatures T'_m/T_m, tapered to constant operation, will be

$$\frac{T'_m}{T_m} = \frac{(v'_b + c_o)^2}{c^2} \qquad (12)$$

Let us use relations (5) and (9) to evaluate the field-free case ($\gamma_b = 0$).

$$\frac{T_m}{T_m} = \frac{(c_o[R-1] + c_o)^2}{c^2} = \frac{c_o^2}{c^2} \cdot R^2 = R \qquad (13)$$

For example, we see from Table I that an 11% improvement in $v_b (R = 5)$ results in a five-fold rise in maximum temperature. If equation (12) is evaluated for $R = 5$ and $\gamma_b = 0.25$, the ratio T'_m/T_m becomes 4.4.

VI MAXIMUM VELOCITY OF TAPERED EXHAUST

The maximum exhaust velocity c'_m of the tapered-c rocket, relative to the fixed exhaust c, is given by

$$\frac{c'_{max}}{c} = \frac{v'_b + c_o}{c_o}$$

Using equations (4) and (9) and the fact that $gt_b = c\gamma_b$ leads to

$$\frac{c'_m}{c} = R^{.5} \cdot \sqrt{1 - \gamma_b^2/12} - \gamma_b/2 \qquad (14)$$

Thus for $R = 5$ and $\gamma_b = 0.25$; $c'_m/c = 2.11$. If $\gamma_b = 0$, $c'_m/c = \sqrt{R} = 2.24$. The total span of exhaust velocities $c'_m/c_o = 3.7$, whereas if $\gamma_b = 0$; $c'_m/c_o = R = 5$. This indicates that c_o is substantially lower in field-free space than on the earth's surface.

VII COMMENTS ON TAPERED EXHAUST ROCKET

The initial exhaust velocity c_o must be determined by equating total energy in the propellant in the uniform and tapered programs. If it is desired that the tapered exhaust be absolutely motionless with respect to an earth observer, it is necessary to start off the rocket with a boost velocity equal to c_o. This will modify equation (4) and all subsequent equations involving (4).

The preceding calculations are of interest primarily in situations where energy is limited in quantity and there is no penalty associated with high rate of release of energy. (i.e. Power or temperature not limiting). This is in fact the reverse of conditions governing present chemical rockets. However, there are propulsion techniques, such as accelerated particle beams, in which the controlling factors may differ from those of present conventional engines.

VIII OPTIMUM MASS RATIO WITH FIXED ENERGY PER UNIT PAYLOAD

Let us assume that a fixed amount of energy E/m_o per unit payload m_o can be distributed over a propellant mass m_p, and that a constant mass flow rate $\dot{m}$ and exhaust velocity c will be used. What mass ratio $R = (m_p + m_o)/m_o$ will provide maximum terminal velocity for m_o?

If the energy E is distributed uniformly over the working fluid mass m_p, then the ideal exhaust velocity c is given by

$$E = (.5)m_p c^2 \qquad (15)$$

Inserting this c into the conventional velocity equation (6) gives

$$v_b = \left(\frac{2E}{m_p}\right)^{.5} \ln\left(\frac{m_p + m_o}{m_o}\right) - gt_b \qquad (16)$$

We may express this v_b in terms of the fundamental quantities mass ratio R and initial acceleration ratio $\alpha = a_o/g$ by means of the following relations:

$$R = \frac{m_p + m_o}{m_o} \qquad (17)$$

$$\left(\frac{1}{m_p}\right)^{.5} = \left(\frac{1}{m_o}\right)^{.5} \left(\frac{m_o}{m_p}\right)^{.5} = \left(\frac{1}{m_o}\right)^{.5} \left(\frac{1}{R-1}\right)^{.5} \qquad (18)$$

$$gt_b = g\frac{m_p}{\dot{m}} = g\left(\frac{R-1}{R}\right)\frac{(m_o + m_p)}{\dot{m}}$$

$$gt_b = g\,\frac{R-1}{R}\,\frac{(m_p + m_o)}{F}\,c$$

$$gt_b = \left(\frac{R-1}{R}\right)\frac{gc}{a_o + g}$$

$$gt_b = \left(\frac{R-1}{R}\right)\frac{c}{1 + \alpha} \qquad (19)$$

Where F = constant thrust, and a_o is the initial acceleration in a direction opposite to the gravitational field, with $\alpha = a_o/g$. Substituting (19) and (18) into (16)

$$v_b = \left(\frac{2E}{m_o}\right)^{.5}\left(\frac{1}{R-1}\right)^{.5}\left(\ln R - \frac{R-1}{R(1+\alpha)}\right) \qquad (20)$$

We shall now examine (20) to see if v_b has a maximum with respect to R. The available energy per unit payload, E/m_o, is presumed to be specified.

IX CALCULATION OF MAXIMUM v_b WITH RESPECT TO R

Taking the derivative of (20) with respect to R, and setting it equal to zero results in

$$\ln R_m = \frac{R_m - 1}{R_m}\left[2 + \frac{1}{1+\alpha}\left(1 - \frac{2}{R_m}\right)\right] \qquad (21)$$

Where R_m is mass ratio for max v_b. We note that in field-free space, $\alpha = a_o/g$ approaches infinity, and that for take-off from earth with 1g upward acceleration, $\alpha = 1.0$. Solving the transcendental equation (21) numerically yields the following Table II for the relation between α and R_m.

X CONCLUSION

We see from Table II that in field-free space a rocket with mass ratio 5 will give greatest terminal velocity to m_o per unit of energy available. To cite an extreme example[1] if m_o = 1 ton, and E is that energy available from the fission of 3.75 pounds of Uranium, then the v_b available by distributing this E into the fission fragments only, could be multiplied more than forty-fold by distributing this same E instead into 4 tons of inert working fluid.

Ref (1) H. S. Seifert and M. M. Mills. Physical Review, 71: 279, 1947, and by same authors, Jet Propulsion Lab Memo 3-4, Jan. 23, 1947.

TABLE I

EFFECT OF R AND γ_b ON BURNOUT VELOCITY RATIO v'_b/v_b

R \ γ_b	0	0.1	0.25	0.5	1.0
			(v'_b/v_b)		
1.5	1.005	1.008	1.015	*	*
2.0	1.020	1.023	1.032	1.072	*
5.0	1.11	1.12	1.13	1.16	1.29
10.0	1.24	1.25	1.27	1.31	1.42
20.0	1.42	1.43	1.46	1.50	1.62

*For these large values of γ_b, both v'_b and v_b are negative; i.e. the rocket is sinking rather than rising at burnout, and the ratio v'_b/v_b is not significant.

TABLE II

TAKE-OFF ACCELERATION VS. OPTIMUM MASS RATIO

$\alpha = \frac{a_o}{g}$	$R_m = \left(\frac{m_p + m_o}{m_o}\right)_{opt.}$
0.0	12.5
0.5	9.7
1.0	8.0
2.0	7.0
4.0	6.0
9.0	5.4
∞	5.0 (Field-Free Case)

Note: $\alpha = 0$ means no initial acceleration. (rocket momentarily balanced against g.)

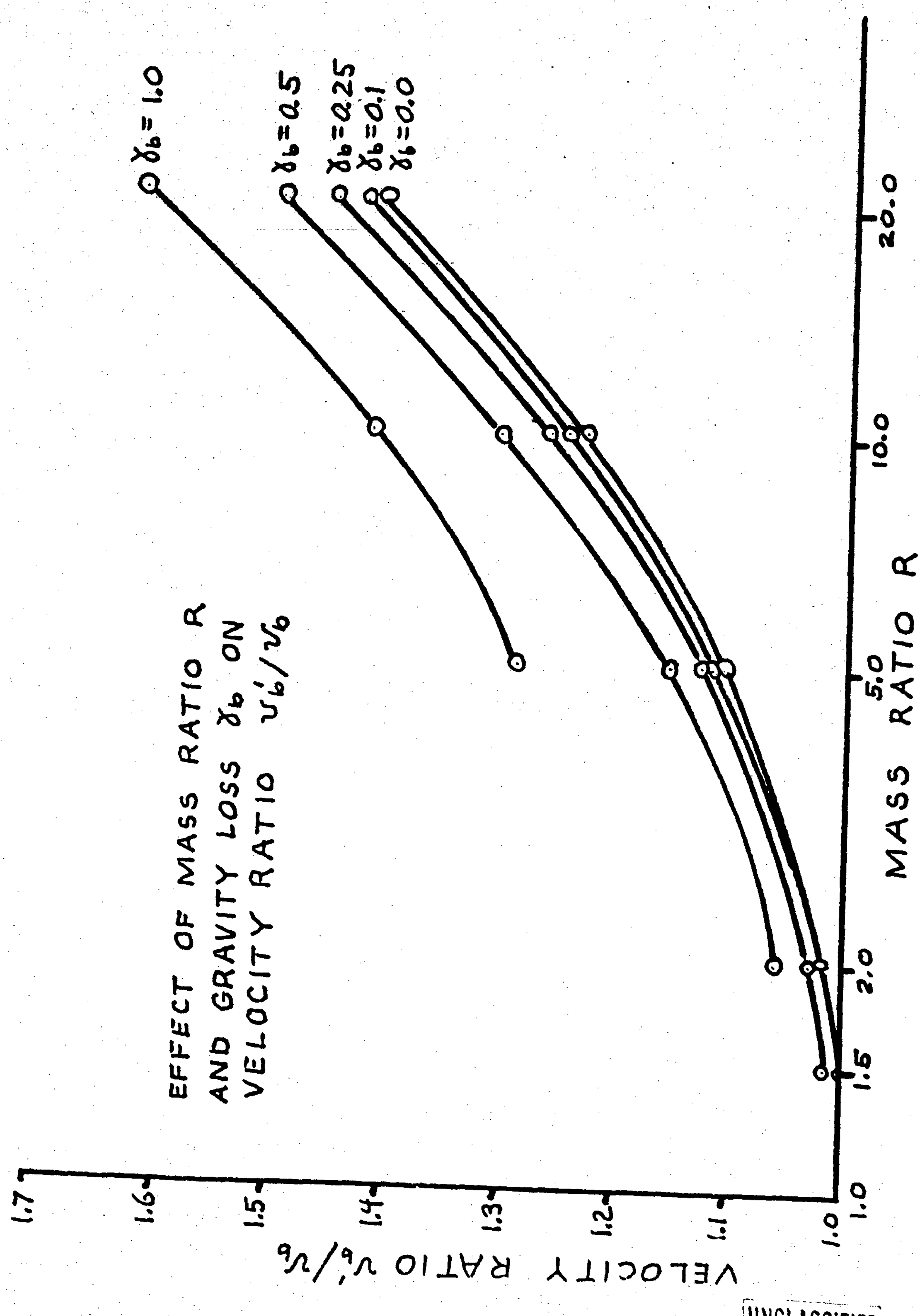
EFFECT OF MASS RATIO R
AND GRAVITY LOSS γ_b ON
VELOCITY RATIO v_b'/v_b
$\gamma_b = 1.0$
$\gamma_b = 0.5$
$\gamma_b = 0.25$
$\gamma_b = 0.1$
$\gamma_b = 0.0$
VELOCITY RATIO v_b'/v_b
1.0
1.1
1.2
1.3
1.4
1.5
1.6
1.7
MASS RATIO R
1.0
1.5
2.0
5.0
10.0
20.0

FIGURE 1

AN EVALUATION OF LIQUID OZONE-OXYGEN MIXTURES AS ROCKET OXIDIZERS

J.P. Layton, I. Glassman, & D. Garvin
James Forrestal Research Center, Princeton University
Princeton, New Jersey

This paper was not received in time to include with the preprints. It will be published with the proceedings, following the symposium.

HYDROGEN PEROXIDE PROPELLANTS

Andrew J. Kubica & John H. Keefe
Becco Chemical Division of Food Machinery & Chemical Corp.
Buffalo, New York

I. INTRODUCTION

Concentrated hydrogen peroxide has been used for many years as an oxidant for rocket propulsion projects and related applications. Many of these applications have been of European origin, principally in war-time Germany and in present day England. In the United States, hydrogen peroxide has found acceptance as a monopropellant. The U. S. Navy has sponsored the development of hydrogen peroxide as an oxidant in underwater propulsion systems and, more recently, as an oxidant in rocket systems especially for superperformance of manned jet aircraft. There is considerable information available on the use of hydrogen peroxide for such applications which will not be presented in this paper. This paper will be confined to a summary of recent research work on hydrogen peroxide and on low freezing hydrogen peroxide-based monopropellants and oxidants.

The propellants which will be discussed are (a) an aqueous solution containing 90% by weight hydrogen peroxide, (b) an essentially anhydrous hydrogen peroxide containing more than 99% by weight H_2O_2, (c) a mixed oxidant consisting of 55% by weight H_2O_2, 39% ammonium nitrate and 6% water and (d) a mixed monopropellant consisting of 67.8% by weight H_2O_2, 6.6% diethylene glycol and 25.6% H_2O (BMP-DEG monopropellant). The properties of these four propellants will be compared. The effects of these properties on handling and on design criteria will be discussed.

II. PROPERTIES OF THE PROPELLANTS

A. Physical Properties

A summary of the important physical properties of the propellants is shown in Table I. Heat capacity vs. temperature for 90 and 100% H_2O_2 is presented in Figure I (SP-2007). It is seen that all four propellants possess the desirable property of being high density solutions. The freezing points shown are, more correctly, the temperature points at which the first crystals appear. All four propellants contract on freezing and all generally supercool at least 20 to 25°F below their true crystallization point. However, for cold weather applications supercooling cannot be depended on to prevent freezing. It is because of this that the H_2O_2-based oxidant and monopropellant solutions are being developed; these solutions have crystallization points of -40°F or lower depending on the water content. For cold weather applications of 90% and 100% H_2O_2, the sensible heat of the solution affords some protection against freezing. A device is presently being developed that will utilize the heat of decomposition of part of the stored H_2O_2 to prevent freezing of the bulk of the solution.

None of the propellants is flammable. All will support combustion of flammable materials. If 90 or 100% H_2O_2 contacts a flammable material containing a catalyst, such as rust, decomposition of the H_2O_2 will occur and the rise in temperature will generally cause ignition of the flammable material. This property is important in providing smooth ignition and combustion in bipropellant systems. The adiabatic decomposition temperature of the H_2O_2-NH_4NO_3 oxidant is shown to be 1479°F. It is difficult to achieve this temperature by catalytic decomposition because complete decomposition of the H_2O_2 and also of the less reactive ammonium nitrate must be obtained. However, pressure, as well as temperature assists in the decomposition of the ammonium nitrate and this is utilized in catalytic decomposers.

The BMP-DEG monopropellant appears to be noninflammable. In a laboratory flammability test, passing a flame over the solution at 77°F and 150°F did not cause either the vapors or the solution to ignite.

If the H_2O_2 present in the BMP-DEG monopropellant is decomposed in a catalyst chamber, the glycol will ignite and an 1800°F flame temperature will be reached.

If a stable BMP-DEG solution is maintained at or near its boiling point, the water, which is the most volatile component, will boil away and the residual mixture will increase in H_2O_2 and fuel concentration. If boiling is continued the change in composition can produce an explosive mixture. Care must be taken to prevent containers of BMP-DEG solutions, as well as other H_2O_2 propellants, from being exposed to external fires.

Other fuel components for monopropellant solutions are being investigated in an attempt to develop a solution whose composition would not change on boiling.

B. Compatibility of Materials

The materials which can be used for handling the hydrogen peroxide oxidants are, in general, the same for all three oxidants. 90 and 100% H_2O_2 have been evaluated more extensively in this respect than has the H_2O_2-NH_4NO_3 solution. However, as might be expected, the results to date indicate that materials suitable for 90% H_2O_2 are also suitable for the H_2O_2-NH_4NO_3 solutions. A partial list of the compatibility of materials with the H_2O_2 oxidants is shown in Table II. A more complete list of materials can be found in Bureau of Aeronautics Handbook NAVAER 06-25-501(1). It should be noted that polyethylene is listed in Table II as a class II material suitable for short-time contact prior to storage or use of the hydrogen peroxide. In previous classifications, polyethylene had been shown as a class I material suitable for long-time contact with H_2O_2. It has been found that, in the presence of a fire, polyethylene will melt and char. Under these conditions, the polyethylene will react explosively with the H_2O_2. Polyethylene could be used as a storage material, but only if there is no possibility of an external fire.

Compatibility tests on BMP-DEG monopropellant with various materials have not been as extensive as the tests with the oxidants. The best material for storage containers for BMP-DEG monopropellants is 1060 (99.6) aluminum alloy. Other alloys of aluminum range between classes II and IV. A factor that must be taken into consideration before making any recommendation of a material of construction is the possible corrosive and solvent property of the organic constituent in the monopropellant. The solvent action of the organic must be considered especially in the case where the use of plastic materials is being contemplated.

C. Stability

The term "stability" embraces a variety of related phenomena including thermal stability, both from the standpoint of storage and of use in regenerative and transpiration cooling, resistance to mechanical or hydrodynamic shock and resistance to adiabatic compression.

A comparison of the storage stability of the four propellants is shown in Table III. Storage stability is directly related to the purity of the solution. 100% H_2O_2 exhibits better storage stability than 90% H_2O_2 because the fractional crystallization process used in manufacturing 100% H_2O_2 results in an increase in purity. The lower stability of the H_2O_2-NH_4NO_3 solution results from the difficulty in obtaining an extremely pure ammonium nitrate and similarly the stability of the BMP-DEG solution depends on the purity of the diethylene glycol and water.

90% hydrogen peroxide has been employed for regenerative cooling of rocket thrust chambers in England and in the United States. Tests at the U. S. Naval Air Rocket Test Station have been reported(2). In the NARTS tests, the maximum temperature recorded at the coolant jacket outlet was 155°F at oxidant to fuel weight ratios from 12.21 to 9.94 and 300 psia chamber pressure. These tests were carried out in a 120 in. L* chamber incorporating commercial hollow-cone spray nozzles made of stainless steel. The six oxidizer nozzles were arranged radially about one fuel nozzle, their axes canted inward at 45°. At these oxidizer-rich ratios a specific impulse of 184 to 189 seconds was realized with an average heat flux to the hydrogen peroxide ranging from 0.75 to 0.89 $BTU/in^2/sec$. The Naval Air Rocket Test Station concluded that 90% H_2O_2 is usable as a regenerative coolant and further study of the problem at higher chamber pressures was recommended.

In porous wall investigations carried out at Becco with 90% H_2O_2, H_2O_2 jacket outlet temperatures were recorded in the order of 380°F when operating at a chamber pressure of 300 psia without incident.

Regenerative cooling by 100% H_2O_2, or by H_2O_2-NH_4NO_3 solution has not been reported. However, the favorably high oxidant to fuel ratios of the 100% H_2O_2 and the H_2O_2-NH_4NO_3 oxidants with JP-4 and their relatively high specific heats would indicate that these oxidants should lend themselves to such cooling provided they are of sufficient thermal stability.

We believe that, if optimum chamber design were employed, local hot spots caused by vortices in conventional helix combustion chambers could be eliminated and higher performance thrust units at higher pressures could successfully be regeneratively cooled with all three oxidants. Actual firing tests under all operating conditions should be performed.

The relatively high thermal stability exhibited by 90% H_2O_2 under transient conditions was shown by tests where the H_2O_2 reservoir was pressurized by hot H_2O_2 decomposition gases. Expulsion tests were carried out by General Electric at their Malta Test Station. A curve of the actual lbs. of 90% hydrogen peroxide expelled from the oxidant tank per lb. of 90% hydrogen peroxide required by the chemical pressurizing gas generator is shown in Figure II (SP-1844). A typical expulsion tank pressure and temperature vs. time curve is shown in Figure III (SP-1812).

The oxidant reservoir was an uninsulated 10-gallon surplus oxygen tank. The duration for total expulsion varied from approximately 25 to 50 seconds depending on the oxidant tank pressure. Maximum tank temperatures realized at the top of the tank were approximately 500°F. In one test, approximately 90 lbs. of 90% H_2O_2

were pressurized with the hot, 1360°F, decomposition gases for approximately 15 minutes before the H_2O_2 was allowed to be expelled from the tank. No build-up in tank pressure was experienced.

The pressure drop through the pressurization gas generator was approximately 20 psi, so that the pressurization system was a pressure sensitive device. If in flight, excessive slosh of the liquid in the propellant tank was experienced, thereby cooling the pressurization gases and causing a slight decrease in the propellant tank of approximately 5 psi, this increased the pressure drop across the gas generator by 25%, automatically increasing the gas generator flow rate to compensate for the cooling effect.

The four propellants have been subjected to a variety of tests to determine their sensitivity to mechanical or hydrodynamic shock and to adiabatic compression. Repeated tests (greater than 50) in a modified Bureau of Mines Liquid Explosive Impact Tester have shown negative results at an impact of 3 kg meters. The temperature of the solution was varied between 70°F and 212°F.

Pipe tests were used to determine the possibility of propagating a detonation wave through a column of each of the propellants. Lengths of schedule 80 stainless steel pipe, 1" diameter, were filled to a depth of approximately two feet. Number 6 electric blasting caps were immersed in the liquid and detonated. No detonations of the propellants were observed. In all cases, there was a barely perceptible bulge in the pipe wall adjacent to the blasting cap. The bulge was approximately the same as when water was used in place of the propellant solutions. Under conditions of higher confinement and greater shock, a partial release of the energy of 90 to 100% H_2O_2 has been observed(3).

Aluminum drums filled with 250 pounds of each of the propellants have been tested by immersing 15 grams of Herkomite No. 2 dynamite at approximately the midpoint of the propellants. The dynamite was then detonated by a No. 6 blasting cap. In all cases the drum walls were bulged and in some cases the rolling hoop adjacent to the dynamite charge was cracked. The tests were conducted with the propellants at ambient temperature (approximately 50°F) and also with the propellants electrically heated to 160°F. Similar results were observed when the drums were filled with water.

Card gap tests(4) were conducted at the Naval Air Rocket Test Station on the four propellants at ambient temperature (approximately 60°F) and with the solutions heated to 160°F. In these tests a sample of the test solution is supported above a detonating charge of 50 grams of tetryl. The space between the detonator and the sample is adjusted by a number of cellulose acetate cards. A steel target plate is placed above the sample. If detonation of the sample occurs, a hole is pierced in the steel plate. The results of the tests in the hydrogen peroxide solutions were confusing. In no case was a hole observed in the target plate. However, some burning or slight melting of part of the target plate was observed, indicative, at least, of partial release of energy of the oxidant. In one series of tests increasing the number of cards caused an increase, rather than a decrease, in the deformation of the target plate. It is planned to repeat the tests using an oxygen balanced detonating charge and noncombustible spacer cards.

Adiabatic compression tests were also conducted at the Naval Air Rocket Test Station on the hydrogen peroxide oxidants and the monopropellant. The results on all four propellants were negative at the maximum pressurization rate of 231,000 psi/sec. obtainable in the NARTS apparatus. The four solutions were tested in triplicate at ambient temperature (approximately 70°F) and at 160°F.

It is concluded that all four propellants are so insensitive to mechanical and hydrodynamic shock and to adiabatic compression which might be encountered in field use that no real hazard exists.

III. 90% H_2O_2, 100% H_2O_2 AND H_2O_2-NH_4NO_3 OXIDANTS IN BIPROPELLANT SYSTEMS

A. Thermal Ignition

Several ignition methods have been employed in bipropellant systems employing 90% H_2O_2, 100% H_2O_2 and the H_2O_2-NH_4NO_3 oxidants. Experience has shown that ignition of the fuel by hot decomposition gases from these oxidants is safer, more reliable and less complex than other ignition systems. No reliance is placed on electric sparks, glow plugs, micro-switches, complicated and critical propellant injection timing devices or other devices. The engine is started "cold," on the decomposition products of the oxidant alone. The decomposition products develop approximately 1/2 the rated thrust giving a first stage thrust level and purging the combustion chamber of any liquid fuel. The fuel is then injected into the combustion chamber and immediate ignition is realized.

Reasonable design decisions on fuel injectors, decomposition gas velocities, chamber volumes and starting pressures must be considered to insure positive ignition. Satisfactory ignition with JP-4 jet fuel has been realized with decomposition gas velocities of approximately 300 feet/sec. and a combustion chamber L* of approximately 80 inches. It is probable that gas velocities can be increased and the L^* decreased with optimum combustion chamber and fuel injection design. These design criteria should be investigated for the particular propellants to be employed.

Thermal ignition employing the decomposition products of the oxidants has the disadvantage of requiring a catalyst to decompose the oxidant. The catalyst weight and volume must be held to a minimum.

B. Factors Affecting Catalyst Decomposition

A typical decomposer, shown in Figure IV (SP-1988), utilizes samarium oxide activated silver screens to decompose 90% H_2O_2. A few comments on the design of such a unit should be mentioned.

The inlet distribution plate is designed to give even propellant distribution over the catalyst bed with an optimum inlet velocity. The diameters of the inlet holes do not exceed 0.125 inches. Stainless steel perforated plates, 1/8" thick, with 20 to 30% open area have been used for both the distribution and bed support plates. High liquid injector velocities can cause erosion of the silver screens. This may cause the downstream section of deep beds to clog resulting in an increase in catalyst bed pressure drop. With minimum depth beds, erosion of the silver screens can cause bed flooding and poor decomposer performance. The catalyst pack must be maintained tight at all times to prevent channeling. In large beds anti-channel baffles should be used, as shown in Figure V (SP-950).

The purity of the hydrogen peroxide required to give satisfactory performance with such catalyst beds has recently been studied. Participants in this program were the Naval Research Laboratory, the Naval Air Rocket Test Station, Reaction Motors, Inc., Rocketdyne, DuPont and Becco. The work was sponsored by the Bureau of Aeronautics. Tentative conclusions concerning the required purity of electrolytically produced 90% H_2O_2 have been reached and are shown in Table IV. Additional work is being done to explore interrelationships between certain of the variables, principally the phosphate-tin-pH relationship, to refine analytical procedures and to study other possible variables in both electrolytically and organically produced H_2O_2.

The 100% H_2O_2 has been decomposed in a catalyst bed similar to the 90% H_2O_2 reactor except that the lower section of the bed, where the temperature exceeded the melting point of the silver, consisted of copper plated stainless steel screens. Catalyst pellets of manganese dioxide and cobalt powder have also been used. High melting silver palladium or silver platinum alloys have exhibited catalyst activity similar to silver in laboratory tests but flow test evaluation has not been performed.

The H_2O_2-NH_4NO_3 catalyst has presented the most difficult development problem of the three oxidants discussed. The difficulty is that most of the standard catalyst materials were dissolved by the hot HNO_3 which is a product of the NH_4NO_3.

Figure VI (SP-1979) shows a catalyst configuration that has been developed by Becco to decompose the H_2O_2-NH_4NO_3 oxidant at a bed loading of approximately 4.3 lbs/in²/min. This is low compared to 20 lbs/in²/min. or higher realized with the 90% and 100% catalyst beds. A typical temperature-time curve at room temperature is shown in Figure VII. Satisfactory on-off ignition at room temperature has also been obtained with the H_2O_2-NH_4NO_3 oxidant and JP-4 and JP-5 fuels as shown in Figure VIII.

Experience with this catalyst at room temperature has indicated that the performance of the catalyst is a function of the reactor pressure. Where low reactor pressures are anticipated (150 psia with decomposition alone or 300 psia with fuel), the bed support plate should have a pressure drop of approximately 74 psi at the rated oxidant flow rate for satisfactory performance.

C. Pilot Combustion Chamber to Minimize Catalyst Size and Weight

A considerable amount of the catalyst might be eliminated in H_2O_2 systems without sacrificing reliability of the conventional H_2O_2-fuel systems, by exploiting the thermal characteristics of the oxidants. With proper design, it appears feasible to reduce the catalyst weight approximately 70 to 85% as shown in Figure IX (SP-922).

Based on test results obtained in the 100% H_2O_2 catalyst development program, there are strong indications that, after the 100% H_2O_2 is initially catalytically decomposed, the 100% H_2O_2 will sustain a high rate of smooth thermal decomposition in the 1824°F atmosphere.

The savings in combustion chamber weight and size that would be realized by this method without great sacrifice of the extreme reliability would make the H_2O_2-fuel combustion chambers compare favorably in size and weight with competing, less reliable propellant combustion chambers. This should be considered especially when large thrust units are anticipated.

D. Performance of Hydrogen Peroxide Oxidants With Various Fuels

Theoretical performance curves of the three oxidants with JP-4 are shown in Figure X. Values for the 90% and 100% H_2O_2 were obtained from the Bureau of Mines(5). Values for the H_2O_2-NH_4NO_3 oxidant were obtained from unpublished data of Rocketdyne, Division of North American Aviation Corp.

Reported information on actual performance of the three oxidants with JP-4 should soon be available from tests which are in progress. Preliminary tests were recently completed at Naval Air Rocket Test Station using the H_2O_2-NH_4NO_3 oxidant and JP-4 and JP-5. Catalytic decomposition of the oxidant and ignition of the fuel were obtained. Additional tests to obtain performance data will be carried out.

Additional theoretical performance curves of 100% H_2O_2 with Diborane, NH_3 and N_2H_4 are shown in Figures XI, XII and XIII (Becco Drawings SP-1995, SP-1996 and SP-1974). Values with the Diborane and NH_3 fuels were obtained from NACA Report Nos. RM E8117a and E8A30, respectively. The N_2H_4 values were obtained from unpublished data of Rocketdyne.

Theoretical performance curves of 98% H_2O_2 with UDMH are shown in Figure XIV (SP-1919). These values were obtained from unpublished data of the General Electric Co., Rocket Section, Aircraft Gas Turbine Division.

Calculations have been published by Dr. Johann G. Tschinkel, Table V, indicating the relative range increase that could be realized in a V-2 type missile if 90% H_2O_2 and 100% H_2O_2 were employed as oxidants instead of liquid oxygen with a common $CH_{1.8}$ hydrocarbon fuel. It is interesting to note that the relative range of a V-2 type missile could be increased by approximately 7 and 16 percent by employing the 90% or 100% H_2O_2, respectively, instead of liquid oxygen.

The simplicity and reliability of systems employing H_2O_2 oxidant are illustrated by the experience of the General Electric Company in the development of a hybrid unit. Several hundred hot runs were made with 90% and anhydrous H_2O_2 with a $C_{11}H_{22}$ (solid polyethylene) fuel without failure. A direct scaling of the 90% H_2O_2 hybrid unit from 200 lb. to 20,000 lb. thrust was accomplished without incident. Simultaneous ignition of nineteen 1050 lb. thrust units verified the reliable ignition and stable combustion characteristics of the H_2O_2-polyethylene system. Another striking feature exhibited by this hybrid propulsion system was the stable combustion experienced with a very low system pressure drop. The total system pressure drop between the oxidant tank and combustion chamber was approximately 50 psi when operating at 400 psia chamber pressure. The estimated catalyst bed pressure drop was about 25 psi.

An H_2O_2-hybrid system employing aluminum or magnesium as the fuel might be investigated for applications where higher impulse is required. The ignition difficulty encountered with the lower decomposition temperatures of the 90% H_2O_2 (1360°F) with aluminum might not be encountered with the higher decomposition temperatures of the 100% H_2O_2 (1824°F).

IV. CONCENTRATED H_2O_2 AND H_2O_2-BASED PROPELLANTS FOR MONOPROPELLANT APPLICATIONS

The Germans utilized approximately 200 lbs. of high strength H_2O_2 per second as a monopropellant in their V-1 launchers without any difficulties. The use of hydrogen peroxide as a monopropellant in the helicopter "Rocket on Rotor," application was developed by Reaction Motors, Inc.(6). This unique system of utilizing the centrifugal force of the rotors for delivering the hydrogen peroxide to the rocket units at high pressures without the use of a pump or gas pressurization system is the utmost in simplicity. The reliability and positive control features of H_2O_2 monopropellant units have been exploited to keep the Glenn L. Martin's "Viking Missile" on course in the stratosphere, where the low air density does not provide sufficient aerodynamic control for the rocket's directional fins. Similar control rockets could be employed to eliminate the aerodynamic control difficulties experienced at extreme altitudes with piloted aircraft.

In gas generator applications, the simplicity and reliability again are attributed to the inherent ease of catalytic decomposition and the density of the concentrated H_2O_2 and H_2O_2 based monopropellants. The specified gas turbine gases can be chosen and held to ± 50°F or closer merely by selecting the appropriate H_2O_2 concentration or the H_2O_2-DEG-water ratio. No reliance is put on electrical or 3rd propellant ignition systems, complex mixture control regulators or critical sequencing systems which is the case with most bipropellant systems. The clean, nontoxic, hot decomposition products of hydrogen peroxide can also be utilized after they leave the turbine for heat exchangers without any danger of fouling with carbon or of corrosion. In piloted aircraft the oxygen-rich exhaust from the H_2O_2 gas generator starter, featuring unlimited starts, could be employed to reignite the oxygen starved turbo-jet engines at extreme altitudes. Where concentrated H_2O_2 is employed as a primary oxidant in the rocket propulsion system, the exhaust products from the H_2O_2 gas generator can be injected into the pilot combustion chamber thereby utilizing additional energy from the gas generator propellant for propulsion.

In order to retain the reliable operating characteristics of H_2O_2 systems, the Bureau of Aeronautics is sponsoring a program to investigate the feasibility of a -40°F freezing point H_2O_2 based monopropellant for reduced temperature application. Satisfactory catalytic starting has been obtained with programmed starts with the H_2O_2-DEG monopropellant at -20°F. Development is being carried out for a catalyst for -40°F operation. Figures XV and XVI (SP-1986 and SP-1985) show the theoretical monopropellant performance curves of the various H_2O_2 concentrations and the -40°F H_2O_2-DEG-H_2O monopropellant.

V. CONCLUSIONS

Recent research has indicated that the following characteristics of concentrated H_2O_2 are advantageous for application in the field of rocket propulsion.

A. The stable combustion characteristics and ignition-purge feature of the H_2O_2-fuel system offer a simple and therefore reliable rocket propulsion system with repeated "On-Off" thrust available if desired.

B. The various oxidant-hydrocarbon fuel systems are not propellant weight ratio sensitive.

C. The relatively low flame temperatures and the favorable specific heats and propellant weight ratios indicate that regenerative cooling with these oxidants appears promising.

D. Concentrated H_2O_2 bipropellant systems demonstrate higher impulse densities than liquid oxygen or nitric acid bipropellant systems with hydrocarbon fuels.

E. The ability to store concentrated H_2O_2 for long periods in plastic bags and diaphragms because it is compatible with plastic materials such as PVC, Kel-F and Teflon make its storage in missiles and aircraft for long periods of time possible. Utilizing an expulsion bladder should be considered in propulsion tankage systems where long-term storage, compatibility, expulsion efficiency, propellant slosh control and control of the center of gravity of the propellants are important.

F. The exhaust products of concentrated H_2O_2 and the H_2O_2-DEG-water monopropellant are not toxic or corrosive.

G. Utilizing the chemical pressurization characteristics of the 90% H_2O_2 and the favorable high temperature stress features of Armco 17-7 PH stainless steel indicate that favorable system weights can be realized with this scheme when competing with costly turbo-pump systems.

H. Hydrogen peroxide is noncorrosive, noninjurious to the skin, nonvolatile and generally easy to handle except for the need for extreme cleanliness and venting of the storage container.

TABLE I

Physical Properties of Hydrogen Peroxide Propellants

Physical Properties	90% H_2O_2	99.6% H_2O_2	H_2O_2-NH_4NO_3	MIP-DEG H_2O
Density at 77°F, g/cc	1.3866	1.4399	1.453	1.295
lb./gal.	11.57	12.04	12.1	10.8
Heat Capacity, BTU/lb. 1°F	0.660	0.628	0.57	-
Refractive Index 77°F	1.3980	1.4063	1.4356	1.3880
Specific Electrical Conductivity 77°F Micromhos/cm.	1.94	0.5	2000	7.4
Vapor Pressure, mm Hg at 70°F	2.57	1.47	-	-
Viscosity, Centipoises, 77°F	1.156	1.156	2.44	1.4
122°F	0.807	0.818	1.98	-
Boiling Point (1.0 ATM), °F	286.4	302.4	410.4	255
Freezing Point, °F	11.3	31.3	-40	-40
Heat of Vaporization, BTU/lb.at 77°F	700.3	652.8	-	-
Surface Tension, dynes/cm.at 68°F	79.33	80.4	-	-
Adiabatic Decomposition Temp. at 1.0 atm, °F	1364	1824	1479	1800
Apparent pH by Glass Electrode	0.1	-2.0	2.8	2.1

TABLE II

COMPATIBILITY OF MATERIALS WITH HYDROGEN PEROXIDE PROPELLANTS

(Partial List)

Material	Long-Time Contact Class 1	Short-Time Contact Prior to Storage Class 2	Short-Time Contact Prior to Use Class 3	Unsatisfactory Class 4
Aluminum Alloys				
1060	X	X	X	X
1100	X	X	X	X
3003		X	X	
2024				X
2024 anodized			X	
5652	X	X	X	
5254	X	X	X	
6061		X	X	
6063		X	X	
43		X	X	
214		X	X	
356		X	X	
Copper				X
Iron				X
Lead				X

TABLE II (continued)

COMPATIBILITY OF MATERIALS WITH

HYDROGEN PEROXIDE PROPELLANTS
(Partial List)

Material	Long-Time Contact Class 1	Short-Time Contact Prior to Shortage Class 2	Short-Time Contact Prior to Use Class 3	Unsatisfactory Class 4
Stainless Steel				
AISI No.				
302		X	X	
304		X	X	
309		X	X	
310		X	X	
316		X	X	
321		X	X	
347		X	X	
400 series				X
Buna				X
Kel-F	X	X	X	
Mylar				X
Polyethylene		X	X	
Silicone Rubber 12650		X	X	
Teflon	X	X	X	
Tygon 3604B		X	X	
Vinylite VG 1914		X	X	

A more complete listing of materials for Hydrogen Peroxide service may be found in Bureau of Aeronautics Handbook NAVAER 06-25-501.

TABLE III

STORAGE STABILITY OF HYDROGEN PEROXIDE PROPELLANTS

	90% H_2O_2	99.6% H_2O_2	H_2O_2-NH_4NO_3 Unstabilized	BMP-DEG 1800-67.8
% Not Decomposed In 24 Hours at 100°C	98 to 99	99	93 to 95	92 to 96
Maximum Recommended Storage Temperature For 300 Lb. Drums	120°F	120°F	100°F	100°F
Maximum Permissible Storage Temperature	145°F	145°F	100°F	100°F

NOTE: The values shown for the H_2O_2-NH_4NO_3 oxidant and BMP-DEG Monopropellant are based on best present data. Unconfirmed data indicates that stabilized H_2O_2-NH_4NO_3 solutions have stabilities similar to that of 90% H_2O_2.

TABLE IV

TENTATIVE PROCUREMENT CRITERIA
FOR 90% HYDROGEN PEROXIDE

	Maximum Content Milligram/Liter
Aluminum	0.6
Nitrate	5.0
Chloride	1.0
Phosphate	0.5
Sulfate	3.25
Tin	4.0
Ammonium	2.25

TABLE V.

Extracted from

"TETRANITROMETHANE AS OXIDIZER IN ROCKET PROPELLANTS"

by Johann G. Tschinkel

which appeared in Industrial and Engineering Chemistry

Vol. 48, Page 732, April 1956

IDEAL CUTOFF VELOCITY FOR SELECTED PROPELLANTS

Oxidizer	uc	SP	Uid uc	Uid	Uid (Relative)	Uid^2 (Relative)	Range (Relative)
H_2O_2 (100%)	2235	1.340	1.379	3082	1.12	1.25	1.16
HNO_3	2153	1.337	1.353	2913	1.06	1.12	1.09
H_2O_2 0.21 H_2O(90%)	2160	1.305	1.337	2888	1.05	1.10	1.07
(O_2) liquid	2400	0.992	1.142	2741	1.00	1.00	1.00

Table V shows the low density propellant (fuel oil-oxygen) to fall off to the last place in the range parameter, Uid^2. Under the assumed ideal conditions, range is proportional to Uid^2. Range calculations were carried out on a V-2 type rocket where necessary adjustments in size of some components, such as pumps, were made, which amounts to adjusting the parameter Vp/Mc. Calculations refer to vertical flight in vacuum. Range came out to be proportional to about 1.5 power of Uid.

REFERENCES

1. Handbook, Field Handling of Concentrated Hydrogen Peroxide, NAVAER 06-25-501, Bureau of Aeronautics, (1955)
2. Blessing, A.H., Ninety-Percent Hydrogen Peroxide as a Regenerative Coolant in a 350 lb. Thrust Rocket Motor, NARTS 84 Technical Note TED-ARTS-SI-5317, February 1956 (Confidential)
3. Jones. L.F., Pope, R., Whitbread, E.G., Report ERDE No. 22R50, Detonability of Liquid Hydrogen Peroxide, Explosive Research and Development Establishment, Waltham Abbey, England
4. Recommended Test No. 1, Card Gap Test for Shock Sensitivity of Liquid Monopropellant, American Rocket Society (July 1955)
5. Brinkley, S.R., Jr., Smith, R.W. and Edwards, H.E., Bureau of Mines Report, Equilibrium Composition, Thermodynamic Properties and Specific Impulse of Combustion Products of Hydrocarbon-H_2O_2 Systems
6. Brown, W.R., Rotor Rockets for Helicopters, Reaction Motors, Inc., Rockaway, New Jersey, American Rocket Society Paper No. 200-55 dated April 21, 1955

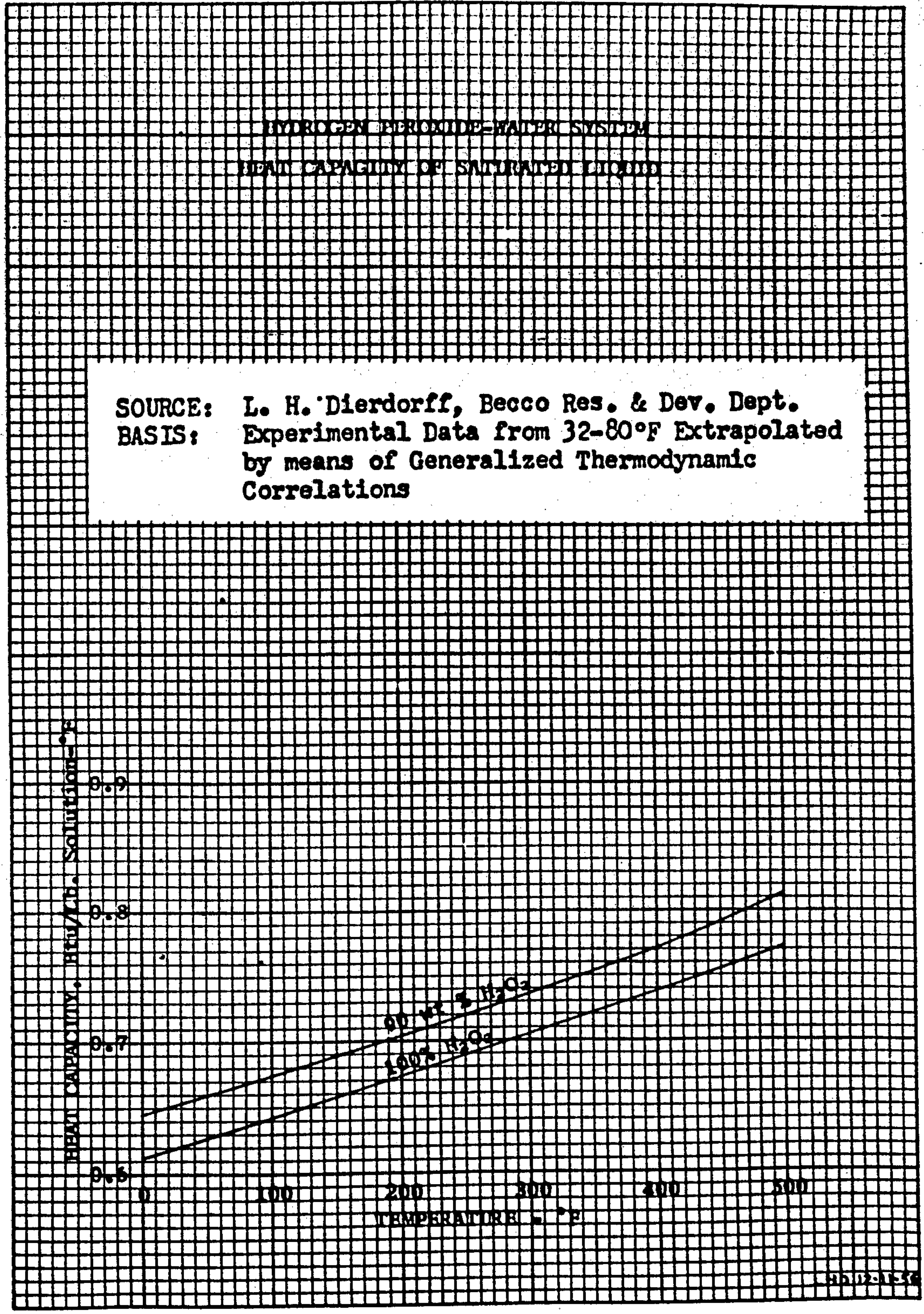

HYDROGEN PEROXIDE-WATER SYSTEM
HEAT CAPACITY OF SATURATED LIQUID

SOURCE: L. H. Dierdorff, Becco Res. & Dev. Dept.
BASIS: Experimental Data from 32-80°F Extrapolated by means of Generalized Thermodynamic Correlations

FIGURE 1
HEAT CAPACITY OF SATURATED LIQUID H_2O_2 WATER SYSTEM

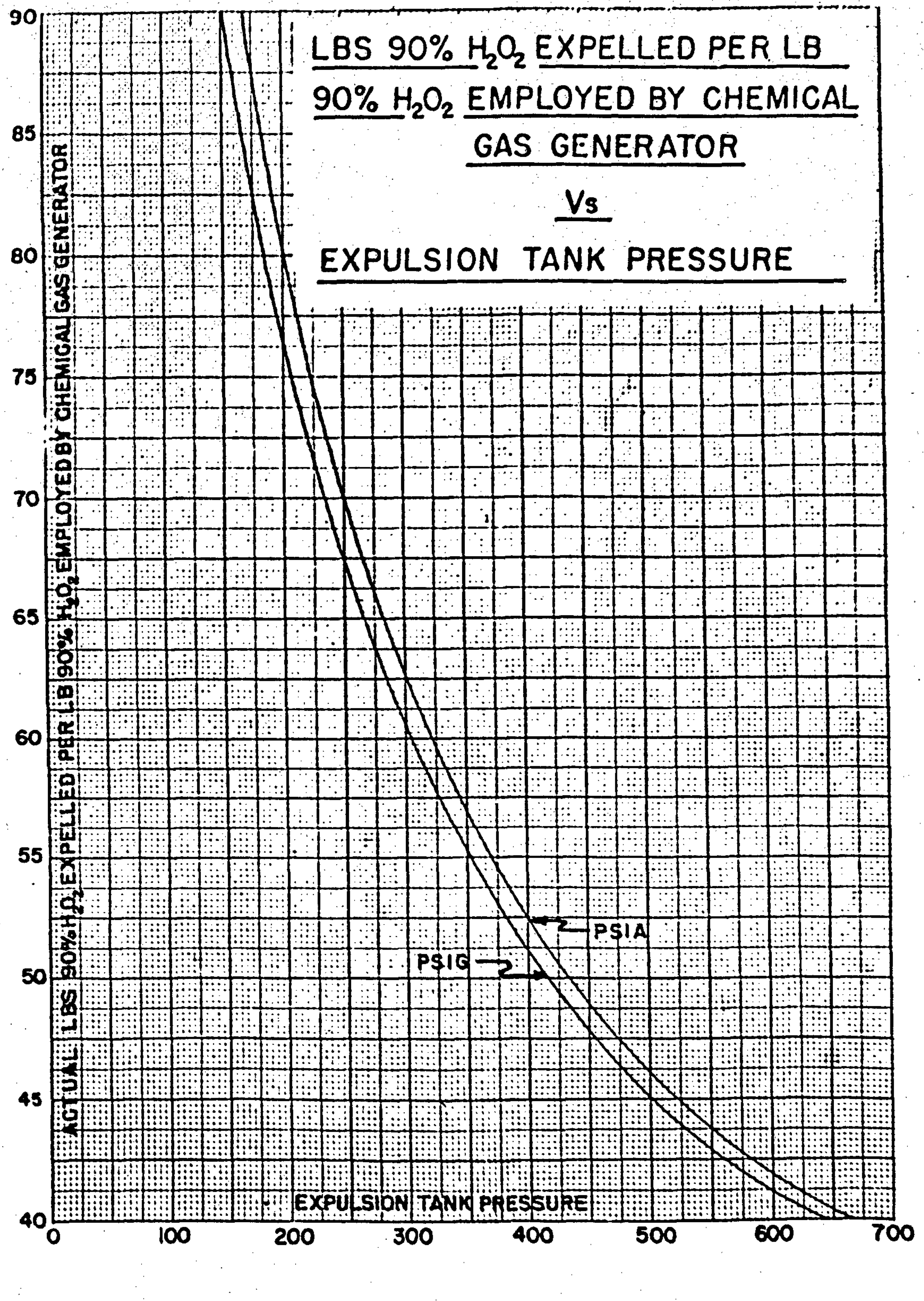

FIGURE 2
90% H_2O_2 EXPELLED
PER LB 90% H_2O_2
EMPLOYED BY CHEM.
GAS GENERATOR

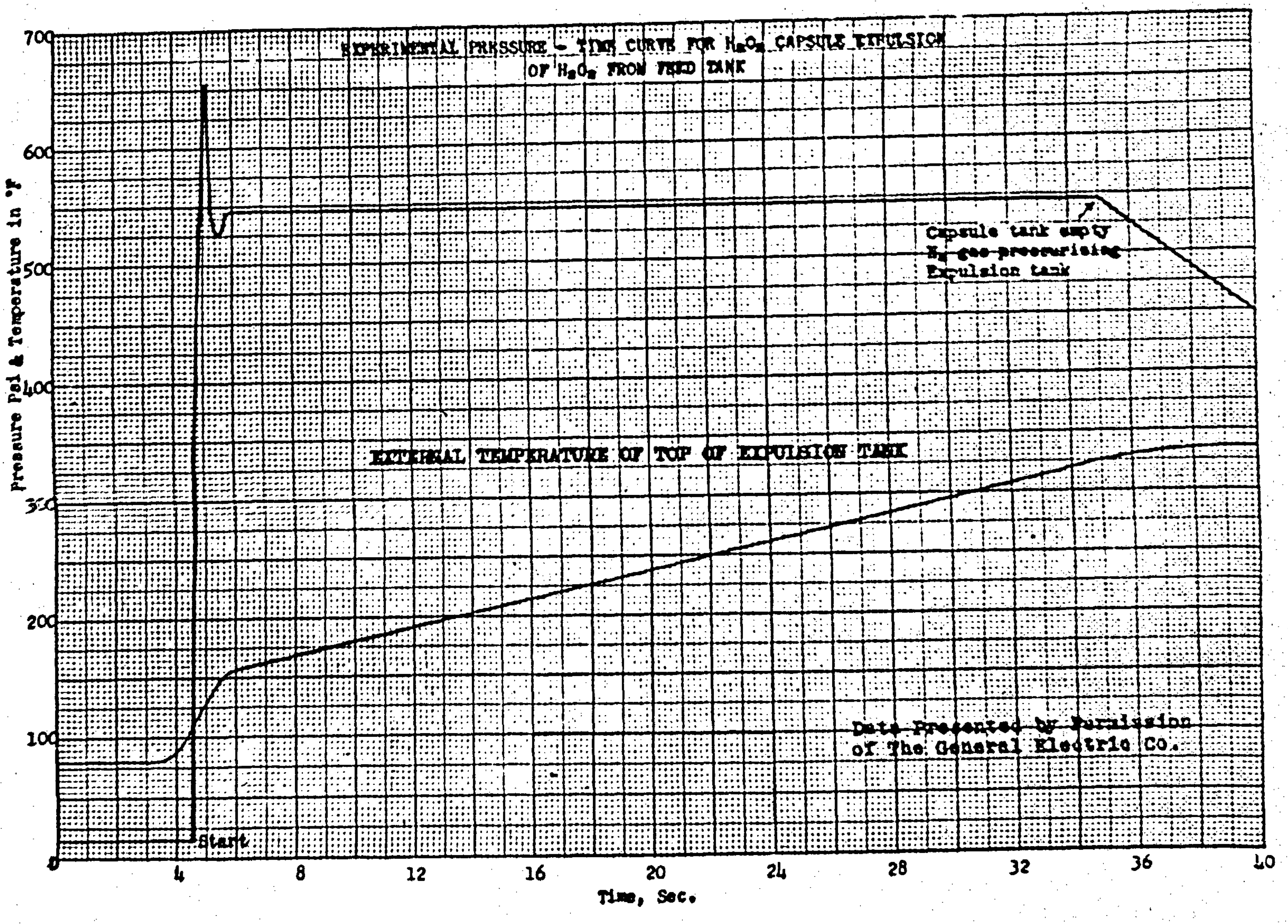
EXPERIMENTAL PRESSURE - TIME CURVE FOR H2O2 CAPSULE EXPULSION
OF H2O2 FROM FEED TANK
EXTERNAL TEMPERATURE OF TOP OF EXPULSION TANK
Capsule tank empty
N2 gas pressurizing
Expulsion tank
Data Presented by Permission
of The General Electric Co.
Start
Pressure Psi & Temperature in °F
700
600
500
400
300
200
100
0
4
8
12
16
20
24
28
32
36
40
Time, Sec.

FIGURE 3

DWG SP-1988

FIGURE 4

TYPICAL GAS GENERATOR DESIGN FOR 90% H_2O_2 AND 100% H_2O_2

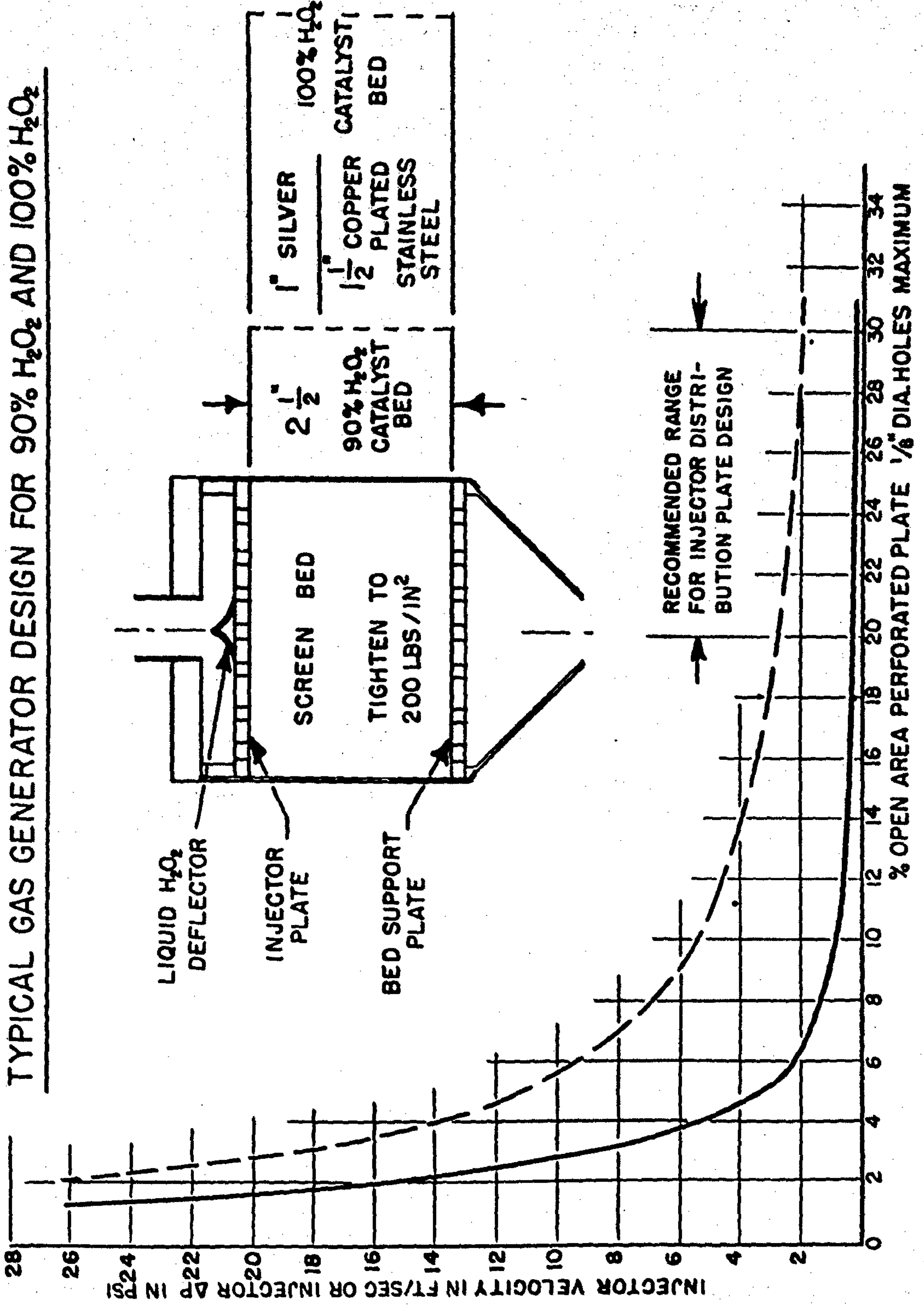
LIQUID H_2O_2 DEFLECTOR
INJECTOR PLATE
BED SUPPORT PLATE
SCREEN BED
TIGHTEN TO 200 LBS/IN^2
$2\frac{1}{2}$"
90% H_2O_2 CATALYST BED
1" SILVER
$1\frac{1}{2}$" COPPER PLATED STAINLESS STEEL
100% H_2O_2 CATALYST BED
RECOMMENDED RANGE FOR INJECTOR DISTRIBUTION PLATE DESIGN
INJECTOR VELOCITY IN FT/SEC OR INJECTOR ΔP IN PSI
28
26
24
22
20
18
16
14
12
10
8
6
4
2
0
2
4
6
8
10
12
14
16
18
20
22
24
26
28
30
32
34
% OPEN AREA PERFORATED PLATE 1/8" DIA. HOLES MAXIMUM

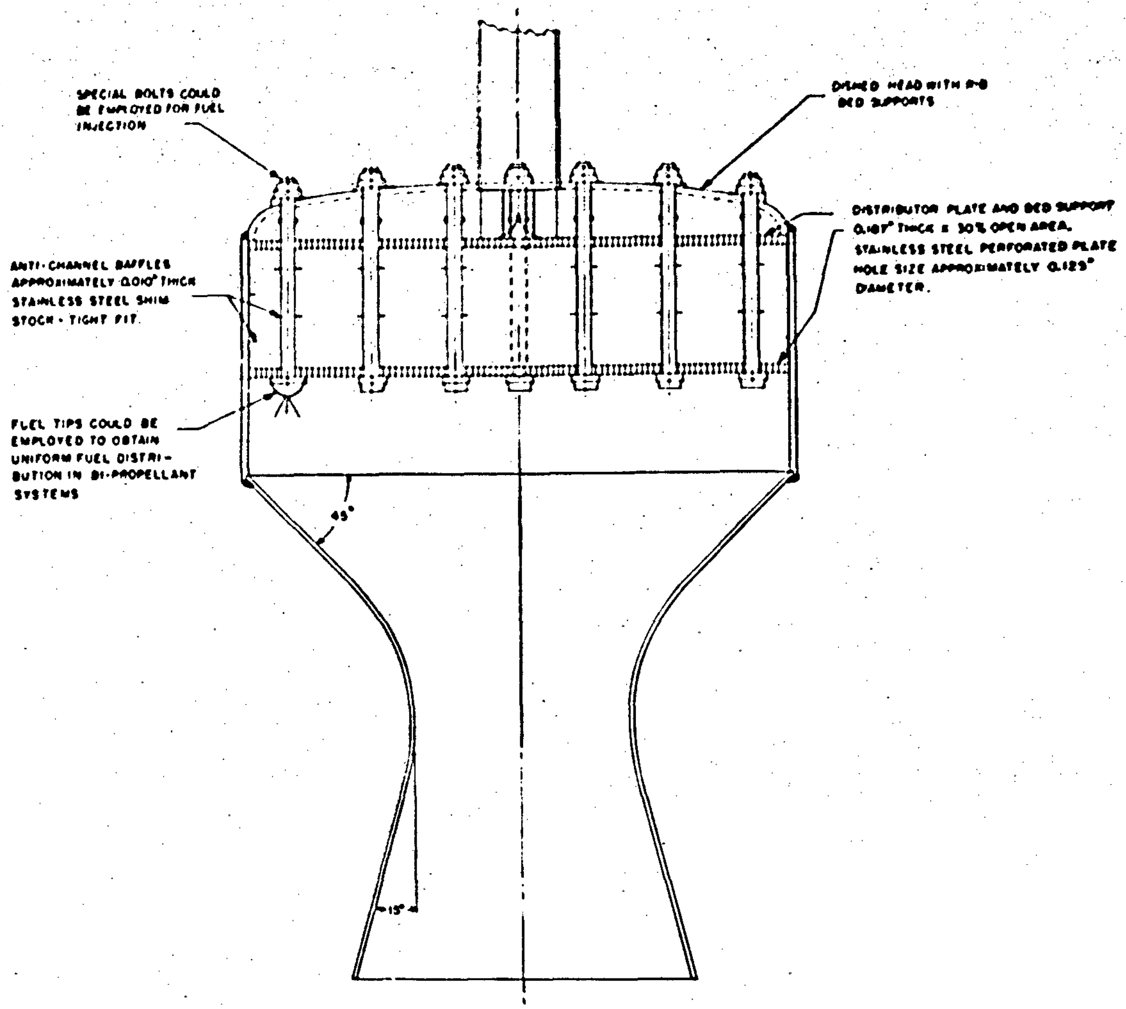
SPECIAL BOLTS COULD BE EMPLOYED FOR FUEL INJECTION
DISHED HEAD WITH R-B BED SUPPORTS
DISTRIBUTOR PLATE AND BED SUPPORT 0.187" THICK x 30% OPEN AREA. STAINLESS STEEL PERFORATED PLATE HOLE SIZE APPROXIMATELY 0.125" DIAMETER.
ANTI-CHANNEL BAFFLES APPROXIMATELY 0.010" THICK STAINLESS STEEL SHIM STOCK - TIGHT FIT.
FUEL TIPS COULD BE EMPLOYED TO OBTAIN UNIFORM FUEL DISTRIBUTION IN BI-PROPELLANT SYSTEMS
45°
15°

TYPICAL 90% H_2O_2 MONOPROPELLANT
ROCKET THRUST CHAMBER

FIGURE 5

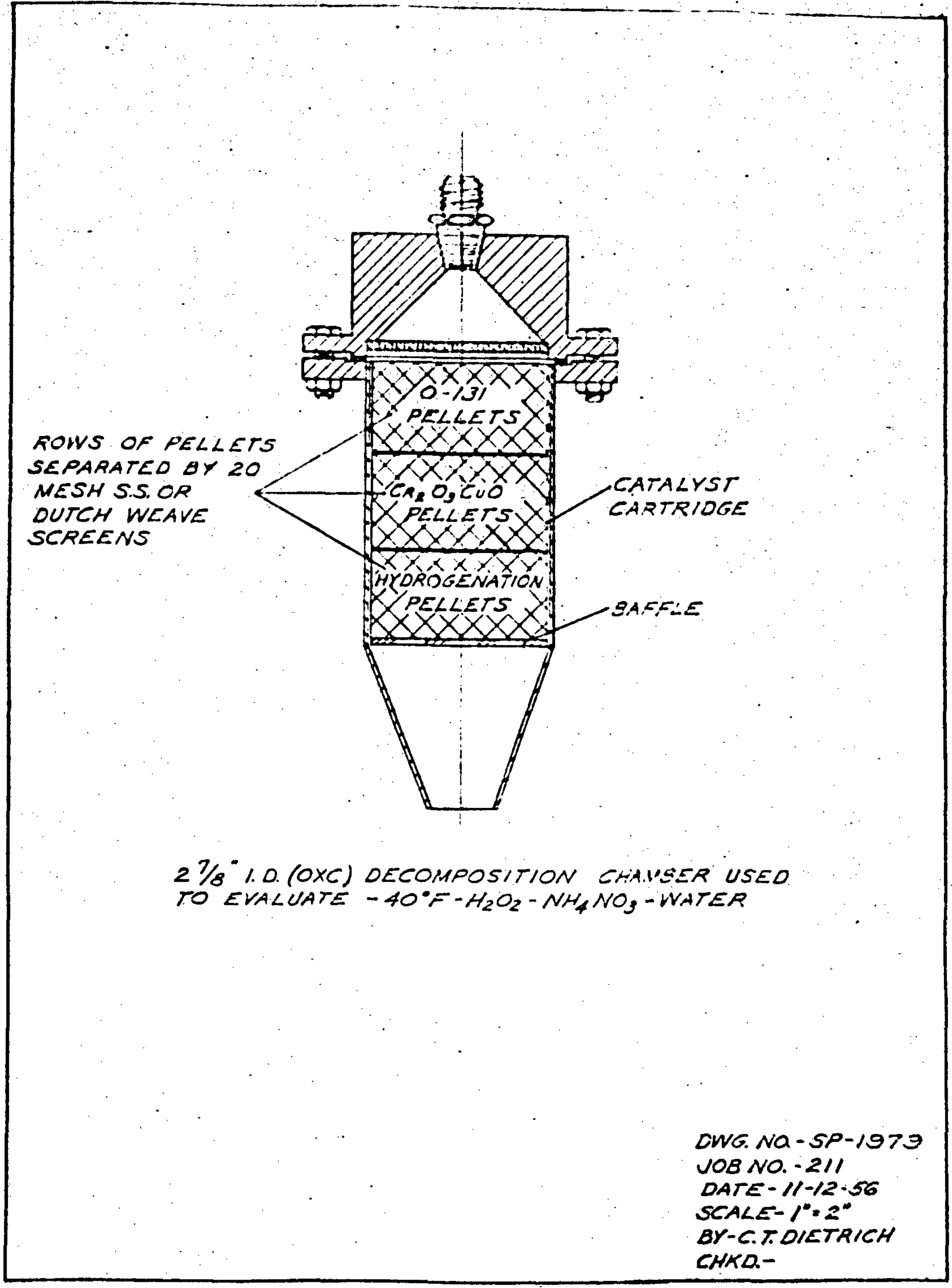
O-131 PELLETS
Cr_2O_3CuO PELLETS
HYDROGENATION PELLETS
ROWS OF PELLETS SEPARATED BY 20 MESH S.S. OR DUTCH WEAVE SCREENS
CATALYST CARTRIDGE
BAFFLE
2 7/8" I.D. (OXC) DECOMPOSITION CHAMBER USED TO EVALUATE -40°F-H_2O_2-NH_4NO_3-WATER
DWG. NO.-SP-1973
JOB NO.-211
DATE-11-12-56
SCALE-1"=2"
BY-C.T. DIETRICH
CHKD.-

FIGURE 6
CATALYST CHAMBER FOR
H_2O_2-H_4NO_3 OXIDANT

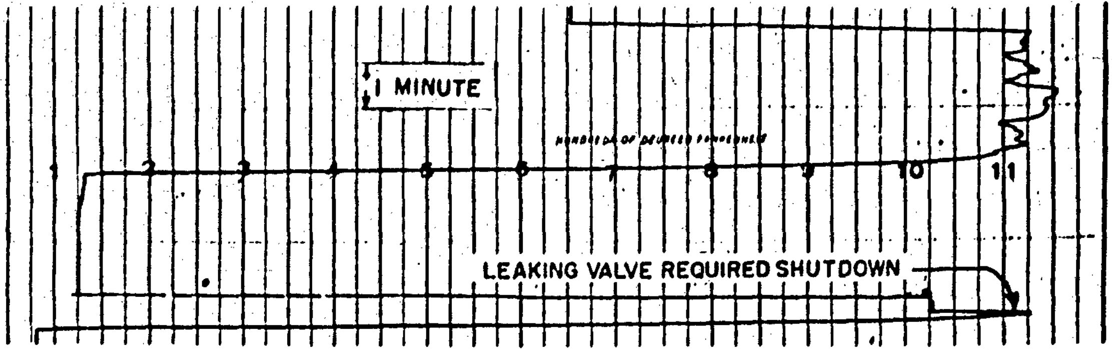

RUN #246

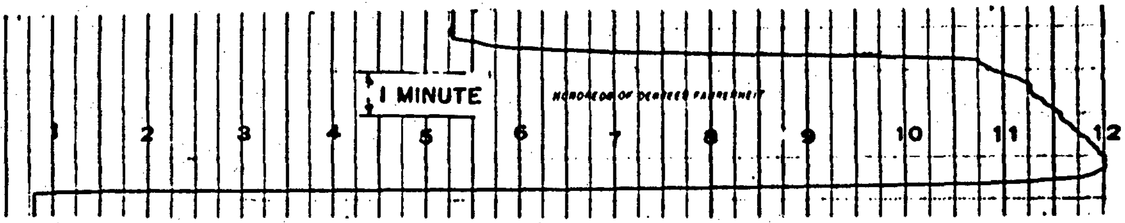

RUN #245

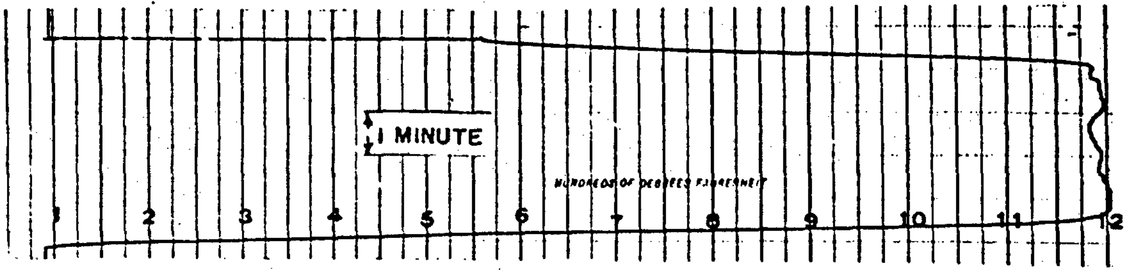

RUN # 243

DECOMPOSITION TEMPERATURE OF -40°F (H_2O_2 - NH_4NO_3 -WATER) OXIDANT IN RUNS 243, 245 AND 246 WHEN USING THE SAME CATALYST BED. TOTAL BED TIME 10 MINUTES THRUPUT WAS 4.3#/SQ.IN./MIN. IN THE OXC 2 7/8" I.D. CHAMBER.

FIGURE 7
TYPICAL DECOMPOSITION TEMPERATURE
OF H_2O_2-NH_4NO_3 OXIDANT

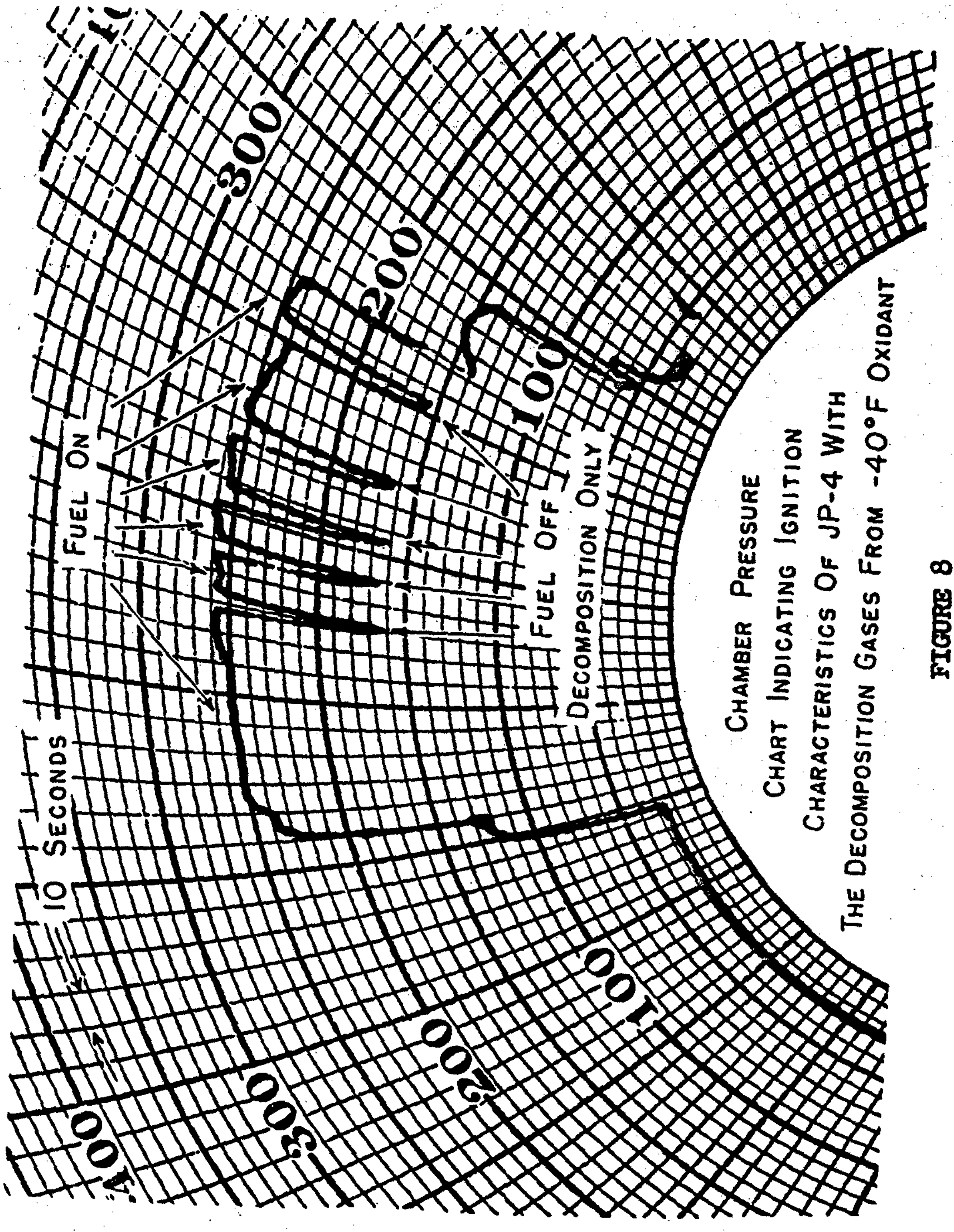

Chamber Pressure Chart Indicating Ignition Characteristics Of JP-4 With The Decomposition Gases From -40°F Oxidant

FIGURE 8

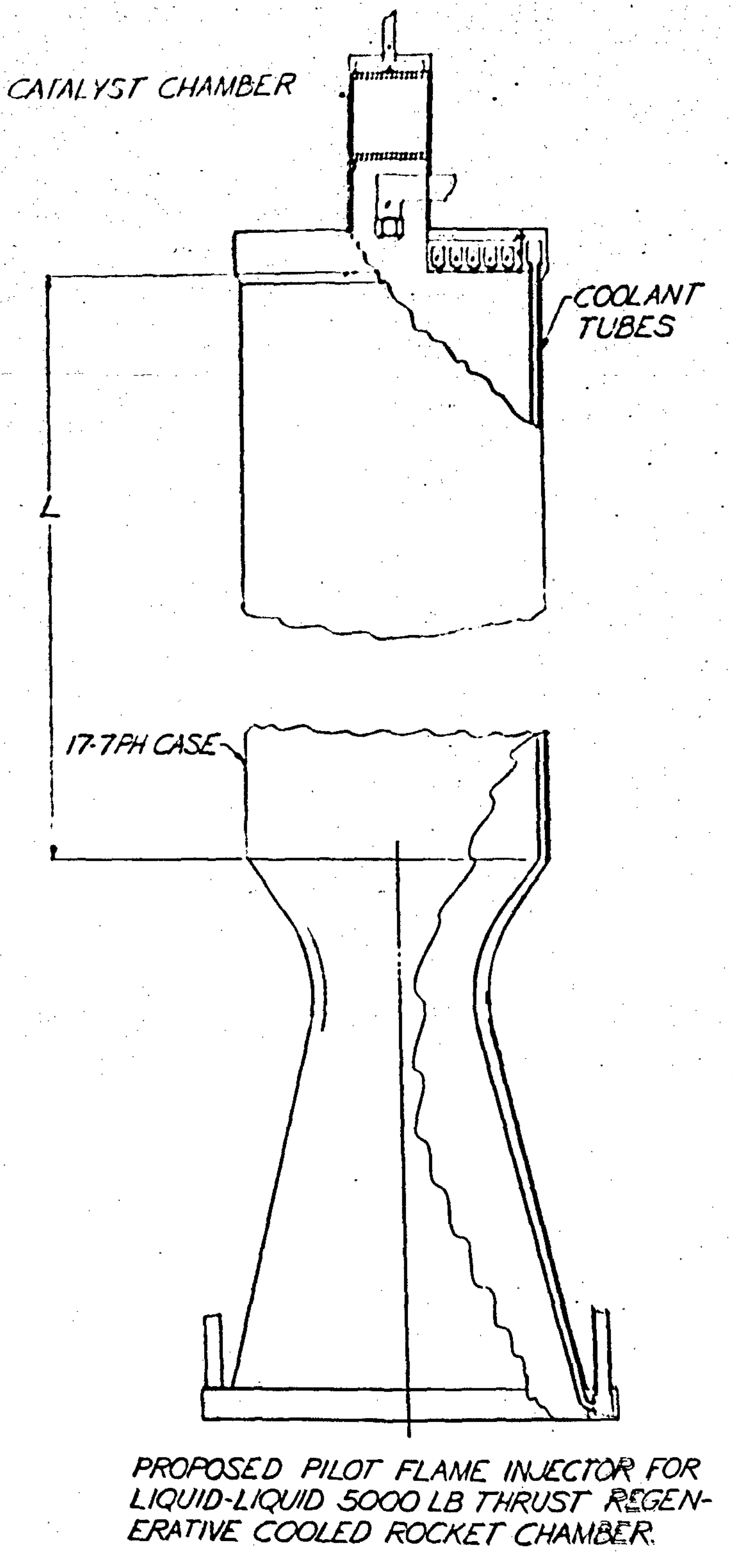
CATALYST CHAMBER
COOLANT TUBES
L
17-7PH CASE
PROPOSED PILOT FLAME INJECTOR FOR LIQUID-LIQUID 5000 LB THRUST REGENERATIVE COOLED ROCKET CHAMBER.

FIGURE 9
ROCKET THRUST CHAMBER WITH
PILOT CATALYST IGNITER

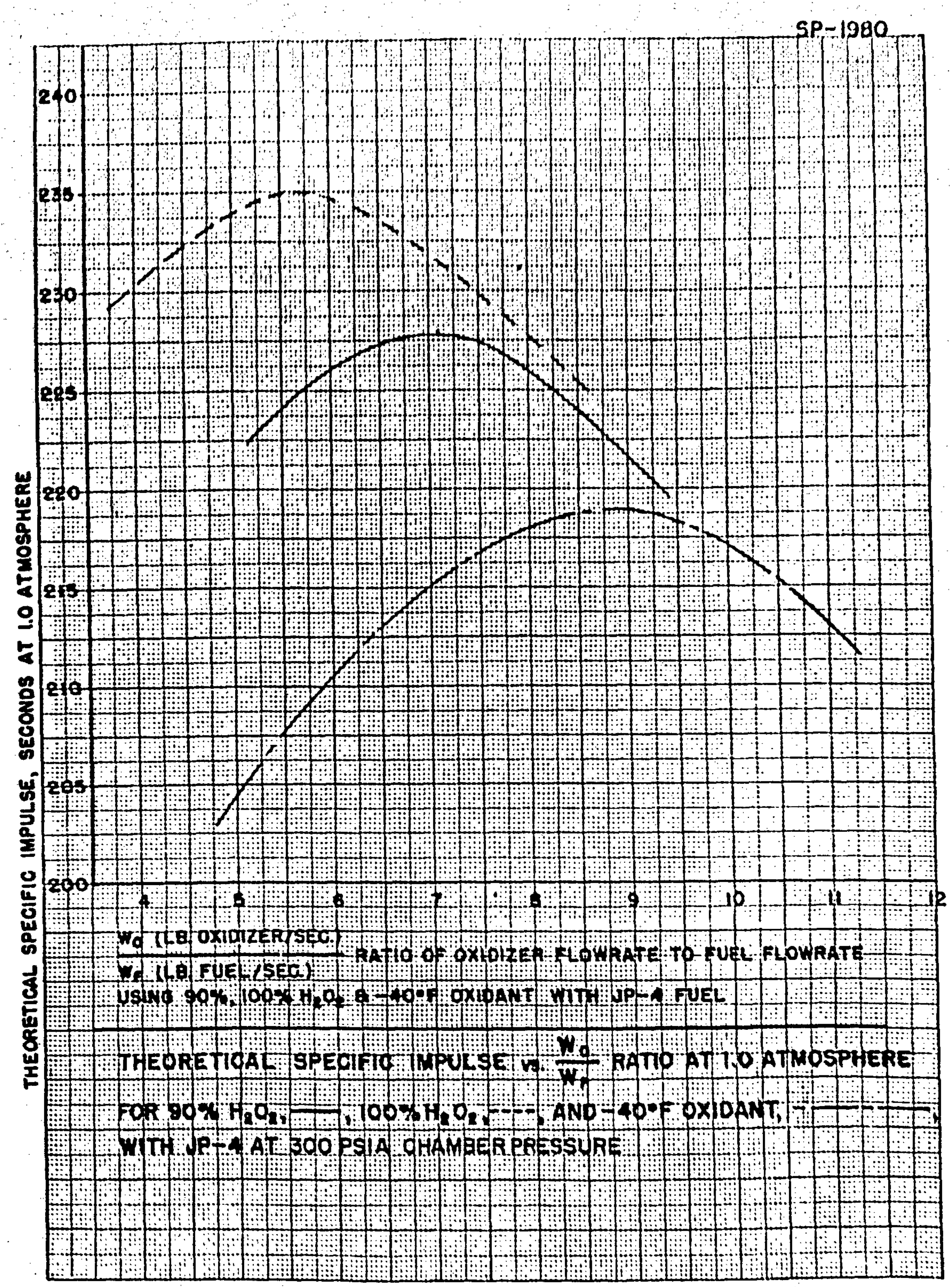

FIGURE 10
THEORETICAL PERFORMANCE OF
H_2O_2 OXIDANTS WITH JP4 FUEL

FIGURE 11

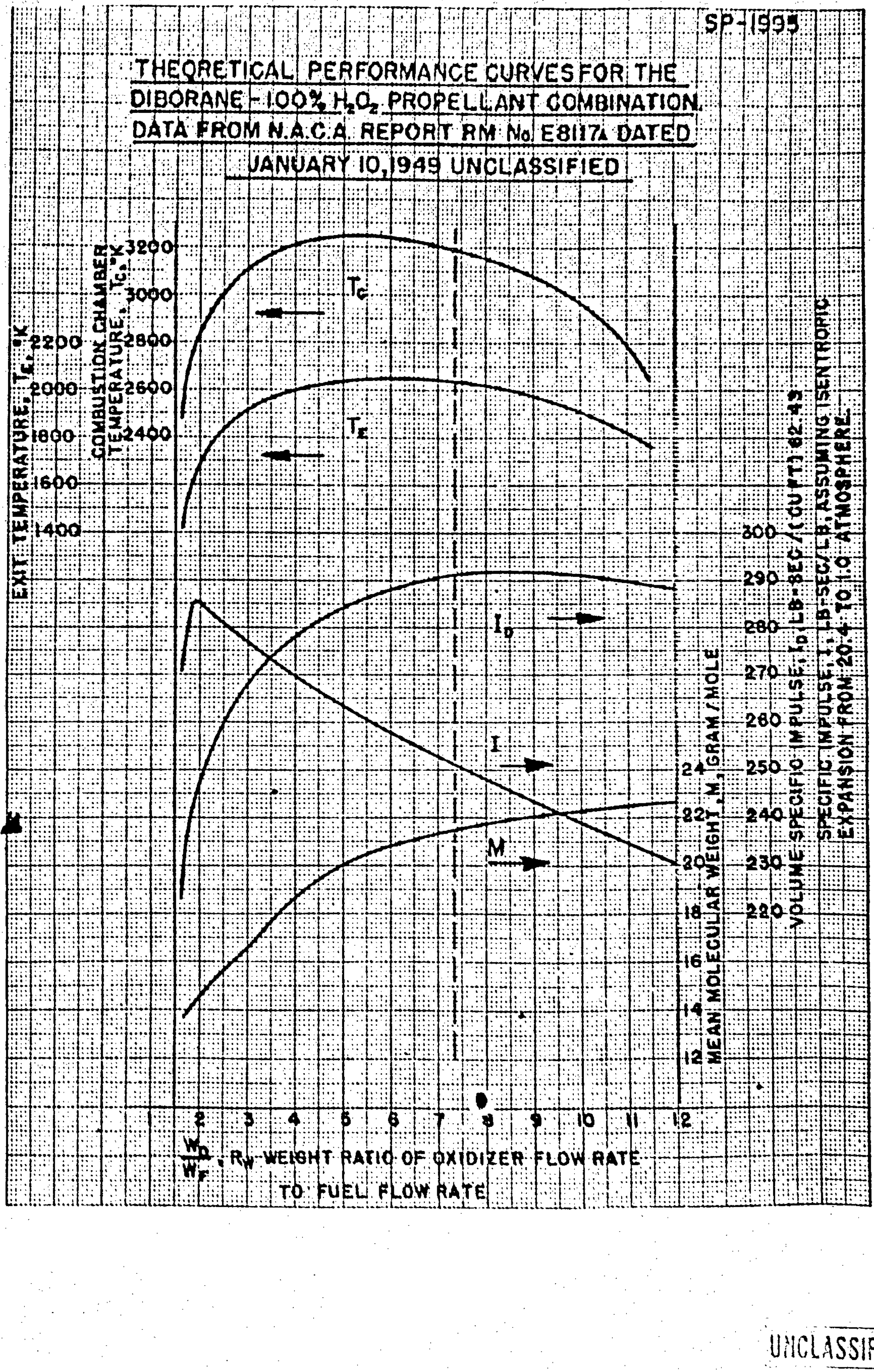
SP-1995
THEORETICAL PERFORMANCE CURVES FOR THE DIBORANE - 100% H2O2 PROPELLANT COMBINATION. DATA FROM N.A.C.A. REPORT RM No. E8I17A DATED JANUARY 10, 1949 UNCLASSIFIED
EXIT TEMPERATURE, TE, °K
1400
1600
1800
2000
2200
COMBUSTION CHAMBER TEMPERATURE, TC, °K
2400
2600
2800
3000
3200
TC
TE
ID
I
M
MEAN MOLECULAR WEIGHT, M, GRAM/MOLE
12
14
16
18
20
22
24
VOLUME SPECIFIC IMPULSE, ID, LB-SEC/(CU FT) 62.43
SPECIFIC IMPULSE, I, LB-SEC/LB, ASSUMING ISENTROPIC EXPANSION FROM 20.4 TO 1.0 ATMOSPHERE
220
230
240
250
260
270
280
290
300
1
2
3
4
5
6
7
8
9
10
11
12
WO/WF, RW WEIGHT RATIO OF OXIDIZER FLOW RATE TO FUEL FLOW RATE

FIGURE 12

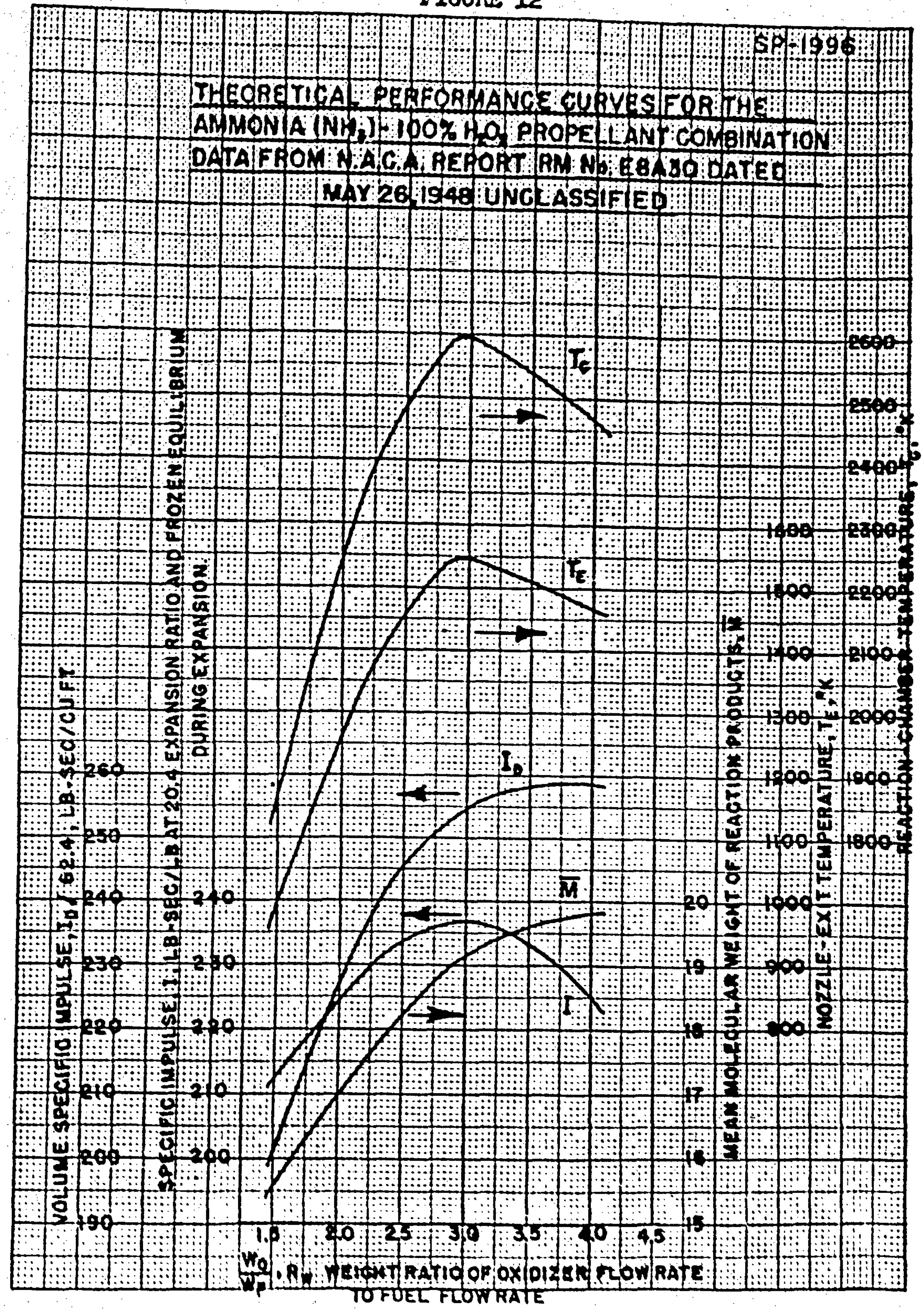
SP-1996
THEORETICAL PERFORMANCE CURVES FOR THE AMMONIA (NH_3) - 100% H_2O_2 PROPELLANT COMBINATION
DATA FROM N.A.C.A. REPORT RM No. E8A30 DATED MAY 26, 1948 UNCLASSIFIED
T_C
T_E
I_D
$\overline{M}$
I
VOLUME SPECIFIC IMPULSE, I_D = I × 62.4, LB.-SEC/CU FT
190
200
210
220
230
240
250
260
SPECIFIC IMPULSE I, LB-SEC/LB AT 20.4 EXPANSION RATIO AND FROZEN EQUILIBRIUM DURING EXPANSION
200
210
220
230
240
1.5
2.0
2.5
3.0
3.5
4.0
4.5
$\frac{W_O}{W_F}$, R_W WEIGHT RATIO OF OXIDIZER FLOW RATE TO FUEL FLOW RATE
MEAN MOLECULAR WEIGHT OF REACTION PRODUCTS, $\overline{M}$
15
16
17
18
19
20
NOZZLE-EXIT TEMPERATURE, T_E, °K
800
900
1000
1100
1200
1300
1400
1500
1600
REACTION-CHAMBER TEMPERATURE, T_C, °K
1800
1900
2000
2100
2200
2300
2400
2500
2600

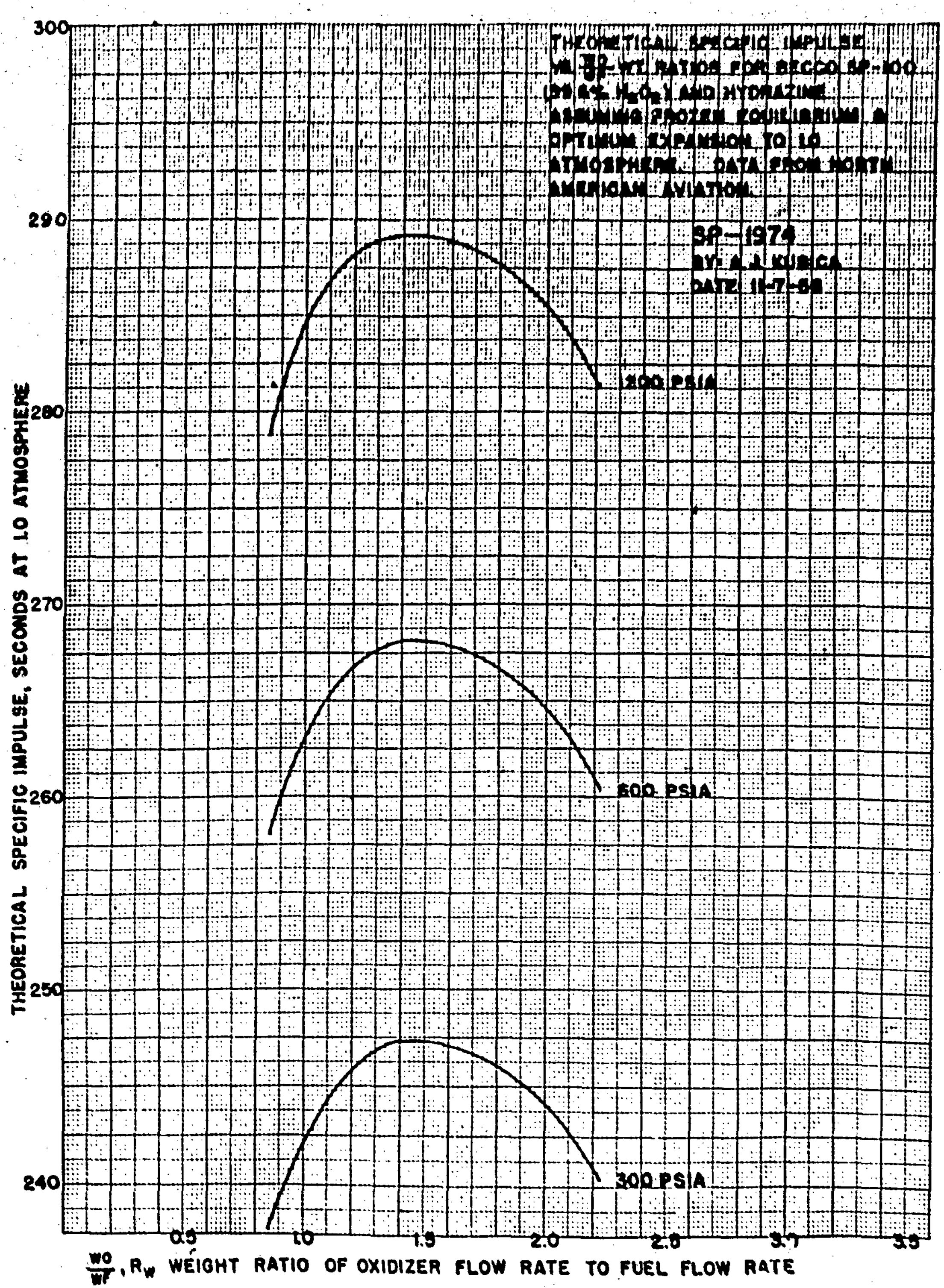

FIGURE 13
THEORETICAL PERFORMANCE FOR
99.6% H_2O_2 AND HYDRAZINE

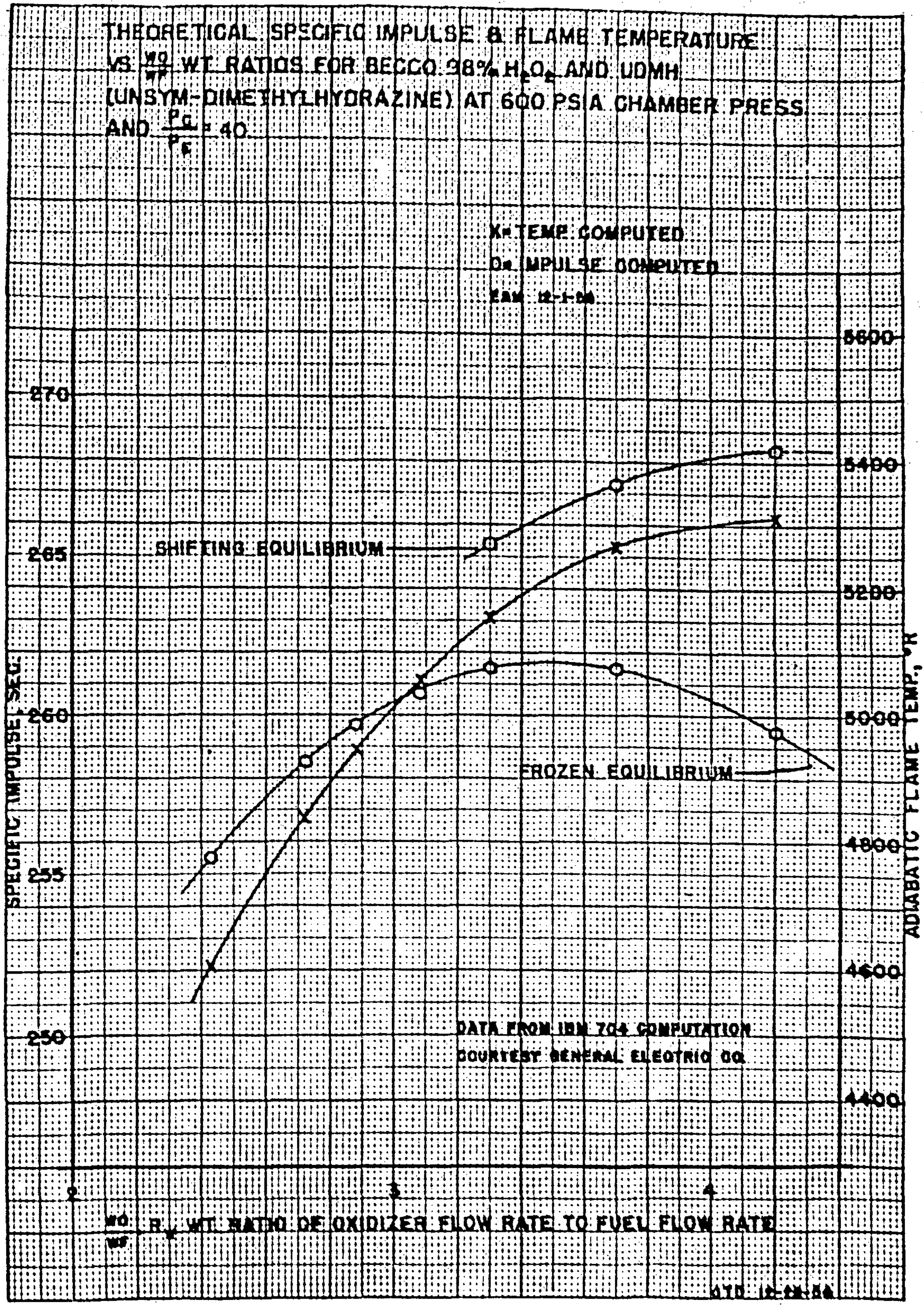

FIGURE 14
THEORETICAL PERFORMANCE
FOR 98% H_2O_2 AND UDMH

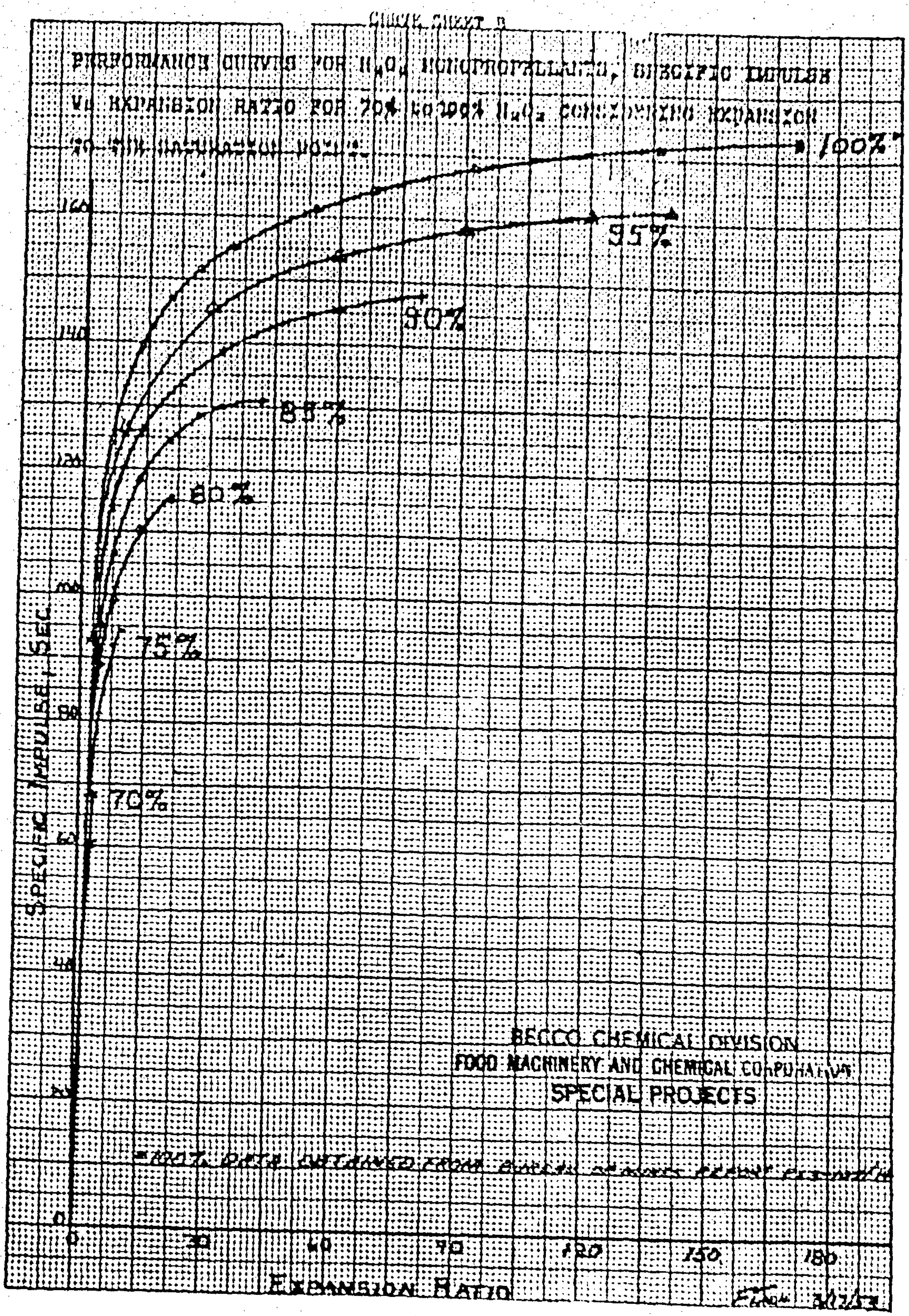

FIGURE 15
THEORETICAL PERFORMANCE FOR
70% TO 100% H_2O_2 MONOPROPELLANT

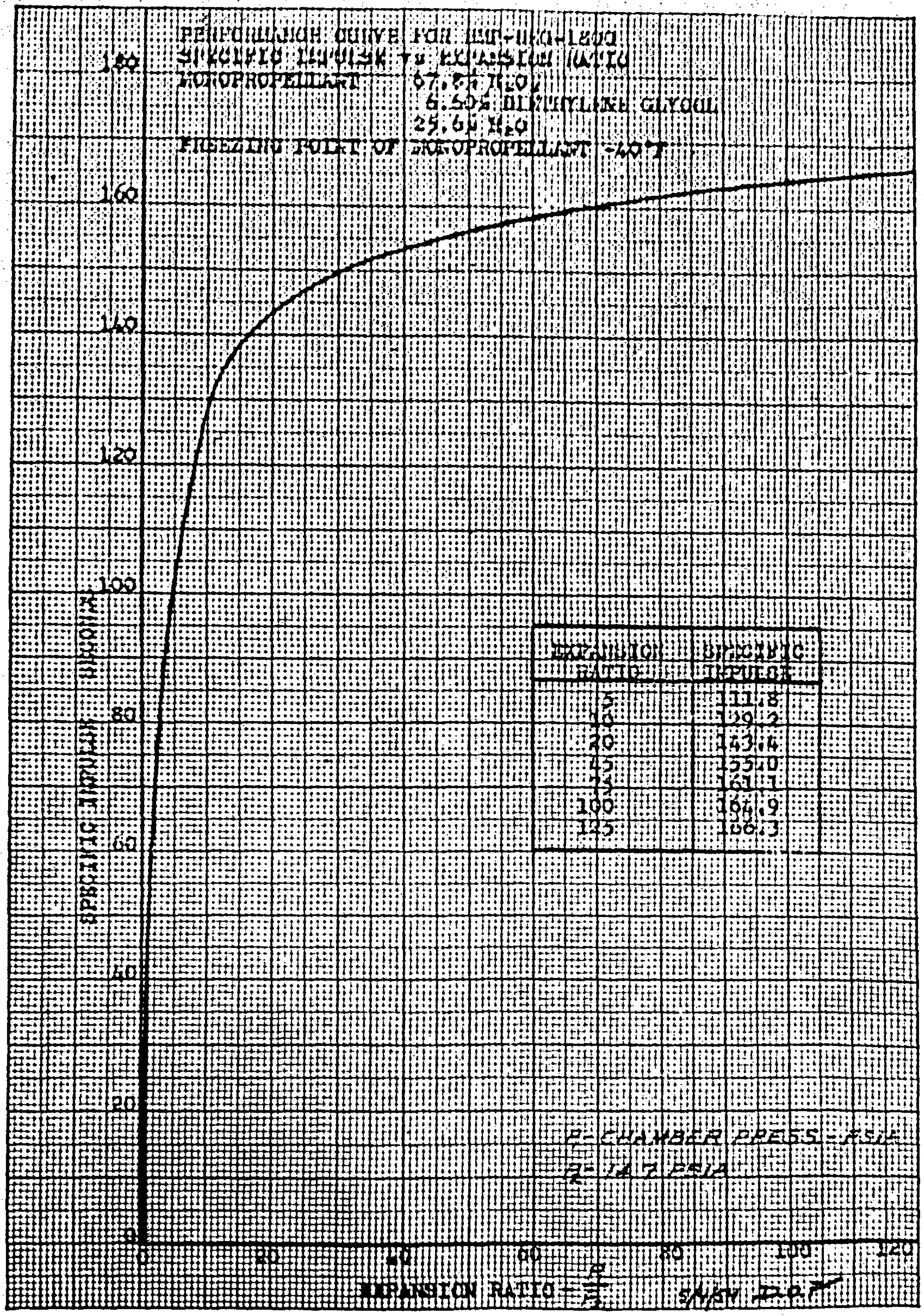

EXPANSION RATIO	SPECIFIC IMPULSE
5	111.8
10	129.2
20	143.4
45	155.0
75	161.1
100	164.9
125	166.3

FIGURE 16
THEORETICAL PERFORMANCE
FOR BMP-DEG-1800

CONFIDENTIAL

PERFORMANCE OF PERCHLORYL FLUORIDE

E. A. Mickle, K. Berman, E. S. C. Gantz
Rocket Engine Section
General Electric Co.
Cincinnati 15, Ohio

In 1952 a new compound, perchloryl fluoride was discovered by Engelbrecht and Atzwanger (1). This compound might be considered the acid fluoride of perchloric acid. The formula for the compound is ClO_3F. The compound is a stable gas at ambient conditions but possesses a high oxidation potential. Since the vapor pressure is not exorbitantly high, this compound is of considerable interest as an oxidizer.

Calculations at the Naval Air Rocket Test Station (2) were made when the heat of formation of the compound had not been measured. However the specific impulse with unsymmetrical dimethylhydrazine was promising. A brief motor evaluation was also made at NARTS (3). This was with monomethylhydrazine in a 50 lb thrust motor. These tests showed that the propellant combination was hypergolic.

Complete thermodynamic calculations have now been made using an IBM 704 calculation for the systems perchloryl fluoride as oxidizer with JP-4, hydrazine and unsymmetrical dimethylhydrazine as fuels. In addition brief motor trials have been made using the perchloryl fluoride - unsymmetrical dimethylhydrazine system. This report presents a summary of the theoretical and experimental results obtained.

Performance Calculations

The method of calculation used was based upon that of Brinkley and Lewis (4). The independent variable that defines the relative proportion of fuel to oxidizer is called the equivalence ratio, R_2, defined as "actual fuel to oxidizer volume ratio divided by stoichiometric fuel to oxidizer volume ratio". The other independent variables were P_c (atm) and T (°R).

A. The JP-4, ClO_3F system

For convenience JP-4 was assumed to be C_9H_{18} and the stoichiometric equation for the reaction was taken to be as follows:

$$4\ C_9H_{18} + 27\ ClO_3F = 9\ H_2O + 36CO_2 + 27\ HF + 27\ HCl$$

The following substances were considered as possible products of combustion: solid carbon in the form of graphite, H_2O, CO_2, CO, HF, HCl, OH, H, O, Cl, F, H_2, O_2, Cl_2, F_2, CH_4 and ClF. Other compounds considered but omitted from the final calculations were CCl_4, ClF_3, F_2O, ClO_2, and CF_4. F_2O and ClO_2 were omitted because of their extremely small equilibrium constants while the other three were dropped from consideration because their effect on equilibrium of the combustion products is negligible.

Values used for R_2 ranged from 0.40 to 4.00, for P_c (atm) from 0.10 to 100.0 and for T_c (°R) from 2000 to 6600 at 100 degree intervals.

Sources of Data of Thermodynamic Properties of Constituents

$C_{(s)}$, H_2O, CO_2, CO, OH, H, O, H_2, and O_2 --- Selected Values of Properties of Hydrocarbons and Related Compounds, Vol. I, American Petroleum Institute Research Project 44.

HF, HCl, Cl, F, Cl_2, F_2, ClF --- NACA Report 1037, Huff, Gordon and Morrell. (Heats of formation at absolute zero are not consistent with the system used in the American Petroleum Institute Report. All heats of formation were put on a common basis by use of N.B.S. Circular 500.)

- CH_4 - Properties through 5000°R taken from General Electric Publications, Properties of Combustion Gases, Powell, Shaffer and Suciu, 1955, General Electric Company Properties above 5000°R were extrapolated.

The heat of formation of ClO_3F was taken as -2.4 kcal/mole at 25°C and for JP-4 as -50.0 kcal/mole.

The results of the calculation for specific impulse are summarized in figure 1 and for chamber temperature in figure 2. More complete data will be found in the General Electric Company publication R56AGT368 by E. A. Mickle issued 28 June 1956.

B. The N_2H_4 - ClO_3F System

The stoichiometric equation was assumed to be

$$2\ N_2H_4 + ClO_3F = 2\ N_2 + 3\ H_2O + HF + HCl$$

The constituents considered were O_2, N_2, H_2O, HF, HCl, O, OH, H_2, N, NO, F, Cl, H, F_2, Cl_2, NH_3, and ClF.

The heat of formation of ClO_3F was taken as -2.4 kcal/mole at 25°C and for N_2H_4 as +12.05 kcal/mole.

The range of P_c was 0.1 atm to 100 atm and for R_2 0.75 to 3.00. The reactants were assumed to enter the combustion chamber at 298.16°K.

The results of the calculation for specific impulse are summarized in figure 3 and for chamber temperature in figure 4. More complete data will be found in General Electric Company publication DF56AGT426 by E. A. Mickle issued 18 July 1956.

C. The UDMH - ClO_3F System

The stoichiometric equation was assumed to be

$$(CH_3)_2\ NNH_2 + 2\ ClO_3F = 2\ CO_2 + N_2 + 2\ H_2O + 2\ HF + 2\ HCl$$

The constituents considered were C (in the form of graphite), H_2O, CO_2, CO, HF, HCl, OH, H, O, Cl, F, H_2, O_2, Cl_2, F_2 N_2, N, NO.

The heat of formation of ClO_3F was taken as -2.4 kcal/mole at 25°C and for $(CH_3)_2\ N_2H_2$ as + 11.3 kcal/mole.

The range of P_c was 1.0 atm to 100 atm and for R_2 was 0.75 to 2.2. As before the reactants were assumed to enter the combustion chamber at 298.16°K.

The results of the calculation for specific impulse are summarized in figure 5 and for chamber temperature in figure 6.

Experimental Results

The amount of perchloryl fluoride available was limited, so the tests made were with unsymmetrical dimethylhydrazine in nominal 1000 lb thrust chambers. These water-cooled engines have an inside diameter of three inches and a throat diameter of 1.75 inches. The nozzle area ratio $\frac{\text{(exit area)}}{\text{(throat area)}}$ was 4. The injector employed was a conventional ring type like-on-like injector with alternate rings being used for fuel and oxidizer injection respectively, starting with fuel on the outside ring.

A small pyrotechnic ignitor, located in the injector, was used to initiate combustion. This was done since, on the account of the high cost of PF, it was deemed inadvisable to attempt any hypergolic starting tests.

In all tests, operation was smooth and stable. Below are summarized the operating conditions for a typical run:

Chamber pressure	322	psia
Oxidizer to fuel ratio	2.27	
Thrust	1025	lbs
Characteristic velocity	5800	ft/sec
Specific impulse	238	sec
Injector pressure drop (oxidizer)	91	psi
Injector pressure drop (fuel)	48	psi
Total Propellant flow rate	4.30	lb/sec
Nozzle heat transfer rate	3.62	$\frac{\text{BTU}}{\text{in}^2\text{sec}}$
Chamber heat transfer rate	2.38	$\frac{\text{BTU}}{\text{in}^2\text{sec}}$

Summary

As can be seen from the performance curves in figures 1, 3 and 5, perchloryl fluoride is almost as efficient an oxidant as is oxygen. However since it does boil at -46°C it seems likely that it will find application in those limited areas which lend themselves to the use of a pressurized system. It is noteworthy that in the limited tests of perchloryl fluoride with unsymmetrical dimethylhydrazine in a 1000 lb thrust chamber that approximately 98% of theoretical performance was obtained.

References

1. Englebrecht, A. and Atzwanger, H., Monatsh. f. Chem., 83, 1087, 1952.

2. Clark, John D., "Properties of Perchloryl Fluoride, A New Oxidizer for Rocket Fuels", NARTS 72, U. S. Naval Air Rocket Test Station, November 1955. (Confidential)

3. Forsten, I., "Experiments With the Oxidizer Perchloryl Fluoride in a Rocket Engine", NARTS 73, U. S. Naval Air Rocket Test Station, November 1955. (Confidential)

4. Brinkley, S. R. Jr. and Lewis, B., "The Thermodynamics of Combustion Gases: General Calculations", U. S. Department of Interior, April 1952.

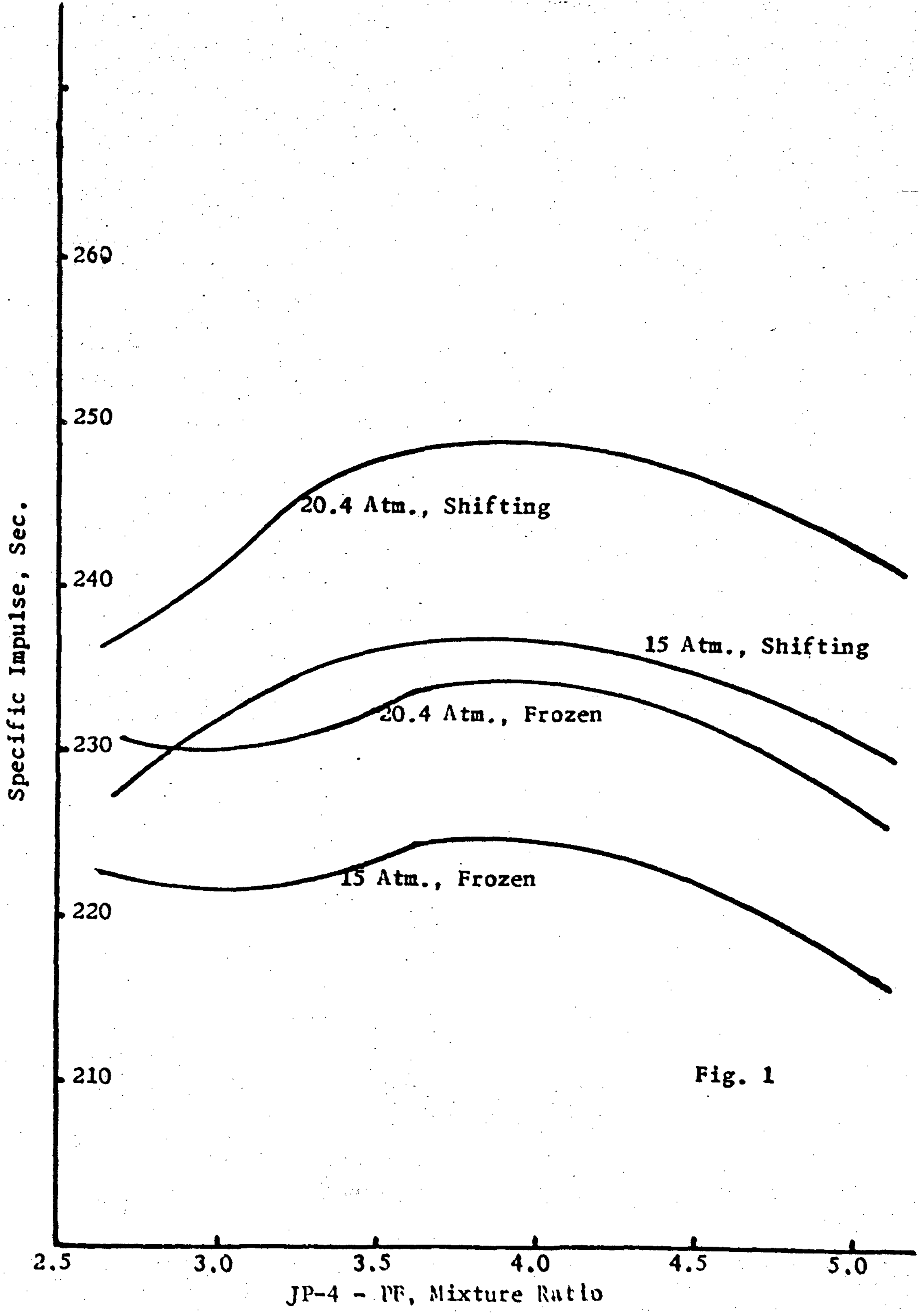
Specific Impulse, Sec.
260
250
240
230
220
210
20.4 Atm., Shifting
15 Atm., Shifting
20.4 Atm., Frozen
15 Atm., Frozen
2.5
3.0
3.5
4.0
4.5
5.0
JP-4 - PF, Mixture Ratio

Fig. 1

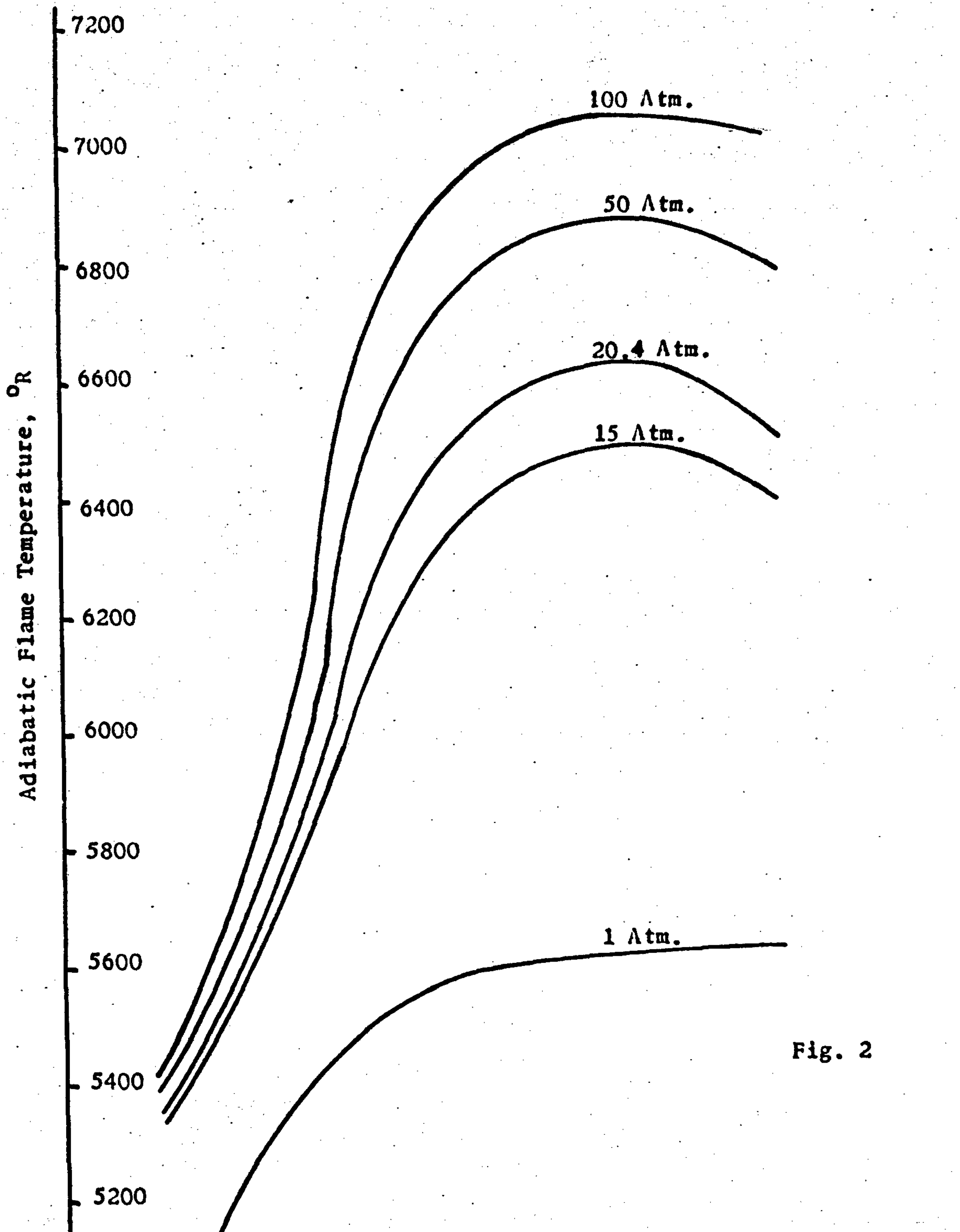

7200
7000
6800
6600
6400
6200
6000
5800
5600
5400
5200
Adiabatic Flame Temperature, °R
100 Atm.
50 Atm.
20.4 Atm.
15 Atm.
1 Atm.
2.5
3.0
3.5
4.0
4.5
5.0
5.5
JP-4 - PF, Mixture Ratio

Fig. 2

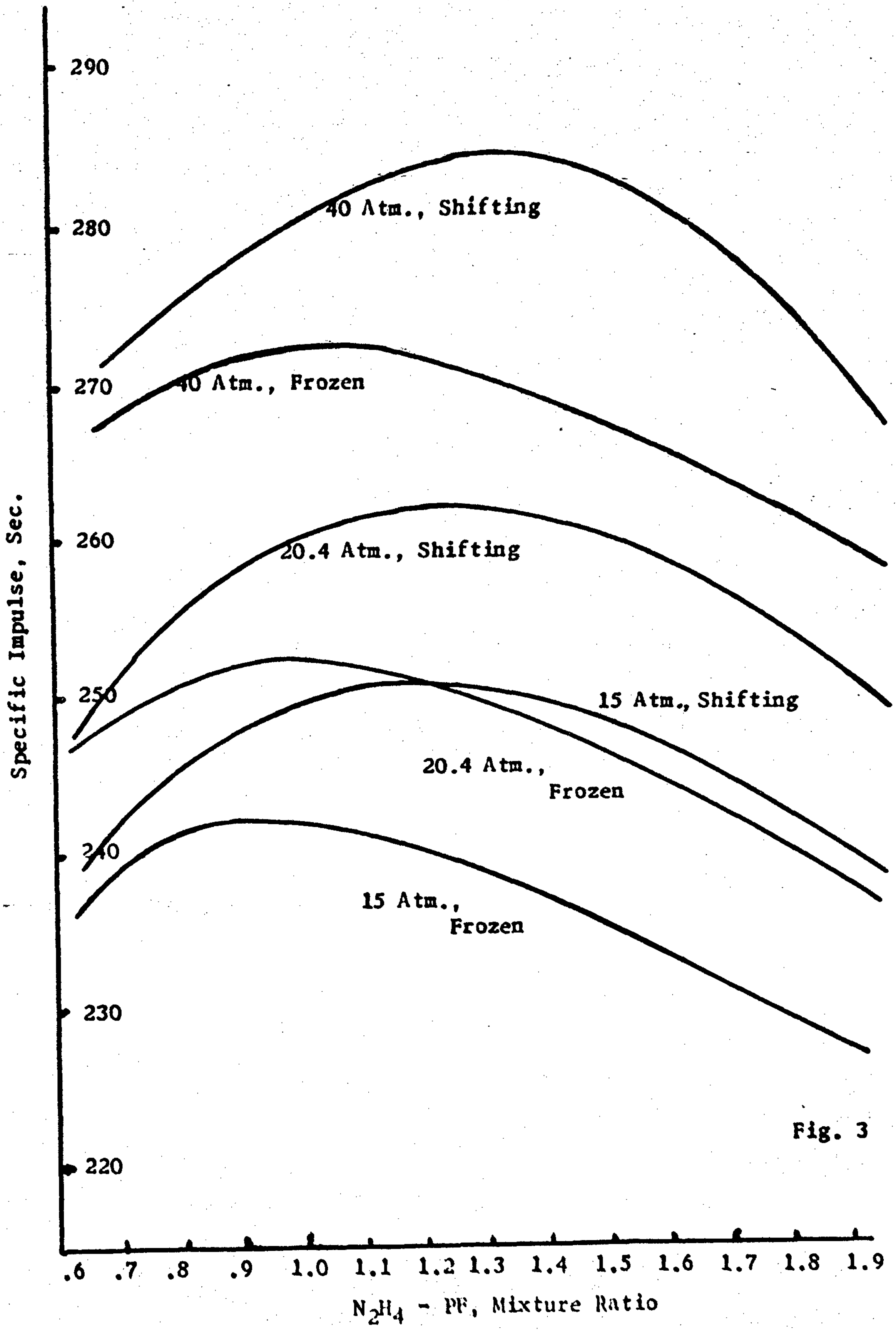
Specific Impulse, Sec.
290
280
270
260
250
240
230
220
40 Atm., Shifting
40 Atm., Frozen
20.4 Atm., Shifting
15 Atm., Shifting
20.4 Atm., Frozen
15 Atm., Frozen
.6
.7
.8
.9
1.0
1.1
1.2
1.3
1.4
1.5
1.6
1.7
1.8
1.9
N_2H_4 - PF, Mixture Ratio

Fig. 3

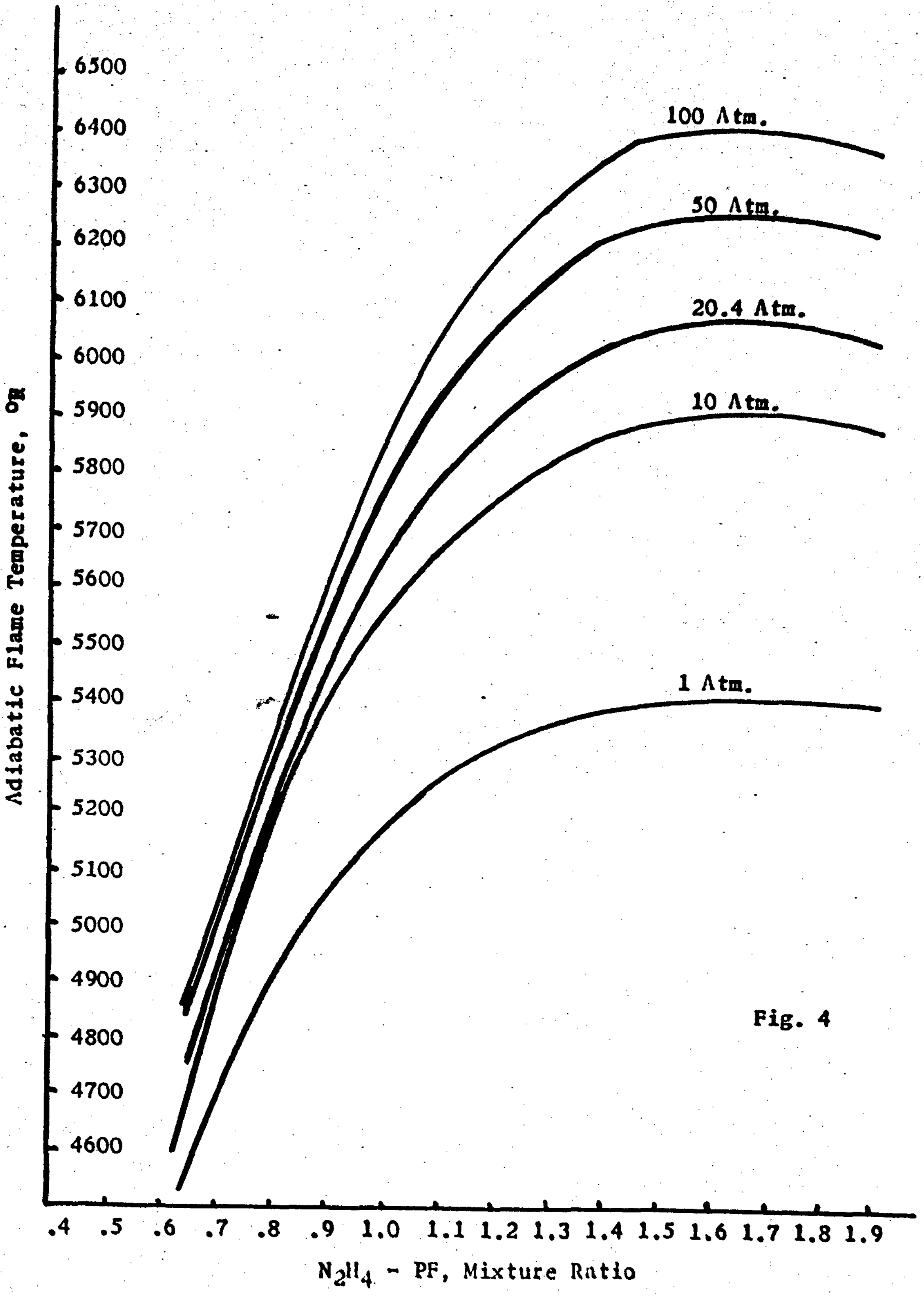
6500
6400
6300
6200
6100
6000
5900
5800
5700
5600
5500
5400
5300
5200
5100
5000
4900
4800
4700
4600
Adiabatic Flame Temperature, °R
100 Atm.
50 Atm.
20.4 Atm.
10 Atm.
1 Atm.
.4
.5
.6
.7
.8
.9
1.0
1.1
1.2
1.3
1.4
1.5
1.6
1.7
1.8
1.9
N_2H_4 - PF, Mixture Ratio

Fig. 4

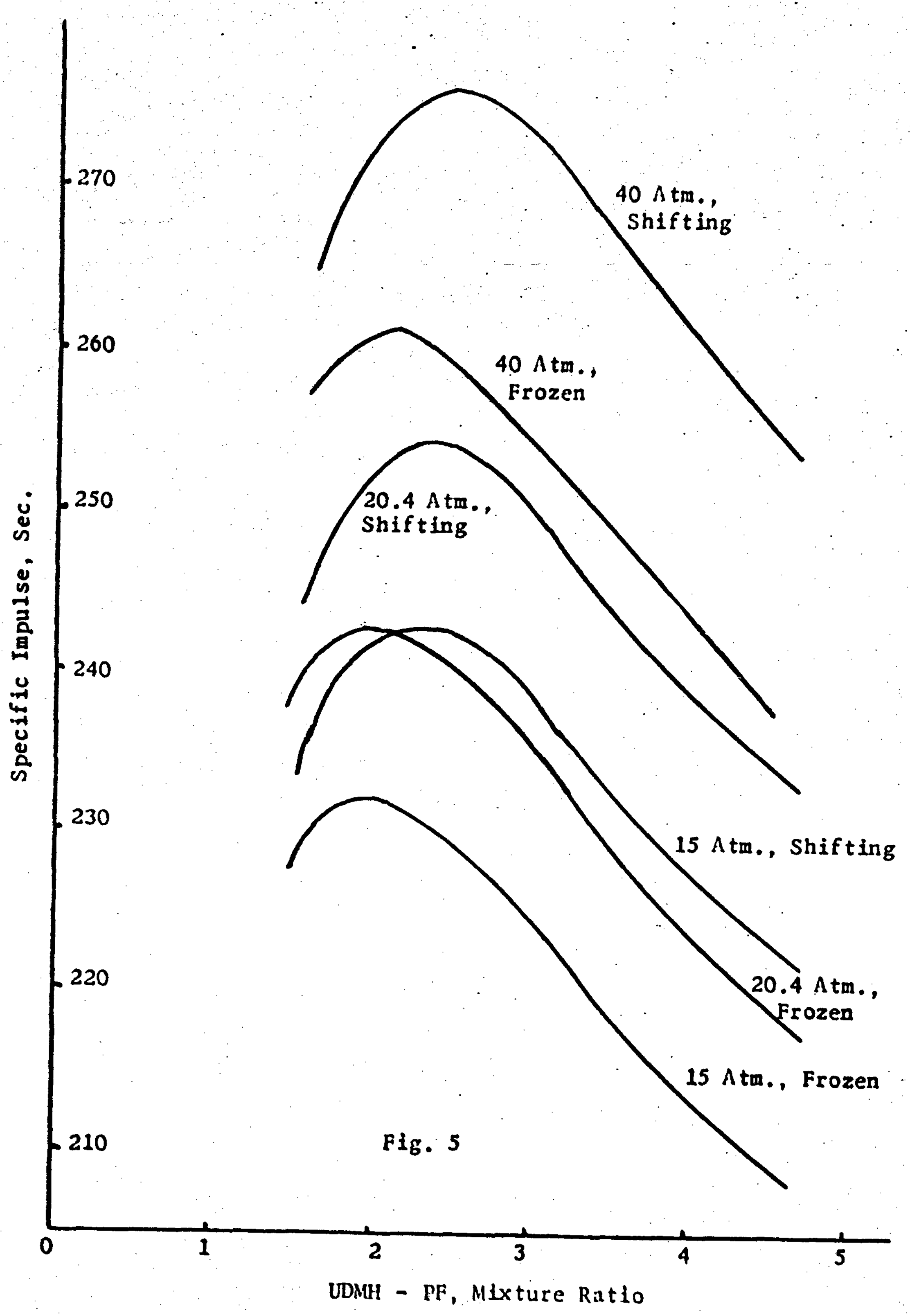
Specific Impulse, Sec.
270
260
250
240
230
220
210
0
1
2
3
4
5
UDMH - PF, Mixture Ratio
40 Atm., Shifting
40 Atm., Frozen
20.4 Atm., Shifting
15 Atm., Shifting
20.4 Atm., Frozen
15 Atm., Frozen

Fig. 5

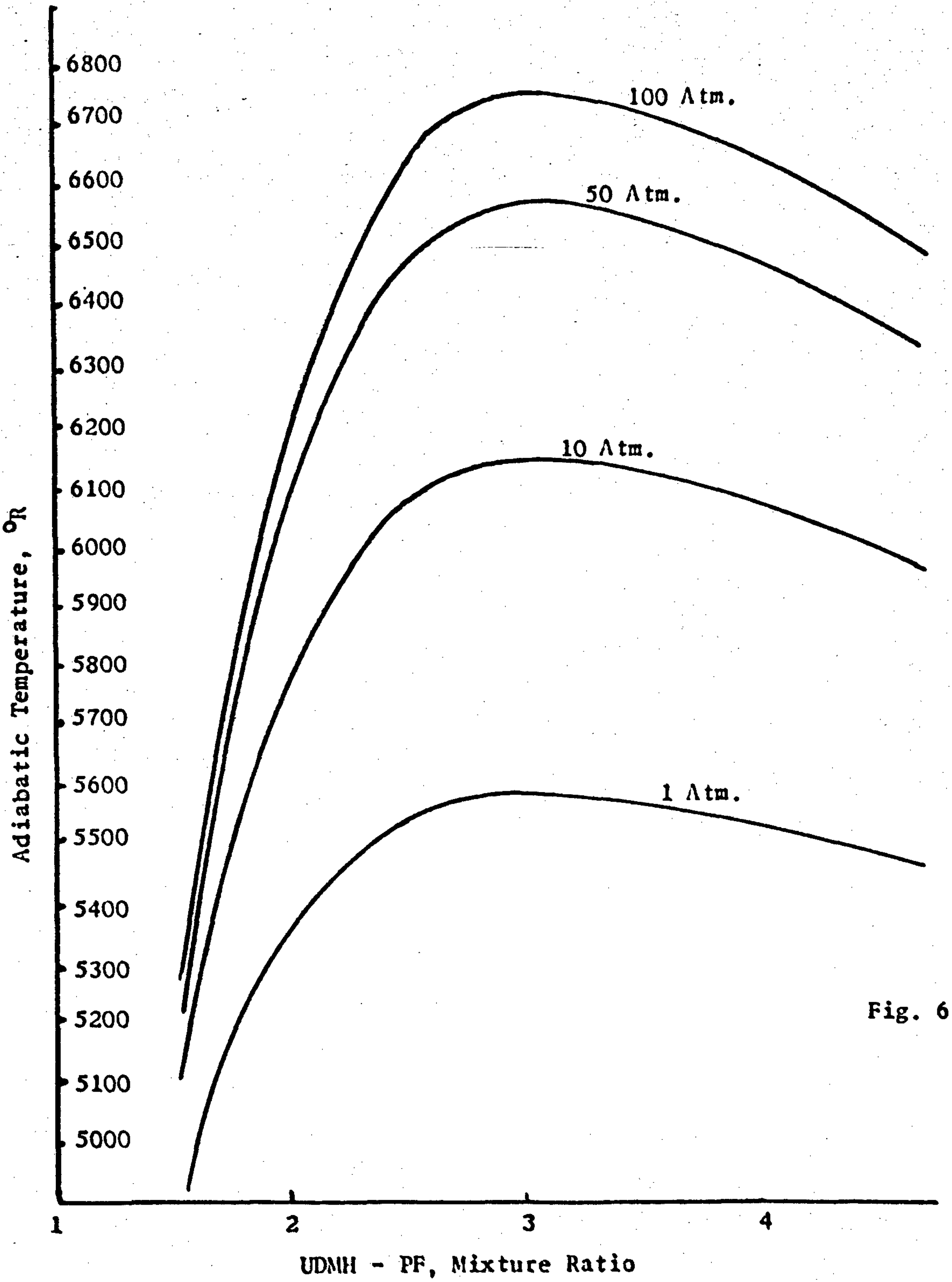
Adiabatic Temperature, °R
6800
6700
6600
6500
6400
6300
6200
6100
6000
5900
5800
5700
5600
5500
5400
5300
5200
5100
5000
100 Atm.
50 Atm.
10 Atm.
1 Atm.
1
2
3
4
UDMH - PF, Mixture Ratio

Fig. 6

UNCLASSIFIED

HIGH TEMPERATURE RESEARCH AT TEMPLE

A. V. Grosse, C. S. Stokes and W. L. Doyle
The Research Institute of Temple University
Philadelphia 44, Pennsylvania

SUMMARY

High temperature research has been carried on at the Research Institute of Temple University for the last eight years. It was originally supported by the Office of Naval Research, later by the Office of Ordnance Research, and at the present time by the Air Force's Office of Research and Development and by Redstone Arsenal.

Methods were developed to produce high temperatures by the combustion of metals, such as aluminum, magnesium, titanium, zirconium, calcium and others. Various techniques and some of the results obtained will be reviewed.

Still higher temperatures were produced by the combustion of such endothermic compounds as cyanogen and carbon subnitride in oxygen. Recently investigations of Dr. A. Streng showed that 100% ozone could be substituted for oxygen in a number of flames. This increases the temperature to some extent, but, in particular, increases the burning velocity significantly.

Considerable effort was devoted to fluorine containing flames. Thus the premixed hydrogen-fluorine flame was shown to be the fastest flame known. The hydrogen cyanide-fluorine-oxygen flame produces the highest temperature which can be achieved with presently available commercial chemicals. It has been used at Temple's high temperature establishment at Reading Furnace Farms, Pa., as a means of aerodynamic heating of samples in a supersonic high temperature jet.

Oxygen fluorides have interesting properties as fuel oxidizers. Thus O_2F_2 is substantially more endothermic than OF_2. Recently ozonefluoride, or O_3F_2 has been isolated, synthesized and definitely identified as a chemical compound. The properties of the oxygen fluorides will be discussed.

UNCLASSIFIED

The various new fuels and oxidizers open new possibilities for the study of detonations in liquid and solid phase. Single individual molecules, such as CO_2, O_2, H_2O, and others, can be made the sole product of detonation. Thus the properties of these molecules at extremely high temperatures and pressures can be determined experimentally.

At the present time there is great interest in the production and study of very high heat fluxes. Such high heat fluxes were accomplished at Temple by means of (a) chemical flames; (b) the high temperature arc, and (c) by radiation sources.

The heat fluxes obtained are in the range of 100-1000 cal/cm^2·sec. The various measuring techniques used will be discussed.

The whole field of inorganic chemistry at temperatures above 3000°K. is a wide open field of research. It should be realized that in this field the time element is of essential importance. Thus from a practical standpoint the materials have to stand up only for comparatively short times, of the order of a few minutes, whereas in our usual technology the service life is measured in years. The various methods that are available at Temple for the study of inorganic chemistry in this range will be discussed.

TOXIC HAZARDS OF LIQUID PROPELLANTS (U)

Keith H. Jacobson
Directorate of Medical Research
Chemical Warfare Laboratories
Army Chemical Center, Maryland

(U) The ability of liquid propellants to release great amounts of energy frequently involves, as a concomitant property, their ability to be hazardous to persons handling them. Many of these propellants are explosive, and many are flammable. Also, many of them are toxic, i.e. their reaction with living organisms produces disease or injury. We are concerned here with the ability of these liquid propellants to produce injury to humans by penetration into or through, or reaction with, various biological fluids and tissues of importance to the human organism.

(U) Every known compound is toxic to some degree, so it is not strictly proper to describe any given material as toxic or non-toxic. However, many materials have a degree of toxicity sufficiently low so that few if any precautions are necessary to prevent poisoning. Other materials, and this unfortunately includes many of the liquid propellants, have a sufficiently high toxicity to require considerable precautions to prevent injury. It is generally true that any material, no matter how toxic, can be safely handled. However, materials of high toxicity usually require greater precautions to permit their safe handling. The usual precautions may involve the use of protective clothing, including respiratory protection. Other precautions involve adequate ventilation, and the use of various devices to prevent spills and leaks.

(U) The most common routes by which toxic chemicals get into the human system are by inhalation of vapors and aerosols, by exposure of the eyes to toxic vapors or liquids, and by exposure of the skin to liquid or solid chemicals, resulting in systemic effects by penetration of the skin or in local reactions on the skin, including sensitization. Another route of accidental absorption involves oral ingestion. This may occur as a result of careless handling of the materials, or by intentional ingestion, usually because of a mistaken belief that the material is potable.

(U) The prevention of exposure involves eye, respiratory and skin protection to minimize the amount of the material in question that comes in contact with personnel. The need for specific protection and type of devices needed depend not only on the effect of the material, i.e. its toxicity, but also on the likelihood of accidental exposure on a given operation.

(U) Reduction in the seriousness of injuries, once exposure has occurred, is normally the responsibility of the physician in charge, and the general principles involved in treatment of exposed persons are not appropriate here. There are a few principles of first aid, including self aid, that might be briefly mentioned. In the case of liquid splash on the skin or into the eyes, the most important thing is to remove the toxic as soon as possible. I emphasize the word remove, because there seems to be too great a tendency to neutralize toxic agents, as if decontamination were similar to a laboratory titration. Speed is usually essential, and in many cases copious quantities of water, or soap and water, will effect adequate removal. The usually ready availability of water facilitates speedy removal; the use of a specific solvent or neutralizer may frequently involve delay that can be fatal. A specific example here involves the frequently seen suggestion that sodium bicarbonate solution be used to decontaminate skin splashed with RFNA. Copious quantities of water will do as good a job, and for various reasons, of which ready availability is an important one, water is undoubtedly superior to bicarbonate solution.

(U) Following this discussion of a few general principles, it may be of interest to describe briefly the action and toxicity of various liquid propellants, as well as a few gaseous or solid propellants, since they may be similar in action to liquid propellants of interest, or might be used in liquid form by alteration of pressure and/or temperature.

Hydrocarbons.

(U) The hydrocarbons (gasoline, kerosene, JP-3, JP-4, etc.) form an important class of propellant fuels. While high vapor concentrations can cause narcosis in exposed personnel, normal operating procedures rarely permit such high concentrations. The main problem comes from the lipid solvent properties of these fuels. When they are in prolonged or repeated contact with skin, they may cause skin irritation. Leaded gasoline is an additional problem, because of the possibility of lead poisoning. Soap and water are useful in removing hydrocarbons.

Hydrazine and Derivatives.

(U) Hydrazine, monomethylhydrazine, and uns-dimethylhydrazine cause local skin and eye damage when spilled on these organs. When the compounds are absorbed into the body by skin penetration or inhalation of vapors or aerosols, in sufficient amounts, they may cause convulsions. Respiratory irritation may result from inhalation of the compounds. Hydrazine has been shown to produce liver damage; while this has not yet been shown to be a toxic effect of uns-dimethylhydrazine or methylhydrazine, it has been presumed that they may also cause liver damage, because of their chemical similarity to hydrazine. Table I shows some data on the comparative toxicity of these compounds. The listing of LD50's to various species of experimental animals does not imply the same values for man; however, it is likely that the ratio of the toxicity of two compounds, if it be similar in several species of experimental animals, will be similar for both man and lower animals.

Table I (U)
Toxicity of Hydrazine and Some of Its Derivatives

	LC50, ppm 4 Hr. Inhalation		LD50, mg./kg. Percutaneous	MAC* ppm
	Rats	Mice	Rabbits	Man
Hydrazine	570	252	93	1**
Methylhydrazine	74	56	110	-
uns-Dimethylhydrazine	252	172	1341	0.5***

---

* Maximum allowable concentration

** Tentative value, Amer. Conf. of Governmental Industrial Hygienists

*** Suggested interim working value

(U) When one of these compounds is spilled on skin or into eyes, copious quantities of water should be used to remove them as soon as possible. Treatment of poisoned persons should be symptomatic; barbiturates or Mesantoin may be useful in controlling convulsions.

Alcohols.

(U) Methyl, ethyl, and furfuryl alcohols are all depressants. With normal ventilation, intoxication by inhalation of the vapors is not common. Their lipid-solvent characteristics are sufficient so that repeated or prolonged skin contact may result in skin irritation. They are irritating to the eyes. Their greatest danger probably lies in the likelihood of their ingestion on the assumption that "alcohol is alcohol". The literature is filled with references to blindness and/or death resulting from ingestion of methyl alcohol. While the personal experience of many of us has shown that ethyl alcohol is indeed potable, the ethyl alcohol used is propulsion is usually denatured, and undesirable effects may result. It might be mentioned that methyl alcohol is a common denaturant in ethyl alcohol.

Boron Hydrides.

(C) The boron hydrides comprise an increasingly important class of propellants. Diborane (a gas at ordinary temperatures and pressures) causes respiratory irritation. The other hydrides under consideration (pentaborane, decaborane, propylpentaborane, and ethyldecaborane) can also produce respiratory irritation by inhalation of the vapors, but also produce profound systemic effects, such as cardiovascular effects, liver and kidney damage, and central nervous system effects, including convulsions. They are highly toxic, as is shown in Table II.

Table II (C)
Toxicity of Some Boron Hydrides (U)

	LC50, ppm 4 Hr. Inhalation		LD50, mg./kg. Percutaneous	MAC ppm
	Rats	Mice	Rabbits	Man
Diborane	40	29	-	0.1*
Pentaborane	6	3	-	0.01**
Propylpentaborane	12	11	1000 - 3200	-
Decaborane	46	12	-	0.05**
Ethyldecaborane	23	6	62	-

* Established value, American Conference of Governmental Industrial Hygienists.

** Tentative value, American Conference of Governmental Industrial Hygienists

(U) No specific treatment is available to counteract the effects of these compounds. Symptomatic treatment should be given by qualified medical personnel. Barbiturates or Mesantoin may be useful in controlling convulsions.

Nitro Compounds.

(U) Among the compounds of interest in this category are nitroglycerine, n-propyl nitrate, and tetranitromethane. There has been considerable experience with the toxic effects of nitroglycerine. It causes vasodilatation with consequent lowering of blood pressure, and a mild methemoglobinemia. It is readily absorbed through intact skin, and may cause severe headache in exposed persons. Large doses may cause nausea, vomiting, colic, and sometimes bloody diarrhea. Persons handling nitroglycerine frequently suffer severe headache during their first few days of contact, but they then adapt rapidly, i.e. they no longer suffer toxic effects, even though exposure continues. Adaptation is temporarily lost on removal from exposure for several weeks.

(U) Animal studies with n-propyl nitrate suggest that it may be similar in nature to nitroglycerine. It produces methemoglobinemia and hypotension, and adaptation has been noted among animals subjected to chronic exposure.

(U) While tetranitromethane has not been studied in as great detail as nitroglycerine and n-propyl nitrate, it does not appear that it has the vascular effects of the first two compounds. Animal studies indicate that inhalation of this vapor causes respiratory irritation and its sequelae.

Miscellaneous Fuels.

(U) Among the miscellaneous fuels of interest in the field of liquid propellants are: ethylene oxide, butyl mercaptan, ammonia, aniline, and methyl acetylene. These are not highly toxic compounds, but they may offer a serious toxic hazard in many operations. Ethylene oxide is a respiratory irritant; aqueous solutions have been shown to cause skin sensitization. Industrial experience has not indicated a serious problem from inhalation of the gas; however, skin sensitization has been a problem in some types of operations. Butyl mercaptan is not highly toxic, either by inhalation of the vapor or by skin exposure. The disagreeable odor of this compound will normally limit exposure to a level well below the toxic level. Ammonia, while normally a gas with respiratory irritant properties, may be handled as a liquid; in that event, precautions to prevent skin splash of the liquid should be taken, since its low temperature in liquid form can cause local freezing. The symptoms of this local action are often similar to those of burns. Aniline is a well-known industrial poison. It is toxic by all common routes of administration, but because of its low volatility, it does not constitute a serious inhalation hazard in most operations. The most common method of poisoning is by skin penetration. It reduces the hemoglobin in the blood to methemoglobin, thus reducing the ability of the tissues to obtain oxygen, with consequent cyanosis and anoxemic changes. Methyl acetylene has a low order of toxicity. In high concentrations, it causes pulmonary irritation.

Table III (U)
MAC's of Various Fuels

	MAC, ppm
Ethylene oxide	100
Butyl mercaptan	10*
Ammonia	100
Aniline	5
Methyl acetylene	1000

The above values are established threshold limit values of the American Conference of Governmental Industrial Hygienists.
* Tentative value, American Conference of Governmental Industrial Hygienists.

Miscellaneous Oxidizers.

(U) While there are some exceptions, most oxidizers are irritants, causing respiratory irritation on inhalation of the vapors; they may also cause eye and skin irritation when the liquid is splashed on those organs. Among the corrosive oxidizers are red fuming nitric acid, white fuming nitric acid, hydrogen peroxide, fluorine, and fluorine oxide. Oxygen, of course, is not toxic in the gaseous form. The liquid, however, because of its low temperature, may cause local damage resembling burns if it is splashed on skin. Perchloryl fluoride is not highly toxic. Preliminary information suggests that this compound may be much more easily handled from the standpoint of toxic hazard than most oxidizers.

Table IV (U)
MAC's of Various Oxidizers

	MAC, ppm
Red fuming nitric acid (as NO_2)	5
90% Hydrogen peroxide	1
Fluorine	0.1

The above values are established threshold limit values of the American Conference of Governmental Industrial Hygienists. No value has been established for fluorine oxide, but it is anticipated that it would be below 0.1 ppm.

(U) The above information is rather general in nature, and will not answer all questions on the toxicity of the various liquid propellants. Somewhat more information is given in a publication entitled "Health Hazards From Propellant Fuels and Oxidizers" (TB Med 242, NavMed P-5035, AFP 160-6-3). The Chemical Warfare Laboratories, at Army Chemical Center, Maryland, have a continuing project "Health Hazards of Military Chemicals", under which studies of the toxicology of various propellants, as well as other military chemicals, are carried out. More detailed information on most of these propellants is published in technical reports of the CW Laboratories. These reports receive a wide distribution within the Department of Defense, and further distribution can be made to anyone in the Armed Services with a need for the information, within prevailing security restrictions. Also, inquiries on the toxicology of any compounds studied in the CW Laboratories will be welcomed at any time.

HEAT TRANSFER PROPERTIES OF ANHYDROUS AMMONIA

T. F. Reinhardt, R. L. Potter, and F. M. Moore
Bell Aircraft Corporation
Rockets Division
Buffalo, New York

Purpose

A program was undertaken recently at Bell Aircraft Corporation under Contract AF33(616)-3570 to investigate the heat transfer properties of anhydrous ammonia. The primary objective of the program was to assess the value of anhydrous ammonia as a regenerative coolant for a rocket thrust chamber. Consequently the program was concerned with measurement of forced convection heat transfer coefficients at high heat flux, in both non-boiling and nucleate boiling regimes.

Introduction

Anhydrous ammonia has been used widely as both a thermodynamic working fluid and a heat transfer medium for many years. Its utilization as a working fluid in mechanical refrigeration systems has prompted thorough investigation of its physical and thermodynamic properties. As a consequence, extensive data are available in the literature on the physical, thermodynamic, and transport properties of anhydrous ammonia.

Interest in anhydrous ammonia as a rocket fuel has developed relatively recently. Since the operating conditions of a rocket engine differ markedly from those of a refrigerator, it is not surprising that some extension of physical data has proved to be necessary. Nevertheless, in most cases existing data have been reliable enough to allow for reasonable extrapolation.

The determination of heat transfer properties of a fluid consists of measuring the coefficient of heat transfer (h) between the moving fluid and a stationary wall, and relating it to the velocity of flow, the dimensions of the flow passage, the pressure, the temperature, and the properties of the fluid. The coefficient of heat transfer is defined by the following equation:

$$h = \frac{q/A}{T_w - T_f} \qquad (1)$$

where q/A = heat flow per unit area (e.g. Btu/in^{2}sec.)

T_w = wall temperature (°F)

T_f = bulk fluid temperature (°F)

Equation (1) is known as Newton's Law of Cooling, and is analogous to Ohm's Law. It may be considered valid as long as the fluid is in one phase, but becomes meaningless if nucleate boiling occurs on the wall. In the latter case, q/A may be increased significantly with little or no change in T_w. There is a maximum value of q/A which can be absorbed in this manner, beyond which the wall becomes blanketed with vapor and T_w undergoes a sudden large increase. The nucleate boiling region, its upper limit, and the conditions of pressure, bulk temperature, and velocity under which stable nucleate boiling may be maintained, are of primary concern to the rocket engineer.

Method of Test

The heat transfer experiments with anhydrous ammonia were conducted in a forced convection apparatus which was designed and built at Bell Aircraft Corporation, and which has been used with several other fluids (Ref. 1, 2, 3). The heart of the apparatus is an electrically heated stainless steel tube 3/16 inch O.D. x .010 inch wall thickness, mounted concentric with a 5/16 inch I.D. heavy walled Pyrex tube. The fluid under investigation flows in the annulus between the two tubes. The heated section of the stainless steel tube is 2 inches long. A photograph of the test section is shown in Fig. 1, and a disassembled view is shown in Fig. 2. Auxiliary equipment includes high-pressure storage and receiver tanks, a heat exchanger to regulate the bulk temperature of the fluid, a 20 KW direct current generator (synchronous motor driven) to supply the heater current, a Potter flowmeter to measure the fluid flow rate, thermocouples to measure heater tube and bulk fluid temperatures, Tabor pressure transducers to measure system pressure and pressure drop across the heater, strip chart recorders to make simultaneous records of heater voltage and current, pressures, temperatures, and flow rate, and the necessary piping, valves, and controls. Gas pressure is applied to the storage tank to force the fluid through the test section. Current is applied to the heater tube in stepwise increments until tube burnout occurs, or until the maximum output of the generator has been reached. At maximum generator output, the heat flux from the heater tube is about 12 Btu/in^{2}sec (6,200,000 Btu/ft^{2}hr). Since the generator is synchronous motor driven, its output is independent of line voltage fluctuations, and the current flow can be maintained at precise values for indefinite periods. A shortcoming of the generator is its large inductance, which causes the heat flux to increase with momentary increases in tube temperature. This phenomenon causes burnouts to occur as soon as any instability develops in the boundary layer.

The heater input can be measured with a high degree of accuracy from the voltage drop and the current through the tube. Due to the annular design of the apparatus, it can be assumed with high accuracy that, under steady state conditions, all of the heat generated in the tube is transferred to the fluid. This can be checked by measuring the flow rate and the bulk temperature rise of the fluid, but the latter measurements are less accurate than the electrical measurements. The inside wall temperature of the heater tube is measured by three chromel-alumel thermocouples located along the axis of the tube, not touching the walls. Since heat can only flow radially outward from the heater tube, the temperature everywhere inside the tube must be equal to the inside wall temperature. The outside wall temperature, which is required for our heat transfer correlation, is calculated from the inside wall temperature, assuming the tube to be heated uniformly through its cross section and to be cooled on the O.D. only by the following formula:

$$T_i - T_o = q/A \frac{X}{K_m} \left(1/2 + \frac{1}{6} \frac{X}{D_o}\right) \qquad (2)$$

where X = wall thickness

K_m = mean thermal conductivity of the wall

The assumption of uniform electrical and thermal conductivities is theoretically in error, but the magnitude of the error is small as the tube wall is very thin. The coolant bulk temperature is obtained by averaging thermocouple readings taken in the inlet and outlet plenum chambers of the test section. Errors due to heat loss from the apparatus to the surrounding air are believed to be very small. Errors in determining bulk temperature are estimated to be ± 2 degrees. Errors in determining T_o are estimated at from ± 2 to ± 5 degrees; the error increasing with increasing heat flux. Errors in determining heat flux are believed to be less than ± 1 percent.

Correlations of heat transfer data may show greater errors than the above due to uncertainties in the values of the transport properties used. For ammonia, the density, heat capacity, and vapor pressure data of National Bureau of Standards, Ref. 4, and the viscosity data of Carmichael and Sage, Ref. 5, appear to be quite accurate. However, the single value of thermal conductivity given by Kardos, Ref. 6, is of doubtful accuracy, and the variation with temperature is not known.

Dean (Ref. 2) calibrated this apparatus with water, and compared results with calculated results from the Sieder-Tate Equation (Ref. 7) in the non-boiling region. Agreement with the constant and exponents of the equation was good; the data showed a "scatter" (standard deviation) of 5.8 percent. Data obtained on RFNA, however, had a standard deviation of 14.8 percent, which was attributed to variations in the acid composition, doubt concerning the physical properties, and to scale formation. The present work on ammonia, when compared with the Dittus-Boelter Equation (Ref. 8) shows a standard deviation of 14.9 percent. The data at low values of Δ T show the greatest scatter, which reflects the limit of accuracy of our temperature measurements. Data for a Δ T less than 10°F are considered to be unreliable.

Discussion of Results

A total of 36 test runs was made with anhydrous ammonia, and a total of 600 data points was obtained. During these tests, the system pressure was varied from 450 to 600 pounds per square inch absolute, the bulk temperature from 35°F to 127°F, and the velocity from 22 to 125 feet per second. The annulus width was 0.0618 inch in all tests, giving a flow area of 0.0486 square inch (0.000338 sq. ft.) and an equivalent hydraulic diameter of 0.1235 inch (0.01029 feet).

In Figure 3 are shown typical uncorrelated results of test runs, with the heat flux (q/A) plotted versus the temperature difference (T_w-T_f) on log-log paper. The slopes of the lines in the non-boiling region should all be equal to unity, in accordance with Equation (1). The zero intercepts of these lines should give values of the heat transfer coefficient, h, which is a function of velocity. The curves show a sharp upward break at the inception of nucleate boiling, and at higher values of q/A, the wall temperature remains nearly constant. This break occurs at a temperature only 2 to 10 degrees above the boiling point of ammonia at the system pressure. The onset of nucleate boiling could be observed only as an apparent discoloration of the tube surface. Bubble formation could not be seen visually until just before burnout. There was no evidence of any chemical interaction between the ammonia and the stainless steel tube.

Burnout points were fairly reproducible, and our correlation efforts are shown in the next section. Burnout always occurred suddenly, without any visual or instrumented warning. There was no stable film boiling region, such as has been observed with JP-4 (Ref. 1) and with RFNA (Ref. 2). It has been noted that fluids which are mixtures of several chemical species and have more or less wide boiling ranges will show more gradual transitions from non-boiling to nucleate boiling, and may show a stable film boiling region. The observed behavior for ammonia is believed to be typical of pure compounds. Another factor accounting for the observed difference is that ammonia has a relatively high critical pressure of 1657 psia, and the difference in specific volume between the liquid and its vapor at 500 psia is quite large. The critical pressures of hydrocarbons making up JP-4 are in the vicinity of 400 psia; hence at this pressure there will be no distinct change in density in passing from the liquid to the vapor phase. The maximum burnout q/A observed during the current tests was 9.03 Btu/in^{2}sec at a velocity of 100 ft/sec, a pressure of 515 psia, and a bulk temperature of 57°F. However, at 125 ft/sec, the tube did not burn out at 9.9 Btu/in^{2}sec.

Some of the raw data show an anomalous decrease of wall temperature with increasing q/A in the nucleate boiling region. This effect was traced to an occasional very slight leakage of ammonia between the heater tube and the copper bus insert. This leakage permitted ammonia vapor to flow to atmosphere past the heater tube thermocouples, causing them to read low. The amount of leakage, and the heat absorbed thereby, was negligible in comparison with the total flow and heat flux; consequently the burnout points obtained on these runs were accepted as valid.

Correlation of Data

The data for heat transfer to ammonia in the non-boiling regime were correlated by means of the dimensionless Nusselt relation of the form:

$$Nu = A \cdot Re^{a} \cdot Pr^{b} \qquad (3)$$

where $Nu = \frac{hD}{K}$ (Nusselt number)

$Re = \frac{VD\rho}{\mu}$ (Reynolds number)

$Pr = \frac{\mu C_p}{K}$ (Prandtl number)

A, a, b = Constants

The above equation is based on the concept of "Reynold's Analogy" relating heat transfer to momentum transfer. Heat transfer data from a wide variety of sources have been compiled by Mc Adams (Ref. 9) Dittus and Boelter (Ref. 8) and others to establish the values of the constants. The Dittus-Boelter Equation is:

$$Nu = 0.027\ Re^{0.8}\ Pr^{0.4} \qquad (4)$$

Figure 4 shows the non-boiling data for ammonia plotted against the Dittus-Boelter Equation. Statistical analysis of our data shows that the constants agree with the Dittus-Boelter Equation, with a standard deviation of 14.9 percent. Physical properties in this correlation are evaluated at the bulk fluid temperature.

Nucleate boiling data for several liquids have been correlated by Rohsenow (Ref. 10) with a relationship similar in form to Equation (3) but using modified parameters. This correlation is based on ΔT_{sat}, or the difference between the wall temperature and the liquid boiling temperature, as the driving potential for heat transfer in nucleate boiling. Attempts to apply this correlation to the present ammonia data were not successful, since the observed values of

ΔT_{sat} were within the limits of accuracy of the wall temperature measurement. It can be concluded qualitatively that ΔT_{sat} was very small in comparison with results obtained for other fluids, e.g. Ref. 2. In general, our qualitative observations agree with those of other observers. Nucleate boiling occurred at a temperature slightly above saturation, and the location and slope of the nucleate boiling line were unaffected by fluid velocity or by bulk liquid temperature. A composite plot of the nucleate boiling data is shown in Figure 5.

Burnout heat flux was found to be related both to fluid velocity and to bulk liquid temperature, or more exactly to ΔT_{sub}, the difference between the bulk temperature and the saturation temperature at the system pressure. Figure 6 shows a plot of the burnout heat flux versus ΔT_{sub}, with fluid velocity as the parameter. These data have been compared with data recently published by the Jet Propulsion Laboratory (Ref. 11). The JPL data show a lower dependence of $(q/A)_{burnout}$ on ΔT_{sub} than is shown on our results.

Ashley (Ref. 3) correlated burnout data for WFNA by an equation of the form

$$(q/A)_{burnout} = A \cdot V^{b} \cdot \Delta T^{c}_{sub} \qquad (5)$$

This form of equation will fit the data over a limited range, but it indicates that $(q/A)_{burnout}$ goes to zero if either V or ΔT_{sub} goes to zero. This is not the case with most liquids.

JPL, Ref. 11 reported burnout heat flux of wires in liquid ammonia. Introducing this value into the data leads to an equation containing a constant term, a term proportional to ΔT_{sub}, and a term proportional to a power of V times ΔT_{sub}.

$$(q/A)_{BO} = 0.00137\ V^{0.6} \Delta T_{sub}{}^{1.2} = 0.0042\ \Delta T_{sub} + 1.71 \text{ But/in}^2\text{sec} \qquad (6)$$

where V is in feet per second, and ΔT is in degrees Fahrenheit. This equation fits the present ammonia data with a scatter of ±0.738 Btu/in^{2}sec. A plot of this correlation is shown in Figure 7.

Conclusion

Forced convection heat transfer data have been measured for anhydrous ammonia over a limited range of pressures in the non-boiling, nucleate boiling, and burnout regimes. These data indicate that ammonia is potentially an excellent coolant. The range of pressures investigated was limited to those of interest for regenerative cooling, and it would be desirable to extend this range in order to get a better picture of the dependence of cooling properties on pressure.

References

1. Dean, L. E. "Heat Transfer Characteristics of JP-4", Bell Aircraft Corp. Report No. 56-982-026, October 1954.
2. Dean, L. E. "Heat Transfer Characteristics of RFNA", Bell Aircraft Corp. Report No. 117-982-004, July 1956.
3. Ashley, E. "Heat Transfer Measurements for WFNA", Bell Aircraft Corp. Report No. 56-982-016, February 1953.
4. Anon. "Tables of Thermodynamic Properties of Ammonia", National Bureau of Standards Circular No. 142, April 16, 1923.
5. Carmichael, L. T. and Sage, B. H., "Viscosity of Liquid Ammonia at High Pressures", Industrial & Engineering Chemistry V. 44, Pt. II, pp 2728-32 (1952).
6. Kardos, A. "Die Warmenleitfahigkeit verschiedenes Flussigkeiten", Zeitschrift fur die gesamte Kalte-Industrie, V. 41, No. 2 (1934).
7. Sieder, E. N. and Tate, G. E. "Heat Transfer and Pressure Drop of Liquids in Tubes", Industrial & Engineering Chemistry, V. 28, p 1429, 1936.
8. Dittus, F. W. and Boelter, L. M. K., "Heat Transfer in Automobile Radiators of the Tubular Type", University of California Publication, Engineering No. 2, p. 433, 1930.
9. McAdams, W. H. "Heat Transmission", McGraw-Hill Book Co. 3rd. ed. 1954.
10. Rohsenow, W. M. "Heat Transfer Associated with Nucleate Boiling", Heat Transfer and Fluid Mechanics Institute, 1953.
11. Anon. "Combined Bimonthly Summary", No. 52, Feb. 1-Apr. 1, 1956, No. 53, Apr. 1-Jan. 1, 1956, No. 54, Jun. 1-Aug. 1, 1956. Jet Propulsion Laboratory, California Institute of Technology.

UNCLASSIFIED

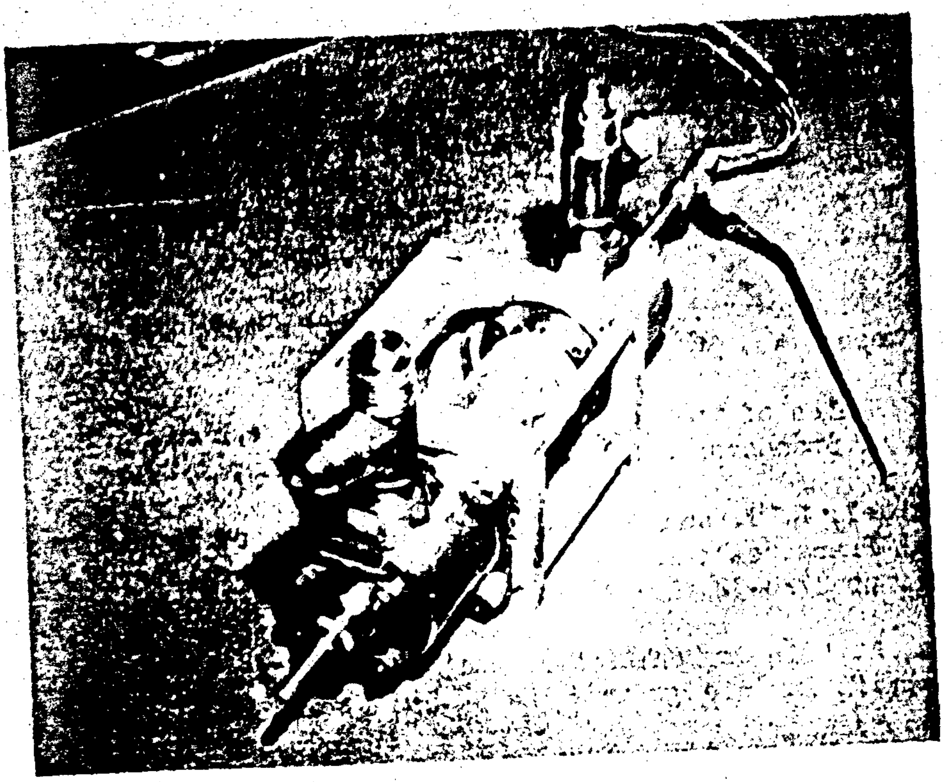

Figure 1 - Heat Transfer Test Section, Assembled View

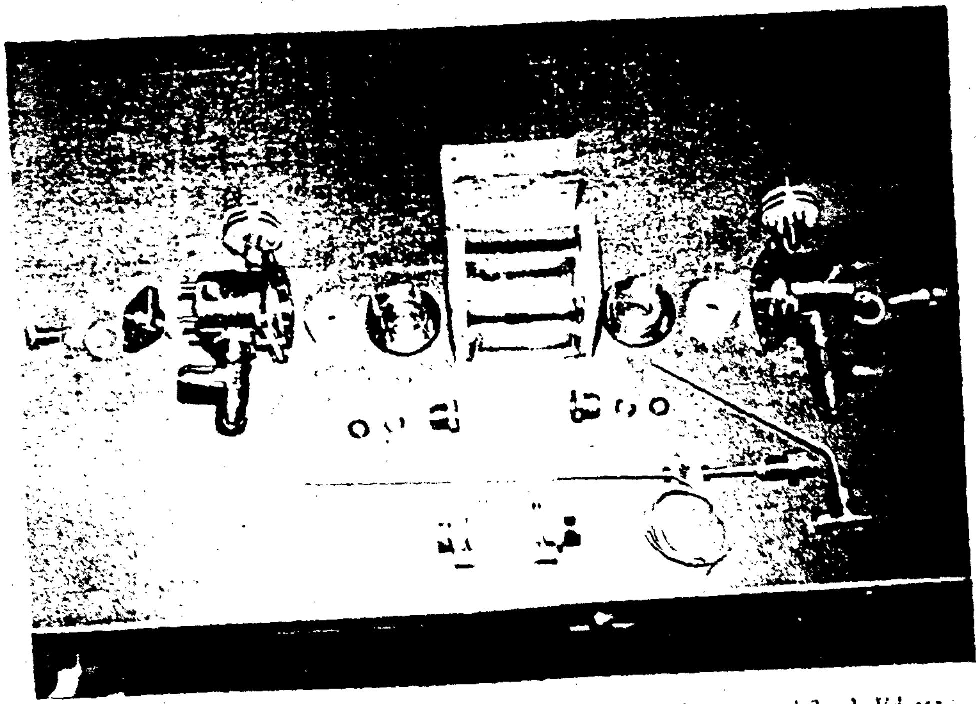

Figure 2 - Heat Transfer Test Section, Disassembled View

UNCLASSIFIED

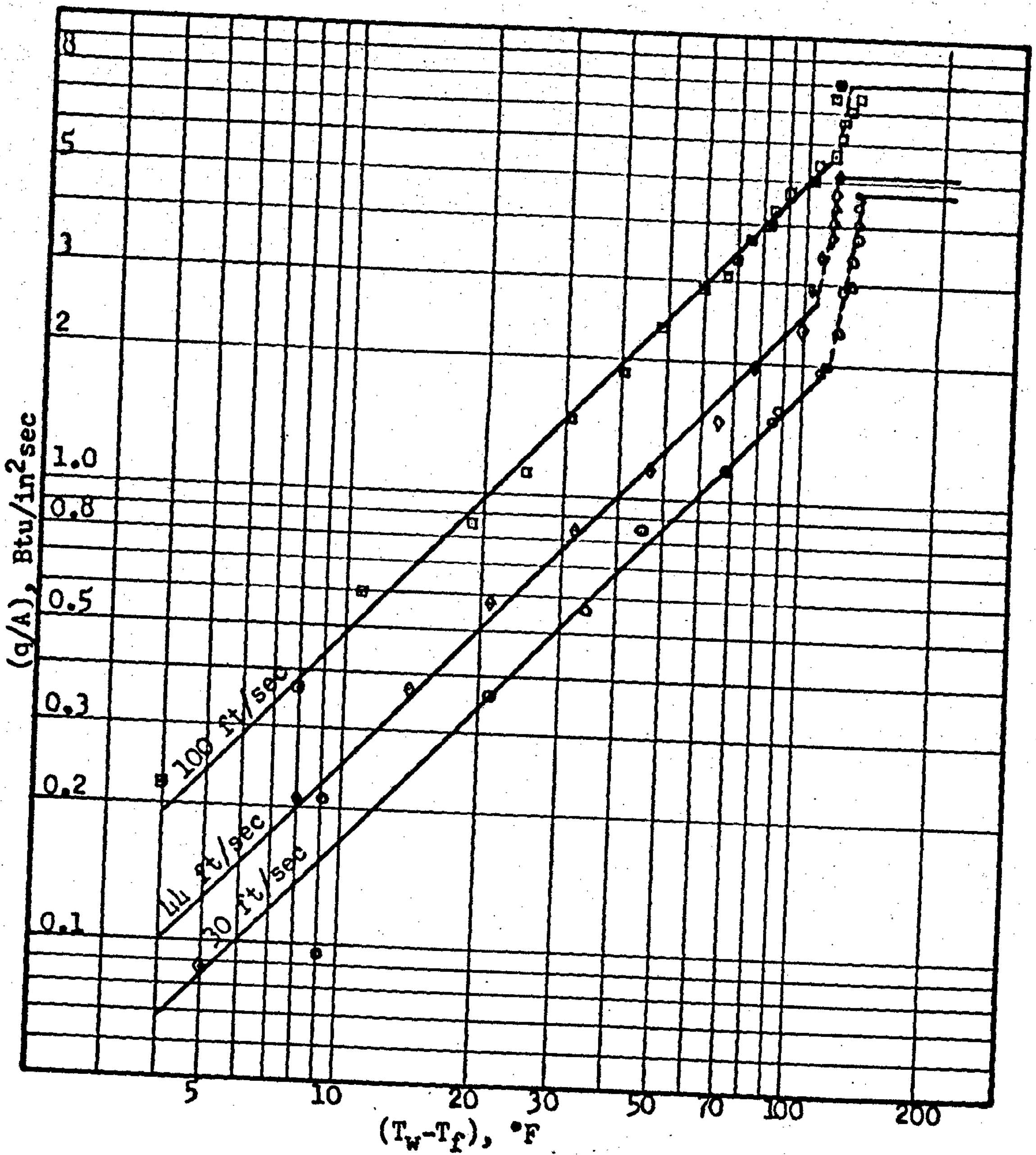

Figure 3 - Liquid Ammonia Heat Transfer
Bulk Temperature 55°F ±5°F
Pressure 500 psia

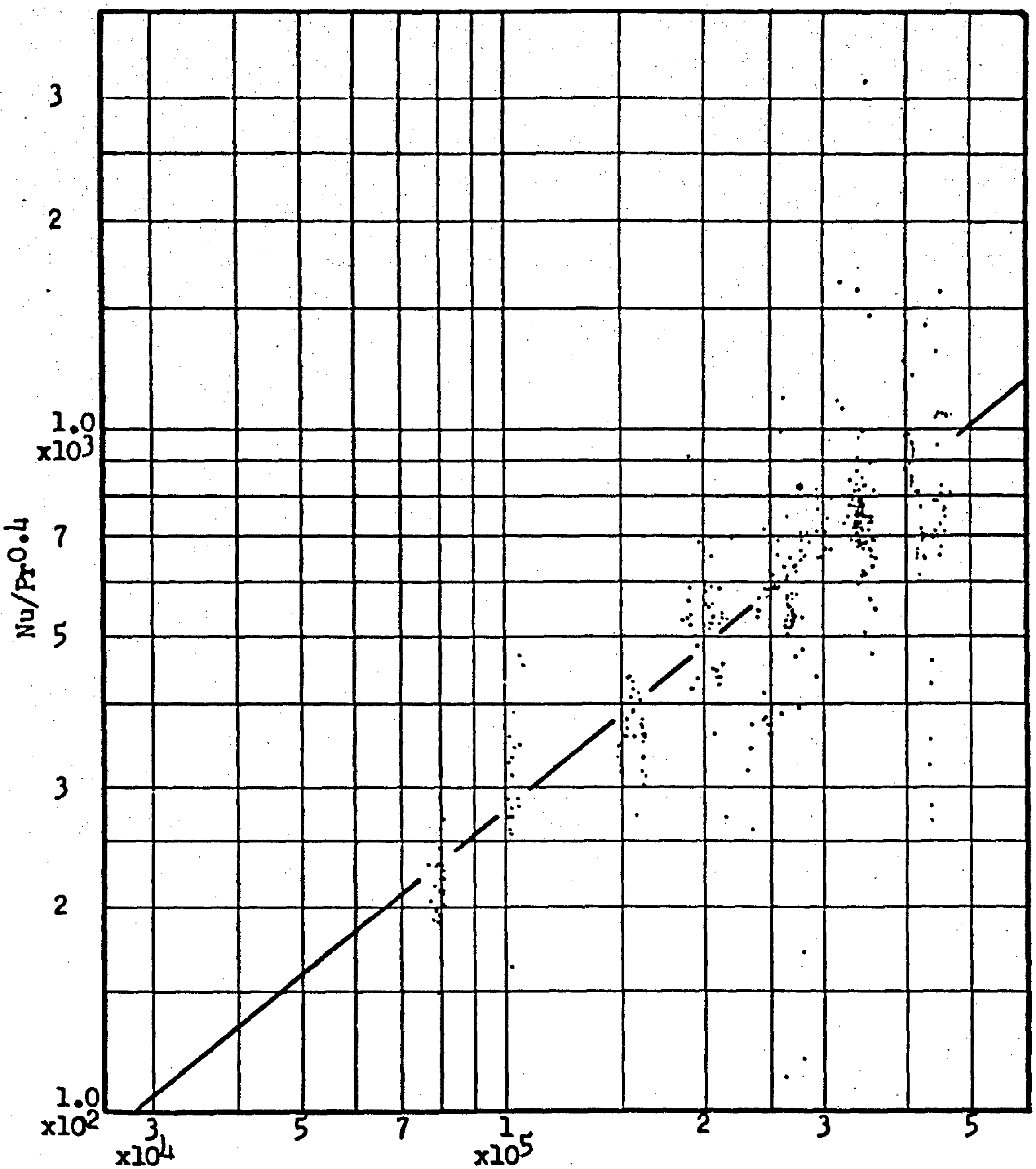

Figure 4 - Correlation of Non-Boiling Data for Ammonia Compared with Dittus-Boelter Equation $Nu = 0.027\ Re^{0.8} \cdot Pr^{0.4}$

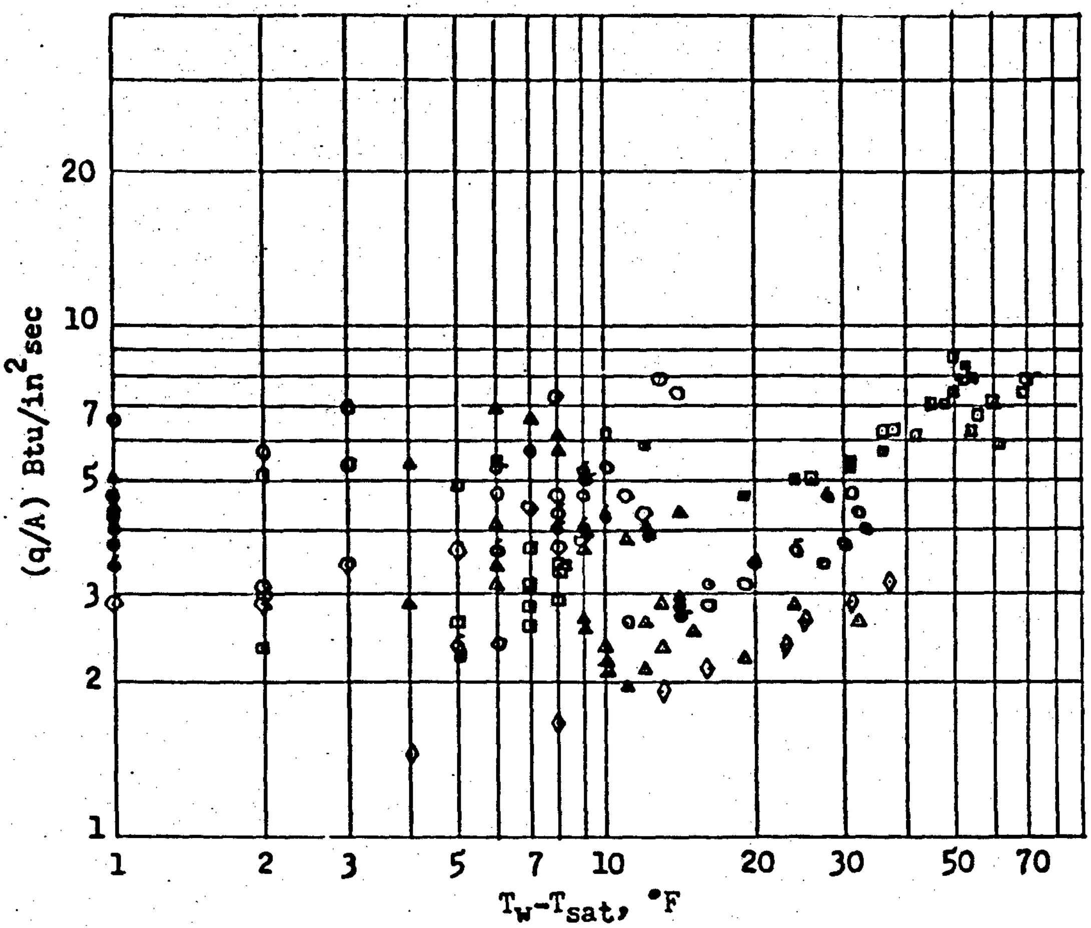

Figure 5 - Composite Plot of Nucleate Boiling Data for Ammonia

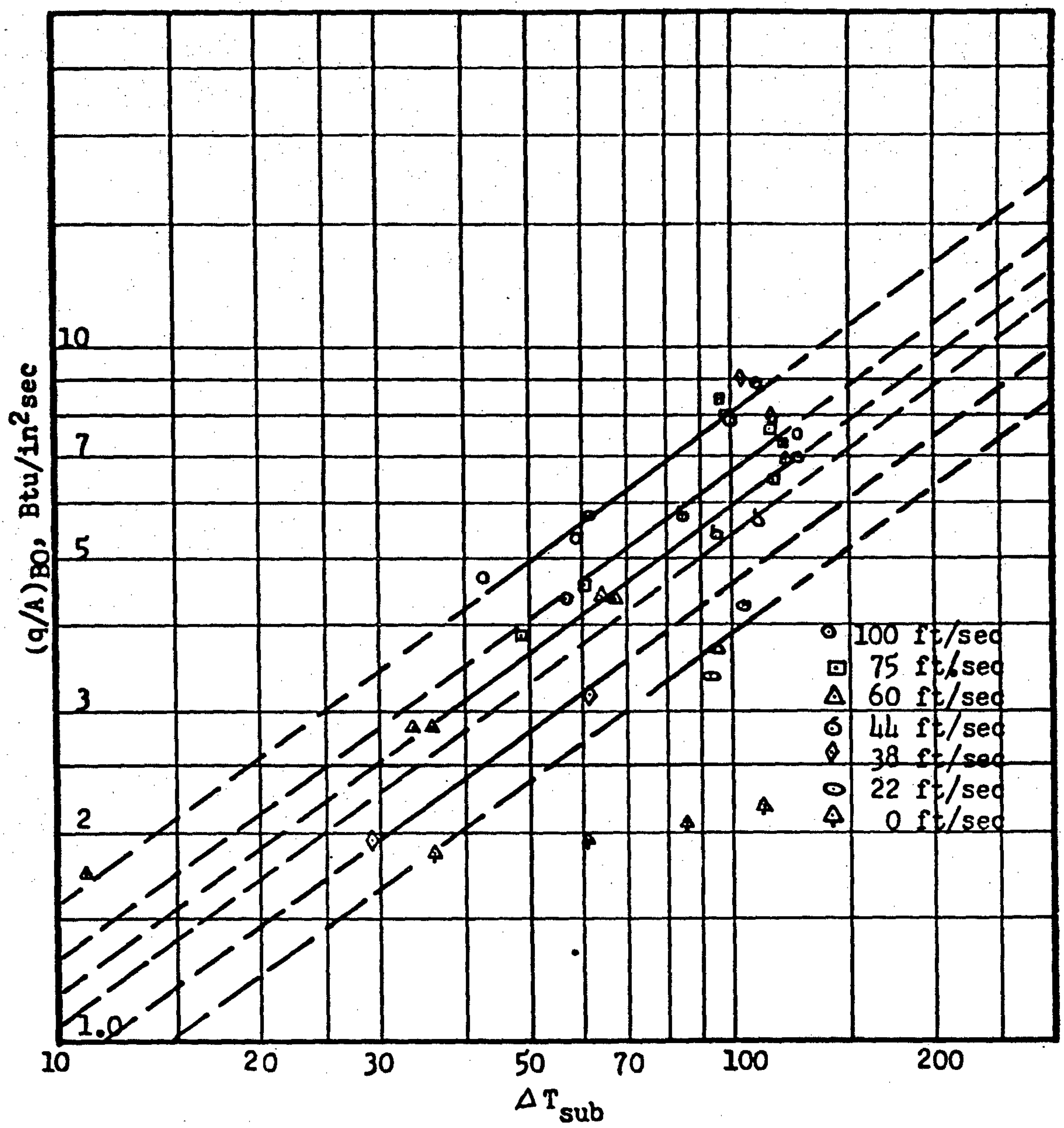

Figure 6 - Burnout Data for Ammonia

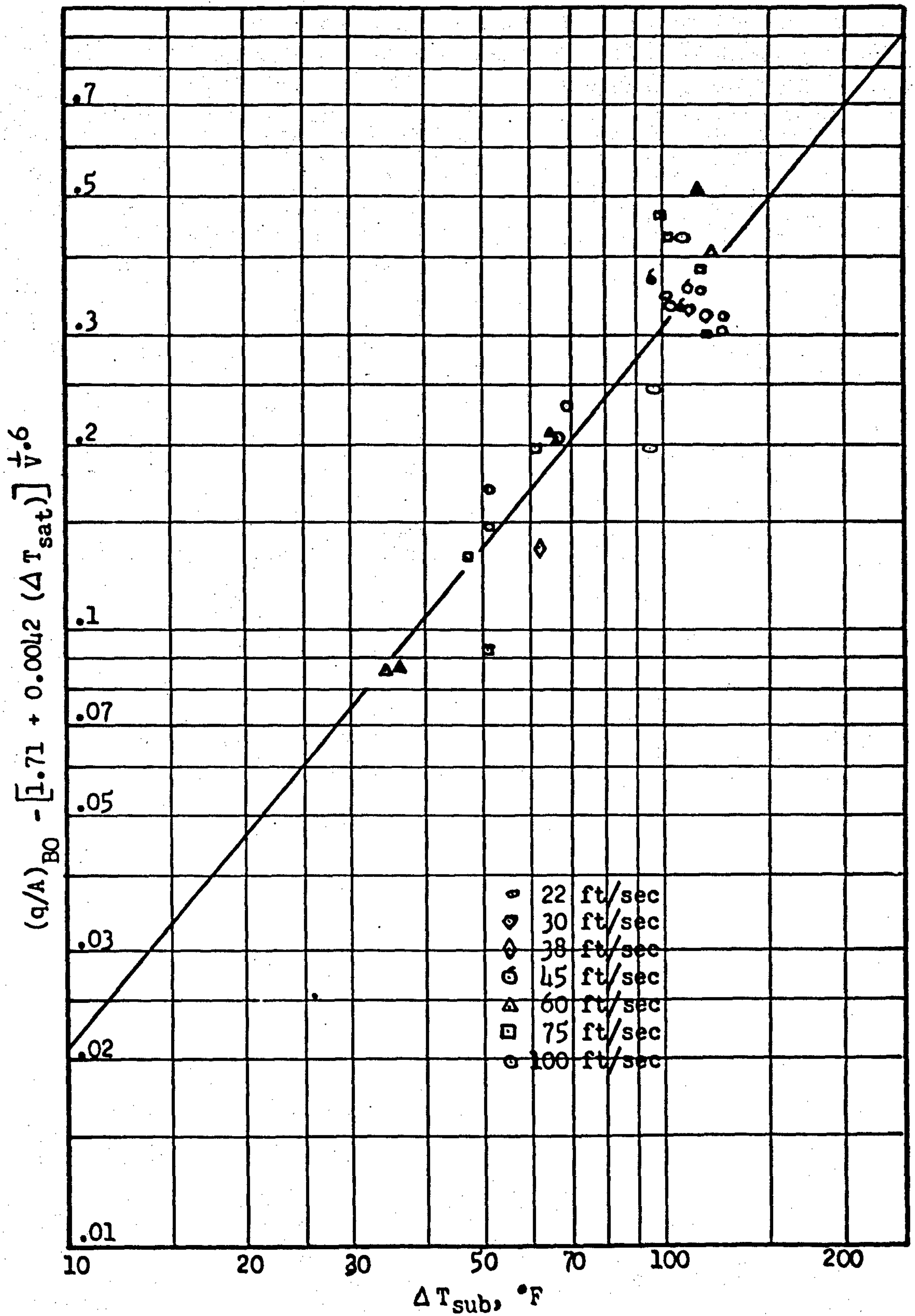

Figure 7 - Correlation of Burnout Data by Equation (6)

CONFIDENTIAL

PETROLEUM DERIVABLE NITROGEN COMPOUNDS AS LIQUID ROCKET FUELS

J. E. Mahan, H. M. Fox, H. W. Bost, O. E. Larsen and R. C. Doss
Phillips Petroleum Company
Bartlesville, Oklahoma

SUMMARY

This is a report of a study of petroleum derivable chemicals as potential rocket fuels. The most promising of the chemicals investigated were the low molecular weight ditertiary diamines. They possess wide liquid ranges (low freezing points, high boiling points) short ignition delays at temperatures as low as -65 F, low viscosities, long-term storage stability, thermal stability at elevated temperatures (500 F plus), efficient combustion with red fuming nitric acid, high bulk performance, ease of preparation, and low cost of raw materials.

A limited study of solutions of the nitrate salts of the diamines in nitric acid as potential high energy monopropellants has been made. These solutions have most of the properties desirable in a monopropellant. Poor thermal stability is the chief problem.

PETROLEUM DERIVABLE NITROGEN COMPOUNDS AS LIQUID ROCKET FUELS

J. E. Mahan, H. M. Fox, H. W. Bost, O. E. Larsen and R. C. Doss
Phillips Petroleum Company
Bartlesville, Oklahoma

I. INTRODUCTION

About six years ago Phillips Petroleum Company began a program under a Navy Bureau of Ordnance contract(1) in search of petroleum derivable materials potentially useful as liquid rocket propellants. Since that time this work has been fairly continuous first under the Bureau of Ordnance contract and later under an Air Force contract(2). The purpose of this report is to summarize the important results of this work, particularly results pertaining to the tertiary diamines which evolved as a promising class of compounds for use as liquid rocket fuels with nitric acid oxidizers.

One of the chief criteria used in screening these potential liquid rocket propellants was the hypergolicity of the fuels with red fuming and white fuming nitric acids. Two measures of hypergolicity were used (a) ignition delay, and (b) maximum tolerance of a diluent, without loss of hypergolicity. An injector-type laboratory apparatus which vigorously and rapidly mixed the propellant and the acid was developed to measure ignition delays. Since shorter ignition delays result in smoother and more dependable ignition and apparently smoother motor operation, materials having the shortest ignition delays were sought. In general, an arbitrary value of 50 milliseconds delay was taken as the upper limit of potential usefulness. Materials which were found acceptable from this standpoint were screened further on the basis of physical properties, storage characteristics, and calculated performance parameters. The physical properties considered to be most important were freezing point, boiling point, density, and viscosity. Theoretical performance parameters were calculated as a function of fuel-oxidizer ratio. Some of these were specific impulse, characteristic exhaust velocity, combustion temperature, and combustion products. From specific impulse and bulk density, overall volume impulse was calculated.

Approximately 500 compounds were evaluated including various types of hydrocarbons; oxygen containing compounds such as alcohols, ethers, carbonates, and epoxides; sulfur containing compounds such as mercaptans, sulfides, and sulfenamides; nitrogen containing compounds including amines, nitriles, pyridines, and pyrroles; and some phosphorous containing compounds such as phosphates and phosphites.

In terms of broad generalities the study of the various classes of compounds was narrowed to a study of the ditertiary diamines through a gradual elimination process on the following basis: Of the hydrocarbons, only those containing multiple unsaturation appeared to hold promise and these compounds were under investigation by other organizations under contract with the Armed Services; the oxygenated compounds as a group did not possess the desired hypergolicity characteristics; many of the sulfur compounds exhibited properties which were good but somewhat less attractive than those of the diamines; many of the phosphorus compounds possessed good ignition properties but these materials as a group lost favor because of low impulse and gum formation and nozzle erosion characteristics found in motor firings. A study of the nitrogen-containing compounds revealed that the ditertiary diamines possessed better low temperature properties than other amines and polyamines in general. These ditertiary diamines as a group were found to have low ignition delays over the temperature range of 75 F to -65 F, excellent physical properties, and good calculated theoretical performance characteristics. From this screening program the ditertiary diamines emerged as the most promising of the fuels investigated and subsequent work was directed toward a study of this class of compounds.

II. TERTIARY DIAMINES AS LIQUID BIPROPELLANT FUELS

A. Preparation

A number of ditertiary diamines were prepared. Special methods were required for the preparation of some of these materials but most of these compounds, particularly those of low molecular weight, were prepared by one of the three following methods:

$$(1)\quad R_2NH + XCHR'(CH_2)_nX \longrightarrow R_2NCHR'(CH_2)_nNR_2 + 2HX$$

$$(2)\quad R_2NH + R'CH = CHCHO \xrightarrow{\text{desiccant}} R_2NCHR'CH = CHNR_2 + H_2O$$

$$(3)\quad R_2NCHR'CH = CHNR_2 + H_2 \xrightarrow[\text{press.}]{\text{cat.}} R_2NCHR'CH_2CH_2NR_2$$

A considerable amount of study was given to the preparation of the diamines through the use of epoxides in the following manner:

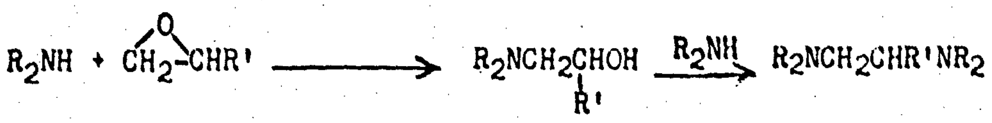

$$R_2NH + \overset{O}{CH_2\!-\!CHR'} \longrightarrow R_2NCH_2\underset{R'}{CHOH} \xrightarrow{R_2NH} R_2NCH_2CHR'NR_2$$

The first step of the reaction proceeded readily but none of the known methods of direct conversion of alcohols to amines were found to be effective in this conversion of a β-aminoalcohol to the corresponding diamine. While it is not known to what this change in the characteristics of the carbon-oxygen bond may be attributed, it is apparent that a marked change has been produced. Similarly, attempts to produce the propene-diamine through the reaction of epichlorohydrin and a secondary amine followed by dehydration of the diaminoalcohol as represented below were unsuccessful.

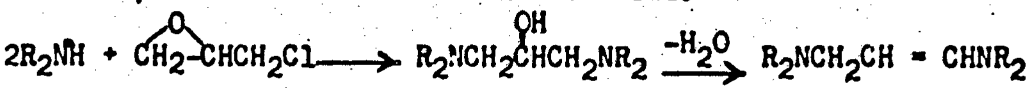

$$2R_2NH + \overset{O}{CH_2-CH}CH_2Cl \longrightarrow R_2NCH_2\overset{OH}{C}HCH_2NR_2 \xrightarrow{-H_2O} R_2NCH_2CH = CHNR_2$$

Again, the first step proceeded readily but the second step is not achieved by any of the usual methods. Comparable intractability of the corresponding diaminoisopropylchloride toward dehydrohalogenation has been reported in the literature. These difficulties eliminated an otherwise promising route to several of these diamines.

B. Laboratory Evaluation

A study of the ignition delays of most of the possible saturated and olefinic diamines and a few of the acetylenic diamines of the general structure $(CH_3)_2N-R-N(CH_3)_2$ where $R = C_1$ through C_4 plus tetramethylhexane-1,6-diamine was made. It was found that of this series of diamines the methylenediamine was unsatisfactory at room temperature and the hexane-1,6-diamine and 2-butyne-1,4-diamine were unsatisfactory at low temperatures. Otherwise almost all of this class of compounds was found to be acceptable from the standpoint of ignition delay characteristics over the range 75 F to -65 F. Figure 1 shows the comparison of the ignition delays of several of these diamines at 75 F. A curve is drawn to show graphically the correlation between the length of the straight chain carbon structure between the nitrogen atoms and the ignition delay. Other comparisons can be drawn from the indications afforded by these limited data: e.g. α-branching appears to be beneficial while β-branching offers no advantage, etc. Since all of these materials are in the range of acceptability both at this temperature and at low temperatures, no particular benefit is to be derived by such comparisons of these materials falling in so narrow a range of ignition delay characteristics. Therefore, preliminary selection of the most desirable fuel is dependent upon the physical and storage characteristics with final selection being necessarily dependent upon the firing and operational characteristics of the fuel in actual motor evaluation.

A study of the storage characteristics of several of the diamines was made. Samples were stored at 140 F in both clear and black containers, under atmospheres of nitrogen and of air, in glass containers alone and in glass containers in contact with various construction materials likely to be encountered in rocket usage. These included 1020 C.R. Steel, 347 stainless steel, 61ST aluminum, copper, Hycar rubber, Teflon, Kel-F, Tygon, Crane Packing, Neoprene and Marlex* polyethylene.

In glass containers the unsaturated materials darkened somewhat on long-term standing but the ignition delay characteristics of these materials did not appear to be changed by this discoloration. At elevated temperatures these materials decompose rather rapidly. It has been found, for example, that N,N,N',N'-tetramethyl-1-butene-1,3-diamine decomposes within a matter of minutes at 500 F. During the heating the presence of a small amount of sodium to remove the last traces of water, however, will allow the butene to be heated at 500 F for one hour without appreciable change. The saturated materials are quite stable and will withstand heating at 500 F for one hour without appreciable change, indicating potential usefulness of these materials in missile skin and rocket nozzle cooling applications.

Storage tests in contact with construction materials showed that, in general, C.R. steel, 347 SS, aluminum, Teflon, and Marlex* polyethylene were found to be acceptable as construction materials for use in contact with these amines. Crane packing is suitable in contact with saturated amines but is attacked somewhat by the unsaturated diamines. Neoprene, Kel-F, Tygon and Hycar rubber are generally attacked by these fuels.

The Naval Ordnance Test Station reported at the Bi-propellants Research Meeting, which was held in Los Angeles in May, 1956, on the thermal stability of the diamines. They used a closed bomb connected with a manometer and determined pressure build-up at a constant bomb temperature of 122 F. On a saturated diamine, N,N,N',N'-tetramethylpropane-1,3-diamine, there was no pressure build-up in storage under these conditions; on the other hand, the analogous propene-1,3-diamine had a pressure build-up of 5.7 mm of mercury per day. However, it has been seen that this material can be stabilized by adding a small amount of sodium to remove the last traces of water.

A limited investigation of the toxicity of the propane and propene derivatives was made. It was found that these materials must be handled with the same precautions as common nitrogen chemicals such as aniline and the methylamines; that is, they are severe skin and eye irritants.

C. Motor Evaluation

Table I summarizes the physical properties and performance data obtained in five of the most promising tertiary diamines investigated. The wide liquid range of these materials is worthy of note. In general, these materials have freezing points considerably below the minimum service requirement, -65 F, and at the same time have high boiling points, much higher in most cases than unsymmetrical dimethylhydrazine, commonly used as a nitric acid hypergol. Consequently, vapor pressures at temperatures encountered in skin and motor cooling applications would be much less. This coupled with the thermal stability of the saturated tertiary diamines appears as an important advantage of these materials. Viscosities vary from compound to compound but they fall well below 40 centistokes at -65 F generally considered adequate for most applications. While the densities of the diamines are lower than desired, they compare favorably with UDMH. It is to be noted that the stoichiometry of the diamines is such that on an overall basis they are considerably superior to UDMH.

---

*A trademark of Phillips' family of olefin polymers.

Recent firing tests of N,N,N',N'-tetramethylpropane-1,3-diamine at NOTS have been reported. These tests were run in a 1500-lb motor designed to simulate LAR. This motor is very severe having a very low L^* and operating under conditions such that one-half pound of propellant per cubic inch of motor volume per second is consumed. Data reported by NOTS on these firings are as follows:

O/F	c^*
2.63	5170
2.90	5255
3.45	4950
3.76	4950
4.03	4905

These data were obtained using an injector designed for UDMH giving 5260 ft/sec c^* at 2.63 O/F nitric acid to fuel ratio. Since this represents the optimum oxidizer to fuel ratio for UDMH it is seen that the propane diamine peaks at roughly the same value of c^* but at a much higher oxidizer to fuel ratio. This confirms in practice the theoretical overall volume impulse advantage of the diamines.

The propene diamine was fired in the LAR in earlier tests and was found to be satisfactory. An impulse of 195 $\frac{lb_f\text{-sec}}{lb_m}$ was reported as compared to 172 obtained under similar conditions for UDMH and 200 for the low freezing hydrazine mixture. This also indicates that the diamines, at least this one unsaturated diamine, are very reactive even under very severe combustion conditions such as the LAR motor.

Firings using N,N,N',N'-tetramethylethane-1,2-diamine, N,N,N',N'-tetramethylpropane-1,2-diamine, N,N,N',N'-tetramethylbutane-1,3-diamine, and N,N,N',N'-tetramethyl-1-butene-1,3-diamine as well as those of the propane and propene diamines have been made at WADC in the 100-lb Aerojet Universal Propellant Tester or in a 200-lb uncooled motor.

Below is a condensed summary of the data obtained in firing tests at WADC in the Aerojet Universal Propellant Tester.

	Max. Isp	Wo/Wf	Overall Volume Isp at Max. Isp
N,N,N',N'-tetramethylethane-1,2-diamine	220.9	3.0	16,774
N,N,N',N'-tetramethylpropane-1,2-diamine	219.3	3.38	16,655
N,N,N',N'-tetramethylpropane-1,3-diamine	212.0	3.4	16,433
N,N,N',N'-tetramethylpropene-1,3-diamine	218.0	3.5	17,261
N,N,N',N'-tetramethylbutane-1,3-diamine	218.7	3.58	17,165
N,N,N',N'-tetramethyl-1-butene-1,3-diamine	219.1	3.28	17,179

D. Most Promising Ditertiary Diamines Evaluated

While all of the low molecular weight ditertiary diamines have most of the characteristics desirable in a nitric acid hypergol, two have been singled out as most promising. These are N,N,N',N'-tetramethylethane-1,2-diamine and N,N,N',N'-tetramethylbutane-1,3-diamine. They are among the ones evaluated rather extensively. They should present no problems in rocket usage from a storage standpoint being thermally stable to at least 500 F, or from a physical property standpoint. Ballistically, they appear as good or better than unsymmetrical dimethylhydrazine. Pertinent properties of these two materials are tabulated below along with UDMH for comparison.

	N,N,N',N'-Tetramethyl-ethane-1,2-diamine	N,N,N',N'-Tetramethyl-butane-1,3-diamine	Unsymmetrical Dimethyl-hydrazine
Boiling Point, F @ 760 mm	246-252	319-320	146(a)
Freezing Point, F	-70	-131	-72(a)
Viscosity, cs @ -65 F	3.0	11.24	5.8(b)
Density, g/ml @ 20/4	0.775	0.795	0.79(a)
Motor Data(c), Universal Propellant Tester, WADC			
Isp @ 300 psi	220.9	218.7	
c*, ft/sec	5170	5181	
Wo/Wf	3.00	3.58	
Est. Per Cent Eff., $\frac{\text{Expt. Isp} \times 100}{\text{Equiv. Theor. Isp}}$	97.6	97.2	
Calculated Performance Data			
Isp @ 300 psi	226.3	225.2	232
c*, ft/sec	5189	5163	5328
Wo/Wf	3.48	3.50	2.42
Vol. Isp, lb_f-sec/cu. ft.	17,577	17,744	17,409
Wo/Wf	4.18	4.00	3.05
Laboratory Ignition Delay, ms			
@ 75 F	7.2	6.7	0.6
@ 0 F	14.5	7.4	0.6
@ -65 F	25.2	12.2	2.3

(a) Ref. 3.
(b) 5.0 cp value of Ref. 3 converted to centistokes using density = 7.2 lb/gal.
(c) Oxidizer used was RFNA, 12-20% NO_2.

III. BLENDS OF TERTIARY DIAMINES AND JP-4 AS LIQUID ROCKET FUELS

From a logistics standpoint it would be desirable to have a material which could be added in small quantities to a jet fuel composition and impart to this less expensive and more readily available fuel the characteristics desired of a rocket fuel. Somewhat less desirable, but also to be considered, is the possibility of adding such jet fuel as an extender to that fuel and thereby reduce the cost of the total propellant. One of the characteristics particularly sought in either case is that of hypergolicity. Toward either of these ends a considerable amount of study was given to the investigation of blends of the diamines with JP-4. The diamines were found to be miscible with JP-4 in all proportions. Series of blends of the diamines and JP-4 were prepared such that the following correlations of the structure of the amines with the effect on the hypergolicity characteristics of the JP-4 blend might be made:

(a) The effect of variations in the length of the carbon chain between the two nitrogen atoms;

(b) Straight chain versus branched chain carbon skeletons between the nitrogen atoms;

(c) The effect of unsaturation versus saturation;

(d) The effect of variations in the N-alkyl substituents.

From this study several generalizations were found in terms of the retention of hypergolicity of the blend as the percentage of the jet fuel was increased. It was found that the substituted ethanediamines imparted more desirable ignition delay characteristics to the blends than did the diamines containing a larger carbon chain skeleton-either straight or branched chain--between the two nitrogen atoms. The dilution tolerance of the saturated diamines to JP-4 appeared greater than that of the unsaturated diamines when the multiple bond and the nitrogen atom were attached to the same carbon atom in a vinyl amine configuration. When only allylic amine configurations were present, the unsaturated amines had greater dilution tolerances than the corresponding saturated amines. One double bond in a diamine molecule did not significantly change the temperature sensitivity of the fuel. The presence of a triple bond or several double bonds in the molecule made the fuel more sensitive to changes in temperature. Variations in the N-alkyl substituents of ethanediamine showed that allylic unsaturation produced better ignition delay properties than saturated terminal groups at room temperature. Blends of the unsaturated fuel, however, were more sensitive to temperature changes than the saturated materials. Further, methyl group substitution was found to produce more desirable dilution properties than larger alkyl groups and blends of tertiary diamines showed less sensitivity to temperature than primary and secondary amines.

In general, N,N,N',N'-tetramethylethane-1,2-diamine was the best diamine tested relative to retention of hypergolicity in jet fuel dilutions over the temperature range of 75 F to -65 F. In this respect UDMH is superior to the diamines. However, on an overall basis where thermal and phase stability of the blend and physical properties of the blend are considered, the diamines may be more favorable.

IV. SALT SOLUTIONS AS LIQUID MONOPROPELLANTS

After sufficient study had been given to the investigation of tertiary diamines to demonstrate that these materials held considerable promise for potential bipropellant usage, the aims of the project were directed toward the study of the possible usefulness of these materials in monopropellant applications. Because of the simplifications in motor design which could be realized through the use of a monopropellant there is currently a great need for an operational high impulse monopropellant. Dr. John Clark and his coworkers at NARTS in recent months have investigated the potential usefulness of nitric acid-monoamine nitrate salt solutions for this application.(4) Extension to the diamine solutions seemed desirable. Calculated performance values indicated that nitric acid solutions of the nitrate salts of these diamines possess theoretical impulse values in the range of 220-225 lb-sec/lb at 300 psi chamber pressure, or in excess of 250 at 1000 psi chamber pressure.

The diamines were converted to their nitrate salts and these salts were dissolved in nitric acid. Anhydrous nitric acid is used in the preparation of these solutions because of the increased rate of decomposition of some of these solutions caused by the presence of the oxides of nitrogen. Stoichiometrically equivalent solutions, i.e., solutions containing a ratio of salt to nitric acid such that all the carbon and hydrogen will be converted to carbon dioxide and water, were used throughout this study. However, in actual usage, solutions containing an excess of salt would be more desirable in most cases.

These solutions were then screened on the basis of physical properties, thermal stability, burning rate, theoretical performance, and shock sensitivity characteristics. Table II lists the properties of three of these acid-salt solutions. In general, the densities, freezing points, and burning rate characteristics of these solutions were good but their thermal stabilities and low temperature viscosities were less desirable.

In many cases a small amount of acetamide (1.4 per cent of the weight of the acid) was added to the solutions to reduce the rate of accumulation of the oxides of nitrogen. In some cases HF was also added. It is recognized that additional variables of undetermined magnitude are introduced by the presence of additives but both of these materials were shown to markedly increase the stability of some of these monopropellant solutions. For the sake of more equitable comparisons, then, these additives were included in some of these propellants before their presence in these solutions was shown to be advantageous. In some cases these additives were shown to exert very little effect on the stability of the solution. And in some cases their effect on other characteristics such as burning rate, card gap sensitivity, etc., have been shown to be advantageous while harmful in others. No clear picture of the role played by such additives has come to light and a considerable amount of work is needed to determine the net worth of such materials in these systems.

In the card-gap tests for hydrodynamic shock sensitivity, stoichiometric solutions of N,N,N',N'-tetramethylpropane-1,3-diamine dinitrate exhibited surprisingly low card-gap sensitivities of 12 cards each. At the same time they had good burning rates (0.303 inch per second at 600 psi for the butane derivative solutions containing acetamide). But on storage at 140 F both solutions decomposed sufficiently in less than three days to cause rupture of a 110 psi blowout disk.

A few generalizations can be drawn with the limited amount of test data available. The nitrate salts of the diamines are insensitive to mechanical shock. Most of these salts exhibit a greater solubility in nitric acid than that required for the preparation of stoichiometrically equivalent solutions. The solubility of N,N,N',N'-tetramethylbutane-1,3-diamine dinitrate at -40 F, for example, is almost two-fold that required for a stoichiometrically equivalent solution. The thermal stability of these solutions has not been found to be particularly encouraging and insufficient data on the effects of additives has been obtained to indicate the potential fruitfulness of investigation of this area.

Limited investigations were made on nitric acid solutions of the picrate and perchlorate salts of a few diamines and monoamines. In general, the picrate solutions were unsatisfactory because of their poor solubility or thermal stability characteristics. The perchlorate solutions on the other hand showed a very surprising degree of thermal stability, considerably greater than that of most of the diamine dinitrate solutions. The only diamine diperchlorate solution tested, however, was more sensitive to shock than the corresponding nitrate solution. But determinations of the sensitivity of the monoamine perchlorates have not been made. The freezing point, viscosity, density, and theoretical specific impulse characteristics of these materials appear promising.

V. REFERENCES

1. Final Report, Contract NOrd 11338, "Petrochemicals as Rocket Propellants", Research Division Report 308-52-53R, CONFIDENTIAL, Phillips Petroleum Company, September 30, 1953.
2. Final Report, Contract AF 33(616)-2675, "Petroleum Derivable Nitrogen Compounds as Liquid Rocket Fuels", Research Division Report 1478-56R, CONFIDENTIAL, Phillips Petroleum Company, in preparation.
3. "Notes on Unsym-Dimethylhydrazine as a Propellant", Development Department, Westvaco Chlor-Alkali Division, Food Machinery and Chemical Corporation, March 1, 1955.
4. Verbal Communications with Dr. John Clark of NARTS, September, 1956.

TABLE I

PHYSICAL PROPERTIES AND PERFORMANCE DATA

Property	(1) Ethane-1,2	(2) Propane-1,2	(3) Propane-1,3	(4) Propene-1,3	(5) Butane-1,3	(6) Butene-1,3
Molecular Weight	116.2	130.2	130.2	128.2	144.2	144.2
Boiling Point, F	253	266-280	294	320-329	319-320	347-351
Freezing Point, F	-70	-175	-176	Glass -130	-131	-126
Viscosity, cs 75 F	0.74	0.44	0.97	1.30	1.25	1.34
-40 F	2.02	3.42	3.35	6.96	5.68	7.35
-65 F	3.00	5.78	5.54	15.06	11.24	16.86
Density, gm/cc at 20 C	0.775	0.795	0.782	0.822	0.795	0.818
Refractive Index, n_D^{20}	1.4170	1.4248	1.4236	1.4600	1.4300	1.4666
Heat of Combustion, Btu/lb,	16,926	17,088	17,020	16,263	17,548	17,219
Ignition Delay, ms, 75 F	7.2	7.3	7.7	14.2	6.7	6.0
0 F	14.5	16.8	9.5	12.9	7.4	8.6
-65 F	25.2	22.6	17.1	17.4	12.2	23.6
Specific Impulse, Max.,						
$I_{sp}, \frac{lb_f\text{-sec}}{lb_m}$	226.3	224.7	224.3	226.3	225.2	225.3

(Continued)

TABLE I (Cont'd)

PHYSICAL PROPERTIES AND PERFORMANCE DATA

Property	(1) Ethane-1,2	(2) Propane-1,2	(3) Propane-1,3	(4) Propene-1,3	(5) Butane-1,3	(6) Butene-1,3
Oxidant/Fuel, O/F (at Max. Isp)	3.48	3.38	3.33	3.13	3.45	3.30
Overall Volume Impulse, Max. I_v, $\frac{\text{lbf-sec}}{\text{ft}^3}$	17,577	17,682	17,567	17,889	17,744	17,832
Stoichiometric$^{(7)}$ Performance						
O/F	4.648	4.452	4.452	4.325	4.543	4.430
Density	1.278	1.291	1.285	1.300	1.294	1.302
Isp	219.9	218.8	218.5	219.5	219.0	218.7
I_v	17,532	17,630	17,522	17,809	17,687	17,763
Combustion Temp., Tc, °K	3,019	3,005	2,999	3,053	3,015	3,040
Gas Composition, Mole %						
CO	7.37	7.34	7.28	8.33	7.59	8.24
H_2	2.59	2.49	2.47	2.61	2.53	2.54
H_2O	44.30	44.27	44.35	41.77	43.89	41.97
N_2	19.80	19.51	19.52	19.65	19.19	19.38
CO_2	17.02	17.68	17.76	17.88	17.83	18.33
OH	3.20	3.11	3.07	3.43	2.19	3.34
O	0.54	0.51	0.50	0.63	0.54	0.61
O_2	3.54	3.52	3.49	3.90	3.62	3.86
H	0.60	0.56	0.56	0.67	0.59	0.63
NO	1.04	1.01	1.00	1.13	1.03	1.10

---

1) N,N,N',N'-tetramethylethane-1,2-diamine.
2) N,N,N',N'-tetramethylpropane-1,2-diamine.
3) N,N,N',N'-tetramethylpropane-1,3-diamine.
4) N,N,N',N'-tetramethylpropene-1,3-diamine.
5) N,N,N',N'-tetramethylbutane-1,3-diamine.
6) N,N,N',N'-tetramethyl-1-butene-1,3-diamine.
7) Assumed Products: CO_2, H_2O, N_2.

TABLE II

PHYSICAL PROPERTIES AND CALCULATED PERFORMANCE OF NITRIC ACID-AMINE SALT SOLUTIONS

	N,N,N',N'-tetramethyl-propane-1,3-Diamine Dinitrate	N,N,N',N'-tetramethyl-butane-1,3-diamine Dinitrate	Triethylamine Perchlorate
Properties of Salt			
Molecular Weight	256.3	270.3	201.6
Melting Point, F	315.5-319.1	239-240.8	168.8-170.6
Heat of Combustion, Btu/lb[(a)]	8349	9056	9236
Impact Sensitivity, in.-lbs.	120	120	120
Solubility in Anhydrous HNO_3, Wt. %			
75 F	-	-	-
32 F	46.6	79.8	-
-40 F	42.3	61.2	
Stoichiometric[(b)] Solutions of Salts in Anhydrous Nitric Acid (Plus 1.4% Acetamide in Nitrate Solutions)			
Salt Content, Wt. %	36.1	33.8	34.0
Acid/Salt	1.766	1.960	1.940
Freezing Point[(c)], F	-81.8	-94	-85.1
Density, gm/ml @ 20 C[(d)]	1.420	1.421	1.3768
Viscosity, cs, @ 75 F[(e)]	6.1	4.7	1.08
-40 F	108	62	3.96
Storage Stability @ 140 F, hrs	145	57	est'd 2 yrs
Burning Rate, inches/sec			
@ 100 psi	-	-	-
200	-	0.063	-
300	0.043	0.172	-
400	0.065	0.208	-
600	0.130	0.303	-
Card Gap Sensitivity, Cards	12.0	12[(f)]	-
Hypergolicity[(g)]	No	Yes	Yes

(Continued)

TABLE II (Cont'd)

PHYSICAL PROPERTIES AND CALCULATED PERFORMANCE OF NITRIC ACID-AMINE SALT SOLUTIONS

	N,N,N',N'-tetramethyl-Propane-1,3-Diamine Dinitrate	N,N,N',N'-tetramethyl-Butane-1,3-diamine Dinitrate	Triethylamine Perchlorate
Calculated Performance Values			
Max. Specific Impulse, $\frac{\text{lb-sec}}{\text{lb}}$	222.2	223.2	
Optimum Acid/Salt	1.30	1.44	
Max. Volume Impulse, $\frac{\text{lb-sec}}{\text{cu. ft.}}$	19,470	19,582	
Optimum Acid/Salt	1.40	1.54	

(a) Calculated: Algebraic addition to the experimental heat of combustion of the amine and heat of combustion of the nitric acid portion of the salt.
(b) Assumed exhaust products: CO_2, H_2O, N_2.
(c) The temperature at which salt crystals began to separate.
(d) Westphal balance values.
(e) Using ASTM-D445 method.
(f) Without acetamide. Value not available where acetamide present.
(g) Determined by adding 0.2 ml. of N,N,N',N'-tetramethylbutane-1,3-diamine to 0.5 ml. of propellant solution.

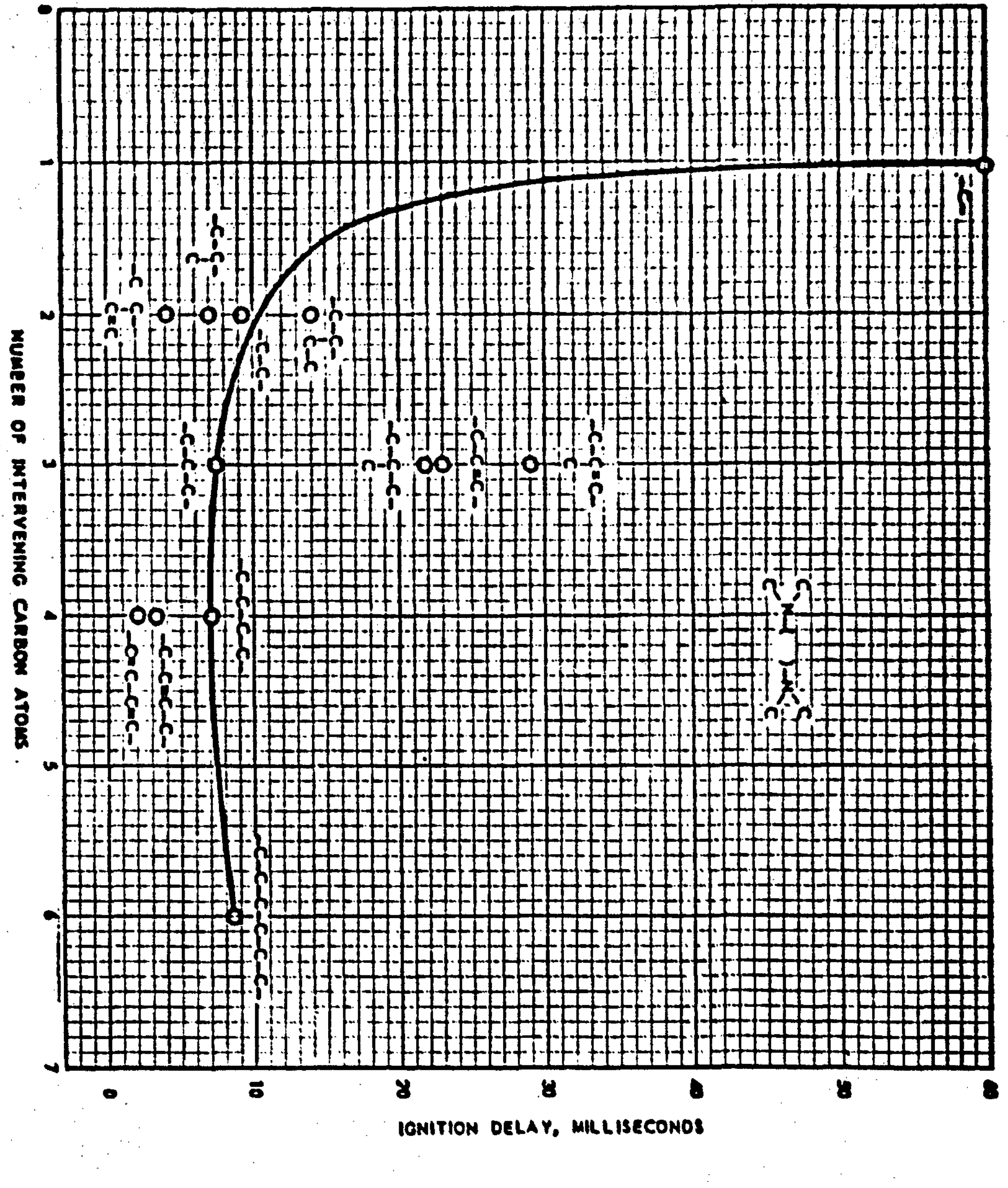

FIGURE 1
CORRELATION OF STRUCTURE
WITH IGNITION DELAY FOR DIAMINES WITH RFNA

THEORETICAL AND EXPERIMENTAL EVALUATION OF SEVERAL AMINE FUELS, WITH FUMING NITRIC ACID

J. S. Gordon
Wright Air Development Center
Wright-Patterson AFB, Ohio

The bipropellant test program of the Rocket Propellant Section, Fuel and Oil Branch, Power Plant Laboratory has been oriented toward hypergols with nitric acid, since 1954. Engines of 100, 200 and 220 pounds thrust have been used. Work at a larger thrust level, or where quantitative measurements of combustion instability are necessary, has been generally done elsewhere by contract. Data are reported here (RFNA oxidizer, pressure ratio $^{300}/_{14.7}$) on:

N,N - dimethylhydrazine (UDMH)
N,N,N',N' - tetramethyl ethane 1,2 - diamine ("ethane)
N,N,N',N' - tetramethyl propane 1,2 - diamine ("1,2 - propane")
N,N,N',N' - tetramethyl propane 1,3 - diamine ("1,3-propane")
N,N,N',N' - tetramethyl propene 1,3 - diamine ("propene")
N,N,N',N' - tetramethyl butene 1,3 - diamine ("butene")
N,N,N',N' - tetramethyl butane 1,3 - diamine ("butane")
diethylenetriamine (DETA)
N,N - dimethylamino 3-propylamine (DMAPA)
methylhydrazine (MMH)
N,N - dipropargyl hydrazine (UDPH)
triethylamine
DETA - UDMH 50-50 blend

In addition, a number of organic nitrogen compounds were given preliminary screening.

N,N - dimethylhydrazine. Because of its extremely short ignition delay, good theoretical performance and potentially unlimited availability, UDMH was of interest to this Laboratory as early as 1950. WADC performance data are summarized in Fig. 1. Peak Isp of 222 and 216 sec. were obtained in 200-lb uncooled and 100-lb cooled engines. Theoretical data of high mixture ratios are shown in Table I.

Tetramethyl diamines. These compounds have the advantage of low freezing point, very high boiling point, good experimental performance and high mixture ratio for peak performance. Properties of six ditertiary diamines are given in Table I. All six have been fired at 100 lb thrust, giving Isp of 216 to 221 sec. "Ethane" and "Butene" were also fired at 200 lb thrust (uncooled motor) and slightly lower performance obtained. "Propene" was also fired in a 220 lb motor with film and water cooling, and C* measured. Performance curves are given in Figures 2 - 7.

Diethylenetriamine. Some work was done with this byproduct fuel. Theoretical performance data are given in Fig. 14. Experimentally, 200 sec. Isp could not be attained (see Fig 8.). Its high freezing point, high viscosity and mediocre performance make it unattractive. A 50-50 mixture of DETA-DMH gave about the average performance of the neat fuels (Fig. 17).

Dimethylaminopropylamine. A comparison of this monotertiary diamine with the tetramethyl diamines is of interest. Theoretical Isp is about the same but, experimentally, 200 sec. Isp could not be attained. See Fig. 9.

Methylhydrazine. At present, interest in MMH is secondary to UDMH. For certain production processes, the cost may be minimized by accepting a mixture of MMH-UDMH as product. The eutectic mixture (60% UDMH, freezing point -112°F) was chosen for study at 100 lb thrust. Performance data are shown in Fig. 10. There is no performance penalty accruing from the addition of UDMH to MMH. The performance of MMH monopropellant was calculated (see Figs. 11, 15-16).

Propargylhydrazines. Theoretical shifting Isp and C* are given in Fig. 12 for dipropargyl hydrazine. Peak Isp is only 2 sec. higher than UDMH. In ignition-delay tests, smooth monopropellant ignition was obtained with UDMH (9 ms delay) by adding one drop of RFNA at ambient pressure. Some monopropellant application might be feasible although the decomposition products are very sooty (67 wt.% carbon). Only 50 grams were available. Monopropargyl hydrazine was also tested but gave unreliable and long ignition delays, confirming some conclusions reached at Aerojet on 5-membered-ring formation in this fuel, leading to decreased reactivity.

Miscellaneous. Dimethylaminoethanol, dimethylamino 2-methoxy propane, dimethylformamide, acetone cyanohydrin and ethylene cyanohydrin were evaluated and judged unsatisfactory. A blend of 25% ethylmercaptol of acetaldehyde - 75% ethylmercaptal of acetone was fired at 100 lb thrust but nozzle corrosion and hard coke deposits were severe.

Conclusions: Saturated ditertiary diamines deserve full consideration for applications requiring good specific performance, good density impulse, high thermal stability and wide liquid range, despite the commanding lead in rocket state of the art enjoyed by UDMH. To this end, a supply of "butane" is to be fired at 5000 lb thrust. Alkyl polyamines without fully methylated N atoms are less satisfactory fuel candidates.

Work in progress. A study is underway at Aerojet, under WADC sponsorship, to advance the state of the art in UDMH with RFNA and oxygen. Some work is underway at WADC with UDMH at chamber pressure as low as 75 psia in support of high-altitude rocket research. A study of amine nitrate and perchlorate salts is being conducted by Phillips Petroleum Company under WADC sponsorship. Work is scheduled at WADC with perchloryl fluoride and several amine fuels, at 100 lb thrust. An oxygen-hydrogen start will be utilized.

TABLE I

Theoretical Performance of UDMH, RFNA (14% NO_2, 2.5% H_2O)
at Shifting Equilibrium
P_c = 300 psia

M.R.	Isp	C*	C_F	T_c °K	T_e °K
20	106.1	2463	1.386	835	395
18	113.5	2631	1.388	949	459
16	122.2	2827	1.390	1085	536
14	132.1	3053	1.392	1250	632
12	143.7	3314	1.395	1454	756
10	157.7	3629	1.398	1715	919
7.5	180.2	4127	1.405	2147	1217
3.75	232.4	5208	1.436	2978	2149
2.5	239.8	5457	1.414	2963	1814

Gordon

TABLE II
Physical-Chemical and Rocket Data for Ditertiary Diamines

Nicknames	TMED "ethane"	1,2-TMPD "propane"	1,3-TMPD "propane"	1,3-TMPD= "propene"	1,3-TMBD "butane"	1,3-TMBD= "butene"
R group is	$-CH_2CH_2-$	$-CH_2\underset{\overset{\vert}{CH_3}}{CH}-$	$-CH_2CH-CH_2-$	$-CH_2CH=CH_2-$	$-CH_2CH_2\underset{\overset{\vert}{CH_3}}{CH}-$	$-CH=CH\underset{\overset{\vert}{CH_3}}{CH}-$
Freezing point, °F	-69.5	-175	-115.6	glass at -130	-132	-126
Boiling point, °F	252	285	294	324	320	350
Viscosity, centistokes						
at 75°F	0.74	0.94	0.97	1.30	1.25	1.34
-40	2.02	3.42	3.35	6.96	5.68	7.35
-65	3.00	5.78	5.54	15.06	11.24	16.86
Gross Heat of combustion, Btu/lb	16,928	17,088	17,020	16,263(?)	17,548	17,219
Heat of formation, liquid Kcal/mole	-18.4	-37	-42	0	-29.9	-7.1
Ignition delay, milliseconds with RFNA						
at 75°F	7	7	8	21	7	6
-40	16	17	14	21	6	7
-65	23	23	17	22	10	8
Density at 75°F, gm/cc	0.775	0.795	0.782	0.822	0.795	0.813
Peak Isp (theoretical frozen equilibrium with WFNA, 300 -- 14.7 psia)	226.3	224.7	224.3	221.7	225.2	225.3
at w_o/w_f =	3.48	3.38	3.33	3.40	3.45	3.30
Peak experimental Isp	221	219	212	218	219	219
Best synthesis yield	78%	45%	60%	73%	70%	85%
Worst features	deposits in cooled nozzles		CO2 pickup forms gum	slowly polymerizes in air or light		decomposes slowly in presence of air or light, thermally sensitive.

FIG. I

UDMH - RFNA

200# THRUST
110" L*
UNCOOLED

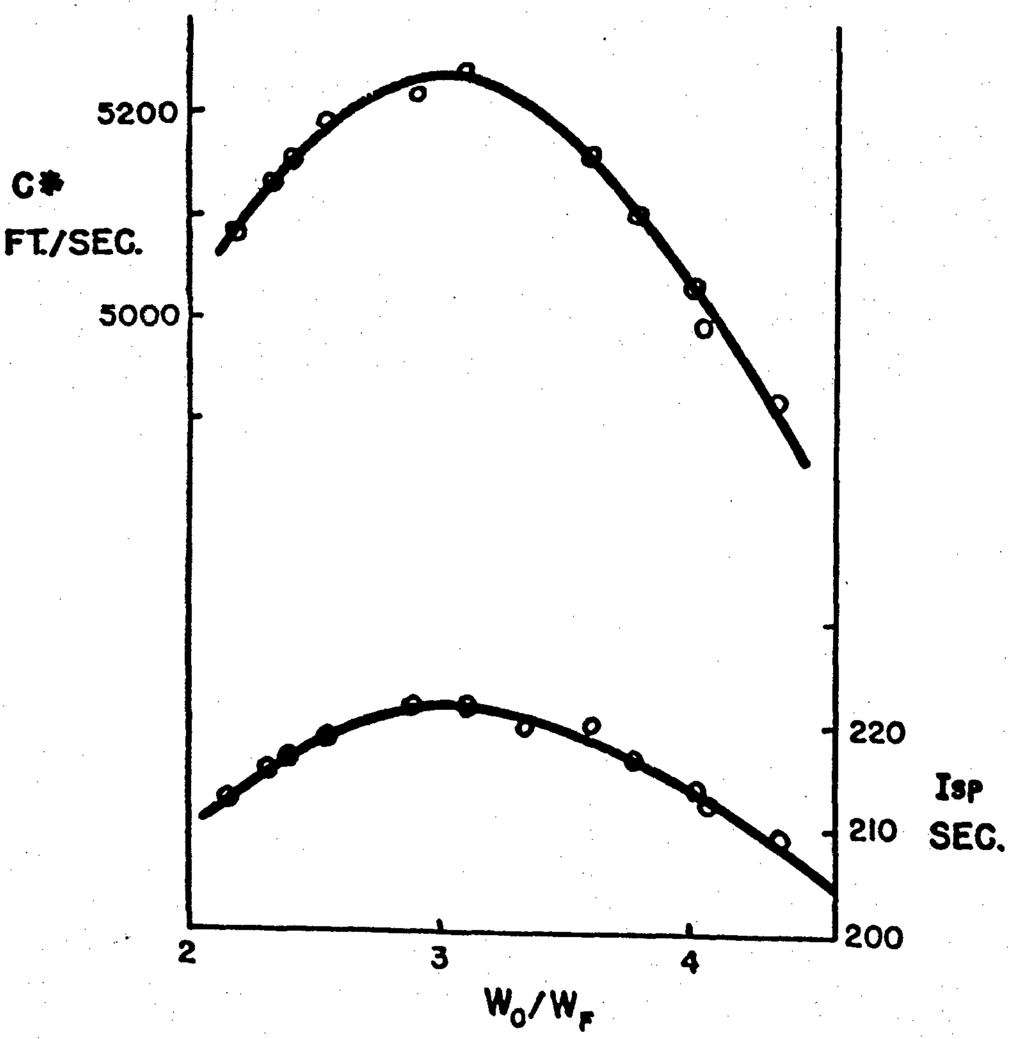

FIG. 2

"ETHANE"-RFNA

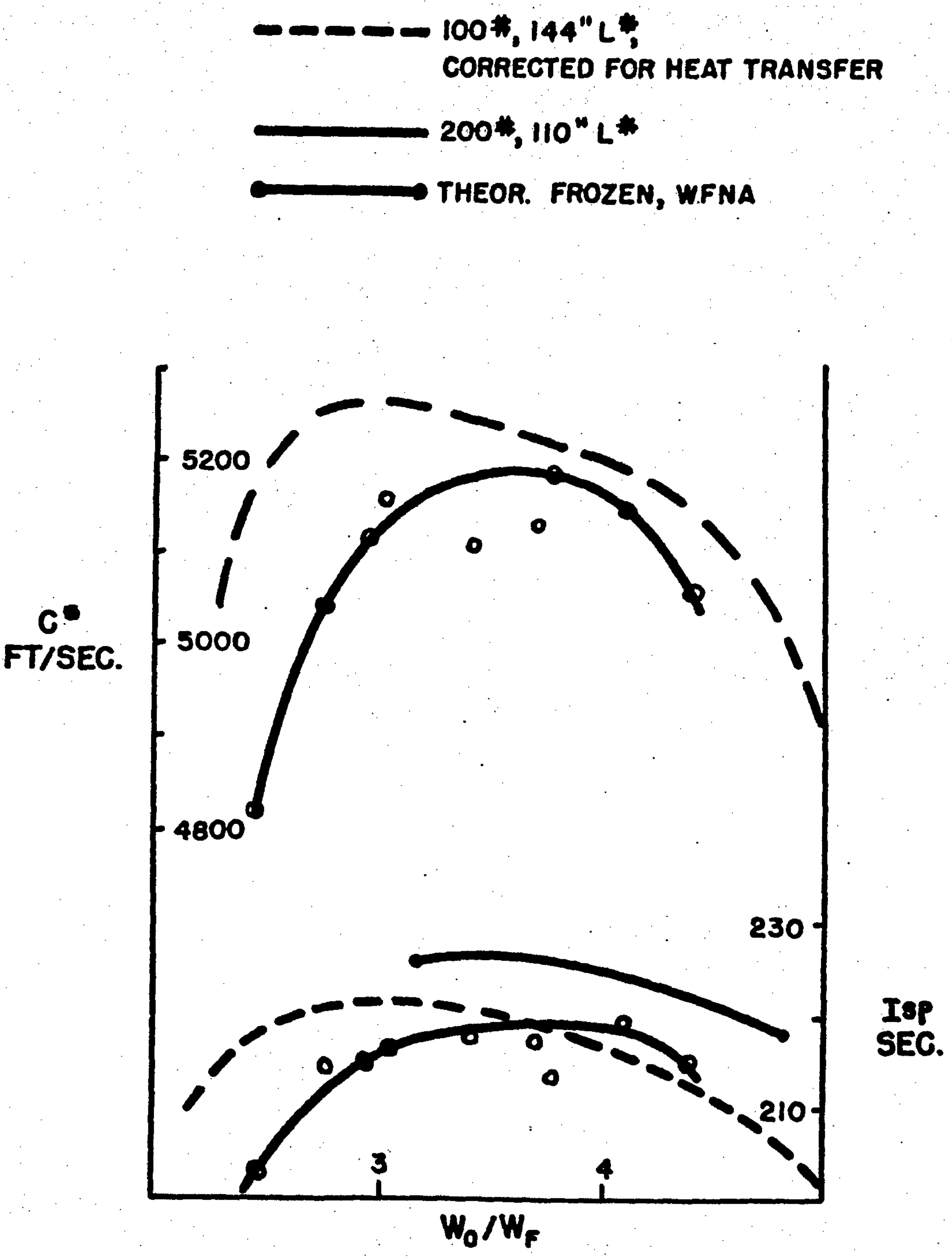

FIG. 3

"1,2-PROPANE" - RFNA

100# THRUST

144" L*

CORRECTED FOR HEAT TRANSFER

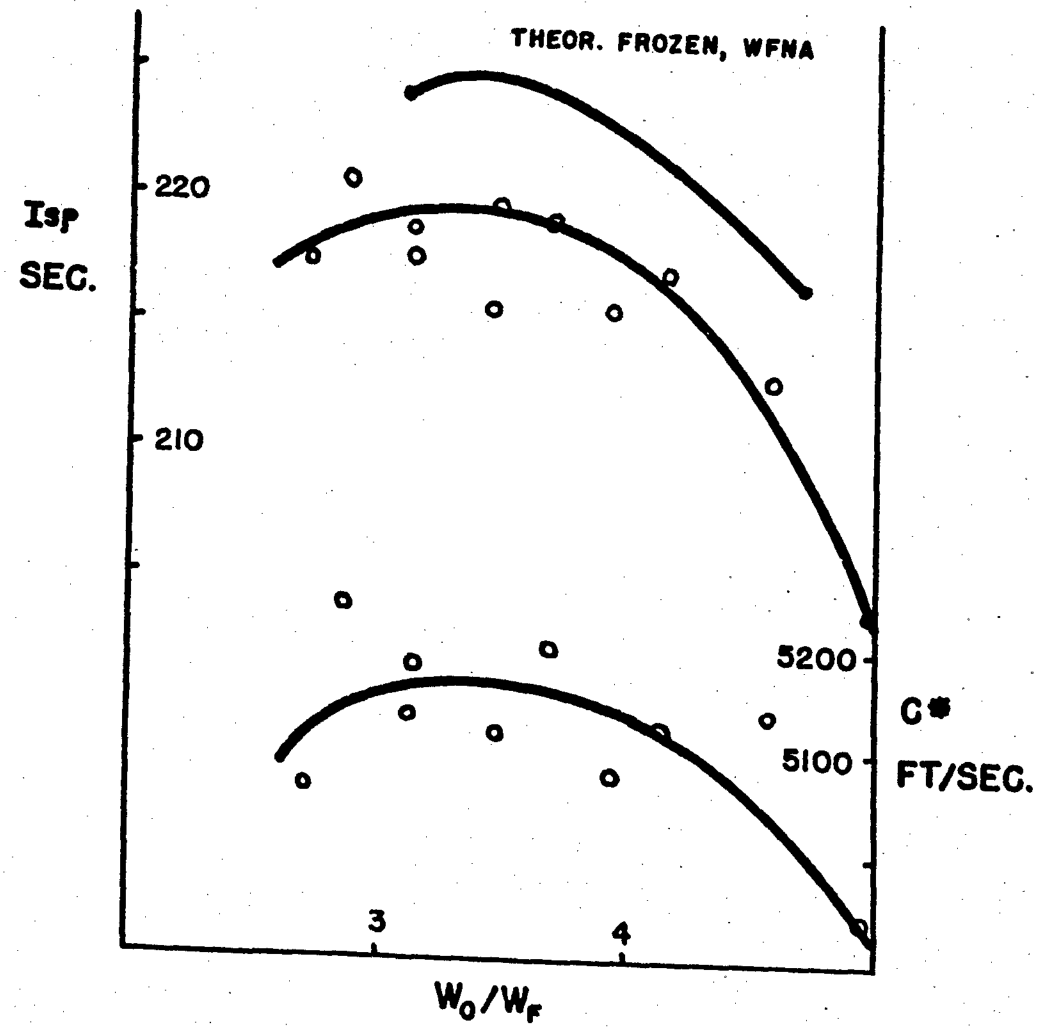

Fig. 4

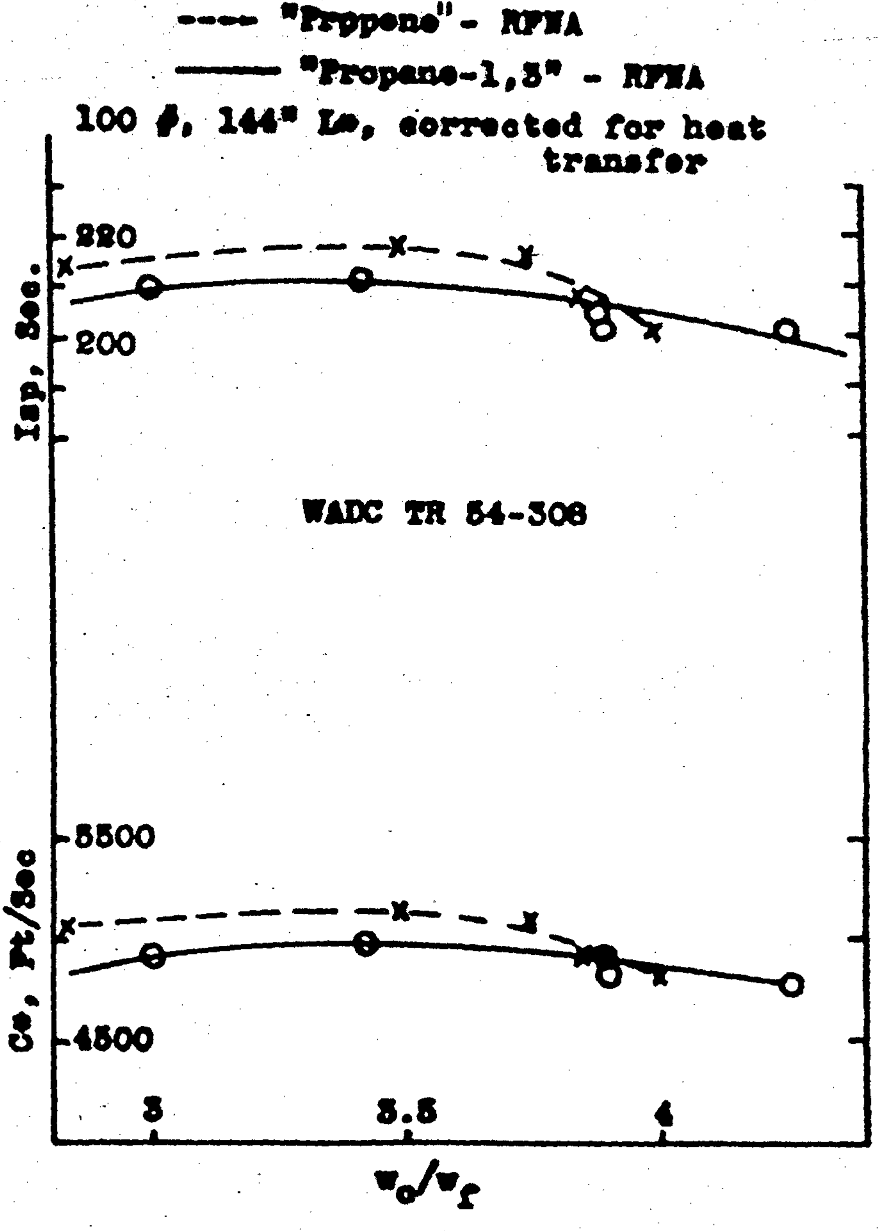
---- "Propene" - RFNA
—— "Propane-1,3" - RFNA
100 #, 144" L*, corrected for heat transfer
220
200
Isp, Sec.
5500
4500
C*, Ft/Sec
3
3.5
4
w_o/w_f

FIG. 5

"PROPENE" - RFNA

220* THRUST
54" L*
FILM AND WATER COOLED

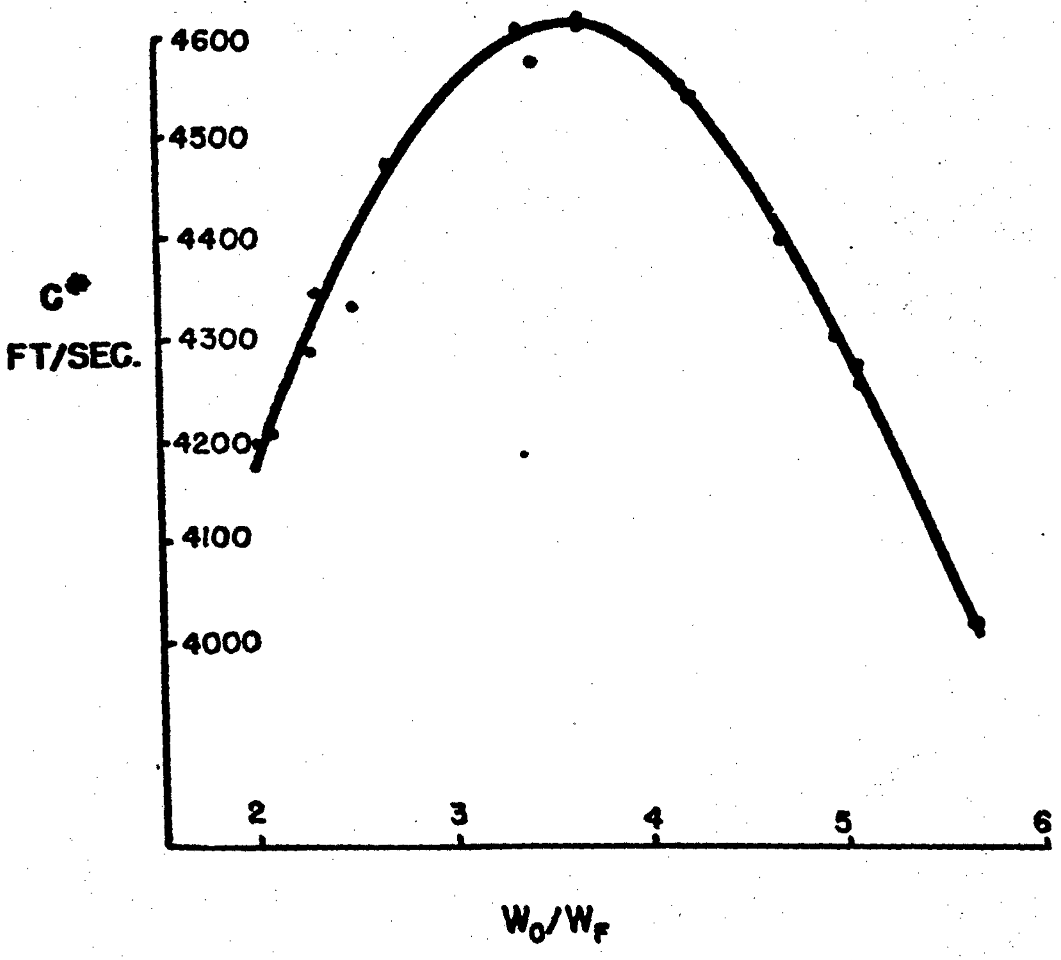

FIG. 6

"BUTENE" - RFNA

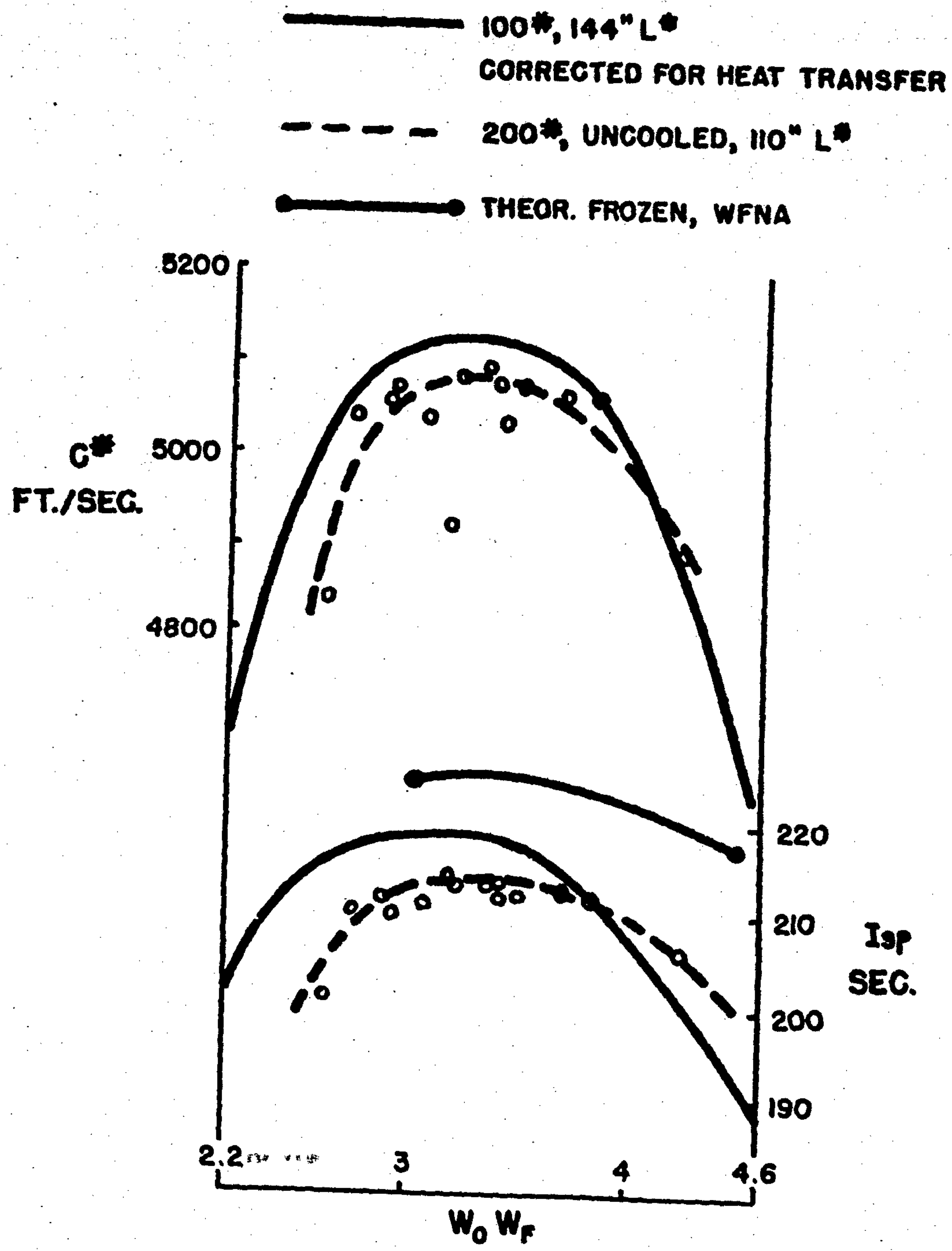

FIG. 7

"BUTANE" - RFNA

100* THRUST

144" L*

CORRECTED FOR HEAT TRANSFER

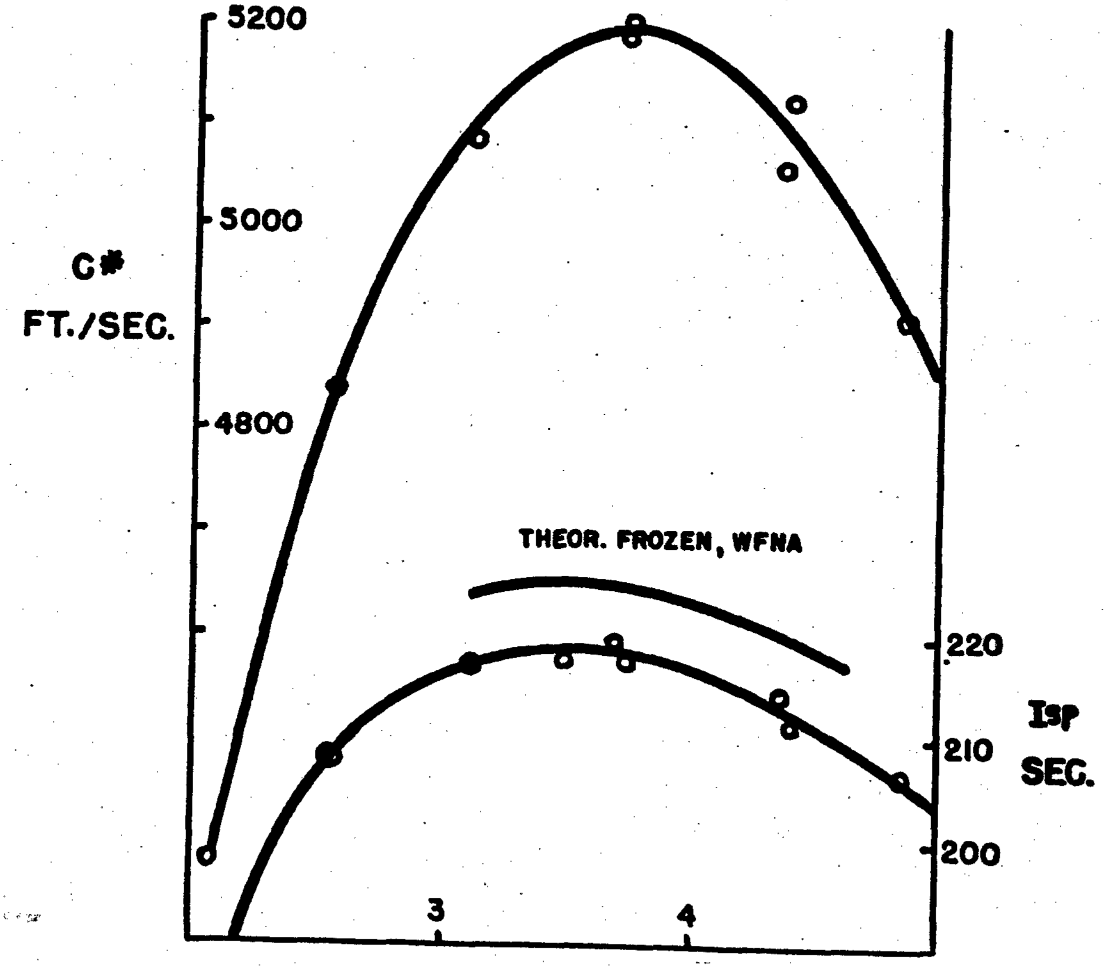

FIG. 8

DIETHYLENETRIAMINE - RFNA

200 # thrust

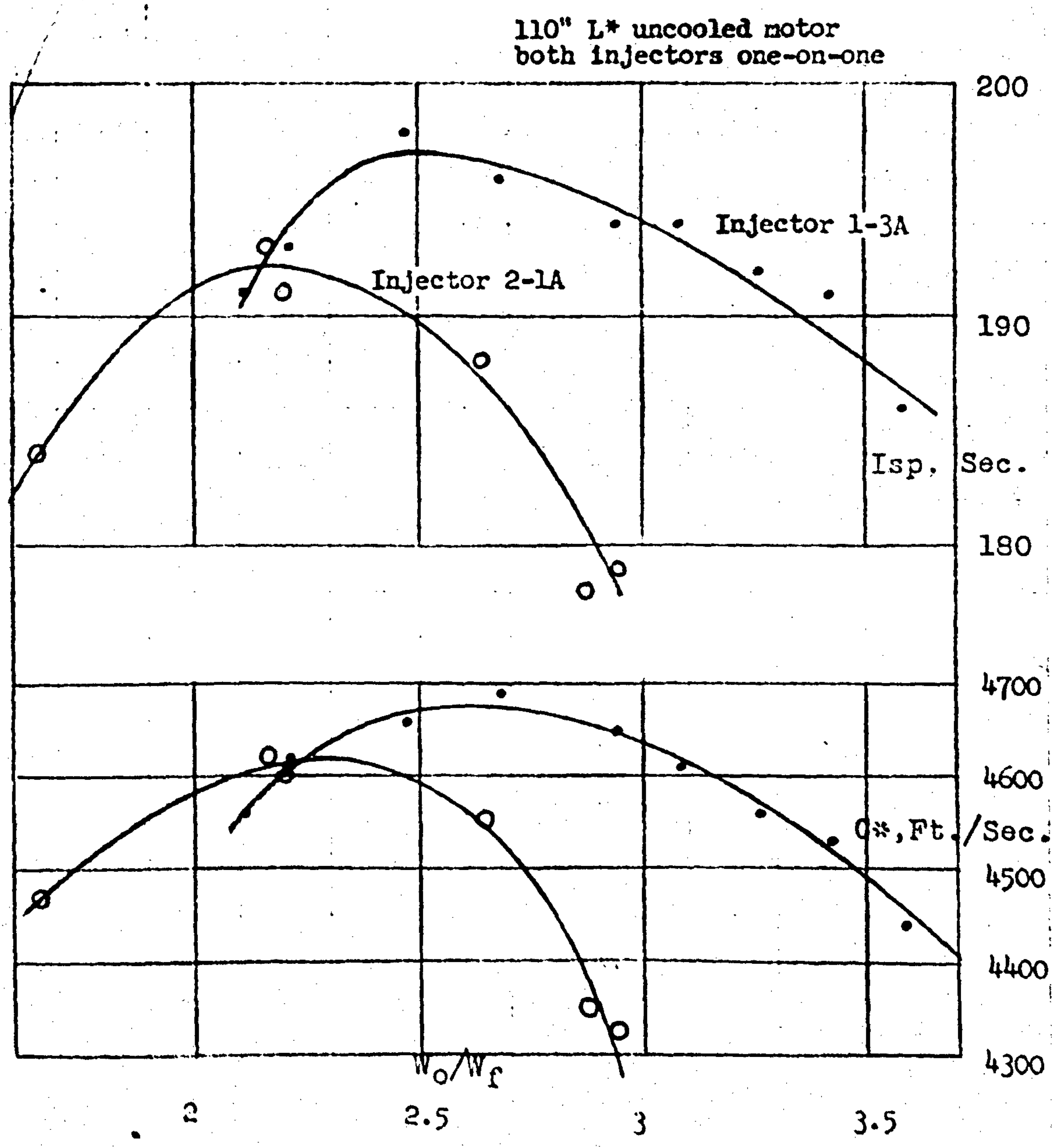

FIG. 9

DIMETHYLAMINOPROPYLAMINE - RFNA

$Q_F = -14.5$

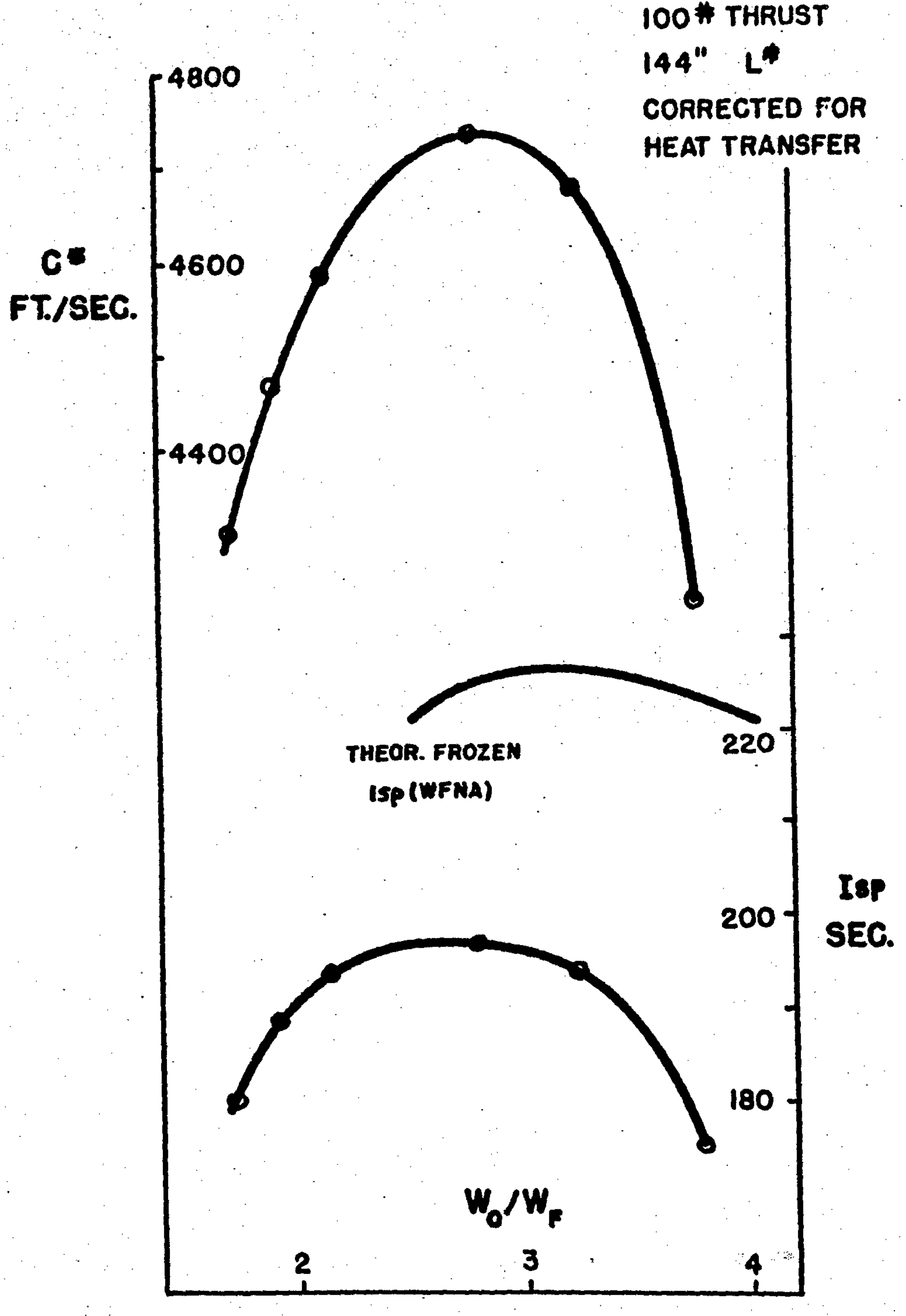

Fig. 10

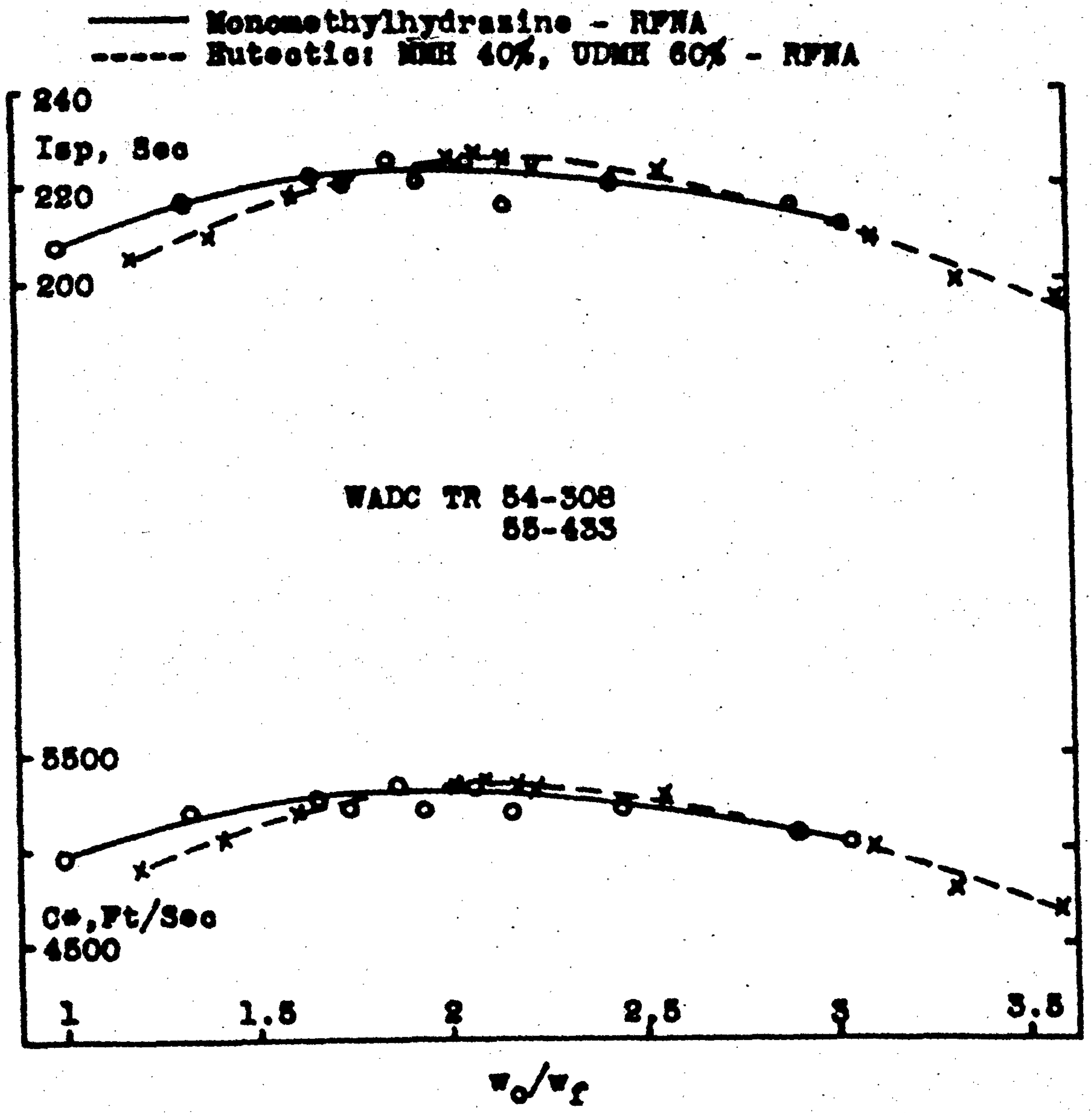
—— Monomethylhydrazine - RFNA
----- Eutectic: MMH 40%, UDMH 60% - RFNA
240
Isp, Sec
220
200
WADC TR 54-308
55-433
5500
C*, Ft/Sec
4500
1
1.5
2
2.5
3
3.5
w_o/w_f

FIG. 11

Theoretical Performance of Methylhydrazine Monopropellant (No Methane Cracked)

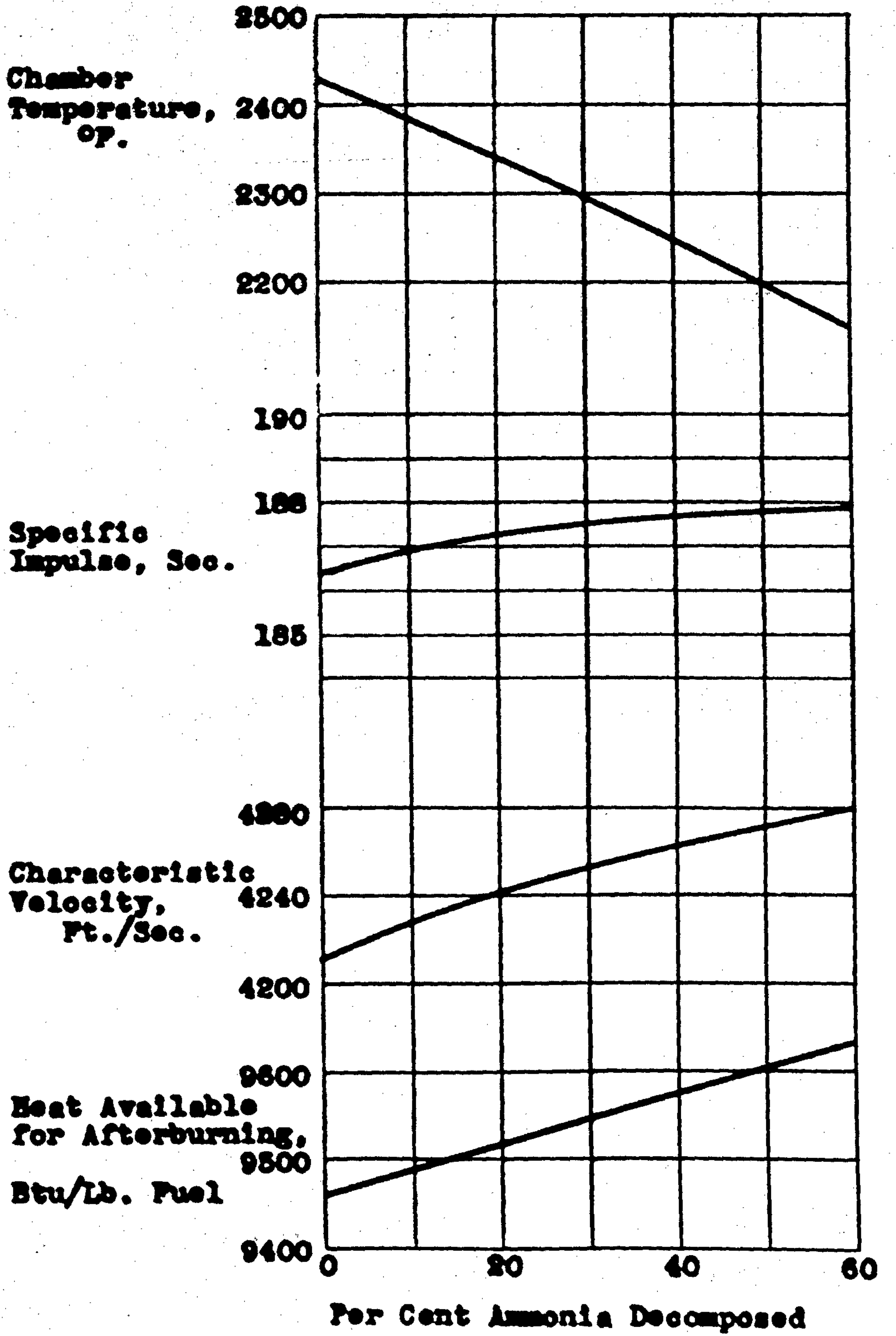

FIG. 12

N,N-DIPROPARGYL HYDRAZINE - RFNA

THEORETICAL SHIFTING PERFORMANCE

$Q_F = +120$

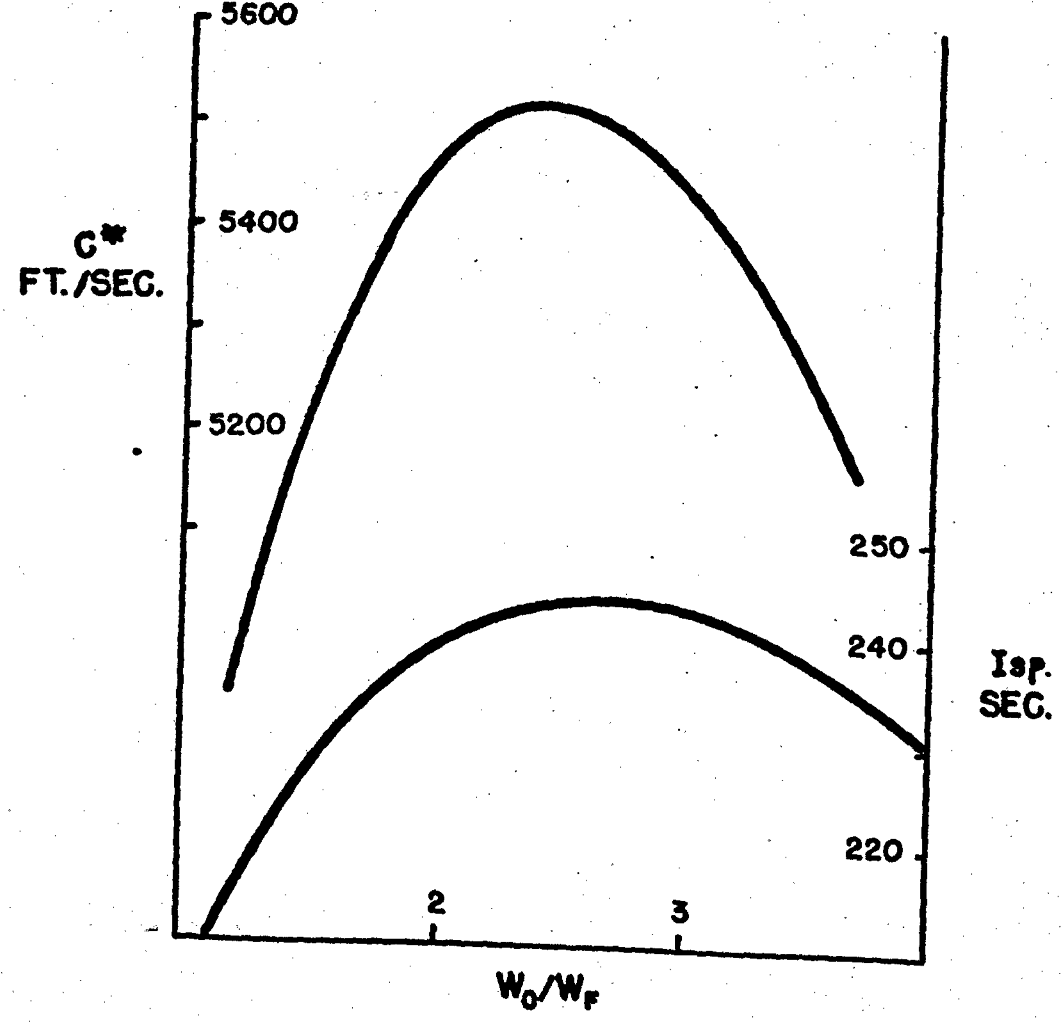

FIG. 13

TRIETHYLAMINE - RFNA

100*, 144" L*
CORRECTED FOR HEAT TRANSFER

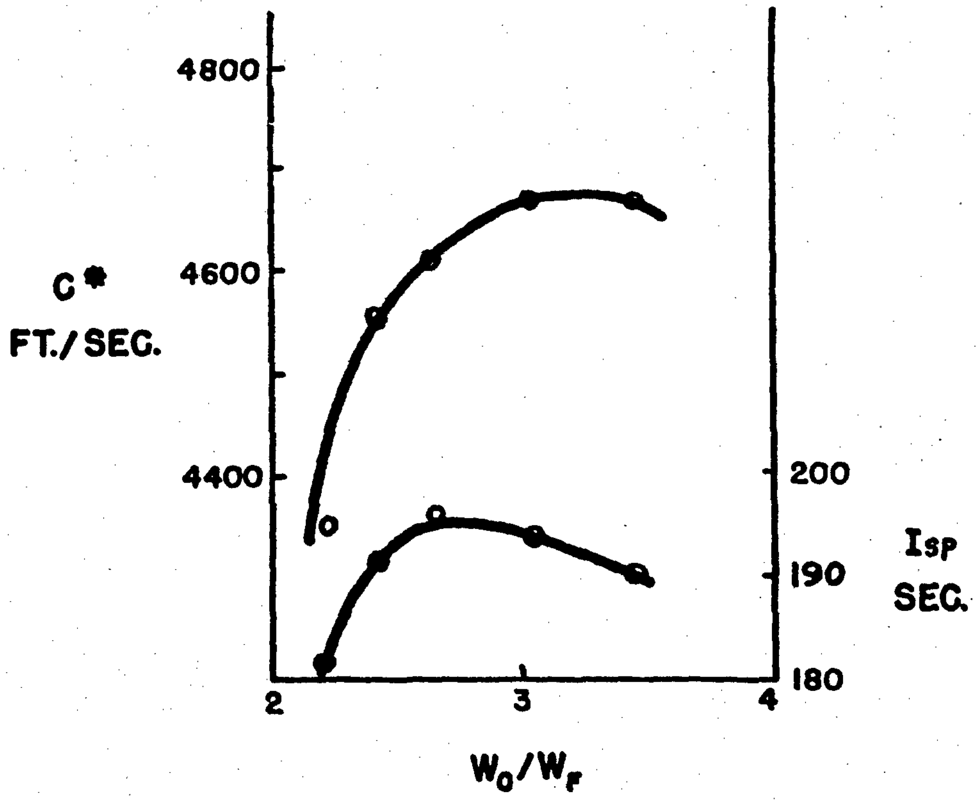

Fig. 14. DETA-RFNA

Theoretical Frozen Performance
ERA - 1103 Digital Computer

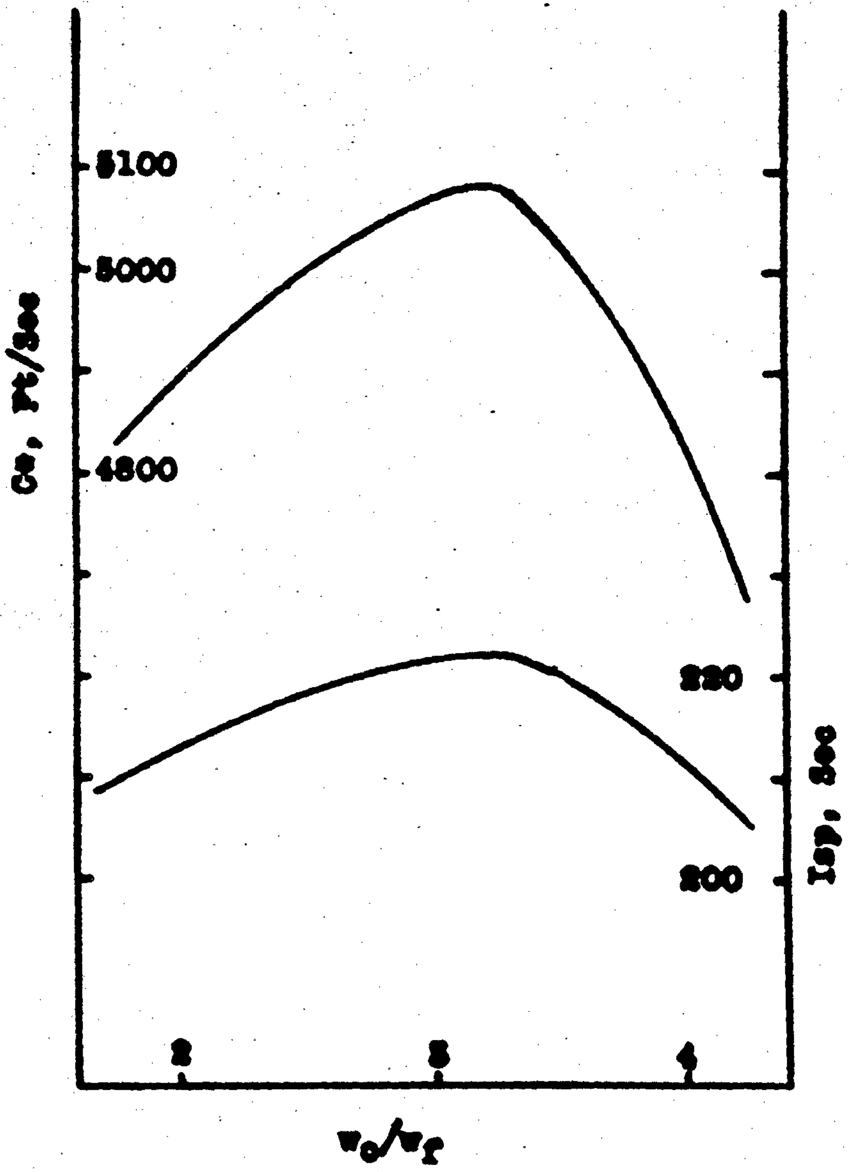

FIG. 15 Decomposition Temperature of Methylhydrazine as a Function of Ammonia and Methane Decomposition

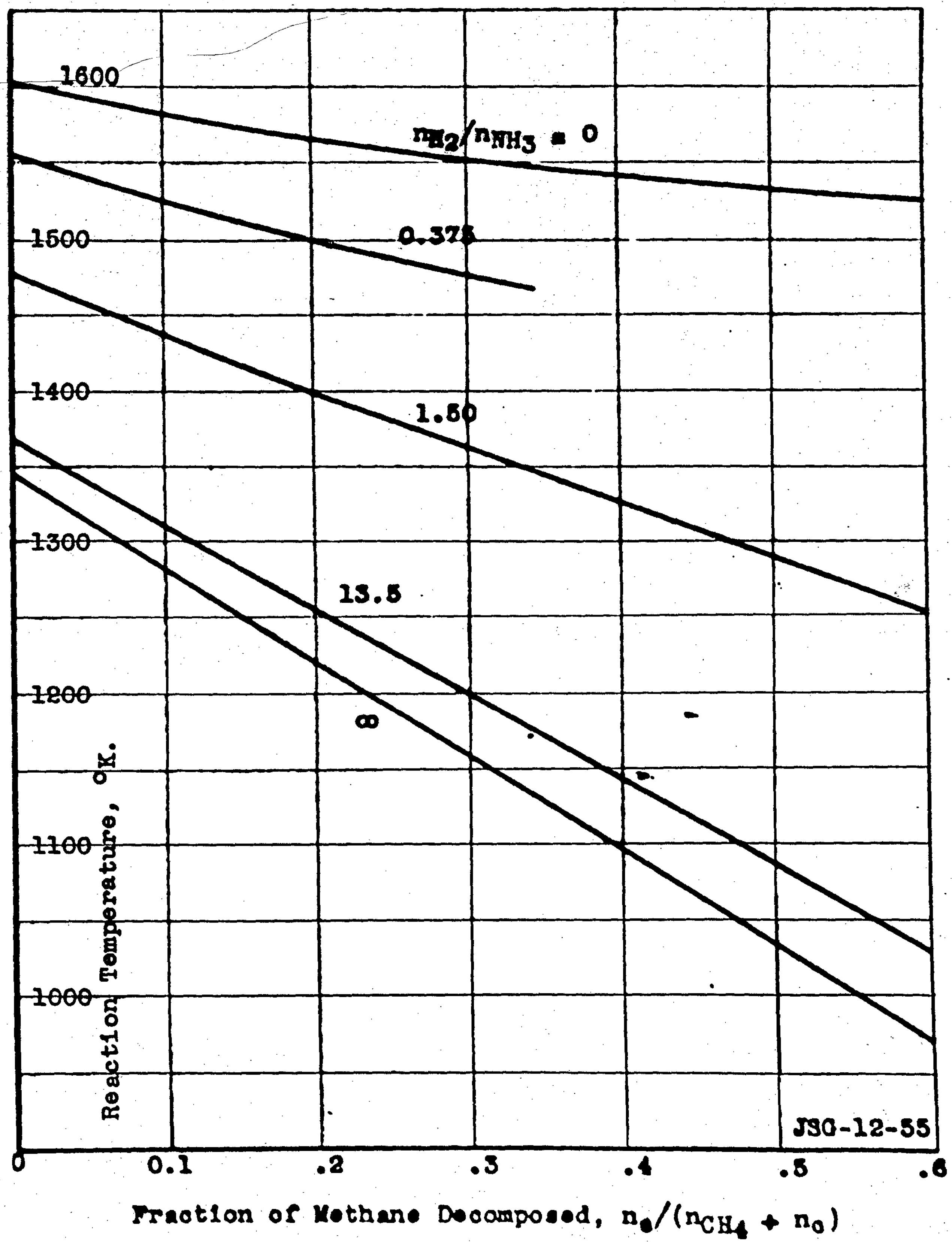

FIG. 16 Specific Impulse of Methylhydrazine as a Function of Ammonia and Methane Dissociation (P_c/P_{ex} = 300/14.696)

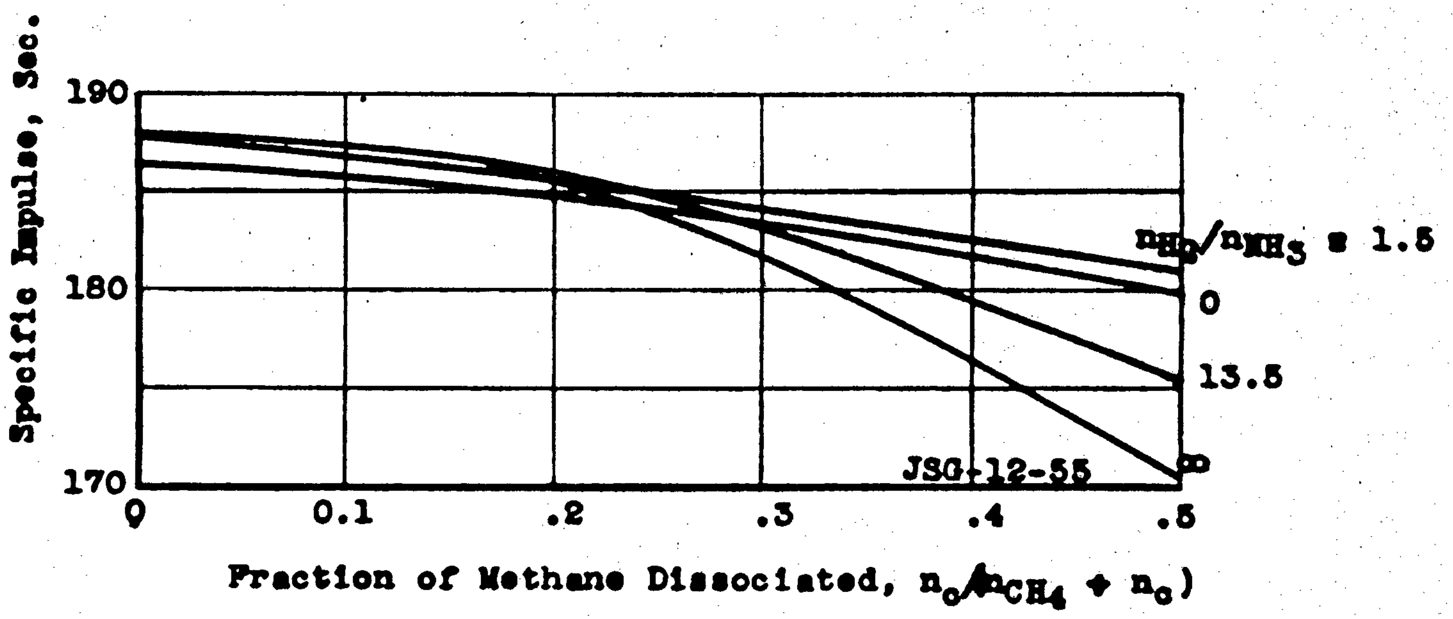

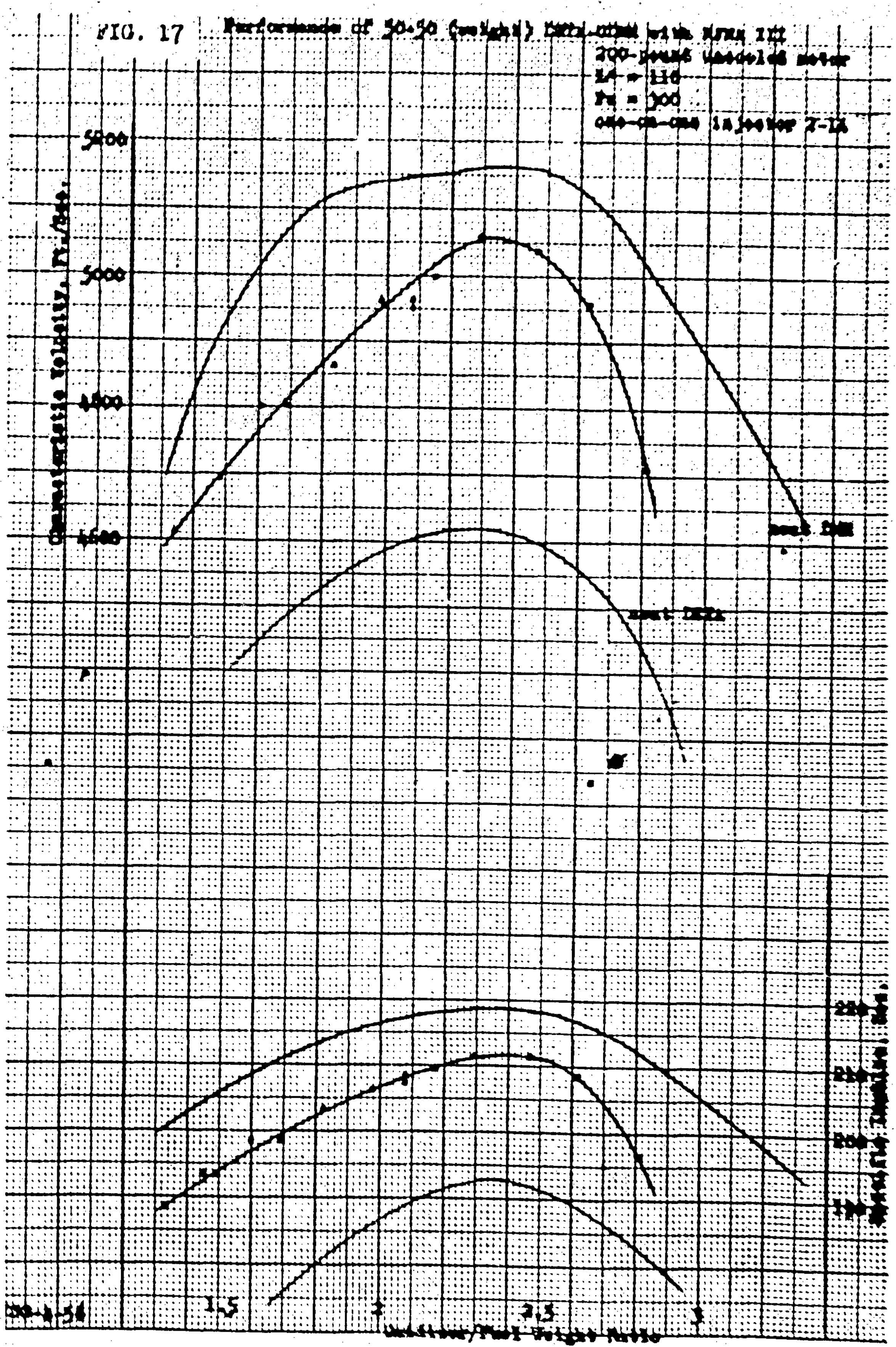

FIG. 17 Performance of 50-50 (weight) [illegible] with RFNA III

DESENSITIZATION OF LIQUID MONOPROPELLANTS TO ADIABATIC AIR COMPRESSION IMPACT BY THE ADDITION OF ETHYLENE OXIDE

C.W. Tait and W.A. Cuddy
Wyandotte Chemicals Corporation
Wyandotte, Michigan

INTRODUCTION

In the first paper of this series (Ref.1), which is to be published in the proceedings of the present symposium, but is not to be presented orally, an apparatus is described for measuring the sensitivity of liquid monopropellants to adiabatic air compression. The tester is a modification of the well-known Bureau of Mines Drop Weight Tester for solid propellants and explosives. The modifications center around three things: an O-ring to contain the liquid and to provide pressure sealing, a rupture disc covering an orifice in the bottom of the liquid holder, and an air cavity in the piston which is plunged into the liquid sample by the drop weight. Details of the apparatus are shown in Figs. 1-3 of Ref. 1.

Using the standardized specifications for the tester which are listed in Ref. 1, data of reasonably good reproducibility were obtained for the drop heights necessary to cause several monopropellants to be consumed because of the application of the impulse by the drop weight. With the particular thickness of the disc used in these tests consumption of the liquid did not lead to rupture of the disc. A bulge was blown in the disc, however. Additional criteria for a positive result in the drop tests were the disappearance of the liquid, the formation of carbon and the mangling of the O-ring. In a negative result on the tester the liquid sample and the O-ring remained intact and undamaged. Also, no carbon was formed. Additional discussion will be presented below of the pressure rise developed in the air cavity during the compression of the air bubble by the falling weight.

Using the above criteria for a positive result in the drop weight test, an evaluation of the sensitivity of several monopropellants in terms of the 50% point for a positive test was obtained. Typical data are given in Table 5 of Ref 1.This preliminary, relative listing of monopropellants appears to be compatible with our practical experience in handling the materials.

In earlier work with the tester, as listed in Table 3 of Ref. 1, we had found that the addition of 10% by weight of ethylene oxide to n-propyl nitrate or to 2-methoxyethyl nitrate increased the 50% point for positive results from a value of 8 or 9 inches to a value of about 50 inches. (A value of 50 inches was the limit of the tester range). Naturally, we were curious about why small additions of ethylene oxide had such a pronounced effect on reducing the sensitivity of these monopropellants as measured in our drop-weight tester. It is the purpose of this paper to present some thoughts and some experimental work associated with the elucidation of this phenomenon.

CALCULATION OF THE PRESSURE DEVELOPED DURING COMPRESSION OF THE AIR BUBBLE

In the use of our drop-weight tester it has been assumed that adiabatic compression of the air bubble present in the cavity of the piston generates a hot spot which leads to ignition and to combustion of the liquid monopropellant contained in the cavity of the O-ring. It appeared desirable, therefore, to calculate the order of magnitude of pressure and temperature that would result in the air bubble at the instant that the velocity of the falling weight was reduced to zero. Such a calculation would indicate if a high enough temperature would be obtained to cause ignition. In the calculation as carried out the assumption was made that all of the kinetic energy that the falling weight possessed when it hit the piston was utilized in compressing the bubble.

The energy available from the falling weight would be equal to the work done in lifting the weight up to the drop height. At a drop height of 3 inches for a 5 pound weight, for example, the energy available would be 1.25 foot-pounds or 0.404 calories.

To derive an expression for calculating the changes that occur during adiabatic compression of the bubble, use is made of the first law of thermodynamics, according to which

$$dU = dq - dw = dq - pdv \qquad (1)$$

where the quantities have their well-known meanings. Since it is also true that

$$dU = C_v dT + \left(\frac{\partial U}{\partial v}\right)_T dv \qquad (2)$$

It is apparent that by combining equations 1 and 2, equation 3 results.

$$dq = C_v dT + \left(\frac{\partial U}{\partial v}\right)_T dv + pdv \qquad (3)$$

If it is assumed that the gas in the air bubble behaves as a perfect gas, then

$$\left(\frac{\partial U}{\partial v}\right)_T = 0 \qquad (4)$$

$$pv = nRT \ , \qquad (5)$$

and

$$dq = CvdT + pdv. \qquad (6)$$

For an adiabatic process, dq = o and equation 6 reduces to

$$CvdT = - pdv \qquad (7)$$

By substituting for the value of p from equation 5 into equation 7 there is obtained the expression

$$\frac{dT}{T} = \frac{-R}{Cv} \frac{dv}{v} \qquad (8)$$

Integration of equation 8 gives the result that

$$T = Kv^{-R/Cv} \qquad (9)$$

In order to put this relationship in a more recognizable form use is made of the relationship

$$Cp - Cv = p\left(\frac{\partial v}{\partial T}\right)_p \qquad (10)$$

which can be obtained by operating on the internal energy and heat content functions.

Since this calculation is to be made for a perfect gas, equation 10 can be simplified by substituting the value of $\left(\frac{\partial v}{\partial T}\right)_p$ which is obtained from equation 5. This substitution leads to the relationship that

$$Cp - Cv = R \qquad (11)$$

Substitution of the value of R from equation 11 into equation 9 results in the relationship

$$T = Kv^{-\frac{Cp - Cv}{Cv}} = Kv^{-\gamma + 1} \qquad (12)$$

which is in the form that is normally used.

In order to find the volume that the air bubble would be compressed to if the drop weight energy were all used in adiabatic compression, an integration was performed according to equation 13.

$$-\text{ Drop Weight energy} = \int_{v_0}^{v} p\,dv \qquad (13)$$

Substitution for p from equation 5 and for T from equation 12 leads to the expression

$$-\text{ Drop weight energy} = nRK \int_{v_0}^{v} v^{-\gamma}\,dv. \qquad (14)$$

Integration yields

$$-\text{ Drop weight energy} = \frac{nRK}{1-\gamma}\left[v^{1-\gamma} - v_0^{1-\gamma}\right] \qquad (15)$$

In the case at hand for a 3 inch drop of a 5 pound weight (0.404 calories of energy) onto a piston containing an air cavity of 0.0869 cc. at 300°K. with a γ for air of 1.40, a final volume of 1.66×10^{-6} cc. would be obtained. Substitution of this volume into equation 12 yields a value of 23,200°K. for the temperature that would result in the bubble if the bubble were compressed from atmospheric pressure. The final pressure in the compression would be several million atmospheres.

The value of temperature calculated above is so high that it seems desirable to check it in some fashion. Another way of estimating the temperature is to compute through the value of the heat capacity at constant volume the rise in temperature that would occur if 0.404 calories were used to heat up the known amount of air. Using the approximate value of 5 calories/mole/degree for the heat capacity of air and 3.53×10^{-6} moles of gas, which the cavity contains, the temperature rise would be 23,000°C. This rough calculation gives a value of temperature which is in good agreement with that obtained in the adiabatic compression calculation.

On the basis of the rough calculations presented above it appeared very unlikely that all of the energy of the drop weight would be used in compressing the air bubble. For one thing, the O-ring underneath the piston has to be deformed in order to force the liquid up into the air cavity to provide the compression of the air bubble. Some of the deformation would be elastic and would convert part of the kinetic energy of the drop weight into potential energy which would cause the weight to rebound. Additional energy would be lost through friction, through the sound waves that result from the impact and scatter in all directions, and through thermal conduction from the compressed bubble. Because of the uncertainty of how much energy would go into compression of the bubble it appeared desirable to attempt to record experimentally the pressure that was developed within the cavity of the piston.

MEASUREMENT OF THE PRESSURE DEVELOPED DURING COMPRESSION OF THE AIR BUBBLE

In designing apparatus for measuring the pressures developed in the cavity of the drop weight tester, emphasis was placed on reproducing accurately the internal configuration and volume relationships in the bomb assembly. The test bomb designed for these studies had the identical internal dimensions after assembly as the test bomb discussed in Ref. 1, which was used to obtain the drop height 50% points for the several monopropellants. In this modified assembly, however, the rupture diaphragm rested directly on a Control Engineering strain gage pressure transducer. The output of this transducer was transmitted through a Control Engineering strain gage amplifier to a DuMont single-beam oscilloscope equipped with a Polaroid Land Camera. The pressure transducer was calibrated, after partially assembling the test bomb, by applying nitrogen pressure to the drop weight piston.

The most rugged pressure transducer that we had on hand for these tests had a maximum pressure rating of 10,000 psia. Because of the uncertainty of the pressure to be recorded, we replaced the liquid monopropellant with an equal volume of water and started the drop tests at low drop heights. In Fig. 1 is shown a recording of the output voltage of the strain gage pressure transducer as a function of time. This particular test was for a drop height of 3 inches. The broad line at the top of the grid in the figure is the repeated trace of the sweep beam which had a sweep time of 5.0×10^{-4} seconds per inch. Single sweep instrumentation which would have given better records, was not used in these experiments. In Fig. 1 the pressure reaches a peak value of 6,240 psia. in 7.5×10^{-4} seconds. The oscillations that appear on the initial portion of the pressure pulse may be associated with the sound waves that reflect through the piston because of the elastic impacts of the several components of the tester. The duration of the small pulses appear to be compatible with the time required for a sound wave to pass through the piston and for the tension wave to return. A slower time base recording was made of the drop, and the record is shown in Fig. 2. It can be seen that a second pulse appears on the record after the initial pulse. The second pulse is attributed to a bounce of the drop weight and represents a pressure of about 1/8 of the original pressure.

It is believed that the frequency response of the instrumentation used in the present experiments is adequate to give an accurate representation of the pressure developed in the air cavity. This opinion is based on the steep slopes associated with some of the oscillations superimposed on the main pressure pulse and on additional experiments wherein the weight was dropped directly on the

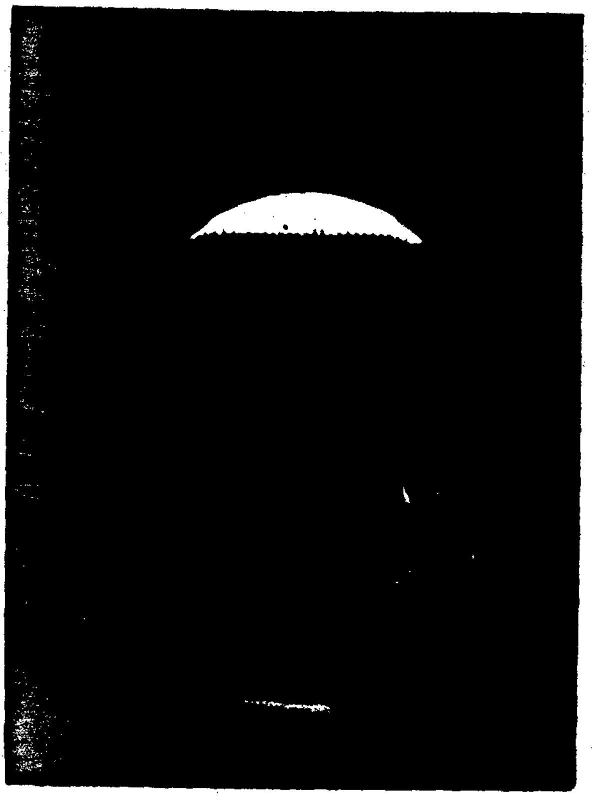

0.06 cc. Water
0.089 cc. Air
Peak Pressure - 6240 PSIA
Time to Peak Pressure - 750 Micro-Seconds

FIG. 1 Drop Weight Test Pressure/Time Record

Tait

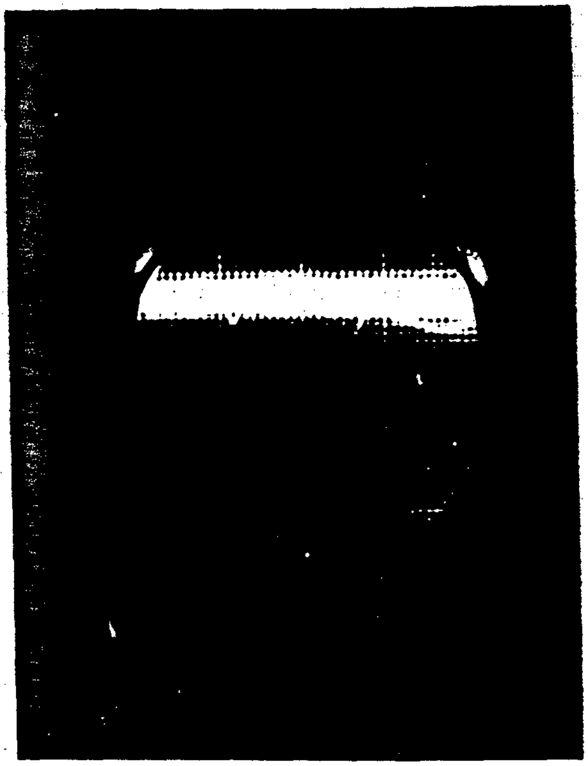

0.06 cc. Water
0.089 cc. Air
Peak Pressure - 6200 PSIA
Bounce Pressure - 800 PSIA

FIG 2. Drop Weight Test Pressure/Time Record

pressure transducer without the presence of an O-ring.

In Fig. 3 is shown a plot of the peak pressure obtained for various drop heights without correction for the bounce of the drop weight. Over the range of heights covered the peak pressure appears to be about a linear function of drop height. If the pressure were a consequence of an elastic impact, the pressure should be a function of the square root of the drop height. Therefore, the pressure does not appear to be a consequence of a completely elastic impact. Also, the fact that the rebound of the drop weight is only a fraction of the drop height is further evidence that elastic impact is not the dominant factor in this test. However, it must be admitted that the impact is partially elastic.

Before the measured peak pressures can be used to calculate the temperature rise in the air bubble it is necessary to know the original pressure in the cavity. As the drop test is performed, a pre-compression of the O-ring is effected in order to insure that there is sealing during the impact to retain the pressure. For the particular bomb assembly used in the tests, the precompression from a 0.012 inch displacement of the piston was employed. This displacement of the piston results in a reduction of volume such that the pressure in the cavity increases from 1.0 atmosphere to 1.29 atmospheres. Because of the slight variation in volume of O-rings used in the tests, the precompression will vary slightly from test to test, but it will be considered to be constant in subsequent calculations.

In order to calculate the temperature associated with the experimentally measured pressures, equations 4 and 12 can be combined to yield the well-known relationship

$$\frac{T_2}{T_1} = \left(\frac{P_2}{P_1}\right)^{\frac{\gamma - 1}{\gamma}} . \qquad (16)$$

In the case of a 6 inch drop that produced 688 atmospheres pressure starting with an initial pressure of 1.29 atmospheres at 293°K., a temperature of 1762°K. would be developed during the compression.

For temperature and pressures of this magnitude it is desirable to question the use of the perfect gas law throughout the calculations. A better approximation to reality might be obtained by using the Van der Waal equation of state. In reviewing equations 1 - 12 by which the temperature - volume relationship for the adiabatic compression was derived, it becomes apparent that a rigorous derivation for a real gas cannot be obtained. The reason for this is that the expression $(\partial U/\partial v)_T$ cannot be evaluated analytically for the real gas. Another difficulty lies in the term $(\partial v/\partial T)_p$, which can be evaluated for the real gas, but which does not give a simple form for the difference in Cp and Cv that is obtained for the perfect gas. Therefore, the exponents for equations 12 and 16 are no longer simple.

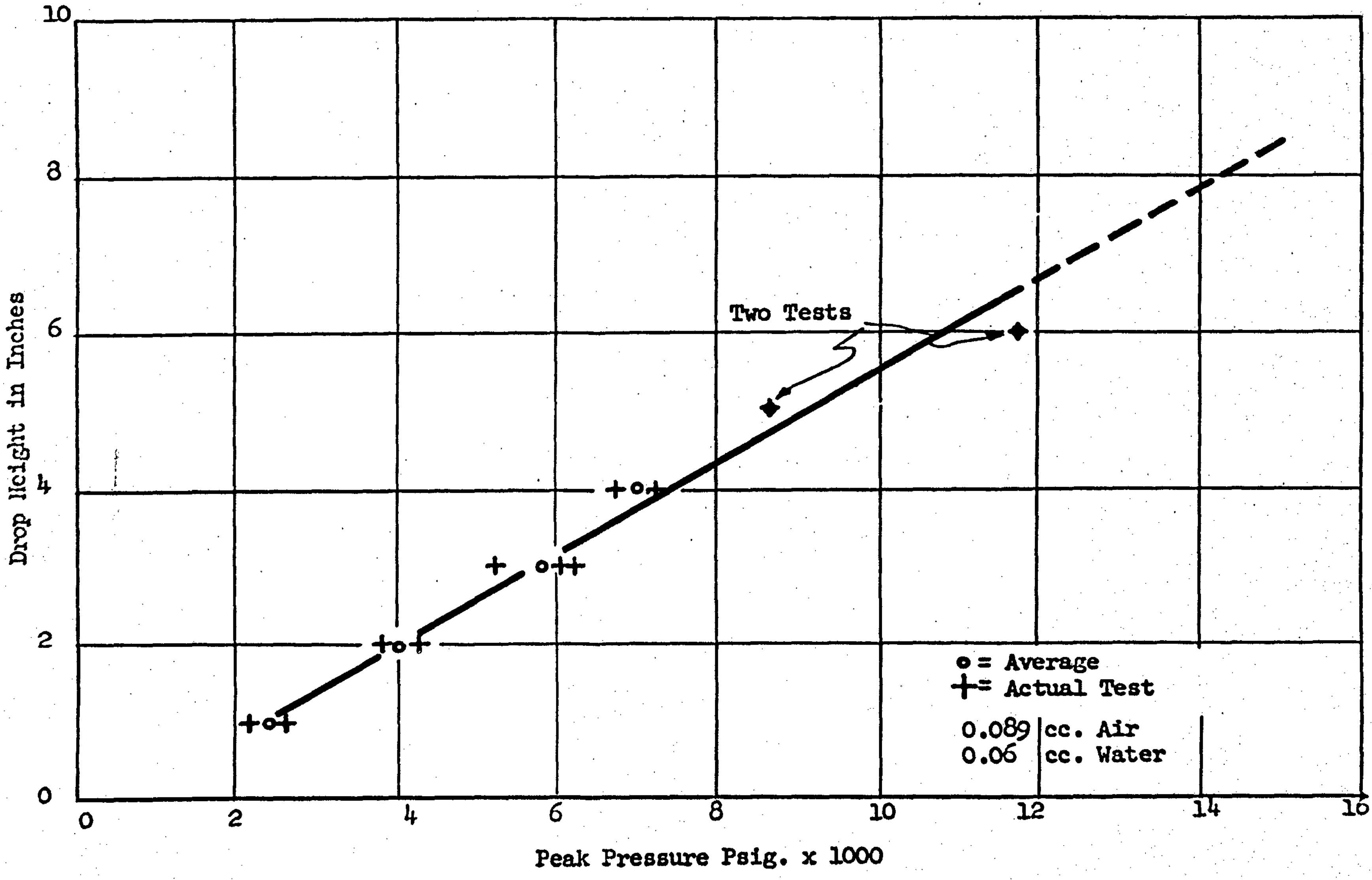

FIG. 3. Pressure vs. Drop Height in Drop Weight Test Apparatus

Bowden[2] approximates a solution to this problem by using the expressions

$$T(v-b)^{\gamma-1} = K, \text{ and } \qquad (17)$$

$$P = \frac{R}{K^{1/(\gamma-1)}} T^{\gamma/(\gamma-1)} - \frac{a}{\left[\left(\frac{K}{T}\right)^{1/(\gamma-1)} + b\right]^2} \qquad (18)$$

where a and b are the constants from the Van der Waal equation.

In the case being considered, after precompression, the initial volume of gas in the bubble is 0.0645 cc., the initial temperature is 293°K. and b for the air in the cavity is 1.32×10^{-4}. For a 6 inch drop, where the recorded pressure was 688 atmospheres and the calculated temperature was 1762°K., use of the perfect gas law (equation 5) yields a final volume of 7.4×10^{-4} cc. For a 3 inch drop, with associated pressure and temperature of 469 atmospheres and 1584°K., equation 5 yields a volume 10^{-3} cc. Therefore, at these conditions the volume of the gas molecules represents a significant portion of the total volume, and correction for this fact should be made. Time did not permit making the calculation for this paper, but the calculation will be made subsequently.

For the time being let us assume that the temperature of 1762°K. or 1489°C. is a valid estimate of the temperature associated with the experimentally determined pressure of 688 atmospheres for a 6 inch drop. In the case of a 3 inch drop a pressure of 469 atmospheres was measured. This pressure, through equation 16, indicates a temperature of 1584°K. or 1311°C. An experiment was also made with a water solution that contained 10% by weight of ethylene oxide. The pressure recorded for a 3 inch drop was 460 atmospheres. To calculate a temperature for this pressure according to equation 16, data from Ref. 3 was used for the vapor pressure of ethylene oxide over water. Because of the ethylene oxide in the vapor, the γ of the vapor now becomes 1.27 instead of 1.40. Substitution of these values into equation 16 gives a temperature of 1021°K. or 748°C. Thus the addition of a small amount of ethylene oxide to the vapor in the bubble lowers the temperature that is calculated from the measured pressures in a very striking manner. This phenomenon is not new; Bowden discusses it extensively in Ref. 2. However, the calculation does shed light on why small additions of ethylene oxide to n-propyl nitrate or to 2-methoxyethyl nitrate had such a pronounced effect on increasing the 50% point in the drop weight tester. The ethylene oxide reduced the γ of the vapors trapped in the bubble so that a lower temperature was obtained during the adiabatic compression of the bubble.

One thing that is still peculiar about the above calculations, however, is the fact that even at drop heights of 3 inches the temperatures calculated were far in excess of that required to cause ignition of the monopropellant. If the temperatures calculated are valid, it would appear that initiation of combustion may be occurring but that propagation throughout the liquid does not occur. When one considers the size of the compressed bubble, 1 μ thick for a pressure of 100 atmospheres and a temperature of 1000°K., and the fact that this hot bubble is probably in direct contact with the relatively massive steel piston, it is not unreasonable to expect that heat would be conducted out of the bubble into the piston at a high rate. The film coefficient at the interface is an obstacle to the calculation of the heat transfer into the piston, but it must be granted that the piston is a sink for draining energy out of the combustion wave that would have to propagate through the liquid. The quenching of flames at reduced tube diameters is a well-known phenomenon in the burning of both gases and liquids. In an attempt to evaluate the significance of heat losses to the piston on the 50% point in the drop weight tester, the cavity of one piston was enlarged and a Teflon insert with 0.015 inch thick walls was inserted. The cavity in the Teflon insert was of the same dimensions as the cavity of a normal steel piston. When tests were made with n-propyl nitrate a 50% point of 7.5 inches was obtained in contrast to the standard value for n-propyl nitrate of 9.6 inches. Therefore, the Teflon cup had a significant effect on the measured sensitivity of n-propyl nitrate. The reason for the increased sensitivity may be that the propagation of the combustion wave through the liquid is aided by a reduced loss of heat to the walls of the cavity in the piston.

An experiment that is planned is to obtain a photograph of the inside of the cavity during the impact in a fashion similar to that used by Bowden with explosives. Such photographs should shed light on the concept of initiation without propagation.

Another factor that requires additional study is the compressibility of the O-ring. In order to obtain the volume reduction of the air bubble in the cavity that is required to develop the high temperatures, it is necessary that the O-ring be squeezed into the bubble cavity. The O-rings used in the drop weight tests are quite hard. Therefore, it is conceivable that they are not deforming adequately at low drop heights, but rather are causing a partially elastic impact. Since the O-ring was sitting directly on the pressure transducer in the experiments where the pressure was recorded, the elastic impact would also be recorded. The bounce pulse shown in Fig. 2 is indicative of this effect. Another way of testing the effect of the rigidity of the O-ring would be to use a reduced depth of the air cavity. In this fashion, the O-ring would not have to deform as much in order to provide compression of the air bubble.

STORAGE STABILITY OF MIXTURES OF ETHYLENE OXIDE AND n-PROPYL NITRATE

In order to see if a practical, desensitized monopropellant could be obtained from these mixtures, the stability of mixtures of n-propyl nitrate and ethylene oxide after storage in sealed glass tubes was investigated. The ethylene oxide and n-propyl nitrate in all the tests reported were purified by distillation prior to testing. It was originally intended to work up the storage product by removing the ethylene oxide by distillation at 30-40°C. at atmospheric pressure. The first distillation, performed in a 30-40°C. bath for 2 hours at atmospheric pressure, failed to remove the ethylene oxide from the mixture. No weight loss was obtained, and there was no variation in drop weight sensitivity.

To determine the possibility of interaction between the two compounds, a sample of the mixture was submitted for infrared analysis to detect hydroxyl groups which would be present in any reaction of ethylene oxide. Infrared proved the absence of hydroxyls.

A refractive index vs. concentration curve was constructed for the mixture. It was found that a straight line was obtained, indicating the absence of any compound formation between the ester and ethylene oxide. The index of refraction was plotted as a function of the storage time in a 30-40°C. bath, and it was found that the index was relatively constant.

The preceding tests indicated that no reaction was occurring between ethylene oxide and n-propyl nitrate and that the evaporation difficulty was arising from the non-volatility of the mixture under the conditions of the test. This was verified by constructing a vapor pressure curve for the 90/10 NPN/EO mixture at 40°C.

At 40°C. the sum of the partial pressures of the components was found to be considerably below the pressure necessary for boiling to occur.

Subsequent evaporations were performed under the reduced pressure of a water aspirator for the complete removal of ethylene oxide.

The results of the storage tests are summarized below:

	Storage Duration	Storage Temp.	Before Evap. n_D^{4}	Before Evap. Drop Wt. Sens. In.	After Evap. n_D^{25}	After Evap. Drop Wt. Sens. In.
90% NPN 10% E.O.						
1	13 days	70°C.	---	50 in.	1.3952	10.0
2	24 days	70°C.	---	50 in.	1.3951	9.7
3	2 months	70°C.	1.3994	50 in.	1.3965	8.6
50% NPN 50% E.O.						
4	3 months	70°C.	1.3803	Could not be contained in tester	1.3922	---
5	3 months	70°C.	1.3764		1.3945	10.1

The index of refraction for:

90-10	NPN - E.O. at 4°C.	= 1.3990
50-50	NPN - E.O. at 4°C.	= 1.3818
Pure	NPN at 25°C.	= 1.3949

Sample No. 3 was submitted for infrared analysis prior to evaporation, and no OH absorptions were observed. This specimen contained 10% E.O. which presumably was lost in performing the IR analysis. A subsequent sample of product stripped under reduced pressure from sample No. 3 was analyzed as "infrared pure" for n-propyl nitrate.

Hence, it appears that mixtures of ethylene oxide and n-propyl nitrate are probably storable for extended periods of time without polymerization of the ethylene oxide. A practical disadvantage to such mixtures, however, is the high vapor pressure of the ethylene oxide over the mixture at elevated temperatures. To be sure it is the vapor pressure of the ethylene oxide which reduces the sensitivity of the mixture to adiabatic compression. But any leak in the system would result in the progressive loss of the desensitizing component.

ACKNOWLEDGMENTS

The work described in this report was carried out under the sponsorship of the Bureau of Aeronautics as partial fulfillment of contract NOas 55-144-c, Amendments 1 and 2. The drop weight tests were made by Stephen P. Ferris and E. McLaughlin, the storage tests were made by R. E. Bacon. Dr. C. T. Lenk originally suggested at

Wyandotte the use of ethylene oxide for desensitizing n-propyl nitrate.

REFERENCES

(1) "An Adiabatic Air Compression Drop Weight Tester for Liquid Monopropellants",by W. A. Cuddy. Wyandotte Chemicals Corporation, Wyandotte, Michigan.

(2) "Initiation and Growth of Explosion in Liquids and Solids", by F. P. Bowden and A. D. Yoffe. Cambridge at the University Press. 1952. page 49.

(3) "Liquid Propellants Handbook". Battelle Memorial Institute, page 8, Phase Properties of Ethylene Oxide. (Confidential)

EFFECT OF HYDROCARBON FUEL COMPOSITION ON ROCKET PERFORMANCE

Jacob Silverman and Robert J. Thompson
Rocketdyne, a Division of North American Aviation, Inc.
Canoga Park, California

ABSTRACT

The significance of composition and physical properties of blended hydrocarbon fuels on the performance of large rocket engines is discussed. Results of a research program conducted at Rocketdyne to study the effects of systematic variation of the fuel molecular type and molecular weight in bipropellant turbine gas generators and model rocket thrust chambers are presented. It is shown that a high aromatic content is deleterious to the performance of these combustion devices. A highly naphthenic fuel in the kerosene boiling range appears to represent the best compromise among satisfactory thrust chamber and gas generator performance and good physical properties. Salient features of the new RP-1 rocket fuel, Specification MIL-F-25576A, are discussed in the light of these results.

EFFECT OF HYDROCARBON FUEL COMPOSITION ON ROCKET PERFORMANCE

Jacob Silverman and Robert J. Thompson
Rocketdyne, a Division of North American Aviation, Inc.
Canoga Park, California

INTRODUCTION

The effect of composition and physical properties of blended hydrocarbon fuels on the performance of conventional combustion engines has long been recognized. An enormous amount of research in the petroleum, automotive and aircraft industries over a period of many years has been devoted to improving hydrocarbon fuels in order to achieve higher power, higher efficiency, greater reliability under all operating conditions, reduced maintenance and longer life of internal combustion engines and, more recently, turbojet engines. When it was found that the optimum engine fuel did not correspond to any fraction which could be produced in quantity by simple distillation or extraction of crude petroleum, a huge chemical industry, modern petroleum refining, was established to reshape the natural hydrocarbon molecules systematically into optimum fuels for each of several designs of engines. More than one fuel had to be produced, for it had been found that the best fuels for automobile engines, diesel engines, aircraft piston engines and aircraft jet engines, for example, were by no means the same. The effort required to tailor the fuel to the engine in these applications is now accepted as quite natural and inevitable.

With this background, it is perhaps the more extraordinary that the possible need of a radically new type of engine, the rocket engine, for a different type of fuel than any used in previous engines was not recognized earlier. However, it is not too difficult to see how this came about. First, the liquid rocket engine introduced a new element in combustion engineering: the liquid oxidizer. The energetic liquid oxidizers are either liquified gases like oxygen, or highly reactive and corrosive liquids like hydrogen peroxide and nitric acid. Such a complex of new problems was introduced by the oxidizer that the relatively pacific fuel tended to be neglected by comparison. Second, much of the earlier rocket development was carried out with commercial grade pure chemicals like ethyl alcohol and aniline, which were selected at least partly because of favorable chemical and physical properties for rocket engine applications. But as the infant rocket industry grew rapidly both in size of engines and in rate of testing, the voracious appetite of this new engine for its chemical fuel became alarmingly evident. For logistic and economic reasons, it appeared desirable to shift large rocket engines to cheap, available hydrocarbon fuels.

When this shift in fuel was attempted, serious difficulties were encountered in the engines employing nitric acid as the oxidizer. This has led to a considerable effort to improve the propellant performance by various means, including additives to the fuel. However, the shift to hydrocarbon fuels was accomplished with relatively little difficulty in engines employing liquid oxygen as the oxidizer. The absence of major difficulties at this stage probably inspired a false feeling of confidence that large rocket engines could satisfactorily employ any current specification jet fuel. The reason for this is now evident. At the time this shift was accomplished, the rocket engine was not yet sufficiently developed and refined to discriminate in its performance between relatively minor fuel differences. Lack of precision of both the engine itself and the test instrumentation produced sufficient scatter to mask variations due to fuel composition. As the engine and its instruments have become more precise, the effects of variation in fuel properties are now readily apparent. In fact, the variations which may occur within the specification range of JP-4 and JP-5 fuels can already produce a greater variation in engine performance than all other engine and operating variables combined. As the drive toward lighter engines operating at higher thrust, higher pressure, higher performance and higher accuracy continues, the requirements on the fuel may be expected to become increasingly stringent. The rocket designer will be relieved of the burden of accommodating his engine to the existing fuel. Rather, the fuel will be tailored to fit the needs of the engine, as has been the case with other combustion engines.

The Fuels Evaluation Program now under way at Rocketdyne was activated by the Air Research and Development Command, Western Development Division in 1955 as an experimental and analytical effort in support of large rocket engine development programs, in order to establish the influence of chemical composition of mixed hydrocarbon fuels on those parameters which are pertinent to the combustion of the liquid oxygen-mixed hydrocarbon propellant system in high thrust rocket engines. The practical need for such a full scale investigation developed with the realization that the compositional and physical variability permitted under the existing specification for JP-5, the originally designated Atlas fuel, might very well be inconsistent with reliably high and reproducible engine and missile performance. Furthermore, it was distressingly evident that little engine and laboratory data existed upon which to base a knowledgeable selection of optimum composition limits for a mixed hydrocarbon fuel. Hence, it became the prime objective of the program to develop systematically the chemical and engineering data necessary to define unambiguously the important behavior differences, if such exist, between the various chemical species which normally occur in petroleum fuels.

Briefly summarized, the program involves research tasks associated with thrust chamber and gas generator combustion and cooling. The tasks which are presently active embrace studies on thrust chamber performance and combustion stability, gas generator combustion characteristics, the real thermodynamic properties of gas generator gases, chemical kinetics of fuel-rich (gas generator type) flames, and the physical and thermodynamic properties and heat transfer characteristics of mixed hydrocarbon fuels.

Parallel with these studies of fuel properties and performance, and as an integral part of the overall program, a chemical laboratory support task of major proportions was initiated, principally to develop highly definitive chemical analytical techniques and thence to provide complete and detailed analytical services to all other phases of the program. Such support involves complete analyses of each of the test fuels as well as of the combustion product gas samples collected under the gas generator and flame study phases. Physical properties and thermal stability are also being studied in the laboratory.

Five specific chemical species are involved in this study:

1. Normal Paraffins (Straight chain saturates)
2. Branched Chain Paraffins
3. Naphthenics (Saturated cyclics)
4. Aromatics (A special class of unsaturated cyclics, i.e., benzene)
5. Olefins (Chain or cyclic unsaturates)

In the JP-5 boiling range, "pure" samples of each of these chemical types are either unavailable or prohibitively expensive; hence, natural or synthetic blends thought to be enriched in each of these general types were procured. However, for correlative purposes, "pure" samples of somewhat higher volatility than JP-5 were obtained and tested. In addition, a large quantity of JP-5, from a randomly chosen source, was procured as a reference fuel; the latter is referred to in the ensuing text as JP-5R.

Until very recently, no specification existed for a hydrocarbon fuel for rocket engines. Specification MIL-F-25576A for RP-1 fuel, originally issued 8 May 1956, represents the first concrete result of this joint effort by the Air Research and Development Command and Rocketdyne to arrive at a hydrocarbon fuel composition which will best suit the needs of today's and tomorrow's large rocket engine. Since time does not permit a full discussion of all aspects of the fuels program, the balance of this report will be devoted primarily to a discussion of the results of the thrust chamber and gas generator studies which influenced the selection of fuel characteristics set forth in this specification.

GAS GENERATOR PERFORMANCE

The heart of the large liquid rocket engine is the high speed turbopump assembly. The thrust of the engine is directly related to the rate of propellant pumping which in turn depends on the power delivered by the gas turbine. The turbine power is itself determined for a given configuration by the flow rate and available enthalpy of the driving gas. The available enthalpy depends essentially on the gas temperature, molecular weight and adiabatic expansion exponent, γ , and on the pressure drop through the turbine nozzles. The gas temperature must also be held within close limits to avoid overheating the highly stressed turbine. The attainment of optimum turbine design and performance evidently requires a quite precise knowledge and control of the combustion process and the properties of the combustion products.

In an air breathing engine, such as the aircraft gas turbine, the bulk of the hot gas is nitrogen: about 70% at stoichiometric ratio, more at the lean mixture ratios characteristic of steady-state operation. The remainder consists of relatively simple molecules with quite accurately known properties, carbon monoxide, carbon dioxide and water. Given the heating value of the fuel and the combustion efficiency, calculation of the required gas properties is straightforward. In contrast, the rocket bipropellant gas generator employs excess fuel as the diluent and coolant to attain the required turbine operating temperature. When this fuel is a complex hydrocarbon mixture of high average molecular weight which is also thermally unstable and can break down into a host of products, the resultant gas properties can no longer be directly calculated. A detailed knowledge of the entire fuel-rich combustion process becomes essential for the establishment of optimum design and operating criteria.

The phenomena which occur during the fuel-rich combustion of a chemically complex hydrocarbon mixture such as jet fuel, under turbulent, non-equilibrium conditions with heterogeneous mixing and enormous thermal gradients, may be conservatively described as poorly understood. The approach to bipropellant gas generation has heretofore been as superficial as it has been direct, involving, in essence, the creation of an oxidizer-fuel adiabatic "oven" which in turn dissipated its sensible enthalpy to pyrolyze large molecules into a moderately low molecular weight, low-temperature turbine drive working fluid. In retrospect, hardly any other approach was feasible during early gas generator development. Since chemical equilibrium is not attained and the nature and extent of the chemical reactions involved are largely unknown, classical thermochemical calculation techniques could not be applied to predict the gas temperature, composition, and other properties.

While the empirical approach to gas generation allowed a rapid initial development, certain inevitable penalties soom became evident. Every change in generator or turbine configuration necessitated a separate development program to attain the desired turbine power output. Experimental mixture ratio-temperature data also had to be obtained for each gas generator and turbine assembly. The performance characteristics of the final assembly are still distinctly sensitive to compositional variations in the fuel. These shortcomings have been further aggravated by the continual demand to upgrade the rocket system and components for smaller volume, lower weight, higher power, and greater reliability.

Today it is generally agreed that systematic engineering research into fuel-rich combustion is virtually mandatory. Such a program is presently under way at Rocketdyne. This program is designed to examine and establish the interdependence between the various fundamental engineering parameters in the fuel-rich combustion of mixed hydrocarbons and oxygen in large rocket engine gas generators. It includes a basic laboratory investigation of the chemical kinetic nature of the combustion processes, and the direct determination in model generators of gas properties of interest and their dependence on pressure, temperature, mixture ratio, flow rate, injector and combustor design, and fuel composition. This comprehensive program is still in its early stages. However, the results of a shorter experimental program, carried out on both model and full scale operational hardware, have clearly delineated the effect on gas generator performance of at least one species of hydrocarbon, the aromatics, which may occur in substantial amounts in jet fuel. Rather less conclusively, performance differences were found which appear to correlate with the average molecular weight and naphthenic ring content of the low aromatic fuels tested.

Experimental Operations and Analysis

The series of experiments herein described were undertaken in order to determine, at least semi-quantitatively, the extent of the differences in the available adiabatic work output among the product gases generated by combustion of liquid oxygen with an excess of each of several hydrocarbon fuels of widely varying composition and volatility. Ideally such a study should reveal the relative influences, if such exist, of fuel volatility, average molecular weight, and of each of the chemical types normally found in the family of jet fuels, i.e., aromatics, olefinics, naphthenics, straight and branched chain paraffinics. Exploratory tests were carried out first on a model scale using an engine system normally employed for engine controls research. The qualitative trends which were uncovered were then confirmed on full scale operational hardware.

The model scale tests were performed on a calibrated engine system operating at the 5,000 lb thrust level. Although the fuels burned in the gas generator were systematically varied, the propellants pumped to the main chamber were always liquid oxygen and JP-5. The gas generator system consisted of a ten pair doublet injector, a splash plate and a combustion chamber 16 in. long by 1.25 in. inside diameter, terminated by a butterfly valve beyond which was a fixed pressure reducing orifice. The engine employed a single stage, partial admission impulse type turbine with direct drive to the propellant pumps. The turbine shaft horsepower per pound of propellant flow per second at any chosen reference value of the measured turbine inlet temperature was taken as the measure of performance. At a fixed operating pressure ratio and turbine efficiency, the specific horsepower depends primarily on the ratio of gas temperature to average molecular weight, T_c/M_c.

The fuels which were selected for this preliminary examination were:

JP-4 (MIL-F-5624C)
JP-5 (MIL-F-5624C)
Kerosene (Standard Oil Co. "Pearl Oil"; MIL-F-25576A)
Amsco Solvent (American Mineral Spirits Co.)
Heptane (Phillips Commercial Grade)
Iso-Octane
Iso-pentane
Toluene
Methylcyclohexane

Standard ASTM analyses for these hydrocarbon fuels are given in Table I. Complete and detailed chemical analyses for kerosene, heptane, iso-octane, toluene, and methylcyclohexane can be found in the body of Tables II and III.

The fuels were selected to provide a reasonably wide range of gas generator performance. JP-4 and JP-5 are, of course, typical of the jet fuel family. Kerosene meets the specification for a wide range JP-5. The analytical data of Table III indicates about 40% naphthenic character; however, this kerosene differs principally from the chosen JP-5 in that its aromatic content is substantially lower (4.8% compared to 22.4%). Amsco solvent is probably similar in general chemical constitution to kerosene but of higher volatility. Of the low boiling fuels, iso-octane and isopentane, toluene, and methylcyclohexane are fairly pure representatives of the paraffins, aromatics, and naphthenics respectively. Commerical heptane is approximately a 40:30:30 mixture by volume of n-heptane, methylcyclohexane, and mixed iso-octanes.

The model scale results did not lend themselves readily to graphical representation and hence are not presented here as such. However, when viewed as a whole, the data fell neatly into three broad but distinctly distinguishable regions which are conveniently designated as 1, 2, and 3.

1. High Performance
    a. light paraffins (iso-pentane, iso-octane, heptane)
2. Intermediate Performance
    a. naphthenes (methylcyclohexane)

b. naphthene-paraffin blends (Amsco solvent, JP-4, kerosene)

c. light aromatics (toluene)

3. Low Performance

a. heavy, aromatic rich fuels (JP-5)

This performance pattern was as interesting as it was surprising. For example, within region 2, despite substantial differences in their physical properties, JP-4, kerosene, methylcyclohexane, Amsco solvent, and toluene were all reasonably similar in performance. From a practical standpoint, these data emphasize that the volatility of a fuel is not a satisfactory criterion of its performance potential in a gas generator. Alternately, it may be concluded that altering the molecular weight of the liquid fuel may not produce a corresponding effect on the molecular weight of the product gas. The average molecular weights of these gases at the same temperature and, hence, their T_c/M_c value, are dependent primarily on the chemistry of the combustion chamber processes which, in turn, depend primarily upon the chemical species present (composition) rather than the physical properties of the fuel.

The paraffins, represented by iso-octane and iso-pentane, certainly appear to be best adapted to gas generator application from an energy standpoint. The markedly higher values for iso-pentane unquestionably are due to the nearly 40% lower molecular weight, reflecting the importance of this property in the case of the very light paraffins although it is quite probable that the behavior differences between homologous paraffins decrease rapidly beyond C_8. It is equally interesting, however, to note that the data for commercial heptane, with a molecular weight intermediate between iso-octane and iso-pentane, fall slightly below those for iso-octane. The reason for this behavior is quite straightforward, i.e., the commercial heptane contains about 30% methylcyclohexane, a gas generant of demonstrated poorer performance.

The behavior of saturated ring systems or naphthenics seems to be uniformly moderate. Naphthene rich fuels of widely varying physical properties, such as JP-4, kerosene, and Amsco solvent are indistinguishable from methylcyclohexane. One might speculate that the performance of the higher boiling JP-4 and kerosene would have been lower than methylcyclohexane were if not for the presence of substantial quantities of paraffinics in the former fuels. However, it must be noted that the performances of Amsco solvent and methylcyclohexane, two fuels of similar volatility, are substantially the same in spite of the presence of paraffinic stock in the former. The conclusion to be drawn is that moderate amounts of naphthenics, at least in the 200-500 F boiling range, are excellent performance levelers in hydrocarbon blends.

Although toluene has been grouped in the central region, its performance was sufficiently low to be considered almost borderline between regions 2 and 3. The great advantage in volatility and molecular weight which this fuel enjoys over such heavy fuels as JP-4 and especially kerosene was apparently of little consequence. On the basis of the toluene data alone, it could have been predicted that fuels containing substantial quantities of heavy, polynuclear aromatics would exhibit exceedingly poor performance.

Finally, and most important, there exists the marked difference in performance between kerosene and JP-5, two fuels which, superficially at least, appear to be almost identical in all respects save one - aromatic content. The very poor performance of this particular JP-5 is unquestionably due to its high aromatic content which, incidentally, still falls within the specification requirements for the fuel.

Thus, these exploratory experiments indicated that the energy availability from liquid oxygen - hydrocarbon gas generators is largely, if not primarily dependent upon the molecular type, i.e., the relative amounts of paraffins, naphthenes, and aromatics in the fuel. Highly paraffinic fuels are best performing; naphthenes and especially aromatics are detrimental, to a degree dependent upon their molecular complexity. The lower naphthenes and aromatics (e.g., methylcyclohexane and toluene) do not differe markedly in performance but the higher molecular weight aromatics appear to be distinctly inferior to their naphthenic analogs. Volatility (ASTM distillation) and average molecular weight by themselves are not reliable parameters for predicting or explaining fuel performance. The more volatile naphthenes and aromatics are no better than the high boiling, low aromatic jet fuels under gas generator combustion conditions. However, within a single molecular type the order of performance is generally inverse to the order of molecular weight.

Two series of corroborating experiments were carried out on large engine operational hardware. The test systems, consisting of a gas generator assembly and turbopump in each series, were of two different types; hence, the absolute performance levels are different. However, it is the relative performance levels between fuels which are the important factors. In each series, the propellant flow rates were similar, i.e., 9 - 12 lb/sec. In series I, all the model engine test fuels were examined except for toluene and iso-pentane. The series II test fuels included iso-octane, heptane, kerosene and three additional high molecular weight fuels whose detailed chemical analyses are contained in Tables II and III. These additional fuels are:

1. Heavy Alkylate Bottoms - an iso-paraffin in the C_{12} - C_{16} molecular weight range.
2. Shell UMF Grade C (RJF; MIL-F-25558) - a low aromatic fuel containing half again as much naphthenic structure as kerosene and having a 50 F higher distillation range.
3. Hi-Cetane Diesel Reference Fuel - a fuel in the

RJF distillation range, highly enriched in paraffins but also containing about 12% aromatic structure.

The graphical data of Figure 1 fully confirm the qualitative conclusions reached previously. The high, intermediate, and low performance levels of heptane, kerosene, and 22.4% aromatic JP-5 respectively are unmistakable. At a reference temperature of 1300 F, the power factor for JP-5 is 5 - 6% less than that of the low aromatic kerosene. On the other hand, the power factor for heptane is 7 - 8% higher than that of kerosene. The latter difference may be attributed both to the 75% greater molecular weight and the approximately 40% higher naphthenic content of kerosene relative to heptane. The curves for Amsco solvent and JP-4 (the latter has been omitted for the sake of graphical clarity) lie very close to that of kerosene, a behavior consistent with their low aromatic content and general compositional similarity. Methylcyclohexane, the only purely naphthenic fuel, shows behavior intermediate between that of JP-5 and kerosene, suggesting strongly that the higher performance of kerosene and other mixed hydrocarbon fuels is due principally to the elevating influence of the paraffinic components. Toluene and iso-pentane were not run in the series of Figure 1. The results with iso-octane in this series were spurious for reasons which are not known, but most probably relate to measurement errors.

The data of Figure 2 are equally consistent with the foregoing postulates. The performances of the paraffin-rich heptane and iso-octane are substantially identical. Note also that in spite of a molecular weight 1.5 - 2 times that of iso-octane, the chemically similar heavy alkylate closely approaches the high performance of iso-octane. Equally significant is the effect of 12% aromatics on the performance levels of the paraffin-rich diesel fuel. The drop in power factor is 5 - 6% below that of heavy alkylate and 3 - 4% below that of the low aromatic kerosene. As in previous tests, the low aromatic (<5%) kerosene containing approximately a 3:2 paraffin: naphthene compositional ratio, takes an intermediate performance position. It is of interest, finally, to note the moderately low performance level of UMF Grade C fuel, probably attributable to both its higher (3:2) naphthene: paraffin ratio and to the high average molecular weight. The relation of UMF Grade C to kerosene is thus similar to that previously noted between kerosene and commercial heptane. One final set of experiments is under way in order to establish unambiguously the quantitative effect on gas generator performance of aromatic content. These tests are being performed under strictly controlled experimental conditions using a specially designed, highly instrumented research gas generator of 1 - 3 lb/sec. propellant flow rate. The aromatic content of the naphthenic-rich RP-1 (corresponding to the low aromatic kerosene of the preceding discussion) and of the entirely paraffinic heavy alkylate are being systematically varied from 1 - 25% (the present MIL-F specification limit for JP-5) using Esso Heavy Aromatic Naphtha (JP-5 boiling range stock with about 85% aromatic content) as the aromatic additive. No reduced data are yet available from these tests.

RESEARCH THRUST CHAMBER PERFORMANCE

The theoretically computed specific impulses with oxygen of the various hydrocarbons in the JP-5 distillation range can differ significantly. Generally, it is advantageous to choose a fuel which has the highest possible heat of combustion or, stated differently, the lowest possible carbon-hydrogen ratio. Thus, a highly paraffinic fuel should be preferable to a more naphthenic or aromatic type. The maximum variation in the theoretically calculated performance of JP-5, based on the variation in aromatic content permitted by the specification (0 - 25%) is actually on the order of 1.5%, a rather significant figure for a long range ballistic missile. In addition, some fuel components may burn more efficiently in a rocket motor than others, producing differences in performance that cannot be computed in advance. The objective, therefore, of the thrust chamber phase of the fuels program was to establish the influence of variations in chemical composition of mixed hydrocarbon fuels on the operational thrust chamber characteristics of the liquid oxygen-hydrocarbon propellant system.

The model thrust chambers were intended deliberately to enhance differences in performance between the various chemical types which normally occur in JP type fuels. In addition, for an intensive program involving a very large number of firings, simplicity and flexibility, as well as high performance, are highly desirable motor characteristics. These features were successfully incorporated in the two operational thrust chambers used during the course of the program, which were water cooled and throatless, i.e., unity contraction ratio. They incorporated removable inner copper liners and differed only in the characteristic length, L*, of 5 in. and 20 in. respectively. Operating conditions were maintained at about 2800 lb. thrust at an injector end chamber pressure of 500 psia.

Nine hydrocarbon fuels, in addition to the reference JP-5, were test-fired in each chamber. Low and high boiling representatives respectively (with one exception), of each of the major chemical species of interest were procured:

1. n-paraffin: n-heptane and Shell High Cetane Reference Diesel Fuel.
2. iso-paraffin: iso-octane and Heavy Alkylate Bottoms (Standard Petroleum Refined Oil).
3. naphthenic: methylcyclohexane and Standard Thinner 425.
4. aromatic: toluene and Esso Heavy Aromatic Naphtha.
5. unsaturate: iso-octene (no high boiling analog was obtained).

In addition, Ram Jet Fuel, specification MIL-F-25558 (Shell UMF Grade C) was run at the 5 in. L* only. The JP-5R conforms to the RP-1 specification MIL-F-25576. Enough of the JP-5R was purchased in a single lot to last through the entire program. Any changes in performance of this reference fuel were attributed to changes in test hardware or variations in instrumentation. The complete analyses of these test fuels are given in Tables II and III.

The experimental portion of this program, comprising 777 thrust chamber firings, has only recently been completed. The detailed analytical treatment of the directly measured data, described in a subsequent section, is designed to evaluate the effect of unavoidable changes of some operating parameters such as injector modifications, thrust chamber variations, calibration variances, etc., as well as the systematic planned changes of mixture ratio, fuel type, and L*.

Experimental Operations

The selection of the thrust chamber hardware was governed by the following considerations:

1. The necessity for enhancing the small differences in performance obtained from the various chemical types which normally occur in JP type fuel.
2. The need for carrying out a very large number of runs, thus making simplicity, reproductibility, and low cost of hardware very important.
3. The need for the hardware to withstand severe operating conditions.
4. The desirability of systematic variation in combustion volume.

The best means for observing differences in performance among the fuels appeared to be the reduction of the time available for combustion to a very small value and the use of a high performing injection pattern in order to obtain maximum performance in this limited burning time. Limitation of the combustion period is accomplished by the reduction of the characteristic length (i.e., the combustion volume) to a minimum value. However, very small combustion volumes are physically feasible only in low contraction ratio motors. Previous use of 1:1 (throatless) contraction ratio motors has indicated that high performance values are obtainable at low characteristic lengths. Consequently, a throatless motor of 5 in. L* was chosen for the thrust cylinder. The fuel comparison was then repeated in a 20 in. L* chamber where the increased reaction time would presumably allow a closer approach to combustion equilibrium. Thus, a direct comparison is available between the performance in the two chambers which should help to elucidate the effect of combustion rate on performance.

The injector was not only required to produce high performance in a very small combustion volume, but also had to be easily fabricated, readily reproducible, and comparatively long-lived. In order to meet these requirements, the injector face was fabricated from a single piece of material, with the oxidizer and fuel manifolds assembled to the face section. Thus, the hole pattern could be changed by making only one new part.

The injection pattern was designed both for ease of drilling (in the interests of reproducibility of injector performance) and for high performance. A ring of triplet holes (two oxidizer streams impinging on one fuel stream) with nearly zero stream length was positioned around the periphery of the injector. A ring of short stream length doublets was placed about half way between the periphery and the injector center. Previous experience had shown this pattern to be high-performing, but to yield very high thrust chamber heat transfer rates. Figure 3 depicts details of the injector.

In order to carry out a large number of runs and still keep the hardware cost to a minimum, a removable liner was incorporated into the thrust cylinder design. In this way the inexpensive liners (average cost about $100.00 each) could be replaced while retaining the more expensive outer shell assembly. The motor hardware cost for the 777 valid data-producing runs made under this program was less than $10.00 per useful run. Copper was specified for the liner material and injector in order to withstand the severe heat transfer conditions. Figure 4 illustrates the complete thrust chamber assembly.

A chamber pressure of 500 psia was chosen to correspond to present practice in large engines. The expansion ratio and thrust level (selected as 2800 lb.) were determined by the availability of the copper bar stock used for the motor liners and also by the test stand capability. An expansion ratio of 2.85:1 was chosen whereas 4.5:1 is the optimum expansion ratio for local ambient pressure; hence there was a 1.7% correction factor to be applied to obtain the thrust corresponding to optimum expansion. The nozzle expansion half angle was set at 15°. Water cooling was employed, since the heat transfer rates and total heat rejection were too great to allow regenerative cooling with the fuel, and the heat transfer characteristics of the fuel are the subject of a separate study.

Standard instrumentation was used throughout the program. Steady state measurements were recorded on Foxboro rotating charts, and transient measurements on oscillographs. The one exception to this practice was the steady state measurement of flows, the cyclic record of the turbine type flow meters being directly reproduced on the oscillograph. Pressures (tank, injector, chamber and coolant) were measured by means of a strain gauge on a Bourdon tube, such as a Statham gauge; temperatures (oxidizer, fuel, and coolant) were measured by means of thermocouples and thermistors. Thrust was measured by means of a Baldwin load cell. Ignition was achieved by means of two pyrotechnic igniters inserted through the throat of the motor.

The general test procedure involved the periodic re-establishment of the performance datum line by test firing JP-5R after each two mixture-ratio versus performance series of test firings of each fuel under study. During the major portion of the 5 in. L* program, nightly calibrations were made of all critical measurements except flow meters. During the 20 in. L* program, calibrations of all critical measurements except flow meters were made on every day that test firings occurred. The flow meters were calibrated twice during the program; no significant change was noted.

The two major changes in hardware which occurred during the firing program were the gradual injector erosion, both on the injector face and at the intersection of impinging injection holes, and the gradual shrinking of the nozzle throat diameter. The injector faces were machined back whenever the hole patterns had changed visibly or whenever combustion vibration became excessive. (This vibration appeared to be sensitive to the subsurface impingement which resulted from erosion between holes.) Motor liners were changed for each new fuel tested. The throat diameter of the used liner was then machined back to its original diameter and the liner reused. Careful measurement of critical thrust cylinder dimensions were made during each series of tests.

Under normal mixture ratio operation, the exhaust flame exhibited the red-yellow color characteristic of LOX-JP for all fuels tested, and required use of dark glasses for visual observation. However, during the very high mixture ratio (3.5-4.0) runs made with the 20 in. L* motor, the flame became almost transparent and could easily be observed directly. Moreover, the carbon deposition on the inside of the chamber was almost completely eliminated under these conditions, with an accompanying increase in heat transfer rate.

For each thrust chamber and for each fuel, the average overall heat transfer rate was about 4-5 Btu/sq in./sec at a mixture ratio of 2.0. Such a high value for heat transfer rate is to be expected from the combination of throatless motor (with attendant high gas velocities in the chamber section), high performance injector, and copper liner walls. At high (4.0 to 4.5) mixture ratios, with consequent reduction of coking on the chamber walls, the heat transfer rate went as high as 8-9 Btu/sq in./sec in the 20 in. L* motor for the majority of the fuels. At these high mixture ratios, conditions giving rise to combustion vibration resulted in heat transfer rates as high as 10-12 Btu/sq in./sec during vibratory combustion in the case of the few tests made.

Mathematical Treatment of Performance Data

The sets of thrust chamber performance data from the Fuels Evaluation Program were curve-fit by means of the "least-squares" technique to the general form $y = \alpha + (\beta x + \gamma)e^{-x^{\delta}}$, where the four parameters α, β, γ, and δ were determined for each set of data. The following procedure was used for I_s, C^*, and C_F vs mixture ratio data from both the 5 in. and 20 in. L^* motors.

1. Since the throat area of the chambers was measured after each run it was possible to correct all C^* and C_F data for the associated changes in expansion and contraction ratios. Thus changes in throat area due to the shrinkage of the chamber linear should not effect the subsequent analyses.

2. The data were then grouped according to injector. An injector was considered to have lost its former identity and become a new injector when the face was milled. By examining the reference fuel firings when applicable, significant performance level shifts for any one injector over the testing period could be detected. If this occurred, it was assumed, whenever possible, tha~~t th~~is shift was linear over the injector testing period, and a straight line which gave the adjustment in performance required for each test in terms of the average for the given injector was established.

To establish all the performance data for each chamber independent of injector changes, the performance data from all injectors used with each chamber were scaled with respect to the average level of one arbitrarily chosen injector by means of the reference fuel firings.

3. After each set of data was completely reduced, it was fitted with a curve of the type $y = \alpha + (\beta x + \gamma)e^{-x\delta}$. The computations and comparisons were carried out using the I.B.M. 704 EDPM.

Results and Analysis

The results of the model thrust chamber specific impulse program are graphically summarized in Figures 5 (5 in. L^*) and 6 (20 in. L^*). The average values of the confidence band radii for the illustrated curves at the 95% confidence level are 1.6% (3.6 sec.) and 1.7% (4.3 sec.) for the 5 and 20 in. L^* data, respectively. Measurements analysis computations indicate that roughly half of each of these figures can be attributed to instrument variation; the balance, therefore, is due to the natural variance of the test fuels and the motor. In general, the impulses of the propellants tested in the 5 in. motor were between 85 and 95% of frozen theoretical; the impulses obtained in the 20 in. chamber were uniformly above 95% of frozen theoretical indicating, incidentally, that excellent performance can be obtained in small motors with proper injector design.

Close examination of the data of Figures 5 and 6 reveals some interesting general trends. The experimental curves of Figure 5 do not resemble in shape the theoretical performance curves since the latter are maximized at lower mixture ratios (i.e., in the vicinity of 2.2). In fact, most of the experimental curves appear to approach or reach peak values near the stoichiometric mixture ratios (3.1 - 3.4

depending on the fuel) at which, theoretically, the highest chamber temperatures occur. This behavior suggests that at the very low gas residence time of the 5 in. L* motor, equilibrium conditions are being approached only at the highest flame temperatures. Since chemical reaction rates and heat transfer rates from burnt gas to incoming propellant both increase with temperature, it appears that the performance in the 5 in. L* motor is rate limited at mixture ratios below stoichiometric and perhaps even at all mixture ratios. Increasing the gas residence time in the chamber (increasing L*) brings about a distinct shift in the peak impulse mixture ratio (Figure 6) although the degree of this shifting varies considerably with the fuel.

The data of Figures 5 and 6 permit several other important general observations. The volatility of the fuels seems to have little correlation with its performance. For example, the performance of RJF, one of the least volatile fuels of Figure 5 (distillation end point 523 F) is at least as high as that of the highest volatility fuel, n-heptane (end point 206 F). Similarly, from the 20 in. L* data (Figure 6) it is seen that the performance of JP-5R (end point 498 F) either exceeds or equals (within the total precision of the data) that of the higher volatility fuels. In fact, the Figure 6 data unambigiously point out that JP-5R, which meets the specification requirements of MIL-F-25576A, is an excellent rocket fuel with liquid oxygen.

Some distinctive performance patterns evolve when the individual families of chemical types are reviewed separately. For example, because of their low heats of combustion and high C/H ratios, the aromatic rich fuels, namely toluene and aromatic naphtha, should have approximately 9 and 12 seconds, respectively, lower specific impulse than either JP-5R or the Hi-Cetane Diesel fuel. (In spite of its higher aromatic content, the diesel fuel does not differ significantly from JP-5R in heating value or C/H ratio since the former also has a 30% higher paraffin content.) Experimentally, however, this predicted theoretical relationship does not entirely prevail. From Figure 7, it is apparent that the performance of toluene in the short L* motor is substantially equal in magnitude to JP-5R and the diesel fuel and considerably higher (4.5 seconds) than the aromatic naphtha. Although this behavior pattern is thermodynamically not predictable, it is kinetically reasonable since it is known from flame study experiments that aromatics are normally faster burning than their aliphatic counterparts. This reasoning can similarly account for the higher than predicted level, relative to JP-5R, of the aromatic naphtha. It is probable that the remaining difference between toluene and the aromatic naphtha can be attributed to physical process rate limiting factors arising from the considerably lower volatility of the latter.

On the other hand, when the gas residence time in the chamber is increased, chemical kinetic influences rapidly diminish. In the 20 in. L* chamber, toluene, heavy aromatic naphtha, and JP-5R have already assumed their thermodynamically predicted relative order, the performance differences between the aromatic fuels and JP-5R reaching

65% of theoretical. On this basis, there appears to be little doubt that the theoretical thermodynamic differences between aromatic-rich and aromatic-free fuels are readily realizable in the combustion volumes characteristic of high thrust chambers.

The Figure 7 data for Hi-Cetane Diesel Fuel are not as readily explainable. Although the 5 in. L* data appear reasonable, the 20 in. L* performance difference of four seconds between this fuel and JP-5R is thermodynamically not predictable. Relative to JP-5R, the diesel fuel has somewhat higher molecular weight and lower volatility, due principally to a considerable quantity of high boiling n-paraffins (C_{16} and higher) (Table III). The aromatic content of the diesel fuel is four times that of JP-5R by volume, but some eighteen times as great by weight. The presence of condensed aromatic ring systems, indicated by this analysis, may inhibit performance. The naphthenic carbon content of diesel fuel is half that of JP-5R; the paraffinic content of diesel fuel is correspondingly higher and, furthermore, the saturate fraction of diesel fuel shows by far the lowest degree of chain branching of any fuel tested. This high n-paraffin concentration may be responsible for the slightly low performance, since the 20 in. L* data for heptane (Figure 8), the only other test fuel high in n-paraffins, is similarly surprisingly low (see below). It appears that a high n-paraffin fuel performs relatively well at minimum combustion volume (5 in. L*) but is somewhat less efficient than an isoparaffinic or naphthenic fuel at moderate combustion volume (20 in. L*).

Figure 8 illustrates the performance characteristics of the paraffinic fuels. Temporary fuel procurement difficulties prevented the experimental completion of the 5 in. L* heptane and iso-octane curves, as well as the 20 in. L* heavy alkylate curve. Nevertheless, sufficient data exist to illustrate a well defined trend. The fuels of Figure 8 should, thermodynamically, show a maximum spread of two seconds so that, within experimental error, all the experimental curves should be substantially identical. Contrary to theory, marked differences occur in both the 5 in. and 20 in. L* motor data. Considering n-heptane and iso-octane to be identical within experimental error, the 5 in. L* motor impulses decrease in the order of increasing volatility, suggesting the predominant influence of physical process rates. However, in the light of the Figure 7 and, as will be seen, Figure 9 data, it is extremely doubtful that the moderately lower volatility of heavy alkylate compared to JP-5R can fully account for the 4 second performance difference. It is more reasonable to hypothesize, as in the case of toluene and heavy aromatic naphtha, that the lower burning rates of highly branched paraffins are real contributory factors.

The 20 in. L* data show the performance levels of JP-5R and iso-octane to be exactly in the order demanded by their combustion thermodynamics without regard to volatility. However, n-heptane is fully 3 seconds lower than expected. This fuel, it will be recalled, is an approximately 40:30:30 mixture of n-heptane, methylcyclohexane and iso-octanes. Since the performance of iso-octane is obviously good and that of methylcyclohexane higher (see Figure 9) than that of commercial n-heptane, one is almost forced to the conclusion that the full performance potential of normal paraffins is more difficult to realize experimentally, although the reasons for this behavior are not immediately apparent. A similar performance pattern has already been noted with Hi-Cetane Diesel, another n-paraffin rich fuel.

Figure 9 illustrates principally the remarkably high performance obtainable from a high boiling, high naphthenic, low aromatic fuel. RJF (MIL-F-25558) was tested only in the 5 in. L* motor, where its specific impulse was 5 seconds higher than JP-5R and apparently higher than the simple, low molecular weight naphthene, methylcyclohexane. The molecular structural characteristics of RJF (Table III) are substantially the same as JP-5R except that the former has 62% of its carbon content in naphthenic structures compared to only 39.4% for JP-5R.

Based on the heats of combustion and C/H ratios, methylcyclohexane and JP-5R should have equal specific impulses. The small superiority of the former under short L* conditions is probably due to its higher volatility, since the order is reversed under 20 in. L* conditions. The latter data indicate that saturated ring systems with numerous and varied substituents are more efficient burners than simple molecules. Exactly how high an L* must be reached before these performance characteristics based on combustion kinetics give way to straightforward thermodynamics, is a provocative question indeed.

The conclusions which may be derived from the foregoing data are few but quite important. First, volatility affects fuel performance somewhat only under extremely short L* conditions, but has already lost its importance even at a 20 in. L*. Under reasonable L* conditions, conventional equilibrium thermodynamics can predict the effect on performance of aromatics; inevitably, because of low heats of combustion and high C/H ratios, the effect of aromatics on performance is deleterious. Fuels in the JP-5 distillation range will benefit from a reasonably high concentration of naphthenics; on the other hand, there is evidence, not conclusive by any means, that n-paraffins are not especially desirable components of mixed fuels for reasons which are not immediately apparent. Branched paraffins appear to behave normally.

The performance behavior of mixed hydrocarbon fuels with liquid oxygen is not, unfortunately, simply the story of paraffins, naphthenes, and aromatics. Little, if anything, is known about the possibility of special, totally unpredictable, combination or synergistic effects of various molecular species. There is the further possibility of the existence of specific molecular "bad actors" whose effect may exceed their concentration by many orders of magnitude. A case in point is the specific impulse behavior of Standard Thinner 425.

Within the limitations of the extensive chemical analyses of Table III, this particular fuel is in all respects equivalent to JP-5R and, like JP-5R, meets the specification requirements of RP-1. Yet its performance (Figure 10) is distinctly lower than JP-5R, especially in the 20 in. motor where the difference is a full 3.5 seconds. This provides further evidence, if any is needed, that mixed hydrocarbon rocket fuel research is still in its infancy.

RP-1 (MIL-F-25576A, USAF)

The immediate goal of the fuels program is the development of sufficient engineering information to establish a rocket engine fuel specification which will insure, insofar as possible, that fuel components detrimental to reliable, consistent, and high performance are eliminated. Furthermore, the specification requirements must be such that no significant variation in operating characteristics can result from any chemical variation of the fuel within the specification. Although an enormous amount of research effort is still in prospect before all the requirements for an ideal mixed hydrocarbon fuel can be evolved, the results of the experiments discussed in the preceding pages were sufficiently definitive to permit the immediate recommendation of several changes in the existing JP-5 specification. These recommendations, together with additional changes designed to secure higher thermal stability and more consistent engine operation, formed the basis for the first specification of a mixed hydrocarbon fuel explicitly intended for rocket engines using liquid oxygen as the oxidizer. These special requirements on the specific gravity, total sulfur, heat of combustion, aromatic content, olefin content, smoke point and flash point are sufficiently important to merit some special comment. For purposes of comparison, Table IV presents a comparison of the requirements for RP-1 and JP-5.

Aromatic Content, vol percent, max.

RP-1, 5.0
JP-5, 25.0

The limitation of aromatic content is a direct consequence of the gas generator and thrust chamber experiments described herein. Although combustion theory is not sufficiently advanced to permit either a quantitative prediction or an unequivocal explanation of the deleterious effect of aromatics on gas generator performance, the phenomenon is undoubtedly real. The effect of aromatics in reducing thrust chamber performance was both thermodynamically predicted and experimentally confirmed. Ideally, of course, it would be desirable to eliminate aromatics entirely; practically, however, such a fuel would either be prohibitively expensive or entirely unavailable. Hence, a practical lower limit was chosen consistent with reasonably high engine performance, i.e., 5%.

Heat of Combustion, Btu/lb, min.

RP-1	18,500
JP-5	18,300

The increase in heating value of RP-1 is a simple consequence of the decrease in aromatic limit. Although few samples of RP-1 will ever have heats of combustion below about 18,600, a conservative value of 18,500 permits a certain margin for safety to accommodate the possible existence of peculiar blends which cannot be anticipated.

Smoke Point, mm, min.

RP-1	28.0
JP-5	20.0

The higher smoke point of RP-1 is also a direct result of its reduced aromatic content.

Flash Point, min.

RP-1	110 F
JP-5	140 F

The reduced flash point of RP-1 also reflects the reduced aromatic and increased saturated hydrocarbon content. It is of interest that over a period of a year's surveillance, the flash points for most fuels varied between 125 F and 135 F; only one or two samples have been found with values as low as 119 F. Thus, the flash point can probably be raised to 120 F, min if desirable.

Specific Gravity,° API

RP-1	42.0 - 45.0
JP-5	36.0 - 48.0

The desirability of narrow specific gravity limits for liquid propellant pump-fed power plants designed for use in unmanned vehicles is probably obvious. As the gravity limits become wider, the requirements placed on the engine propellant utilization system become increasingly burdensome, since close mixture ratio control is required for optimum performance. A narrow specific gravity requirement for a mixed hydrocarbon fuel permitting up to 25% aromatic content is unrealistic inasmuch as aromatics and saturates of similar distillation characteristics are quite different in density, the aromatics being much the heavier. On the other hand, the much tighter aromatic limitation for RP-1 compared to JP-5 permits a similar tightening of the specific gravity range. Thus, the narrow gravity range is not of itself a very stringent requirement. In the case of RP-1, physical property correlation studies favored the 42.0 - 45.0 range and to date, no sample has failed to meet this requirement.

Sulfur, total, percent wt., max.

RP-1	0.05
JP-5	0.4

Mixed hydrocarbon fuels which meet the aromatic requirement for RP-1 are generally sulfuric acid or sulfur dioxide treated fuels. A natural and favorable consequence of this treatment is the practically complete elimination of non-hydrocarbons, including sulfur compounds. It is widely recognized that organic sulfur and nitrogen compounds are largely responsible for adverse effects on the thermal stability of the fuel. There are indications even in today's engines, operating in the 500 - 700 psia chamber pressure range, that the thermal stability limits of hydrocarbon fuels are being rapidly approached. The higher heat rates associated with higher chamber pressure operation may very well soon exceed the thermal limits of many fuels. Hence, any action, however small or empirical, which will increase the thermal stability limits of hydrocarbon fuels, should be encouraged. The lowering in the total sulfur requirement is such a step.

Olefins, vol percent, max.

RP-1	1%
JP-5	5%

The olefin content of most JP fuels rarely exceeds 2 - 3%. In the particular case of RP-1, olefin content is reduced practically to the vanishing point for the same reasons (sulfuric acid or SO_2 treatment) as apply to total sulfur. The limit of 1% is quite liberal since RP-1 rarely assays more than 0.5%. However, the practical reason for restricting this species again has to do with thermal stability since, under pressure and at moderate temperatures, olefins are known to polymerize extensively. The occurrence of such pyrolysis reactions in thrust chamber coolant passages would be disastrous. The probability of this occurrence will increase markedly as rocket chamber pressures are increased in the quest for higher performance.

The RP-1 fuel specification thus represents a first major step in recognizing and to a considerable extent providing for the special requirements of large, advanced liquid propellant rocket engines. This specification still represents a considerable compromise between desirability and availability. As the importance of the rocket engine gains recognition, the application on a large scale of refining techniques already available, such as hydrotreating, and the introduction of new techniques will no doubt permit the specification of fuels of ever improving performance characteristics which can also be made available in adequate quantity at a reasonable cost.

TABLE I. Physical Properties of Hydrocarbon Fuels

	JP-5	JP-4	Kerosene	Amsco Solvent	Methyl cyclo hexane	Heptane	Isooctane	Toluene	Isopentane
Specific Gravity*	0.8380	0.7919	0.8125	0.7528	0.7720	0.7297	0.6950	0.8710	0.6239
API Gravity *	37.35	47.18	42.65	56.47	51.79	62.42	72.10	30.96	95.30
Viscosity, cs *	2.77	1.42	2.61	0.80	0.99	1.83	0.76	0.72	0.417
ASTM Distil., °F									
10%	390	200	377	206	209	202	205	222	81
50%	434	362	417	250	209	203	206	222	85
90%	498	436	471	268	209	204	206	222	89
Reid V.P.,Psi	0.15	2.05	0	0.68	1.55	1.84	1.79	1.13	> 15
Aniline PT, °F	133	132	157	128	102	128	176	< 80	
Smoke PT., MM	22	21	27	36	34	> 50	38	9.5	> 50
Flash PT., °F	147	< 78		< 75	< 70	< 15	< 70	< 55	< 75
Total Sulphur, %	0.34	0.09	0.03	0.02	0.09	0.02	0.26	0.04	0.01
Composition, %									
Saturates	77.1	90.8	94.7	92.9	97.8	95.7	99.5	0	100
Aromatics	22.4	8.8	4.8	6.6	1.9	3.8	< 0.5	100	0
Olefins	0.5	0.4	0.5	0.5	0.3	0.5	< 0.5	0	0
Net ΔH_c, BTU/lb	18460	18600	18640	18700	18640	19000	19080	17424	19303

* at 60 F

TABLE II Analytical Results for the Low Boiling Fuels

	Toluene (Phillips)	N-Heptane Phillips Comm. Gd.	Iso-octane (Phillips)	Methyl-Cyclo Hexane (Phillips)	Iso-octene (Phillips)
Density 40 F	0.8813	0.7322	0.7060	0.7809	0.7310
60 F	0.8709	0.7229	0.6968	0.7713	0.7216
68 F	0.8668	0.7192	0.6931	0.7675	0.7179
100 F	0.8501	0.7044	0.6784	0.7520	0.7028
API Gravity	30.98	64.24	71.58	51.95	64.59
Refract. Index, "D", 60 F	1.49421	1.40626		1.42267	1.4115
"F"	1.50527	-	-	1.42802	-
"C"	1.48932	1.40384	-	1.42022	-
Sp. Dispersion	184.0	-	-	101.6	-
Sp. Refraction	0.3360	0.3417	0.3584	0.3316	0.3462
Viscosity, Cks, 60 F	0.731	0.731	0.847	1.00	0.787
100 F	0.574	0.579	0.620	0.769	-
Reid V. P., PSI	0.8	1.7	1.8	1.6	1.4
Aniline Pt., F	-	129.2	176.0	102.2	109.0
Flash pt., F	<76	<70	<77	<80	<70
Total Sulfur, %	-	0.009	0.19	0.015	-
Mercaptan S, %	0.0003	0.0014	0.0009	0.001	0.0006
Copper Strip Cor.	0	-	0	-	-
Freezing pt. F	<-90	<-90	<-80	<-92	<-90
Water Reaction	1	1	1	1	1
Water Tolerance	0	0	0	0	0
Smoke pt., mm.	8.4	>50	44	>50	25
Exist. Gum, mg/100 ml	1.7	2.4	0.1	1.0	2.8
Potential Gum, mg/100 ml	7.2	3.6	2.7	2.4	-
Ht. of Comb. Net, Btu/lb	17,670	18,880	19,130	18,500	18,680

TABLE II Analytical Results for the Low Boiling Fuels (Contd.)

	Toluene (Phillips)	N-Heptane Phillips Comm. Gd.	Iso-octane (Phillips)	Methyl-Cyclo Hexane (Phillips)	Iso-octene (Phillips)
Diesel Index	-	105.3	126.0	53.09	70.40
Characterization F.	10.1	12.0	12.0	11.3	12.1
Refract. Intercept	1.0608	1.0467	1.0647	1.0389	1.0526
A.S.T.M. Dist.					
IBP., F	221	203	204	205	204
10%	225	203	206	207	208
20%	225	203	206	208	208
30%	225	203	206	208	208
40%	225	204	206	208	208
50%	225	204	206	208	208
60%	225	204	206	208	208
70%	226	205	206	208	210
80%	226	205	206	208	210
90%	226	206	206	208	210
95%	226	206	207	209	-
End pt.	275	263	258	260	218
Residue, %	0.5	0.2	0	0.3	0.5
C/H, wt.	10.5	6.05	6.02	7.06	-
Aromatics, V. %	99.6	3.4	0.5	1.1	<0.5
Olefins, V.%	<0.4	<0.4	<0.5	<0.5	99.5
Saturates, V. %	<0.4	96.2	99.5	98.4	<0.5
N-paraffins, V. %	<0.4	39	1	<1	-
Naphthenes V. %	<0.4	31	2	95.2	<0.5
I-paraffin, V. %	<0.4	26.2	97	2.2	<0.5

TABLE II Analytical Results for the Low Boiling Fuels (Contd)

	Toluene (Phillips)	N-Heptane Phillips Comm. Gd.	Iso-octane (Phillips)	Methyl-Cyclo Hexane (Phillips)	Iso-octene (Phillips)
			AROMATIC FRACTION		
Benzene, V. %	1	0.9	1.0	37.5	-
Toluene, V. %	99	99.1	99.0	62.5	-
			SATURATE FRACTION		
Propyl Benzene					
Density, 60 F	-	0.7256	0.6965	0.7706	
68 F	-	0.7220	0.6929	0.7668	-
100 F	-	0.7077	0.6783	0.7514	-
API Gravity		63.51	71.66	52.12	
Aniline pt., F	-	131.7	174.9	104.0	-
Refract. Index "D" 68 F	-	1.40391	1.3917	1.42204	-
"F"	-	-	-	1.42708	-
"C"	-	1.40158	-	1.41960	-
Sp. Refraction	-	0.3387	0.3434	0.3314	-
Sp. Dispersion	-	-	-	97.55	-
Refract. Intercept	-	1.0429	1.0453	1.0386	-
Ht. of Comb. Net.	-	18,820	19,250	18,510	-
Naphthene, V. %	-	32	2	97	-
N-Paraffin, V. %	-	41	1	1	-
Iso-paraffin, V. %	-	27	97	2	-
Major Constituent	-	41	97	97	96
Pentane	-	-	-	-	-
Hexane	-	-	-	0	-
Heptane	-	41	1	1	-
Octane	-	-	-	-	-
Methylcyclohexane	-	32	0.6	97	-

TABLE II Analytical Results for the Low Boiling Fuels (Contd.)

	Toluene (Phillips)	N-Heptane Phillips Comm. Gd.	Iso-octane (Phillips)	Methyl-Cyclo Hexane (Phillips)	Iso-octene (Phillips)
Iso-Octanes	-	24	97.4	1	-
Methylcyclopentane	-	-	-	-	-
Cyclohexane					
All other	-	3	1.0	1	4

TABLE III Analytical Results for the High Boiling Fuels

Test	Reference JP-5	RP-1 (Std. Oil of Calif.-Pearl Oil)	High Cetane Ref. Fuel	Heavy Alk. Bottoms	Heavy Arom. Naptha	UMF Grade C	St'd. Thinner No. 425
Density, 40 F	0.8119	0.8184	0.8101	0.8042	0.9395	0.8590	0.8141
60 F	0.8039	0.8106	0.8023	0.7965	0.9311	0.8516	0.8061
68 F	0.8008	0,8075	0.7992	0.7934	0.9277	0.8493	0.8030
100 F	0.7879	0.7950	0.7867	0.7811	0.9144	0.8368	0.7933
Refractive Index at 68 F "D"	1.44300	1.44577	1.44734	1.4449	1.53809	1.46326	1.44412
"F"	1.44879	1.45106	1.45370	1.45020	1.55195	1.46850	1.44934
"C"	1.44148	1.44323	1.44457	1.44178	1.53284	1.46050	1.44154
Specific Dispersion, 68 F	91.3	96.9	114.0	106.0	206.0	94.4	97.0
Specific Refraction	0.3317	0.3300	0.3345	0.3351	0.3372	0.3245	0.3309
API Gravity	44.52	42.98	45.00	46.15	20.50	34.52	44.03
Viscosity, CKS, 60 F	2.53	2.64	3.23	7.20	2.68	4.85	2.83
100 F	1.71	1.75	2.21	3.98	1.77	2.90	1.86
Reid V.P. PSI	0	0.1	0	0	0	0.1	0.1
Aniline Pt. F	161.1	159.8	167.2	196.0	<80	158.0	165.0
Flash Pt. F	142	135	181	181	156	196	137
Total Sulfur, %	0.007	0.007	0.11	0.018	-	0.017	0.009
Mercaptan S, %	0.0009	0.0014	0.04	0.001	0.0003	0.004	0.0005
Cop. Strip Corr.	0	0	0	1	0	0	1
Freezing pt., F	-58	-58	-14	-82	-62	-80	-48
Water Reaction	1	1b	1	Emulsion	1	1	1
Water Tolerance	0	0	0	-1	0	0	0
Smoke pt. mm	32	31	31	29	5.5	21	33
Gum, Existent (mg./100 m.)	1.4	4.2	2.6	123	7.2	2.5	2.5

TABLE III Analytical Results for the High Boiling Fuels (Contd.)

Test	Reference JP-5	RP-1 (Std. Oil of Calif.- Pearl Oil)	High Cetane Ref. Fuel	Heavy Alk. Bottoms	Heavy Arom. Naptha	UMF Grade C	St'd. Thinner No. 425
Gum, potential (mg./100 ml.)	3.2	5.8	3.2	125	8.3	5.2	2.8
Diesel Index	71.72	68.68	75.24	90.45	-	54.54	72.65
Characterization Factor	11.9	11.8	12.2	12.2	10.4	11.4	11.9
Refract. Intercept.	1.0437	1.0419	1.0477	1.0478	1.0742	1.0386	1.0427
Molecular wt.	178	179	191	232	165	185	181
Ht. of Combustion Gross, BTU/lb	-	19,940	19,990	20,050	18,440	-	20,010
Ht. of Combustion Net, BTU/lb	18,690	18,660	18,690	18,730	17,570	18,520	18,700
ERDCO Thermal Stability, min./28" HG	>300	>300	>300	59	280	>300	>300
ASTM Distillation							
IBP, F	354	356	414	408	382	436	372
10%	380	379	436	431	388	452	400
20%	392	390	446	439	407	455	410
30%	398	400	454	450	425	461	418
40%	409	409	464	458	440	466	426
50%	419	419	473	466	451	471	433
60%	427	430	482	478	461	477	440
70%	437	440	492	494	471	483	450
80%	452	454	504	521	481	496	460
90%	473	472	524	574	488	513	477
95%	498	491	544	598	502	532	492
End Point	527	506	560	598	533	546	506
Residue	1.1	1.4	1.3	0.5	1.1	1.5	1.2

TABLE III Analytical Results for the High Boiling Fuels (Contd.)

Test	Reference JP-5	RP-1 (Std. Oil of Calif.- Pearl Oil)	High Cetane Ref. Fuel	Heavy Alk. Bottoms	Heavy Arom. Naptha	UMF Grade C	St'd. Thinner No. 425
Aromatics, Vol. %	2.7	2.3	11.8	(3)	85.1	2.6	2.9
Olefins, Vol. % (By chromatography)	0.5	0.5	0.4	(0.6)	0.8	0.3	0.5
Bromine No.	0.01	0.02	1.2	6.0	0.62	0.07	0.07
Vol. % Olefins based on Bromine No.	0.01	0.02	1.4	8.7	0.56	0.09	0.08
Saturates, Vol. %	96.8	97.2	87.8	96.1	14.1	97.1	96.6
N-paraffins, Vol. %	16.0	11.0	20.0	1	2	<1	15.5
Iso-paraffins Naphthenes, Vol. %	80.8	86.2	67.8	95.1	12.1	96.1	81.8
Arom. C, st. %	0.4	0.5	7.3	3	57	2	0.5
Naph. C, wt. %	39.4	42.7	18.0	8.4	9.0	62	38.4
Paraffin C, wt. %	60.2	56.8	74.7	88.6	34	36	61.1
Aromatic Rings/mol.	0.01	0.01	0.17	0.09	1.18	0.03	0.013
Napthene Rings/mol.	0.88	0.96	0.44	0.24	0.31	1.60	0.87
Total Rings/mol.	0.89	0.97	0.61	0.33	1.49	1.63	0.88
SATURATE FRACTION							
Density, 60 F	0.8051	0.8061	0.7927	0.7943	-	0.8509	0.8054
68 F	0.8019	0.8039	0.7896	0.7912	0.7978	0.8478	0.8022
100 F	0.7891	0.7913	0.7771	0.7789	-	0.8355	0.7895
Refract. Index "D" 68 F	1.44186	1.44430	1.44728	1.44345	1.44162	1.46232	1.44308
"F"	1.44719	1.44965	1.45334	1.44921	1.44688	1.46802	1.44823
"C"	1.43936	1.44178	1.44463	1.44088	1.43918	1.45973	1.44057
Sp. Dispersion, 68 F	98.1	97.9	110.0	105.0	90.5	97.8	95.7
Molecular Wt.	175	176	191	233	151	185	181

TABLE III Analytical Results for the High Boiling Fuels (Contd.)

Test	Reference JP-5	RP-1 (Std. Oil of Calif.- Pearl Oil)	High Cetane Ref. Fuel	Heavy Alk. Bottoms	Heavy Arom. Naptha	UMF Grade C	St'd. Thinner No. 425
Aniline pt., F	164.7	164.7	177.1	197.6	171.1	159.4	167.3
Ht. of Comb, Net	18,730	18,700	18,810	18,900	-	18,520	18,720
Refract. Intercept.	1.0427	1.0424	1.0525	1.0479	1.04272	1.0384	1.0420
Degree of Branching	0.62	0.41	0.14	0.56	0.16	0.62	0.39
CH/mol	1.0	2.2	0.9	1.8	0.7	0.8	0.95
CH2/mol.	5.0	7.3	11.8	5.4	8.6	7.8	8.7
CH3/mol.	8.4	5.0	2.8	11.8	3.1	6.6	5.1
		N-PARAFFIN FRACTION					
V. % °F N-paraffins							
C-9	1	1	-	-	-	-	1
C-10	5	4	5				5
C-11	12	7	10				11
C-12	30	17	18				21
C-13	24	27	23				25
C-14	15	23	15				18
C-15	9	9	10				8
C-16 & Higher	4	12	19				11
		AROMATIC FRACTION					
Density, 60 F	0.9001	0.9055	0.9465	0.813	0.9416	0.9224	0.9063
68 F	0.8968	0.9028	0.9430	0.809	0.9411	0.9196	0.9037
100 F	0.8848	0.8894	0.9301	0.794	0.9391	0.9082	0.8907
API Gravity	25.86	24.77	18.00	42.60	18.06	21.90	24.63

TABLE III Analytical Results for the High Boiling Fuels (Contd.)

Test	Reference JP-5	RP-1 (Std. Oil of Calif.- Pearl Oil)	High Cetane Ref. Fuel	Heavy Alk. Bottoms	Heavy Arom. Naptha	UMF Grade C	St'd. Thinner No. 425
Refract. Index "D", 68 F	1.50582	1.5119	1.5455	1.45037	1.55928	1.5150	1.5113
"F"	1.51544	1.5222	1.5591	1.45590	1.57503	1.5246	1.5214
"C"	1.50170	1.5077	1.5400	1.44759	1.55325	1.5110	1.5071
Sp. Dispersion	154	161	203	104	232	148	159
Sp. Refraction	0.3309	0.3323	0.3355	0.3324	0.3432	0.3279	0.3317
Molecular Wt.	168	157	162	233	165	189	162
Arom. Rings/mol.	0.98	1.0	1.32	0.6	1.55	1.0	1.0
Naph. Rings/mol	0.45	0.47	0.44	0.60	0.03	0.85	0.82
C-atoms/mol.	12.4	11.6	12.1	16.9	12.3	13.9	12.0
Naph. C-atoms/mol.	1.8	1.9	1.76	2.5	0.1	3.4	3.3
Par. C-atoms/mol.	4.6	3.7	3.06	10	4.0	4.5	2.7
Arom. C-atoms/mol.	6.0	6.0	7.28	4.4	8.2	6.0	6.0
C/H, Wt.	7.6	7.8	8.6	6.5	8.8	8.4	8.0
H/C, mol.	1.58	1.54	1.4	1.8	1.4	1.44	1.5
Substituents/mol	2.75	2.90	2.94	3.40	2.88	2.74	2.80
Double Bonds/mol.	3	3	3.6	2.2	4.1	3	3
CH_3/mol.	4.4	4.1	3.6	9.3	3.2	5.0	4.0
CH_2/mol.	3.9	3.6	3.8	4.6	2.5	4.7	3.6
CH/mol.	4.1	3.9	4.7	3.0	6.6	4.2	4.4
Total Rings/mol.	1.43	1.47	1.76	1.24	1.58	1.84	1.82
Arom. C, Wt. %	45	52	60	26	66.4	44	50
Naph. C, Wt. %	15	16	15	15	1.0	24	27.5
Par. C, Wt. %	40	32	25	59	32.6	32	22.5
Degree of Branching	0.54	0.56	0.57	0.65	0.29	0.61	0.62
Refract. Intercept.	1.0565	1.0605	1.0740	1.0459	1.0887	1.0552	1.0595

TABLE IV. Comparative Requirements for RP-1 and JP-5

Requirements	RP-1 (MIL-F-25576A)	JP-5 (MIL-F-5624C)
Distillation		
Initial boiling point		
10% distillation point, min °F	365	400
10% distillation point, max °F	410	
50% distillation point		
90% distillation point		
End point, max °F	525	550
Residue, volume percent, max	1.5	1.5
Distillation loss, volume percent, max	1.5	1.5
Gravity °API - Min (sp gravity, max)	42.0 (0.815)	36.0 (0.845)
Gravity °API - Max (sp gravity, min)	45.0 (0.801)	48.0 (0.788)
Existent gum, mg/100 ml, max	7	7
Potential gum, mg/100 ml, max	14	14
Sulfur, total, percent wt. max	0.05	0.4
Mercaptan-Sulfur, percent wt, max		0.005
Freezing point, °F, max	-40	-40
Thermal value		
Heat of combustion (lower or net) BTU/lb/min	18,500	18,300
Viscosity, centistokes at - 30°F, max	16.5	16.5
Aromatics, Volume percent, max	5.0	25.0
Olefins, volume percent, max	1.0	5.0
Smoke point, mm, min	28.0	20.0
Corrosion		
Water reaction		
Flash point, min	110°F	140°F
Aniline point, °F		

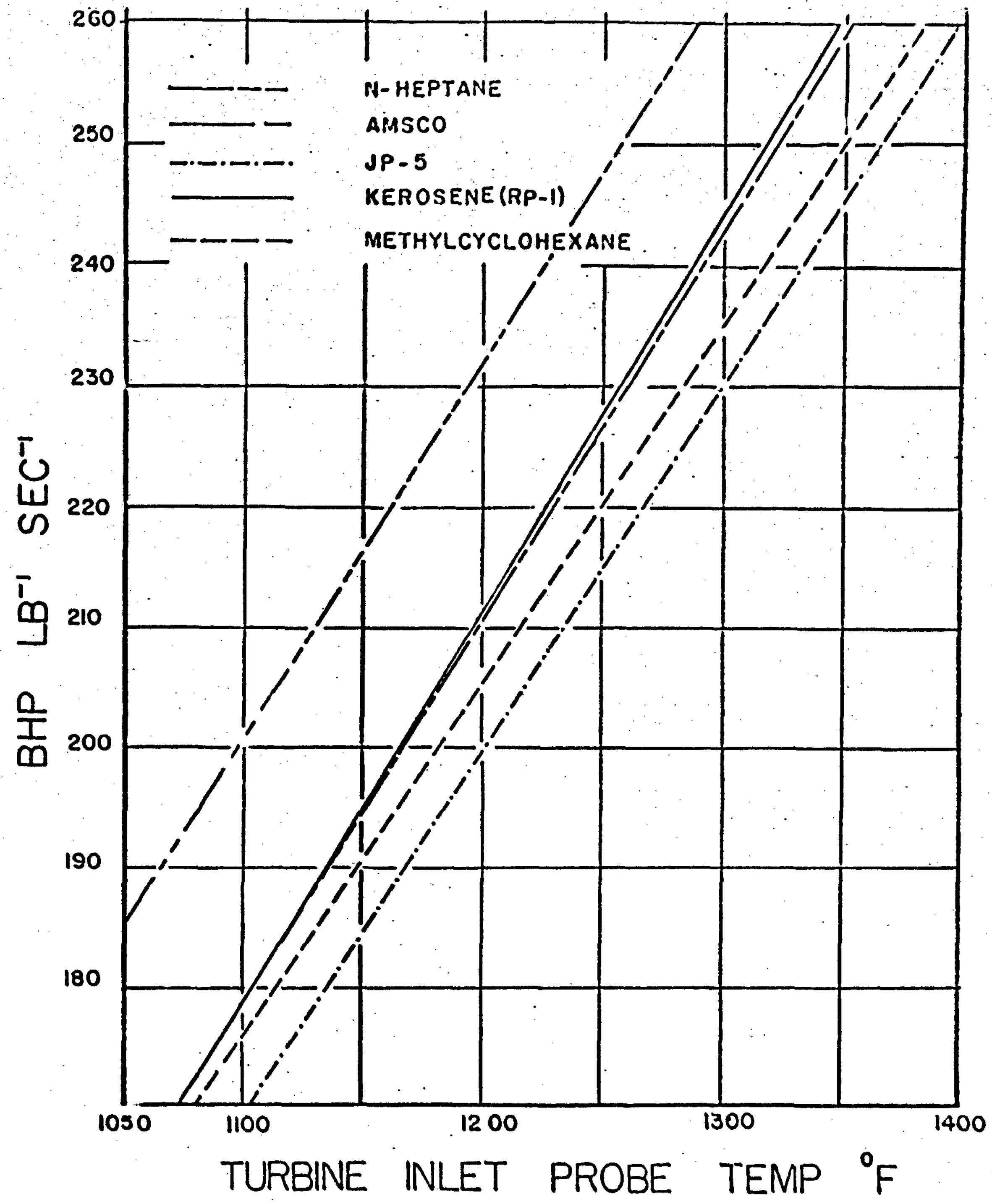

FIG. 1. Turbine Inlet Temp. vs Available Energy
(Large Engine Gas Generator)

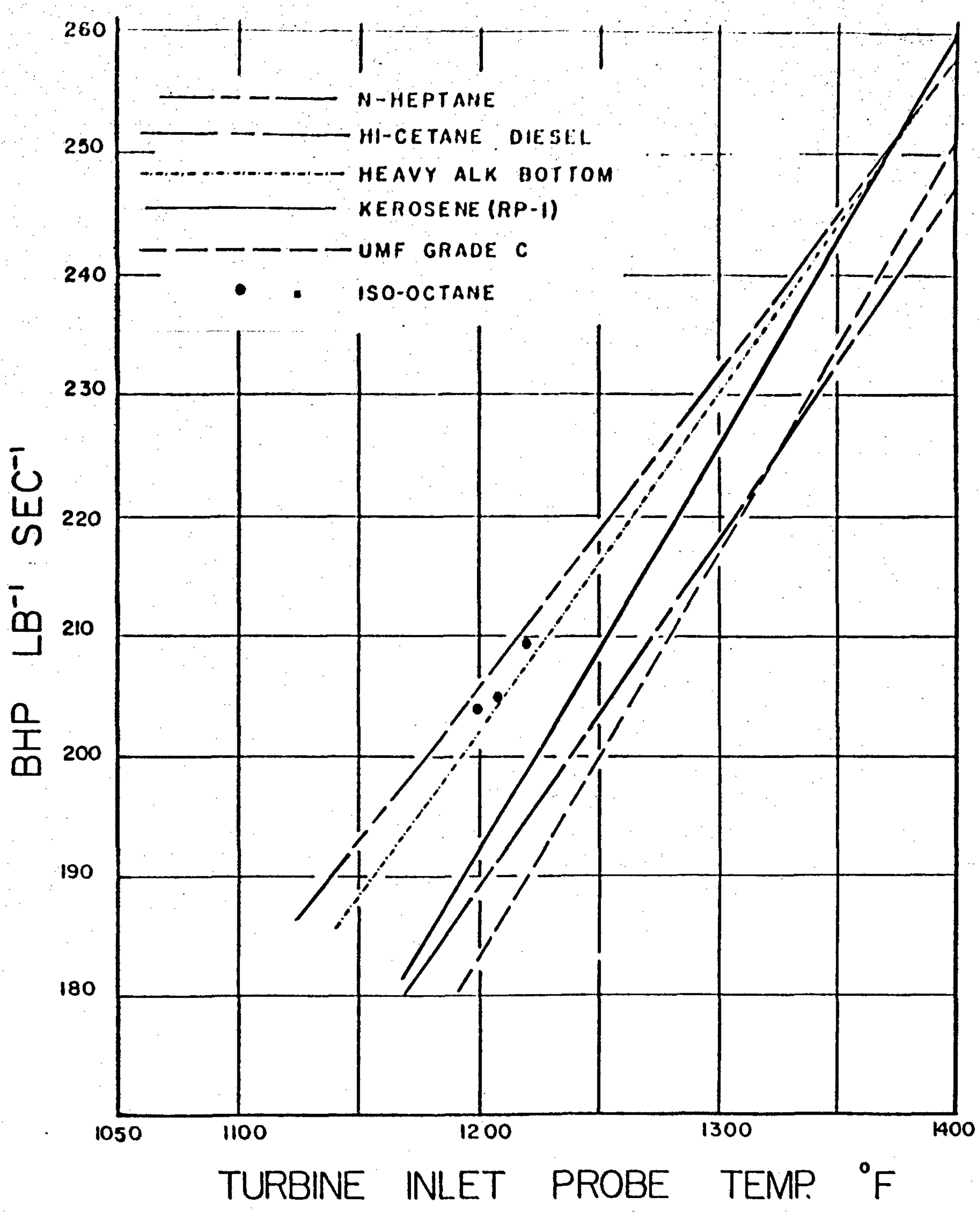

FIG. 2. Turbine Inlet Temp. vs Available Energy
(Large Engine Gas Generator)

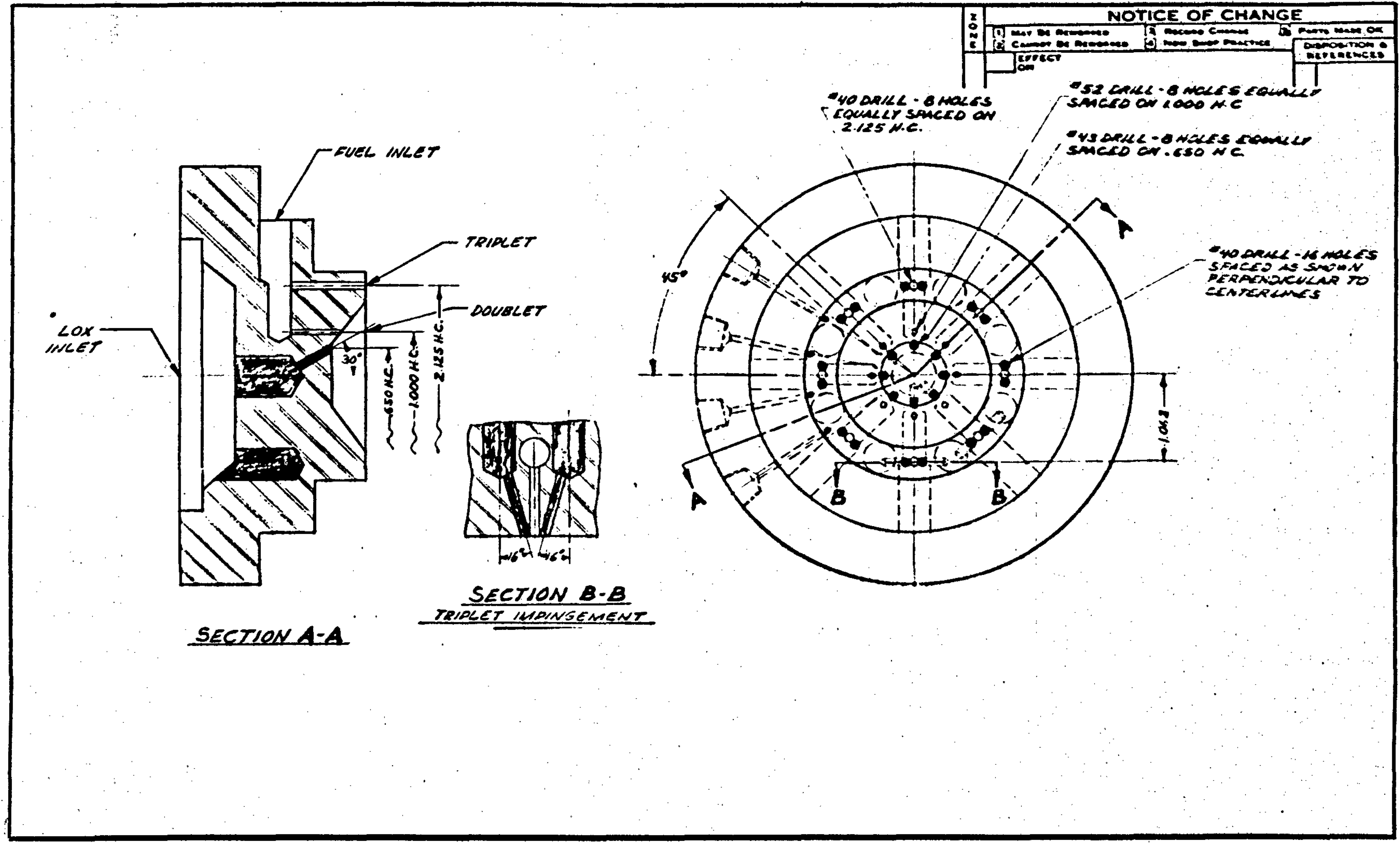
NOTICE OF CHANGE
ZONE
Record Change
New Shop Practice
Parts Made OK
Disposition & References
Effect On
#52 DRILL - 8 HOLES EQUALLY SPACED ON 1.000 H.C
#43 DRILL - 8 HOLES EQUALLY SPACED ON .650 H.C
#40 DRILL - 8 HOLES EQUALLY SPACED ON 2.125 H.C.
#40 DRILL - 16 HOLES SPACED AS SHOWN PERPENDICULAR TO CENTERLINES
45°
A
A
B
B
1.043
FUEL INLET
TRIPLET
DOUBLET
LOX INLET
30°
.650 H.C.
1.000 H.C.
2.125 H.C.
SECTION A-A
16°
16°
SECTION B-B
TRIPLET IMPINGEMENT

FIG. 3. Fuels Evaluation Motor Spoke Injector #1 - Reversed Triplet-Doublet

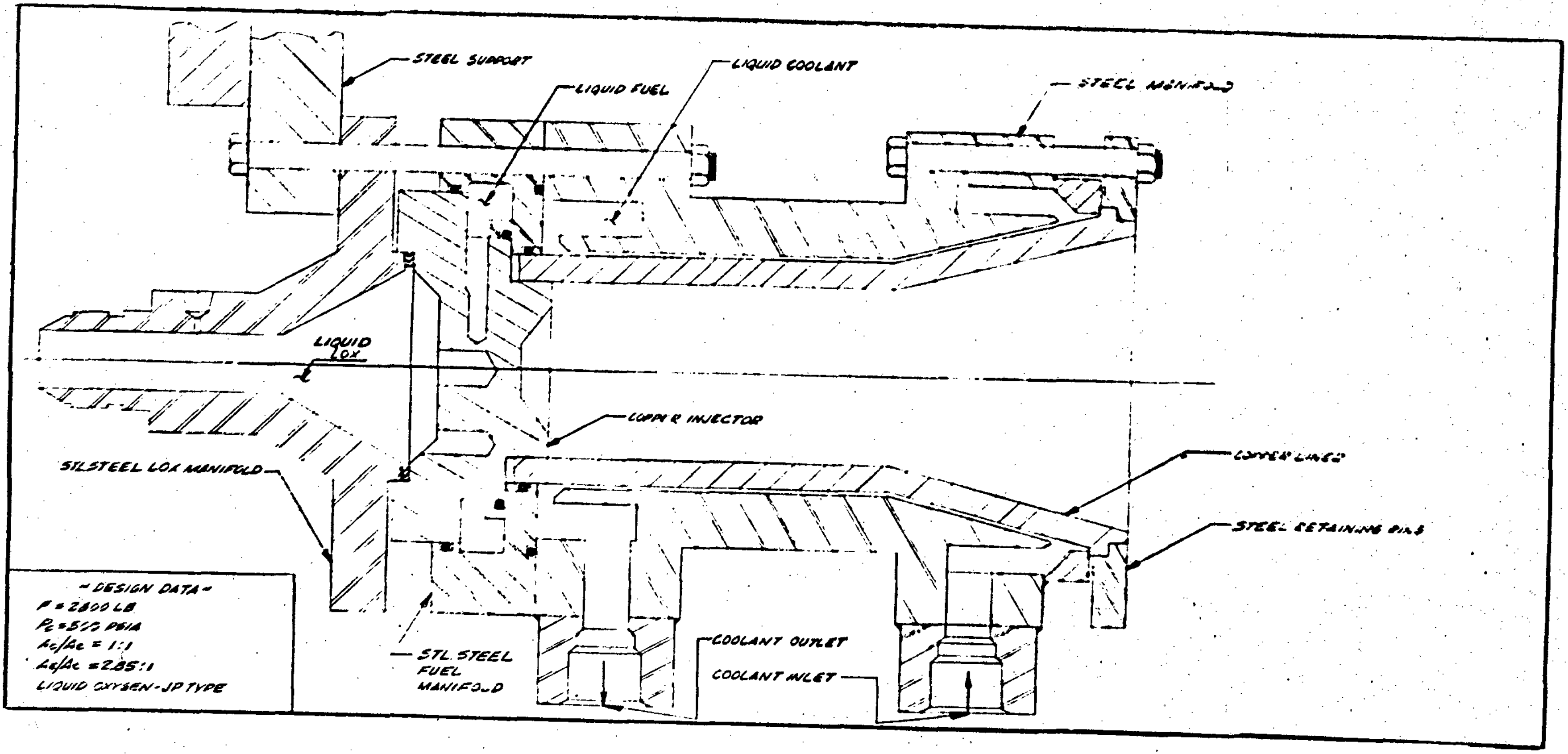
STEEL SUPPORT
LIQUID FUEL
LIQUID COOLANT
STEEL MANIFOLD
LIQUID LOX
COPPER INJECTOR
COPPER LINER
STEEL RETAINING PINS
STLSTEEL LOX MANIFOLD
STL STEEL FUEL MANIFOLD
COOLANT OUTLET
COOLANT INLET
~DESIGN DATA~
F = 2800 LB
Pc = 500 PSIA
Ac/At = 1:1
Ae/At = 2.85:1
LIQUID OXYGEN-JP TYPE

FIG. 4. Fuels Evaluation Motor Assembly

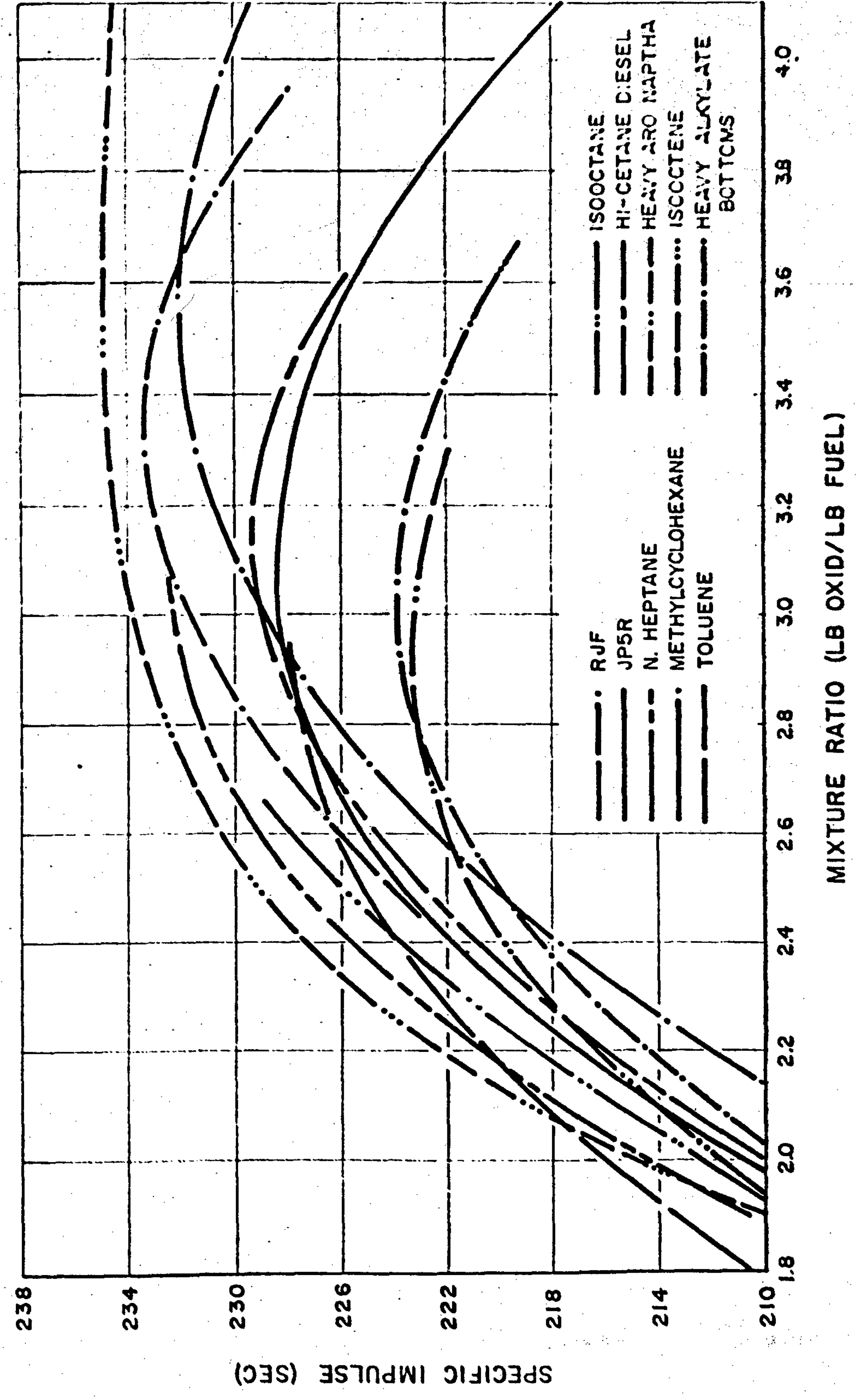

FIG. 5. Statistical Curve - Fits for Adjusted Data from the Fuels Program 5"L* Fuels Evaluation Motor

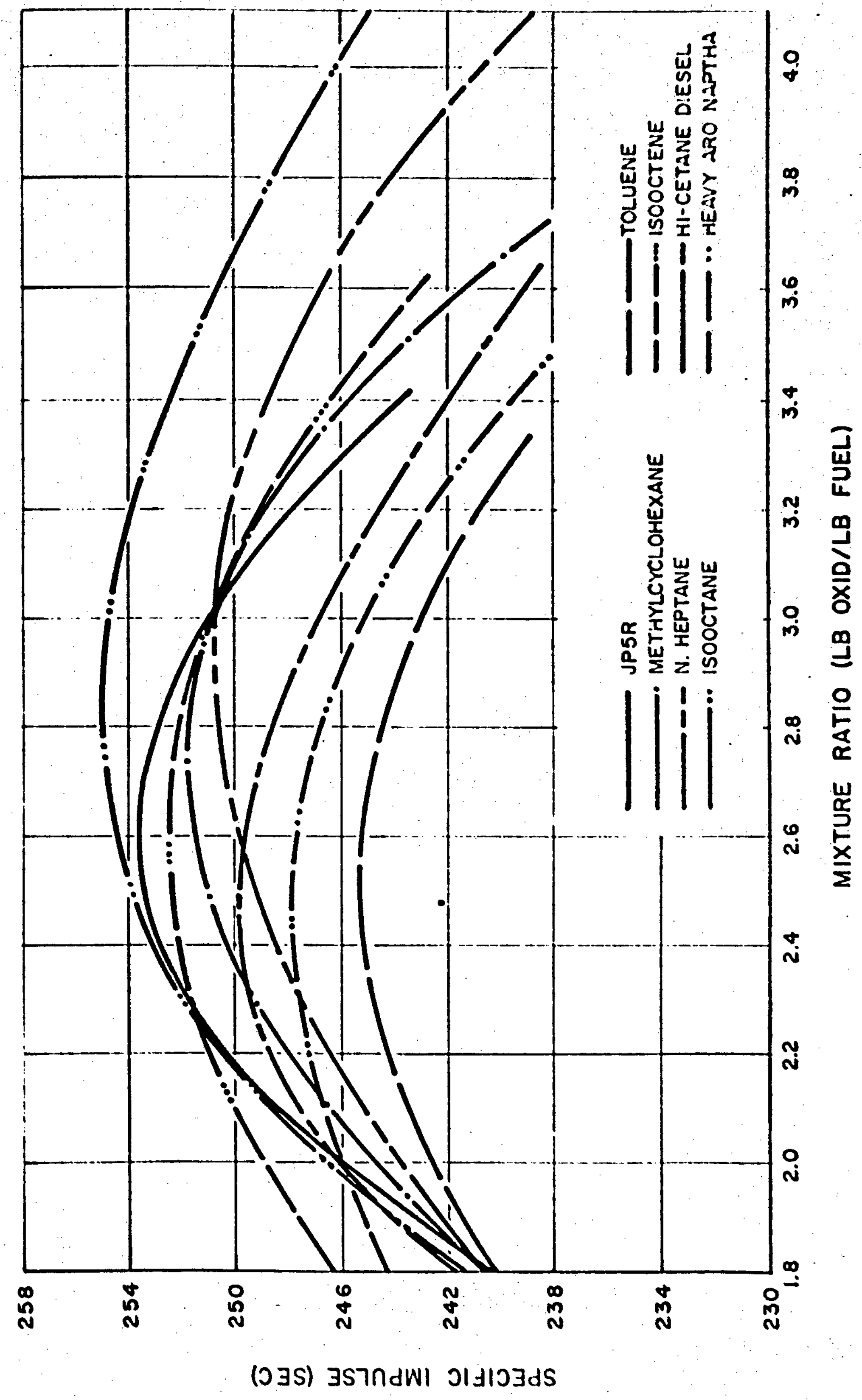

FIG. 6. Statistical Curve - Fits for Adjusted Data from the Fuels Program 20"L* Fuels Evaluation Motor

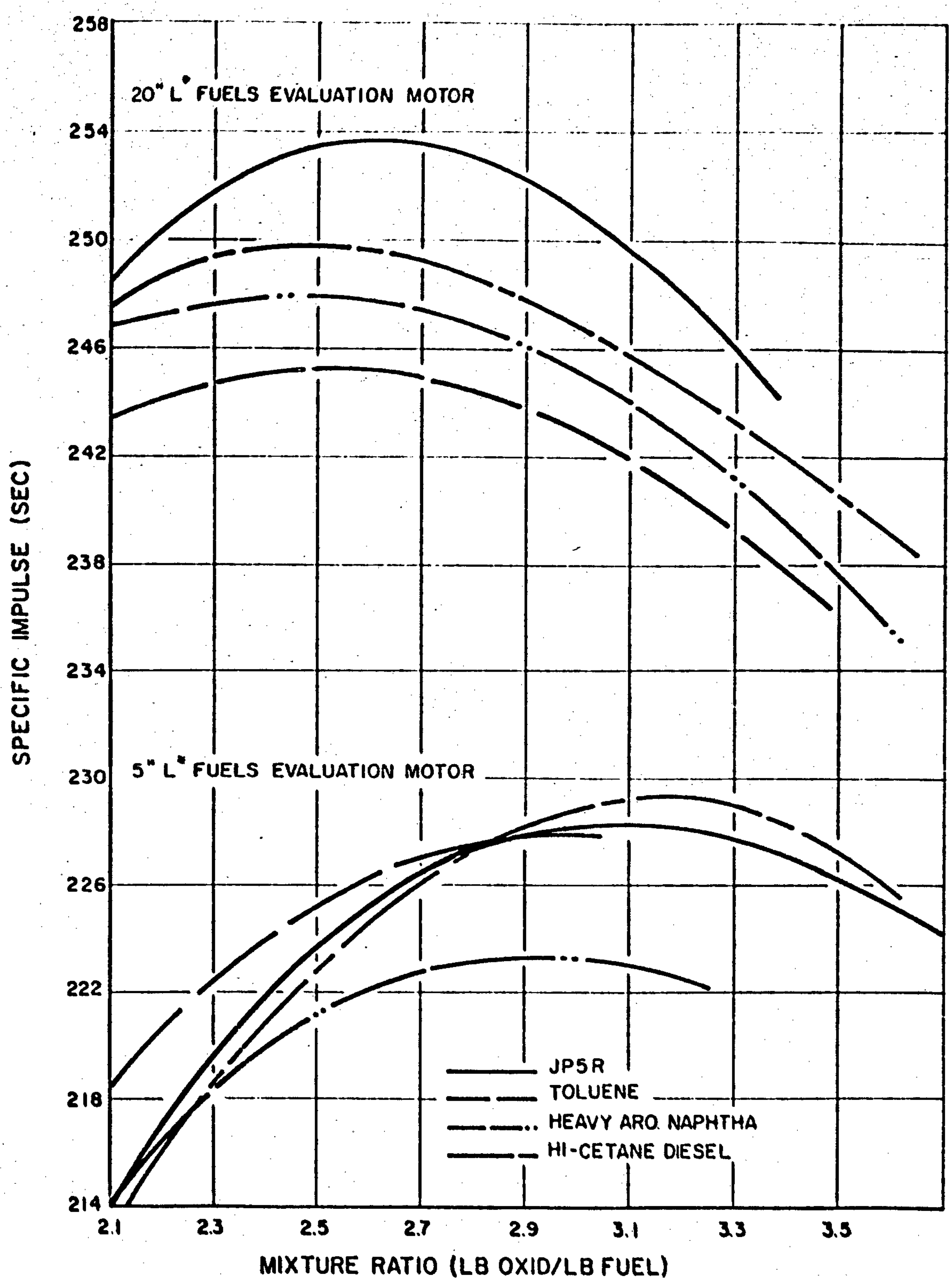

FIG. 7. Statistical Curve - Fits for Adjusted Data from the Fuels Program

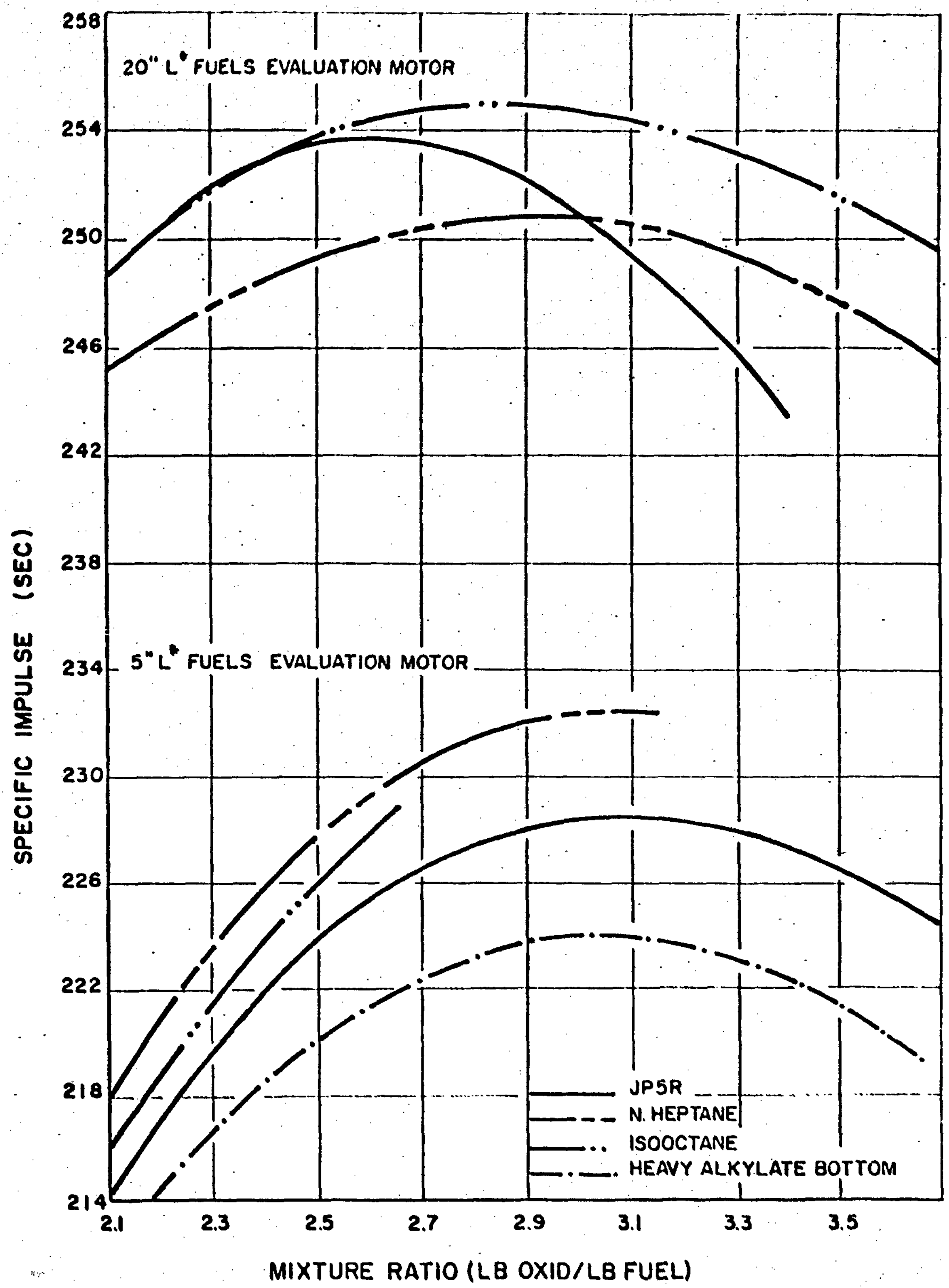

FIG. 8. Statistical Curve - Fits for Adjusted Data from the Fuels Program

CONFIDENTIAL

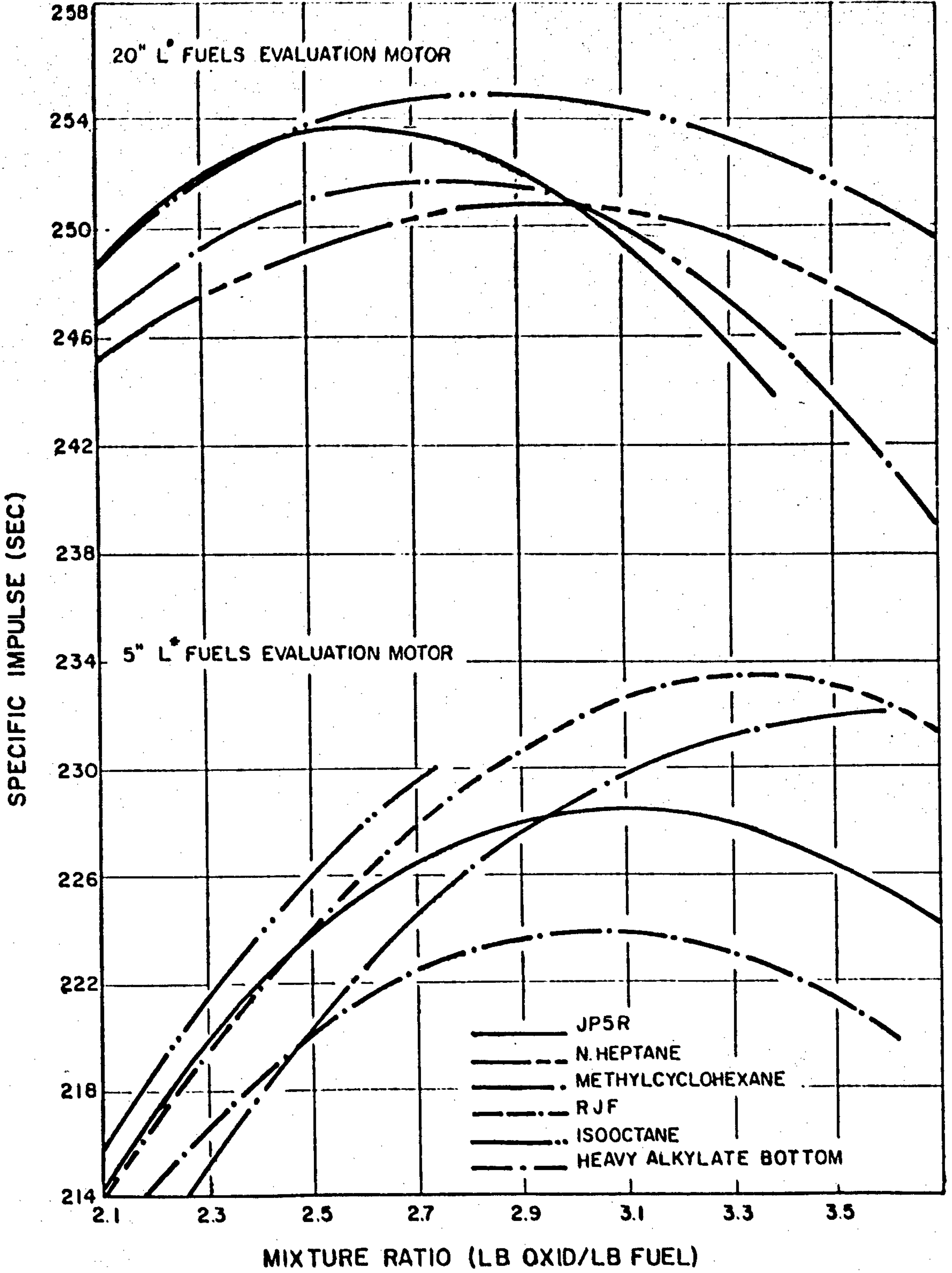

FIG. 9. Statistical Curve - Fits for Adjusted Data from the Fuels Program

CONFIDENTIAL

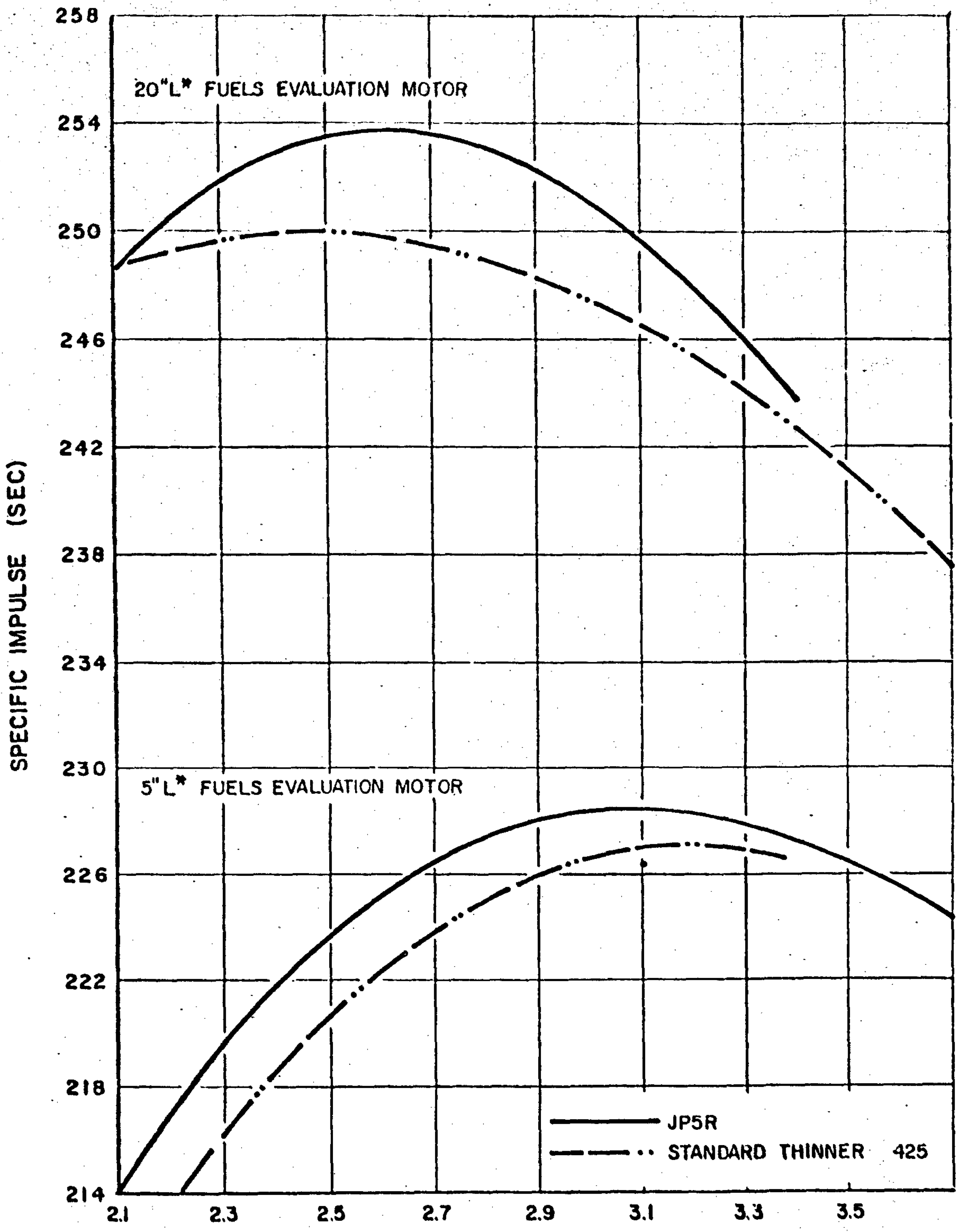

FIG. 10. Statistical Curve - Fits for Adjusted Data from the Fuels Program

THE PERFORMANCE OF UNSYM-DIMETHYLHYDRAZINE-RED NITRIC ACID IN A MOTOR AT VARYING THRUST LEVELS

N. J. Sippel, D. H. Couch, and Stanley Singer
U. S. Naval Ordnance Test Station
China Lake, California

The study of the 5.0-Inch Liquid-Propellant Aircraft Rocket (LAR) at the U. S. Naval Ordnance Test Station was concerned with development of a liquid propellant motor with distinctive characteristics (1). High thrust was required from a small combustion chamber. In the program beginning in 1950 studies were directed to motors operating at 1,500-1,800 psi chamber pressures with characteristic chamber length (L*) of 8.5-20 inches. In terms of propellant consumption, performance specifications required study of propellant loading density rates in the combustion chamber in the range 0.5-3.0 pounds per second per cubic inch of chamber volume. As development progressed performance obtained from the bipropellant systems used in the rocket gradually improved from 62% to almost 90% of theoretical. The increase in performance largely followed improvements in the design of the injector.

With impending requirements for motors capable of supplying continuously variable thrust on demand, attention turned to application of the LAR motor for this purpose. Initial studies were directed to investigation of combustion stability and performance in a motor with fixed injector and nozzle area.

In this simple approach thrust variation in the missile would ostensibly be obtained by variation of the force used in transferring the propellants or by variation of the pressure drop in propellant flow upstream of the injector. This contrasts with methods which control propellant flow by variation of injector orifice area and nozzle throat area, which may make available significantly higher performance over wide ranges of thrust (2, 3, 4).

The PEMLAR

The combustion and performance tests were made in a static test motor modeled on the LAR and used for propellant evaluation, the

PEMLAR. A schematic diagram of the motor in its test stand is shown in figure 1. High-pressure nitrogen gas is used to feed the propellants in parallel oxidizer and fuel tanks and propellant lines for the tests. The propellant lines are firmly braced. The motor used in propellant evaluation tests is shown in figure 2.

The injector is illustrated separately by figure 3. The injector contains 36 alternating oxidizer and fuel orifices in a single ring with a diameter of 1.7 inches. For the usual tests propellant mass flow is controlled largely by the orifice dimensions. The propellants are injected into the combustion chamber axially; they are deflected toward its center by the deflector ring. The action of the injector may thus be compared with that of an optical system. The angle of the deflector surface provides a means of focusing or concentrating propellants toward a point at a selected distance from the plane of the injector.

This motor, which is somewhat improved over the LAR, has given somewhat higher performance. For example, up to 99% of theoretical c* has been obtained with unsym-dimethylhydrazine (DMH) and red fuming nitric acid containing 20% nitrogen dioxide (RFNA). Some propellant investigations in the motor with 20-inch L* shown in figure 2 are summarized in table 1 to illustrate typical studies and performance results.

TABLE 1.

PEMLAR Propellant Studies

Fuel[a]	Deflector[b]	Oxidizer: Fuel Ratio[c]	R_c[d] lb/in^3/sec	P_c[e] psi	c*[f], fps
DMH	Mod 1	2.35-2.93	0.45	1490	5165 ± 25
DMH	Mod 2	2.60	0.45	1465	5255 ± 40
Hydrazine 32% Ammonium Thiocyanate	Mod 1	1.33-1.57	0.47	1460	5050 ± 10
1,3-Bis(dimethylamino)-propane[g]	Mod 2	2.90-3.46	0.45	1460	5230 ± 15
Aniline[h]	Mod 1	1.92-2.67	0.45	1320	3995 ± 145
Tetramethyltetrazene[i]	Mod 1	2.33-2.57	0.45	1460	5130 ± 80

a. The oxidizer used had the nominal composition HNO_3 77%, NO_2 20%, HF 0.5%, H_2O 2.5%. b. Two deflector rings were

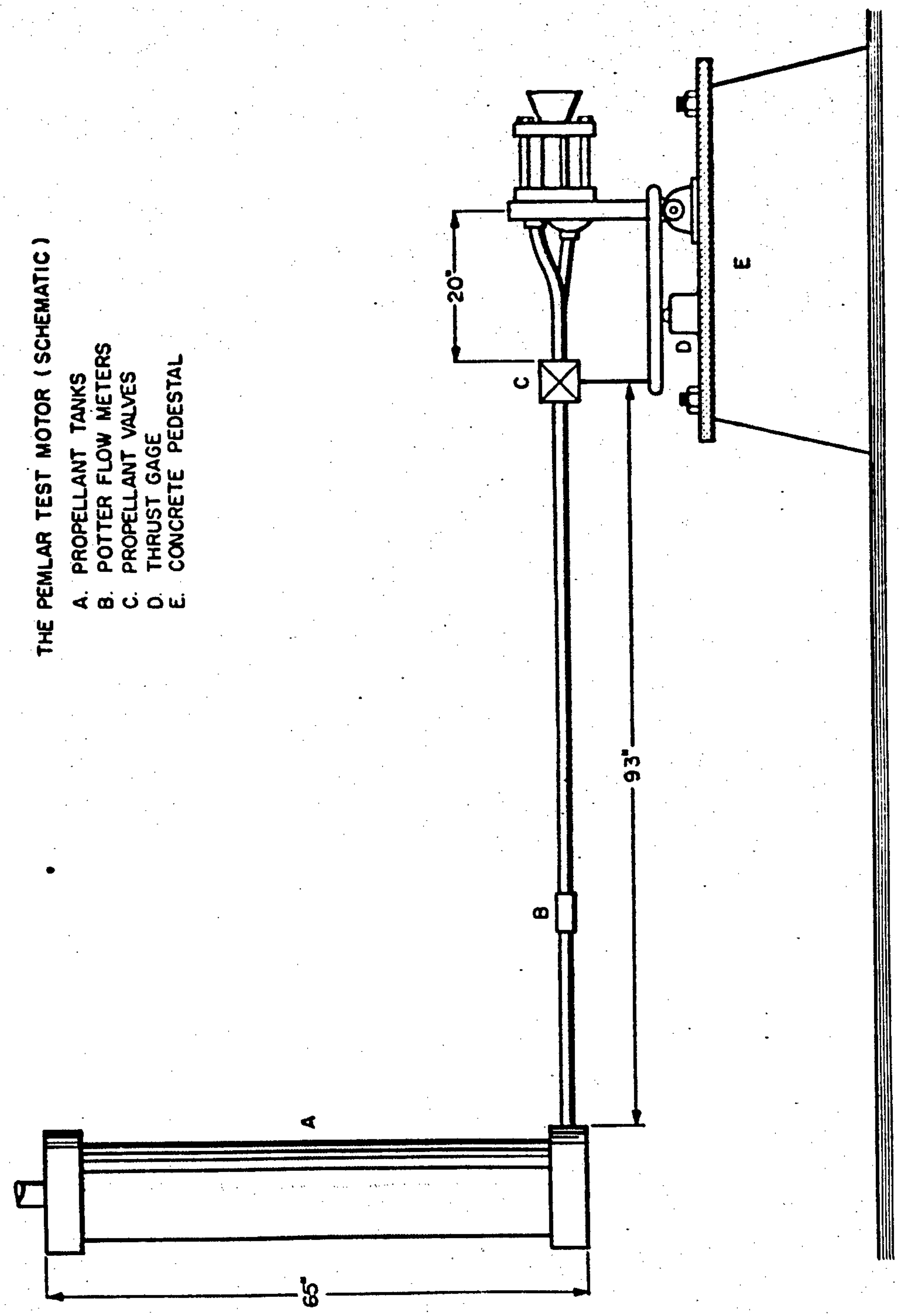
THE PEMLAR TEST MOTOR (SCHEMATIC)
A. PROPELLANT TANKS
B. POTTER FLOW METERS
C. PROPELLANT VALVES
D. THRUST GAGE
E. CONCRETE PEDESTAL
A
B
C
D
E
20"
93"
68"

Figure 1. The PEMLAR Test Motor

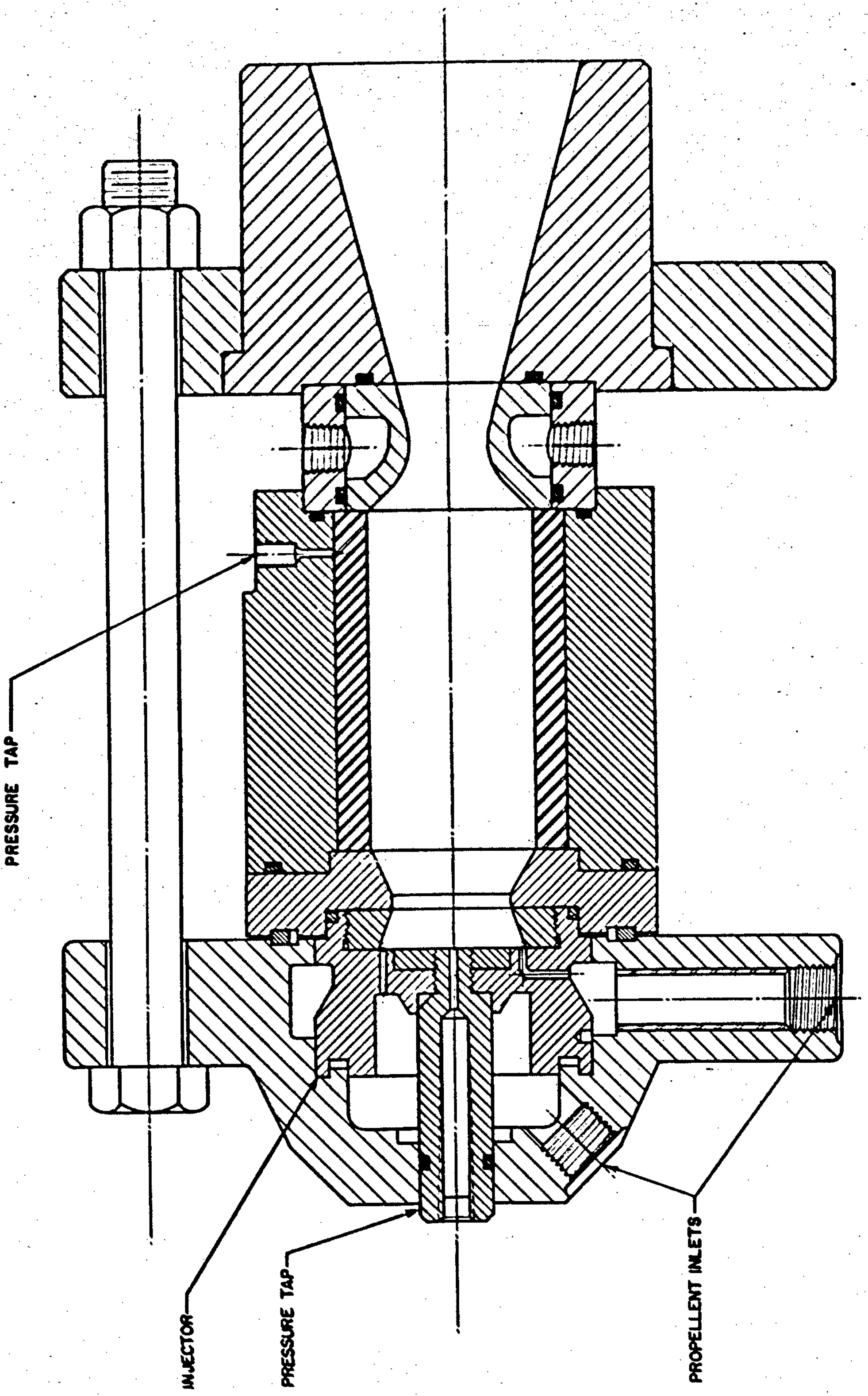
PRESSURE TAP
INJECTOR
PRESSURE TAP
PROPELLENT INLETS

Figure 2. The PEMLAR Small-Diameter Motor
Internal Dimensions: 2" X 4"

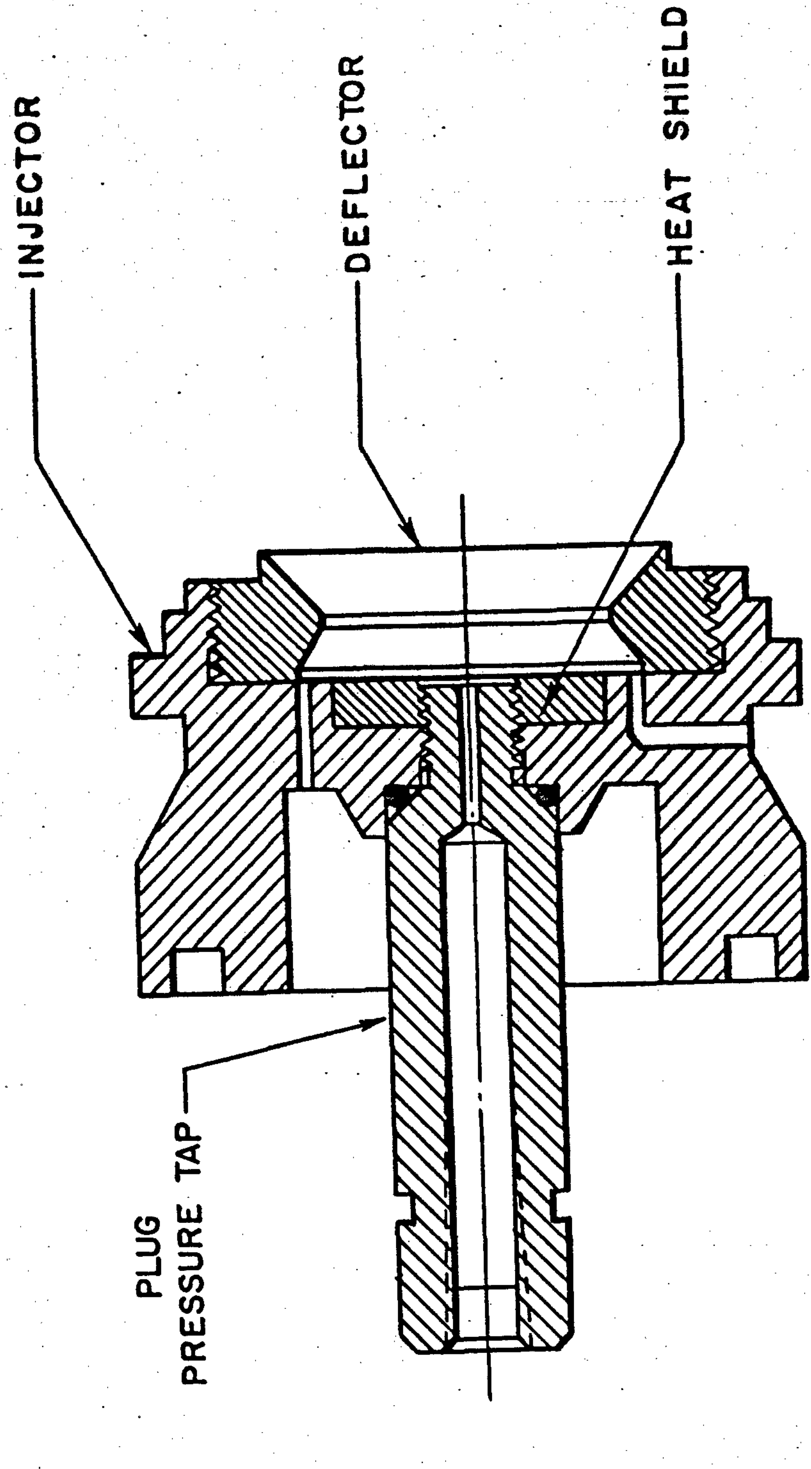
INJECTOR
DEFLECTOR
HEAT SHIELD
PLUG
PRESSURE TAP

Figure 3. PEMLAR Injector

used in these studies; "Mod 1" indicates a ring with a single surface at 60° to the face of the injector, "Mod 2" was a ring with a surface at 60° followed by another at 45°. c. The computed (stoichiometric) O/F weight ratios are as follows. For each fuel two values are given, the first for complete oxidation of all carbon to CO_2, the second for oxidation to 50% CO and 50% CO_2: DMH 3.30, 2.89; hydrazine-32% ammonium thiocyanate 1.67, 1.62; bis-(dimethylamino)propane, 4.37, 3.70; aniline 4.11, 3.32; tetramethyltetrazene 2.98, 2.56. d. The chamber loading density. e. Chamber pressure. f. Characteristic exhaust velocity with standard deviation of the mean. g. Supplied by Phillips Petroleum Company-Wright Air Development Center. h. The oxidizer contained 3% ammonium vanadate in the studies of aniline. i. Supplied by Drs. W. R. McBride and H. W. Kruse, Inorganic Chemistry Branch, U. S. Naval Ordnance Test Station.

The conditions indicated in these studies are representative of those discussed previously as applied in the LAR. Thus, chamber pressures of 1400-1500 psi, loading density rates of 0.45 $lb/in^3/sec$, and an L* of 20 inches were used. The studies of DMH show the effect of the deflector ring on performance. Increase of performance available by variation of the deflector design, usually by a decrease in the angle, is limited by the appearance of combustion roughness.

These tests were insufficient to establish a variation of c* with O/F ratio in the ranges studied. No correlation of the two parameters exceeding the standard deviation reported appeared in the ranges given.

Similar tests were made with DMH in a combustion chamber with a length of 2 inches, a diameter of 2 inches, and an L* of 10 inches. Performance equal to that obtained in the motor with 20-inch L* was obtained with a loading density rate of 0.88 $lb/in^3/sec$. Under these conditions the motor is delivering a thrust of 1600 pounds. A thrust coefficient of 1.63 is assumed since thrusts were not measured in these studies. Tests at loading rates up to 1.00 $lb/in^3/sec$ gave satisfactory combustion. At the maximum loading rate of 1.00 performance decreased by approximately 14% from the optimum rate of 0.88.

The hydrazine-32% ammonium thiocyanate fuel is a low freezing solution which was of interest until the introduction of DMH (5).

The 1,3-bis-(dimethylamino)propane, also known as N,N,N',N'-tetramethylpropane-1,3-diamine, gave performance comparable with that of DMH but with rougher combustion. Initiation of combustion was also rougher. Oscillations in a typical test occurred with a frequency of approximately 250 cps. Roughness occurred in repetitive cycles of 0.1 sec with the amplitude of pressure oscillations gradually increasing to approximately 130 psi. Characteristically, there was no erosion of motor parts during such tests. The rough combustion as well as the high performance may be attributed to the deflector ring used.

Aniline, studied with RFNA containing 3% ammonium vanadate to secure hypergolic ignition with a short delay time (9 millisec), gave markedly lower performance as noted in table 1. Combustion was variably rough on occasion.

Tetramethyltetrazene gave very smooth combustion and high performance comparable with that of DMH. This compound is structurally similar to DMH, from which it is prepared (6). Its properties include: boiling point, 125°C (extrapolated); melting point, -22.0°C; density, 0.8895 g/cc (25°C); viscosity, 0.7 cp (25°C); and ignition delay with RFNA of 2 milliseconds.

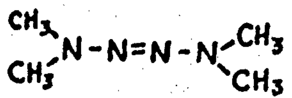

Tetramethyltetrazene-2

Varying Thrust Level Experiments

DMH was selected for the studies of performance at different flow rates in the PEMLAR. The motor shown in figure 4 was used with the standard injector of figure 3 and a deflector angle of 70°. The L* of the combustion chamber was 15 inches. In these tests a flat nozzle with no expansion cone was used; performance assessment was based on characteristic exhaust velocity. Thrust was not measured. The attitude of the motor was somewhat different from that shown in figure 1, the nozzle being directed at an angle of 45° to the horizontal. Performance was not affected by this change.

Chamber pressure recordings were obtained with two Wiancko pressure transducers in the pressure taps shown on figure 4, one placed in the face of the injector and the other at the side of the chamber near the nozzle. The response of the galvanometers in the recording oscillograph is fairly limited, with flat response up to 180 cps. Indications of frequencies up to 500 cps and above can be obtained. The sensitivity of the pressure measurement is dependent on the pressure being measured. Thus, in figure 5a rough combustion indicated at the side tap shows maximum peak-to-peak oscillations of approximately 110 psi at a chamber pressure of 540 psi. The minimum pressure oscillation which would be visible is estimated at 25-30 psi. This sensitivity applies to record 5b also. In record 5c an oscillation of approximately 7 psi could be observed if it occurred in the chamber pressure, which is 90 psi.

Propellant flow in the tests was measured with the well-known Potter turbine flowmeter. (7, 8).

The materials used in the combustion chamber (figure 4) include: 1020 mild steel for injector plug, heat shield, and chamber liner; 304 stainless steel for injector, deflector ring and the chamber wall containing the injector; and copper for the nozzle. The nozzle is cooled with water. Transite is also used as chamber liner.

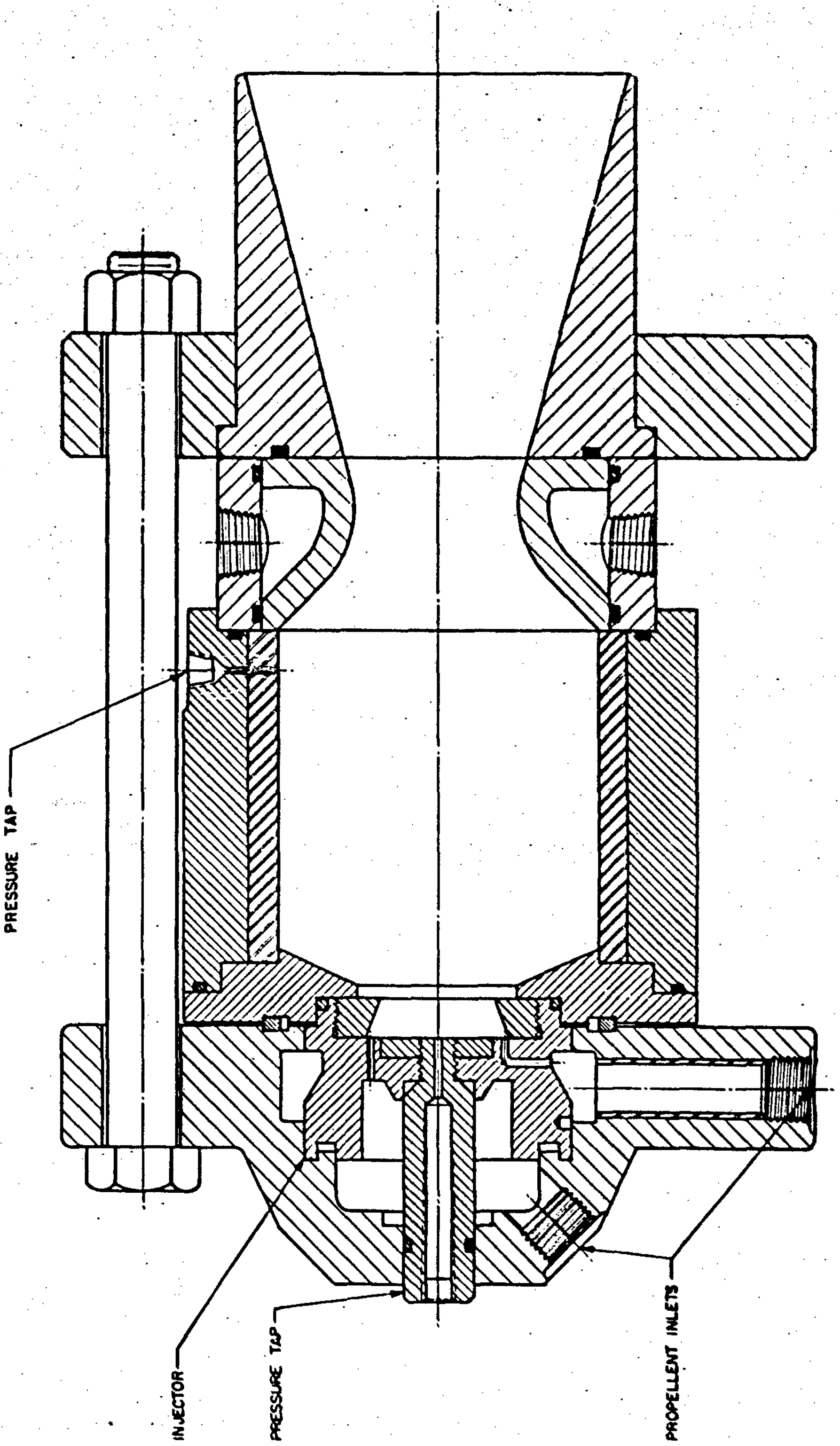
PRESSURE TAP
INJECTOR
PRESSURE TAP
PROPELLENT INLETS

Figure 4. The PEMLAR Large-Diameter Motor Chamber Dimensions: 4" X 4"

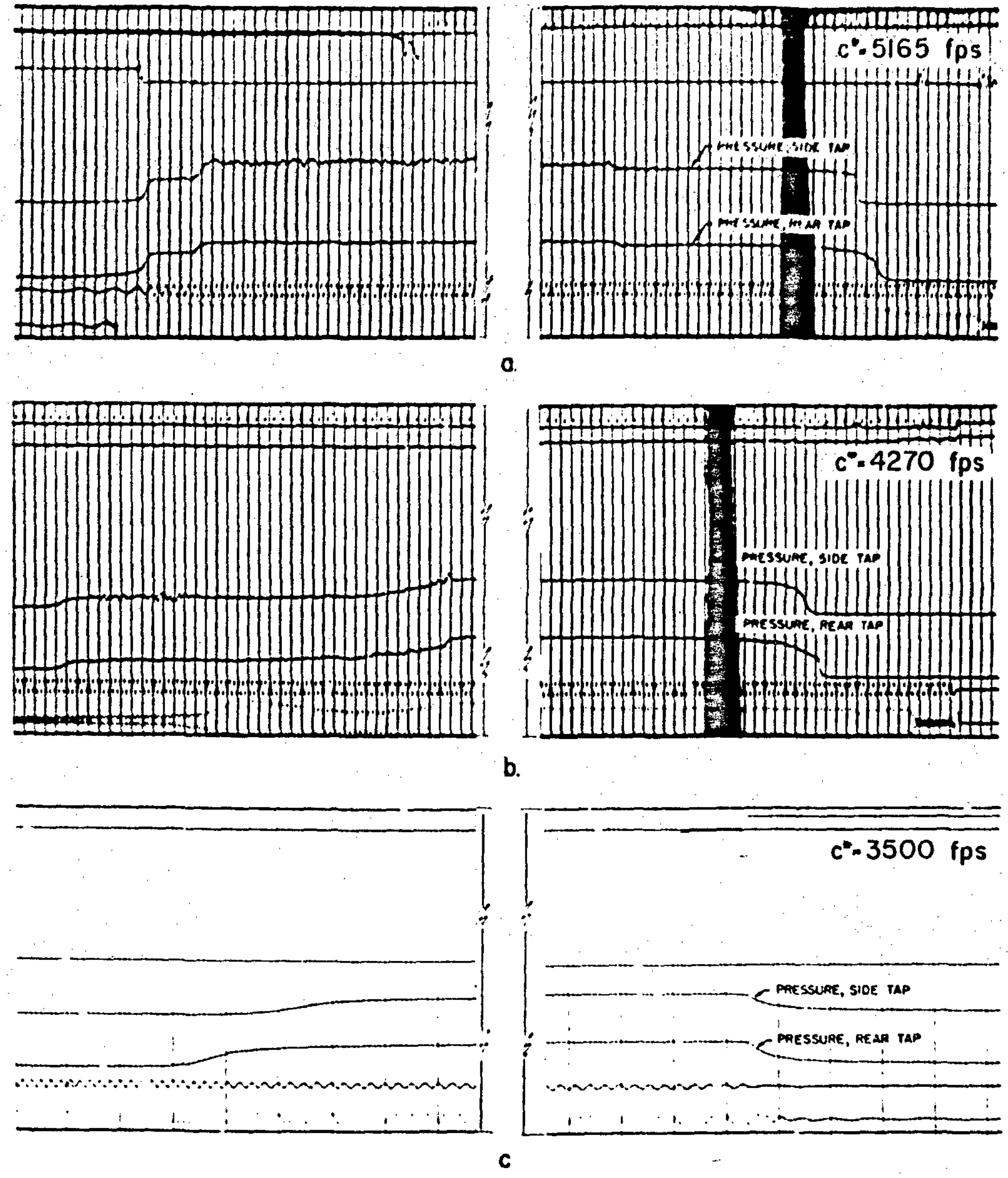

Figure 5. Thrust Level Test Records
Reduction factor in reproduction: 1:3

Propellants: DMH-RFNA
Injector: STM 2A; Mod 6(70°)

a. PEMLAR Test 130; chamber pressure, 510 psi; 0.55 sec of run deleted from middle of trace.

b. PEMLAR Test 149; chamber pressure, 467 psi; 5 sec of smooth run continued from right section deleted from center of trace; extended rough shut-down in left section caused by exhaustion of oxidizer.

c. PEMLAR Test 151; chamber pressure, 72 psi; 22 sec of run deleted from middle of trace.

In a propellant test the propellant lines between the PEMLAR and the propellant valves shown in figure 1 were filled with 5 cubic inches of a slurry of Bentonite containing approximately 90% water. The propellant tanks were pressurized with nitrogen, and the valves opened for the firing. Performance tests were in general between 1 and 3 seconds in length as in the propellant evaluation studies discussed previously. Maximum firing times of 6 seconds at the highest flow rate and 25 seconds at the lowest were studied to observe effects on the motor parts. The firing times were limited by propellant tank capacity. Lack of a variable gas pressure control required separate tests at each pressure. The applied gas pressure was adjusted to give the desired propellant flow and chamber pressure.

Results of Thrust Level Studies

The following observations were made to evaluate the results: the magnitude of the pressure transients on initiation of combustion, the smoothness of the pressure traces, performance (as c*), and regions and depth of erosion of motor parts.

The flow of water from the PEMLAR injector was investigated at the gas pressures applied in the varying thrust tests. Figure 6a-h shows these tests. The "lens" effect is clear. At lower pressures flow is weak and mixing relatively poor. Little change in the flow appears above applied pressures of 900 psi. At the higher pressures an oscillation occurs near the "focal point". The rough combustion observed in tests at high pressures may be a reflection of this fluctuation in liquid flow. Pressure oscillations are usually recorded at the side of the chamber at the position closest to the region where this characteristic fluctuation occurs. Pressure observed at the other position is usually very stable. In smooth combustion no oscillations are observed at either position.

In addition to the difference in stability occasionally observed at the two pressure stations, a discrepancy in the magnitude of pressure was usually observed. In most tests the station in the injector face indicated markedly higher pressures than the side station. Differences up to 70 psi were observed at the highest thrusts studied. The discrepancies decreased generally with decreasing flow rate. In a few tests the higher pressure was noted at the side station. These observations can for the most part be attributed to a combination of the various effects of the flow patterns, velocities, and propellant reaction. The chamber pressures reported are unweighted averages of the two readings; and characteristic exhaust velocities were computed with the averages.

The boundaries of the liquid seen in figure 6 up to the focal point remain within the dimensions of the small-diameter chambers used in the propellant evaluation discussed previously.

The results of a series of tests made at varying thrust

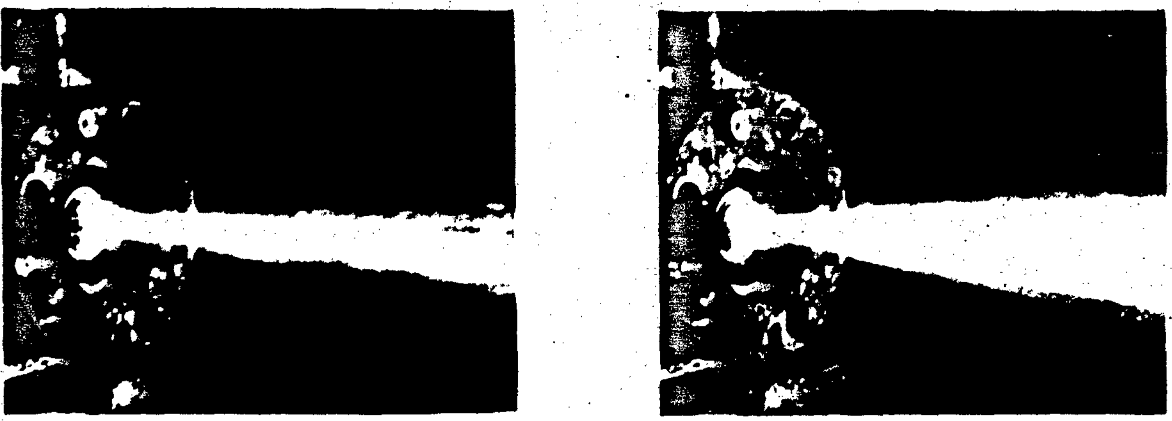

a. P_A 100 psi

b. P_A 300 psi

c. P_A 500 psi

d. P_A 700 psi

Figure 6. Injector Flow Studies
Injector STM 2A, Mod 6(70°)

levels are summarized in table 2. The thrust variation in these tests is indicated in the final column of table 2 by the variation in the product of propellant mass flow rate and the characteristic exhaust velocity, $\dot{w}\ c^*$. This parameter is computed from experimental variables and is used because thrust was not measured. The variation in thrust indicated is a factor of 16 to 1 over a region of stable non-erosive combustion. If thrust is computed with estimated thrust coefficients, a variation of 22 to 1 is indicated from 2990 lb down to 135 lb. In this estimate a thrust coefficient of 1.52 was used for the maximum thrust and a coefficient of 1.1 for the lowest.

Smooth combustion was obtained at chamber pressures from 569 psi down to 35 psi. In short tests over the thrust range no erosion was noted in a cumulative firing time of 65 sec. In the tests run at maximum firing times of 6 sec at maximum thrust in non-oscillatory combustion there was slight erosion of the deflector ring, and at low thrust level there was little or no erosion in 25 sec.

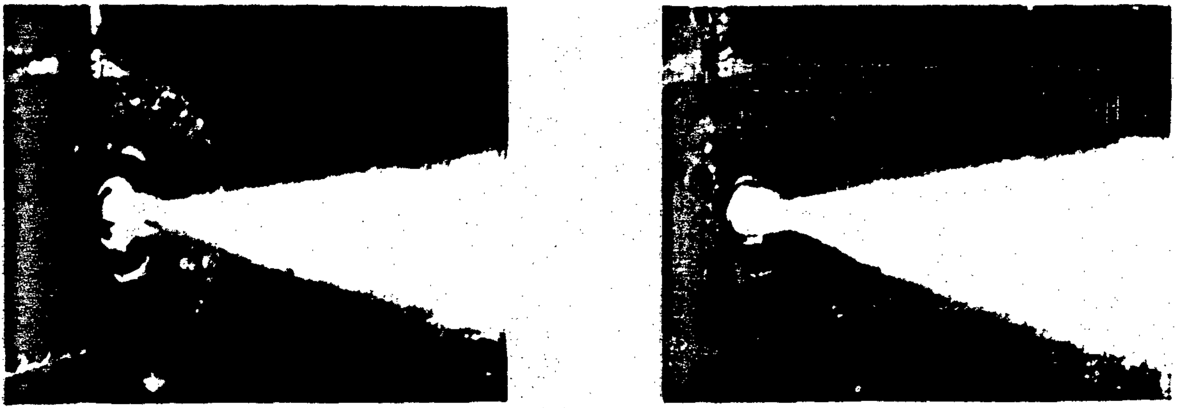

e. P_A 900 psi

f. P_A 1100 psi

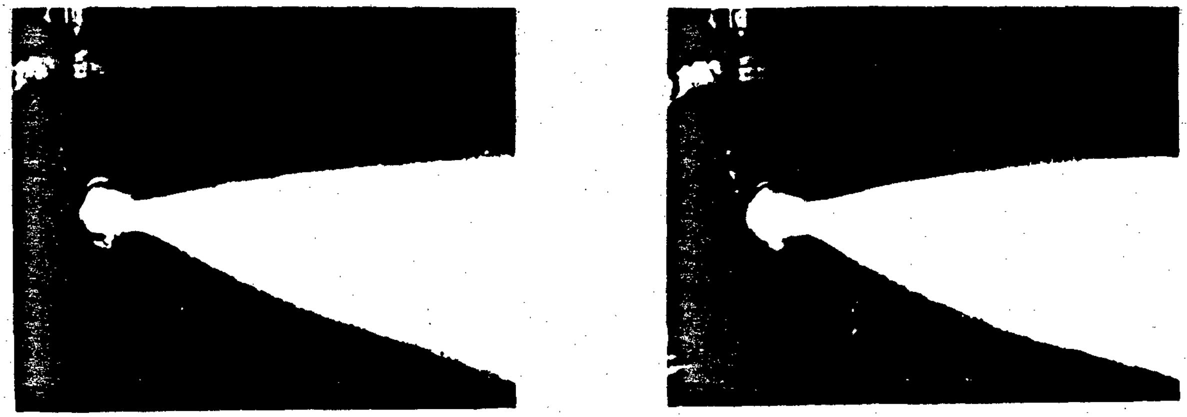

g. P_A 1300 psi

h. P_A 1500 psi

Figure 6(contd.) Injector Flow Studies
Injector STM 2A, Mod 6(70°)

Propellant flow rate decreased linearly with the square root of the pressure drop in injection. The pressure drop reported in these studies was that observed between the propellant tanks and the combustion chamber. The drop in pressure varied approximately linearly with the pressure applied to the propellants over the range studied.

As the data in table 2 indicate, the thrust change is only in part caused by the change in propellant flow rate, which varies by a factor of 6 to 1. In addition, there is a decrease of combustion efficiency reflected in c* as flow rate and chamber pressure decrease. The variation of c* with chamber pressure is shown in figure 7. The curve indicated on this figure is a second degree function representing all the data with a least-mean-squares fit. The experimental results appear to show somewhat higher combustion efficiencies than indicated by this function at chamber pressures from 100-200 psi, with c* decreasing sharply at lower pressures. The wide variation among results seen in figure 7 at the higher chamber pressures may be caused by the use of pressure averages as described in the previous discussion.

TABLE 2

Thrust Level Studies[a]

Propellants: unsym-dimethylhydrazine, red fuming nitric acid (20% NO_2)
L*: 15"
Deflector Ring Angle: 70°

$\dot{w}$ lb/sec	O/F	R_c lb/in^3/sec	P_A psi	P_c psi	ΔP psi	c* fps	$\dot{w}$ c*
12.38	2.70	0.24	1675	569	1106	5120	63,400
12.37	2.98	0.24	1665	467	1198	4270	52,800
10.97	2.86	0.21	1675	508	1167	5140	56,400
10.91	2.81	0.21	1655	478	1177	4850	52,900
10.35	3.12	0.20	1150	349	801	3810	39,400
10.01	3.26	0.19	1150	340	810	3830	38,300
8.12	3.10	0.16	770	292	478	4100	33,300
8.11	3.14	0.16	795	296	499	4120	33,500
6.04	2.82	0.12	515	237	278	4350	26,300
5.85	3.15	0.11	495	189	306	3600	21,100
5.52	2.81	0.11	510	237	273	4760	25,300
5.05	2.98	0.10	400	179	221	3960	20,000
5.05	2.98	0.10	400	174	226	3840	19,400
4.25	2.97	0.08	305	144	161	3790	16,100
4.20	2.93	0.08	300	145	155	3870	16,200
3.28	3.00	0.06	205	108	97	3690	12,100
3.23	2.99	0.06	205	105	100	3640	11,800
2.51	3.92	0.05	135	54	81	2420	6,070
2.37	3.14	0.04	130	77	53	3670	8,700
2.35	3.90	0.04	130	56	74	2680	6,290
2.33	3.09	0.04	124	72	52	3500	8,160
2.14	4.63	0.04	95	35	60	1840	3,940
2.01	4.29	0.04	100	54	56	3030	6,086

[a] $\dot{w}$ is the total mass flow rate of propellants into the combustion chamber. O/F is the mass ratio of RFNA to DMH. P_A is the gas pressure applied to the propellants. P_c is the combustion chamber pressure obtained as the average of pressures measured at the two locations in the chamber. ΔP is the pressure drop between the propellant tanks and the combustion chamber. Theoretical c* from exact computations for RFNA containing 14% nitrogen dioxide is 5360 fps at O/F 2.5, 5330 at 3.0, and 5250 at 3.45 (9).

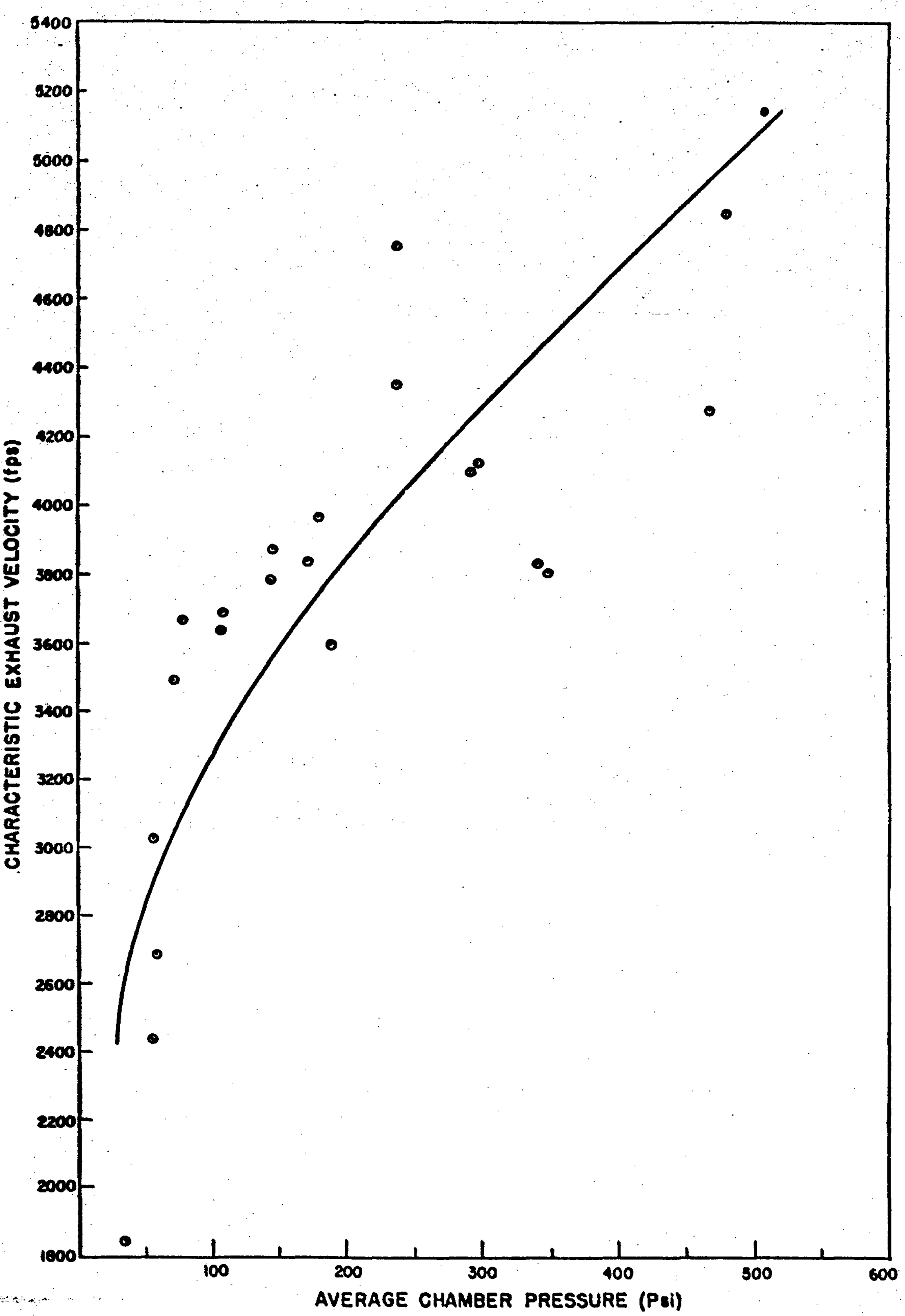

Figure 7. Variation of Performance with Chamber Pressure

In terms of missile performance these results would mean that range for a flight at the lower or intermediate thrusts with this motor would be significantly decreased over that obtainable with better combustion efficiency. An alternate interpretation is that for a given low propellant flow rate the thrust is significantly reduced from theoretical.

The reduction in performance may be explained in part by the observations in the water flow tests (figure 6). In addition, the injector configuration or, more specifically, the deflector angle selected for this study was based on high performance compatible with smooth combustion without erosion at the maximum flow rates. Further improvement through optimization of the deflector design is possible. For example, in exploratory tests a deflector ring with two surfaces, the first at 70° followed by another at 60°, has been studied. (The surfaces are specified in the order in which liquid flowing from the injector orifices hits them.) With use of the two-angle deflector an average c* of 4420 fps at 104 psi chamber pressure was obtained, an increase of approximately 21% over that obtained with the 70° deflector. In the region of 225 psi c* is approximately 4450 fps; combustion is non-erosive, but very small oscillations are visible in the pressure records, and a whistle is audible during the test. At 565 psi oscillations are intense; the injector face and regions of the chamber erode even during 1-2 second tests. Performance based on c*, however, is equivalent to that with the 70° deflector. Future studies thus give promise of improved performance at the low thrust levels and chamber pressures investigated here, combustion stability and motor erosion at high thrust defining a limit to this approach.

REFERENCES

1. G. R. Makepeace, "A Status Report on the 5.0-Inch Liquid-Propellant Aircraft Rocket (LAR), NOTS TM 1464, 23 March 1956. CONFIDENTIAL

2. William A. Tomazic, "Rocket-Engine Throttling", NACA RM E55J20, December 19, 1955. CONFIDENTIAL

3. J. A. Bolt, et al, "Third Progress Report on Rocket Motor Throttling", UMM-109, University of Michigan, May 1953. CONFIDENTIAL

4. F. R. Hickerson, "Investigation of Methods for Varying Thrust in Rocket Engines", Report No. 88, April 1956, Naval Air Rocket Test Station, Dover, New Jersey. CONFIDENTIAL

5. E. D. Campbell, H. P. Jenkins, Jr., and Wm. Cohen, "A Low-Freezing-Point Hydrazine Fuel for the LAR", NOTS TM No. 1478, U. S. Naval Ordnance Test Station, China Lake, California. CONFIDENTIAL

6. W. R. McBride, D. G. Nyberg, Arnold Adams, and H. W. Kruse, "Tetramethyltetrazene as a Potential Liquid Propellant", pp C5-C8, Research in Chemistry, September-October 1956; NOTS 1628, NAVORD 5381, 31 October 1956. CONFIDENTIAL

7. Bulletin S-1, Potter Aeronautical Company, Union, New Jersey.

8. Jerry Gray, "Transient Response of the Turbine Flowmeter", Jet Propulsion 26, 98-100 (1956).

9. G. W. Elverum, Jr., Personal Communication, Jet Propulsion Laboratory, Pasadena, California.

THE TANGENTIAL MODE OF COMBUSTION INSTABILITY *

R. S. Pickford and H. B. Ellis
Aerojet-General Corporation
Azusa, California

ABSTRACT

The tangential combustion instability in liquid-propellant rocket motors has been investigated. A physical-process mechanism for fully developed instabilities has been proposed and a system established for the various front modes. The axial and radial distribution of the front, occurring in the experimental chamber, is discussed. Luminosity, instantaneous pressure, and front motion have been correlated, and an estimate has been made of the movement of chamber gas during unstable combustion.

I. INTRODUCTION

The tangential mode of combustion **instability** has been one of the more severe combustion problems, and is capable of damaging or destroying a thrust chamber within a relatively short period of time. The majority of thrust-chamber developments by the various rocket engine contractors have encountered the tangential mode in one form or another. Usually the project has been delayed until stable combustion is achieved.

The purpose of the investigation discussed in the following text is to define the nature of the tangential mode of combustion instability and to determine the physical processes associated with this phenomenon. The results outlined represent an increment in a continuing research project.

---

*The research work discussed in this paper was supported by the United States Air Force, through the Combustion Dynamics Division, AF Office of Scientific Research, Air Research and Development Command, Contract No. AF18(600)-1155. See References 1, 2, and 3.

II. EQUIPMENT

In order to conduct an experimental investigation of the tangential-combustion instability, it was necessary to develop a suitable laboratory tool. The combustion chamber should be able to reproduce any desired mode and should suffer a minimum of physical damage, thus requiring little or no maintenance. For the greatest significance in results, the experimental tests should be comparable with full-scale thrust-chamber operation.

For the experimental tests, thrust chambers were designed, favoring the tangential mode by confining the propellant injection to an annulus extending radially inward from the circumference of the combustion chamber. To facilitate changes in injection patterns, the injector was divided into replaceable sections, which resulted in a discontinuous injection pattern around the chamber circumference. A view of a typical research motor injector face is given in Figure 1. To initiate combustion instability, a gas pulse was created by burning desired weights of smokeless gunpowder behind burst diaphragms of appropriate thickness. The weight of the powder charge required to initiate instability was used as a relative measure of the resistance level to the initiation of high-frequency instability offered by the test configuration. The velocity of the wave front and the circumferential velocity of the chamber gases during the front passage are used as a measurement of the front severity or strength. For the initial phases of the testing, these two measurements were considered to be adequate in describing the front and for indicating the degree of reproducibility.

Physical damage to the hardware was kept at a minimum by restricting the full-thrust operation under high-frequency instability to 0.120 sec or less, which was found by experience to be a satisfactory duration.

Three different sizes of thrust chambers were constructed having diameters of 15, 22-1/2, and 30 in. The smallest size incorporated eight removable injector elements; the second, 12 elements; and the largest, 16 elements. The relationship of the injector elements to each other and to the chamber wall was the same for all chamber sizes. Circumferential windows were placed approximately 1.7 in. downstream of the injector face. A 15 in. diameter thrust chamber was modified so that an axial window could be clamped along the full length of the chamber. The injector was split along a diameter, and a window was incorporated here also. A schematic of the split chamber is illustrated in Figure 2 and a view of the test installation is shown in Figure 3. The 22½ in. dia thrust chamber and the 30 in. dia chamber appear in Figures 4 and 5.

Most of the data used in the technical discussion was obtained by the slit window, strip film technique and with high-response pressure transducers. Figure 6 illustrates the photographic technique for recording luminosity from a circumferential window. General Radio cameras were used which were capable of film velocities of 100 ft/sec. Timing dots were placed on all films simultaneously at 0.001-sec intervals. On the pressure records, the timing dot and corresponding event are side by side, whereas, on the slit window records the event is recorded 15 sprocket holes ahead of the corresponding timing dot. Pressure was sensed with a Li-Liu pressure gauge and recorded by a strip-film camera exposed to the face of an oscilloscope. The pressure-sensing diaphragm of the gauge was mounted flush with the chamber wall in all cases.

All of the tests were made with red fuming nitric acid, type III-A (MIL N-7254B-USAF Specification) and JP-4 propellants and were used with a showerhead injection pattern.

III. TECHNICAL DISCUSSION

A. MOTION OF TANGENTIAL FRONT IN CHAMBER

The tangential front revolves around the chamber and is concentrated in an annular zone, the outer boundary of which is formed by the chamber wall. The location of the front within an axial segment of the chamber was obtained through photographic records taken at approximately 90° to each other, as illustrated in Figure 7. These two records furnish coordinates by which the front position in the chamber can be found. Figure 8 shows a strip-film photograph from each camera and locates the front position in the chamber from the films. A continuous single-front instability is present in this example. The points A, B, and C which are marked on the film are related to the corresponding points on the schematic of the chamber shown at the bottom of the figure. Point A appears at the bottom of camera record No. 1. At the same time, it appears on the far side of the chamber to camera No. 2. When the front arrives at point B, midway between A and C, it is approaching the peak excursion point as viewed from camera No. 1 and will soon pass around to the far side of the chamber. From camera No. 2, the front, at point B, has just passed the peak excursion point and has just appeared on the near side of the camera. As the front moves on to position C, it appears on the far side of the chamber to camera No. 1, and at the second peak excursion point to camera No. 2. Thus, the front is shown to propagate circumferentially around the chamber.

The period of most intense luminosity was found to coincide with the peak pressure excursion measured at the chamber wall. The zone of this intense luminosity has been defined as that of the front location. A typical pressure trace taken during a severe single front instability is shown in Figure 9. This record, which was taken as the propellant valve begins to close, indicates there is no true "step-function" pressure rise with the passage of the front. However, the tangential front propagates at velocities up to Mach 3 with respect to the chamber wall and behaves like a detonation front in many respects.

B. DISTRIBUTION OF TANGENTIAL FRONT IN CHAMBER

The shape of the tangential front has been determined with the aid of slit-window photographs taken through all three dimensions of the chamber. The radial and axial records taken with the split chamber and injector were combined with previous work utilizing a chamber containing a circumferential window. Of course, similar test conditions were used for the two chamber designs, so that comparisons could be made.

The axial distribution of the front is illustrated in Figure 10 for a continuous, single-front instability. Notice that only a portion of the front is parallel to the axis of the chamber and that the luminosity level is higher in this area than over the rest of the window length. The major portion of the energy release takes place in this zone, which for this test condition extends approximately 3.5 to 4.0 in. from the injector face. The axial penetration of the liquid-propellant streams during 1 cycle of the front is less than the axial depth of the high-energy zone. Assuming the velocity of the liquid stream remains constant, the fuel will have penetrated 0.62 in. into the chamber, and the acid 0.27 in. during the cycle period.

Downstream of the high-energy zone, the front is not parallel to the axis of the chamber, and the nozzle end of the front lags behind the injector end. A reflection of the front extends from the entrance of the nozzle back toward the injector. All portions of the front maintain the same cyclic relationships, which would indicate a cyclic propagation in the zone viewed through the window.

There are no discernible fluctuations in the axial movement of the chamber gases upon passage of the front, although it is possible that the photographic resolution is too poor to reveal any such motion. The calculated chamber gas velocity at the nozzle entrance during stable combustion is only Mach 0.04 or 140 fps.

If the axial window record is considered separately, a question might arise as to whether the sloping front is actually caused by a wave which is moving axially through the chamber. The axial velocity for such a wave, computed from the slope of the "tail", would be approximately 8700 fps, whereas the usual velocity of an axial front existing during this type of combustion system seldom exceeds an average of 4500 fps. In any event, an axial front system could not produce the circumferential distribution of light obtained in the radial and circumferential-window photographs.

If it is assumed that the velocity of the front is dependent upon the energy available for consumption in the front, the propagation velocities downstream of the high energy zone should be less than that within the zone. Therefore, the following model may be constructed:

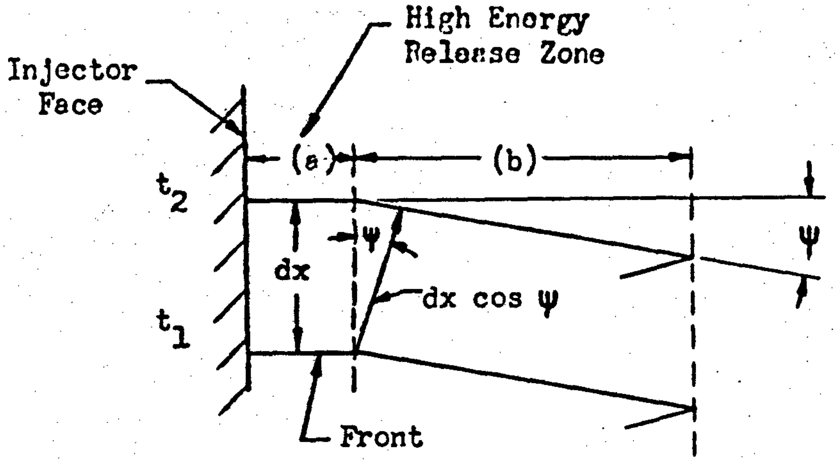

$$v_a = dx/dt$$

$$v_b = \frac{dx}{dt} \cos \psi$$

$$v_b = v_a \cos \psi \qquad (1)$$

where

v_a = front velocity in high energy zone
v_b = front velocity of "tail"

dx = distance of front propagation in time, dt

The high energy portion of the front shown in Figure 10 has a velocity of 6900 fps while the "tail" velocity is 6883 fps. This latter velocity is based upon the difference in velocities between the front in the high energy zone and the "tail," which can be calculated accurately from Equation (1). Of course, the error in absolute front velocity can be larger than the calculated differences in propagation velocity as obtained from the relative slope of the front in axial window records. However, the differences in front propagation velocity can be measured within a few feet per second.

The light pattern shown in Figure 11 was produced by a slit-window photograph across a diameter of the injector. The dark strip in the center of the photograph was caused by the propellant valve, which was mounted off-center to expose the window to within 2.7 in. of the chamber centerline. The front appears alternately on one side of the chamber and then the other. The greatest luminosity occurs near the chamber wall at the time the front arrives, even though this area emits relatively little light during stable combustion or between front arrivals. This supports the belief that the front is concentrated near the chamber wall in these test chambers in which the propellant injection is in a 3-in. wide annulus and where the wall curvature continually forces a change in the front direction. The record in Figure 11 was taken when the propellant valve was partially closed and the propellant flow reduced so that most of the background light from combustion was removed. Notice the sudden emission of light upon arrival of the front, and that the distribution of the front is radially inward toward the center of the chamber. Distinct luminosity streaks, showing radial motion of the chamber gases, appear between the fronts.

A radial-window record taken during full propellant flow is shown in Figure 12, in which the method of determining the radial movement of chamber gases is given. Unfortunately, considerable detail is obscured in the reprinting process, and the luminosity streaks are not seen as well as in the original negative.

A typical circumferential-window view of a tangential instability is shown in Figure 8. The luminosity streaks between the front arrivals are easily discerned. A detailed discussion of this type of record has been given previously in References 2 and 3.

C. CHAMBER-GAS MOTION AND PRESSURE DISTRIBUTION

An analysis of the records taken from the slit-window experiments has yielded a picture of the chamber-gas-velocity distribution and pressure profile for a segmental element of the chamber near the injector face. Figure 13 indicates what is believed to take place during a continuous, single-front instability of the tangential mode. Before discussing the diagram, the methods upon which these conclusions have been made will be set forth.

Several assumptions have been made, as follows:

1. The luminous streaks which appear between front arrivals and through the fronts themselves represent the velocity of luminous particles. There is some evidence that this assumption may be valid. Investigators at NAA Rocketdyne have found that the

luminosity streaks from an axial window record have the same velocity as the chamber gases (Reference 4). The movement of the chamber-gas was established by the difference in velocity of an axial mode front as it traveled between the injector and the nozzle.

2. The front velocity is constant, and each cycle is the same.

3. Any axial movement of the chamber gases plays an insignificant part in the instability process. It is believed that there is little axial movement of chamber gases induced by the passage of the front, because the pressure fluctuations along any axial element of the chamber are small. Thus, a thin, circular segment of the chamber will be studied.

4. The circumferential vectors and velocities of the gas movement are the same along any radius of the chamber. This seems reasonable, as very little crossing of the luminosity streaks can be found. As to the depth into the chamber which can be seen, it should be noted that the front is discernible on the far side of the chamber.

From the radial and circumferential records, a plot of the chamber gas velocities and the resultant vectors may be constructed for any given instant of time. Because the front is moving at a constant velocity and each cycle is the same as the next cycle, the phenomena observed through the slit windows during one cycle period will be identical with the phenomena occurring throughout the chamber at any given instant. The segment of the chamber to be considered is within the high-energy release zone and parallel to the injector face. The radial and circumferential velocities from the film records were resolved into a resultant vector velocity for every part of the cycle. A plot of these velocities and the vector angles is given in Figure 14.

When the vectors are drawn in a cross-sectional chamber segment, a diagram such as that shown in Figure 13 emerges. Around the chamber segment are polar plots of the gas-velocity magnitude and the pressure profile as measured at the chamber wall. It is interesting to note that there is an abrupt movement of the chamber gases, radially outward, just prior to the arrival of the front. One of the most significant points revealed by the diagram is that in the typical test considered, the chamber gases never travel across the injector face at less than 800 fps, and even reach velocities as high as 2450 fps. Yet, the pressure profile and front velocity of 6860 fps are considered to be of medium strength. Stronger fronts in this size of chamber, in which acid-JP4 propellants were used, have traveled in the neighborhood of 7500 fps. With such high-velocity gas movement, the atomization and the heat-transfer input to the liquid-propellant streams become very effective and can account for the exceedingly short time required for the preparation of a mixed-and-heated combustible media. Of course, these velocities can also partially account for the high rates at which heat is transferred to the chamber walls during this type of combustion instability.

D. GAS-PARTICLE PATH

To obtain a better picture of the tangential instability phenomenon, the path of a gas particle was calculated during one revolution of the front around the combustion chamber. The particle mass would be that of the particles which cause the luminosity streaks on the film records. Figure 15 shows the estimated path of a particle existing in the front system previously considered, and the method used to derive the path is discussed below.

The motion of a particle from one position to another was set forth by the diagram shown immediately below.

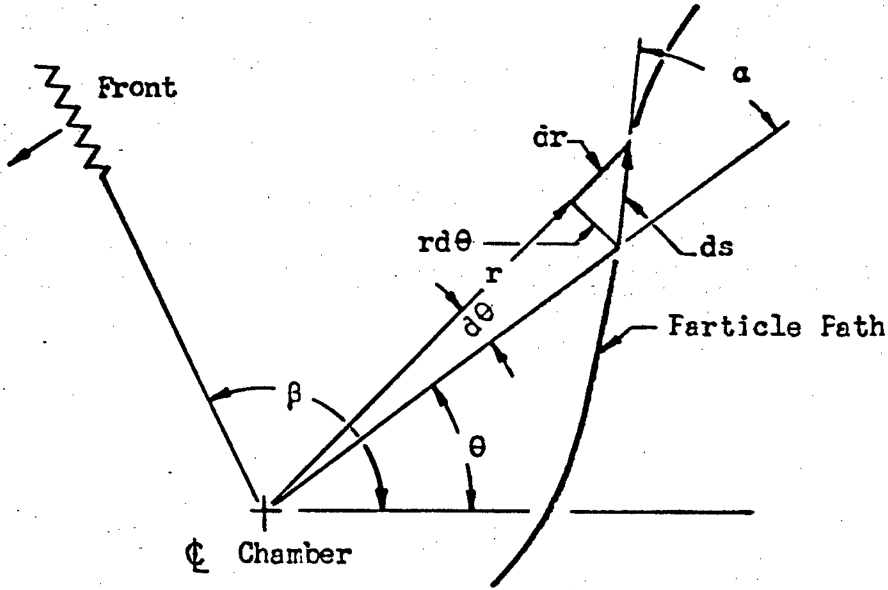

where

β = angular position of front
θ = angular position of particle
r = radial position of particle
α = vector direction of particle motion
ds = distance particle moves in time increment, dt
dθ = change in angular position in time, dt
dr = change in radial position in time, dt

then

$$ds = \sqrt{(dr)^2 + (rd\theta)^2} \qquad (2)$$

$$ds = vdt$$

$$dr = ds \cos \alpha = vdt \cos \alpha \qquad (3)$$

$$rd\theta = ds \sin \alpha = vdt \sin \alpha \qquad (4)$$

where v = particle velocity

An examination of the phenomena taking place in the chamber reveals that the particle vector angle, α, is dependent upon the relative position of the particle and the front. The particle velocity, v, is established when the angle α is ascertained.

Integration gives:

$$r = \int v \cos \alpha \, dt \qquad (5)$$

$$\theta = \int \frac{v}{r} \sin \alpha \, dt \qquad (6)$$

where

$$v = f(\alpha)$$

$$\alpha = f(\beta - \theta)$$

$$\theta = \int w_f \, dt$$

where

w_f = angular velocity of front
t = time elapsed when $\phi = 0$

The above equations for the particle position, expressed in terms of r and θ, were solved by summation over relatively small time increments. The curves which represent the gas velocity and vector direction, with respect to the front position, are generally non-linear and the time increments used were smallest in the areas of greatest curvature. The solution was made in two parts, as determined by the sign of cos α, which determines whether r is increasing or decreasing.

For increasing values of r, α varies from 0 to 90° and from 270 to 360° :

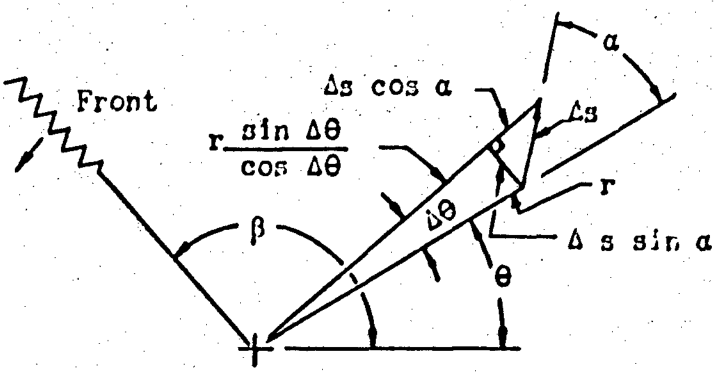

$$r + \Delta r = \Delta s \cos \alpha + r \frac{\sin \Delta \theta}{\tan \Delta \theta} \qquad (7)$$

but $\sin \Delta \theta = \frac{\Delta s \sin \alpha}{r}$

By substitution $r + \Delta r = \Delta s \ (\cos \alpha + \frac{\sin \alpha}{\tan \Delta \theta})$

$$= v \ (\cos \alpha + \frac{\sin \alpha}{\tan \Delta \theta}) \ \Delta t \qquad (8)$$

If each incremental position of r is assigned a subscript, then

$$r_1 = r_o + \Delta r_1$$

$$r_2 = r_1 + \Delta r_2$$

$$= r_o + \Delta r_1 + \Delta r_2$$

$$r_n = r_o + \Delta r_1 + \Delta r_2 + \ldots + \Delta r_n$$

$$= r_o + \sum_{n=1}^{n} \Delta r$$

where r_o = initial radial position of particle

Thus $r_n = r_{n-1} + \Delta r_n$

Substituting Equation 8

$$r_n = v \ (\cos \alpha + \frac{\sin \alpha}{\tan \Delta\theta_n}) \ \Delta t \qquad (9)$$

where $\Delta\theta_n = \text{arc sin} \ (\frac{v \sin \alpha}{r_{n-1}}) \ \Delta t$

$$v = f\ (\alpha) = \sqrt{(v_r)^2 + (v_\theta)^2}$$

$$\alpha = f\,(\beta - \theta)$$

$$= f\left[\int_0^{n-1} w_r \;\Delta t - \sum_{n=0}^{n-1} \;\Delta\theta\right]$$

For decreasing values of r, α varies from 90° to 270°:

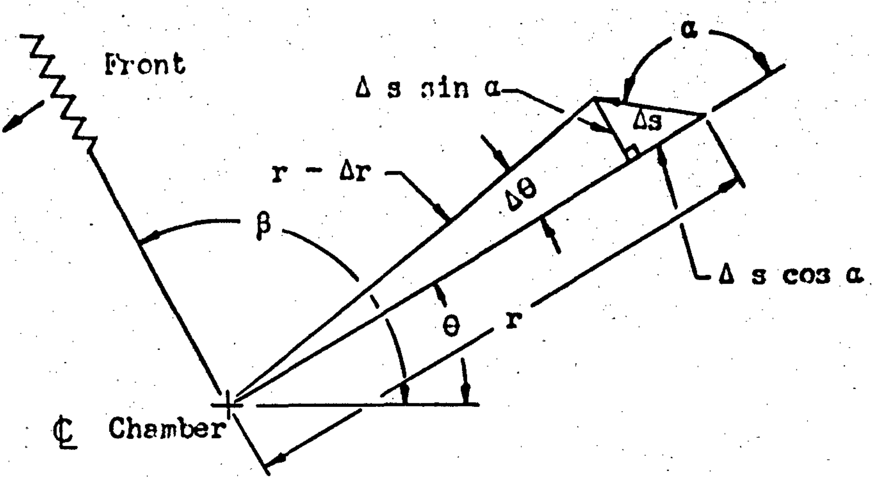

$$\tan \Delta\theta = \frac{\Delta S \sin \alpha}{r - \Delta S \cos \alpha}$$

$$\sin \Delta\theta = \frac{\Delta S \sin \alpha}{r - \Delta r}$$

$$r - \Delta r = (r - \Delta s \cos \alpha)\,\frac{\tan \Delta\theta}{\sin \Delta\theta}$$

$$r_n = r_{n-1} + \Delta r_n$$

$$= (r_{n-1} - v \cos \alpha\, \Delta t)\,\frac{\tan \Delta\theta_n}{\sin \Delta\theta_n} \qquad (10)$$

where

$$\Delta\theta_n = \text{arc tan}\,\frac{v \sin \alpha\, \Delta t}{r_{n-1} - v \cos \alpha\, \Delta t}$$

$$v = f\,(\alpha)$$

$$= \left[(v_r)^2 + (v_\theta)^2\right]^{\frac{1}{2}}$$

$$\alpha = f\,(\beta - \theta)$$

$$= f\left[\int_0^{n-1} w_f \;\Delta t - \sum_{n=0}^{n-1} \Delta\theta\right]$$

The initial conditions were chosen with the particle 1 in. from the chamber wall and with the particle and front at the same angular position in the chamber. The path of the particle was then calculated during the time the front revolved around the chamber. The last calculation was made when the front and particle locations again coincided during the second revolution of the front. Because all errors are accumulative and are carried through to the last calculation, care was used to achieve reasonable accuracy. The computations of the angular positions were carried out to 0.001 of a degree and the radial locations to 0.001 in.

The particle path is illustrated in Figure 15 which shows a portion of the segmental chamber section used in Figure 13.

At Position 1, the front and the particle under consideration have the same angular position. As the front passes by, the particle is accelerated in the same direction as the front movement. However, the sudden release of combustion gases, after the front, causes the particle to be deflected toward the center of the chamber. By the time the front has revolved 180° around the chamber, the particle is traveling in a direction opposite to its original path and begins to move radially outward and toward its initial angular position. The particle velocity is lowest during this period. Prior to the arrival of the front, the particle is again accelerated circumferentially in the direction of the front, which passes the particle for the second time at Position 5.

For the calculations determining the particle path, the circumferential velocity component of the gas movement was assumed to be the same along any radius at a given time. This assumption may entail less error than would initially be supposed, as an examination of the velocity vectors in Figure 13 indicates that a similar flow direction prevails within the chamber in most places. Thus, there are not likely to be many large velocity gradients along any given radii, except during the very high velocities which are associated with the front arrival and passage. At this time, the particle is closest to the wall, and the observed velocities are subject to the least error.

E. MECHANISM OF THE TANGENTIAL FRONT

The tangential mode of combustion instability is composed of three major phases: (1) preparation of the front supporting media, (2) accumulation and distribution of the supporting media, and (3) combustion and release of the stored energy upon arrival of the front. The first phase is composed of injection of new propellants, mixing, and heating. The second phase begins when enough time has elapsed to form a front-supporting medium, and ends upon arrival of the front. The third phase of the instability cycle occurs when the front arrives and the available energy is released, thus aiding in the propagation of the front. The processes involved in the three phases are dependent upon each other and can become quite complex in their relationships.

Before the discussion is continued, the various terms that have been used will be defined.

1. A tangential front results when the release of chemical energy in the combustion chamber takes place in a manner that causes a circumferential propagation of a high intensity, luminous region and pressure front.

2. A supporting medium is an explosive mixture in which the energy content and availability are sufficient to propagate a tangential front.

3. Minimum propellant preparation time is the minimum time required to form a supporting medium, as measured from the moment a tangential front passes through the area under consideration.

4. Auto-ignition is the spontaneous ignition of a supporting medium. Auto-ignition as defined must automatically result in a tangential front as it occurs in a supporting medium.

5. Auto-ignition time is the propellant preparation time required for the spontaneous development of a tangential front through auto-ignition of a supporting medium as measured from the moment a tangential front passes through the area under consideration.

The character of the tangential front can be discussed, with these definitions in mind, by examining the phenomena from a given point on the chamber wall near the injector face. As the front moves by, the immediate area is subjected to high pressures and temperatures, but meanwhile, the injection of new propellants continues. As these liquids enter into the combustion chamber, they are atomized, mixed and vaporized at a much higher rate than during stable combustion, for the large mass of combustion products released by the front is now sweeping across the injector face at velocities that may be as high as 2400 ft per sec. Soon, the energy added satisfies the requirements for the minimum preparation time, and a supporting medium is formed. Assuming the wave completes one cycle at this moment, and again passes the point in question, a continuous cyclic process would result. A simple block diagram of this condition is illustrated in System (a) of Figure 16.

If the wave takes longer than the minimum propellant preparation time to make one revolution, more chemical energy will have been stored and prepared for release, and the front becomes stronger, as indicated in System (b) of Figure 16. To extend the cycle period further would eventually cause the wave to arrive at the instant the supporting medium reaches the point of auto-ignition. Under this condition, it is believed that the energy release time is the shortest and the energy available for release the greatest, with the result that the front reaches its maximum destructive power.

The effect of again increasing the time for the front to make one revolution is to allow auto-ignition at the point of observation, before the front arrives. Thus, a new front is created, and the old front arrives at a time when there is little energy available, which results in its attenuation and demise (see System (c) of Figure 16). Further extension of the front cycle period would allow two waves to exist, each under conditions similar to those for the first front type discussed (System (d) of Figure 16.

The above interpretation of the combustion phenomena for the tangential front was derived from the study of data taken under various test conditions. A continuous spectrum of the wave forms shown in Figure 16 is given in the diagram in Figure 17. In applying this concept to actual thrust-chamber-hardware performance, the factors affecting the absolute cycle time must be taken into consideration. These factors include thrust-chamber circumference, variations of the minimum propellant preparation time (as affected by injector patterns), chemical properties, and the fact that the front does not necessarily travel at a constant velocity.

To date, the tangential wave phenomena recorded can be correlated, as illustrated in Figure 17. In the right-hand diagram, time has been chosen as the abscissa, and is used in the relative sense only. The heavy line slanting downward and to the right represents one cycle period as measured from the "Y" axis along any ordinate. This cycle period is basically simple for uniform conditions, representing the time required for the front moving at a velocity v to make a circuit of the chamber, a distance, πD,

$$T = \frac{\pi D}{v} \tag{11}$$

where

T = cycle period (sec)

v = front velocity (ft per sec)

D = thrust chamber diameter (ft)

However, in actual conditions, the front velocity, v, is a complex variable. In general, it can be said that, the greater the amount of energy released in the front, the higher the front temperature and velocity. The front has a characteristic of rapid response to the nature of the media through which it passes. If the nature of the media at the time the front passes through the region is described as a function of the position around the combustion chamber, β, a more exact formula for the cycle period can be written

$$T = \frac{\int_{0}^{2\pi} R \, d\beta}{v} \tag{12}$$

where

R = combustion chamber radius (ft) and is a constant

v = front velocity (ft/sec), a variable considered as a function of β

β = angular position of front around chamber (rad)

The mechanism in preparing the front-supporting media from the liquid fuel and **oxidizer** that are injected should now be discussed in greater detail. For simplicity, it is assumed that the front consumes all of the propellant in the region through which it passes. The production of the front-supporting media appears to be controlled largely by the nature of the preceding front, as it passes through the volume element of the combustion chamber under consideration, and as long as the gases produced in the front sweep across that region. The gases released by the chemical combustion reaction in the front can provide a source of heat for raising the temperature and vaporizing the liquid propellants, that are injected, as well as furnishing the kinetic energy required to atomize, transport, and mix the propellant components so as to produce a supporting medium.

A suggested relationship between the rate of the injected liquid propellant being converted into mixed gaseous media from a finite element of injection, as a function of time after the passage of a front, is shown in Figure 18. Immediately after the injection stream element has left the injector face, no front supporting gaseous media can be formed from its contents in a bi-propellant system as no mixing has been immediately accomplished. Assuming some vapor is immediately available at the instant of injection the initial mixing will begin after a time period, "a"

$$a = \frac{S}{12 \, V_g} \tag{13}$$

where

a = time period (sec)

S = distance between bi-propellant injection streams (in.)

V_g = component of gas velocity between injection stream points (ft per sec)

When the time period, "a," has elapsed, mixing begins, and the rate would be expected to increase in some manner with respect to time. After a portion of the injection stream elements had been mixed, the rate would logically be expected to fall off in some manner, possibly of the general nature of a log-decrement approaching zero as a limit. To evaluate this rate versus time relationship, the effect of numerous factors must be considered, including the injection stream atomization, heating and vaporization, the initial characteristics of the hot-gas cross flow (such as mass velocity and temperature), as well as the transport of atomized liquid and vapors at various rates. Consideration of these processes leads to the construction of the relationship shown in Figure 19. It is expected that monopropellants would begin to produce a supporting medium immediately, as the transport and mixing required of bi-propellant systems is not present. This is shown by the dashed line (A) where the rate of production of a gaseous monopropellant may be presumed to be largely effected by the heat-transfer rate into the injection spray. Some types of injection spray (such as a fine atomization) will probably show a higher production rate of supporting media than coarser spray types. After the peak production rate is reached, the decline will probably be faster, and will become zero sooner for the monopropellant than for a bi-propellant, where the mixing of widely separated components is an important factor.

In contrast, a bi-propellant showerhead injector stream would have a finite time, "a," before any front supporting media would be produced, and the production rate would depend upon such factors as the jet diameter, injection velocity, etc. A liquid-phase-mixing injector (such as an unlike pair or a two-on-one) could be expected to give a different type of curve. If the impingement length were long enough, the showerhead curve would be approached; for zero impingement length, the monopropellant curve would be approached. For a short impingement length, there would be a reduced time, "a," before any supporting media would be produced, followed by a rapid rise in the production rate, depending upon the fineness of atomization and the heat-transfer input. This would be followed by a decline, largely controlled by the mixing of separated quantities of fuel and oxidizer. The amount of supporting media produced from each element of an injection jet stream is a function of the total time of exposure.

$$W_m = \int_0^{t_e} \epsilon \, dt \qquad (14)$$

where

W_m = amount of front supporting media produced from injection stream element

ϵ = production rate of supporting media as a f(t)

t_e = total time of exposure for any given element

The integration of the production rate of the supporting media function in Equation (14) gives the total amount of the supporting media derived from an element of the injected propellant stream. A summation of these integrated amounts, for all the elements in an injection stream for the time period between fronts, will give the amount of supporting media available for the front.

These injection-stream elements (Δm or dm) are distributed along the length of the stream penetration. The following summation may be made:

$$W_e = \sum_{l=o}^{l=l_p} W_m \Delta m \qquad (15)$$

where

W_e = amount of supporting media produced from an injection stream during the time between fronts
Δm or dm = elemental portion of injection stream under consideration
l = axial distance along injection stream path
l_p = maximum axial penetration of stream during time between fronts

The limit of this summation becomes

$$W_e = \int W_e \, dm = \int\int \epsilon \, dt dm \qquad (16)$$

To make this a more useful parameter of the energy available for immediate release in the front, it can be converted into the terms of the amount of supporting media per unit of volume. The volume concerned will be bounded by the area of the injector-face pattern sector associated with the injection stream element integration in Equation (15), and of the injection penetration axially into the combustion chamber, l_p.

$$Vol = \Delta A \, l_p \qquad (17)$$

The simplified assumption would be a uniform distribution of the supporting media in this volume. This condition is probably non-existent, but may be approached as the degree of turbulence in the gas flow increases. For the case of uniform distribution

$$W_m = \frac{\int\int \epsilon \, dt dm}{\Delta A \, l_p} \qquad (18)$$

Where l_p is short, this may be found to be a suitable parameter. Where l_p is long, the distribution along l_n may be significant, and thus warrant consideration. Figure 20 presents curves to show those points.

From the preceding discussion of the preparation of a front-supporting medium, a significant parameter appears, namely, the period of time elapsing between the passage of a front and the minimum preparation of new media that will support a second tangential front. This parameter is represented on the tangential front model diagram (Figure 17) as the vertical dashed line to the right of the zero-time line. As time is relative in this diagram, the minimum propellant-preparation time is constant relative to the increasing cycle time, which is indicated by the heavy cycle-period line slanting to the right. An important consideration is the relationship between these two, the minimum propellant-preparation time (MPPT) and the cycle period, as this can be expressed in terms of the angular position of the front in the combustion chamber in relation to the point under consideration after the minimum propellant-preparation time has elapsed. A diagram of this is shown in Figure 21. The distance the front has gone around the circumference is

$$D = \int_0^{MPPT} v_f dt \qquad (19)$$

where

D = distance traveled (ft)
v_f = front velocity (ft/sec) which can be a variable
t = time, sec

The angular position of the front is obtained by dividing D by the radius, R, of the combustion chamber, giving

$$\beta = \frac{1}{R} \int_0^{MPPT} v_f dt \qquad (20)$$

where β = angle front travel (rad)
R = combustion chamber radius (ft)

The difference between the position of the front and the point under consideration at the time a supporting media is formed at the point has been termed the "lead angle," and is

$$\emptyset = 2 \pi - \beta \qquad (21)$$

It can be seen that, in the regions where

1. $\emptyset$ is positive, supporting media can be present, and conditions are favorable for the continuous propagation of a front

2. ϕ is less than zero, supporting media will not be present and, therefore, no energy is available for the continued propagation of the front.

This leads to a statement of one stability condition:

"When ϕ is negative, and remains continuously negative for all positions around the circumference of the chamber, the tangential front cannot exist." This condition is represented by the plot in Figure 22a. This is the top region in the diagram in Figure 17, and is exemplified by the strip film Sample 0.

When ϕ is zero, a continuous single front can be supported, and as the amount of energy available for release in the front is at a minimum, the front will be relatively slow and weak. This condition is represented by the plot in 22b, and by the strip-film Sample 2 in Figure 17.

Experimentally, a front has been encountered that can be explained by a lead angle ϕ, which varies from less than zero to positive and back in a cyclic manner. An example is shown in strip-film Sample No. 1 in Figure 17. This strip of film shows a strong, fast front changing into a weaker, slower, more diffuse front, and at a later time, regaining its strength and speed, only to revert to the slower front again in a cyclic manner. It is postulated in this case that when the strong front completes a circuit of the chamber, it arrives before the minimum propellant preparation time has elapsed (negative ϕ), and therefore attenuates and slows down. However, before it attenuates to the extent that the front disappears, it enters a region where the minimum propellant preparation time has elapsed. At this position in the chamber, ϕ becomes positive, and the front becomes strong and fast once more. A diagram of this condition showing a two-revolution cycle is presented in Figure 22c. This phenomenon may explain the "subharmonics" encountered by several observers utilizing electronic gauges. These strong fronts and associated peak pressures come at appreciably longer time intervals (and hence, lower frequencies) than that associated with a continuous front. While it is not necessarily at half the frequency of a continuous tangential front, specific instances can be at half of some presumed natural acoustic frequency, and thereby create the condition of a "subharmonic."

As the relative cycle time becomes progressively greater than the minimum propellant preparation time (increasing positive ϕ), more energy is released in the front, resulting in a stronger and faster front. Examples of this are shown by the progression in strip film Samples 2 through 5 in Figure 17, which show progressively faster fronts with increasing concentration of the luminosity in the front. This trend is followed until the cycle period reaches the auto-ignition time.

The auto-ignition time is represented by the second vertical line in the diagram shown in Figure 17. This phenomenon is one often encountered in diesel and Otto-cycle internal-combustion engines. From the previous discussion of the preparation mechanism of the front supporting media, it can be seen that, in many conditions, heating can continue until an auto-ignition temperature is reached. When this occurs, in a supporting medium, a combustion front forms. In addition, when the cycle period is greater than the auto-ignition time, a change in the character of the front is noted.

The strip film Sample 6 in Figure 17 shows an example in which the cycle period is slightly longer than the auto-ignition time, and the formation of an auto-ignition front precedes the arrival of the original front by a small time period. When these time periods are short enough, and in close proximity of each other, the effect on propellant injection and the subsequent preparation of a new supporting medium is similar to that of a single front. This condition has been termed a "pre-ignited front." Thus the ϕ angle is increased to the extent that, before the front completes the circuit to the point under consideration, auto-ignition occurs at that location. The angle between the position of the front and the point (at the instant of auto-ignition at the point) has been termed the σ angle. The auto-ignition front becomes separate and distinct from the initial front. The strip film Sample 7 in Figure 17 shows an example of the above condition. This phenomenon is discussed in the next section.

As the cycle period becomes still longer, relative to the minimum propellant preparation time, a point is reached where

$$\beta = \frac{1}{R} \int_{0}^{MPPT} v_f \, dt = \pi \tag{22}$$

It may be seen that the time for a front to make one-half a revolution in the chamber equals the minimum propellant preparation time. When this condition is reached, two identical continuous fronts can be supported as shown in strip-film Sample No. 8 in Figure 17. Figure 23 represents the condition when the fronts have maximum strength, with the auto-ignition time coinciding with the arrival of the front.

F. THE DISCONTINUOUS DOUBLE FRONT

The discontinuous front system is considered separately as this type of instability is frequently encountered, particularly in larger diameter chambers. Tangential instabilities which occur as a result of perturbations in the combustion process are believed to be of a complex multiple front nature in the initial stages.

Many of those fronts are discontinuous. The following discussion deals with a simple discontinuous front system which never involves more than two fronts in the chamber at a given time.

A circumferential-window photograph of a discontinuous double front is shown in Figure 24. The fronts are marked by the white lines, which are solid when the front is on the near side of the chamber and broken when the front is on the far side of the chamber. It will be noted that, when a new front is born, the existing front dies out when it reaches the birth point. The time which has elapsed after the passage of the new front is insufficient to create a supporting media; thus, there is not enough energy available for the original front when it arrives in this area. The birth point of the new fronts is not always located at the same point in the chamber. This may be attributed to the movement of high-velocity gases carrying a supporting medium into the non-supporting zone and to a changing angular relationship between the new and old fronts. A difference in angular position of the fronts will affect the time when the next front is born. In Figure 24, the birth point, A, appears to shift over the bottom rear quadrant of the chamber.

A diagram of an idealized, double, discontinuous front is shown in Figure 25. This cyclic relationship was first proposed in Reference 3, and it closely follows the actual front mechanism of Figure 24. At a random instant (shown in Interval A of Figure 25), a front (F_1) is progressing in a counter-clockwise direction with a positive ϕ angle, represented by the preceding shaded sector. An attenuating front (F_0) is just disappearing in the form of a shock front in a region where the supporting medium has been exhausted by the preceding front (F_1), and insufficient time has passed to allow the formation of new supporting media. The medium at Position a is always the one that has progressed the most in the state of preparation. At a slightly later time (diagrammed in Interval C of Figure 25), the preparation of front supporting media has progressed sufficiently to cause auto-ignition, and a new Front (F_2) is born. Each new front must propagate in a counter-clockwise direction, as supporting media are not present immediately clockwise to the front. At a later interval, Front F_1 approaches Point a (see Interval D of Figure 2.5) and attenuates and disappears in the same manner as did Front F_0 which preceded it (Interval E of Figure 25). In the meantime, F_2 has been progressing in a normal manner. Sometime after F_1 has passed by Point a, the minimum propellant-preparation time(after the passage of F_2) is reached, resulting in the appearance of supporting media which are progressively increasing in extent as Point b advances until auto-ignition once more occurs, resulting in the introduction of Front F_3, as shown in Interval F of Figure 25.

G. SCALING CONSIDERATIONS

The mode of the tangential front system is dependent upon chamber diameter. To ascertain whether the front system would behave as predicted by the tangential-mode diagram shown in Figure 17, tests were conducted in 15, 22 1/2, and 30-in. dia. chambers. This diagram indicates that, as the cycle period becomes longer with respect to the minimum propellant preparation time, more complex front systems are allowed to propagate in the chamber. The cycle period was varied by the use of different chamber diameters. Relative changes in preparation time were minimized by using identical injector elements and similar operating conditions, such as chamber pressure, mixture ratio, and injection velocities. A comparison of circumferential-window photographs for the three chambers is given in Figure 26. In all chambers, the instability can be divided into two parts, a transition period and a "steady-state" period. The predominance of the transition period varies greatly for different thrust-chamber conditions.

When the tangential instability was initiated for a particular set of conditions in the 15-in.-dia chamber, a continuous single front resulted. The transition period lasted for approximately 25 millisec before one of the stronger fronts predominated and emerged as a continuous wave. This instability was of intermediate strength and would fall about where film strip No. 3 is located on the model diagram of Figure 17.

Under similar test conditions, a continuous single front also developed in the 22 1/2-in-dia chamber. The front velocity was found to be slightly higher than that of the 15-in.-dia chamber and thus the front was considered to be stronger. The transition period was nearly trebled, extending for approximately 70 millisec. During this time, a prounounced discontinuous-front system revolved around the chamber in one direction, while a weaker multiple-front system appeared at intervals, revolving in the opposite direction. Eventually, the weaker front system attenuated and a continuous single front instability developed as shown in Figure 26. The transitional period of the weaker front system was composed of six fronts equally spaced around the chamber. Apparently, these fronts can exist because the cycle period has been increased and, thus, energy is available for front propagation during a greater part of the cycle. Also, it is believed that these very weak fronts do not combust all of the energy available, which allows them to propagate in close proximity to each other. As the dominant discontinuous front gains strength and leaves less energy for the weaker fronts, the whole system transforms into a continuous-front phenomenon. The increase in cycle period, with respect to the minimum propellant-preparation time, was not enough to shift the mode type into the double, discontinuous region.

When the chamber diameter was increased to 30 in., a continuous-front system was not attained. There was a long transitional period during which it is difficult to analyze what was taking place. Once the steady-state instability condition had been reached, a discontinuous system developed, in which it appears that counter-revolving fronts were always present. The front velocity given in Figure 26 for this chamber was measured over 1/2 cycle on one of the more predominant fronts.

It is interesting to note that, despite the large differences in chamber diameter, the front velocities are approximately the same. When the cycle period is increased in a given injection system, more energy is allowed to accumulate between front arrivals. However, if this additional energy is not reflected in a stronger front, it is possible that it is distributed further from the injector face in such manner that there is little change in the energy per unit volume. Such an extension of the high-energy zone from the injector face would mean that the front velocity would be approximately the same, although its active zone would be extended for a greater axial distance. Of course, if the cycle period is increased enough, auto-ignition occurs and a different front system will develop, as illustrated by the 30 in.-dia record in Figure 26.

An increase in chamber pressure and the resulting increase in the density of the chamber gas cause greater atomization of the liquid propellants and higher evaporation rates. The minimum propellant-preparation time would then decrease, and the instability system should move toward the more complex front system shown in the model diagram, Figure 17. Thus, a chamber-pressure increase of 180 psi in the 22-1/2-in.-dia motor caused the continuous, single-front system to change into a discontinuous, double-front system. A definite change in the instability of the 30-in.-dia chamber was also noted when the chamber pressure was increased from 238 to 343 psia. The counter-revolving fronts at the lower pressure were changed to a strong, discontinuous, multiple-front system. There appears to be a cyclic front which at times behaves like a discontinuous, double-front system. Other weak fronts appear at random intervals between the stronger fronts. In the 15-in.-dia chamber, a pressure increase from 210 to 365 psia did not change the preparation time enough to shift the front system out of the continuous, single-front region.

As the chamber diameter increases with respect to the minimum propellant preparation time, it was found that a continuous double front may not develop. Apparently, in larger chambers this front system might be rejected in favor of a discontinuous, multiple-front system which owes a part of its existance to the fact that weak fronts do not combust all of the available energy.

H. CONCLUSIONS

The investigation of the tangential mode of high-frequency combustion instability has revealed many characteristics of the phenomenon, including various mode types and physical processes. A brief summation of the major conclusions and results from the investigation includes the following:

1. A model diagram, Figure 17, of the tangential instability has been constructed which depicts the major modes encountered.

2. The suggested physical-process mechanism for supporting fully developed tangential instabilities is harmonious with noted effects, including those of chamber diameter and combustion pressure.

3. The radial and axial distribution of the tangential front in the experimental chamber has been defined.

4. The motion and pressure distribution of the chamber gas during a single-front tangential instability have been outlined (Figure 13) for an experimental thrust chamber.

5. The estimated path of a luminous particle has been defined during a single-front tangential instability occurring in an experimental thrust chamber, Figure 15.

6. The physical processes established and the testing techniques developed in the experimental investigation can be applied to large-scale thrust-chamber development problems (Reference 5).

REFERENCES

1. Pickford, Krieg, and Ellis, Basic Research of Combustion in Liquid Rocket Thrust Chambers Aerojet-General Report No. 1193 November 1956. (Confidential)

2. Research for Improvement of Combustion in Liquid Rocket Thrust Chambers Aerojet-General Progress Reports 1217-1 through 1217-8, September 1954 to July 1956. (Confidential)

3. Ellis and Pickford, High-Frequency Combustion Instability Aerojet-General Report TN-17 September 1956. (Confidential)

4. Liquid Propellant Rocket Combustion Instability Study, Rocketdyne Report R-312-1, 30 September 1956. (Confidential)

5. Kalt, Investigation of Effectiveness of Gas-side Baffles in 2nd Stage Injector Aerojet-General Internal Report TCR-56, Liquid Rocket Plant, Sacramento, 27 September 1956. (Confidential)

SYMBOLS

A = Area of injector face pattern
D = Combustion chamber diameter, ft.
$MPPT$ = Minimum propellant preparation time, sec
P = Pressure, psia
R = Combustion chamber radius, ft
S = Distance between bi-propellant streams, in.
T = Cycle period, sec
W = Weight or mass, lb

a = Time period, sec
l = Axial distance along injection stream path, in.
r = Radial position of particle in combustion chamber, in.
s = Length of particle path, ft
t = Time, sec
v = Velocity, ft/sec

α = Vector direction of particle motion, deg
β = Angular position of front in combustion chamber, deg or rad
Δ = Finite change of a property or position
ϵ = Production rate of supporting media
θ = Angular position of particle in combustion chamber, deg
ϕ = "Lead angle" or angle ahead of front to the point where supporting medium is just appearing, deg
ψ = Difference in direction of front propagation, deg
w = Angular velocity of front, rad/sec

SUBSCRIPTS

a = High energy portion of front
ave = Average
b = "Tail" of front
e = Exposure
f = Front
g = Gas or vapor
m = Supporting media or elemental portion of injection stream
n = Position at n^{th} increment change
p = Maximum penetration
o = Initial position or condition
1 = Position at first increment change
2 = Position at second increment change

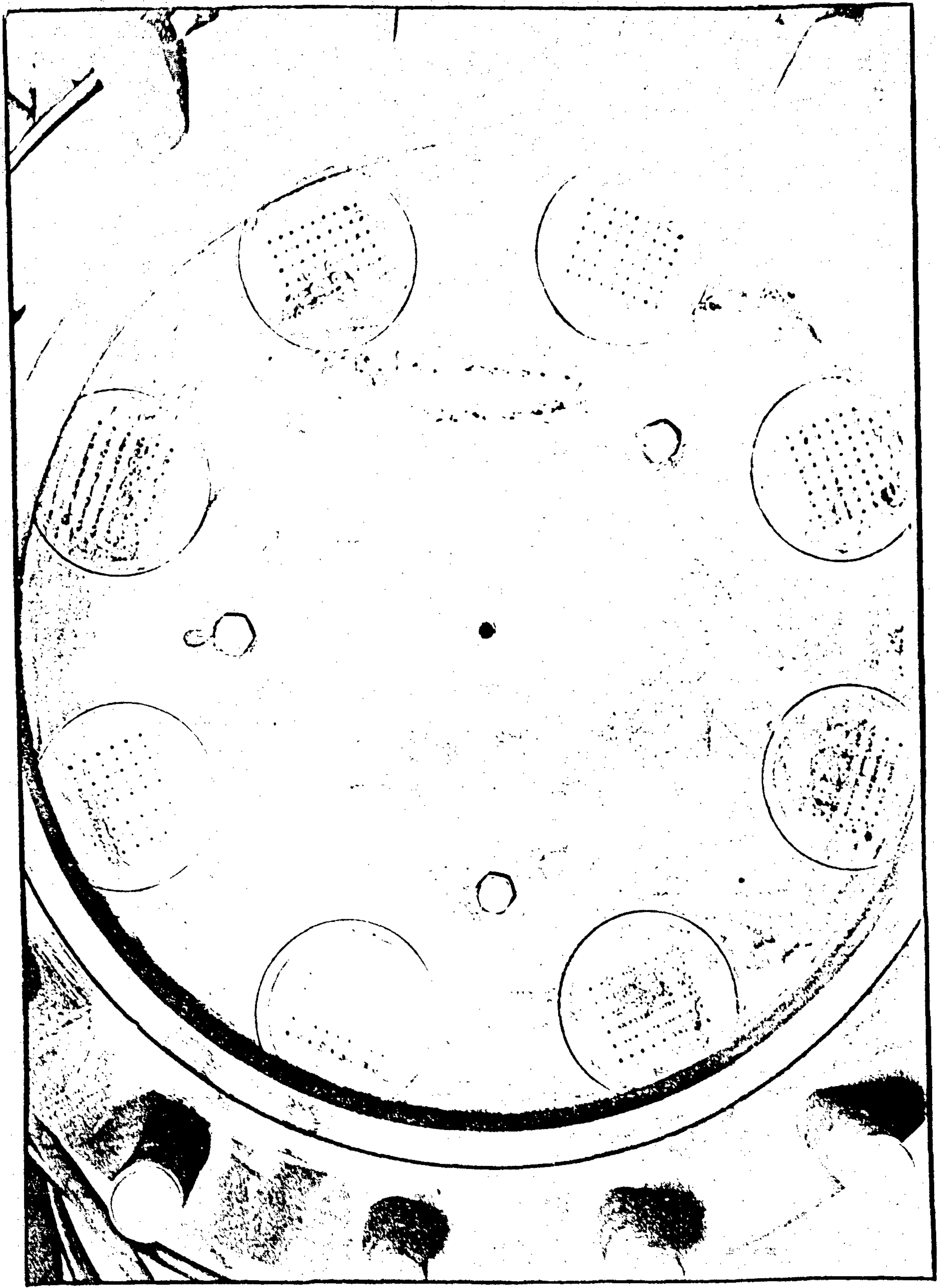

INJECTOR CONFIGURATION
FIGURE 1

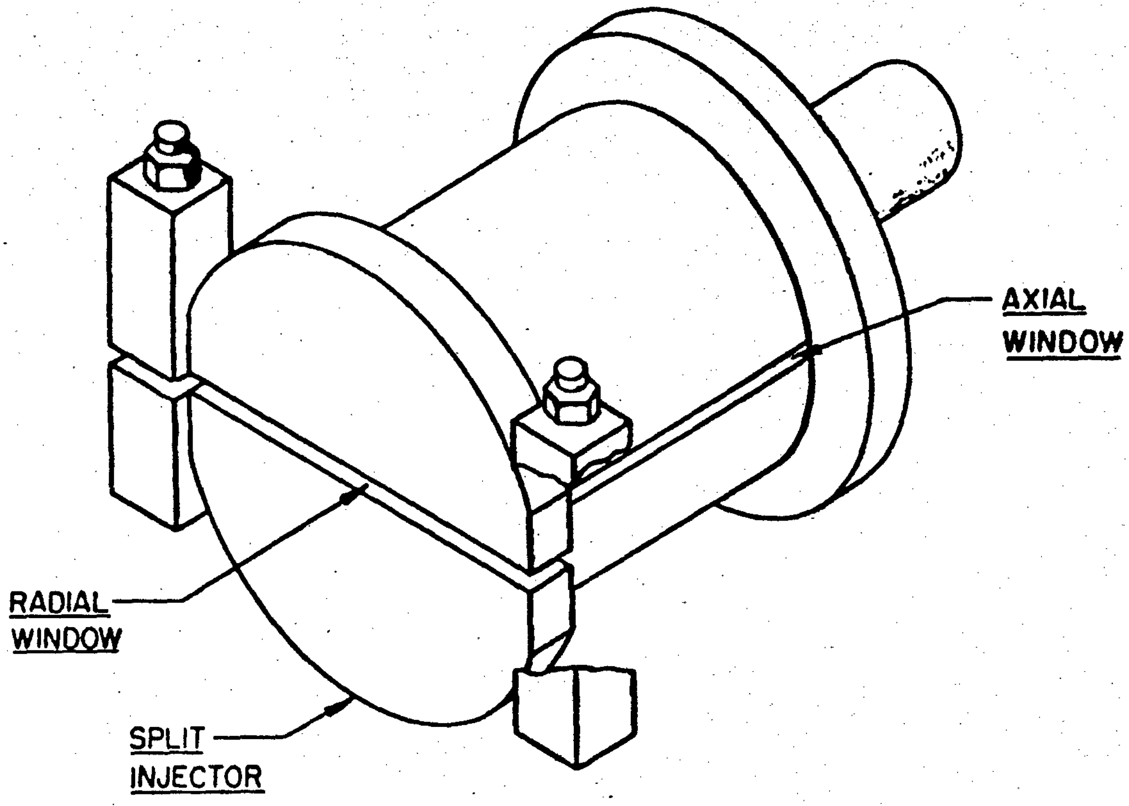
AXIAL WINDOW
RADIAL WINDOW
SPLIT INJECTOR

SLIT WINDOW MOTOR

SCHEMATIC OF SPLIT THRUST CHAMBER

FIGURE 2

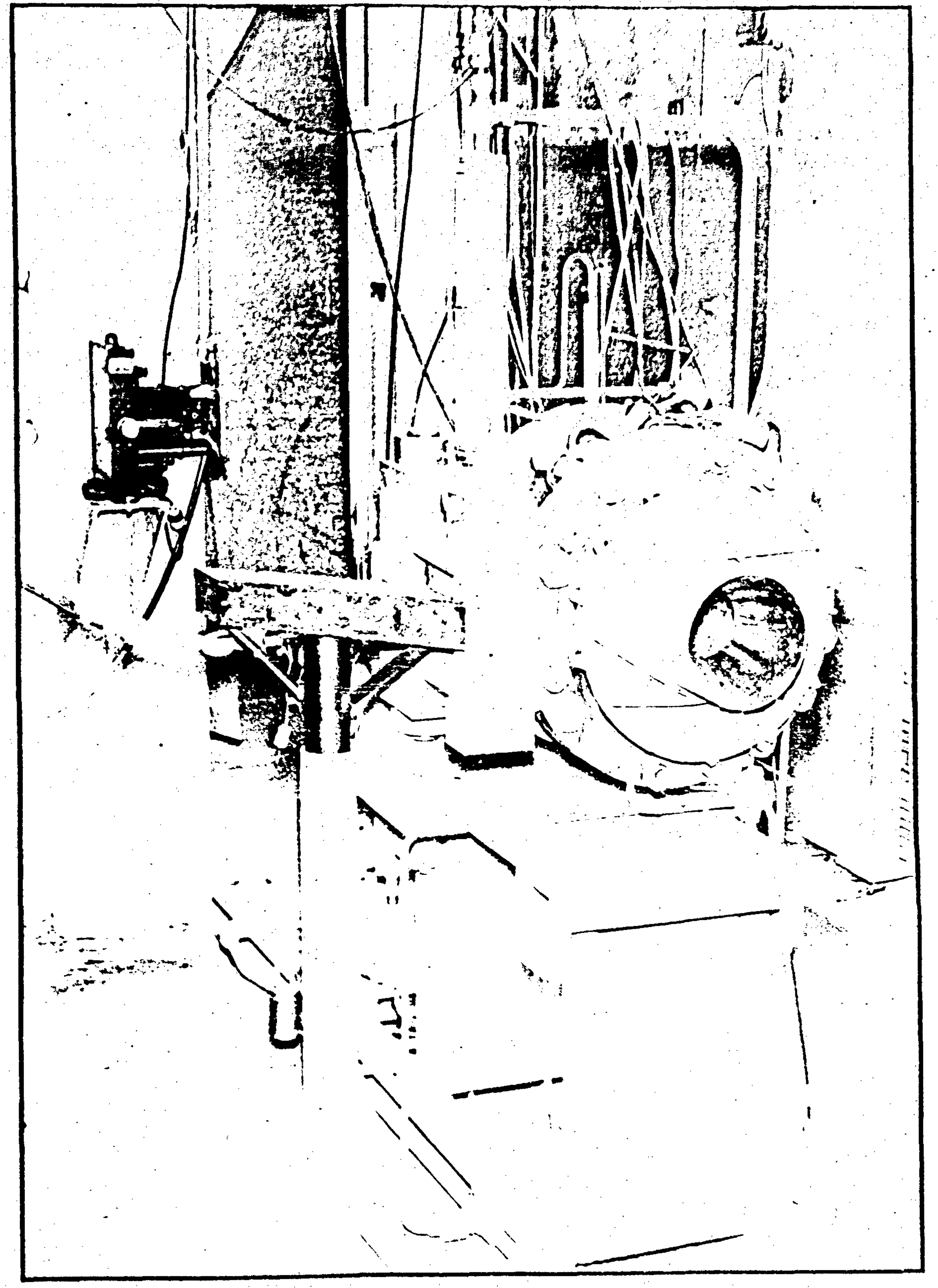

15" DIA. SPLIT THRUST CHAMBER INSTALLATION
FIGURE 3

[illegible]

UNCLASSIFIED

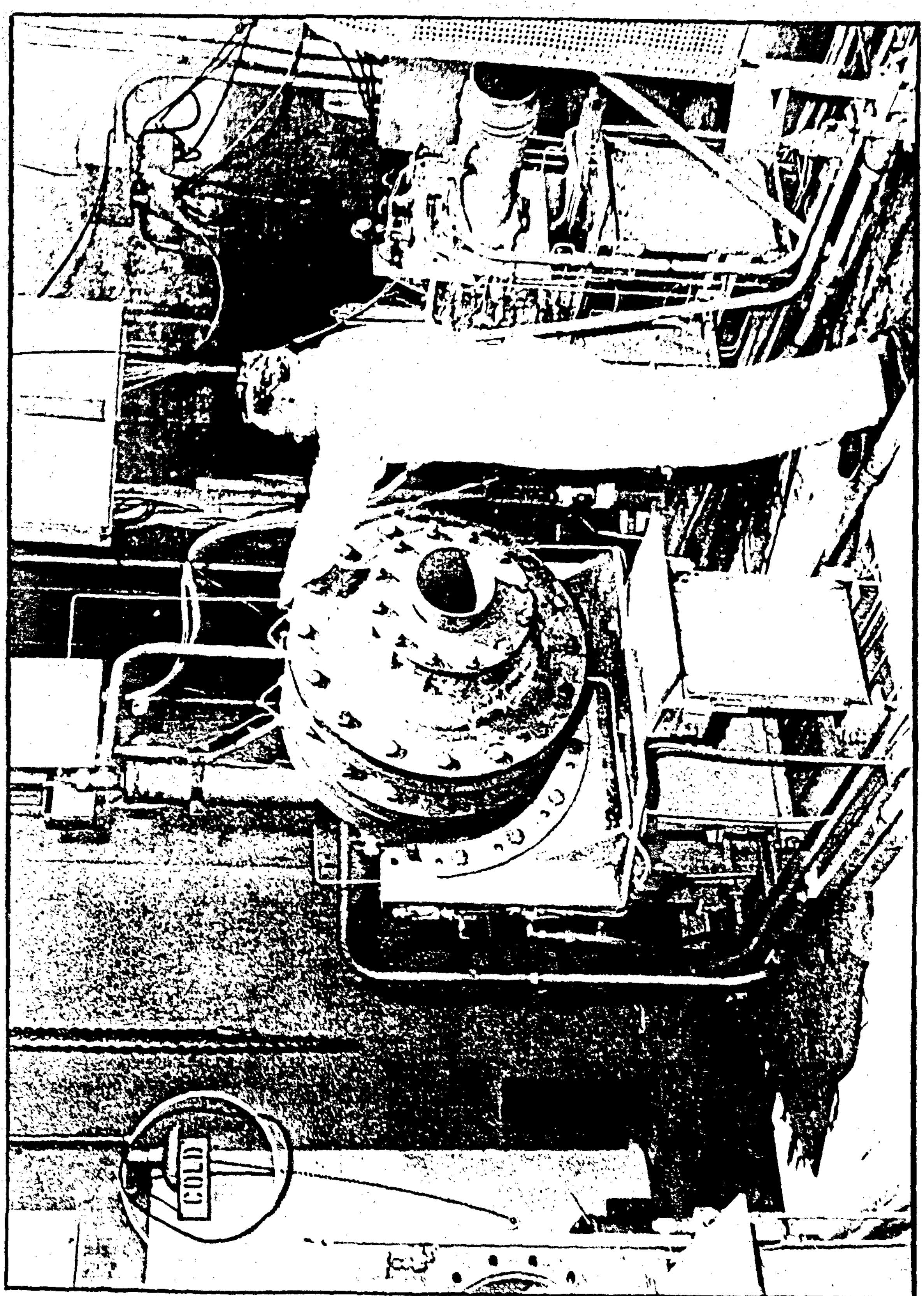

[illegible]" DIA. THRUST CHAMBER
FIGURE 4

UNCLASSIFIED

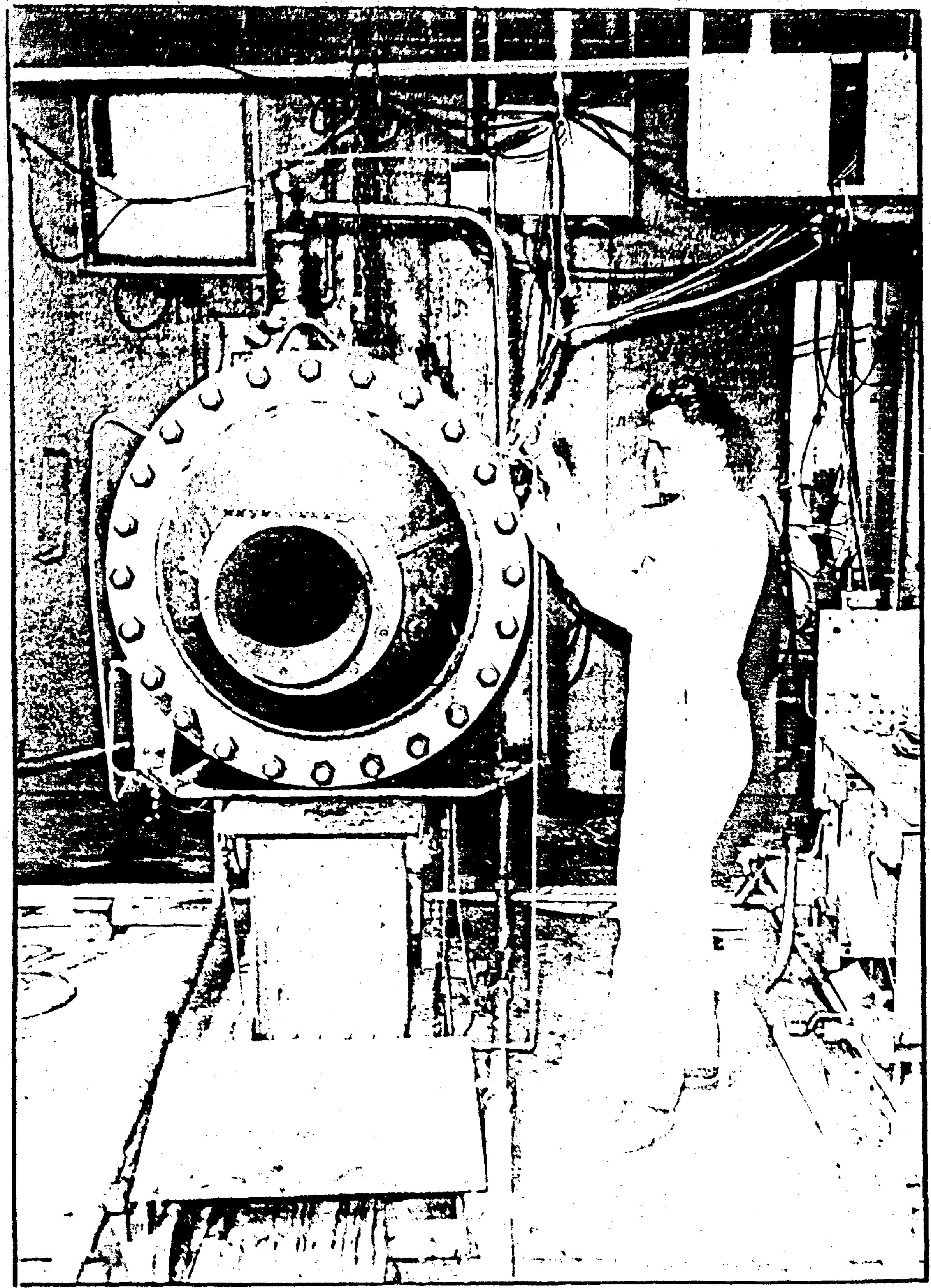

30" DIA. THRUST CHAMBER
FIGURE 5

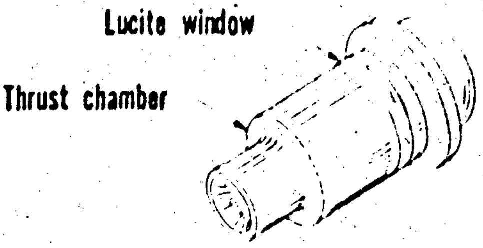
Lucite window
Thrust chamber

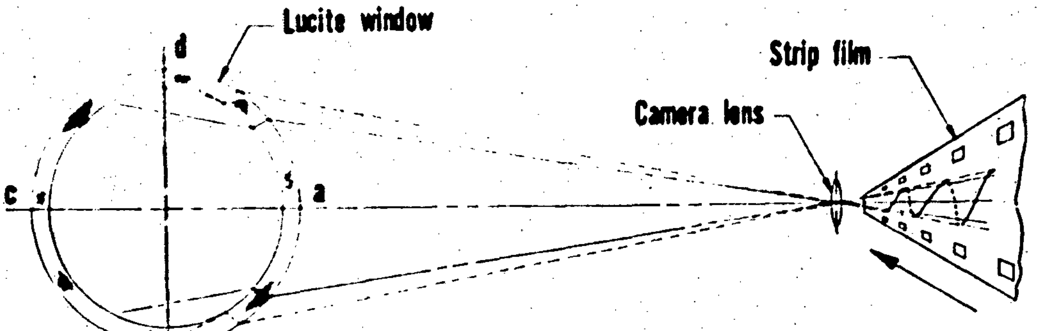
Lucite window
d
Strip film
Camera lens
c
a
b

OPTICAL RAY DIAGRAM

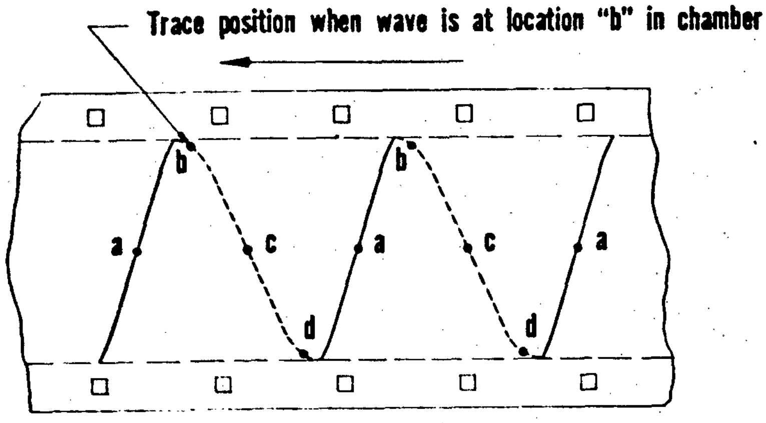
Trace position when wave is at location "b" in chamber
b
a
c
d
b
a
c
d
a

EXPECTED WAVE FORM

Assume: Constant velocity of detonation front & film travel

CORRELATION OF STRIP FILM RECORD
WITH
TRUE POSITION OF CIRCUMFERENTIAL WAVE IN CHAMBER

PHOTOGRAPHIC TECHNIQUE
FIGURE 6

UNCLASSIFIED

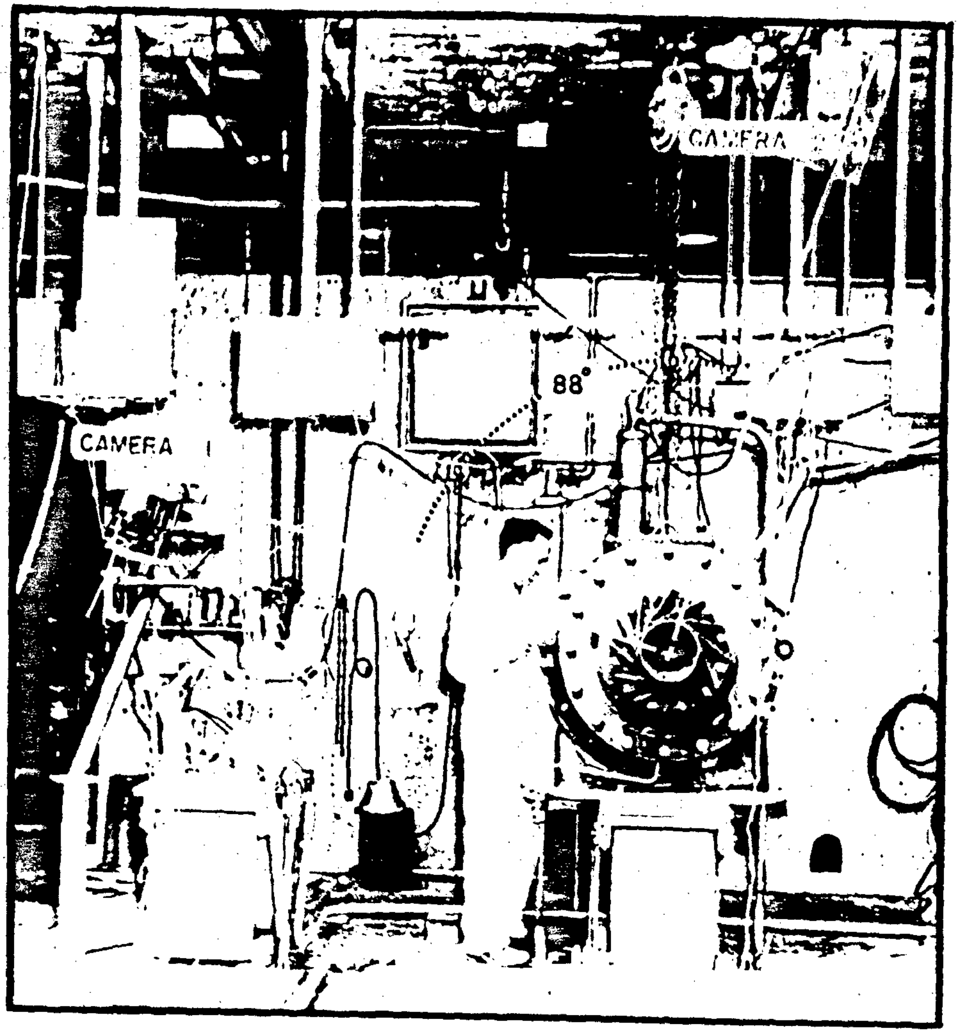
CAMERA
88°
CAMERA

CAMERA LOCATION
FOR
22½ in. dia CHAMBER

FIGURE 7

UNCLASSIFIED

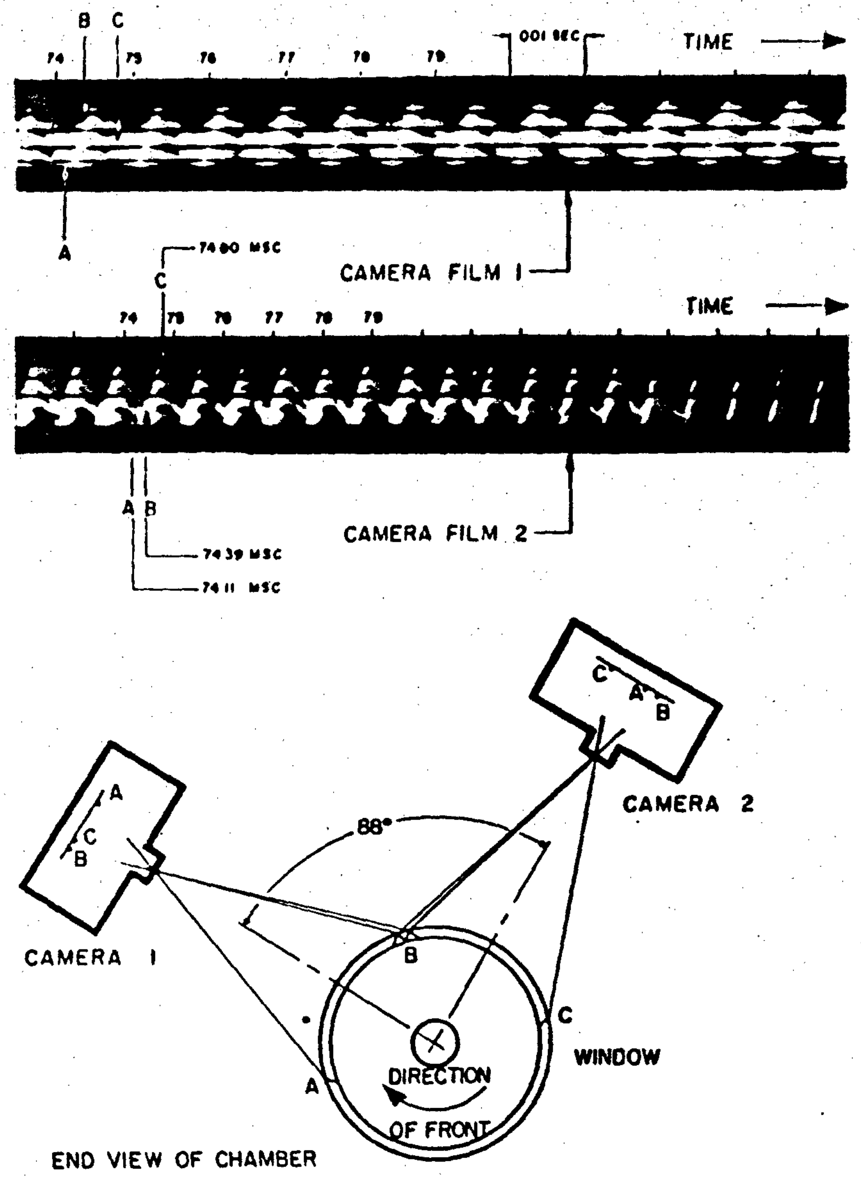
B
C
74
75
76
77
78
79
.001 SEC
TIME
A
CAMERA FILM 1
74.00 MSC
C
74
75
76
77
78
79
TIME
A
B
CAMERA FILM 2
74.39 MSC
74.11 MSC
C
A
B
CAMERA 2
A
C
B
88°
CAMERA 1
B
C
WINDOW
A
DIRECTION OF FRONT
END VIEW OF CHAMBER

CIRCUMFERENTIAL PROPAGATION OF SINGLE FRONT TANGENTIAL INSTABILITY AS SHOWN BY SIMULTANEOUS SLIT WINDOW PHOTOGRAPHS

FIGURE 8

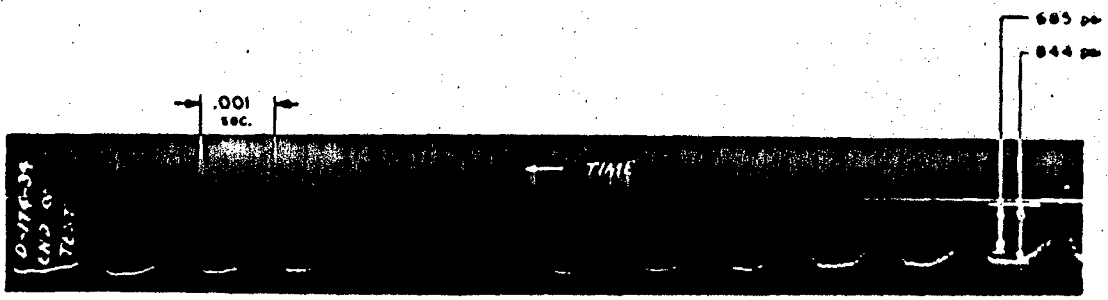

RATE OF PRESSURE RISE; $\frac{dp}{dt} \approx 22.6 \times 10^6$ psi/sec.

FRONT VELOCITY = 5200 ft/sec.

PRESSURE FRONT DURING SHUTDOWN

CONTINUOUS SINGLE FRONT

FIGURE 9

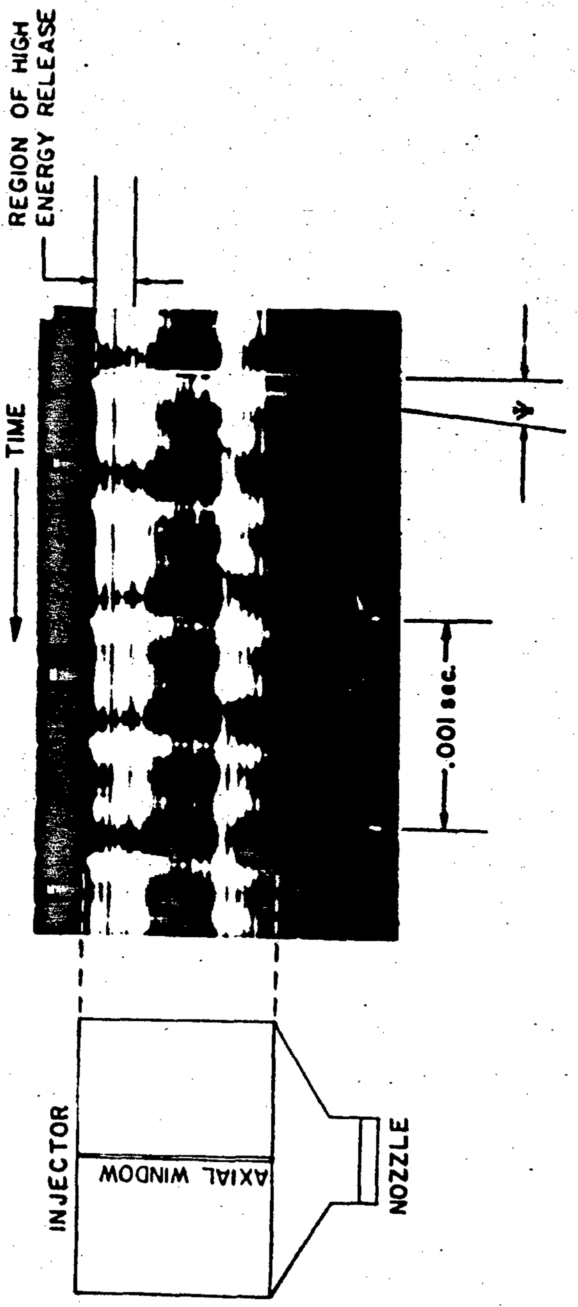
REGION OF HIGH ENERGY RELEASE
TIME
ψ
.001 sec.
INJECTOR
AXIAL WINDOW
NOZZLE

AXIAL DISTRIBUTION OF TANGENTIAL FRONT

FIGURE 10

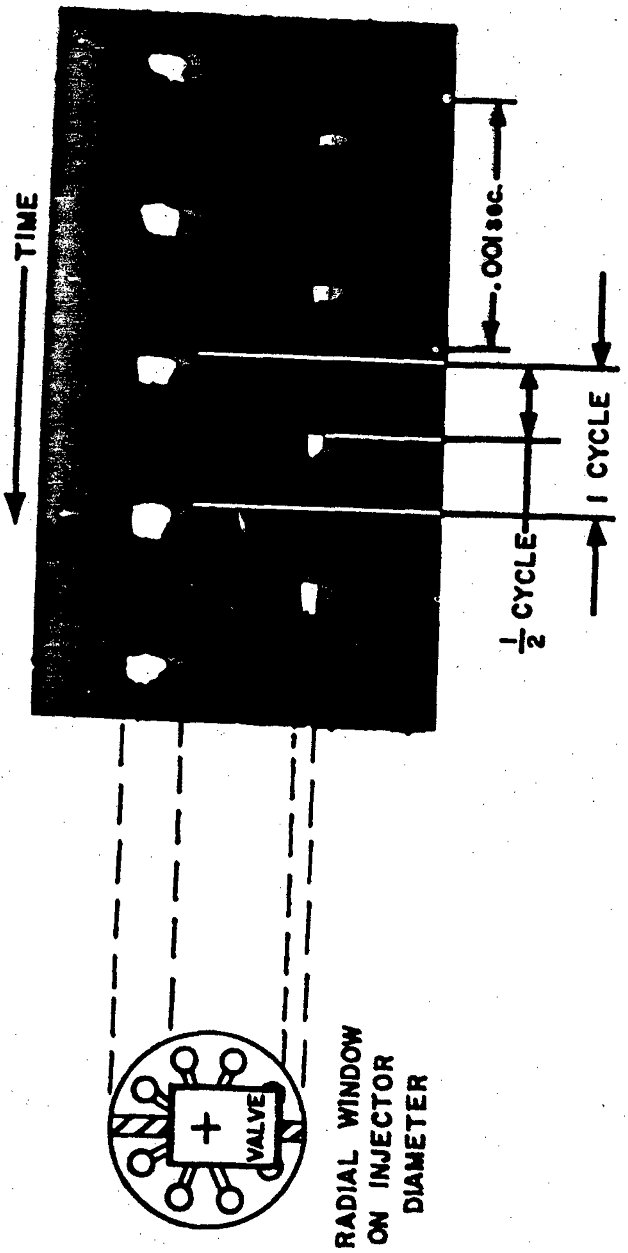
TIME
.001 sec.
I CYCLE
½ CYCLE
VALVE
+
RADIAL WINDOW
ON INJECTOR
DIAMETER

RADIAL DISTRIBUTION
OF TANGENTIAL FRONT

FIGURE 11

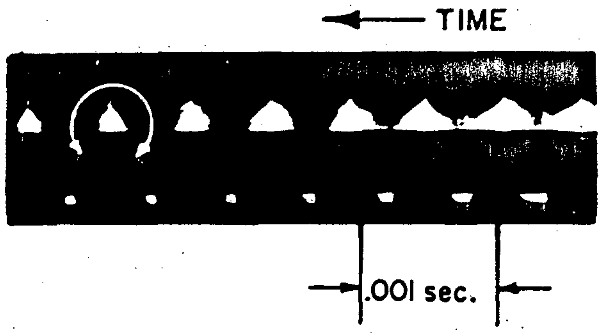
TIME
.001 sec.

RADIAL SLIT WINDOW RECORD
OF
CONTINUOUS SINGLE FRONT INSTABILITY

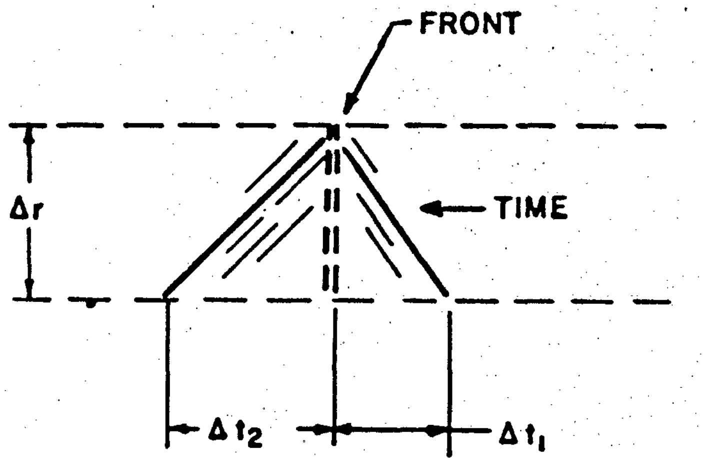
FRONT
TIME
Δr
Δt_2
Δt_1

RADIAL VELOCITY OF LUMINOUS STREAKS
BEFORE FRONT, $V_1 = \Delta r / \Delta t_1$
AFTER FRONT, $V_2 = \Delta r / \Delta t_2$

RADIAL MOVEMENT OF CHAMBER GASES

FIGURE 12

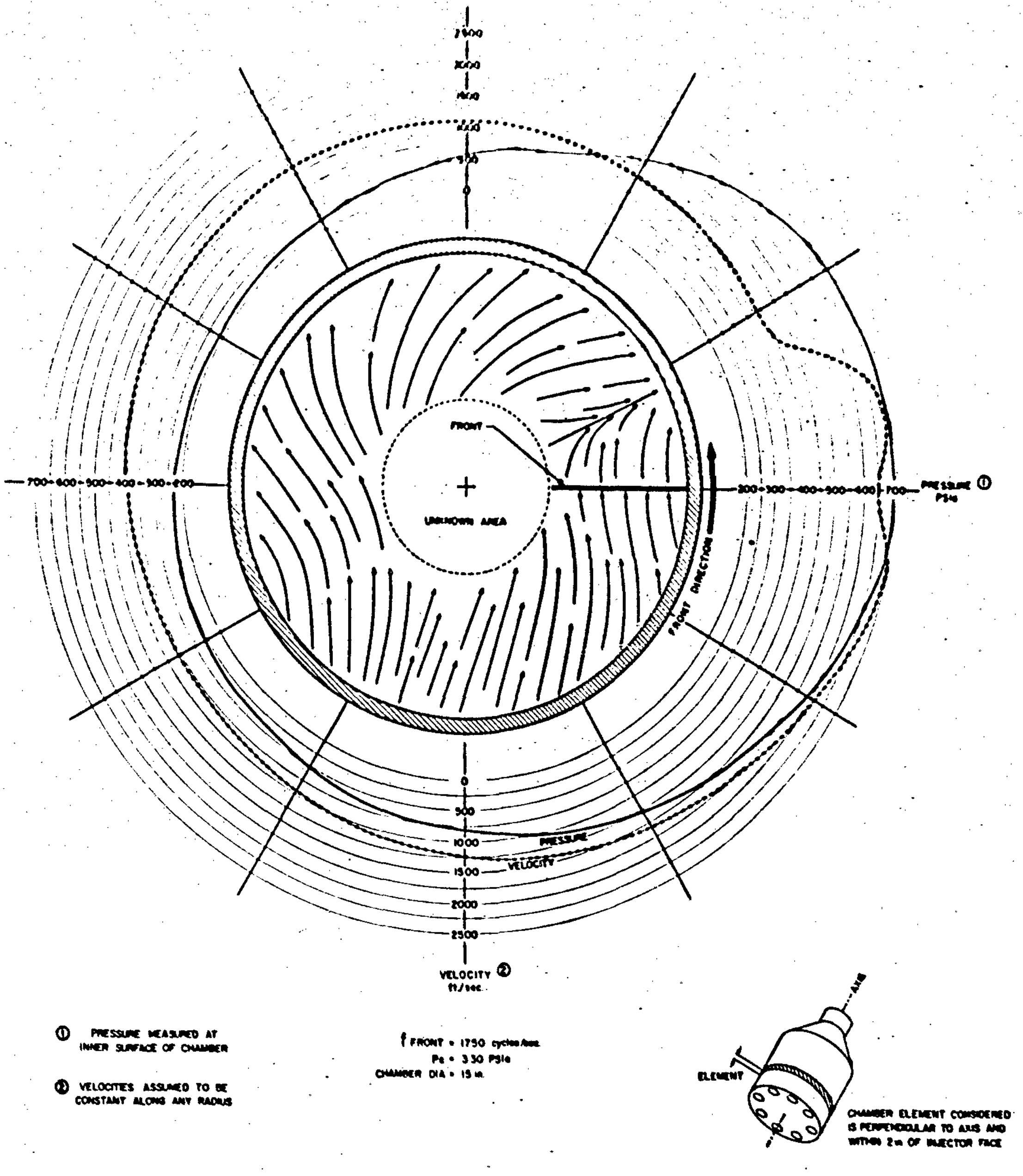
2500
2000
1500
1000
500
0
FRONT
UNKNOWN AREA
700-600-500-400-300-200
200-300-400-500-600-700
PRESSURE ①
PSIA
FRONT DIRECTION
0
500
1000
1500
2000
2500
PRESSURE
VELOCITY
VELOCITY ②
ft/sec.
AXIS
ELEMENT

① PRESSURE MEASURED AT INNER SURFACE OF CHAMBER

② VELOCITIES ASSUMED TO BE CONSTANT ALONG ANY RADIUS

f FRONT = 1750 cycles/sec.
Pc = 330 PSIA
CHAMBER DIA = 15 in.

CHAMBER ELEMENT CONSIDERED IS PERPENDICULAR TO AXIS AND WITHIN 2 in OF INJECTOR FACE

INSTANTANEOUS PRESSURES & VELOCITIES
IN A
CROSS—SECTIONAL ELEMENT OF CHAMBER

FIGURE 13

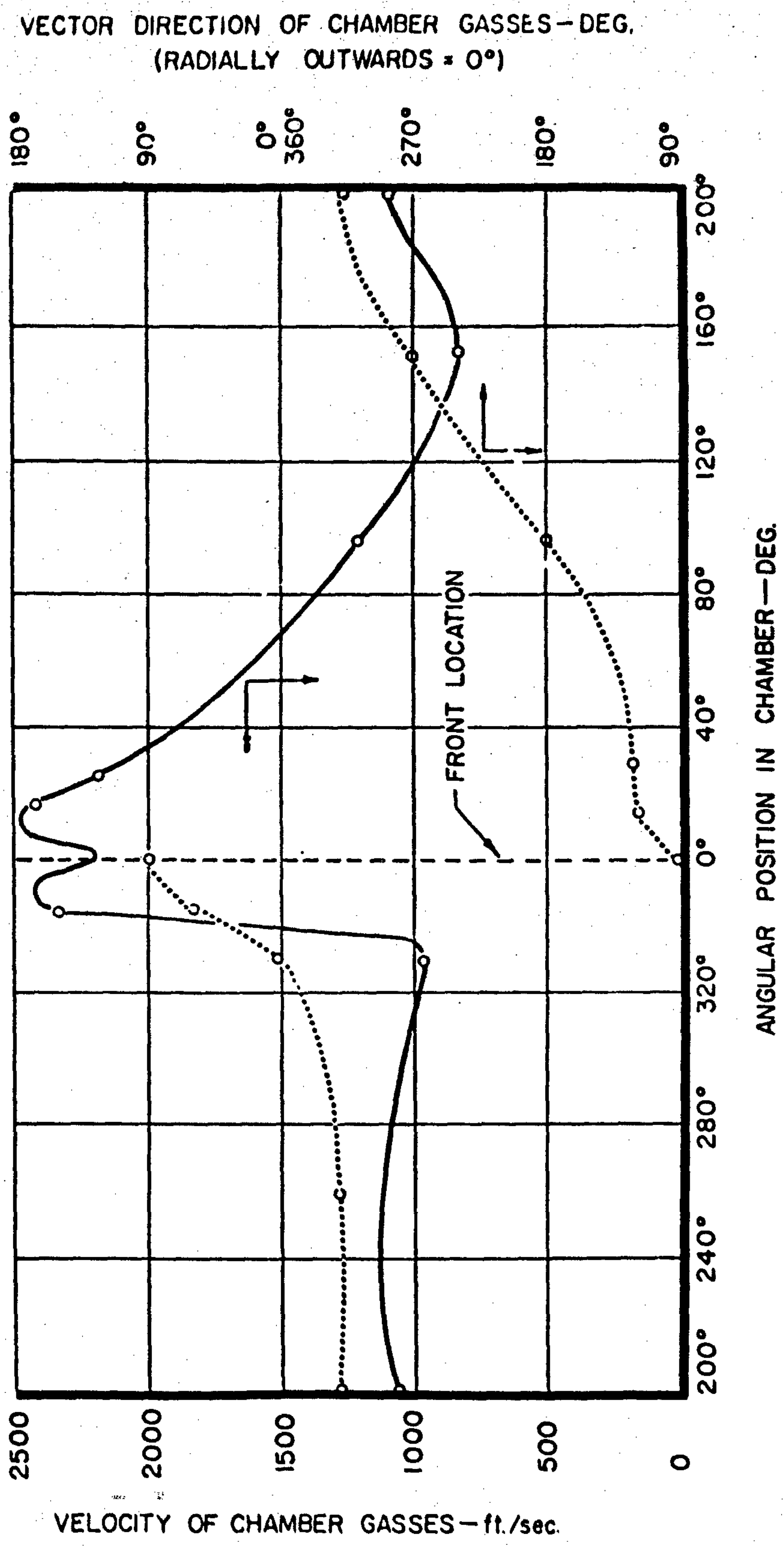

INSTANTANEOUS VELOCITY & VECTOR DIAGRAM
GASSES IN AXIAL SEGMENT OF CHAMBER

FIGURE 14

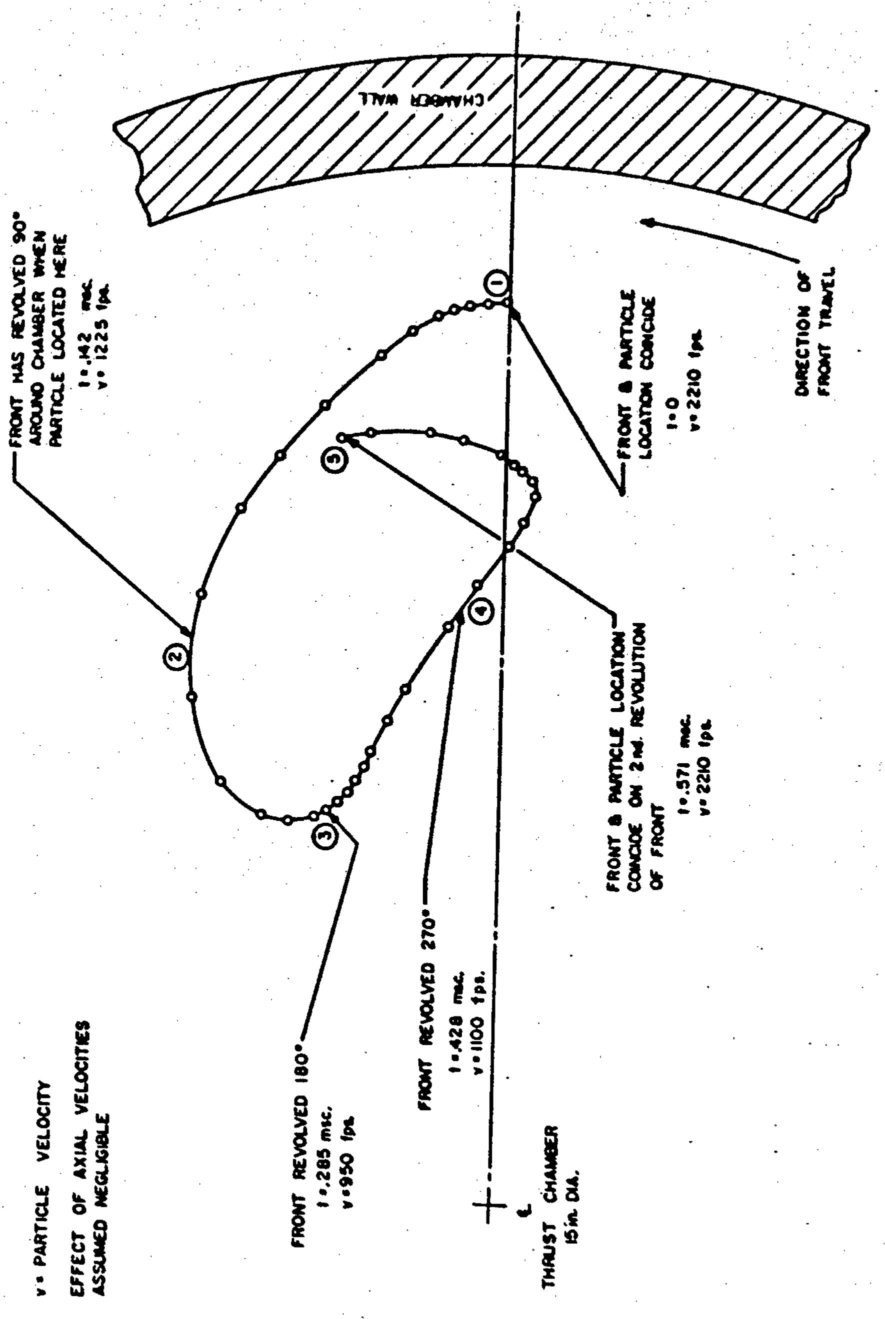
CHAMBER WALL
DIRECTION OF FRONT TRAVEL
① ② ③ ④ ⑤
FRONT & PARTICLE LOCATION COINCIDE
t = 0
v = 2210 fps.
FRONT HAS REVOLVED 90° AROUND CHAMBER WHEN PARTICLE LOCATED HERE
t = .142 msc.
v = 1225 fps.
FRONT REVOLVED 180°
t = .285 msc.
v = 950 fps.
FRONT REVOLVED 270°
t = .428 msc.
v = 1100 fps.
FRONT & PARTICLE LOCATION COINCIDE ON 2nd. REVOLUTION OF FRONT
t = .571 msc.
v = 2210 fps.
℄ THRUST CHAMBER
15 in. DIA.
v = PARTICLE VELOCITY
EFFECT OF AXIAL VELOCITIES ASSUMED NEGLIGIBLE

GAS PARTICLE PATH
DURING TANGENTIAL SINGLE FRONT INSTABILITY

FIGURE 15

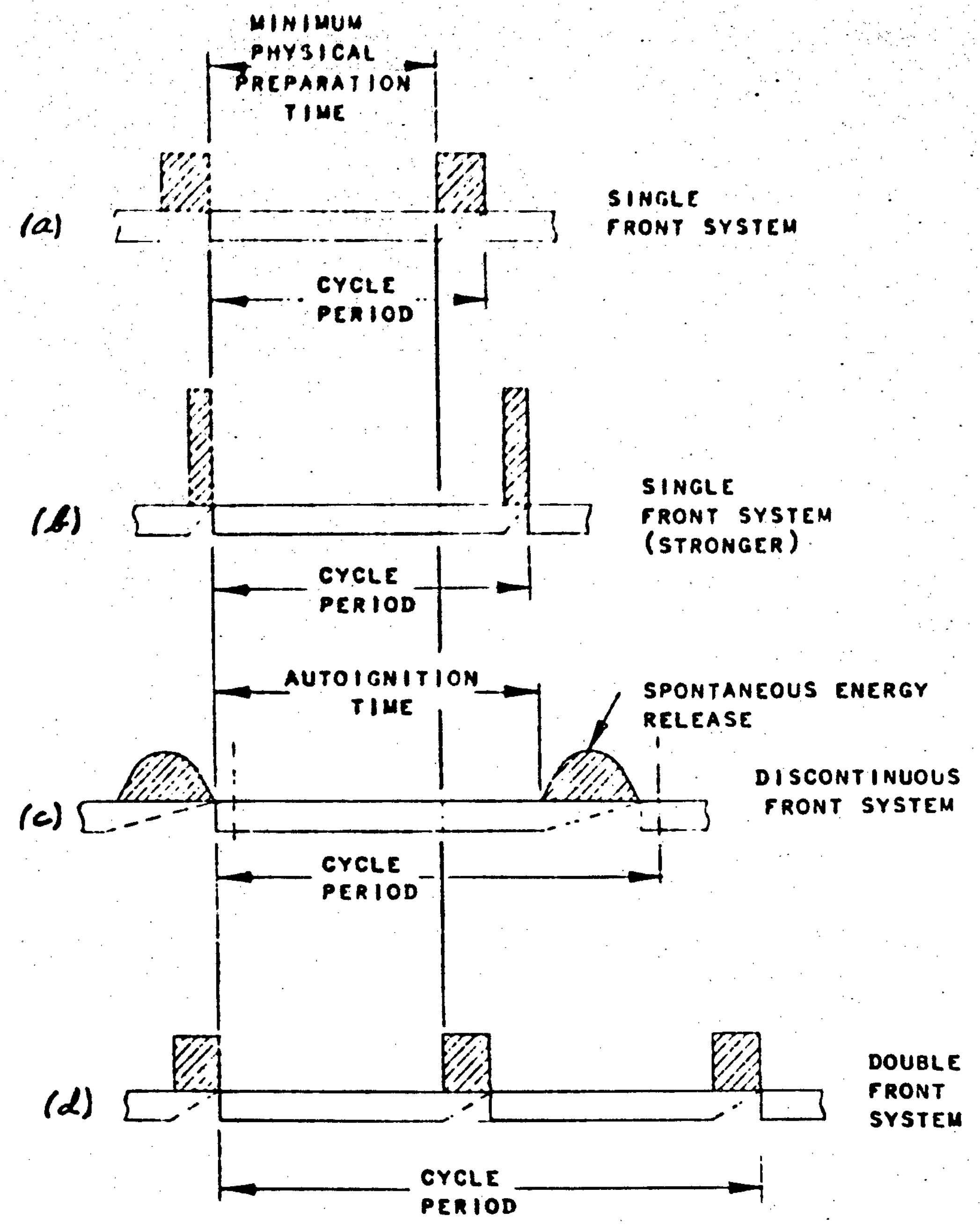
MINIMUM PHYSICAL PREPARATION TIME
(a)
SINGLE FRONT SYSTEM
CYCLE PERIOD
(b)
SINGLE FRONT SYSTEM (STRONGER)
CYCLE PERIOD
AUTOIGNITION TIME
SPONTANEOUS ENERGY RELEASE
(c)
DISCONTINUOUS FRONT SYSTEM
CYCLE PERIOD
(d)
DOUBLE FRONT SYSTEM
CYCLE PERIOD

BLOCK DIAGRAM
OF
CHARACTERISTIC TANGENTIAL FRONT MODE FORMS
OF
THRUST CHAMBER HIGH FREQUENCY COMBUSTION INSTABILITY
IN THE REGION FROM ONE TO TWO FRONTS

FIGURE 16

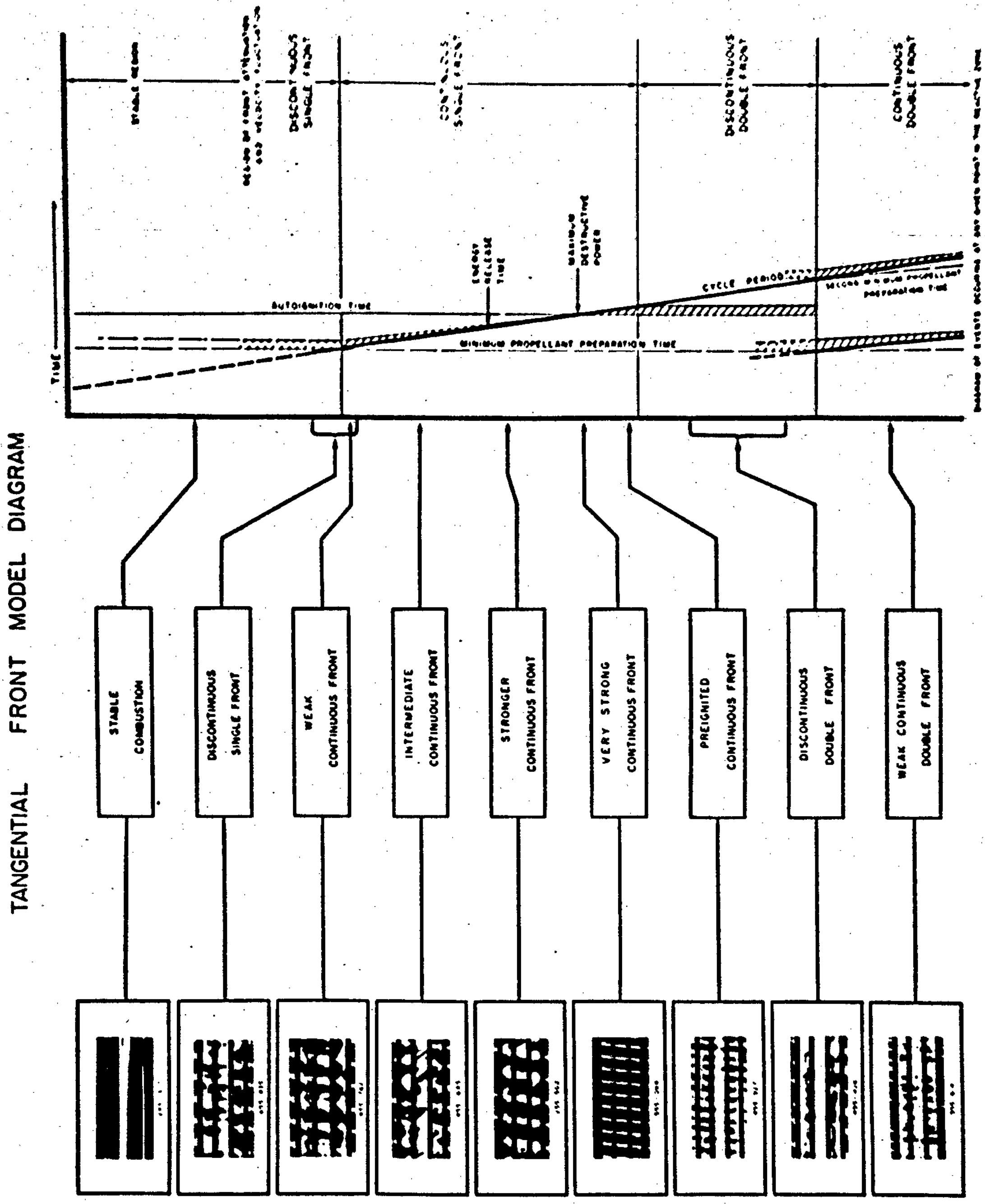
TANGENTIAL FRONT MODEL DIAGRAM
TIME
STABLE REGION
DISCONTINUOUS SINGLE FRONT
CONTINUOUS SINGLE FRONT
DISCONTINUOUS DOUBLE FRONT
CONTINUOUS DOUBLE FRONT
AUTOIGNITION TIME
MINIMUM PROPELLANT PREPARATION TIME
ENERGY RELEASE TIME
MAXIMUM DESTRUCTIVE POWER
CYCLE PERIOD
PREPARATION TIME
STABLE COMBUSTION
DISCONTINUOUS SINGLE FRONT
WEAK CONTINUOUS FRONT
INTERMEDIATE CONTINUOUS FRONT
STRONGER CONTINUOUS FRONT
VERY STRONG CONTINUOUS FRONT
PREIGNITED CONTINUOUS FRONT
DISCONTINUOUS DOUBLE FRONT
WEAK CONTINUOUS DOUBLE FRONT
0
1
2
3
4
5
6
7
8

FIGURE 17

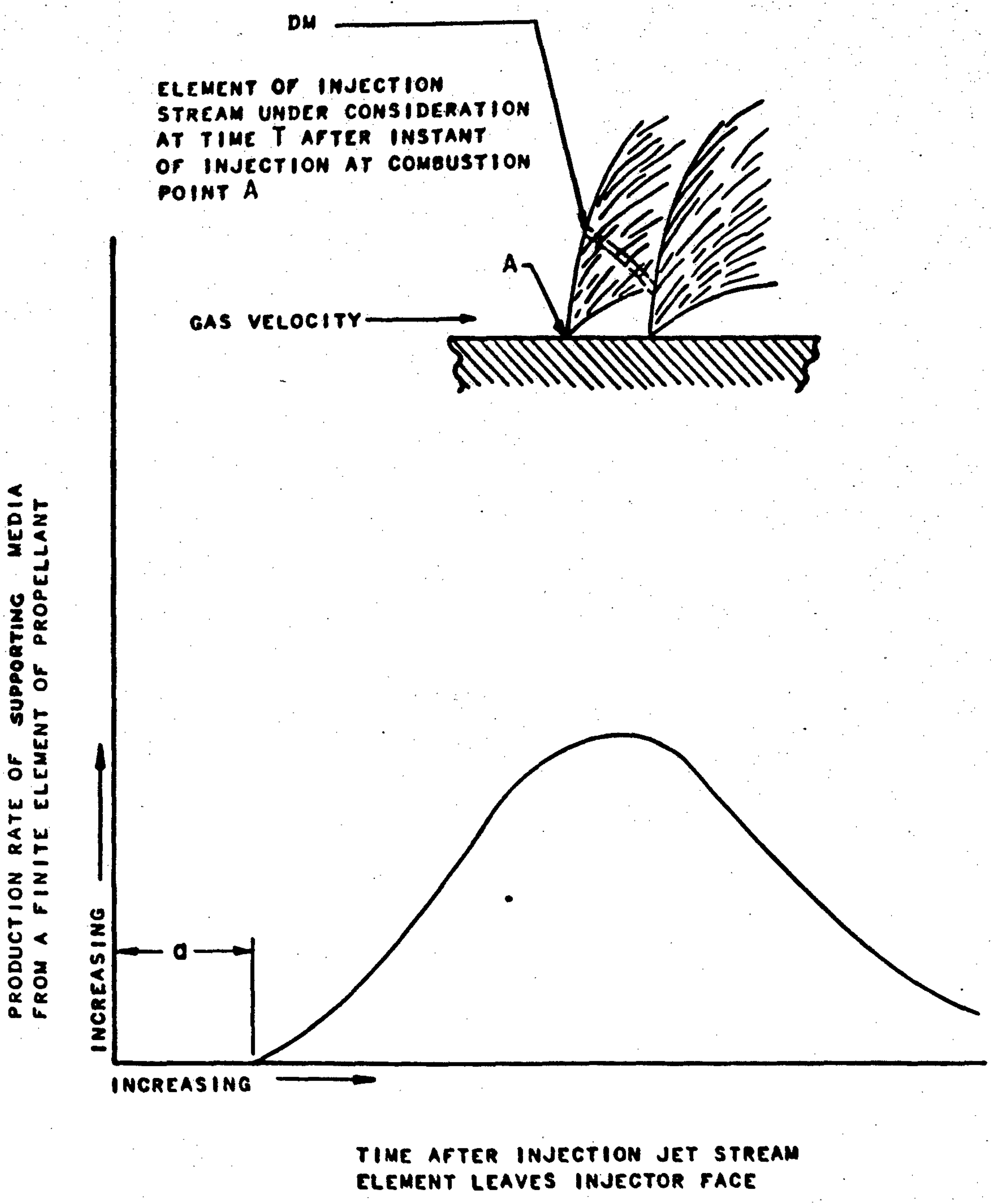
DM
ELEMENT OF INJECTION STREAM UNDER CONSIDERATION AT TIME T AFTER INSTANT OF INJECTION AT COMBUSTION POINT A
A
GAS VELOCITY
PRODUCTION RATE OF SUPPORTING MEDIA FROM A FINITE ELEMENT OF PROPELLANT
INCREASING
a
INCREASING
TIME AFTER INJECTION JET STREAM ELEMENT LEAVES INJECTOR FACE

PRODUCTION RATE OF A FRONT SUPPORTING MEDIA

FIGURE 18

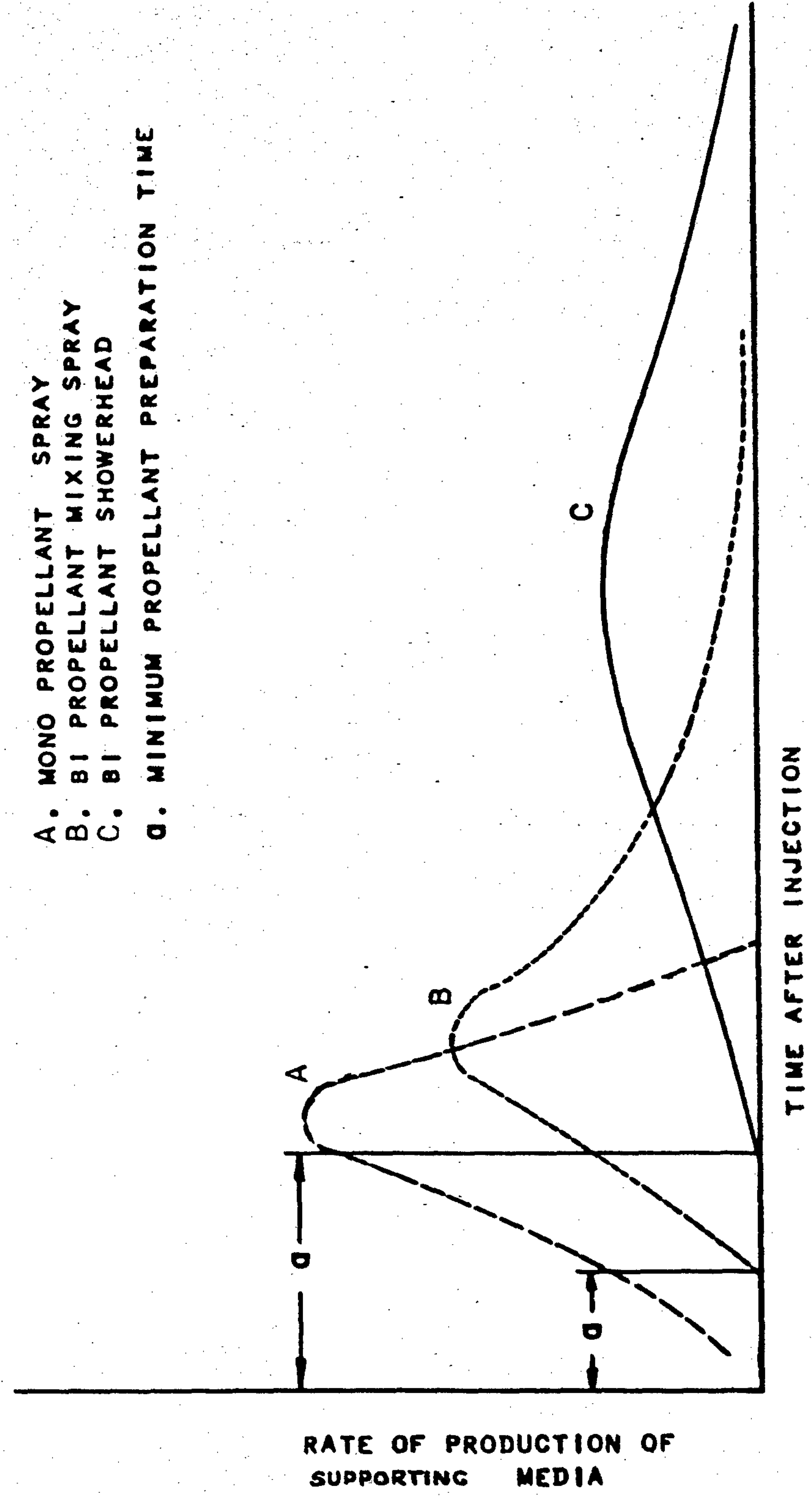

COMPARISON OF INJECTION SYSTEMS ON PRODUCTION RATE OF FRONT SUPPORTING MEDIA

FIGURE 19

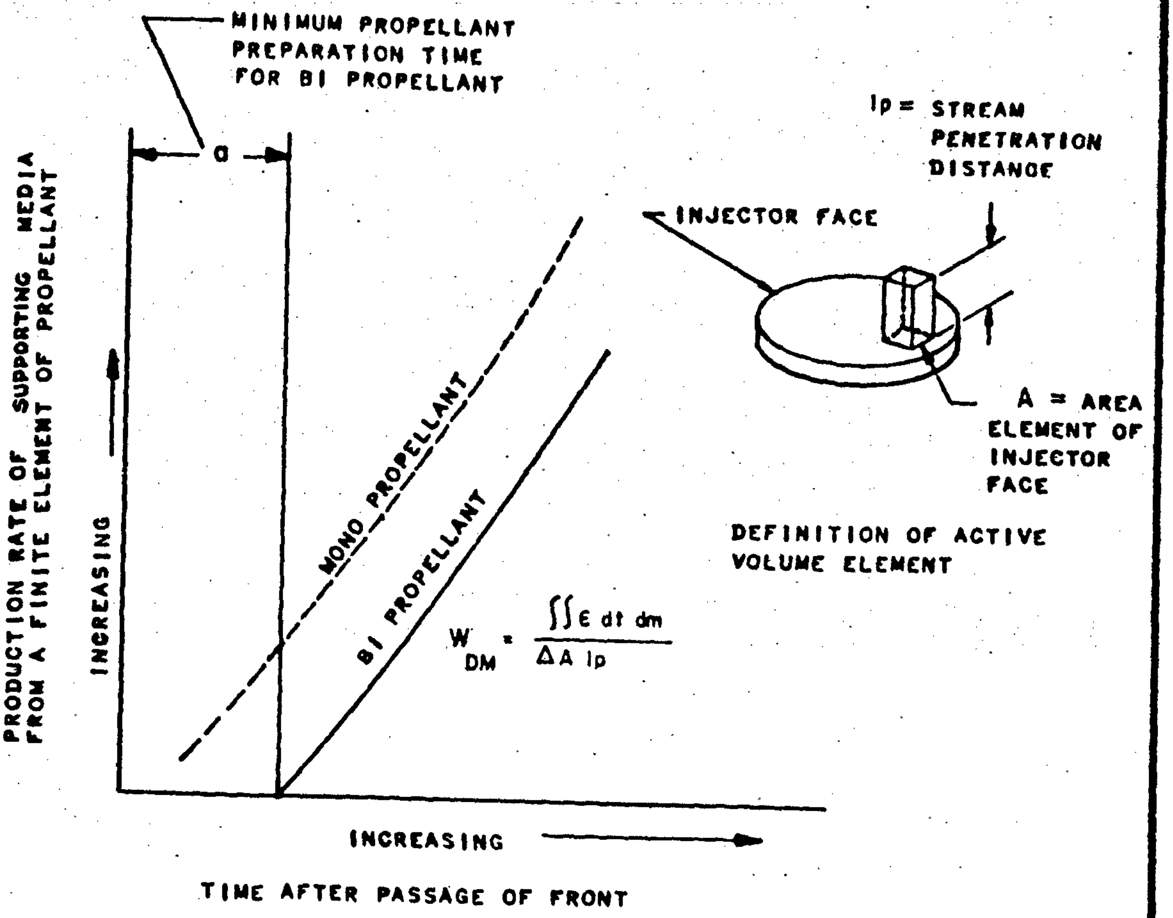

QUANTITY OF FRONT SUPPORTING MEDIA PRODUCED IN A VOLUME ELEMENT OF THE COMBUSTION CHAMBER

FIGURE 20

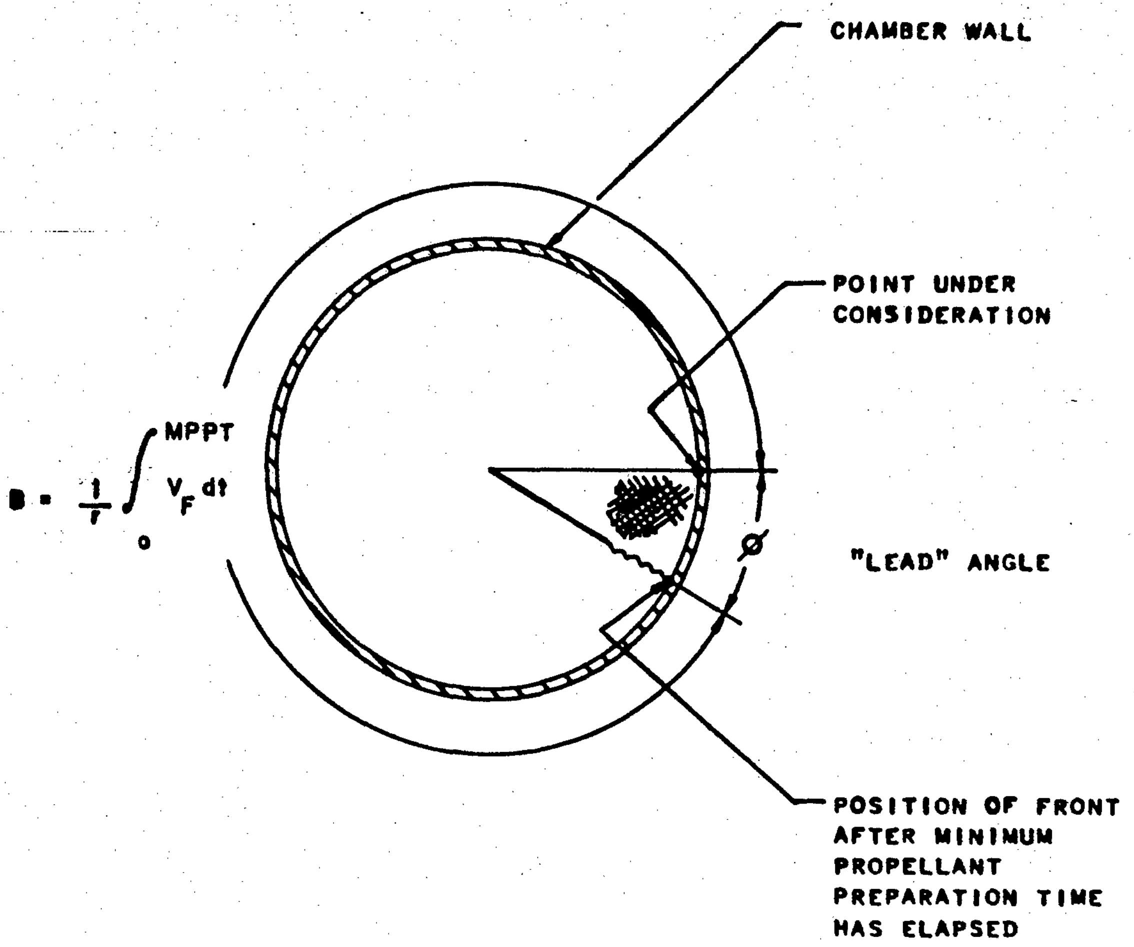

$$\phi = \frac{1}{r}\int_{0}^{MPPT} V_F \, dt$$

CHAMBER WALL
POINT UNDER CONSIDERATION
"LEAD" ANGLE
POSITION OF FRONT AFTER MINIMUM PROPELLANT PREPARATION TIME HAS ELAPSED

LEAD ANGLE DIAGRAM SHOWING RELATIONSHIP OF MINIMUM PROPELLANT PREPARATION TIME CYCLE AND PERIOD

RELATIONSHIP OF MPPT AND CYCLE PERIOD

FIGURE 21

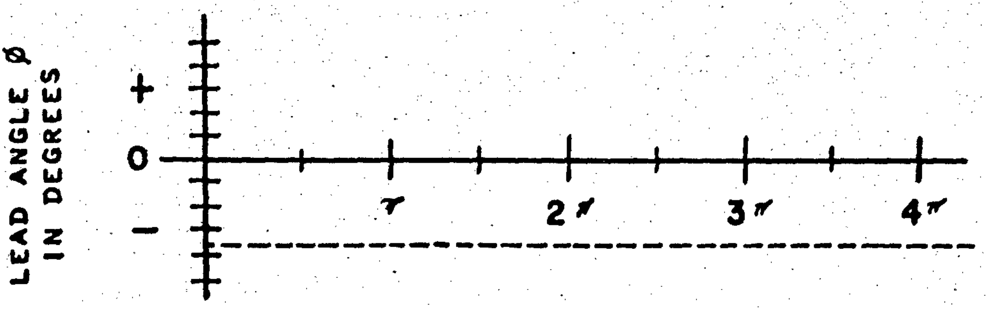

(A) CONDITION FOR STABLE COMBUSTION, ∅ IS CONTINUOUSLY LESS THAN ZERO

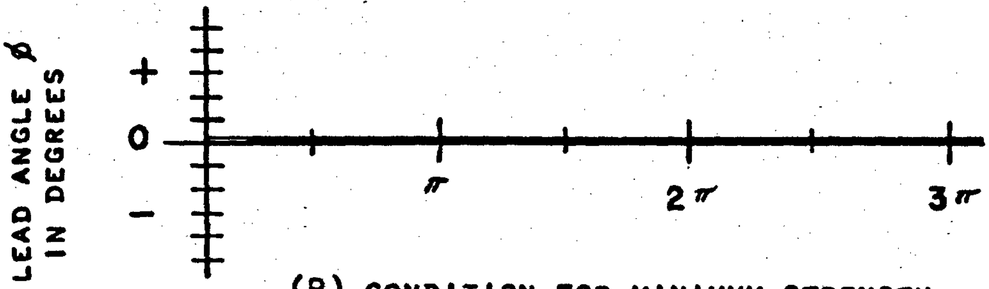

(B) CONDITION FOR MINIMUM STRENGTH, FRONT IS CONTINUOUSLY EQUAL TO ZERO

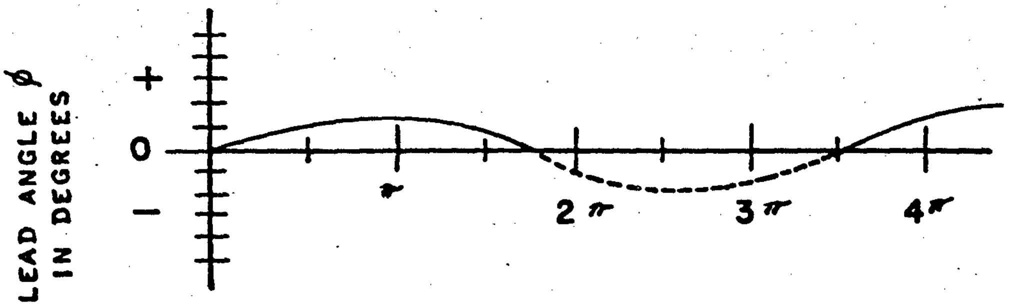

(C) CONDITION OF DISCONTINUOUS SINGLE FRONT ∅ VARIES FROM POSITIVE TO LESS THAN ZERO

LEAD ANGLE RELATIONSHIP
TO COMBUSTION STABILITY

FIGURE 22

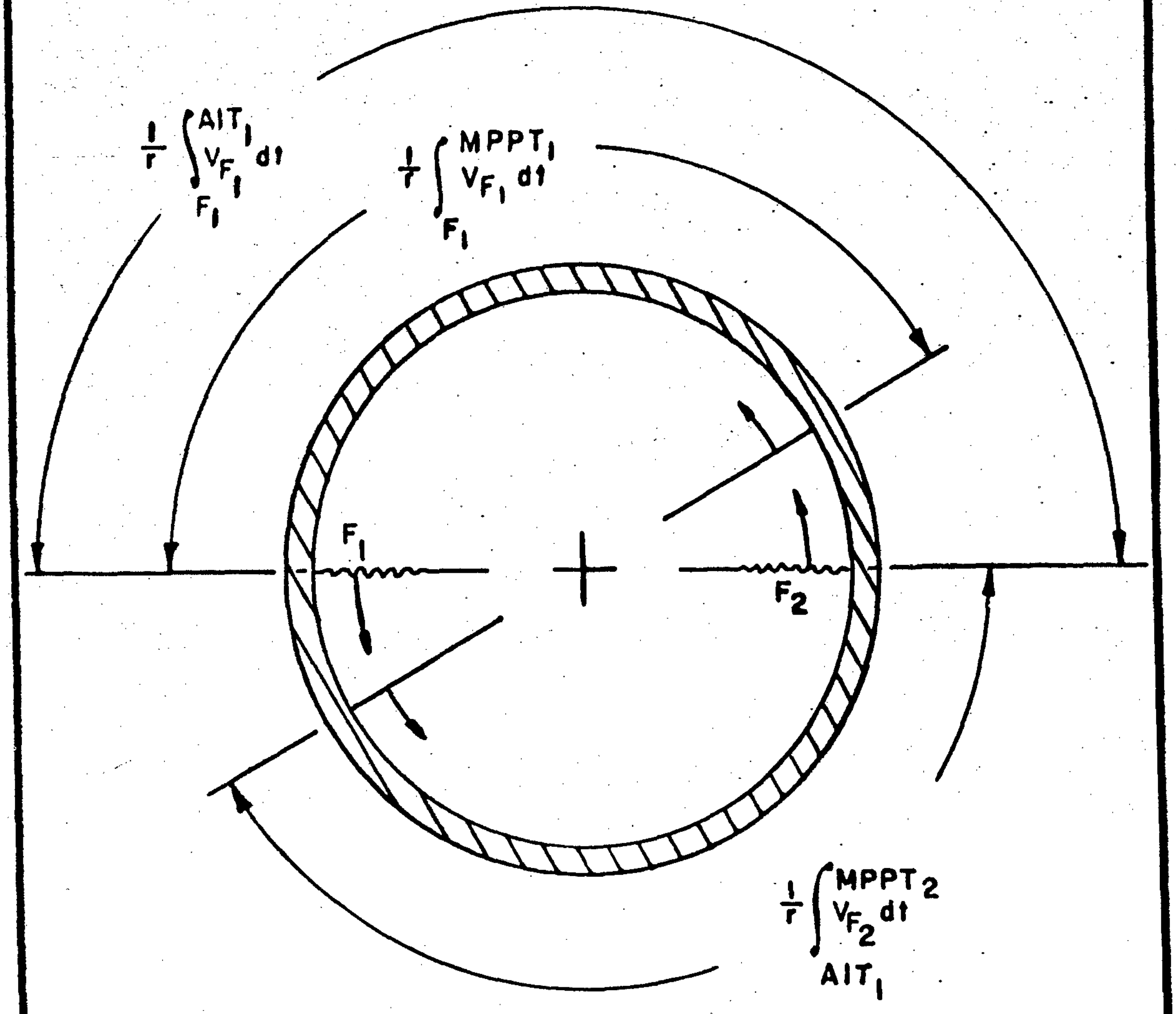
$\frac{1}{r}\int_{F_1}^{AIT_1} V_{F_1}\,dt$
$\frac{1}{r}\int_{F_1}^{MPPT_1} V_{F_1}\,dt$
F_1
F_2
$\frac{1}{r}\int_{AIT_1}^{MPPT_2} V_{F_2}\,dt$

CONDITION FOR CONTINUOUS DOUBLE FRONT

FIGURE 23

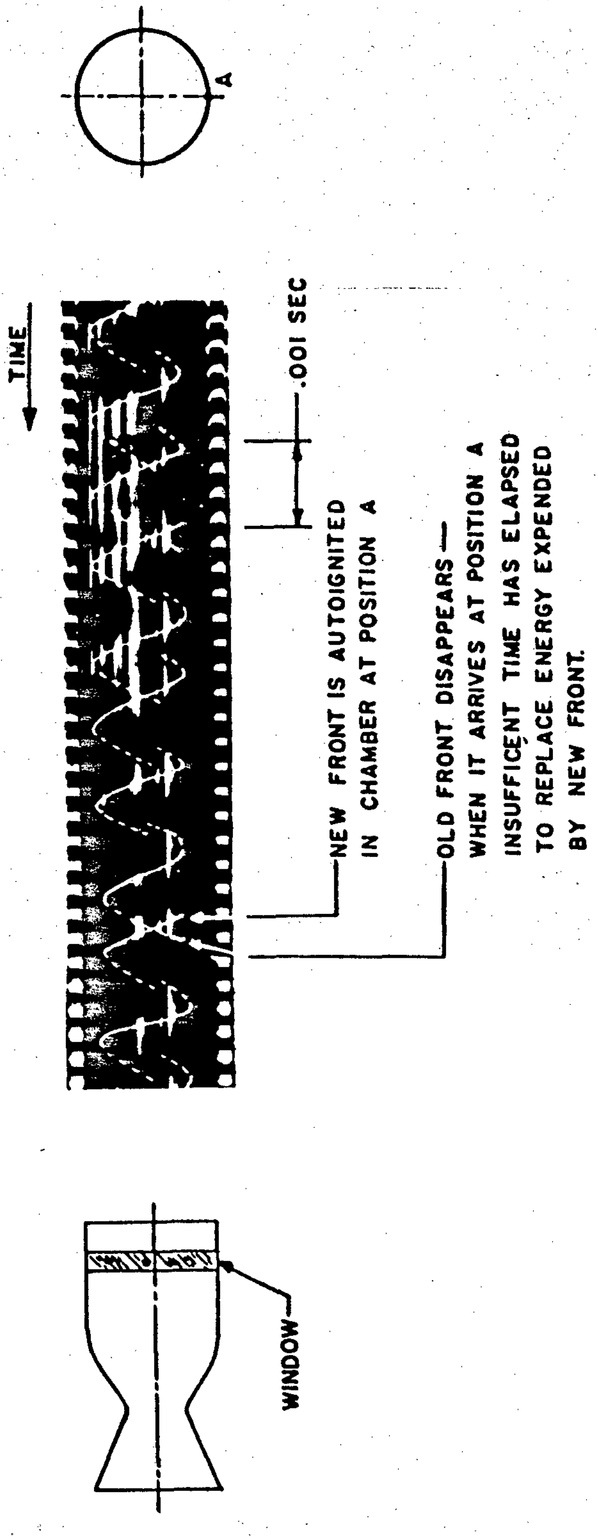
A
TIME
.001 SEC
NEW FRONT IS AUTOIGNITED IN CHAMBER AT POSITION A
OLD FRONT DISAPPEARS— WHEN IT ARRIVES AT POSITION A INSUFFICENT TIME HAS ELAPSED TO REPLACE ENERGY EXPENDED BY NEW FRONT.
WINDOW

AUTOIGNITION AND ATTENUATION OF TANGENTIAL FRONTS

DISCONTINUOUS DOUBLE FRONT SYSTEM

FIGURE 24

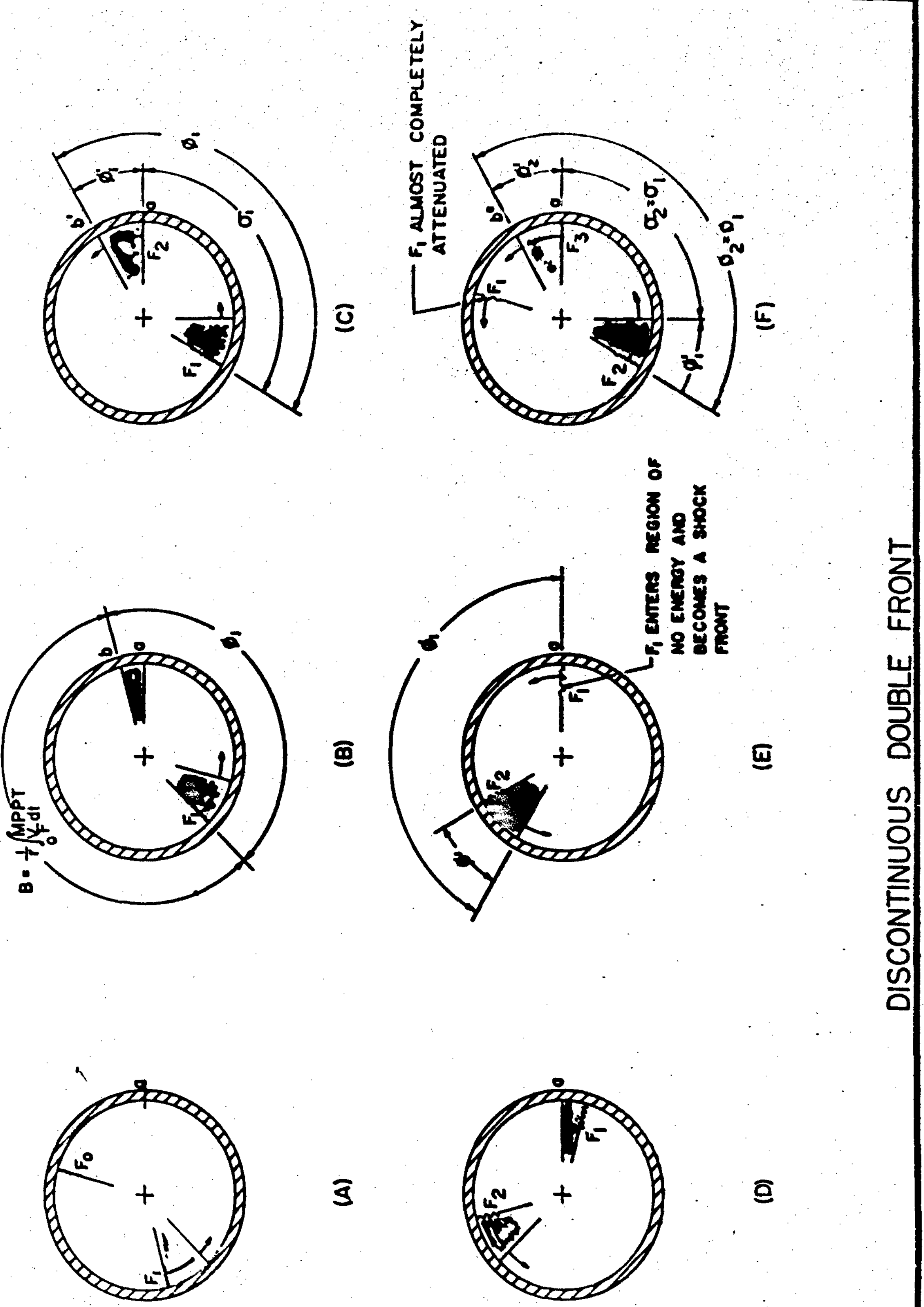
(A)
(B)
(C)
(D)
(E)
(F)
F_0
F_1
F_2
F_3
a
b
b'
ϕ_1
ϕ_1'
ϕ_2'
ϕ'
σ_1
$\sigma_2 = \sigma_1$
$\phi_2 = \phi_1$
$B = \frac{1}{\tau}\int_0^{\tau}\sqrt{\frac{MPPT}{F}}\,dl$
F_1 ENTERS REGION OF NO ENERGY AND BECOMES A SHOCK FRONT
F_1 ALMOST COMPLETELY ATTENUATED
DISCONTINUOUS DOUBLE FRONT

FIGURE 25

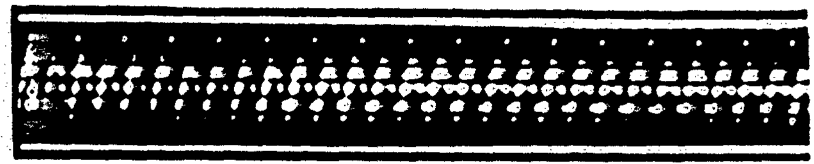

Pc = 210 psia. MR = 3.76 W_f = 22.03 lbs/sec.

CONTINUOUS SINGLE FRONT — VELOCITY = 6740 ft./sec.

15 in. DIA. CHAMBER

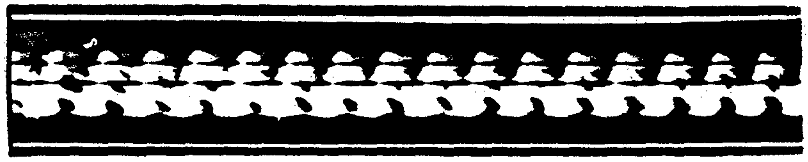

Pc = 242 psia. MR = 3.65 W_f = 36.68 lbs/sec.

CONTINUOUS SINGLE FRONT — VELOCITY = 6900 ft./sec.

22.5 in. DIA. CHAMBER

Pc = 238 psia. MR = 3.54 W_f = 48.1 lbs/sec.

DISCONTINUOUS MULTI - FRONT SYSTEM — TYPICAL VELOCITY = 6860 ft/sec.

30 in. DIA. CHAMBER

SHOWERHEAD INJECTOR # O-007098A
PROPELLANTS: IRFNA-JP4

EFFECT OF CHAMBER DIAMETER
ON
TANGENTIAL MODE

FIGURE 26

FACTORS WHICH INFLUENCE THE SUITABILITY OF LIQUID PROPELLANTS AS ROCKET MOTOR REGENERATIVE COOLANTS[1]

D. R. Bartz
Jet Propulsion Laboratory
California Institute of Technology
Pasadena, California

ABSTRACT

A brief review of methods of utilizing liquid propellants as rocket-motor coolants is given, and criteria for acceptable cooling are established. Methods of analytical and experimental determination of the pertinent heat-transfer characteristics of propellants are described. The measured maximum rates at which liquid ammonia can satisfactorily accept heat are presented to show typical trends with variations of fluid pressure, temperature, and velocity. Measured maximum rates for several propellants are compared with predictions of heat fluxes from the combustion gases of these propellants when producing the same thrust in a hypothetical rocket motor. From this comparison, an insight into the importance of various propellant properties and operating conditions is gained.

I. INTRODUCTION

A major problem confronting the designers of long-duration liquid-propellant rocket systems is designing motor walls compatible with the extreme temperatures resulting from the combustion. Three methods for achieving the desired resistance to the high temperatures are in common use. They are refractory liners, regenerative cooling, and film or transpiration cooling. Of the three, regenerative cooling is most commonly utilized in propulsion systems currently in production or development. Regenerative cooling is accomplished by flowing one or both propellants through motor-wall coolant passages on their way from the propellant tanks to the injector. The missile performance penalty of regenerative cooling is the additional turbo-pump weight and power consumption or additional gas pressurization required to overcome the coolant passage pressure drop. In order to select the method best suited for a contemplated design, this penalty must be compared with the additional dead weight and fabricational difficulties associated with refractory liners and with the penalty of additional propellant consumption associated with film or transpiration cooling. The limitations of each of these methods are such that for extremely high performance motors, optimal combinations of all three methods may be necessary. The purpose of this paper is to present and to discuss the factors which determine the suitability of a given propellant as the coolant for a completely regeneratively cooled motor.

---

[1] This paper represents the results of one phase of research carried out at the Jet Propulsion Laboratory, California Institute of Technology, under Contract No. DA-04-495-ORD 18, sponsored by the Department of the Army, Ordnance Corps.

The criterion for adequate cooling is simply that the coolant flow must maintain the walls of the motor at temperatures above which failure might occur due to melting and/or stress. For metals commonly used for rocket motor walls, such as stainless steel, nickel, inconel, or mild steel, the limiting combustion side surface temperature is in the region from 1500 to 2000°F. Thus, with combustion temperatures from 3000 to 8000°F, resultant differences between the free-stream gas temperature and the wall temperature are from 1500 to 6000°F. The consequence of such high driving potentials are heat fluxes to the wall, which, in units of Btu/in^2 sec, range from about 1 to 20. Such fluxes are orders of magnitude higher than encountered in conventional heat exchange equipment and even significantly higher than encountered in most nuclear reactors.

These levels of heat flux in conjunction with conditions of coolant velocity, temperature, and pressure are such that, over most of the cooled surface, heat is transferred by boiling when the pressure of the system is below the critical pressure of the coolant. Some coolants, however, are necessarily operated at pressures above their critical pressure; hence, both the boiling and super critical heat-transfer characteristics of a wide variety of liquids are of interest in connection with rocket-motor regenerative-cooling applications. A qualitative description of the characteristics of the various pertinent regimes of heat transfer and methods utilized for theoretical and experimental evaluation of these characteristics will serve to define terms and to introduce the problems involved. Such descriptions are best illustrated by a plot of heat flux as a function of wall temperature for constant pressure, bulk temperature, and velocity (Fig. 1).

Considering first a liquid at a pressure below its critical pressure, and a bulk temperature well below its saturation temperature, the line segment A-B represents the range of heat fluxes which can be sustained without boiling. The wall temperature at B exceeds the saturation temperature by anywhere from 10 to 100°F, which constitutes superheating of the liquid. At heat fluxes slightly higher than B, a few bubbles are formed at favored nucleation spots on the hot wall, and they grow rapidly out into the cold liquid stream. They continue to grow until condensation at the cold liquid surface begins to exceed the rate of vaporization at the base of the bubble, whereupon the bubbles begin to collapse. The inertia of the fluid following the collapsing bubble is responsible for completely collapsing the bubble. This process, which occurs at exceedingly high frequencies, is called nucleate or surface boiling. As still higher heat fluxes are encountered in the region B-C, an increasing number of nucleation sites are brought into play, thus increasing the bubble population. This is accomplished with only slight increases in wall temperature. The resulting increase in heat-transfer coefficient represented by the near vertical part of the curve (B-C) is believed by many, although not unanimously (see Ref. 1), to be the result of increasing turbulent mixing or stirring created by the growth and collapse of the bubbles. Unfortunately, this favorable situation has a limit. At this limit C, a slight increase in the heat flux leads to such a dense bubble population that the bubbles coalesce into a vapor film with an attendant large decrease in heat transfer coefficient. The resulting shift in wall temperature, C-D, is for many liquids so high that failure of commonly employed metal surfaces occurs. Hence, this transition from nucleate to film boiling has been used synonymously with the term "burnout." However, for many other liquids, notably light hydrocarbons and alcohols, the temperature at D is not much above 1000°F, and failure does not occur. Thus, the term "burnout" becomes misleading. To avoid this difficulty, point C shall be referred to as the upper limit of nucleate boiling with the symbol $q_{u\ell}$. At heat fluxes above C, even for liquids which do not cause failure, the wall temperature increases rapidly with increases in heat flux (D-E) so that for practical purposes the value of the heat flux at the upper limit of nucleate boiling must be used as the design limit for regenerative cooling systems.

The picture for supercritical pressure liquids is much simpler. Since no boiling can occur, the wall temperature increases monotonically with increasing heat flux (F-G), the heat transfer coefficient remaining essentially constant until the wall temperature reaches the critical temperature. At higher heat fluxes (G-H), the heat is transferred through a gas layer adjacent to the hot wall, resulting in somewhat lower heat-transfer coefficients. Failure temperatures are usually reached at much lower heat fluxes when a liquid is operated above its critical pressure than when operated below its critical pressure.

II. DETERMINATION OF HEAT TRANSFER CHARACTERISTICS

A. Analytical Methods

The relationship between heat flux and wall temperature, i.e., the heat transfer coefficients, in the nonboiling, subcritical temperature regions of both subcritical and supercritical pressure liquids (A-B and F-G of Fig. 1) can be predicted with sufficient accuracy for design purposes by the Sieder-Tate equation (see Ref. 2). The data for a wide variety of liquid propellants have been well correlated by this equation. It has successfully predicted the effects of pressure, velocity, and bulk temperature. The principal difficulty in applying this equation to new propellants is the need of values of the transport properties, viscosity and thermal conductivity. They generally cannot be predicted from theory. While measurement of viscosity is a rather simple laboratory procedure, measurement of thermal conductivity of liquids is considerably more difficult.

The point at which boiling is initiated (B of Fig. 1) can usually be predicted to within about 50°F if the relation between saturation temperature and pressure is known for the liquid. The amount of superheat for most liquids is from 10 to 100°F, the higher values corresponding to higher liquid velocities although no general correlation is known. For design purposes, it is sufficiently accurate to assume the wall temperature at the inception of nucleate boiling is 50°F above saturation temperature. It should be noted that bulk temperature has only a second-order effect on superheat. Saturation temperature curves for most pure liquids are given in the literature. Low pressure data are best extrapolated by plotting log p versus reciprocal of absolute temperature. For many multicomponent liquid mixtures, especially those which decompose at elevated temperatures, the saturation temperatures (or more properly the bubble-point temperatures) are not known and, hence, must be measured.

The slope of the heat flux versus wall temperature curve in nucleate boiling (B-C of Fig. 1) is not correlated for various liquids except that it is generally steeper than the third power of the difference between wall temperature and saturation temperature. Fortunately, this defines the wall temperatures within about 100°F over the range of heat fluxes covered by nucleate boiling of most liquids. It should be noted that the position of the boiling line is independent of either velocity or bulk temperature except through second-order effects on superheat which are probably less than 20 or 30°F in most instances.

The determination of the characteristic curve up into nucleate boiling is thus possible from the considerations mentioned, but this is not of much utility in predicting the limitations of the liquid as a regenerative coolant. This is because the resulting wall temperatures in nucleate boiling are, for most liquids, well below limiting temperatures for successful cooling. The real limitation from a practical view point is the heat flux at the upper limit of nucleate boiling, $q_{u\ell}$, since at heat fluxes above this level, the wall temperatures are generally beyond the limit for successful cooling. Unfortunately, this limiting heat flux cannot be predicted as yet from knowledge of a liquid's physical or transport properties. This is still the unfulfilled goal of a great deal of boiling heat transfer research throughout the world. Definite progress has been made toward this goal in recent years through considerations of the dynamics of bubble growth and collapse (see Refs. 1, 3, and 4).

The shift in wall temperature (C-D of Fig. 1), the heat transfer coefficients in film boiling (D-E of Fig. 1), and the heat transfer coefficients in the region near the critical temperature (G of Fig. 1) are also unpredictable from fluid properties with reasonable accuracy. Prediction of the first two characteristics is not particularly essential if $q_{u\ell}$ is considered to be the limitation. However, predictions of the supercritical heat transfer coefficients are essential since they determine the design limitation directly for some coolants. Such predictions are particularly difficult near the critical temperature because of unusual variations of fluid properties with temperature.

B. Experimental Methods

In order to determine the heat-transfer characteristics of propellants that cannot be predicted by analytical means, a number of experimental programs have been conducted by various organizations on a variety of liquid propellants. An index of references to these data, including ranges of variables investigated and types of data reported, is given in Table I.

Most of these data were obtained by flowing the propellant through electrically heated tubes or annuli at velocities, pressures, and bulk temperatures common to rocket motor cooling passages. Generation of heat by use of the tube wall as a resistance element was found to be the most practical means of achieving and controlling the level of heat fluxes required. Measurements required for determination of the desired heat-transfer characteristics are power consumption for computation of heat flux, flow rate, inlet and outlet pressures and temperatures, and tube-wall temperatures. Because the hydraulic diameters of most rocket motor coolant passages, even up to very large scale, are between 1/8 and 1/2 inch, tests made with tubes and annuli in this range of sizes suffer nothing in scaling. Fortunately, from an experimental standpoint, it is not necessary to scale channel length for boiling heat transfer measurements, since uniform heat transfer conditions are established very close to the entrance of a forced velocity boiling system. Tubes and annuli of 10 to 20 diameters in length are commonly used for such measurements. A necessary, but complicating part of some of these experimental investigations, has been measurements of such adverse effects as deposition of solids on the heated wall, decomposition of the liquid, and corrosion.

C. Typical Results of Experimental Investigations

Since there is rather complete experimental confirmation of the methods described for predicting the nonboiling curve, the inception of nucleate boiling and the wall temperatures in nucleate boiling, the most significant results of experimental investigations are values of $q_{u\ell}$, as a function of the three system variables: pressure, bulk temperature, and velocity. Although, as mentioned, no general correlation of this quantity has been achieved, certain trends have been fairly well established. These trends are well represented by data recently obtained by Noel for anhydrous liquid ammonia (see Ref. 15).

1. Effect of pressure on $q_{u\ell}$: It has been found that maximum values of $q_{u\ell}$ are obtained at pressures which are about 0.4 to 0.6, the liquid critical pressure for given constant bulk temperatures and velocities. The curve usually slopes quite gently on both sides of the peak. The maximum value for $q_{u\ell}$ for ammonia at 60°F was obtained at a pressure of about 850 psi or about 52% of critical pressure (Fig. 2).

2. Effect of bulk temperature on $q_{u\ell}$: It has been found that values of $q_{u\ell}$ decrease with increasing bulk temperature, reaching a near-zero value at saturation temperature. (The only exceptions to this trend have been observed at bulk temperatures less than about 40°F, where it is believed that viscous effects begin to control the boiling mechanism; see Refs. 5 and 16). For some liquids, the decrease is nearly linear with bulk temperature; for others, the values of $q_{u\ell}$ are greater than for a linear decrease. The data for ammonia (Fig. 3) exhibit this latter trend. Several correlations, notably for water, (Refs. 23 and 24) have successfully made use of a correlation variable called subcooling, which is the difference between saturation temperature and bulk temperature. For such correlations, $q_{u\ell}$ decreases linearly or less than linearly with decreasing subcooling.

3. Effect of velocity on $q_{u\ell}$: The $q_{u\ell}$ data for ammonia plotted for constant pressure and various bulk temperatures in Figure 4 show trends with increasing velocity, which are typical of several propellants investigated. The values of $q_{u\ell}$ increase linearly with velocity from zero-velocity-values which are dependent on pressure and bulk temperature. The slope of the curves is found to be dependent on subcooling with lower slopes at lower subcooling.

4. Effect of deposition on $q_{u\ell}$: Deposition of carbon by JP-3 (Ref. 21), and deposition of metallic salts by fuming nitric acids (Refs. 5 and 6) have been observed to cause rather rapid increases in wall temperatures both with and without nucleate boiling. The effect

of such deposition on $q_{u\ell}$ from these tests is not clear, but the general conclusion drawn from the data of Reference 6 is that it did not particularly affect the values of $q_{u\ell}$.

III. DEPENDENCE OF $q_{u\ell}$ ON SYSTEM OPERATING CONDITIONS

Having previously discussed the reasons for considering $q_{u\ell}$ as the practical limiting heat flux and having shown the manner in which $q_{u\ell}$ depends on pressure, bulk temperature, and velocity, it is now of interest to show the effect of the rocket motor operating conditions on the regenerative cooling problem.

The pressure at the outlet of the coolant system is established by the combustion pressure and the injector pressure drop. It is not generally economical to operate the coolant passage at any higher pressure than necessary. It was noted that pressure affected the value of $q_{u\ell}$ only slightly over the pressure range from about 0.3 to 0.7 of critical pressure. On the other hand, the net heat flux from the combustion gas to the motor wall is expected to increase with pressure to about the 0.8 power (see Ref. 25), the effect of pressure on nucleate boiling wall temperatures being of second order in determining the heat transfer driving potential, (T_c-T_w).

The coolant bulk temperature at any point in the coolant passage is simply the sum of the inlet bulk temperature and the temperature rise to that point. The temperature rise is determined by the heat transfer to the wall, the coolant flow rate, and coolant specific heat. Since the higher values of $q_{u\ell}$ are associated with the lower values of bulk temperature, it is desirable to utilize the largest coolant flow rate possible. The total propellant consumption being fixed operation at high mixture ratios (O/F) favors cooling with the oxidizer, and operation at low mixture ratios favors cooling with the fuel. Since both propellant consumption and heat flux increase nearly linearly with chamber pressure, bulk temperature rise is not particularly influenced by changes in chamber pressure. Hence, the result is that bulk temperature rise is principally dependent on selection of motor configuration and propellant combination.

With pressure and bulk temperature rise essentially determined by the selection of motor configuration, propellant combination and combustion pressure, only velocity, of the three parameters affecting $q_{u\ell}$, is left for manipulation to gain cooling advantage. Fortunately, $q_{u\ell}$ can be readily increased by increasing velocity. However, since total coolant flow rate is fixed, velocity can only be increased by decreasing the net flow area of the cooling passage. With axial flow cooling in thin annular passages, it is found that velocity is inversely proportional to the coolant passage height, t, and that the coolant passage pressure drop increases with the third power of velocity for turbulent flow. A sample calculation for a 300 psi chamber pressure, turbo-pumped, ammonia-cooled rocket motor (summarized in Table II) shows the cooling advantage and performance penalty resulting from doubling the coolant velocities. While the calculation is of necessity not general, the results are considered to be typical. They show that the value of q_{ul} can nearly be doubled for as little as about 2% increase in propellant consumption (for turbopump) and only a moderate increase in system dead weight. Hence, such changes should receive full consideration during preliminary design of a regeneratively cooled rocket propulsion system.

IV. DEPENDENCE OF PRESSURE DROP ON HEAT TRANSFER

Considerations of coolant-passage pressure drop such as discussed in the previous section require knowledge of the manner in which the pressure drop varies with type and magnitude of heat transfer. A convenient method of showing this variation is through the use of the ratio of pressure drop per unit length with heat transfer to that without heat transfer for equal bulk temperature, and mass flow rate. This ratio is plotted versus heat flux in Figure 5 from experimental data for two propellants, (1) RFNA, and (2) CORPORAL fuel (a mixture of aniline, furfuryl alcohol, and hydrazine). The results for RFNA from Reference 5 showed that $\Delta p/\Delta p_{q\,=\,0}$ decreased about 15% over the heat flux range from zero to the inception of nucleate boiling (point B of Fig. 5). This decrease is somewhat less than would be predicted by the Sieder-Tate friction factor correction $(\mu_w/\mu_b)^{0.14}$ which is usually recommended. Data presented in Reference 8 for WFNA were correlated with this viscosity ratio to the 0.12 power.

Pressure drop data measured in the nonboiling region for n-butyl alcohol (Ref. 20) and the CORPORAL fuel (Ref. 16) decreased with increasing heat flux to a much greater extent than would be predicted by the factor $(\mu_w/\mu_b)^{0.14}$, the resultant exponents being 0.3 and 0.2, respectively. Curve A'B'C' (Fig. 5) drawn from data for the latter fuel at 100°F bulk temperature shows experimental values of the pressure drop ratio as low as about 0.4 at the inception of nucleate boiling.

With heat fluxes increasing into the nucleate boiling range, the values of the ratio level off, then increase. Maximum values of the pressure drop ratio at the upper limit of nucleate boiling both above and below unity have been observed, depending upon particular conditions of bulk temperature and pressure. The amount of pressure drop data measured during the programs referenced was insufficient to achieve a correlation. Since the total pressure drop is an integration of friction on the cool wall under adiabatic conditions and on the hot wall both with and without boiling the general conclusion drawn from the data was that a calculation based on the adiabatic conditions would be high by less than about 10% for the acid cooling and 25% for the CORPORAL fuel cooling and hence would satisfy design needs.

Unfortunately, very little data on pressure drop have been reported from which to establish correlations or draw general conclusions. This is partially due to the fact that pressure drop measurements must be made over short sections since at nucleate boiling heat fluxes the bulk temperature rise per unit length is quite large. Such pressure drop measurements are difficult to make with acceptable accuracy. Additional measurements are definitely needed to settle the questions concerning coolant passage pressure drops.

V. OPERATIONAL COMPARISON OF COOLING CAPABILITIES OF SEVERAL PROPELLANTS

Having discussed various aspects of the utilization of propellants as regenerative coolants, it is still not possible to calculate a parameter which will characterize the potentialities of a particular propellant as a coolant relative to other propellants. This situation is a result of (1) the apparently complex relation between $q_{u\ell}$ and liquid properties and (2) the variables which are closely related to the selection of the combustion system, motor configuration, and combustion pressure. Although the final evaluation of the merits of a particular coolant must await a detailed design analysis, some measure of comparison between propellants can be achieved by considering several propellants as potential coolants for a hypothetical motor of given configuration, computing the margin between the local values of $q_{u\ell}$ and the heat flux to the wall in a critical region such as the throat.

Such a comparison was made using the propellants listed in the first column of Table III as the coolants. The propellants listed in the second column were considered to react with the coolant-propellant at peak-performance mixture ratios with resulting values of c* which were 95% of theoretical values, based on equilibrium composition expansion. The propellant consumption was such as to produce 50,000 lbs of thrust at chamber pressure near 300 psia with each combination burning in the same motor.

The pertinent configurational parameters of the motor selected were L* 40 inches, throat area 117 in^2, 2:1 contraction area ratio, 7:1 expansion area ratio, 30-degrees contraction half angle, 15-degrees expansion half angle, throat radius of curvature equal to throat diameter. The motor was assumed to have an annular coolant passage of height t which was constant along the whole length of the motor. The value of t was allowed to vary from coolant to coolant so as to result in a 75-psi coolant-passage pressure drop for the appropriate flow rate of each particular coolant. Since the manner in which the friction factor for each coolant varies with heat flux is unknown, the adiabatic value was used for this comparison, using values of viscosity and density which were the average between inlet and outlet bulk temperatures.

An inlet bulk temperature of 100°F was assumed for each of the coolants except liquid ammonia, which it was assumed could be reduced to 32°F by venting the tank prior to flight. The bulk temperature rise of the coolant from the nozzle exit end to the throat, and over-all bulk temperature rise were calculated from the coolant flow rate and specific heat and heat flux to the wall computed with the following assumptions. Chamber gas temperatures, 90% of theoretical equilibrium combustion chamber temperature were assumed, the fraction being the result of assuming c* to be 95% of its theoretical value. Wall temperature was 50°F (superheat) above coolant saturation temperature at 410 psi, the average coolant passage pressure. This wall temperature results from assuming the combustion-side wall to have negligible thermal resistance, and assuming the mechanism of heat transfer along the whole passage to be nucleate boiling. The local heat flux was computed by multiplying the difference between chamber gas temperature and wall temperature by heat transfer coefficients computed by the methods of Reference 25. For reasons discussed in Reference 25 and in Reference 26, the values of the computed heat flux are expected to be generally too high in the chamber, and throughout the nozzle as well, for carbonaceous systems which deposit carbon on the gas side walls during combustion. On the other hand, computed heat flux values are expected to be too low for systems burning either with appreciable dissociation or with unstable combustion or both. These complicating factors cannot be accounted for analytically at present, but it is believed that values predicted on the basis of pure convection are still useful for the comparison of this report; however, in drawing specific comparative conclusions between systems calculated, qualitative allowances should be made for these uncertainties.

With these assumptions, it was possible to compute the values of pressure, velocity, and bulk temperature of each coolant at the throat. Values of $q_{u\ell}$ at these conditions, $q_{u\ell}$*, were computed and compared with computed values of throat heat flux, q*. These results are presented in Table III and Figure 6.

B. Results

It is most significant to note that the computed bulk temperature rise with $C\ell F_3$ system, is such that saturation temperature is exceeded by the bulk temperature within the coolant passage, and saturation temperature is nearly reached with the NH_3 systems. Successful cooling even in the chamber under such conditions is extremely unlikely since values of $q_{u\ell}$ drop well below 1 Btu/in^2 sec when bulk temperature reaches saturation temperature. This is a good point at which to start checking a proposed regenerative cooling design.

Of the systems calculated, it appears that the RFNA, the CORPORAL fuel, and DETA coolants offer the best margins for cooling, the values of $q_{u\ell}^*$ being comfortably above throat heat flux values. It must be remembered that the expected throat heat flux for the JP-3--O_2 system would probably be as much as 50 to 100% lower than predicted because of expected effects of carbon deposition. Hence, in practice, this system would also have a satisfactory but very unpredictable margin for cooling. Systems d, e and f were predicted to be marginal within the uncertainties in predictions of heat flux to the wall. For most fuel-cooled systems, shifts toward lower mixture ratios, and for most oxidizer cooled systems, shifts toward higher mixture ratios, could be made to gain cooling advantage with only negligible penalties in performance.

As indicated by the calculation in Table II, even a coolant with apparently poor cooling capabilities such as isopropanol could be employed successfully if significantly greater coolant passage pressure drop is allowed in order to increase coolant velocity.

VI. CONCLUSIONS

From such calculations and comparisons as presented in this paper, some general conclusions can be drawn relative to liquid physical and chemical properties and to motor operating conditions which are favorable for regenerative cooling.

In order to achieve successful regenerative cooling in a rocket motor with propellants below their critical temperature and pressure, sufficient coolant flow must be provided to achieve local values of the heat flux at the upper limit of nucleate boiling $q_{u\ell}$ which, everywhere throughout the motor, exceed corresponding local heat fluxes from the combustion gases to the wall.

The total heat rate that can be absorbed by a coolant at bulk temperatures below saturation temperature is equal to the product of flow rate, specific heat, and difference between saturation temperature and coolant inlet temperature. This total heat rate must be safely above the total expected heat-rejection rate from the combustion gases to the motor wall since values of $q_{u\ell}$ decrease sharply as bulk temperatures approach saturation temperature, becoming too low for successful cooling even back near the injector. For this reason a high specific heat, and/or a saturation temperature at least about 300°F is desirable. However, higher saturation temperatures than about 700°F allow wall temperatures to climb too high before being limited by nucleate boiling. Even this temperature would prohibit the use of aluminum as a wall material and would significantly reduce the allowable stresses of steel materials.

A liquid critical pressure such that coolant passage pressures are from about 0.3 to 0.7 of critical pressure is desirable. Liquids operating in this pressure range usually exhibit a maxima in values of $q_{u\ell}$ for given velocity and bulk temperature. Fluids which must be used at pressures above their critical pressure are usually poorer coolants than those operated below critical pressure, especially if the bulk temperature goes from subcritical to supercritical somewhere in the coolant passage.

A low viscosity is a favorable liquid physical property, since for a given mass flow rate it permits higher coolant velocities for a given pressure drop. Furthermore, increasing viscosity is believed to be the explanation for the two cases mentioned where $q_{u\ell}$ was observed to decrease with decreasing bulk temperature, contrary to the normal trend.

Liquids which decompose either at limited rates, or explosively, which deposit salts or carbon on the hot wall, or which corrode the wall are generally inferior to liquids which are essentially chemically inert.

The cooling of a motor with the oxidizer is best accomplished by operating the motor at high oxidizer to fuel mixture ratios. Conversely, cooling with the fuel is best accomplished at low mixture ratios. For many systems, significant changes in mixture ratio from the peak performance value can be made to gain cooling advantage with but little sacrifice in performance.

The only design parameter that is available to the designer to improve cooling conditions once the propellants, mixture ratio, combustion pressure, and motor configuration are selected, is the coolant velocity which may be advantageously increased by decreasing coolant passage flow area with an attendant increase in coolant passage pressure drop. For some systems, cooling with both propellants may be required.

REFERENCES

1. Bankoff, S. G., Colahan, W. J., and Bartz, D. R., *Summary of Conference on Bubble Dynamics and Boiling Heat Transfer Held at the Jet Propulsion Laboratory, June 14 and 15, 1956*, Memorandum No. 20-137. Pasadena: Jet Propulsion Laboratory, December 10, 1956.

2. Sieder, E. N. and Tate, G. E., "Heat Transfer and Pressure Drop of Liquid in Tubes," *Industrial and Engineering Chemistry*, V28: pp. 1429 - 1436, 1936.

3. Ellion, M. E., *A Study of the Mechanism of Boiling Heat Transfer*, Memorandum No. 20-88. Pasadena: Jet Propulsion Laboratory, March 1, 1954.

4. Forster, H. K., and Zuber, N., "Dynamics of Vapor Bubbles and Boiling Heat Transfer," *Journal American Institute of Chemical Engineers*, 1, 531, 1954.

5. Dean, L. E., *Heat Transfer Characteristics of RFNA*, Report No. 117-982-004. Buffalo: Bell Aircraft Corporation, July 1956.

6. Combined Bimonthly Summary, Nos. 36, 37, 38, 39, 40, 41, 42, 43, and 50. Pasadena: Jet Propulsion Laboratory (Confidential). 1953-55.

7. Wolf, H., Gray, F. L., Reese, B. A., "Heat Transfer and Friction Characteristics of Red and White Fuming Nitric Acid," *Jet Propulsion*, V26 (No. 11): 979, November 1956.

8. Reese, B. A., Graham, R. W., *Experimental Investigation of Heat Transfer and Fluid Friction Characteristics of White Fuming Nitric Acid*, Technical Note 3181. Washington: National Advisory Committee for Aeronautics, May 1954.

9. Reese, B. A., Graham, R. W., "Heat Transfer and Friction Pressure Drop Characteristics of White Fuming Nitric Acid," *Jet Propulsion*, V24 (No. 4): 228, July-August, 1954.

10. Ashley, E., *Heat Transfer Measurements for White Fuming Nitric Acid*, Report No. 56-982-016. Buffalo: Bell Aircraft Corporation, February 1953.

11. Hatcher, J. B., and Bartz, D. R., *High Flux Heat Transfer to JP-3 and RFNA*, External Publication No. 119. Pasadena: Jet Propulsion Laboratory, November 1951.

12. Combined Bimonthly Summary No. 56. Pasadena: Jet Propulsion Laboratory (Confidential). 1956.

REFERENCES (Cont'd)

13. Powell, W. B., Heat Transfer to Fluids in The Region of the Critical Temperature, Progress Report No. 20-285. Pasadena: Jet Propulsion Laboratory, April 1956.

14. Banchero, Baner, and Ball, Heat Transfer Characteristics of Boiling Oxygen, Fluorine, and Hydrazine, Report 51-11. Ann Arbor: University of Michigan Engineering Research Institute.

15. Combined Bimonthly Summary Nos. 52, 53, and 54. Pasadena: Jet Propulsion Laboratory (Confidential). 1956.

16. Combined Bimonthly Summary Nos. 44, 45, 46, and 47. Pasadena: Jet Propulsion Laboratory (Confidential). 1954-1955.

17. Combined Bimonthly Summary No. 36. Pasadena: Jet Propulsion Laboratory (Confidential). 1953.

18. Combined Bimonthly Summary Nos. 41, and 51. Pasadena: Jet Propulsion Laboratory (Confidential). 1954-1956.

19. Kreith, F. and Summerfield, M., Heat Transfer From an Electrically Heated Tube to Aniline at High Heat Flux, Progress Report No. 4-88. Pasadena: Jet Propulsion Laboratory, February 1949.

20. Kreith, F., and Summerfield, M., Investigation of Heat Transfer at High Heat Flux: Experimental Study of Heat Transfer and Friction Drop with n-Butyl Alcohol in an Electrically Heated Tube. Progress Report No. 4-95. Pasadena: Jet Propulsion Laboratory, May 1949.

21. Hatcher, J. B., High Flux Heat Transfer and Cone Deposition of JP-3 Fuel Mixture, Progress Report No. 20-157. Pasadena: Jet Propulsion Laboratory.

22. Beighley, C. M., and Dean, L. E. "Study of Heat Transfer to JP-4 Jet Fuel," Jet Propulsion, V24 (No. 3): 180, May-June 1954.

23. Gunther, F. C., "Photographic Study of Surface-Boiling Heat Transfer to Water with Forced Convection," Transactions of the American Society of Mechanical Engineers, 73: 115-123, 1951.

24. Rohsenow, W. M., and Clark, J. A., Technical Report No. 4, DIC Project No. 6627. Cambridge: Massachusetts Institute of Technology, 1952.

25. Bartz, D. R., "A Simple Equation For Rapid Estimation of Rocket Nozzle Convective Heat Transfer Coefficients." Jet Propulsion V27 (No. 1), January 1957.

REFERENCES (Cont'd)

25. Bartz, D. R., An Approximate Solution of Compressible Turbulent Boundary Layer Development and Convective Heat Transfer in Convergent-Divergent Nozzles. Progress Report No. 20-234. Pasadena: Jet Propulsion Laboratory, July 1954 (also Transactions of the American Society of Mechanical Engineers, V77 (No. 8) 1235, November 1955).

Bartz

UNCLASSIFIED

TABLE I. INDEXED MEASUREMENTS OF HEAT TRANSFER TO PROPELLANTS WITH AND WITHOUT BOILING UNDER FORCED VELOCITY, SUBCOOLED CONDITIONS

Propellant		Authors	Organization	Reference	Pressure Range (psi)	Bulk Temperature Range (° F)	Velocity Range (ft/sec)	Data*
Designation	Nominal Composition							
Oxidizers:								
Type III-A RFNA	83% HNO_3, 14% NO_2, 2.5% H_2O, 0.6% HF	Dean	Bell Aircraft	5	100 - 910	-65 to 170	5 to 100	FC, NB, $q_{u,b}$, Dep.
RFNA	92 1/2% HNO_3, 6 1/2% NO_2, 1% H_2O	Bartz, Noel	JPL	6	50 - 500	90 to 300	15 to 40	FC, NB, $q_{u,b}$, ΔP, Dep.
SFNA	83% HNO_3, 14% NO_2, 2.5% H_2O, 0.6% HF				60 - 500	80 to 335	30	FC, NB, $q_{u,b}$, Dep.
WFNA	97% HNO_3, 1% NO_2, 2% H_2O				300 - 800	90 to 247	20 to 90	FC, NB, $q_{u,b}$
Type III RFNA	82% HNO_3, 15% NO_2, 2% H_2O, 0.5% HF	Wolfe, Gray,	Purdue	7, 8, 9	90 - 815	25 to 95	5 to 35	FC, NB, Dep., ΔP
WFNA	98% HNO_3, 0.5% NO_2, 1.5% H_2O	Reese			65 - 710	67 to 190	18 to 130	FC, NB, Dep., ΔP
WFNA	97.5% HNO_3, 0.5% NO_2, 2.0% H_2O	Ashley	Bell Aircraft	10	65 - 400	60 to 90	5 to 60	FC, NB, $q_{u,b}$
RFNA	92 1/2% HNO_3, 6 1/2% NO_2, 1% H_2O	Hatcher, Bartz	JPL	11	50 - 500	70 to 90	10 to 50	FC, NB, $q_{u,b}$
ClF_3	Commercial grade	Noel	JPL	12	150 - 800	0 to 200	15 to 60	FC, NB, $q_{u,b}$
Liquid Oxygen	-	Powell	JPL	13	300 - 1100	-280 to 340	(3 to 40)*	FC, subcritical, supercritical
Liquid Oxygen Liquid Fluorine	- -	Banchero, Banor, Ball	University of Michigan	14	-	-	-	-
Fuels:								
Liquid Ammonia	99% NH_3, 1% H_2O	Noel	JPL	15	100 - 1000	30 to 130	8 to 137	FC, NB, $q_{u,b}$
Corporal fuel	46% An, 46% FA, 7% N_2H_4, 1% H_2O	Noel	JPL	16	300 - 400	13 to 45	-10 to 400	FC, NB, $q_{u,b}$, ΔP
	80% An, 20% FA	Noel	JPL	17	400	30	125	FC, NB, $q_{u,b}$
	50% An, 50% FA							
	33% An, 67% FA							
	47.5% An, 47.5% FA, 5% N_2H_4							
	45% An, 45% FA, 10% N_2H_4							
	40% An, 40% FA, 20% N_2H_4							
Diacetone Alcohol	Commercial grade	Noel	JPL	17	400	30	125	FC, NB, $q_{u,b}$
Isopropyl Alcohol	Commercial grade	Noel	JPL	17	400	30	125	FC, NB, $q_{u,b}$
DETA (Diethylenetriamine)	90.4% diethylenetriamine 9.6% amine-ethyl-piperazine	Noel	JPL	18	400	30 to 40	10 to 350	FC, NB, $q_{u,b}$
Aniline	96% aniline, 4% H_2O	Kreith, Summerfield	JPL	19	35 to 365	21 to 37	90 to 135	FC, NB, Dep.
n-Butyl Alcohol	99.5% n-butyl alcohol, 0.5% H_2O	Kreith, Summerfield	JPL	20	30 to 200	24 to 41	85 to 100	FC, NB, ΔP
JP-3	Mil-F-5627	Hatcher	JPL	11, 21	30 to 500	8 to 80	60 to 150	FC, NB, $q_{u,b}$, Dep., ΔP
JP-4	Mil-F-5624A	Beighley, Dean	Bell Aircraft	22	30 to 300	2 to 40	75	FC, NB, $q_{u,b}$
Liquid Hydrogen	-	Powell	JPL	13	750	-390 to 700	(0.9 to 1.9)	FC, supercritical
Hydrazine	-	Banchero, Banor, Ball	University of Michigan	14	-	-	-	-

*UNITS: lb/in² sec, FC = nonboiling forced convection, NB = forced velocity nucleate boiling; $q_{u,b}$ = upper limit of nucleate boiling; ΔP = pressure drop; Dep. = deposition or coking; An = aniline; FA = furfuryl alcohol.

UNCLASSIFIED

TABLE II

EFFECT OF COOLANT VELOCITY ON VALUE OF $q_{u\ell}$ AND ON TURBOPUMP POWER REQUIREMENTS

	First Design	Second Design
Coolant Velocity at Throat (ft/sec)	50	100
Coolant Bulk Temperature at Throat (°F)[a]	100	100
Chamber Pressure (psia)	300	300
Injector Pressure Drop (psia)	75	75
Coolant Passage Pressure Drop (psi)[b]	75	600
Turbopump Outlet Pressure (psi)	450	975
Pressure at Throat in Coolant Passage (psia)	423	675
Value of $q_{u\ell}$ at Throat (Btu/in^2 sec)[c]	4.2	7.7
Total Propellant Consumption Required for Fuel Turbopump[d]	2.0%	4.25%
Increase in Value of $q_{u\ell}$	---	83%
Increase in Total Propellant Consumption Required for Fuel Turbopump		2.25%

[a] Calculation for NH_3 cooled motor

[b] Coolant passage pressure drop proportional to V^3

[c] Interpolated from figures (2) and (4)

[d] For constant mass flow rate turbopump power requirement assumed proportional to head; assuming constant efficiency, propellant consumption is proportional to power.

TABLE III

COMPARISON BETWEEN CALCULATED CONVECTIVE THROAT HEAT FLUX AND THROAT VALUES OF $q_{u\ell}$ FOR TEN PROPELLANT SYSTEMS

	coolant	reactant	1 r	2 c* (ft/sec)	3 T_c (°R)	4 q_* (Btu/in^2 sec)	5 $W_{coolant}$ (lb/sec)	6 t (in.)	7 V_* (ft/sec)	8 T_{L_*} (°F)	$q_{u\ell}$ value (Btu/in^2 sec)	$q_{u\ell}$ ref	T_{sat} °F at 375 psi	$T_{L_{out}}$ (°F)
a	RFNA	UDMH	2.5	5083	4796	5.85	158.0	0.109	60.8	179	8.8	6	355 †	242
b	CORPORAL fuel	SFNA	3.0	4763	4938	5.07	59.3	0.0716	49.3	243	8.20	16	580 †	358
c	DETA	SFNA	3.0	4930	4808	5.02	57.3	0.0724	58.6	214	7.20*	16	740	306
d	50 An-50 FA	SFNA	3.0	4740	4955	4.90	59.6	0.0719	50.0	236	5.40*	17	680 †	346
e	JP-3	N_2O_4	3.0	5069	5206	4.91	55.8	0.0712	63.4	238	5.25*	21	670 †	349
f	NH_3	RFNA	2.2	4997	4224	5.58	70.7	0.0614	72.5	92	5.30	15	140	140
g	Isopropanol	SFNA	3.3	4757	4744	5.24	55.3	0.0744	63.0	207	4.50*	17	550	293
h	NH_3	O_2	1.41	5499	4882	6.52	85.3	0.0688	78.0	92	5.80	15	140	135
i	JP-3	O_2	2.25	5593	5577	6.00	62.2	0.0762	67.1	276	5.15*	21	670 †	376
j	ClF_3	N_2H_4	2.50	5546	5881	5.83	145.0	0.0912	57.8	213	4.25	12	258	304

*Extrapolated from lower velocity and lower bulk temperature values.

†Estimated from nucleate boiling wall temperature measurements.

NOTES:

1. Approximately peak performance (I_{sp} @ 300 psi) mixture ratio, oxidizer/fuel.
2. 95% of theoretical value based on equilibrium expansion.
3. 90% of theoretical value.
4. Computed from $q_* = h_{g*} (T_{c_s} - T_w)$
   h_{g*} computed from Ref. 25, C_p based on constant composition value from thermochemical performance calculation.
   T_w taken to be 50°F higher than saturation temperature of the codant at throat pressure, 410 psia.
5. Value based on total utilization of propellant for regenerative cooling.
6. Computed coolant passage height for 75 psi coolant passage pressure drop, using isothermal friction factor values, and average values of density and viscosity between inlet and outlet temperatures.
7. Coolant velocity of throat.
8. Coolant bulk temperature at throat, based on 100°F inlet bulk temperature for all coolants except NH_3 where 32°F was used.

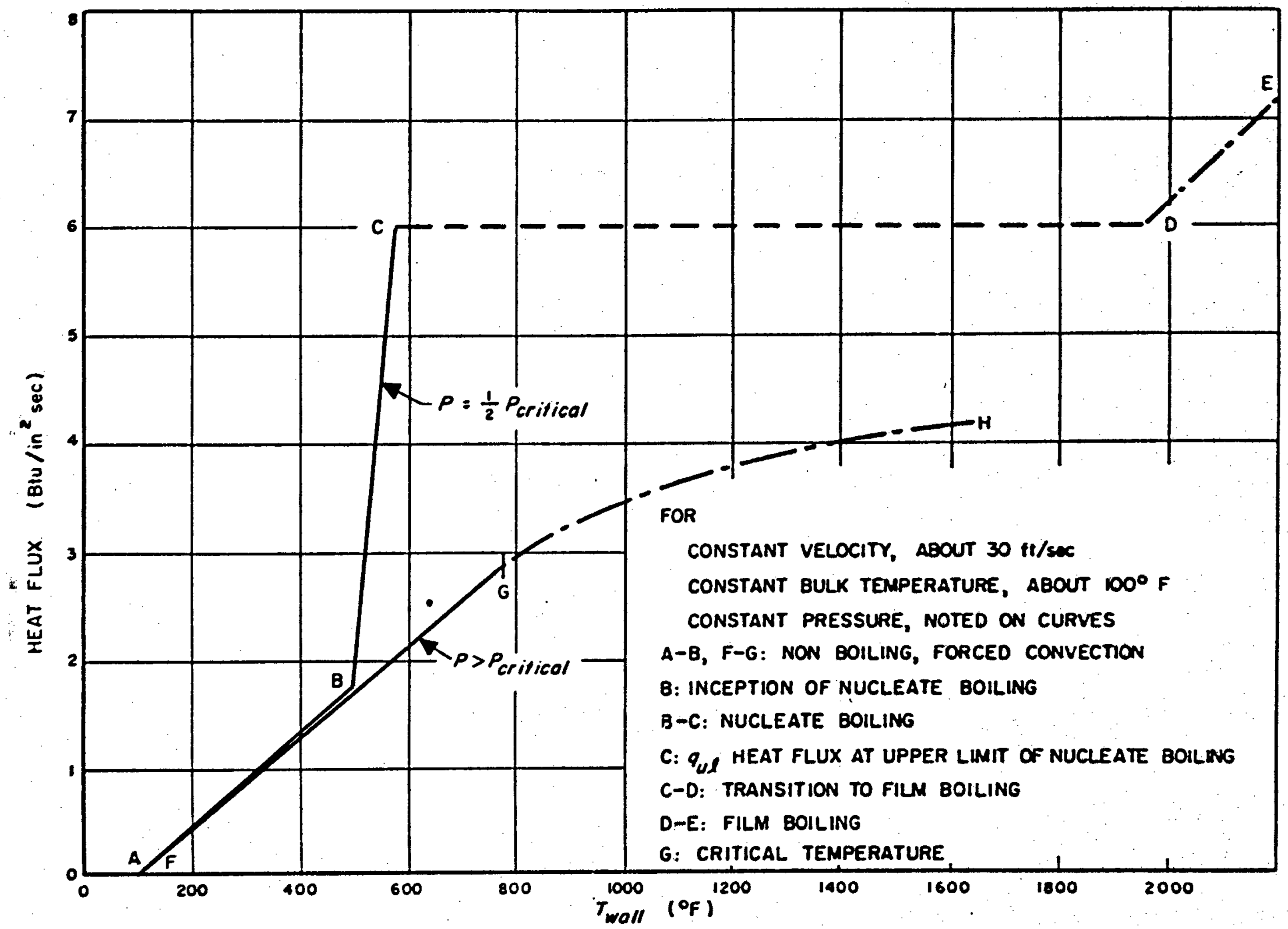

Figure 1. Heat Flux vs Wall Temperature of Typical Liquid Propellant in Various Heat Transfer Regimes

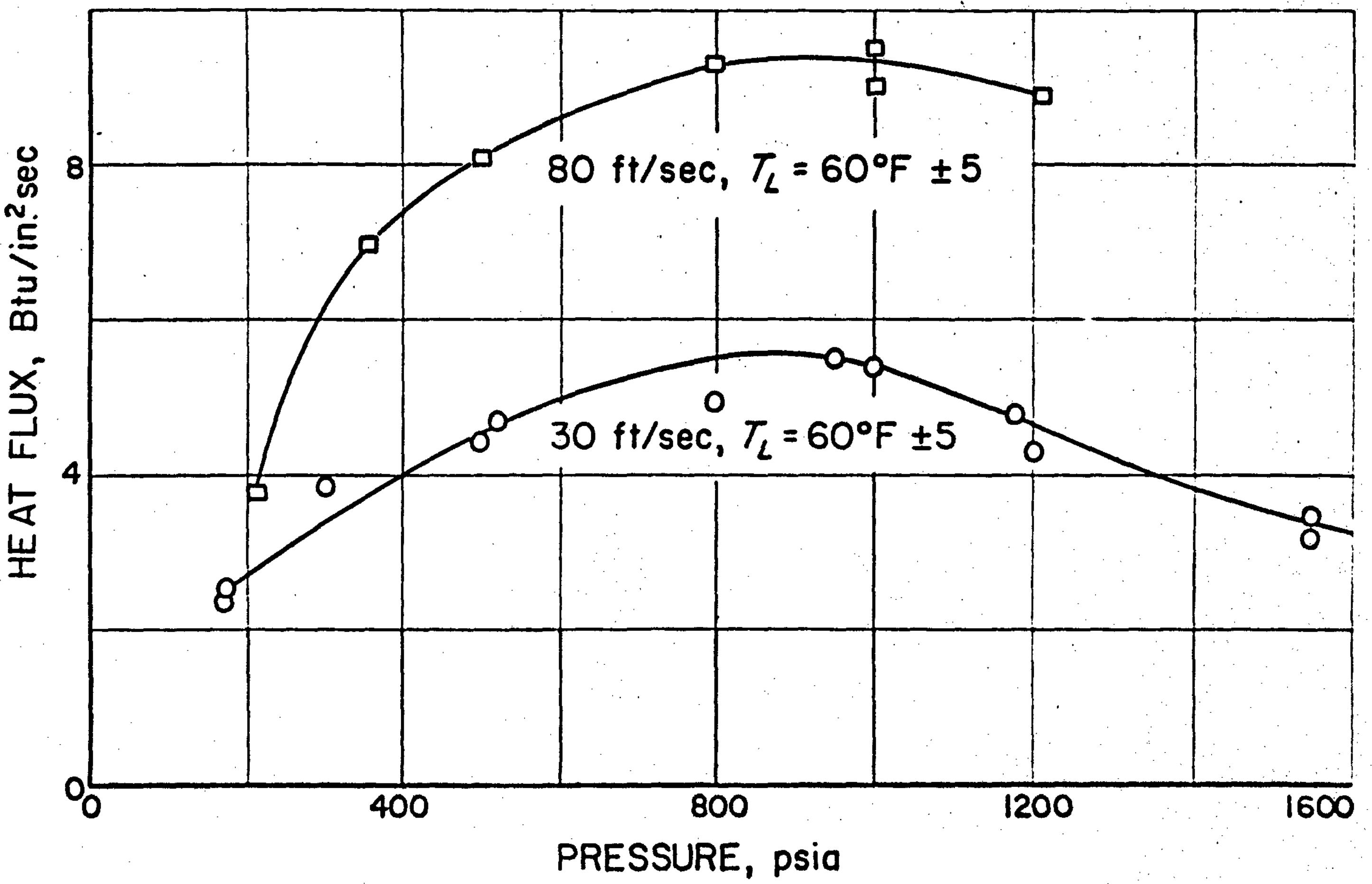

Figure 2. Heat Flux at the Upper Limit of Nucleate Boiling as a Function of Pressure for Ammonia at Bulk Temperature 60°F ±5

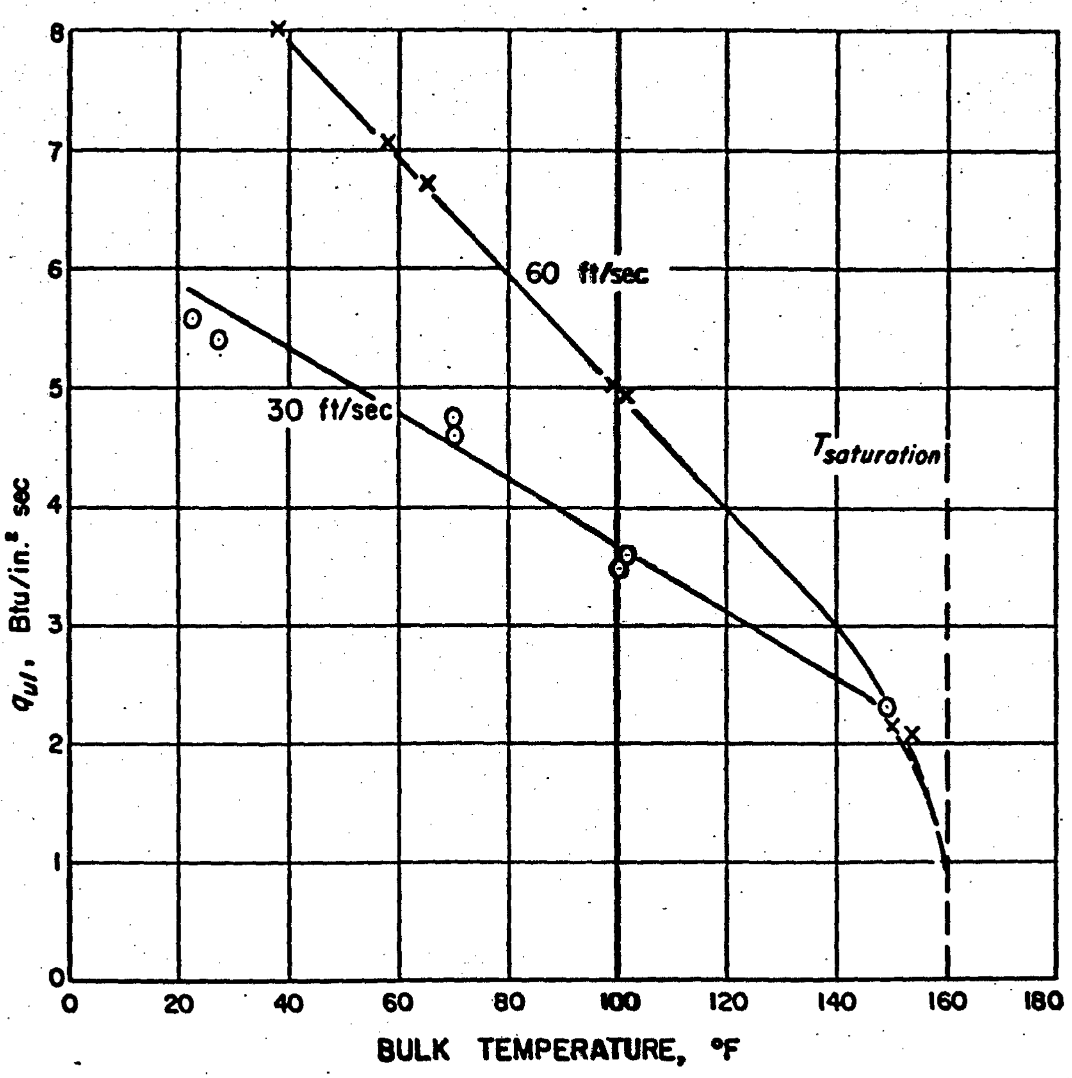

Figure 3. Heat Flux at the Upper Limit of Nucleate Boiling as a Function of Bulk Temperature for Ammonia at Pressure 500 psi, Velocities of 30 and 60 ft/sec

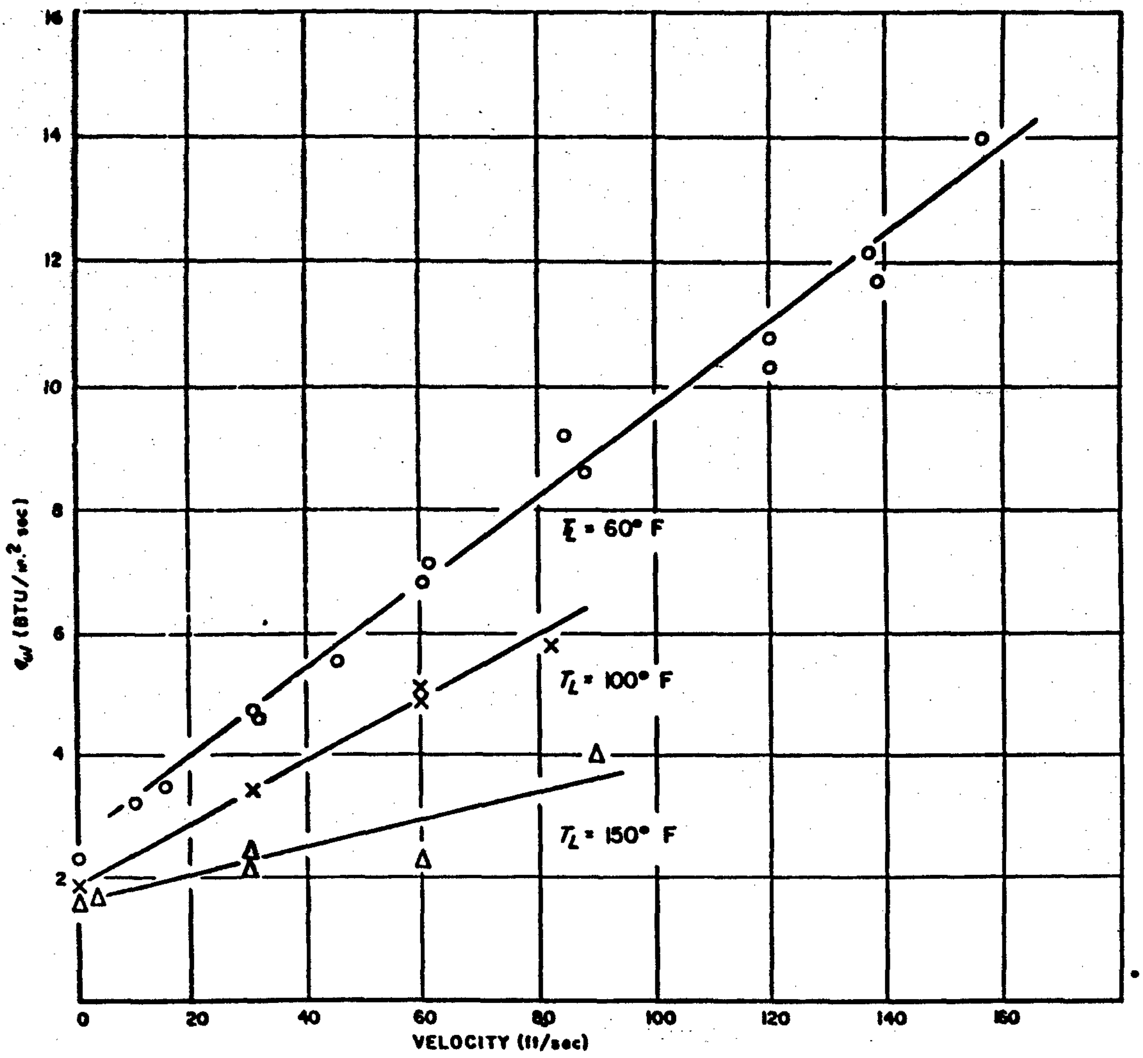

Figure 4. Heat Flux at the Upper Limit of Nucleate Boiling as a Function of Velocity for Ammonia at Pressure 500 psi

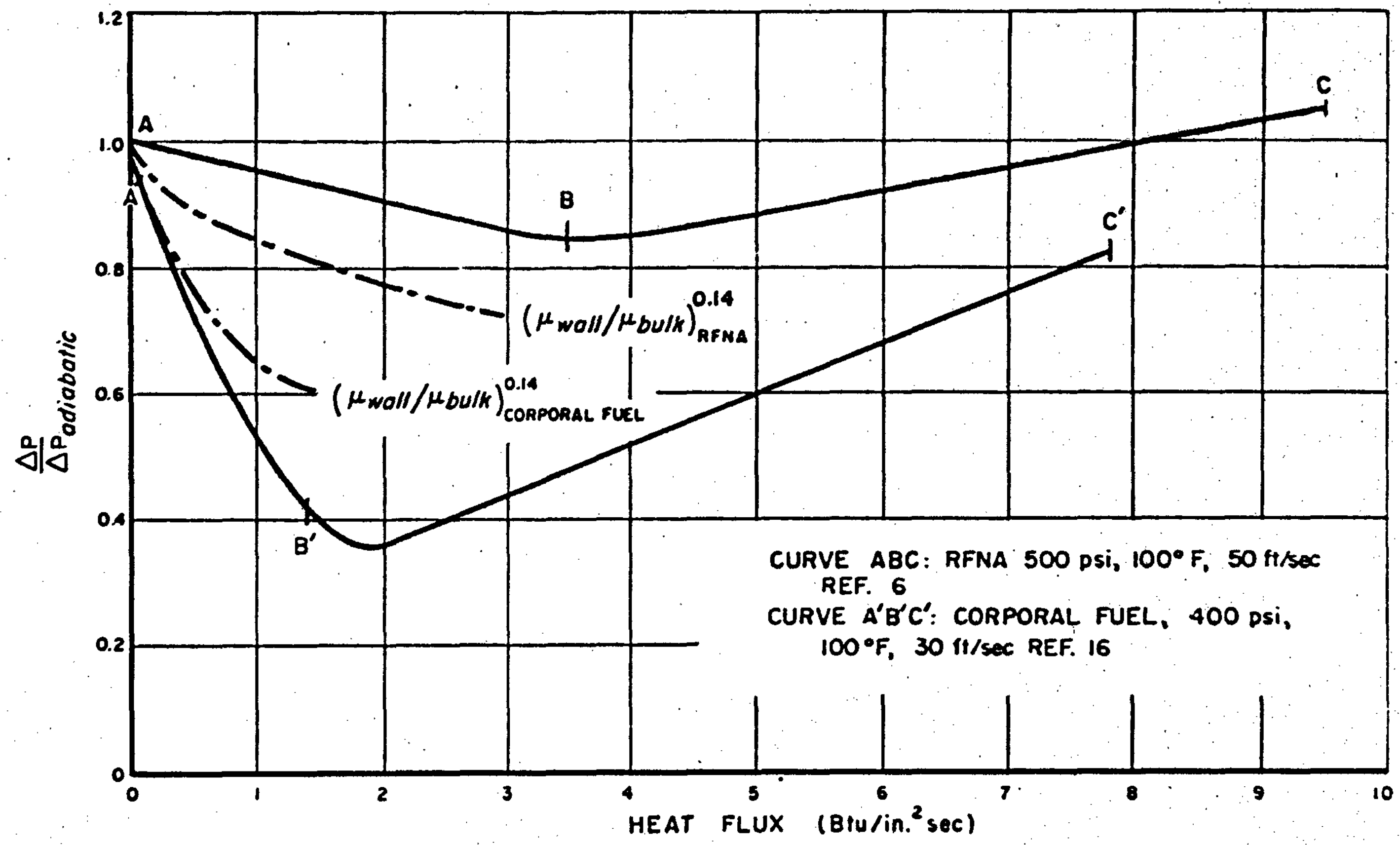

Figure 5. Ratio of Pressure to Adiabatic Pressure Drop vs Heat Flux for RFNA and for CORPORAL Fuel

UNCLASSIFIED

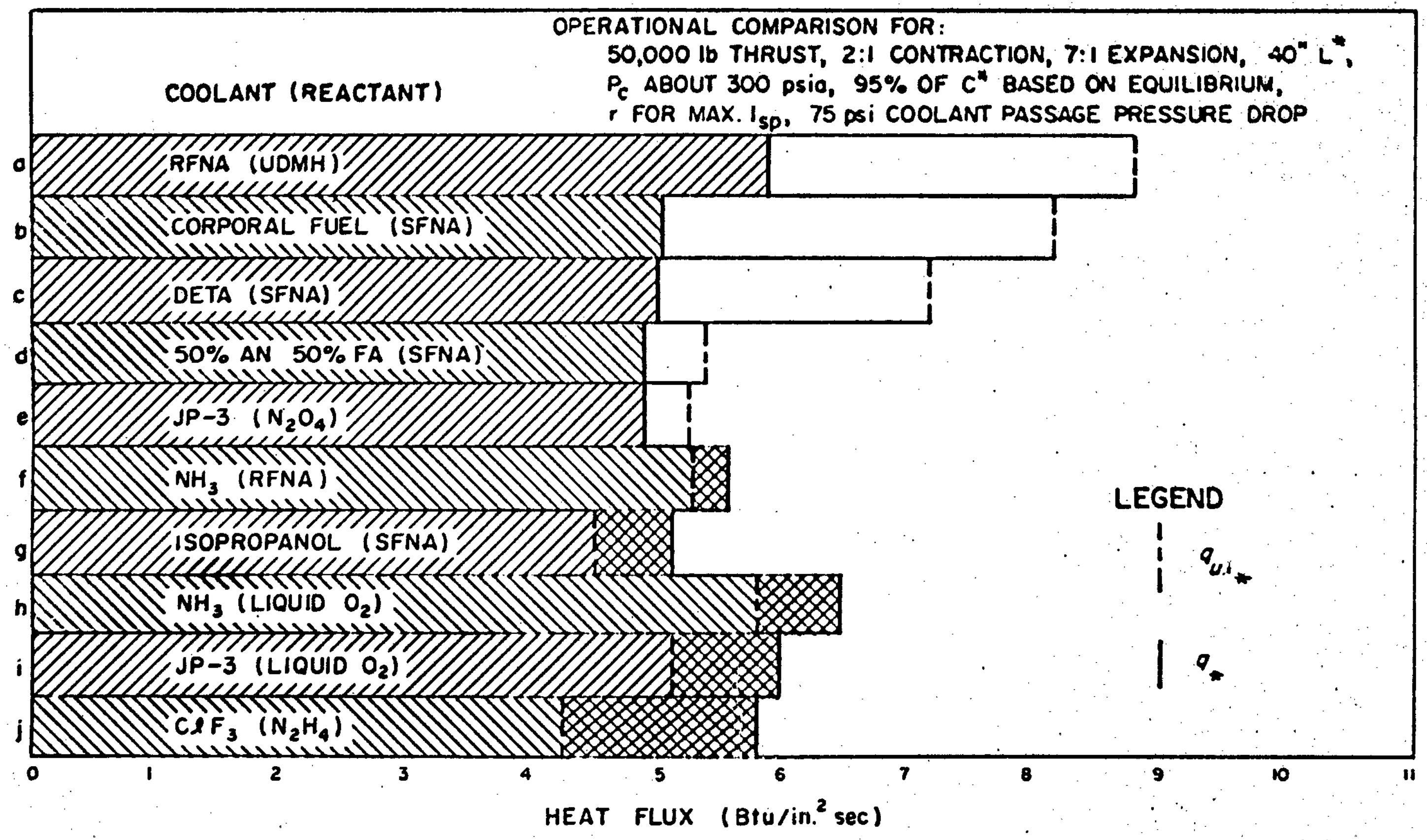

Figure 6. Comparison Between Calculated Throat Convective Heat Flux and Throat Values of q_{ul} of Ten Propellant Systems (see Table III for Performance and Mixture Ratio

UNCLASSIFIED

FACTORS INFLUENCING THE MONOPROPELLANT SPECIFIC IMPULSE OF ACETYLENIC COMPOUNDS

Lloyd E. Line, Jr.
Experiment Incorporated
Richmond, Virginia

The employment of acetylenic-type monopropellants in ram-rocket and turborocket applications involves a two-phase working fluid consisting primarily of carbon and hydrogen with unusually high weight-percentages of finely divided carbon. Thus the working fluid from propyne decomposing according to the equation

$$C_3H_4 \rightarrow 3C + 2H_2 \qquad (1)$$

would contain 90% by weight of solid, which very nearly equals that corresponding to chemical equilibrium at the flame temperature. Other acetylenic compounds of higher molecular weight that decompose in a similar fashion have been considered. These include (1, 2) methylvinylacetylene, methyldivinylacetylene, 1,6-heptadiyne, 1,7-octadiyne, dipropargyl ether, dipropargylamine, and isopropenylacetylene.

The motivation for the studies reported in this paper lies in the fact that no acetylenic monopropellant tested thus far has shown a measured specific impulse greater than about 80% of the theoretical (1, 2). It therefore seemed necessary to consider the physicochemical properties of the two-phase system consisting of carbon and hydrogen with a view to uncovering the probable source or sources of trouble. The problem has also been considered by Glassman (2).

It is the purpose of this paper to list and examine the potential sources of low impulse efficiency, using propyne as an example, and where the results are clear-cut, to indicate those factors that seem most important. These factors are probably common to all acetylenic monopropellants that decompose to give a solid-gas working fluid.

1. Sources of Low Impulse Efficiency

The theoretical calculation of the specific impulse of propyne (189 seconds) assumes that chemical equilibrium is achieved in the chamber and that there is no shift in chemical equilibrium during expansion. Carbon is assumed to be in the graphitic form, and the composition of products is very nearly that represented by Equation 1. It is further assumed that the expansion is adiabatic and that the particles and gas are in thermal equilibrium and leave the nozzle with the same exhaust velocity.

In view of the above assumptions, the following factors seemed to require investigation:

(a) difference in exhaust velocities for the two phases,
(b) lack of thermal equilibrium between the phases,
(c) enthalpy losses due to radiation from the particulate matter,
(d) tie-up of enthalpy in the chemical and physical state of the product carbon, and
(e) failure of the two-phase working fluid to attain chemical equilibrium.

In the following sections the probable importance of each factor operating alone is examined.

2. Velocity Difference Between Phases

If there is a substantial slip of gases past the particles in the expanding mixture, the specific impulse will be lower than that calculated ideally, for the theoretical calculation assumes that particles and gas are in directed-velocity equilibrium. This slip, or velocity difference, has been calculated to a first approximation for the decomposition products of propyne at the flame temperature as given by Equation 1, expanding through a pressure ratio of 20 to 1 in a rocket nozzle having the geometry shown in Figure 1. Thermal equilibrium between the phases was assumed during the expansion.

The procedure was to determine the velocity profile of a single carbon particle being accelerated in the nozzle by a gas which has all the characteristics of hydrogen except the ratio of specific heats, γ, and the molecular weight. The ratio of specific heats is that appropriate to the heterogeneous mixture and the molecular weight (20 grams/mole) is equal to the mass of the products (Equation 1) in grams divided by the number of moles of gas.

The velocity profile of this hypothetical gas is shown by the solid line of Figure 2 and was obtained in the manner usually employed for gas of known γ, temperature, and molecular weight. The velocity profile of a single carbon particle 0.1 micron in diameter (see section 5) was calculated by a process which involved breaking up the gas profile into convenient intervals, each having a constant gas velocity (equal to the terminal gas velocity for the interval) and finding the terminal particle velocity for each successive interval by means of hydrodynamic drag equations. A drag coefficient of 10 was chosen. It was then assumed that each particle has the velocity lag given by the difference shown in Figure 2, and this difference was then interpreted in terms of impulse efficiency. A velocity profile for 1-micron particles is also shown in Figure 2.

For a 0.1-micron particle at the exit the particle velocity, V_p, is 18×10^4 cm/sec, while the corresponding gas velocity, V_g is 19×10^4 cm/sec. Assuming now that these are the actual exit velocities of the phases, the specific impulse of the mixture is obtained from

$$I_{sp} = \frac{1}{g} \left(\frac{r\, V_s^2 + V_g^2}{r\, V_s + V_g} \right) \tag{2}$$

where r is the mass ratio of solid to gas and g is the acceleration due to gravity. Equation 2 is readily derived from the definition of the specific impulse and the equation of continuity for each phase. For the case under consideration $I_{sp} = 180$ sec for 0.1-micron particles, or a probable loss of some 9 seconds due to the slippage factor. This loss is probably a high figure because V_g would actually be higher than that corresponding to no slippage. Moreover, the drag coefficient is probably much greater than 10. Glassman (2), employing the method of Gilbert, Davis, and Altman (3) but a velocity profile for a gas having all the properties of hydrogen except γ, concludes that the effect of velocity lag is negligible.

The above treatment is intended to furnish only a rough idea of the importance of the factor under consideration and simply shows that it cannot account for the discrepancy entirely. A better estimate of the velocity lag would involve a complicated stepwise process which would take into account the interactions of particles and gas in such a manner that the actual gas and particle velocities would be estimated at selected intervals and hence at the exit. In this case the gas- and particle-velocity profiles would lie, respectively, above and below the profile given by the solid line of Figure 2. Equation 2 would then be more nearly applicable than it was in the present analysis.

3. Temperature Difference Between the Phases

When a two-phase system assumed to be initially at thermal equilibrium at the flame temperature expands in a nozzle, it is possible that the expansion is so rapid that the rate of heat transfer does not keep pace with the expansion, so that hot particles are ejected with cooler gas. The result would be a loss in enthalpy.

The degree of heat transfer between particles and gas was evaluated for a working fluid corresponding to $3C + 2H_2$ (flame temperature, 1655°K; carbon particles 0.1 micron in radius) expanding through a pressure ratio of 20 to 1 in a nozzle having the geometry shown in Figure 1. Details of the method are reported elsewhere (4). The procedure involved a stepwise evaluation of the particle and gas temperatures at selected positions along the nozzle axis, resulting in an exit gas temperature from which I_{sp} could be evaluated. At each point the heat transfer was calculated by means of the kinetic theory of gases and a reasonable value of the thermal-accommodation coefficient. Employment of the kinetic theory of gases in this case is justified by the fact that the carbon particles are of the order of the mean free path of hydrogen. Thus it is possible to calculate heat transferred from the number of **collisions per unit area per unit time.** The results of calculations applied to propyne are summarized in Table I.

It is apparent that the computed loss in impulse due to partial heat transfer is quite low. In fact this is an upper figure, since every questionable assumption that had to be made in the analysis was on the side of low heat transfer. Also, for the case of no heat transfer the computed loss in impulse is surprisingly low. This is due to a combination of two factors, one being the high specific heat of hydrogen as compared to carbon and the other being the tendency for the hydrogen to overexpand. From these calculations it would appear that the importance of heat transfer is not serious.

4. Radiation Losses

Since particulate matter is present in the working fluid, it is necessary to evaluate the loss of enthalpy due to radiation. The evaluation given here is a maximum figure for the rocket configuration chosen, since drastic assumptions favoring heat loss were employed in the interest of simplification.

In the calculation it is assumed that all the carbon particles are at the flame temperature (1655°K) and that the wall temperature is 0°K. It is further assumed that steady-state conditions prevail and that the total effective radiating surface equals the wall area of the rocket chamber and nozzle (taken to be 1200 square centimeters). This is the maximum radiating surface.

From the Stefan-Boltzmann Law and the assumption of black-body radiation, the rate of radiant heat loss is found to be 12 kcal/sec. Assuming a propyne fuel decomposition rate of 1 lb/sec (11.3 g-mole/sec), one finds that the rate of heat evolution is 39.2 kcal/mole x 11.3 mol/sec = 443 kcal/sec. The maximum loss in enthalpy, therefore, is about 2.7%, corresponding to a flame temperature of 1627°K and a loss in specific impulse of less than 1%.

The above calculation shows that the loss of enthalpy by radiation from hot carbon particles is probably not a serious factor.

TABLE I

EFFECT OF HEAT TRANSFER ON MONOPROPELLANT SPECIFIC IMPULSE OF PROPYNE

Gas Phase: Hydrogen, 1 part

Solid Phase: Carbon 9 parts, 0.1μ radius

$T_f = 1655^\circ K$

Nozzle Geometry: Figure 1

		ΔI_{sp}	
	I_{sp}	Seconds	Percent
Complete Heat Transfer	189	0	0
Partial Heat Transfer	187	-2	-1.0
No Heat Transfer	173	-16	-8.5

5. Characteristics of Product Carbon

The theoretical monopropellant specific impulse for propyne and for other acetylenic hydrocarbons is calculated on the assumption that the carbon is pure graphite. This section deals with the question of whether this assumption is a valid one and with the general characteristics of the carbon including particle size, chemical composition, and x-ray diffraction patterns.

a. Particle Size

Samples of exhaust carbon were collected through cold probes placed in the chamber and in the exhaust stream of a rocket motor employing propyne. In one run the fuel temperature was 29°F, and in the other it was preheated to 110°F. The chamber pressure was about 250 psi. The run in which the fuel was at ambient temperature gave a specific impulse of 140 seconds; the one with preheated fuel gave a specific impulse of 150 seconds. The electron micrographs show clusters 1 or 2 microns in size consisting of apparently spherical particles 0.1 to 0.2 microns in diameter (Figure 3). The ultimate particles are somewhat larger than those of industrial carbon blacks and of carbon in premixed or diffusion flames. It is impossible to say whether or not these clusters exist during the expansion, but calculations employing a relationship developed by von Smoluchowski (5) show that little agglomeration can occur via a Brownian movement mechanism during the residence times of particles in the rocket motor. The extent of agglomeration due to turbulence is hardly predictable.

Examination of the electron micrographs show no difference in particle size between a sample taken from the chamber and one taken from the exhaust stream. Also there was little difference in ultimate size or shape between particles for which the fuel was preheated and those for which the fuel was at ambient temperature.

b. X-ray Examination

Graphitic carbon has a characteristic x-ray pattern which is well-known. The patterns of product carbon samples taken from the chamber and the exhaust stream (with and without fuel preheating) show broad bands and lines that correspond in general to the graphitic spacing. However, the broadness would seem to indicate a lack of regularity in the structure and/or exceedingly small crystal size combined with spreading of the lattice structure by impurities that are too small to give their own diffraction pattern. The samples did not show marked differences from each other.

c. Heat of Combustion

The heat of combustion of the product carbon is an important quantity, since from this one can compute the enthalpy difference, if any, between this carbon and graphite and relate it to the specific impulse.

Samples of the exhaust carbon were submitted to the National Bureau of Standards for determination of the percentages of carbon and hydrogen and the heat of combustion of the carbon. The percentages of carbon and hydrogen were determined gravimetrically as CO_2 and H_2O, respectively. The heat of combustion of the carbon was obtained calorimetrically, the mass of carbon being obtained from the mass of carbon dioxide found. The heat of combustion was corrected for the presence of hydrogen using the mass of hydrogen in the sample and its heat of combustion per gram, assuming the hydrogen to be physically absorbed.

The results show an average heat of combustion for six samples of 8015 cal/g carbon, whereas the present best value for graphite is 7831 cal/g (6). This means that enthalpy is tied up in the particular form of carbon produced in the decomposition, and only 32.57 kcal are evolved for the decomposition of one mole of liquid propyne at 298°K instead of 39.2 kcal when graphitic carbon is formed. The excess energy resident in this carbon may be associated with its high state of subdivision.

Assuming that this product carbon has the same heat capacity as that of graphite (and neglecting the effect of the removal of hydrogen from the working fluid), one obtains $I_{sp} = 178$ seconds for the ideal specific impulse or a loss of 11 seconds associated with the type of carbon formed.

d. Percentage of Hydrogen

The carbon samples contained an average of 0.75% hydrogen by weight. A calculation of the specific impulse for a graphite-hydrogen working fluid with this much hydrogen removed (temperature, ratio of specific heats and pressure ratio assumed to remain unchanged) gives $I_{sp} = 182$ seconds or a loss of about 7 seconds due to removal of hydrogen. Small weight-percentages of hydrogen in the carbon increase considerably the molecular weight of the working fluid.

6. Analyses of Product Gases

Analyses of exhaust gases from a rocket motor utilizing propyne indicate a high percentage (around 30%) of methane together with hydrogen and smaller percentages of alkenes and alkynes (1-2%). The gases from the decomposition of 1,6-heptadiyne in a rocket show about 38% methane with the remainder largely hydrogen. The amount of methane for an equilibrium distribution of products in the decomposition of acetylenic hydrocarbons is about 2%.

Closed-bomb ignitions (with a fuse wire) of various acetylenic monopropellants in the vapor phase at 260°C also show considerable quantities of methane (Table II).

The question arises, how important is the formation of methane? The specific impulse of the product mixture from the decomposition of propyne according to

$$C_3H_4 \rightarrow 2.5C + H_2 + 0.5\ CH_4 \qquad (3)$$

which corresponds to 33% CH_4, was calculated. In the calculation it was assumed that the decomposition is complete in the chamber and that there is no shift in equilibrium on expansion. The carbon was assumed to be graphitic. To obtain the flame temperature, the enthalpy of the above reaction, obtained from the heats of formation of propyne and methane, was distributed over components considered to be in thermal but not in chemical equilibrium. The result, 182 seconds, shows a loss of only about 7 seconds due to the formation of 33% methane. While the specific impulse should be lowered appreciably by the increased molecular weight (20 to 26.7), this tends to be cancelled by the increase in flame temperature (1655°K to about 2050°K). This latter fact arises because the formation of methane from carbon and hydrogen is exothermic. The slightly different ratios of specific heats for the two cases were neglected.

The question arises whether the 30% methane found in the exhaust gases is the percentage that existed in the working fluid. Assuming no shift of equilibrium in expansion, any change in the gas composition will be that due to cooling of the mixture during sampling. This, however, should increase the percentage of methane, since the equilibrium

$$2H_2 + C \rightleftharpoons CH_4 \qquad (4)$$

shifts to the right on cooling. From these considerations it would appear that the discrepancy of 7 seconds due to the methane found in the exhaust gases is a maximum.

Glassman (2) found only about 7% methane in the exhaust gases from the decomposition of propyne in a rocket motor and concluded that the effect of methane was slight.

Experiments with preheated propyne (7) have been conducted at Experiment Incorporated. Preheating of the fuel by 100°F appears to yield an increase of 10-15 seconds in the specific impulse. Since this is considerably greater than that which would be expected from the preheating alone, the importance of reaction kinetics seems to be indicated.

TABLE II

ANALYSIS OF GASEOUS DECOMPOSITION PRODUCTS FROM SMALL BOMB EXPERIMENTS AT 260°C

Fuse-wire Ignition

Monopropellant	Samples Averaged	Components, mole percent					
		Alkynes	Alkenes	CO	H_2	CH_4	Residual*
Methylvinylacetylene	2	5.8	2.5	1.1	53	30	7.6
Methyldivinylacetylene	3	0.22	2.2	1.7	48	43	4.9
1,6-Heptadiyne	2	1.3	1.8	2.4	60	25	9.5
1,7-Octadiyne	8	0.67	3.1	0.52	56	34	5.7
Dipropargyl ether	1	0.52	4.1	27	36	13	20
Dipropargylamine	5	1.0	4.2	1.1	57	22	15

---

* Residual gases include O_2, CO_2, and N_2. Some ammonia may have been formed when dipropargylamine was decomposed.

Summary and Discussion

The foregoing results, summarized in Table III, show that the discrepancy between the theoretical and measured specific impulse for propyne is distributed over several possibilities. Of these, the least reliable estimate is the one given for the velocity difference between the phases. This estimate is probably high for 0.1-micron particles; for 1-micron particles this factor would become quite important. It is well-nigh impossible to estimate the degree of agglomeration of the 0.1-micron particles in the working fluid.

Heat transfer and radiation from particulate matter appear not to be important. The estimated effects are probably maximum values.

The influence of the state of the carbon may be surprising, yet carbon blacks in general have a higher energy content than graphite (6). This may be due to the high state of subdivision. In any case, the assumption of graphite as the form of carbon produced in the decomposition of acetylenic compounds appears to be in error.

The fact that 0.7% hydrogen (about 8 atom-percent) exists in the solid and about 30% methane in the gases demonstrates that the system does not attain chemical equilibrium. These results, together with the fact that the carbon contains more energy than massive graphite, account for about 25 seconds of the discrepancy between measured and theoretical values.

It is hoped that future work can be directed toward studying the chemical mechanism of decomposition of propyne and other acetylenic monopropellants.

Acknowledgments

The writer wishes to thank Felix von Gemmingen, Jr., and Carl J. Likes of the Virginia Institute for Scientific Research, Richmond, Virginia, for electron micrographs and x-ray patterns of the carbon particles. He wishes also to thank E. J. Prosen and James I. Minor, Jr., of the Thermochemical Laboratory of the National Bureau of Standards for precise measurements of the heat of combustion of carbon and of the percentages of hydrogen and carbon.

The following personnel of Experiment Incorporated have also contributed in various ways to this paper: Elizabeth Wilson Gauldin, Peter L. P. Dillon, D. H. York, H. B. Forney, and Spencer M. King.

The work reported herein was done under the sponsorship of the Bureau of Ordnance, Department of the Navy, under contract NOrd-15337.

TABLE III

SUMMARY OF FACTORS INFLUENCING THE SPECIFIC IMPULSE OF PROPYNE

Factor	Estimated Effect $-\Delta I_{sp}$, seconds
Velocity Difference Between the Phases	9 max.
Lack of Thermal Equilibrium	3 max.
Radiation from Carbon	2 max.
State of the Carbon	11
Removal of Hydrogen by Carbon	7
Formation of Methane	7 max.

Theoretical Specific Impulse (Pressure ratio 20 to 1)	189 sec
Measured value (Without preheating of fuel)	140-150 sec

References

(1) Spencer M. King, George J. Gibbs, and Lloyd E. Line, Jr., "Evaluation of Acetylenic Monopropellants," Experiment Incorporated TP-106, July 1, 1956.

(2) I. Glassman, "Evaluation of Acetylenic Compounds for Ram Rocket Applications," Princeton University Aeronautical Engineering Laboratory Report No. 343, March 15, 1956.

(3) M. Gilbert, L. Davis, and D. Altman, Jet Propulsion, 25, 26-30 (1955).

(4) Peter L. P. Dillon and Lloyd E. Line, Jr., Jet Propulsion, 26, 1091-1097 (1956).

(5) "A General Discussion on Disperse Systems in Gases, Dust, Smoke, and Fog," Trans. Faraday Soc., 32, 1041-1297 (1936).

(6) Private communication from E. J. Prosen of the National Bureau of Standards.

(7) E. C. Wilkerson, "Monofuel Ramrocket Development," Experiment Incorporated TP-96, 31 October 1955.

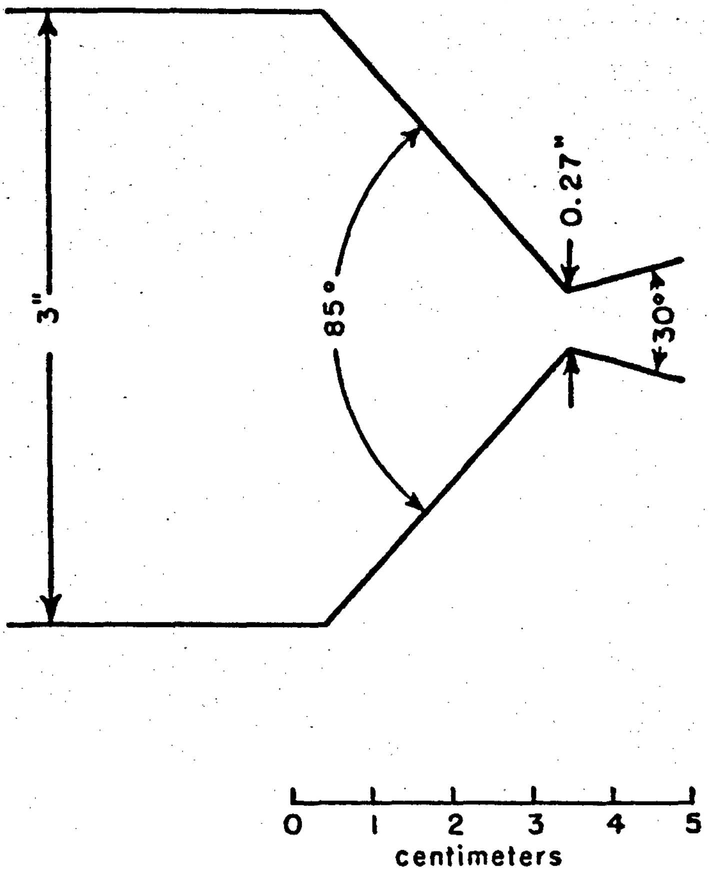
3"
85°
0.27"
30°
0
1
2
3
4
5
centimeters

FIGURE I. ROCKET NOZZLE ASSUMED FOR CALCULATIONS OF PARTICLE VELOCITY LAG. FULL SCALE

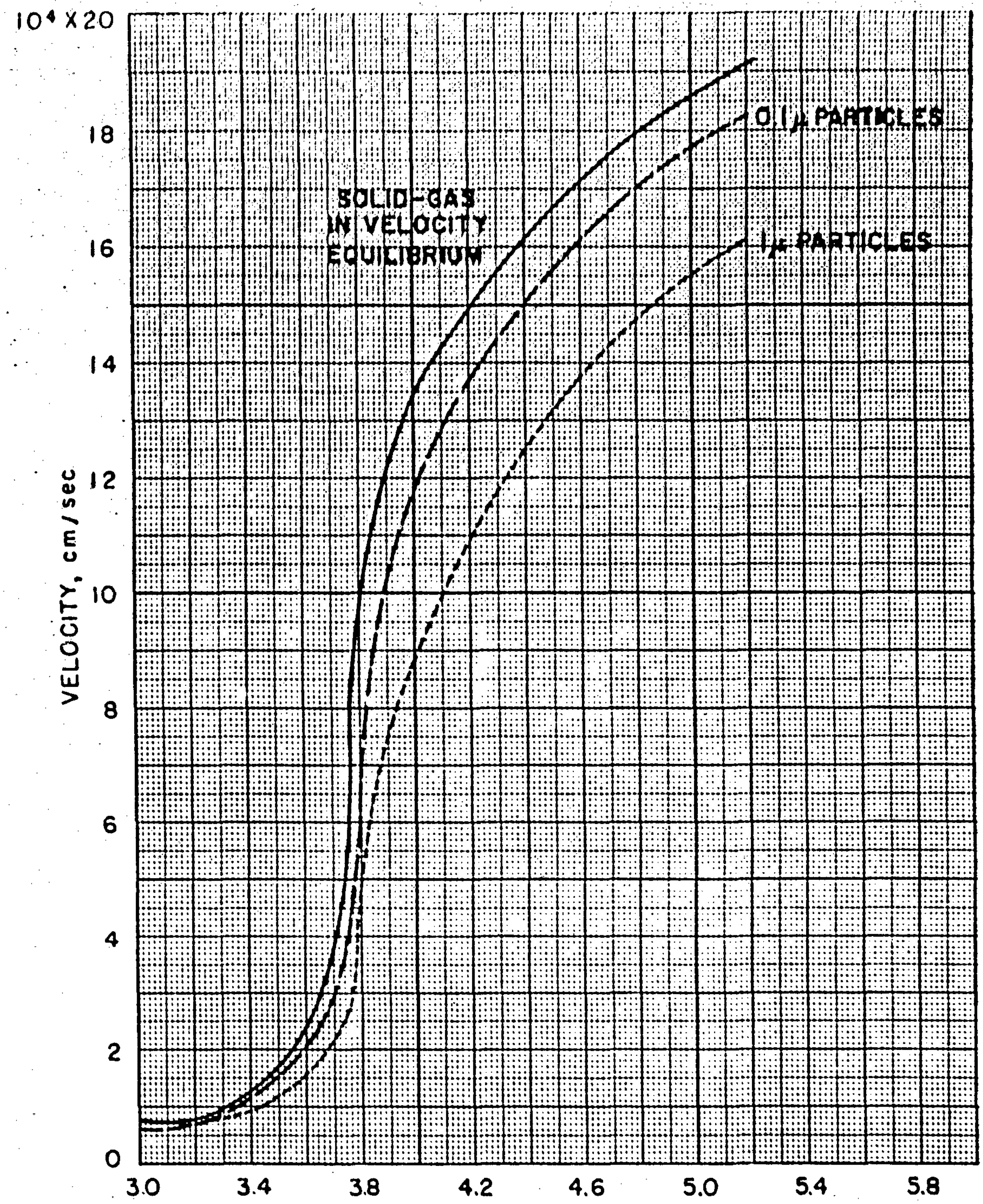

FIGURE 2. GAS AND PARTICLE VELOCITIES ALONG A PROPYNE ROCKET NOZZLE

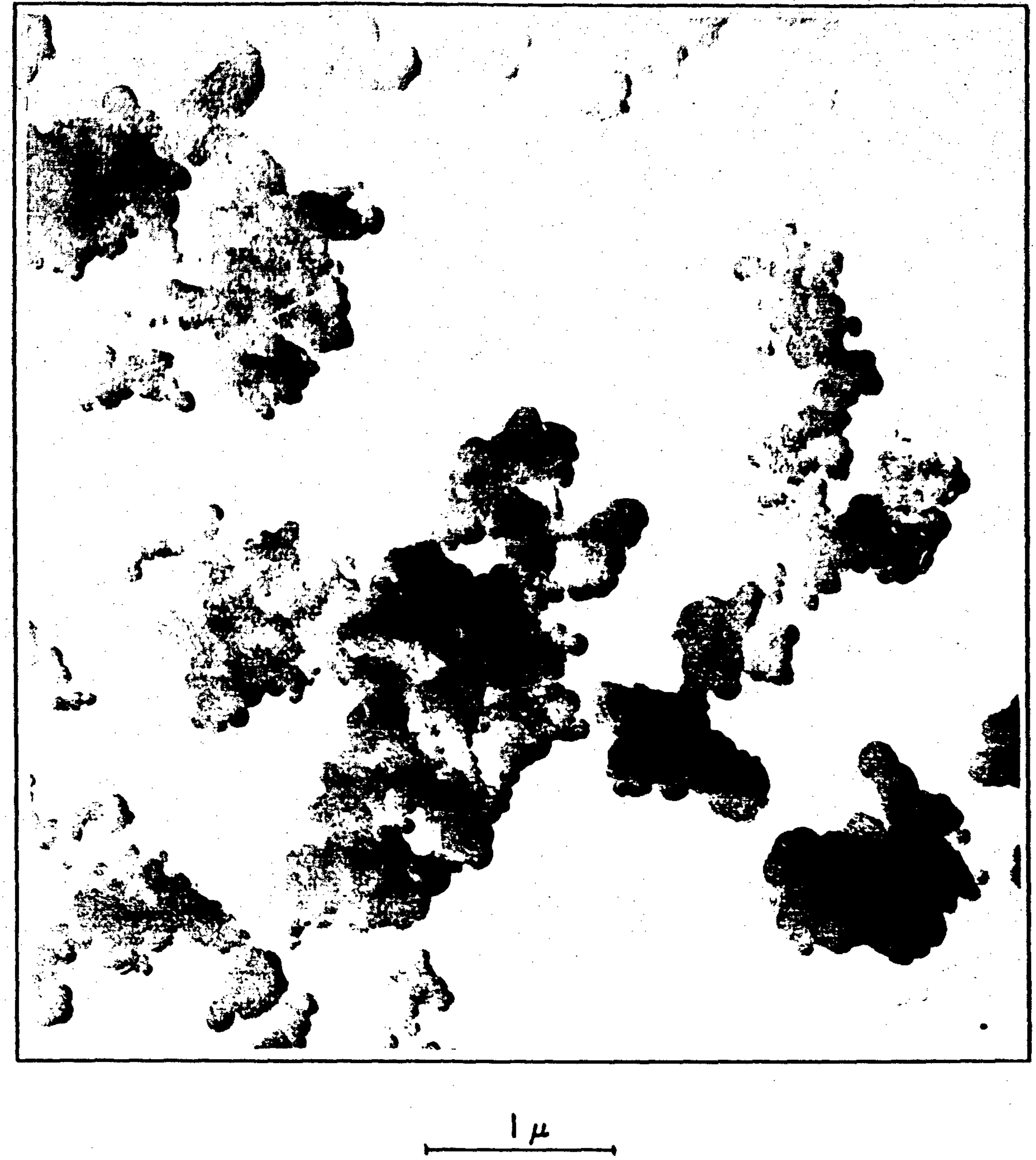

FIGURE 3. ELECTRON MICROGRAPH OF CARBON FROM CHAMBER DURING FIRING OF RAMROCKET

"EFFECT OF HYPERGOLICITY OF THE PROPELLANTS ON THE OPERATION OF A LARGE MISSILE ROCKET"

R. F. Tangren
Aerojet-General Corporation
Azusa, California

INTRODUCTION

A review of the experience gained in the development of a large, liquid-propellant booster-rocket for the BOMARC interceptor reveals the existence of three problems not usually considered in the selection of propellants. Two of these problems are directly associated with the hypergolicity of the propellants and its effect on the operation of the rocket during the shutdown sequence and reignition under conditions of interrupted propellant flow. The third problem which is also affected by the hypergolic characteristics of the propellants, is the combustion time lag and its relationship to the overall system stability.

Propellants for the booster rocket were originally selected to be JP-3 and white fuming nitric acid. Shortly after the inception of the program, the fuel was changed to JP-4 and later the oxidizer was changed to red fuming nitric acid for better storability. After a rather extensive development program with the JP-4, the fuel was changed to JP-X, a hypergolic mixture of JP-4 and the unsymmetrical dimethylhydrazine. A marked improvement was noted in the operation of the rocket in changing the fuel because of the effect of the fuel on the problems listed above.

The utilization of a hypergolic propellant combination makes possible the attainment of a "chemical safety" as distinguished from the "mechanical safety" required for rocket systems dependent on the maintenance of close control tolerances to avoid hazardous malfunctions. The detonation of accumulated propellants within a rocket combustion chamber has been the source of a number of destructive explosions. The proper selection of propellants to minimize this danger allows a greater freedom in the design of the rocket and permits the development of simple overall system.

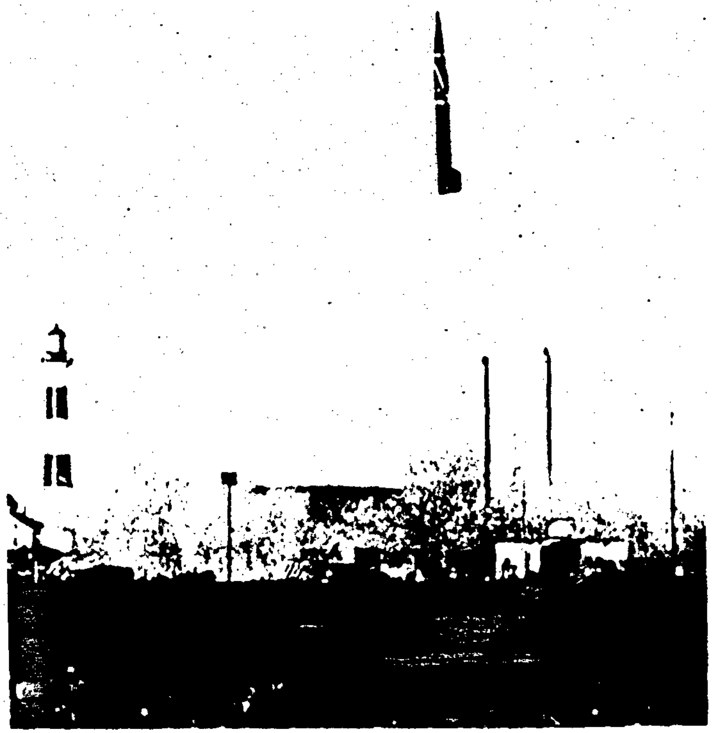

Figure 1 Takeoff of IM-99 Test Vehicle

BOMARC BOOSTER ROCKET

The booster for the BOMARC IM-99 Interceptor is a liquid, bipropellant rocket with a normal rating of 35,000 lbs of thrust. Figure 1 shows the takeoff of one of the vehicles constructed to test the operation of the booster rocket. More than fifteen successful flights have been accomplished. The rocket engines used for these flights all utilized a helium-gas, pressure-fed system shown in Figure 2. The arrangement of the tanks was varied between groups of vehicles to comply with the individual requirements of the groups. The rocket system is operated in the following manner: A solenoid operated control valve admits pressure to the dome of the main gas regulator. As pressure rises in the main tanks, a pressure switch signals the thrust-chamber valve to open. Propellants ignite spontaneously in the thrust chamber, and combustion continues until the propellants are exhausted.

Full scale, "captive" testing of complete rocket systems, simulating actual flight conditions as closely as possible, was found to be a necessary element of the development program. Figure 3 shows the test installation at the Experimental Rocket Engine Test Station

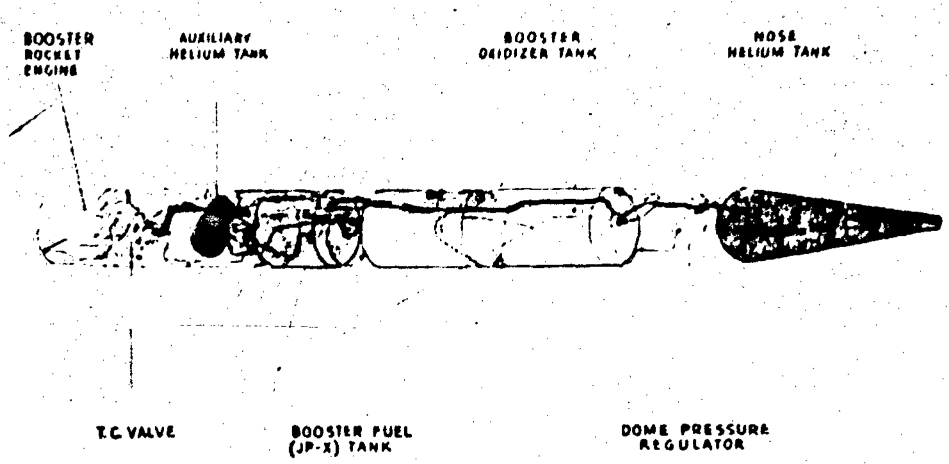
BOOSTER ROCKET ENGINE
AUXILIARY HELIUM TANK
BOOSTER OXIDIZER TANK
NOSE HELIUM TANK
T.C. VALVE
BOOSTER FUEL (JP-X) TANK
DOME PRESSURE REGULATOR

Figure 2 Helium Gas Pressurized Rocket System

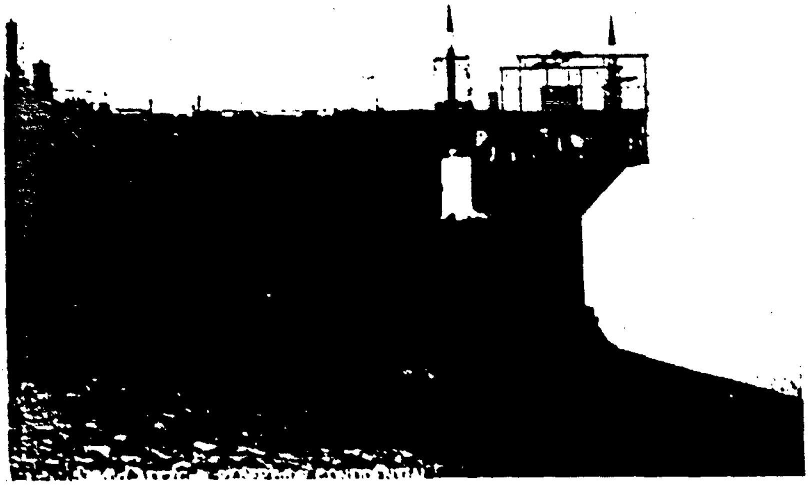

Figure 3 Testing at Edwards Air Force Base

at Edwards Air Force Base with two flight-type vehicles installed, the one nearest the camera firing.

REVIEW OF EXPERIENCE WITH JP-4

With the exception of an adequate shutdown control, the development of the rocket using JP-4 was successful under the conditions existing at the Azusa test facilities of Aerojet-General. At the time that JP-4 was abandoned as a fuel, a total of 944 tests of all kinds has been conducted on the subject rocket and its components, of which 85 were tests of the complete system. Work was in progress on the solution of the shutdown problem, the problem being to stop fuel flow into the combustion chamber in such a manner as to prevent the accumulation and subsequent explosion of a hazardous quantity of mixed fuel and oxidizer. Since JP-4 and nitric acid do not react readily at low pressure, this implies the need for rapid, clean shut-off of fuel flow.

One of the problems encountered was unique to the flight environment, wherein sloshing of propellants in the tanks, caused by pitch and yaw oscillations of the missile, resulted in an uncovering of the outlet port and a momentary interruption of the flow of propellant to the thrust chamber. "Flame out" and subsequent reignition of accumulated propellants resulted in destructive malfunctions. This problem was solved by the mechanical means of adding baffles to the tanks, but indicated the desirability of spontaneously ignitable propellants.

The most critical problem, and the problem dictating the change in fuel, was one of low frequency (approximately 100 cps) combustion instability of the prototype rocket system. The successful system tests described above involved heavy and very rigid thrust-chamber mounts and a feed system designed for test stand use with heavyweight plumbing and tankage. On none of these tests was low frequency instability encountered. However, when the rocket was assembled into a flight-type test vehicle, with the thrust chamber mounted on a lightweight, highly-stressed structure and with the actual configuration of lines and plumbing as designed for the interceptor, low-frequency instability of damaging intensity occurred. It was concluded that the combination of the dynamic characteristics of the structure and the feed system coupled with the characteristic combustion time lag of the propellants were responsible for the instability.

Although it would have been possible to add improved control devices for shutdown control, a continuous flow of propellants was assured for all vehicle motions, and modifications could be made to the feed system and vehicle structure to obtain combustion stability; it was realized that these changes would still result in a system with marginal reliability. It was decided, therefore, to change the fuel to one that was hypergolic with nitric acid.

INVESTIGATIONS WITH JP-X

The evaluation of various mixtures of UDMH and JP-4 (JP-X) was conducted on a very small scale (50 lbs thrust) to determine ignition lag characteristics, on an intermediate scale (5,000 lbs) to determine the operating characteristics of a thrust chamber with an interrupted flow, and on the full scale (35,000 lbs) to demonstrate the feasibility of JP-X as a fuel and to determine the rocket performance. The UDMH content of the fuel for these series of tests was varied between 20% and 50%.

The ignition delay tester consisted of a small combustion chamber and nozzle incorporating a simple one-to-one impinging stream injector with a splash plate immediately downstream from the impingement point. The results of the tests conducted with this tester were considered to be qualitative only, but did indicate that mixtures with 40% or more UDMH had ignition lags equal to, or less than the lag for the 30-70 aniline-furfuryl alcohol mixture previously found to be successful.

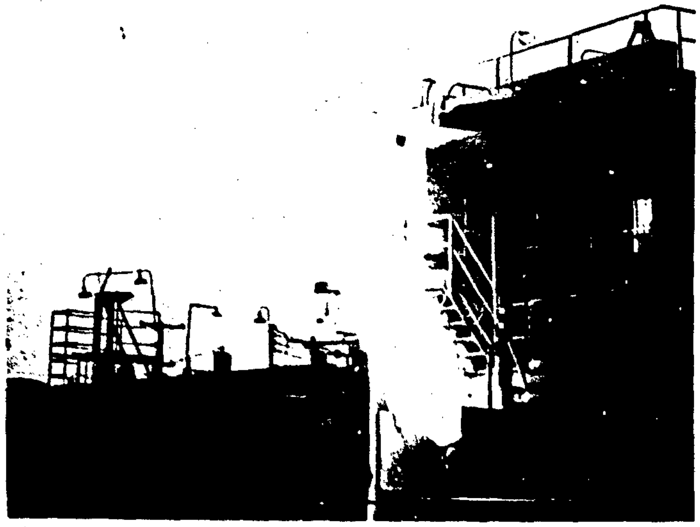

Figure 4 Nozzle-Up Firing (60°)

Because explosive malfunctions would be less costly and hazardous on a small scale than on the full scale rocket, tests with interrupted propellant flow were conducted using thrust chambers rated at 5,000-lb of thrust. As would be expected, the interruption of the oxidizer flow was found to be a more serious condition than interruption of the fuel flow. The tests indicated that safe reignition of the propellants could be accomplished on this scale with a fuel containing 40% UDMH and 60% JP-4 if either fuel or oxidizer were shut off for a period of 0.5 sec.

Full scale (35,000-lb) testing indicated a small improvement in overall performance of the 40-60 fuel mixture over JP-4 at the same oxidizer to fuel ratio and a large improvement over ANFA, therefore, the 40-60 mixture was selected and denoted as JP-X.

A negative acceleration occurs at the end of boost with the BOMARC vehicle designed for booster testing in as much as no sustaining thrust is provided. One of the tests conducted with the 35,000 lb system simulated the shutdown condition by firing a full scale thrust chamber with the thrust axis 60° up as shown in Figure 4.

Very extensive development tests have been successfully conducted using JP-X in the 35,000-lb-thrust chamber for three supersonic sled programs as well as for the IM-99 interceptor. Several tests were made using ANFA (Aniline-Furfuryl Alcohol) with equally satisfactory rocket system operation but with a lower propellant specific impulse than for JP-X. The problems of shutdown, reignition after interrupted propellant flow, and combustion stability were solved by the use of hypergolic propellants.

A word of caution is necessary to point out that the low frequency combustion instability is a function of the whole dynamical system including the feed system, the structure, and the combustion process and must be treated as such. Although the BOMARC system became very stable by changing the fuel, modifications to the structure or feed systems using JP-X fuel can make the overall system unstable.

CONCLUSION

Well over 300 tests of complete systems using hypergolic propellants including "captive firings" of experimental and prototype systems and flight tests have proven the BOMARC booster rocket to be stable and reliable using hypergolic propellants. No significant problems were encountered and the success of the flight test program (the proof of the pudding) has been outstanding. The use of a hypergolic propellant combination has contributed markedly to the success of the BOMARC program by providing a "chemical safety" or reliability that has proven to be of great importance.

SOME PROPELLANT PROPERTIES THAT INFLUENCE THE DESIGN OF ROCKET PROPULSION SYSTEMS

K. N. Watts
Rocketdyne, A Division of North American Aviation, Inc.
Canoga Park, California

1. INTRODUCTION

The liquid propellant rocket engine is essentially a jet propulsion device that derives its thrust force from the reaction to a high-speed jet of ejected matter. This ejected matter, or propellant, is the primary working fluid of the rocket propulsion system, and is contained completely within the propulsion system prior to its ejection. Since it carries its complete propellant mass, the rocket, unlike air-breathing engines, may operate independent of the surrounding atmosphere. From this fact arises the obvious advantage of the rocket engine as a means of propulsion, in vacuo, beyond the earth's atmosphere.

The propulsive jet represents the conversion of the chemical energy of the propellants into useful energy and is initiated by injection of the propellants, at controlled flow rates, into the combustion chamber where combustion occurs. The resulting high-pressure, high temperature combustion gases are then allowed to expand (to low pressure and high velocity) through a nozzle, wherein the thermal energy is converted efficiently into kinetic energy of flow. The resulting increase in momentum of the ejected propellant mass (from low-velocity injection into the thrust chamber to high-velocity gaseous-phase ejection from the nozzle exit) must, in turn, be imparted by reaction to the thrust chamber in order to conserve total momentum. It is this reaction that provides the primary propulsive thrust force of the rocket propulsion system. This thrust force may be generated as long as the propellants are delivered to the thrust chamber at the required conditions of flow rate and high pressure.

As stated previously, the entire propellant mass is contained within the rocket propulsion system prior to its delivery to the thrust chamber. This mass of fuel and oxidizer must be pressurized, pumped, throttled, injected, heated, vaporized, burned, and expanded to supersonic velocity as it passes through the rocket engine at prodigious flow rates. Since the propellant must be controlled and transported at high flow rates and pressures by propulsion system components and sub-systems, it is apparent that physical and chemical properties of the propellant may influence the design requirements of the propulsion system and components to a significant degree. It is the primary objective of this paper to discuss some of the effects on propulsion system design requirements that may result from variations in the properties of the propellants.

2. SCOPE AND LIMITATIONS

Certainly most of the properties of liquid propellants affect, in some way, the design requirements of rocket engine components or systems. However, this discussion is limited arbitrarily to a few of those properties or characteristics that result in obvious or pronounced effects.

For example, while consideration is given to the general effects of specific impulse on the propulsion system, the detailed performance of specific propellants is omitted entirely. The determination of the theoretical performance of various propellant combinations has become a formalized computational process, aided greatly by the recent emergence of the high-speed electronic computer as an analytical tool. To this end, much excellent work has been done to further the evaluation of combustion processes while fundamental research has added to the knowledge of fluid mechanics, gas dynamics and the transport properties of high-temperature rocket combustion gases. It is not the intent of the paper to relegate these extremely important technological data to the status of the obscure or unimportant. Rather, it is the purpose of this paper to isolate a few of those propellant properties that affect, directly, the operation of rocket engine components or systems, and to evaluate the magnitude of these effects.

2.1. SYSTEMS UNDER CONSIDERATION

Consideration will be confined to bipropellant liquid rocket propulsion systems as generally conceived for the propulsion of missiles and other vehicles. Figure 1 presents simplified schematic diagrams of a pressure-fed system (a), and a pump-fed system, (b). The essential elements are seen to be the thrust chamber and the propellant feed system. Although the propellant tanks merely provide the source of propellants, they are integral parts of the propulsion system and are shown as such in Figure (1). The pressure-fed system (1a) requires that the propellant tanks be capable of withstanding the high feed pressures necessary to overcome the thrust chamber pressure and the hydraulic flow resistance of the propellant feed system. However, in the case of the pump-fed system, the required pump inlet pressures are low, and the propellant tanks of the pump-fed system may be of light-weight construction.

The pump-fed system (lb) includes a typical gas turbine-driven pump unit in which a turbine, utilizing an auxiliary working fluid, drives the oxidizer and fuel pumps directly. The auxiliary working fluid is assumed to be supplied from a monopropellant gas generator, or from a bipropellant gas generator utilizing the main propellants fed-back from the main pump discharges. In special applications, e.g., an aircraft rocket engine, the motive power may be derived from other means such as turbojet compressor bleed air or ram air.

The schematic diagrams of Figure 1 show the hydraulic resistance elements of the propellant feed system such as lines, valves, injectors, and regenerative cooling jackets, to be lumped into single equivalent resistances. Details of control systems and other major sub-systems are omitted in the interests of generality.

2.2. SYSTEM INTERACTIONS

The design requirements of a practical system seldom incorporate ideal operating conditions for all of the components or subsystems. (For example, rocket engine turbomachinery rarely includes optimal thermodynamic design of the turbine stages. First, the stringent weight limitations on airborne engine components limit the number of stages to a maximum of two or three. This fact, coupled with the employment of high pressure ratios and unusual working fluids of high available energy, result in relative gas velocities through the rotor blading in the transonic and supersonic ranges generally avoided in more conservative designs.) Therefore, in the interests of overall system reliability and efficiency, engineering compromises are effected in order to achieve the nearest practicable approach to optimum conditions for the majority of components. However, in order to achieve such an optimalization of the entire propulsion system, the designer must be able to evaluate accurately the "exchange ratios" between important parameters such as component efficiency and weight. A few such "exchange ratios", arising from propellant characteristics, are derived and presented herein.

3. GENERAL REQUIREMENTS FOR ROCKET PROPELLANTS

The properties and characteristics of a propellant may be established completely by a set of specifications presenting the chemical and physical data that define a specific propellant. In review, some general characteristics that may be considered to be ideal in evaluating a rocket propellant are:

a) high available energy of combustion gases,
b) stable combustion characteristics,
c) thermal and shock stability,
d) high logistic availability at low cost,
e) low vapor pressure,
f) low freezing point,

- g) low toxicity, and,
- h) low corrosivity.

High available energy of the combustion gases is desirable since this energy is converted directly to useful propulsive energy by the momentum transfer during nozzle expansion. Stable combustion characteristics are desirable in order to attain reproducible engine performance and avoid erratic operation or pressure oscillations that may result in burnout or structural failure of the combustion chamber. High degrees of thermal and shock stability ensure reliable engine operation and safety under the conditions of high temperature and vibration intensity encountered in rocket engines. Logistic availability is a factor that must be given a great deal of consideration, especially for large-scale military operations. And of course the ubiquitous economic consideration -- low cost -- is always desirable. Problems of storing and pumping liquid propellants are reduced greatly by the use of a propellant with a low vapor pressure. A low freezing point is desirable since the operating temperature range may be extended to cover wider environmental conditions. The advantages of low toxicity and corrosivity are obvious from the standpoint of personnel safety, handling complexity and deterioration of hardware.

The general definitive propellant characteristics, listed above, all affect the design requirements of a rocket engine. However, further consideration will be given to certain of these general properties, and a more detailed evaluation will be made of the effects of additional specific characteristics.

4. EFFECTS OF PROPELLANT PROPERTIES ON PROPULSION SYSTEM DESIGN

4.1. GAS PROPERTIES OF THE WORKING FLUID

The primary working fluid of the rocket engine is the high energy gas resulting from the combustion of the propellants in the combustion chamber. Since the thermal energy of this gas is utilized for propulsive purposes by expansion of the gas to high velocity, it is obvious that the thermodynamic properties of the gas will influence the overall design of the propulsion system to a large extent by establishing required flow rates, pressures and thrust chamber geometry for the desired thrust level.

The performance of a specific propellant combination may be expressed in terms of its specific impulse. The specific impulse, I_s, may be considered to be equivalent to the inverse of the specific propellant consumption and may be defined as the total propulsive impulse developed per unit weight of propellant consumed using symbols defined at end of text:

$$I_s = \frac{\int F \, dt}{\int \dot{w} \, dt} , \qquad \text{———} \tag{1}$$

or, instantaneously,

$$I_s = \frac{F}{\dot{W}} \,. \qquad \text{———} \quad (2)$$

The specific impulse of a propellant undergoing ideal expansion, i.e., with the static pressure at the nozzle exit equal to the ambient pressure, may be expressed in the familiar terms of the thermodynamic properties of the combustion gases,

$$I_s = \frac{1}{g_c}\sqrt{2\,\frac{\gamma}{\gamma-1}\,R_u\,\frac{T_c}{M_c}\left[1-\left(\frac{P_e}{P_c}\right)^{\frac{\gamma-1}{\gamma}}\right]} \,. \qquad \text{———} \quad (3)$$

Since, for a perfect gas, $\frac{\gamma}{\gamma-1} R_u \frac{T_c}{M_c} = C_P T_c$, which in consistent units, is equal to the total enthalpy or available energy of the gas measured above zero degrees absolute, it is apparent that the available energy must be a maximum for high performance. This indicates that maximum specific impulse will be obtained near the stoichiometric mixture ratio of oxidizer to fuel.

A survey of the specific impulse of various propellant combinations will indicate that even the most advanced chemical propellants will yield only about a 50% increase in performance over current operational propellants. The nuclear rocket power plant has the potentiality of increasing the specific impulse obtainable by several-fold. For approximate comparisons, Equation (3) may be rewritten,

$$I_s \cong \sqrt{\frac{T_c}{M_c}} \,. \qquad \text{———} \quad (4)$$

If we assume that gas temperatures in a nuclear power plant will not exceed those currently attained in rocket combustion chambers (approximately 6000R) due to material limitations, the specific impulse ratio will be (assuming molecular hydrogen as a nuclear-heated working fluid),

$$\frac{I_{s\,nuc.}}{I_{s\,chem.}} \cong \sqrt{\frac{25}{2}} = 3.54 \qquad \text{———} \quad (5)$$

Therefore, the advent of a successful nuclear rocket power plant utilizing molecular hydrogen as the working fluid would increase the specific impulse by approximately a factor of three over current chemical propellants having combustion gas molecular weights of the order of 25. However, such gains in specific impulse may be partially offset by the increase in empty weight of a vehicle employing a nuclear power plant as compared to a chemical-powered rocket. In addition, the low mass ratio that is inherent in a liquid hydrogen system (because of the low density, sp. gr. = 0.07) results in additional losses in missile performance as will be discussed later.

In summary, it may be seen from Eq. (3) that the thermodynamic properties of the combustion gases are of primary importance in establishing the performance level of a given propellant combination. In addition to determining the specific impulse, or impulse per unit of propellant mass flow, these gas properties (specific heat ratio, molecular weight, and combustion flame temperature) exert considerable influence in establishing design data such as nozzle throat area, expansion area ratio, and regenerative coolant requirements. Since the potential increase in the performance of chemical propellants is apparently not great (even nuclear rockets employing molecular hydrogen would increase current performance by a meager factor of three), an evaluation must be made of the effects of specific impulse changes on the characteristics of rocket-powered vehicles.

4.1.1. THRUST CHAMBER GAS PROPERTIES (After Reference (1)

In order to evaluate the effects of changes in the available energy of the primary working fluid (or specific impulse) on rocket propulsion system performance, a reasonable performance parameter must be evolved upon which to compare the efficacies of such systems. Furthermore, such a general parameter should be applicable to the complete spectrum of rocket-powered vehicles, from booster applications with low effective mass ratios to long-range ballistic missiles or multi-staged vehicles of high mass ratio. The rocket propulsion system is such an integral part of the vehicle in which it is installed, that the performance may be evaluated only with respect to its intended application, and each engine - vehicle combination must be considered separately.

Although it first appears that the powered flight characteristics of a low-mass-ratio rocket-powered booster vehicle may vary significantly from those of a high-mass-ratio ballistic vehicle, a closer examination indicates a great similarity. The objective of the booster vehicle is to produce sufficient impulse to boost a specified payload to a desired terminal velocity, independent of range considerations. Indirectly, the range objectives of a ballistic vehicle dictate the similar need for a specified payload velocity at the end of the propellant burning period. It thus appears that terminal (or burnout) velocity constitutes a reasonable parameter upon which to base a comparison of propulsion system designs.

In the consideration of small changes in a specific trajectory, the initial acceleration, the work done against gravity, and vehicle drag may be considered as small constant quantities without incurring significant errors. Neglecting these terms, the expression for the burnout velocity reduces to the familiar expression for the ideal terminal velocity,

$$V_b = v_e \ln \frac{M_o}{M_e}, \qquad \text{(6)}$$

which may be written,

$$V_b = g_c \bar{I} \ln R_m . \qquad (7)$$

The ideal terminal velocity, as defined by Eq. (7), may then be used as a criterion of relative merit for the evaluation of competing propulsion systems for a specific application.

Eq. (7) may be expressed in logarithmic differential form for convenience in determining partial effects of specific impulse and mass ratio on the terminal velocity,

$$\ln V_b = \ln g_c + \ln \bar{I} + \ln (\ln R_m) . \qquad (8)$$

Differentiating and forming the linearized error equation,

$$\frac{dV_b}{V_b} = \frac{dI}{I} + \frac{dR_m}{R_m \ln R_m} . \qquad (9)$$

Since $R_m = \frac{W_0}{W_e}$, substituting in Eq. (9), $\frac{dR_m}{R_m} = \frac{dW_0}{W_0} - \frac{dW_e}{W_e}$,

$$\frac{dV_b}{V_b} = \frac{dI}{I} + \frac{1}{\ln R_m}\left(\frac{dW_0}{W_0} - \frac{dW_e}{W_e}\right) . \qquad (10)$$

Since all changes are considered to be small in magnitude for this study, performance changes may be expressed in finite differential form,

$$\frac{\Delta V_b}{V_b} = \frac{\Delta I}{I} + \frac{1}{\ln R_m}\left(\frac{\Delta W_0}{W_0} - \frac{\Delta W_e}{W_e}\right) . \qquad (11)$$

If the various missile systems to be evaluated are assumed to have the same gross weight at take-off, then $\frac{\Delta W_0}{W_0} = 0$.

Equation (11) then becomes,

$$\frac{\Delta V_b}{V_b} = \frac{\Delta I}{I} - \frac{1}{\ln R_m}\left(\frac{\Delta W_e}{W_e}\right) . \qquad (12)$$

Equation (12), plotted indirectly in Figure 2, shows the relationship existing between weight and impulse variations, along with their resulting effects on the relative parameter (V_b). The partial effects of specific impulse are seen to be independent of mass ratio, whereas the empty weight variation has a different curve for each mass ratio. It is interesting to note that the "break-even" point at which a specific impulse change has an effect equal to, but algebraically opposite from, an empty weight change of the same amount occurs at the "natural mass ratio," or $R_m = e = 2.718+$.

It is also evident from Figure 2 that, for mass ratios greater than "e", specific impulse changes have a greater effect on performance than weight changes, while the converse is true for mass ratios less than "e". This indicates that, in general, the greatest improvements in range can be realized, for vehicles with large mass ratios such as long-range ballistic missiles, by increasing the overall specific impulse, even at the expense of added weight. At the same time, for small-mass-ratio vehicles, such as "assist take-off" units or booster rockets, the greatest improvements in performance may be realized by reducing the vehicle empty weight. Both of the foregoing conclusions are based on the assumption that efficiency changes and weight changes would require equal effort to achieve.

The approximate method of evaluation developed herein should produce accurate results for the changes of small magnitude considered. A comparison showed that the results of this method of evaluation agreed almost exactly with digital computer solutions of the weight vs. impulse relations for two rocket-powered vehicle applications as determined from complex step-by-step analyses of the trajectories. The linear approximations are valid within the range of about ± 3 per cent variation in vehicle terminal weight.

Figure 2 may then be used to evaluate the effects of changes in propellant specific impulse on missile performance. This method is confined to the study of events occurring during a single stage of rocket engine operation. However, multi-staged vehicles may be studied also, since the final velocity is the sum of the velocity changes for each stage. The overall performance may then be evaluated by considering each stage separately and combining the results.

Figure 2 may be used also to evaluate the effects of small changes in vehicle empty weight due to structural or component weight changes. In addition, the "exchange ratios" may be established between weight and small impulse changes due to variations in propellant energy, chamber pressure, combustion temperature, molecular weight, mixture ratio, etc.

4.1.2. AUXILIARY GAS PROPERTIES (After Reference (1)

The overall specific impulse of a rocket propulsion system is affected to a significant degree by the consumption of propellants by components and sub-systems other than the main thrust chamber. Therefore, the efficiency and propellant consumption rate of auxiliary drives -- typified by the main turbopump turbine of Figure 1b -- assume importance. However, the loss in energy, represented by the auxiliary propellant consumption, may be partially recovered, since some thrust may be derived from the exhaust products of the auxiliary drive system. The effects of auxiliary flow rates and energy recovery from the exhaust may be evaluated in the following manner:

Overall system specific impulse may be expressed in terms of the thrust and propellant flow rates of both the main thrust chamber and the auxiliary drive system:

$$I_o = \frac{F_n + F_{aux}}{\dot{W}_n + \dot{W}_{aux}}, \tag{13}$$

which may be expressed as,

$$I_o = \frac{F_{aux}\left(1 + \frac{F_n}{F_{aux}}\right)}{\dot{W}_{aux}\left(1 + \frac{\dot{W}_n}{\dot{W}_{aux}}\right)}, \tag{14}$$

or

$$I_o = I_{aux}\left[\frac{1 + \frac{F_n}{F_{aux}}}{1 + \frac{\dot{W}_n}{\dot{W}_{aux}}}\right]. \tag{15}$$

The ratio of overall system specific impulse to the basic thrust chamber specific impulse may then be written,

$$\frac{I_o}{I_n} = \frac{I_{aux}}{I_n}\left[\frac{1 + \frac{F_n}{F_{aux}}}{1 + \frac{\dot{W}_n}{\dot{W}_{aux}}}\right]. \tag{16}$$

Since $I \equiv \frac{F}{\dot{W}}$, $\frac{I_o}{I_n} = \frac{I_{aux}}{I_n}\left[\frac{1 + \frac{I_n \dot{W}_n}{I_{aux} \dot{W}_{aux}}}{1 + \frac{\dot{W}_n}{W_{aux}}}\right]$. ——(17)

or, combining,

$$\frac{I_o}{I_n} = \left[\frac{1 + \frac{I_{aux} \dot{W}_{aux}}{I_n \dot{W}_n}}{1 + \frac{\dot{W}_{aux}}{\dot{W}_n}}\right]. \tag{18}$$

Finally, if the generalized, non-dimensional form is denoted by allowing the superscript * to designate the ratio of a parameter to the identical parameter for the main thrust chamber,

$$I_o^* = \left[\frac{1 + \dot{W}^*_{aux} I^*_{aux}}{1 + \dot{W}^*_{aux}}\right]. \tag{19}$$

The non-dimensional equation (19) is plotted in Figure 3, with generalized overall specific impulse, I^*_o, plotted vs the generalized auxiliary flow rate, $\dot{W}^*_{Aux}$, with generalized auxiliary exhaust impulse, I^*_{aux}, as a parameter. Figure 3 is useful in determining the effects of auxiliary propellant consumption rate and exhaust energy recovery on the overall performance of a rocket propulsion system.

The curves of generalized auxiliary exhaust impulse illustrate graphically the effects of thrust recovery from the auxiliary exhaust system by covering the range from zero energy recovery ($I^*_{aux} = 0$) to that equalling the specific thrust of the main thrust chamber ($I^*_{aux} = 1$). The case of zero energy recovery ($I^*_{aux} = 0$) would occur if no attempt were made to derive thrust from the auxiliary drive exhaust, or if the exhaust were expelled in a radial direction - normal to the main thrust axis. The limiting condition wherein I^*_{aux} equals unity could occur in an ideal "topping turbine" application, wherein the auxiliary drive system would exhaust into the injector end of the main thrust chamber, thereby imposing no auxiliary flow rate penalty on the system.

Figure 3 then presents the effects of variations in auxiliary gas flow rates on overall propulsion system performance. Such flow variations may result from either variations in available energy of the auxiliary gases at a given power level or from variations in the power level itself. Figure 3 may be used in conjunction with Figure 2 to evaluate the overall effects of a change in auxiliary power components or working fluid. Figure 3 would be used to evaluate the change in overall specific impulse resulting from a change in auxiliary flow rate. Figure 2 would then be used to determine the allowable weight change for the desired change in burnout velocity. In this manner, reasonable decisions can be made regarding the weight and efficiency, or available energy of the auxiliary working fluid. This is especially important in the consideration of rocket engine turbomachinery since the turbine working fluid may have unusual properties resulting from off-stoichiometric combustion of bipropellants in a gas generator. Excess fuel is generally used in such cases as a diluent to provide temperatures low enough for turbine use. This excess fuel vapor in the combustion gases may produce unusual gas properties, especially if the vaporized fuel is of the heavy hydrocarbon type having very low values of specific heat ratio ($\gamma \cong 1.02 - 1.05$) and low compressibility factors ($Z \cong .75$).

4.2. VAPOR PRESSURE

The vapor pressure of liquid rocket propellants is of major importance in establishing design requirements for the rocket propulsion system. Rocket propellant systems are somewhat unique in this respect, as it is common for a propellant to be a liquefied gas or other low-boiling-temperature fluid with high vapor pressure; for example, liquid oxygen has a normal boiling temperature (vapor pressure equals 14.7 psia) of -297° F.

In addition to the effects on combustion resulting from atomization of propellants during injection into the combustion zone, the vapor pressure exerts its influence in two regions of interest:

(a) the main propellant tanks, and,
(b) the propellant feed system.

4.2.1. MAIN PROPELLANT TANKS

The ullage space above the propellant in the main tank is pressurized (usually with a pressurant gas) for several reasons which are outlined below.

Tank pressure is employed, in some cases, as a load-carrying medium to strengthen integral tank-airframe structures against the compressive and bending loads imposed by flight accelerations, maneuvers, or aerodynamic forces. The degree to which tank pressure is utilized for this purpose is dependent upon many factors and should result from a study of the materials and type of structure used and the "rate of exchange" between the combined weight of the gas pressurization system and the savings in structural weight resulting from the employment of tank pressure as a structural augmentation.

Tank pressure is also employed to suppress vaporization of low-boiling-temperature propellants. Such vaporization may result from adiabatic boiling of a propellant (initially near its saturation temperature) during a climb to high altitude and low ambient pressure, or from aerodynamic heating during static or flight conditions. The large area-to-volume-ratio cylindrical tanks generally employed in missile configurations, together with the extreme boundary layer temperatures encountered during high speed flight, may result in high rates of heat transmission into the tanked propellant. However, heat transfer analysis should indicate the expected maximum propellant temperature during flight, from which the maximum vapor pressure may be determined. Boiling of the tanked propellant, with its attendant loss in propellant mass due to "boil-off" or over-board venting of evolved vapor, may then be prevented by pressurization of the tank to a pressure level in excess of this maximum vapor pressure. An inert gas, such as nitrogen or helium, is used as a pressurant in many instances to prevent the possible formation of a combustible vapor mixture in the tank, with the subsequent explosive hazard.

In addition to the above, tank pressure is also maintained to provide an adequate "suppression head" in order to prevent cavitation and subsequent "vapor-lock" in the propellant feed system or propellant pumps. This factor is extremely important to the design requirements of the pumps and the inlet ducting.

4.2.2. PROPELLANT FEED SYSTEM

In general, the high-pressure feed lines of a pressure or pump-fed system do not present any difficulties arising from propellant vapor pressure. The critical region of the propellant feed system is in the low-pressure inlet ducting upstream of the main propellant pumps.

At the pump inlet "eye", the relative velocity between the low-pressure propellant flowing into the pump and the high-speed rotating impeller may result in local pressures approaching the vapor pressure of the propellant. This condition is generally accompanied by a phenomenon termed "cavitation", wherein cavities, or bubbles, of evolved vapor are formed in the fluid. If the degree of cavitation is severe enough, the mass of vapor evolved may "vapor-lock" the pump, reducing its performance. Figures 4a and 4b show typical cavitation performance curves for a centrifugal and axial pump, respectively. At constant conditions of pump speed and flow, the head developed by the pump is seen to decrease as the suction head to the pump is decreased. However, the characteristics of the head decrease caused by cavitation are significantly different, as shown by Figure 4a and 4b. The head developed by the axial pump decreases gradually as suction pressure decreases, whereas the centrifugal pump shows relatively little effect until a critically low value of suction head is reached, at which time the head breaks down completely as the impeller "vapor-locks". This operating characteristic is extremely important in rocket engine systems as the pumping requirements are such that centrifugal pumps are employed almost universally, with axial pumps being relegated to special use purposes.

4.2.3. PUMP INLET PRESSURE REQUIREMENTS

As shown in Figure 4a the head developed by a centrifugal pump is relatively unaffected by pump inlet pressure, provided the inlet pressure is high enough to suppress cavitation entirely. A parameter that is used to express the approach of pump inlet pressure to a cavitating condition is the net positive suction head (NPSH or H_{sv}). The NPSH is defined as the total absolute pump inlet pressure in excess of the propellant vapor pressure, expressed in feet of the fluid,

$$H_{sv} \equiv H_{is} + \frac{v_i^2}{2g} - H_v \,. \tag{20}$$

In order to suppress cavitation with its accompanying loss in pump performance, it is necessary to maintain a minimum or required value of NPSH. This required NPSH is usually defined arbitrarily as the value equivalent to a small decrease in head (usually 1%) prior to the cavitation break-down of a centrifugal pump (Point a, Fig 4a). The required NPSH is coupled to pump operational characteristics by the parameter, suction specific speed(s), which is defined:

$$s \equiv \frac{n\sqrt{Q}}{H_{sv}^{3/4}} . \qquad \text{———} (21)$$

The suction specific speed(s) is an expression of the steady-state cavitation resistance or suction performance of a pump, and is used primarily for comparisons:

$s = 8{,}000$ (good commercial design),
$s = 12{,}000$ (excellent for radial impellers),
$s = 16{,}000$ (theoretical maximum for radial impellers).

Rocket engine propellant pumps are often required to operate with suction specific speeds in excess of 12,000 because of the high pump speeds and low inlet pressure necessary to minimize the empty weight of the missile system.

4.2.4. STARTING TRANSIENTS

The starting of a pump-fed rocket engine involves the rapid acceleration of the column of liquid in the inlet duct during the period of time when the pump speed is increasing from zero to steady-state operating rpm. Since a portion of the available inlet head is absorbed as a momentum loss during the transient acceleration of the liquid column, the total pump inlet head required prior to starting must be higher than is indicated from steady-state operating conditions. Therefore, exact details must be known regarding inlet duct length, diameter and frictional characteristics as well as instantaneous values of pump speed and flow rate before the minimum value of starting NPSH may be established.

The acceleration of the column of liquid in the inlet duct during the pump starting transient is an unsteady flow condition that may be approximated and analyzed as follows:

Three major effects must be accomplished during the transient flow condition; namely,

a) overcome system friction and other hydraulic losses
b) impart velocity head to the liquid column, and
c) accelerate the liquid column from rest to the steady-state flow velocity.

Therefore, neglecting any system impedances except frictional resistance, entrance losses, etc., the static head loss required to accomplish the above three effects may be expressed from non-steady flow considerations,

$$H_l = \left(\frac{4fl}{d} + K\right)\frac{v^2}{2g_c} + \left(\frac{v^2}{2g_c}\right) + \left(\frac{l}{g_c}\frac{dv}{dt}\right). \qquad \text{———} (22)$$

Since total head is more meaningful in the consideration of NPSH, Eq. (22) may be modified by neglecting velocity head changes,

$$H_\ell' = \left(\frac{4f\ell}{d} + K\right)\frac{v^2}{2g_c} + \left(\frac{\ell}{g_c}\ \frac{dv}{dt}\right). \qquad \text{———} (23)$$

The pump inlet pressure required prior to engine starting may then be determined by a simultaneous solution of the conditions for required and available inlet pressures.

The required NPSH during rocket engine starting may be plotted versus time by employing equation (21), assuming a constant suction specific speed. Theoretical and test results indicate that the assumption that suction specific speed is constant during the pump starting transient is probably conservative. It is presumed that test data have established accurate knowledge of pump suction specific speed, together with transient values of pump speed and propellant flow rates versus time. Figure 5a shows a typical plot of required NPSH versus time.

Total head loss due to inlet duct and momentum losses during the starting period may then be determined in a similar manner, employing equation (23), inlet duct length, diameter, and frictional characteristics. Figure 5b shows a typical plot of total head loss required to satisfy the required duct flow conditions.

The NPSH required prior to engine starting in order to ensure non-cavitation of the propellant pumps during the starting transient may then be determined by superimposing the transient head loss curve (Figure 5b) on the required NPSH curve (Figure 5a) as shown in Figure 6. (Note the inversion of the head loss curve to make the algebraic signs compatible.) The ordinate of the head loss curve should then be adjusted in such a manner that the "inertial dip" that will occur in the region of maximum duct flow acceleration lies above (or just touches) the pump required NPSH curve. In this manner the NPSH available at time zero and throughout the starting transient may be determined (Figure 6). The total pump inlet head required at zero time may be determined by adding the propellant vapor pressure head to the NPSH value. Actual tank pressure requirements may then be determined from the hydrostatic and pressure head relations.

From the discussions in the several preceding sections, it is apparent that the propellant vapor pressure plays a very important role in establishing the requirements for propellant tank pressures in order to minimize the amount of propellant loss due to rapid vapor evolution under static or flight conditions. In addition, it was seen that the vapor pressure must also be given careful consideration in conjunction with the propellant feed system to insure adequate "suppression head" at the pump inlets and thus avoid extreme cavitation or "vapor-lock" of the propellant pumps during the starting transient as well as steady-state engine operation. It may then be concluded that the propellant vapor pressure exerts a great influence on the design requirements of an integrated rocket engine and propellant feed system and also on individual feed system components such as pumps, tanks, ducts, etc.

4.3. PROPELLANT DENSITY

In addition to determining the volumetric propellant tank capacity of a rocket-powered vehicle, liquid propellant density has many effects upon the propulsion system. Since an optimalization of the tank volume requirements involves a detailed study of the densities of both the oxidizer and fuel and the mixture ratio of the specific propellant combinations under consideration, the effects on tank storage volume will not be discussed herein. A general statement may be made to effect that, in order to minimize the overall size of the vehicle and propellant tanks, a high propellant density in the liquid form is considered desirable.

4.3.1. EFFECT OF DENSITY ON PUMP DESIGN

The fluid head developed by a centrifugal pump is generated by virtue of the energy transmitted by the impeller to the fluid as it passes through the pump. The developed head is therefore dependent upon the impeller rotational speed or peripheral velocity. The pressure rise across the pump is then equal to the product of the developed head and density of the fluid.

In order to minimize pump weight and complexity, it is desirable to limit rocket engine propellant pumps to single-stage designs. However, for propellants of extremely low density, for example, liquid hydrogen (Sp. gr = 0.07), it may be necessary to employ multi-stage pump designs in order to attain the discharge pressures required for moderate thrust chamber pressures, yet not exceed reasonable impeller velocities.

The head development characteristics of a pump may be expressed in terms of the dimensionless head coefficient, $\psi = \frac{Hg_c}{u^2}$, (Reference 2). For a typical value of $\psi = 0.60$ at the design point, we may write,

$$\psi = 0.60 = \frac{Hg_c}{u^2} . \qquad (24)$$

Substituting for the pump pressure rise in terms of developed head and propellant density, equation (24) may be rewritten as,

$$u = \sqrt{\frac{\Delta p \, g_c}{0.60 \, \rho}} \; . \qquad \text{———} \; (25)$$

Equation (25) is presented graphically in Figure (7). Stress limitations on the impeller vanes and shrouds will limit the allowable impeller peripheral velocity to a maximum value, typically about 500 feet per second. The cross-hatched area of Figure (7) indicates a maximum impeller velocity of 500 feet per second as the approximate limit for single stage pump designs. It may be seen that for even moderate chamber pressures (requiring a pump pressure rise of 500 psia, say) a fluid specific gravity of 0.20 or less will require a multi-stage pump design. For example, a liquid hydrogen (sp. gr. approximately 0.07) pump operating under these conditions would require a two-or-three stage design, depending upon the exact impeller design speed.

Thus, it may be seen that the propellant density may exert a significant effect on the detailed design requirements of rocket engine components, such as propellant pumps.

4.3.2. EFFECTS OF PROPELLANT DENSITY ON OVERALL ENGINE SYSTEMS

It is of further interest to evaluate the effects of propellant densities on the steady-state operating conditions of a rocket propulsion system. This may be accomplished by means of "influence coefficients", that express the effects of engine independent variables such as propellant densities, atmosphere pressure, inlet pressures, etc., on engine dependent variables such as thrust, pump speed, propellant flow rates, mixture ratio, etc.

The determination of engine influence coefficients is accomplished by solving the system of simultaneous equations that describe the characteristics of each component and sub-system of the rocket engine. The system of equations may be linearized first by partial differentiation and then solved for the dependent variables in terms of the independent variables. Non-linear solutions are also useful but, for the consideration of small changes in independent variables, the advantages of a linearized analysis are significant, e.g.,

(a) The set of linearized equations may be solved by formalized methods such as matrix methods and may be solved directly on a high-speed digital computer.

(b) The principle of superposition is valid for a linearized system and allows the total effect of simultaneous changes in two or more independent variables to be obtained by simple algebraic addition of the individual effects.

(c) The results of a linearized analysis may be presented in a compact table of "influence coefficients", expressing the effects of generalized (percentage) changes in any of the independent variables.

If a system equation expressing the functional relation between a dependent variable and several independent variables is of the form,

$$y = f(x_1, x_2, \ldots\ldots, x_n), \qquad \text{———— (26)}$$

differentiation yields

$$dy = \frac{\partial f}{\partial x_1} dx_1 + \frac{\partial f}{\partial x_2} dx_2 + \cdots + \frac{\partial f}{\partial x_n} dx_n. \qquad \text{———— (27)}$$

Generalization may be accomplished, in order to express the effects of percentage changes among the variables, by rewriting equation (27),

$$\frac{dy}{y} = \left(\frac{x_1}{y}\frac{\partial f}{\partial x_1}\right)\frac{dx_1}{x_1} + \left(\frac{x_2}{y}\frac{\partial f}{\partial x_2}\right)\frac{dx_2}{x_2} + \cdots + \left(\frac{x_n}{y}\frac{\partial f}{\partial x_n}\right)\frac{dx_n}{x_n}. \qquad \text{—— (28)}$$

The influence coefficients at any specific operating condition (design point, say) may then be determined by substituting the design values of the dependent variable, y, the independent variables, x_i, and the partial derivatives obtained during linearization of the equations. The result will then be a numerical relation between the variables of interest of the form,

$$\frac{dy}{y} = a_1\frac{dx_1}{x_1} + a_2\frac{dx_2}{x_2} + \cdots + a_n\frac{dx_n}{x_n}. \qquad \text{———— (29)}$$

The coefficients, a_1, a_2, ..., a_n, are the "influence coefficients" that describe the relation between percentage changes of the variables. These values are exact only at the design point but are assumed to be constant throughout small perturbations about the design points.

Tables I and II present typical influence coefficient tables for a pressure-fed and pump-fed system, respectively. It may be of interest to note that Tables I and II are small portions of complete tables of influence coefficients that describe the characteristics of two current Rocketdyne production engines. The nominal values of operating conditions have been omitted. It should be noted further that, although they characterize typical engines, the influence coefficients of Tables I and II may not be considered typical, but, rather, as examples. The influence coefficient values depend upon the nominal operating conditions and the interactions of the various system elements; therefore each propulsion system must be considered as a unique, integrated system having its own individual characteristics. The influences of control systems are especially strong because of the constraints imposed on the engine by mixture ratio controls, thrust controls, or other special control systems.

5. CONCLUSION

In the foregoing sections, a few of the effects of propellant properties on the design requirements of rocket propulsion systems have been discussed. Some of the aspects of the thermodynamic properties of the working fluids have been evaluated, both the main thrust chamber combustion gas and the auxiliary power system gas flow. The propellant vapor pressure has been shown to exert considerable influence on the design requirements of rocket propulsion systems and components. These effects have been discussed with regard to main propellant tanks, propellant feed systems and pump operation during transient and steady-state conditions. The effects of propellant density on pump design and overall engine systems are discussed. The general methods of analysis presented should allow the system designer to make design compromises on the basis of approximate exchange ratios between important parameters and thus effect the progress of a system design toward optimality.

REFERENCES

(1) K. N. Watts, Factors Affecting the Selection of Airborne Turbomachinery for Rocket Power Plants, (Development Memo No. 29), North American Aviation, Inc., 1954.

(2) A. J. Stepanoff, Centrifugal and Axial Flow Pumps, New York, John Wiley and Sons, 1948.

ACKNOWLEDGMENT

The author wishes to express his appreciation to members of the Systems Design Analysis Unit of Rocketdyne, a Division of North American Aviation, Inc., for their aid in preparing this paper, especially the numerical data of Tables I and II.

NOMENCLATURE

Symbol		Units
d	diameter, propellant duct	consistent
F	thrust	lb force
F_{aux}	thrust, auxiliary exhaust	lb force
F_n	thrust, main thrust chamber	lb force
f	friction factor, Fanning	dimensionless
g_c	gravitational conversion factor	lb-ft/sec^2-lb
H	head, developed	ft fluid
H_{is}	head, pump inlet static	ft fluid (abs.)
H_l	head loss, duct frictional	ft fluid
H_{sv}	head, net positive suction (NPSH)	ft fluid (abs.)
H_v	head, vapor pressure	ft fluid (abs.)
I_{aux}	specific impulse, auxiliary exhaust	lb-sec/lb
I_n	specific impulse, main thrust chamber	lb-sec/lb
I_o	specific impulse, overall engine	lb-sec/lb
I_s	specific impulse	lb-sec/lb
K	hydraulic loss coefficient	dimensionless
l	length, propellant duct	consistent
M_c	molecular weight, combustion gas	gram/mole
M_e, W_e	empty mass, weight	consistent
M_o, W_o	takeoff mass, weight	consistent
n	rotational speed	rpm
P_c	pressure, thrust chamber stagnation	psia
P_e	pressure, nozzle exit	psia
ΔP	pressure change	psi
Q	flow rate, volumetric	gal/min
R_m	mass ratio, takeoff to empty	dimensionless
Ru	gas constant, universal	consistent
s	suction specific speed,	consistent
T_c	temperature, combustion gas	°R
u	velocity, tangential	ft/sec
V_b	velocity, missile burnout	ft/sec
v	velocity	ft/sec

NOMENCLATURE (Continued)

Symbol		Units
v_e	velocity, nozzle exit	ft/sec
v_i	velocity, pump inlet	ft/sec
$\dot{w}$	flow rate, gravimetric	lb/sec
$\dot{w}_{aux}$	flow rate, auxiliary gas system	lb/sec
$\dot{w}_n$	flow rate, main thrust chamber	lb/sec
γ	ratio of specific heats	dimensionless
ρ	density	consistent
ψ	Euler's head coefficient	dimensionless

Superscripts

-	denotes effective average value
*	denotes ratio of parameter to that of main thrust chamber

TABLE I.

Influence of Propellant Densities on the Characteristics of a Typical Pressure-Fed Rocket Propulsion System

Affected Variable	EFFECT Percent Change Due to 1 Percent Increase In: Oxidizer Density	Fuel Density
Oxidizer Flow Rate	+0.313	-0.048
Fuel Flow Rate	-0.151	+0.471
Mixture Ratio	+0.464	-0.519
Thrust	+0.243	+0.076
Specific Impulse	+0.096	-0.062
Chamber Pressure	+0.220	+0.056

TABLE II.

Influence of Propellant Densities on the Characteristics of a Typical Pump-Fed Rocket Propulsion System

Affected Variable	EFFECT Percent change due to a 1 percent increase in: Oxidizer Density	 Fuel Density
Oxidizer Flow Rate	+1.05	-0.59
Fuel Flow Rate	-0.48	+0.99
Mixture Ratio	+1.53	-1.58
Thrust	+0.58	-0.02
Specific Impulse	0.00	+0.09
Thrust Chamber Pressure	+0.47	+0.01
Pump Speed	-0.12	-0.24
Turbine Power	+0.24	-0.42
Turbine Gas Temperature	+0.13	-0.59

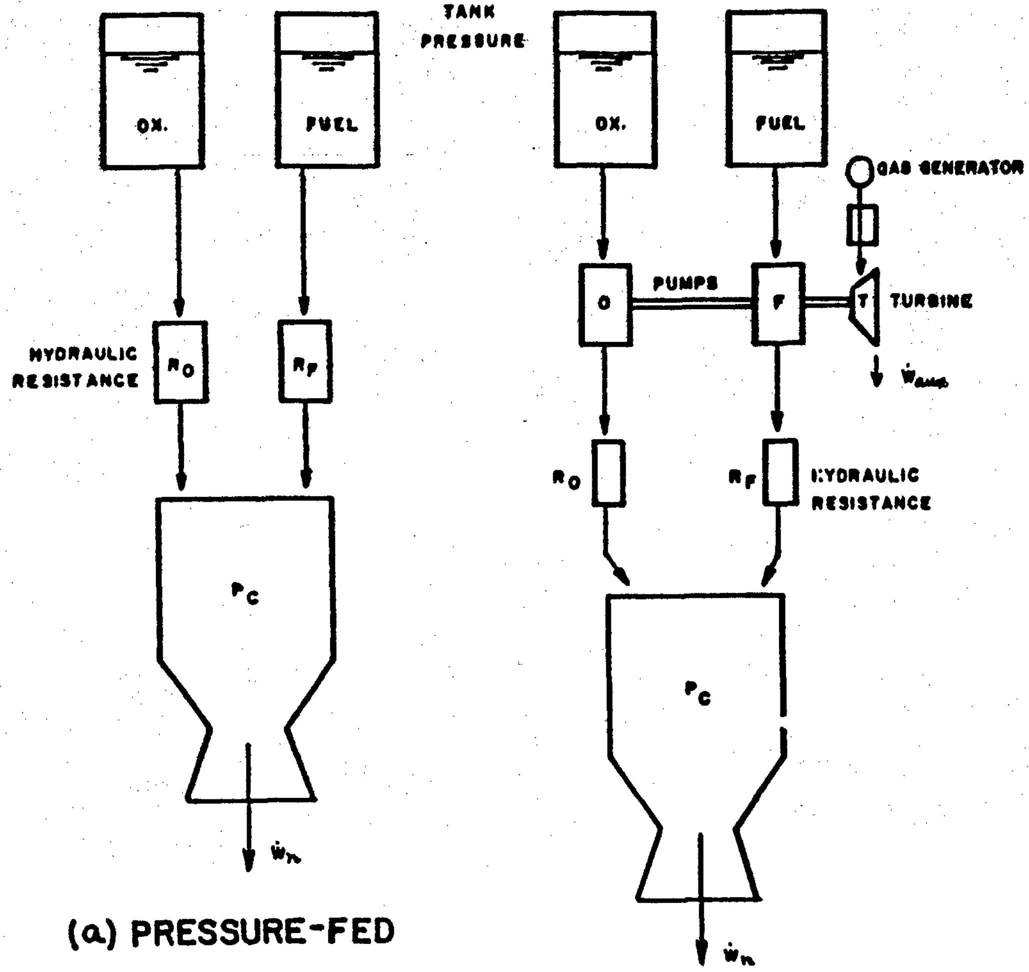
TANK PRESSURE
OX.
FUEL
OX.
FUEL
GAS GENERATOR
PUMPS
O
F
T
TURBINE
HYDRAULIC RESISTANCE
R_O
R_F
R_O
R_F
HYDRAULIC RESISTANCE
P_C
P_C
$\dot{w}_n$
$\dot{w}_n$

(a) PRESSURE-FED

(b) TURBOPUMP-FED

Figure 1

PROPULSION SYSTEM SCHEMATICS

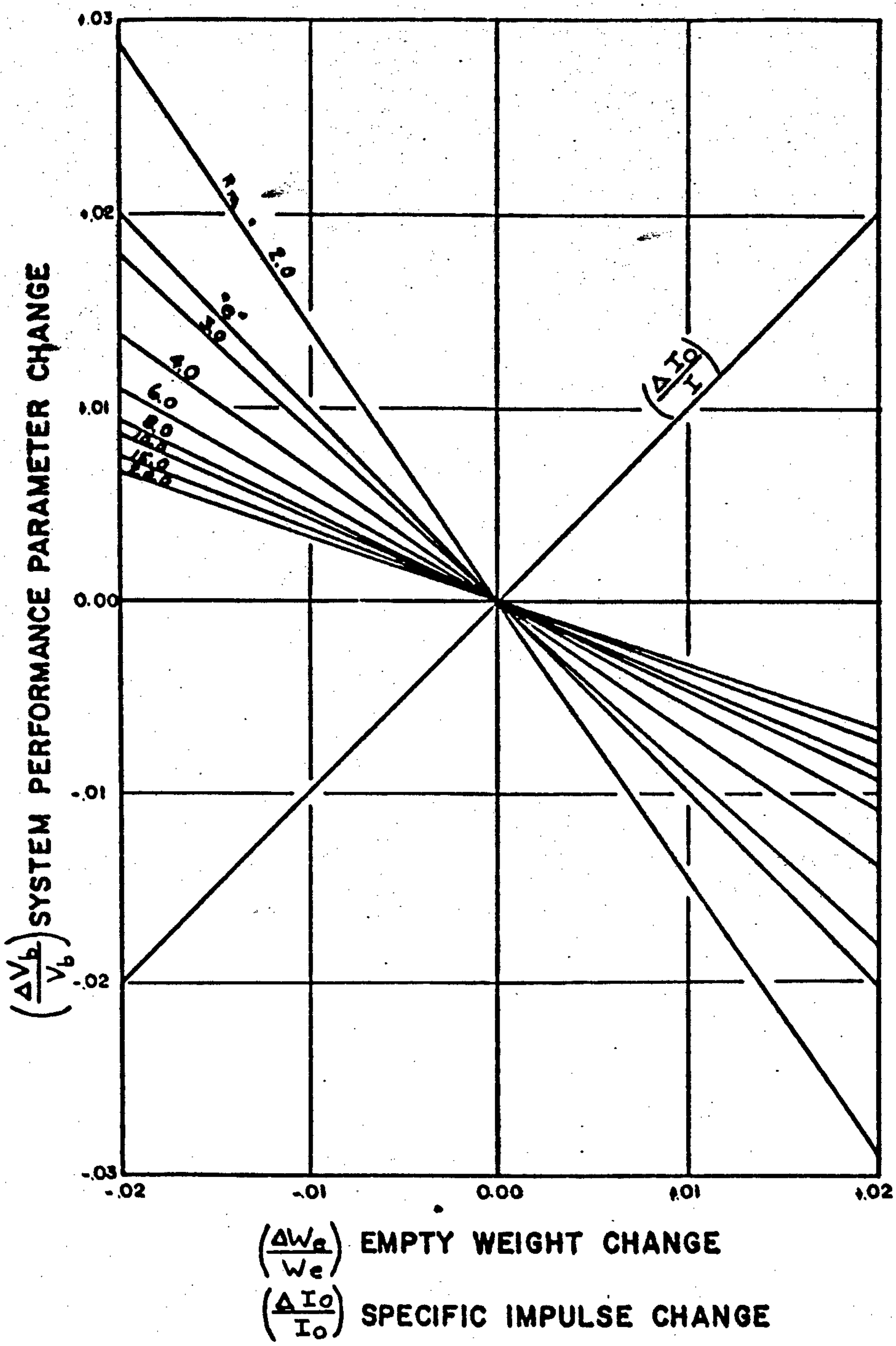

Figure 2

INFLUENCE OF EMPTY WEIGHT AND
SPECIFIC IMPULSE ON VEHICLE PERFORMANCE

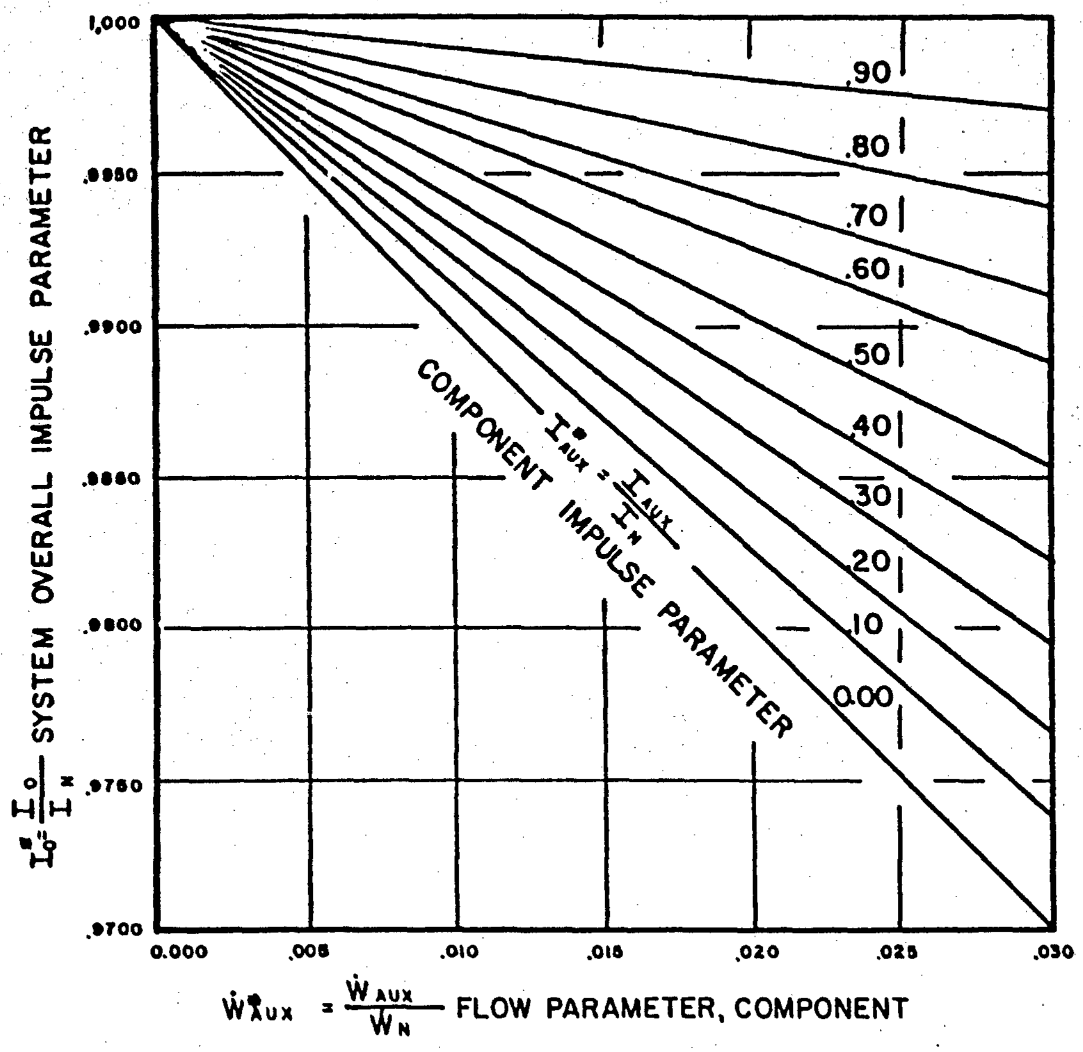

Figure 3

GENERALIZED INFLUENCE OF AUXILIARY FLOW AND IMPULSE ON OVER-ALL SYSTEM PERFORMANCE

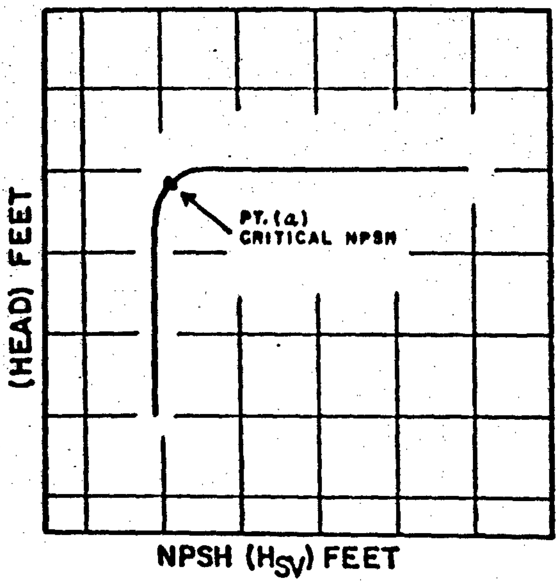

(a) CENTRIFUGAL PUMP

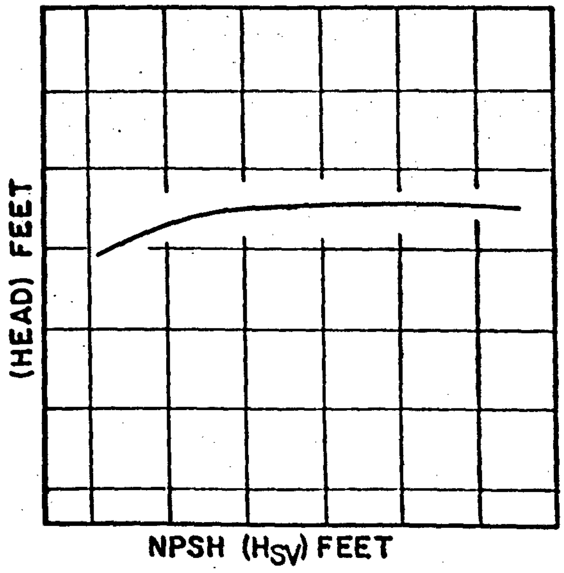

(b) AXIAL PUMP

Figure 4

TYPICAL PUMP CAVITATION CHARACTERISTICS

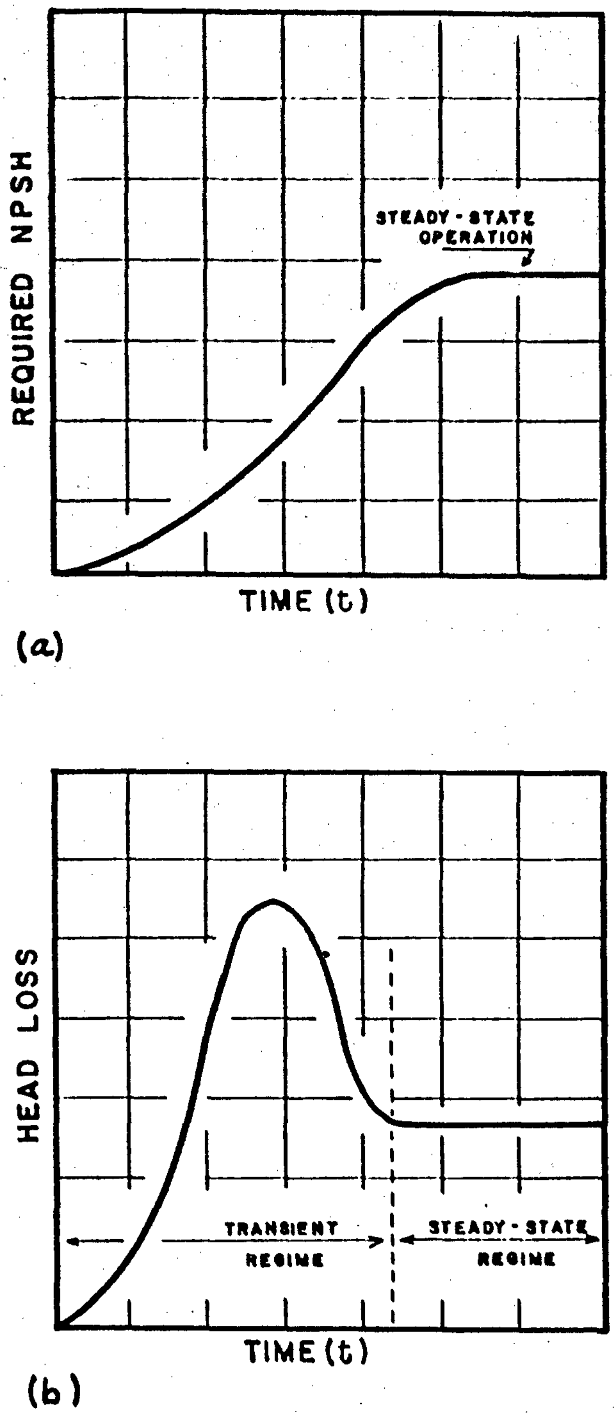

Figure 5

PROPELLANT FEED SYSTEM TRANSIENTS

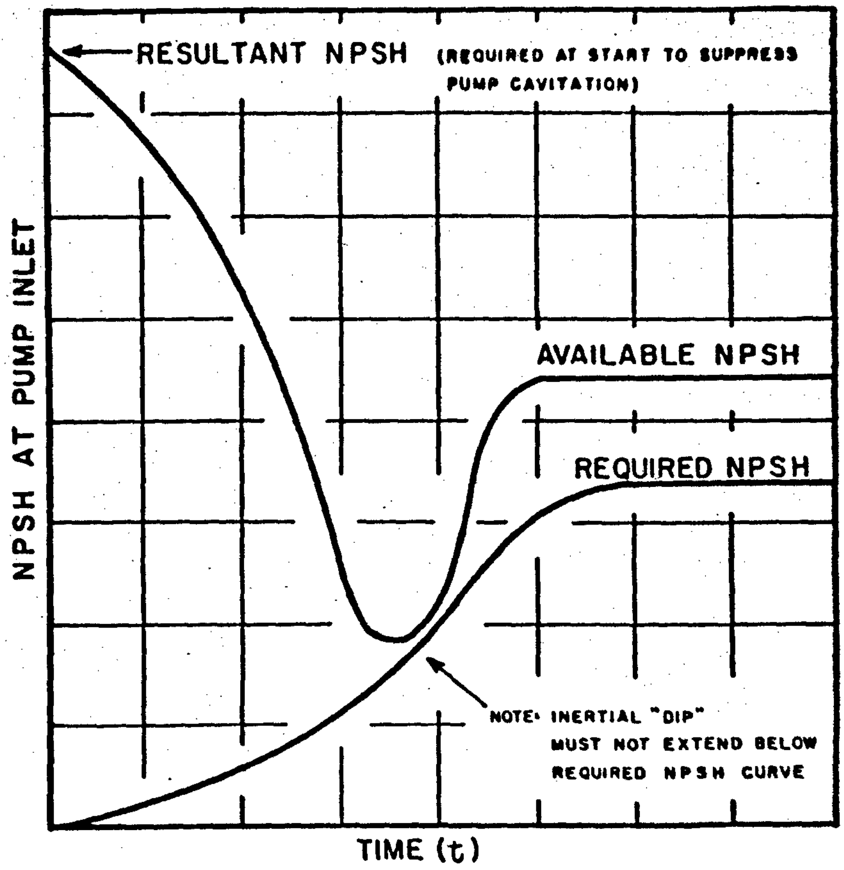

Figure 6

PUMP INLET CONDITIONS DURING
STARTING TRANSIENT

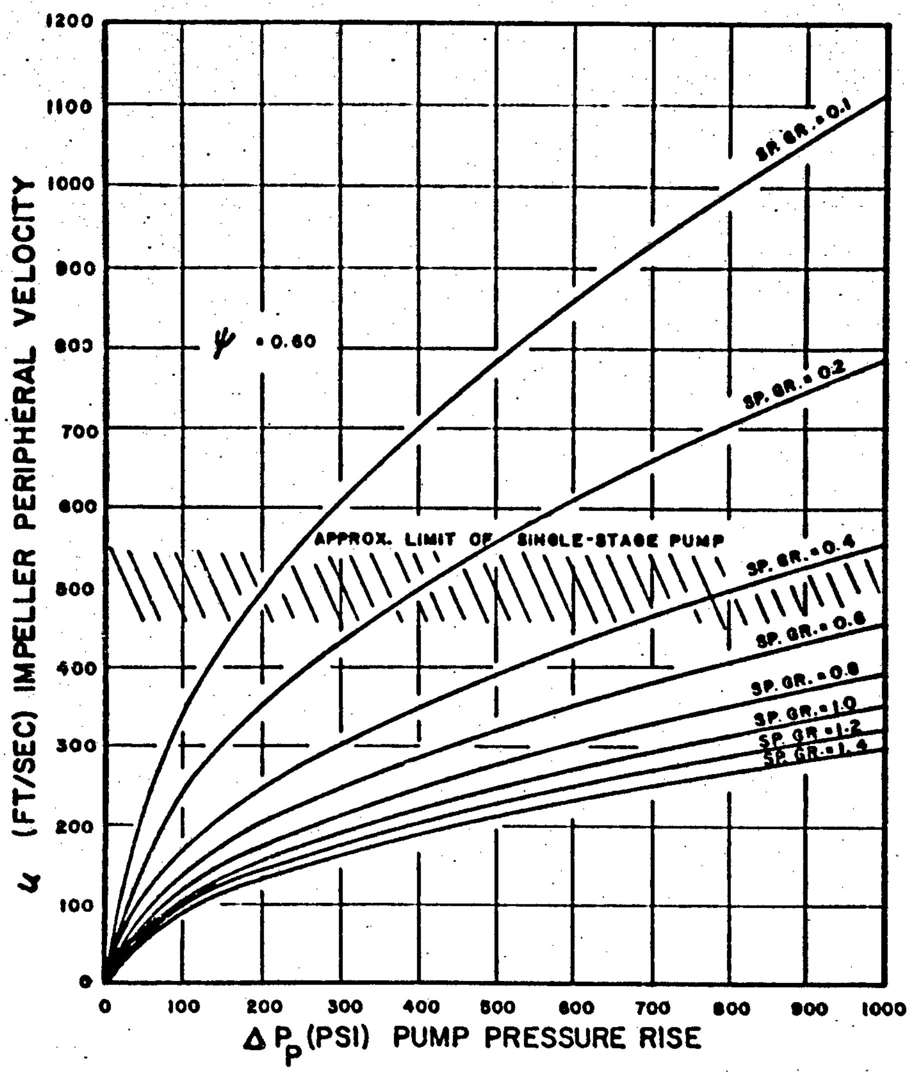

Figure 7

TYPICAL PUMP CHARACTERISTICS

A NON-COKING ETHYLENE OXIDE REACTOR

Loren C. Smith
Wyandotte Chemicals Corporation
Wyandotte, Michigan

INTRODUCTION

The broad objective of the work to be discussed was the development of a practical method for starting ethylene oxide monofuel reactors by means of a glow wire with no oxidizer being present. In carrying out that work, the achievement of non-coking operation of the hardware being developed soon emerged as an important secondary objective in the program.

The decomposition of ethylene oxide entails a heat transfer into the fuel of roughly 500 BTU/lb. to heat the fuel to its auto-decomposition temperature of 571°C; this amounts to a heat input of about 9000 watts/lb./min. Then if, for example, 1000 watts of heat is expended into a stream or spray of fuel injected into a reaction chamber, it is apparent that, if the flowrate of fuel is several lb./min., an even distribution of energy would result only in a rise in the fuel temperature with no decomposition at all. But, if the added heat is confined to a small enough fraction of the total stream, it will effect the decomposition of that fraction; and the heat release from the decomposed fraction can effect the decomposition of another larger fraction, etc., until the entire stream is decomposed. In general, that process occurs in every electrical start; enough of the injected fuel is decomposed by the heat source to effect the decomposition of the remaining portion.

In pursuing this problem at Wyandotte, it has been the practice to have the wattage of the glow wire roughly equal to the rate at which the fuel absorbs heat from the glow wire. This is in contrast to the method whereby heat is stored at low wattage over a period of time and withdrawn by the fuel quickly at a much higher wattage. The practice used at Wyandotte was adopted because it entails the most efficient use of the electrical energy and brings into view the possibility of almost instantaneous starts.

Test results obtained early in the program indicated that the power requirement would be excessive for substantial flowrates in conventional reactors; attention was, therefore, given to a multistage design in which each stage was started by hot gases from the preceding stage, with electrical heat energy applied only to a small, low flowrate primary chamber. Not only does the multistage reactor constitute an apparently sound theoretical basis for achieving electrical initiation, but it entails other important advantages as well. It offers more extensive control of the many variables involved in electrical initiation than does a conventional reactor. The controlled impingement of streams of hot gas from one stage upon cold liquid streams entering the next stage should result in increased rates of heat transfer from reacted gases to incoming fuel needed to improve reaction stability at low operating pressures and to permit the operation of ethylene oxide reactors of lower L*. Another important advantage is that the multistage design may permit the experimental determination of design parameters needed to design ethylene oxide reaction chambers for specified flowrates and operating conditions with a high probability of success.

In the development of the primary chamber for the multi-stage reactor the usual coking problem appeared, and the entire development has thus far centered around the solution of this coking problem. The coke deposition was so severe that reactors would fail after only a few minutes running time. The cooler surfaces in the reaction chamber were free of coke deposits, in sharp contrast to adjacent surfaces at higher temperatures. It was, therefore, believed that the coking problem might be solved by regeneratively cooling the surfaces in the reactor. This idea was the basis of several successive designs; and in the latest design the problem of coke deposits has been virtually eliminated.

The principle of eliminating coke deposits by regenerative cooling was pursued also in the concurrent development of a very small ethylene oxide reactor, designed to operate at a flowrate of less than 1 lb./hr. for a period of eight hours. The problem there was more severe, but the results have been the same; the coking problem is effectively solved by regeneratively cooling the reactor surfaces.

ELIMINATION OF COKING BY REGENERATIVE COOLING

Primary Chamber A.

The first approach to the problem was the design of a two stage reactor (see Fig. 1) comprising primary chamber A and a secondary chamber. A 1/8" diameter carbon rod about 1" long was chosen as the heater because of its rigidity and high melting point. The primary chamber design was unconventional in that the internal metal parts were designed to play a major role in the heat transfer from reacted gases to incoming fuel. The preheat channel in this design was solely for the purpose of heating the fuel, with no concern for

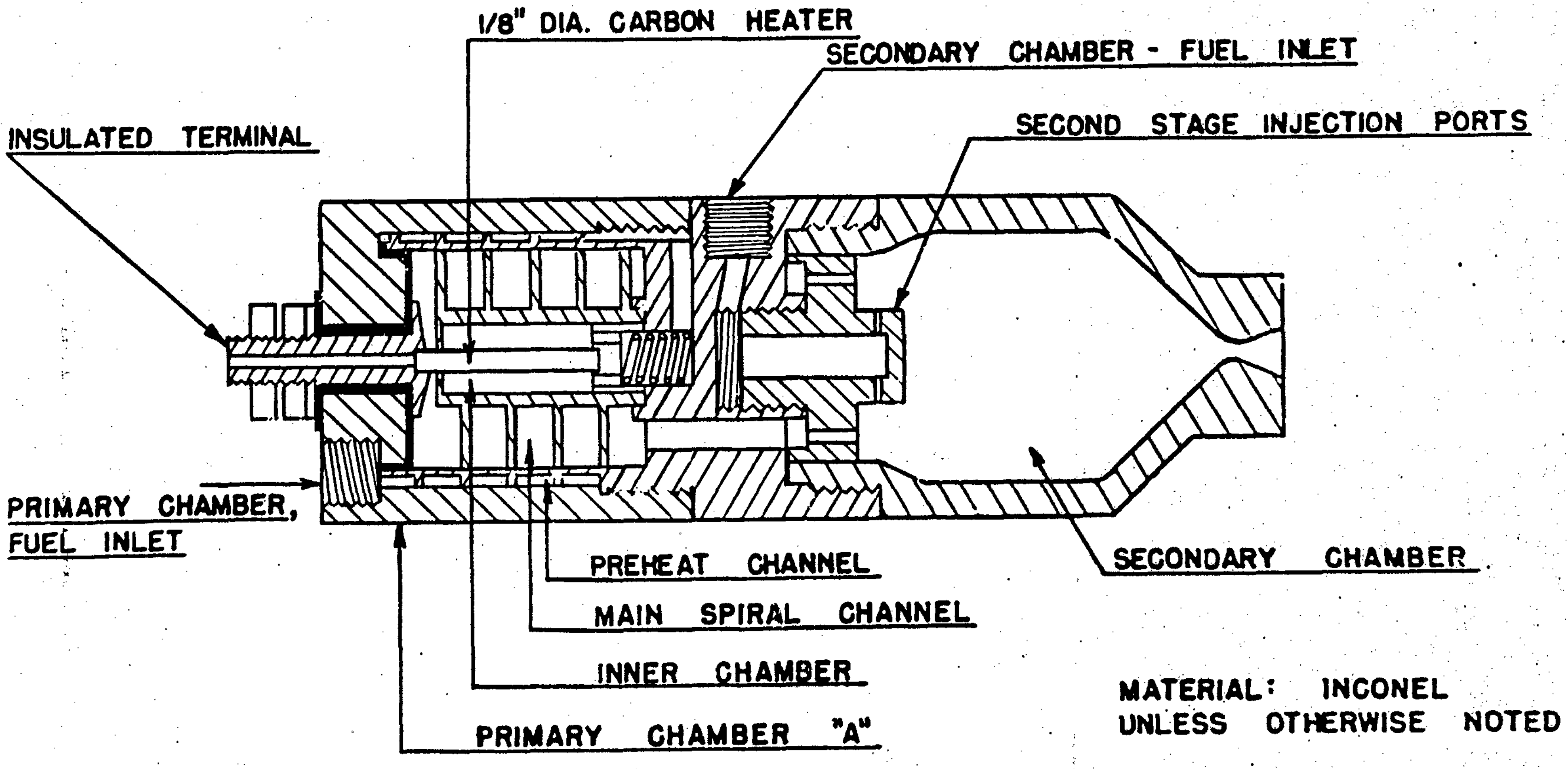
1/8" DIA. CARBON HEATER
SECONDARY CHAMBER - FUEL INLET
INSULATED TERMINAL
SECOND STAGE INJECTION PORTS
PRIMARY CHAMBER, FUEL INLET
PREHEAT CHANNEL
SECONDARY CHAMBER
MAIN SPIRAL CHANNEL
INNER CHAMBER
MATERIAL: INCONEL UNLESS OTHERWISE NOTED
PRIMARY CHAMBER "A"

FIG. 1. TWO-STAGE REACTOR INCORPORATING PRIMARY CHAMBER "A"

cooling the walls. The injector for the second stage was a mixing injector designed to effect impingement of hot gas streams from the primary chamber on streams of liquid entering the secondary chamber.

The primary chamber was first tested alone to determine its running characteristics; and a coking problem arose which was so severe that it was almost prohibitive as far as testing the secondary chamber was concerned. The primary chamber could be operated for only a few minutes before the coking process would force a shutdown. At extremely low flowrates, polymer residue and crumbs of carbon would form in the preheat channel and carbon would form in the inner chamber. If the flowrate was increased, the deposition did not occur in the preheat channel but moved entirely into the inner chamber. When the flowrate was increased further, the carbon formation (and apparently the reaction zone) moved out of the inner chamber into the main spiral channel. The increase in flow was associated with a drop in temperature at the exit of the central chamber. In runs where the inner chamber was found to be fairly clean, the deposition on the carbon rod itself appeared to increase with increasing heater operating time. The most conclusive result obtained from primary chamber A was the deposition of carbon in the main spiral channel. The design is such that this main exhaust channel is essentially a square pipe with one of its four walls, the preheat channel wall, cooled and in poor contact with the other three walls. All four walls were heated by the exhaust gases passing through the channel, and the reaction conditions would appear to be the same for each wall; but coke deposits were formed on the three uncooled walls but not on the cooled wall.

It appeared that the chamber could be started and operated well enough, with a nozzle which would give a flowrate of 0.75 lb./min. at 500 psi., to permit a few tests with the two stage reactor. The flow measurement and control equipment was not adequate, but after many attempts it was started and both stages operated smoothly for 30-40 seconds at a pressure of 350 psi. with a 0.113" diameter exhaust nozzle. The operation then became rough and the reaction failed. The work with this primary chamber was so tedious that, a two stage start having been demonstrated, attention was turned to the development of a reliable primary chamber before pursuing the two stage studies further.

Primary Chamber B.

The next step in the development was the design of a 0.75 in^3. regeneratively cooled chamber ignited by a tungsten resistor. This design was unsuccessful because of poor flow patterns; however, it was operated once or twice with great difficulty at flowrates of about 0.1 lb./min. The only result of importance with this chamber was a single 11 minute run which left the cooled walls of the chamber very clean in contrast to the hard thick deposit on the tungsten heater. The operating time on the heater during that run was about 4 minutes.

Primary Chamber C.

In designing primary chamber C, (see Fig. 2) one of the major objectives was to keep ethylene oxide out of contact with hot surfaces. In the region near the exhaust nozzle, cooling was not considered critical because in previous work a clean exhaust pipe was a normal condition. This chamber ran quite well, and many runs were made with it, but running time was limited to about ten minutes. The uncooled exhaust channel invariably clogged with carbon, terminating the operation. This was attributed to the passage of ethylene oxide from the injector directly into the exhaust stream, due to the nearness of the point of injection to the chamber exhaust port. Coking on the inner walls of the chamber varied from none at all to a very thin deposit, depending upon the reactor operating conditions. More severe deposits occurred on the asbestos gasket at the insulated terminal, a region which could not be effectively cooled. Deposits on the resistor ranged from none at all to heavy, the amount and type depending upon heater operating time, and flowrate and pressure conditions during the run.

Primary Chamber D.

The design of primary chamber D (see Fig. 3) is very similar to that of primary chamber C except that all of the chamber walls are regeneratively cooled. The chamber is larger and the points of injection are further removed from the chamber exhaust ports. Except for deposition on the heater wire, the problem of coking in this reactor is, for all practical purposes, non-existent. At low flowrates and high L*, small amounts of carbon formed in the chamber. Once, after a 20 minute run at about 1 lb./min. a few flakes of carbon were found in the chamber downstream in the nozzle region; this was attributed to a small liquid leak from the injector out over the steel nut which holds the injector in place. This nut is difficult to cool and is believed to run quite hot. After one series of runs made to determine the starting characteristics of primary chamber D, consisting of twenty brief runs averaging 1 minute each and twenty-two starting failures, a small amount of very low density carbon was found in the nozzle region; the main chamber was fairly clean. The large majority of the tests were conducted at higher flowrates and lower L*, and the deposits under those conditions ranged from nothing at all to thin films which could be easily wiped away.

From the test results obtained with primary chamber D, it is believed that, as far as coke deposition on the walls is concerned, trouble-free operation will be realized under the conditions anticipated in a fully developed reactor. The problem of deposition on the heater wire is a more serious one and is discussed in a subsequent section of the paper.

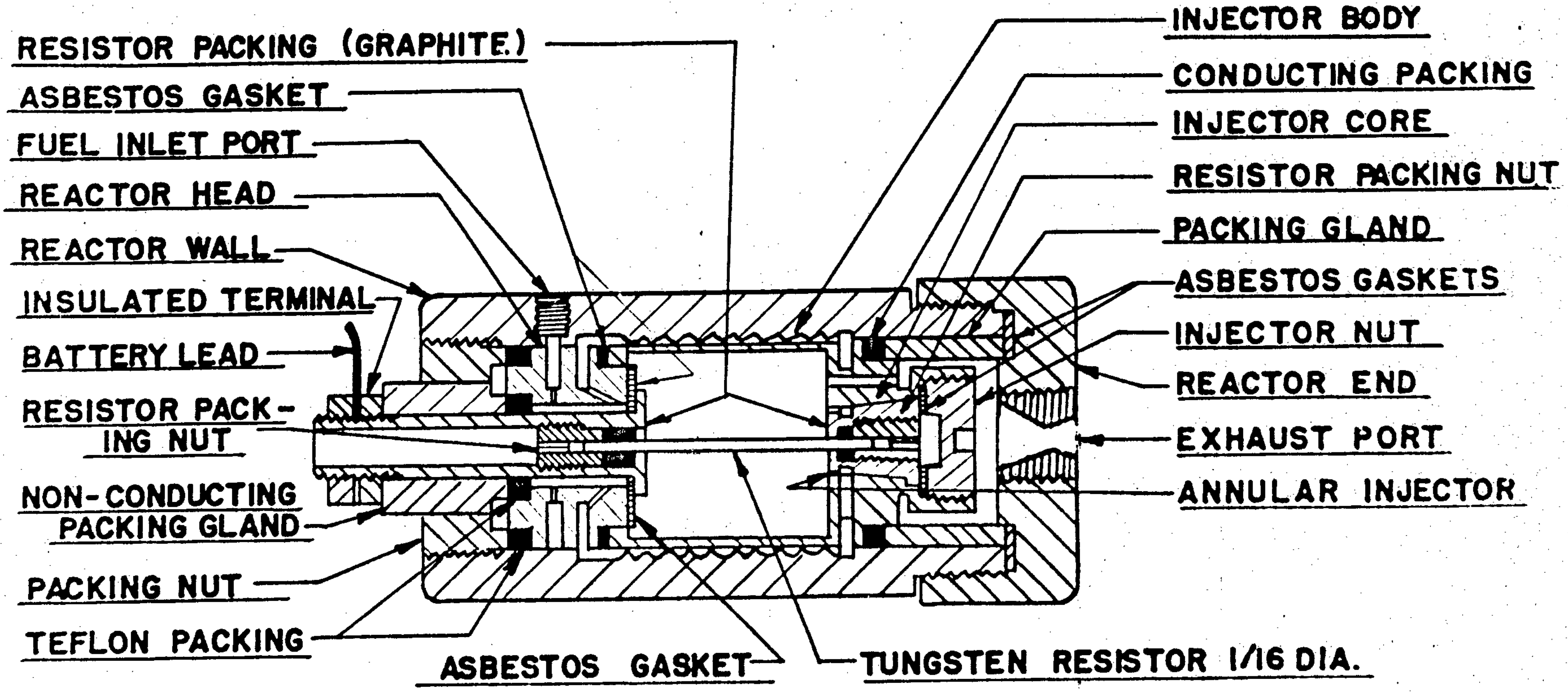
RESISTOR PACKING (GRAPHITE.)
ASBESTOS GASKET
FUEL INLET PORT
REACTOR HEAD
REACTOR WALL
INSULATED TERMINAL
BATTERY LEAD
RESISTOR PACKING NUT
NON-CONDUCTING PACKING GLAND
PACKING NUT
TEFLON PACKING
ASBESTOS GASKET
TUNGSTEN RESISTOR 1/16 DIA.
INJECTOR BODY
CONDUCTING PACKING
INJECTOR CORE
RESISTOR PACKING NUT
PACKING GLAND
ASBESTOS GASKETS
INJECTOR NUT
REACTOR END
EXHAUST PORT
ANNULAR INJECTOR

MATERIAL: Inconel Unless Otherwise Specified

FIG. 2. PRIMARY CHAMBER "C"

CONFIDENTIAL

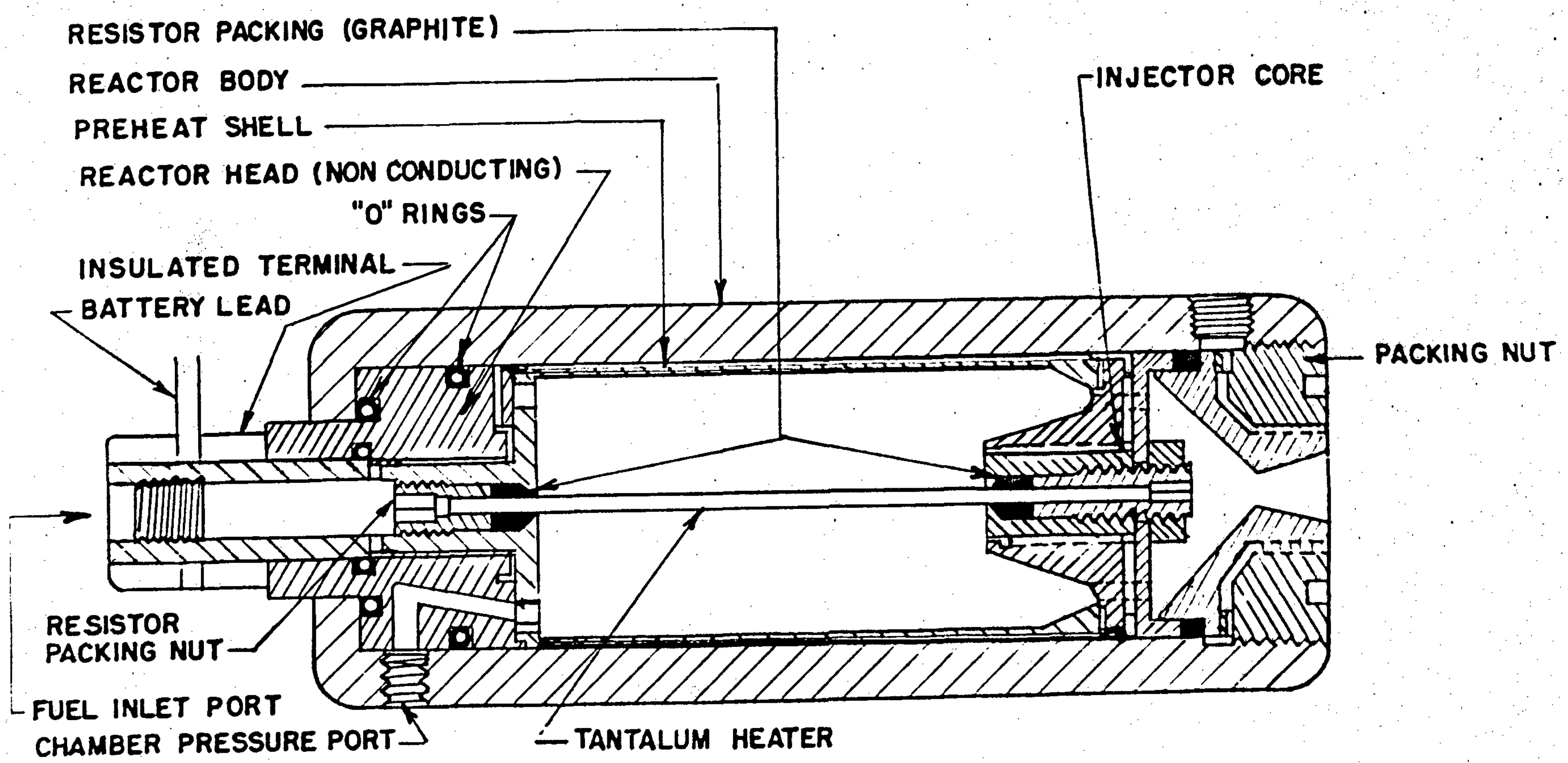
RESISTOR PACKING (GRAPHITE)
REACTOR BODY
PREHEAT SHELL
REACTOR HEAD (NON CONDUCTING)
"O" RINGS
INSULATED TERMINAL
BATTERY LEAD
RESISTOR PACKING NUT
FUEL INLET PORT
CHAMBER PRESSURE PORT
TANTALUM HEATER
INJECTOR CORE
PACKING NUT

MATERIAL: INCONEL UNLESS OTHERWISE SPECIFIED

FIG. 3. PRIMARY CHAMBER "D"

CONFIDENTIAL

Miniature Gas Generator

The principle of eliminating coke deposits by regenerative cooling was pursued also in the concurrent development of a very small ethylene oxide reactor made of brass and inconel with a chamber volume of about 0.013 in.^{3} and designed to operate at a flowrate of less than 1 lb./hr. for a period of several hours. In this reactor, the problem of applying regenerative cooling was more difficult because the ratio of surface area to fuel flowrate is so high that the reactors have a tendency to overheat, even when the incoming fuel is completely vaporized in the preheat channels. Cooling was finally achieved, however, by reducing the size of the reactor and selecting the proper conditions of flowrate and pressure for a given design. In the latest design, coking in the reaction chamber itself has been eliminated. A problem does remain of coking in the brass preheat channels; whether the deposit is a carbonized residue from boiling off the fuel from polymer present in the commercial ethylene oxide or from polymer formed in the hot, brass preheat channels has not been resolved. It is known that brass does cause polymerization of ethylene oxide, and therefore, is a poor material to use as a reactor.

Tests With Special Apparatus

A series of tests was conducted with specially designed apparatus, expressly to determine the effect of wall temperature on carbon formation. Commercial ethylene oxide at ambient temperature was sprayed on the walls of a stainless steel reactor heated to as high as 500°C. with no carbon being deposited at all. Sometimes slight traces of carbon were deposited at temperatures as low as 470°C. and as high as 600°C. When a sustained decomposition was started in that reactor, a marked increase in deposition on the walls resulted. This was not a regeneratively cooled reactor, and, therefore, the wall temperature reached values during sustained reaction considerably in excess of those used in the preliminary tests.

Conclusions

From the test results obtained, it is concluded that the predominant mechanism of coking in ethylene oxide reactors is the degradation of carbon containing molecules on hot surfaces of the reactor. Carbon will deposit from ethylene oxide at temperatures in the region of its auto decomposition temperature. Some polymers of ethylene oxide, which may be formed under the conditions prevailing in a reactor, undergo exothermic degradation strongly in the region of 340°-360°C; this is believed to be the coking process occurring in the preheat channels of the miniature reactor discussed above. There are several different carbon containing molecules which may be present in the chamber, each with its characteristic degradation tendencies. Among these are ethylene oxide, carbon monoxide, methane, polymers of ethylene oxide and possibly intermediates which occur in the decomposition reaction. Also, there are many different situations which can exist in ethylene oxide reaction chambers. In the light of this, it is not surprising that the various investigators involved in this problem have had widely diversified experiences. Another phenomenon worth noting is that, at L' values of about 5000, the formation of soot was observed on the walls of primary chambers C; this might have resulted from the combination of carbon monoxide to form carbon dioxide and carbon.

The existence of surface catalytic effects on the degradation processes must be recognized. At higher surface temperatures, marked differences in the coking tendencies of different surfaces have been demonstrated by other investigators. When reactor surfaces are cooled, these differences diminish to the point where almost any surface is non-catalytic to the degradation process.

It must also be recognized that situations exist where the role of surface catalysis in the polymerization process is of more significance than it is in the degradation process, because non-volatile polymers formed in the reactor have a tendency to adhere to the wall and they will undergo degradation to carbon unless they are cooled to sufficiently low temperatures.

The results indicate that the coking problems in these reactors can be effectively dealt with by regenerative cooling of the reactor surfaces. It also appears that, among the carbonaceous monofuels, ethylene oxide may be unique in its ability to operate in a regeneratively cooled reactor. Its high auto decomposition temperature (571°C) and its low critical temperature (196°C), permit heating the fuel even to the point of complete vaporization with no possibility of auto decomposition in the preheat channels. In the case of monofuels with low auto decomposition temperatures and higher boiling ranges, it is doubtful whether the metal surfaces can be maintained at low enough temperatures to prevent decomposition in the preheat channels; or, if it is possible, it may be difficult to achieve. If regenerative cooling is not practical with a given monofuel, coking problems must be dealt with by fuel additives, surface selection, chamber geometry or secondary cooling systems. Then, in this respect, it may appear that ethylene oxide has a distinct advantage over many of the other monofuels.

DISCUSSION OF MULTI-STAGE REACTOR

A two stage reactor incorporating primary chamber D in its present state of development is shown in Fig. 4. A detailed discussion of the primary chamber will be given first, followed by a discussion of the unit as a whole.

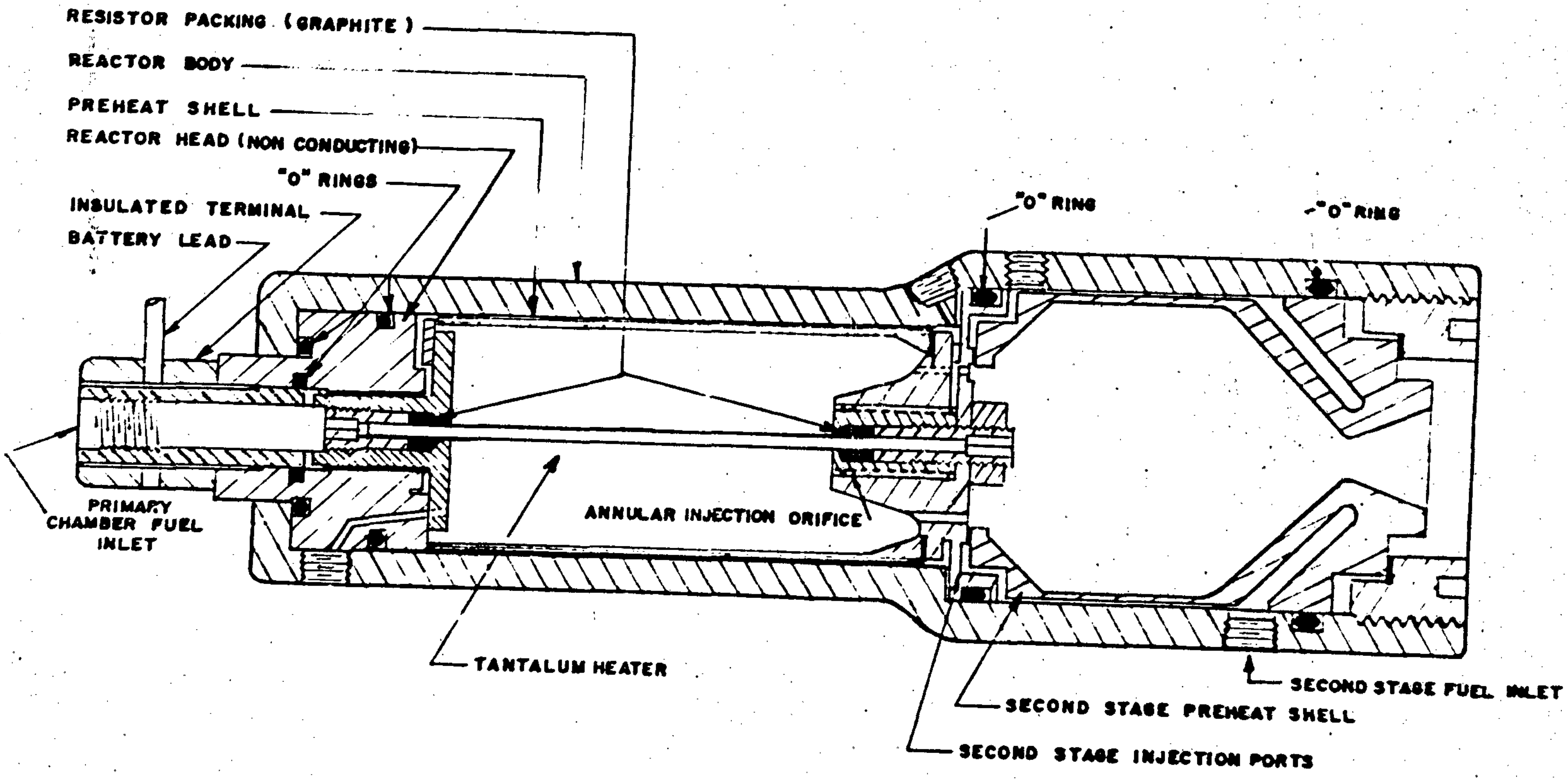
RESISTOR PACKING (GRAPHITE)
REACTOR BODY
PREHEAT SHELL
REACTOR HEAD (NON CONDUCTING)
"O" RINGS
INSULATED TERMINAL
BATTERY LEAD
PRIMARY CHAMBER FUEL INLET
"O" RING
"O" RING
ANNULAR INJECTION ORIFICE
TANTALUM HEATER
SECOND STAGE FUEL INLET
SECOND STAGE PREHEAT SHELL
SECOND STAGE INJECTION PORTS

FIG. 4. TWO STAGE REACTOR INCORPORATING PRIMARY CHAMBER "D"

Primary Chamber D

An effective method of transferring heat from the glow wire directly to the fuel has been developed which insures the transfer of heat necessary to start the chamber. The heater is located axially at the center of the chamber and the fuel injection is axial in a cylindrical pattern surrounding the heater but not contacting it. The heat generated has only three paths by which it may leave the heater. Some of the heat will pass by conduction out into the heater terminals. A small fraction of it will escape through the fuel by radiation. The remainder must necessarily pass from the heater to the fuel by convection. Then, if the heater is operating at a given wattage and the flowrate of fuel is low enough, decomposition of the injected fuel must occur. The reliability inferred in the above argument has been confirmed in practice; starting failures could always be traced to excessive flowrate, faulty injection pattern or failure of the heater.

The injector vs. heater orientation described above is potentially capable of relatively fast starts. The starting time is determined by the time required for the heater to reach its operating temperature and the time required to throttle up the flowrate. At a heat input of 2200 watts, primary chamber D was started repeatedly in three seconds using a 0.1" diameter discharge nozzle. This entailed 2.5 seconds heat up time for the 0.094" diameter heater wire with 0.5 seconds required for manually throttling up the flowrate; the total heater operating time was 5.5 seconds. The starting flowrate was about 1 lb./min.; this was increased during that half second to about 3 lb./min. It is recognized that the primary chamber should be scaled down to employ a more acceptable wattage. And, at a constant heat flux at the surface, as the diameter of the heater wire is reduced to obtain lower wattage, the heat-up time can be reduced and possibly approach the time required for an ordinary incandescent lamp to light. With a smaller wire and an automatically throttled start, a starting time of one second or less does not seem unreasonable to expect.

Tantalum is believed to be the most satisfactory material for the heating element in the primary chamber. This estimate is based upon physical properties alone; if chemical properties are shown to be important, other materials may be superior. Only the high melting point materials were given serious consideration because it seemed improbable that materials with melting points of the region of 1500°C could withstand the sharp temperature rise in the chamber which occurs upon starting. Carbon resistors were used in primary chamber A but the terminal problems were rather severe. Moreover, carbon has a negative temperature coefficient of resistance which gives it undesirable operating characteristics. Tungsten was used successfully in many of the tests, but it is quite fragile after it has been heated. Tantalum is soft and easily worked, and the selection of tantalum here is consistent with the practice of using tantalum filaments in light bulbs subjected to shock. The mechanical problems associated with the heater are the maintainance of good contact at the terminals and making provision for thermal expansion of the wire.

The problem of carbon deposition on the heater wire is cause for some concern; in most of the tests conducted, the deposition was quite severe. However, it is encouraging to note that in some of the tests with primary chamber C, no deposit at all was formed on the heater. The current belief is that the deposits are due to the spraying of fuel on the heater, because open air tests of the injectors showed that, in general, they did not effect the straight cylindrical injection pattern for which they were designed. Moreover in many of the tests conducted, the heater operating time was excessive and starting failures frequently occurred resulting in a flooded chamber. The solution to the problem appears to involve the development of an injector which effects the required cylindrical spray pattern. Then with fuel kept out of contact with the heater, and with the short heater operating time and reliable starting anticipated in a fully developed reactor, the prognosis seems good for obtaining a large number of repetitive starts.

Primary chambers C and D both have good running characteristics. This is of interest particularly because one would expect that an injection pattern designed expressly to effect heat transfer from the resistor to the fuel might not be adequate to effect the heat transfer necessary to sustain a reaction after the heater is turned off. The preheating of the fuel entailed in cooling the primary chamber may be an important factor, because preheating the fuel will make the manner of injection less critical. On the other hand, the injector and the hot gas exhaust ports in these chambers are so located that they both promote a smooth recirculation of hot gases in the chamber. In any case, the result was that both primary chambers C and D did operate at approximately 110 L* at chamber pressures as low as 100 lbs./in.^{2} which is exceptional for ethylene oxide reactors. Moreover, the operation of these chambers has been very smooth over a wide range of operating conditions.

Two Stage Reactor.

In addition to the elimination of coking problems, regenerative cooling of the multistage reactor introduces other advantages. The outer shell temperatures in the case of primary chamber D were found to be in the region of 200°C. This permits the use of light weight alloys for the outer shell, and internal parts of aluminum may also prove to be feasible. At these temperatures, "O" ring seals of silicone rubber or other heat resistant elastomers can be used; this renders the internal sealing problems in the multistage design readily capable of solution. One would expect a regeneratively cooled multistage reactor to be complex, but the design shown in Fig. 4 is very simple and can be readily fabricated.

It is intended that the multistage reactor should operate with low pressure drops between stages. This would require that all of the stages start at low pressure and come up to the operating pressure simultaneously. To do this, it is visualized that a small flow control and distributing device will be located at the reactor and will be actuated by the reactor chamber pressure. This type of start is somewhat difficult to achieve by manual throttling and thus far it has been done only in the two stage reactor shown in Fig. 1.

The present status of the development is the attempt to run the two stage reactor shown in Fig. 4 and to learn its starting and running characteristics, so that an automatic start can be developed for it. Subsequent development should consist of scaling down sharply the primary chamber to a lower wattage unit with faster starting characteristics, the determination of the optimum ratios of hot gas to incoming fuel at the second stage injector under various operating conditions, and the determination of chamber volume required to effect the reactions in the second chamber.

Means of ignition other than a glow wire could be applied to a multistage reactor; and the advantages offered by the multistage design over the conventional design are apparent in each case, because starting of the primary chamber is all that is required. In the case of a start by means of a solid propellant cartridge, a very small charge would be required. In a combustion start, the oxidizer requirement would be negligible. The multistage principle would appear to be the only hope of achieving a start by means of a spark. A different primary chamber would, of course, be developed for each method of starting.

It is hoped that the multistage design will permit the experimental determination of design parameters which can be used to design similar reactors for any specified flowrate and set of operating conditions with a high probability of success. This seems reasonable to expect, because the entire reactor is based upon a stream of hot gas impinging on a stream of incoming fuel, repeated many timesthrough the reactor; and data pertaining to one point of impingement should be applicable to all points of impingement. The process of impinging a stream of hot gas on the stream of fuel should lend itself to isolated study, and any improvements which emerge could be incorporated at once into any multistage reactor. Thus, it is reasonable to expect that a complete line of reactor designs could emerge from this program, from which one could build an ethylene oxide reactor for any flowrate and any set of operating conditions, with any desired means of ignition, which would be useful in a large percentage of the applications of ethylene oxide as a monopropellant.

ACKNOWLEDGEMENTS

Nearly all of the work reported herein was sponsored by the Department of the Navy, Bureau of Aeronautics, under Contracts No. NOa(s) 52-1042-c and No. NOa(s) 55-144-c. The work pertaining to the miniature reactor was sponsored by the Department of the Army, Office of the Quartermaster General under Contracts No. DA44-109-qm-1506 and No. DA19-129-qm-552. The writer wishes to acknowledge the work of Mr. Harold R. Tyler of Wyandotte Chemicals Corporation who played a major role in all of the work discussed herein subsequent to the testing of primary Chamber B. The work with special apparatus designed to determine the effect of wall temperature on coking was entirely done by Mr. Tyler. The writer also wishes to thank Mr. Tyler and Dr. C. W. Tait for their careful study and constructive criticism of this paper.

HIGH ENERGY FUELS IN AIR BREATHING ENGINES

E. A. DeZubay and S. M. King
Research Division
Curtiss Wright Corporation
Quehanna, Pa.

Since the range of a given aircraft is dependent on the specific fuel impulse, which as a first approximation is directly proportional to the heating value of the fuel, the desire to obtain fuels containing high combustion values per unit mass and volume is obvious. In order to obtain the minimum weight of a vehicle, it is necessary to use air as the oxidizer. Thus, in contrast to a rocket motor, the air breathing engine is limited in its domain of operation but benefits from the reduced demands on the working medium by being able to obtain oxygen from the surroundings. At speeds less than hypersonic and at altitudes below 100,000 feet the composition of air can be considered fixed in regards to the oxygen to nitrogen ratio. In the hypersonic range the possibility of a chemical reaction that would produce nitric oxide during the deceleration and compression of air exists while above 100,000 feet and the presence of atomic oxygen may also alter the characteristics of the available oxidizer.

In the search for high energy fuel three possibilities exist. These are; normal chemical fuels, fuels utilizing molecular bonding energies and fuel using electronic bonding energies. If we examine the chemical elements for potential fuels (1) we find that, as shown on Figure 1, the heating value of the elements falls from a maximum of 51,600 BTU/lb. for hydrogen to the range of 13,000 BTU/lb. for the heavier elements such as aluminum and silicon. Obviously from this standpoint hydrogen would be the ideal fuel, but a boiling point of 37° R and a density of 4.36 pounds per cubic foot means that formidable tankage problems will be encountered. The next elements in ascending atomic numbers such as lithium, beryllium, boron and carbon are all solids. Logistic as well as engineering considerations require the use of liquid fuels for aircraft applications. As a result it is desirable to combine elements containing the highest heating value with as much hydrogen as chemical synthesis can achieve to obtain liquid fuels with desirable characteristics. An element of zero atomic weight with an infinite valence would make an ideal hydrogen carrier.

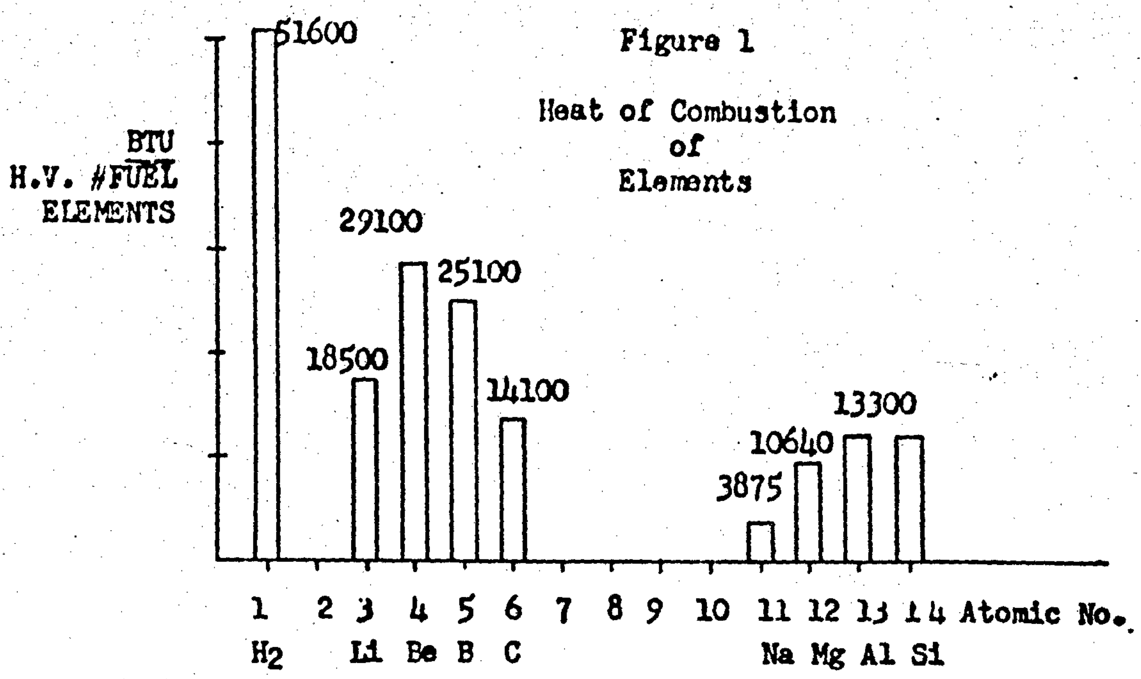

Nature has endowed us with a large supply of carbon hydrides varying in heating value from 21,600 BTU/lb. for methane to approximately 16,000 BTU/lb. for the heavy unsaturated oils. These fuels have been the backbone of our power plants. In an effort to obtain more chemical energy per unit weight hydrides other than those of carbon have been investigated. Figure 2 shows the range of heating values of various hydrides.

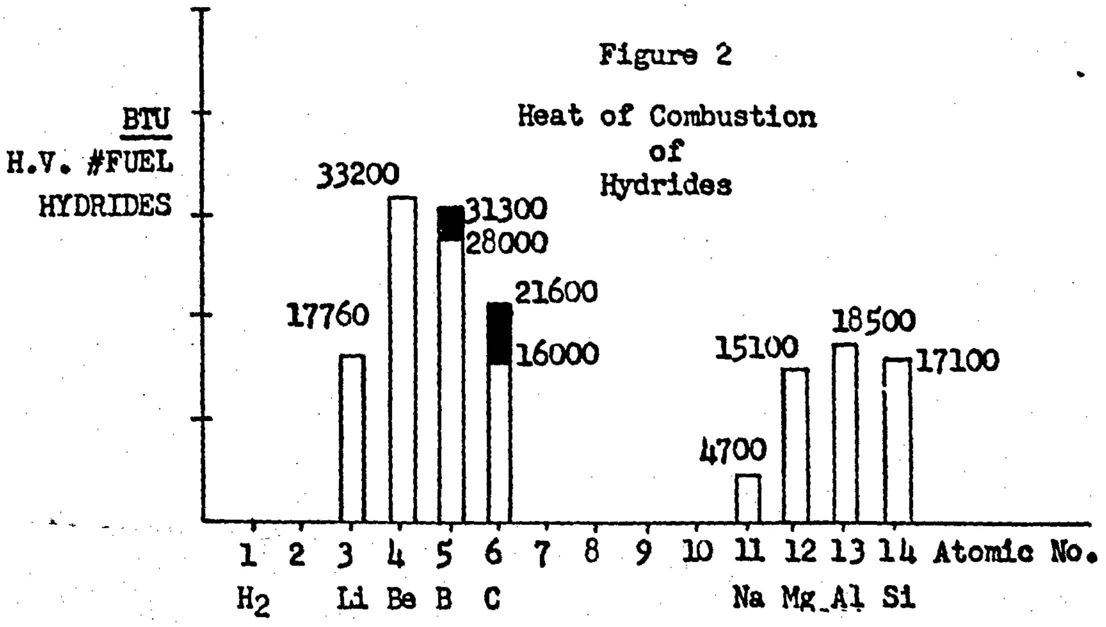

It is evident that only two of these hydrides represent large potential increases in heating values. These are beryllium hydride and the entire family of boron hydrides. Beryllium hydride or beryllium hydride derivatives, because of the extreme toxicity, unknown chemistry (2) and low availability can not be considered as an economically feasible fuel. This leaves only boron hydrides as the other possibility. The pure boron hydrides have heat value ranging from a high of 31,300 BTU/lb. for diborane to about 28,000 BTU/lb. for the higher hydrides (1). However, because of their toxicity and other physical properties, these boron hydrides have had to be modified with alkyl groups. For example, the addition of an ethyl radical to decarborane results in a reduction in heating value from 28,300 for pure decaborane to 26,500 BTU/lb. for monoethyldecaborane. These modifications were necessary to obtain liquid fuels with reasonable handling properties.

The boron hydrides and their derivatives have been given the most active attention since their potential properties such as density, vapor pressure and viscosity could be modified to resemble that of the hydrocarbons presently used as fuels. Fortunately boron-hydrogen compounds form an "organic" type of chemistry which though structurally more complex than that of the hydrocarbons, permits wide variations in composition and physical properties,especially when the alkyl radicals are permitted to replace a selected few of the hydrogen atoms of a normal boron hydride. Chronologically, the boron, carbon, hydrogen type fuels have had an evolutionary trend that started with diborane (B_2H_6), and progressed to pentaborane (B_5H_9), ethyl and propyl pentaborane ($C_2H_5B_5H_8$ or $C_3H_7B_5H_8$), the present ethyl decaborane ($C_2H_5B_{10}H_{13}$), and eventually will end as methyl decaborane ($CH_3B_{10}H_{13}$), the ultimate hope of these synthetic fuels.

There are positive indications that the lower boron hydrides, and their derivatives have a high reactivity with air. This high reactivity has been confirmed by their high laminar flame speed which at stoichiometric fuel-air ratios varies between 200 cm/sec. to 600 cm/sec. (3) compared to a typical hydrocarbon value of 35 cm/sec. This high reactivity has not been verified for decaborane and its derivatives. Furthermore, the activation energy for an oxidation reaction must be considerably lower than the usually accepted value of 30K cal/mole for hydrocarbons. Hydrocarbon flames can be sustained at flame temperatures as low as 2600°R, while borane flames can be sustained at temperatures as low as 1500°R (4). From an aircraft standpoint such properties mean that the combustion space requirements can be reduced, and that wider limits of fuel to air ratios can be used. During the combustion process, zones ranging from fuel rich to below the lean flammability limits are present. It is possible that other boron compounds such as boron carbide may be formed in the fuel rich zones and complete combustion to boric oxide and carbon dioxide may not be obtained. Thus the end products of combusion of the alkyl boranes will have to be examined if appreciable losses in combustion efficiency are observed.

A problem, not encountered with hydrocarbon fuels, is found in the products of combustion of boron-containing high energy fuels. With complete combustion, boric oxide is produced at a rate of about two and a half times that of the fuel consumed, and is a viscous liquid in the normal jet engines mainburner range from 1600 to 850°F (5). At temperatures below 850°F the solid oxide deposits and builds up on every exposed surface even to the extent of closing some passages. At the higher temperatures the situation is alleviated to some extent but the thick liquid still forms traveling waves which destroy the efficiency of aerodynamically shaped surfaces. Methods of preventing the deposition of boric oxide on engine parts are being investigated.

Expansion processes, involving a two-phase system as a mixture of ideal gases and condensible boric oxide present rather complex thermodynamic systems. As an example (6), Figure 3 presents the pressure-temperature conditions for an isentropic expansion from an initial condition of 4200°R and 20 psia to 4 psia with an initial concentration of 0.106 lb. gaseous boric oxide per pound of air. As the expansion line indicates the mixture behaves as a mixture of gases until a pressure of 9 psia is reached. At this point the boric oxide would begin to condense under conditions of equilibrium. At this point of initial condensation the condition line changes slope and proceeds along a new path in which the gaseous components are reheated by the condensing boric oxide. This process results in the gases at the end of the expansion being considerably hotter than gases expanding without condensation. This is exemplified by the condition line of pure air which is included as a comparison. If non-equilibrium conditions exist during the expansion and the boric oxide vapor becomes super saturated, measurable differences in the available enthalpy occur. For ex-

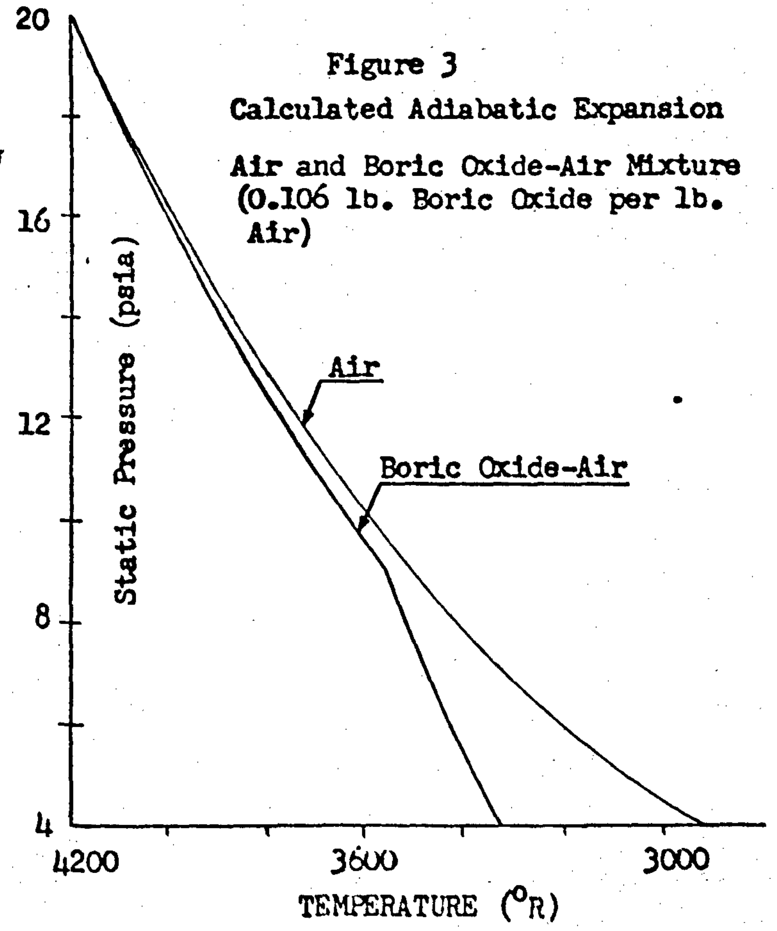

Figure 3

Calculated Adiabatic Expansion

Air and Boric Oxide-Air Mixture (0.106 lb. Boric Oxide per lb. Air) ample, in the case cited in Figure 3 an increase of 4% in the enthalpy available from the expansion would be possible if maximum condensation rather than maximum super saturation of the boric oxide vapor would occur.

Now that boron fuels have passed from the laboratory, hydrogen is receiving consideration. Having no synthesis problem and backed by the development of suitable liquefaction equipment and storage vessels, the investigation of hydrogen can proceed toward its application in present engines, as well as experimental investigations directed toward advanced propulsion systems. Even though hydrogen faces the disadvantage of an extremely low boiling point and density it is quite possible that the actual use of hydrogen in air breathing engines will be realized before the problems associated with the boron fuel can be met successfully.

If the necessity of handling materials at very low temperatures (7 to 100°R) is accepted, an entirely new field of potential fuels can be considered. The obvious choice for a low temperature, high energy fuel, is of course, molecular hydrogen. At present it can be produced in large quantities relatively economically and stored easily. There are also indications that in the cryogenic region, radical fuels may present possibilities. These radical fuels consist essentially of normal fuel molecules from which one or more atoms have been stripped. As a result of such a removal, the available energy is not only the chemical energy usually associated with the combustion process but also the energy expended in breaking the molecular bond of the previously attached molecule or molecules. The best candidate for a radical fuel would again be hydrogen. With its chemical energy of 51,700 BTU/lb. and its dissociation energy of 93,000 BTU/lb., a total energy content of 144,700 BTU/lb. could be realized. Even higher energies can be obtained from ionic forms, where not only the molecular bonds are separated, but also the intra-atomic bond between the nucleus and the planetary electrons are broken. As shown on the following table, these ionic fuels contain fantastic energies.

Table of Energy Values of Ionic Fuels

Fuel	Energy Content
H^+	707,000 BTU/lb.
C^+	78,800 "
C^{++}	163,000 "
CO^+	24,800 "
B^+	80,600 "
B^{++}	177,000 "

For ionized hydrogen, the proton in returning to its molecular state would yield an energy of 655,000 BTU/lb. This value could be increased to a value of 707,000 BTU/lb., if the molecular hydrogen would then be oxidized in air.

If such energies could be realized the specific fuel consumption would be reduced by a factor of roughly 30 from that of conventional hydrocarbon. It should be emphasized that as the energy of dissociation and ionization becomes large in comparison to the energy attainable by combustion, the need for an air breathing engine becomes progressively less. Since the energy obtained by association and deionization can be absorbed by the fuel itself in the form of either thermal or kinetic energy, the need for air as either an oxidizer or working medium becomes almost trivial; as the fuel itself acts as a monopropellant.

The use of both radical and ionic fuels cannot be considered in the immediate future because of the elementary state of knowledge of their production, stabilization (7) and storage for any amount save microscopic quantities. As a consequence of these considerations the immediate future can consider only the boron hydride fuels with their derivatives and liquified hydrogen.

An inspection of the Breguet range equation modified for jet driven aircraft in the form

$$R = S_f \, Ma(L/D) \, \mathrm{Log}_e (W_f/W_e)$$

where R = range (miles)
S_f = specific fuel impulse (# Thrust/#fuel/hr.)
M = Mach No
a = acoustic velocity (miles/hr.)
L/D = lift drag ratio
W_f = weight of vehicle fully fueled
W_e = weight of vehicle empty

can be used as a basis for discussing the range of aircraft utilizing the various fuels discussed previously. Since the density of both hydrocarbons and alkyl boranes are approximately the same, the possibility of interchangeability of these fuels exists. If an alkyl borane fuel is to replace a hydrocarbon fuel the specific fuel impulse would be increased in direct ratio of their heating value, providing that the engine (either turbo or ram jet) would be operated at the same conditions of mass flow and energy input. As a first approximation the range would also increase in the same ratio as the specific impulse, if only the fuel and not the geometry and flight conditions was changed. In the previously cited Breguet equation, only S_f, the fuel dependent variable, and not L/D, M, a, W_f or W_e, the flight and airframe dependent variables, would be changed. For example, an increase in heating value from a hydrocarbon fuel (18,600 BTU/lb.) to ethyl decaborane (26,500 BTU/lb.) would increase the range of an aircraft by about 40%. If liquid hydrogen is to be used as an aircraft fuel no interchangeability with existing vehicles is possible, since hydrogen with its low boiling point and its low density requires large volume, well insulated tanks. These requirements are such that both the airframe geometry and flight condition must be modified, that is, at least L/D and M must be changed to minimize the effect of the bulkier fuselage. Although the specific impulse of hydrogen theoretically is 2.78 times that of a representative hydrocarbon, the required redesign reduces the range increase to about 100%. The relative ranges, as determined by heating values and airframe design requirements are shown on Figure 4. For the fuels which can be utilized at present and in the immediate future, namely hydrocarbons, alkyl boranes and liquid hydrogen; the relative sizes of the required airframes are presented in silhouette form. No attempt was made to estimate the airframe size for such futuristic fuels as radical or ionic hydrogen, since the auxiliary equipment requirements to stabilize such a fuel are unknown. The range of an ionic hydrogen fuel aircraft is included on Figure 4 only to indicate an order of magnitude.

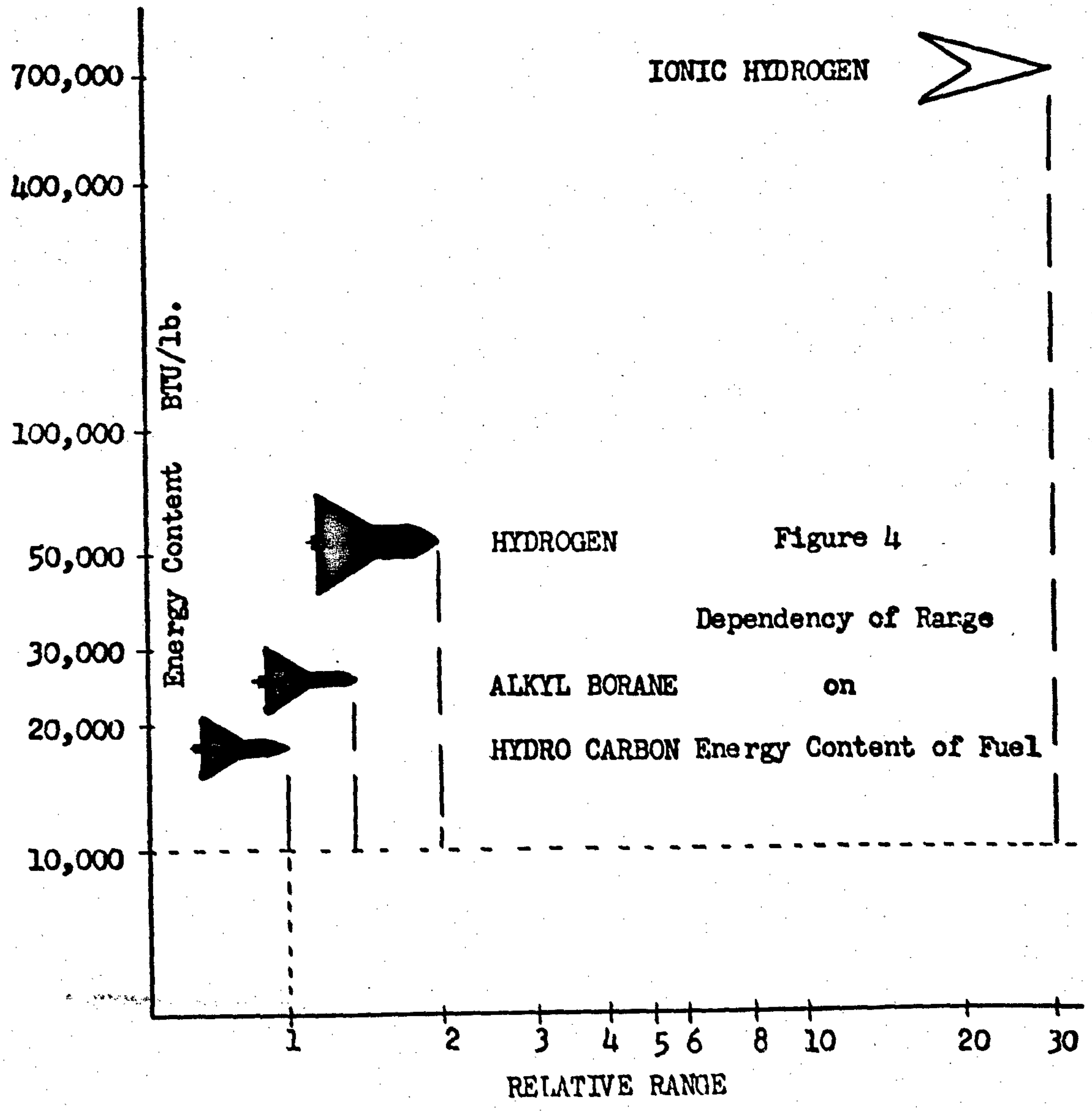

Figure 4

Dependency of Range on Energy Content of Fuel

In conclusion, then, the potential extension of range and performance through the application of fuels with energy contents higher than hydrocarbons will probably follow an evolutionary pattern. The alkyl borane fuels can be used with existing airframes and engines if the problems posed by their products of combustion can be solved. Liquid hydrogen will require complete redesign of airframes, but should present no major problems in existing or future engines. Radical or ionic fuels can only be treated from a theoretical side since no requirements are yet available for the equipment that might possibly stabilize such futuristic fuels.

REFERENCES

1. U. S. Bureau of Standards Circular 500: "Selected Values of Chemical Thermodynamic Properties." February, 1952.

2. Hurd, D. T.: "Chemistry of the Hydrides." New York, John Wiley and Sons, Inc., 1952.

3. Berl, W. G.: Discussion on "Boron Hydride Combustion." Applied Physics Laboratory, Silver Spring, Md., October 25 and 26, 1956.

4. Wolfhard, H. G.: "Combustion Properties of Diborane." Fuel September, 1956.

5. Mackenzie, J. D.: "Viscous Flow and the Constitution of Liquid Boric Oxide." J. Chem. Phys. 24, 925-926 (1956)

6. DeZubay, E. A. and Lacz, J. A.: "Isentropic Expansions of Condensible Vapors." Curtiss-Wright Research Division, Technical Report CWR-327, December 15, 1956.

7. Broida, H. P.: "Stabilization of Free Radicals of Low Temperatures." Paper presented at conference on "Unstable Chemical Species," at the New York Academy of Sciences, March 15-16, 1956.

COMPARISON OF LOX/KEROSENE, LOX/HYDRAZINE, AND LF_2/HYDRAZINE MISSILE SYSTEMS FOR LONG-RANGE MISSIONS

Johann G. Tschinkel
Army Ballistic Missile Agency
Huntsville, Alabama

This paper was not received in time to include with the preprints. It will be published with the proceedings, following the symposium.

STUDIES WITH TWO-STAGE ROCKET ENGINES[1]

Anthony Briglio, Jr.
Jet Propulsion Laboratory
California Institute of Technology
Pasadena, California

ABSTRACT

The operation of a rocket engine is dependent upon complicated inter-relationships of the processes of mixing, atomization, evaporation, and combustion. These relationships are not well understood at present. The designer of rocket engines is hampered by a lack of basic data on how to design high-performance, smooth-operating engines, and considerable effort is generally spent on a trial-and-error basis. The gas-atomizing technique has been applied in an effort to circumvent some of these current unknowns. In this approach, a portion of the propellant is reacted in the first chamber, or stage, of a two-stage engine and converted into high-velocity hot-gas streams which are suitable for atomizing and heating the balance of the propellant. This type of injection does not rely on casual eddy velocities or liquid-phase reactions to accomplish heating of the propellants injected into the main chamber.

A number of two-stage engines, of both 1,000-pound and 20,000-pound thrust, have been tested to investigate the gas-atomizing injection principle. The following parameters were varied: the fraction of propellant burned in the first stage, the gas velocity in the mixing jet, the engine L*, and the orifice pressure drop. In both the 1,000-pound-thrust and the 20,000-pound-thrust engines, high percentages of peak theoretical performances and very smooth combustion were obtained with a number of different bipropellant systems using fuming nitric acid as the oxidizer. The L* required for comparable

---

[1] This paper represents the results of one phase of research carried out at the Jet Propulsion Laboratory, California Institute of Technology, under Contract No. DA-04-495-ORD 18, sponsored by the Department of the Army, Ordnance Corps.

performance was larger for the 20,000-pound-thrust engines than for the smaller scale. Further testing is being directed toward reducing the engine size without sacrificing performance.

Tests to date have shown that utilization of the gas-atomizing principle is a powerful tool in promoting the combustion process in rocket engines for both hypergolic and nonhypergolic systems.

STUDIES WITH TWO-STAGE ROCKET ENGINES

The Jet Propulsion Laboratory has been conducting studies of rocket engines and propellants for several years in the course of developing useful systems for medium-range, surface-to-surface missiles for Army Ordnance. Much of this work was carried out using the fuming nitric acid-isopropyl alcohol propellant system because these propellants, being relatively difficult to burn in rocket engines with impinging jet injectors, served as a useful tool in studying combustion processes. Early in 1953, some high-speed motion pictures were taken of a transparent-walled 1000-lb-thrust engine operating on fuming nitric acid and isopropyl alcohol in an effort to determine the cause of low performance which was being obtained with some 40-inch L* engines of 2-to-1 area ratio (chamber-to-throat).[a] When a splash plate was used in conjunction with a multi-orifice injector, the flame front in the transparent-walled engine, as indicated by the position of initial luminosity in the chamber, was relatively steady at a position about 5 inches downstream from the injector face. Under these conditions, the characteristic velocity c* was about 4400 ft/sec. With the splash plate removed, the flame front oscillated between the injector face and a position about 9 inches downstream from the injector face. Under these conditions the c* was lower than 4000 ft/sec. Consideration of these results led to the hypothesis that the relatively low performance of these engines was due to insufficient heat transfer to the propellant being injected into the chamber.

To test this hypothesis, a two-stage engine was built, consisting of two combustion chambers, or stages, joined by an interstage nozzle (see Fig. 1). A portion of the total propellant flow was burned in the first stage. The resultant gas stream issued forth from the face of the mainstage injector and served as a source of heat in the vicinity of injection of the major portion of the propellant. The first-stage chamber had a volume corresponding to 10 in. L* of the main stage and had the same diameter. The total L* of the engine was 50 in. L* and the chamber-to-throat cross-sectional area ratio was 2. With 10% of the total propellant burning in the first stage, the gas velocity and stay time in the first stage were the same as for an engine having a 20-to-1 chamber-to-throat area ratio and a 100-inch L*.

---

[a] The nomenclature used in this paper is presented in Table I.

Therefore, conditions were such as to assure near-complete combustion and high temperature of the gas coming from the first stage. With this engine, a c* of 4800 ft/sec was attained at r = 3.3, corresponding to an increase in performance of about 9%. This large improvement in performance with relatively little increase in L* indicated that use of the two-stage principle was a powerful tool with which to promote good combustion and hence to circumvent some of the complicated and little-understood inter-relationships of the processes of mixing, atomization, evaporation, and combustion.

A number of different configurations of 1000-lb-thrust two-stage engines were built and tested to obtain design information. Detailed results of these tests are presented in References 1 through 12. The engines were all uncooled, to simplify fabrication and to permit rugged heavy-walled construction. All tests were of short duration, about 2 to 4 seconds, to prevent overheating of the engine components. In all of the engines, triplet sets of orifices were employed, two oxidizer streams impinging on a central fuel stream, so that the direction of the resultant momentum would not change as mixture ratio was varied.

In one design, no interstage nozzle was employed, 15% to 30% of the total propellant being injected into the head end of the chamber and the remainder being injected into the resulting low-velocity (about 200 ft/sec or less) gas stream. The low performance obtained with this configuration indicated that the main-stage propellant should be injected into a gas stream of relatively high velocity, say 600 ft/sec or more.

Ultimately, small-scale two-stage engines were designed which gave c* values of 4800 ft/sec or higher using a wide variety of fuels with fuming nitric acid of different compositions, including SFNA (see Table II). With these engines, high performance was not critically dependent upon chemical composition, as is sometimes the case with rocket engines.

Most of the performance tests just described were made with engines having a 68-inch L*. Since this L* might be excessively large for practical application, some recent tests were made with a high-performance two-stage engine of 1000-lb-thrust (see Figure 2) in which reductions were made in the combustion chamber volumes of both stages, to investigate the effect on performance. With one engine, decreasing the first-stage L* to 15 in. and the second-stage L* to 24 in. (for a total L* of 39 in.) resulted in little loss in performance with SFNA-diethylenetriamine, the c* being 5070 ft/sec and the I_{sp} 208 sec (cf. Table II). Combustion during these tests was smooth.

In addition to the small-scale tests, several configurations of two-stage engines have been tested on the 20,000-lb-thrust scale to obtain design information for possible future application. These tests are described in more detail in References 11 and 12. The tests at 20,000-lb-thrust were all of short duration in uncooled engines. The test installation is shown in Figure 3 with a two-stage engine mounted ready for firing, and some test data are presented in Table III.

The 20,000-lb-thrust engines had two general configurations, one having annular, and the other having circular interstage nozzles. These interstage nozzles, as well as the ones used in the 1000-lb-thrust engines, all had sharp edges at the downstream end to induce separation of the gas stream. In the first type, shown in Figure 4, the propellants were introduced from an injector body which was located on the central axis of the engine. Ten sets of triplet orifices injected one-third of the total propellant flow into the first stage. Each triplet consisted of two oxidizer jets impinging on one central fuel jet. The main-stage injector likewise had ten triplet elements, and the spray produced was directed outward toward the wall intersecting the annular gas stream coming from the first stage. The interstage nozzle was replaceable, making it possible to vary the interstage gas velocity and thereby determine the effect of this variable on performance. Two interstage nozzle velocities were tested (600 ft/sec and 1000 ft/sec), two main-stage L* values (49 in. and 75 in., the first-stage L* being 22 in. in both cases), two different injector body configurations (cf. Figs. 5 and 6), and several different propellant combinations, SFNA with the following fuels: diethylenetriamine, Corporal fuel (46.5% wt aniline, 46.5% furfuryl alcohol, and 7% hydrazine), 50% aniline - 50% furfuryl alcohol, 80% diacetone alcohol and 20% furfuryl alcohol. The combustion obtained in these tests was generally very smooth. Combustion instabilities occurred in none of the tests with injectors of the type shown in Figure 5 and in only one test with injectors of the type shown in Figure 6, the one test being with diacetone alcohol - furfuryl alcohol fuel.

In the tests at the smaller main-stage L* (49 in.), the measured values of chamber pressure appear erroneously high since the values of C_F are 2 to 4% lower than predicted and the values of c* are exceptionally high. The isentropic stagnation pressure p_c for calculating performance was based on measurements of p_2, at the side of the chamber wall a short distance upstream from the start of the converging section of the nozzle. If appreciable combustion were taking place downstream of the p_2 tap and upstream of the nozzle throat, then p_2 and hence p_c would be erroneously high, for the relationship between p_2 and p_c was based on the assumption that combustion was completed in the chamber. When the L* of the main stage was increased to 75 in., the discrepancy in C_F disappeared. For example, using the propellants SFNA-DETA, the specific impulse increased from 204 seconds to 213 seconds, an increase of about 4 1/2%, whereas the c* increased from 4920 ft/sec to 5040 ft/sec, an increase of only 2 1/2%. With the 75-in. L* chamber, C_F values were about 1.36, being identical with theory, whereas the C_F for the engine with the 49-in. L* main stage was about 1.32. Larger discrepancies of this type were obtained in small-scale tests in which the engine L* was reduced to low values. These results emphasize the desirability of measuring thrust in experimental and development testing, since agreement of the experimental values of thrust coefficient C_F with the theoretical values is a good check on test data.

The first injector body which was built (see Fig. 5) had its triplet elements canted so that the spray fans produced by the stream inpingements did not intersect each other before intersecting with the gas stream from the first stage. It was believed desirable to avoid excessive mass concentrations such as might form if the edges of the fans were allowed to mix. The second injector (cf. Fig. 6) was simpler to fabricate, the orifices of each triplet being located in radial planes. The performance of this injector was identical to that of the earlier one, indicating that there was no adverse effects from allowing the spray from the fans to intersect.

In tests with the simplified injector in the engine having a 75-in. L* main stage, a loss in I_{sp} of 6 seconds resulted from enlarging the injector orifices and thereby decreasing the injector pressure drop to 50 psi compared with its previous drop of 125 psi.

More recently, the two-stage engine shown in Figure 7 was tested. This 65-in. L* engine was similar in layout to the best performing small-scale engine (cf. Fig. 2). Some differences between the large-scale and small-scale engines should be pointed out. The 20,000-lb-thrust engine had three triplets in the first stage and six triplets in the second stage. Since one-third of the total propellant was burned in the first stage, an average of over 2000 lbs of thrust was obtained from each triplet element, as compared to a maximum of 220 lbs per triplet in the 1000-lb-thrust engine. The chamber-to-throat area ratio of the large engine was 2, whereas that of the small engine was 4.

The large-scale engine of Figure 7 has been tested with SFNA-diethylenetriamine and with Corporal propellants (SFNA and 46.5% aniline--46.5% furfuryl alcohol--7% hydrazine fuel). Using SFNA-DETA, the peak performance obtained at a p_c of 300 psia is as follows: $c^* = 4850$ ft/sec and $I_{sp} = 203$ seconds at $r = 3.1$. This performance is appreciably below that of the small-scale engine after which it was modeled. Combustion was very smooth during starting, steady-state operation, and shutoff in all but one test of this engine. In the exception, a test with SFNA and diethylenetriamine, a combustion instability occurred, and the engine suffered damage due to burning.

It is planned to make additional tests with the two-stage engine of Figure 7 using orifices which will give reproducible stream characteristics, as predicted by hydraulic studies which are being conducted at the Jet Propulsion Laboratory (cf. Refs. 13 and 14). These studies have shown that control over the distribution of both mass and mixture ratio in the spray resulting from impingement of free liquid streams can be exerted only if the dynamic characteristics of the streams are controlled. It has been demonstrated with nonreacting fluids simulating propellants that the streams must possess controllable dynamic characteristics, i.e., similar and symmetrical velocity profiles in a stable free stream. It appears that the most satisfactory method of controlling the velocity profile is to assure that the streams are fully turbulent. The length of smooth bore required to produce a fully developed turbulent velocity profile is excessively large for practical application in a rocket engine, amounting to about 50 or more diameters. However, it has been found that by utilizing a proper approach section and uniformly roughening a portion of the bore of the orifice, say by threading, the required orifice length can be reduced to about 20 diameters.

In one set of scheduled tests, the two-on-one orifices of the engine shown in Figure 7 will be threaded to investigate the effect on performance of obtaining stable and reproducible stream characteristics. Hydraulic testing revealed that the liquid streams produced by the unthreaded orifices gave relatively poor stream characteristics partly because of the bends in the feed tubes (cf. Figure 8). Threading of the orifices will give more ideal stream characteristics.

In a second series of scheduled tests, the two-on-one triplet sets of orifices will be replaced by one-on-one doublet sets of orifices satisfying the requirements for producing fully developed turbulent streams and in addition having diameters required to produce uniform mixture ratio of the propellants in the spray produced by impingement. The criterion to be satisfied to obtain uniform mixture ratio with one-on-one impinging stream pairs is the relation

$$\delta_{ox} V^2_{ox} D_{ox} = \delta_f V^2_f D_f$$

which was empirically determined using inert fluids simulating propellants, carbon tetrachloride simulating the FNA, and water simulating the fuel (cf. p. 5 of Ref. 14).

Some other organizations have studied two-stage engines. In one series of experiments (cf. Ref. 15), a two-stage engine was operated on the mixed oxides of nitrogen - ammonia propellant system. Compared with some other types of injectors (a swirl type and a triplet impinging type), the two-stage injector gave appreciably lower performance. In other tests (cf. Ref. 16), an effort is being made to determine the major design parameters affecting the jet mixing processes and the effect of these parameters on combustion chamber ignition, performance, and stability. The investigation was stimulated by highly promising results obtained by applying the jet mixing injection technique in other programs.

CONCLUSION

In conclusion, smooth combustion and high performance have been obtained in some experimental rocket engines by burning a portion of the propellant in a separate combustion chamber and injecting the rest of the propellant into the resulting hot, high-velocity gas stream. These so-called two-stage engines have been operated under wide ranges of conditions, such as propellant composition and mixture ratio, and the combustion has been characteristically smooth and free from instabilities. Performance closely approaching the theoretical values was obtained with each of several different two-stage engines, using fuming nitric acid and a wide variety of fuels.

These results are considered highly promising and justify additional study of two-stage engines. This type of engine might be particularly useful for certain specialized applications, for example where throttled operation is required.

Excellent performance was obtained in relatively small L* two-stage engines of 1,000-lb-thrust. In applying the same principle to 20,000-lb-thrust engines, smooth combustion was obtained, but the performance was appreciably lower than that obtained on the small scale. The differences in performance obtained at the two thrust levels and the results of other investigations of two-stage engines (as well as one-stage engines) point up our lack of basic knowledge of the processes affecting rocket-engine operation.

Additional testing of a 20,000-lb-thrust two-stage engine is planned with two different sets of injector orifices to investigate the effect of using triplets which give more stable free streams and with doublet sets of orifices which will give stable free streams and uniform mixture ratio of the propellants in the spray produced by impingement. Test data for both orifice configurations are expected to be available for presentation at the Symposium in March 1957. The effect on combustion of obtaining different mass concentrations of propellants in these new configurations is not known. However, it should be emphasized that unless the liquid streams have predictable dynamic characteristics, little hope can exist for predicting either mass or mixture ratio distribution of propellant. The use of orifices which will at least control mixture ratio distribution is considered a necessary step in the direction of better controlling the processes taking place in rocket engines.

REFERENCES

1. Powell, W. B., and Wilson, E. L., Fuming Nitric Acid - Diethylenetriamine as a Rocket Propellant, Progress Report No. 20-262. Pasadena: Jet Propulsion Laboratory, January 28, 1955 (Confidential).

2. Combined Bimonthly Summary No. 36 (April 20, 1953 to June 20, 1953). Pasadena: Jet Propulsion Laboratory, July 20, 1953 (Confidential).

3. Combined Bimonthly Summary No. 40 (December 20, 1953 to February 20, 1954). Pasadena: Jet Propulsion Laboratory, March 20, 1954 (Confidential).

4. Combined Bimonthly Summary No. 43 (June 20, 1954 to August 20, 1954). Pasadena: Jet Propulsion Laboratory, September 20, 1954 (Confidential).

5. Combined Bimonthly Summary No. 44 (August 20, 1954, to October 20, 1954). Pasadena: Jet Propulsion Laboratory, November 20, 1954 (Confidential).

6. Combined Bimonthly Summary No. 46 (December 20, 1954 to March 31, 1955). Pasadena: Jet Propulsion Laboratory, April 15, 1955 (Confidential).

7. Combined Bimonthly Summary No. 48 (June 1, 1955 to August 1, 1955). Pasadena: Jet Propulsion Laboratory, August 15, 1955 (Confidential).

8. Combined Bimonthly Summary No. 49 (August 1, 1955 to October 1, 1955). Pasadena: Jet Propulsion Laboratory, October 15, 1955 (Confidential).

9. Combined Bimonthly Summary No. 50 (October 1, 1955 to December 1, 1955). Pasadena: Jet Propulsion Laboratory, December 15, 1955 (Confidential).

10. Combined Bimonthly Summary No. 52 (February 1, 1956 to April 1, 1956). Pasadena: Jet Propulsion Laboratory, April 15, 1956 (Confidential).

11. Combined Bimonthly Summary No. 53 (April 1, 1956 to June 1, 1956). Pasadena: Jet Propulsion Laboratory, June 15, 1956 (Confidential).

12. Combined Bimonthly Summary No. 55 (August 1, 1956 to October 1, 1956). Pasadena: Jet Propulsion Laboratory, October 15, 1956 (Confidential).

REFERENCES (Cont'd)

13. Rupe, Jack H., The Liquid-phase Mixing of a Pair of Impinging Streams, Progress Report No. 20-195. Pasadena: Jet Propulsion Laboratory, August 6, 1956.

14. Rupe, Jack H., A Correlation Between the Dynamic Properties of a Pair of Impinging Streams and the Uniformity of Mixture-ratio Distribution in the Resulting Spray, Progress Report No. 20-209. Pasadena: Jet Propulsion Laboratory, March 28, 1956.

15. Tomazic, William A., and Kinney, George R., Experimental Performance of the Mixed-oxides-of-nitrogen-ammonia Propellant Combination with Several Injection Methods in a 1000-lb-thrust Rocket Engine, NACA RM E55A07. Washington: National Advisory Committee for Aeronautics, March 28, 1955 (Confidential).

16. Greenberg, E., Lovingham, J. J., and Kircher, H. J., Jet Mixing Investigations. Report RM1-038-Q7. Denville, New Jersey: Reaction Motors, Inc., April 25, 1956 (Confidential).

TABLE I

NOMENCLATURE

c^* = characteristic velocity = $\frac{p_c f_t g}{w}$

C_F = thrust coefficient = $\frac{F}{p_c f_t}$

D = internal diameter of injector orifice

f_t = cross-sectional area of throat

F = thrust

g = acceleration due to gravity

I_{sp} = specific impulse = $\frac{F}{w}$

L^* = characteristic length = V_c/f_t

p_c = isentropic stagnation pressure in nozzle

p_o = external pressure

r = mixture ratio = w_{ox}/w_f

V = injection velocity of propellant

V_c = combustion chamber volume

w = propellant flow rate

δ = propellant density

Subscripts:

f = fuel
ox = oxidizer

TABLE II

Experimental Performances[a] of 1,000-lb-thrust Two-stage Rocket Engines[b].

Fuel[c]	Chamber-to-Throat area ratio		Nominal Interstage Nozzle Velocity (ft/sec)	L* (inches)		Total (inches)	P_c (psia)	r	c* (ft/sec)	Peak Theoret Frozen c* (%)
	First Stage	Second Stage		First Stage	Second Stage					
Hydrazine	4:1	4:1	1000	24	44	68	300	1.07	5200	94
CORPORAL Fuel	4:1	4:1	1000	24	44	68	300	2.82	4900	99
Isopropyl Alcohol	4:1	4:1	1000	24	44	68	300	3.5	4810	97
Unsymmetrical Dimethylhydrazine	4:1	4:1	1000	24	44	68	300	3.06	5020	96
Diethylenetriamine	4:1	4:1	1000	24	44	68	300	3.0	5070	99
Diethylenetriamine	4:1	4:1	1000	29	40	69	300	3.0	5090	99
Diethylenetriamine	4:1	4:1	1000	21	40	61	300	3.1	5020	98
Diethylenetriamine	4:1	2:1	1000	21	24	45	300	3.0	5010	98
Diethylenetriamine	2:1	2:1	1000	15	24	39	300	3.0	5070	99

[a] The tests were made at mixture ratios at or near the peak performance points for the various propellant systems.

[b] The engine used is shown in Figure 2.

[c] The oxidizer was stabilized fuming nitric acid (SFNA), nominal composition 14% wt NO_2, 2.5% H_2O, 0.6% HF, the remainder HNO_3.

TABLE III

Experimental[a] Performances of 20,000-lb-thrust Two-Stage Rocket Engines

Fuel[b]	Type of Engine or Injector	Chamber-to-Throat Area Ratio	Nominal Interstage Nozzle Velocity (ft/sec)	L^*(in.)		P_c (psia)	r	c^* (ft/sec)	C_F[c]	I_{sp} (sec)	Peak Theoretical Frozen I_{sp} (%)	Peak Theoretical Equilibrium I_{sp} (%)
				First Stage	Second Stage							
Diethylenetriamine	cf.Fig.5	3.56:1	1000	22	49	300	3.0	5000	1.31	203	90	88
Diethylenetriamine	cf.Fig.5	3.56:1	1000	22	49	360	2.9	5040	1.34	210	-	-
Diethylenetriamine	cf.Fig.6	3.56:1	600	22	49	300	3.1	4920	1.33	204	91	88
Diethylenetriamine	cf.Fig.6	3.56:1	1000	22	49	300	3.1	4920	1.33	204	91	88
Diethylenetriamine	cf.Fig.6	3.56:1	600	22	75	300	3.1	5040	1.36	213	95	92
Diethylenetriamine	cf.Fig.6[d]	3.56:1	600	22	75	300	3.1	4940	1.35	207	92	89 1/2
Diethylenetriamine	cf.Fig.6[d]	3.56:1	600	22	75	360	3.1	4990	1.38	214	-	-
Diethylenetriamine	cf.Fig.7	2:1	600	25	40	300	3.1	4810	1.33	199	88.5	86
Diethylenetriamine	cf.Fig.7	2:1	1000	25	40	300	3.1	4850	1.34	203	90	88
CORPORAL fuel	cf.Fig.6$_d$	3.56:1	1000	22	75	300	2.8	4910	1.38	210	97	94
CORPORAL fuel	cf.Fig.6[d]	3.56:1	1000	22	75	300	2.8	4830	1.36	205	94 1/2	92

[a] Performances represent peak values taken from smoothed curves drawn through the test data.

[b] The oxidizer was stabilized fuming nitric acid (SFNA), nominal composition 14 wt% NO_2, 2.5% H_2O, 0.6% HF, the remainder HNO_3.

[c] Exhaust nozzle expansion ratio = 4.53, P_o = 13.6 psia. The theoretical C_F for these conditions is nearly identical to that of an optimum expansion nozzle at P_o = 14.7 psia. Therefore, the values of Isp represent those which would have been obtained using an optimum expansion nozzle at P_o = 14.7 psia.

[d] These tests were made using low-pressure-drop orifices (about 50 psi). The remaining tests were with orifices having a pressure drop of about 125 psi.

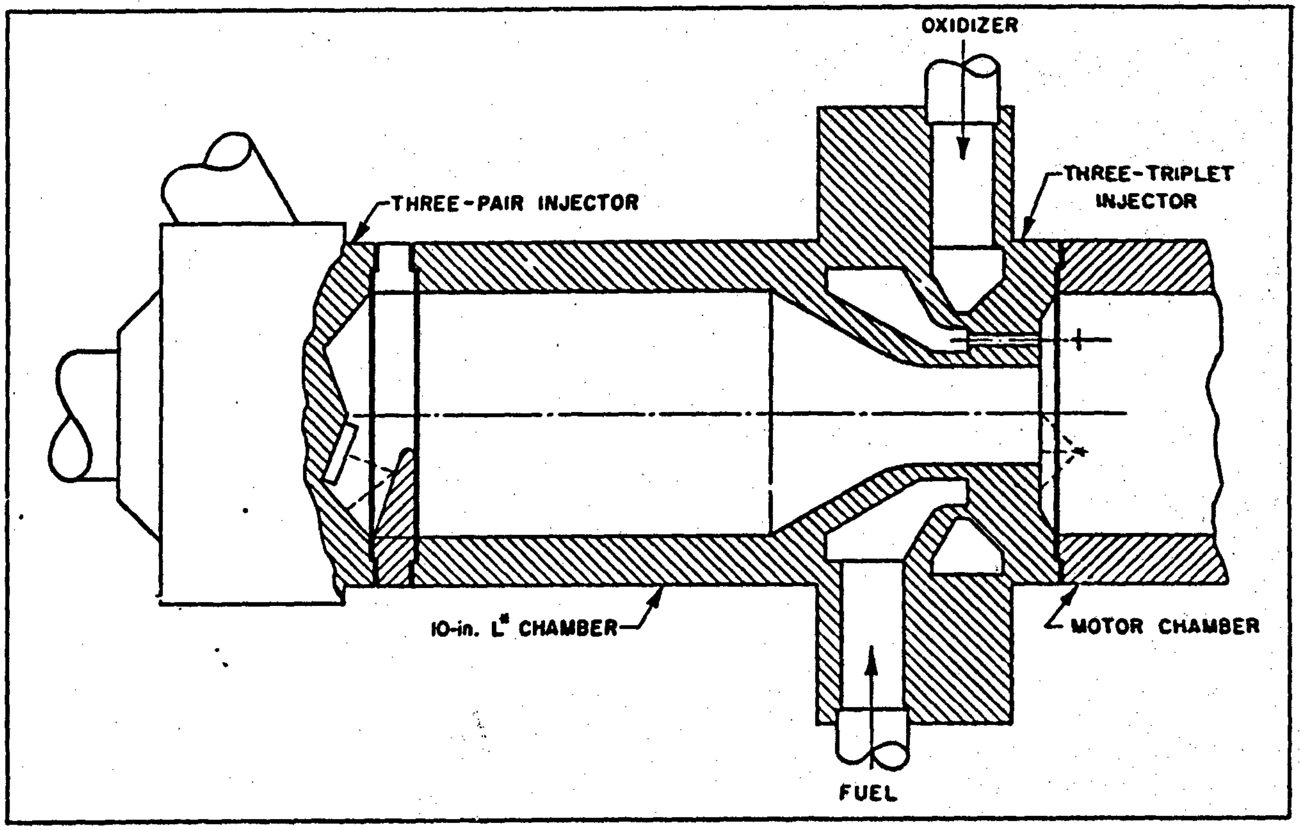
OXIDIZER
THREE-TRIPLET INJECTOR
THREE-PAIR INJECTOR
10-in. L* CHAMBER
MOTOR CHAMBER
FUEL

Figure 1. Configuration of Original Two-Stage 1,000-lb-thrust Rocket Engine

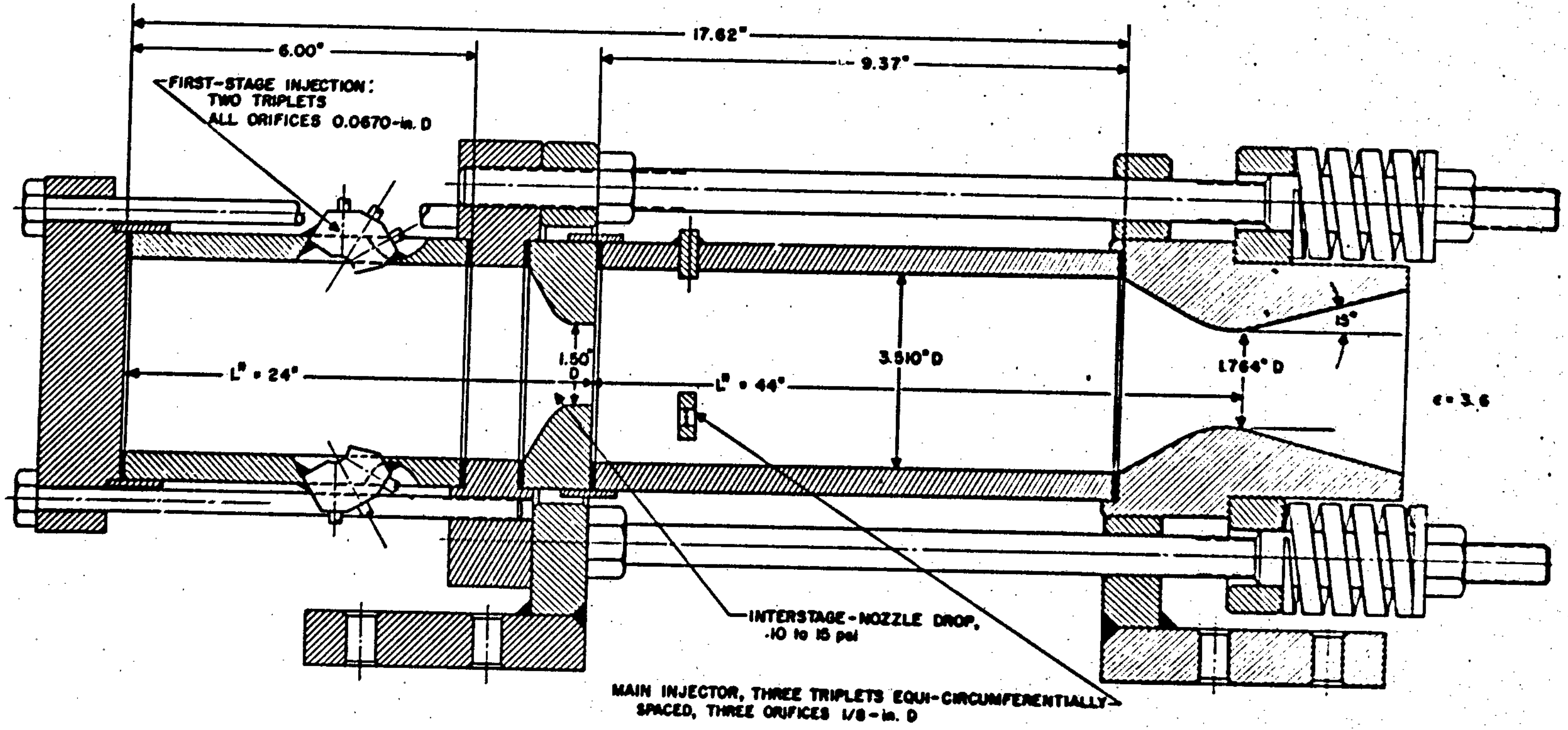
17.62"
6.00"
9.37"
FIRST-STAGE INJECTION:
TWO TRIPLETS
ALL ORIFICES 0.0670-in. D
1.50" D
3.510" D
1.764" D
15°
ε = 3.6
L* = 24"
L* = 44"
INTERSTAGE-NOZZLE DROP,
.10 to 15 psi
MAIN INJECTOR, THREE TRIPLETS EQUI-CIRCUMFERENTIALLY SPACED, THREE ORIFICES 1/8-in. D

Figure 2. Configuration of High-Performance Two-Stage 1,000-lb-thrust Rocket Engine

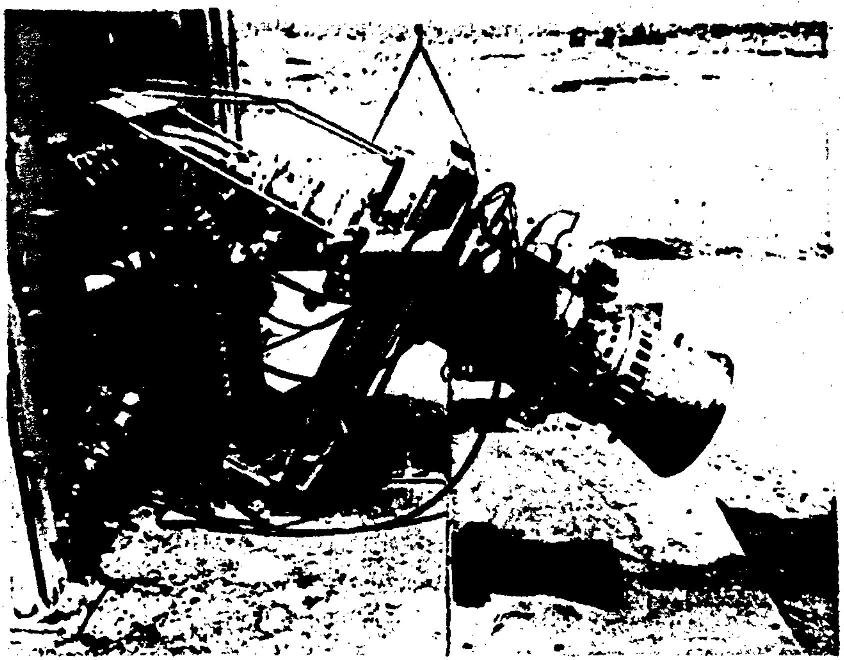

Figure 3. Static-Test Installation of Uncooled Two-Stage 20,000-lb-thrust Rocket Engine

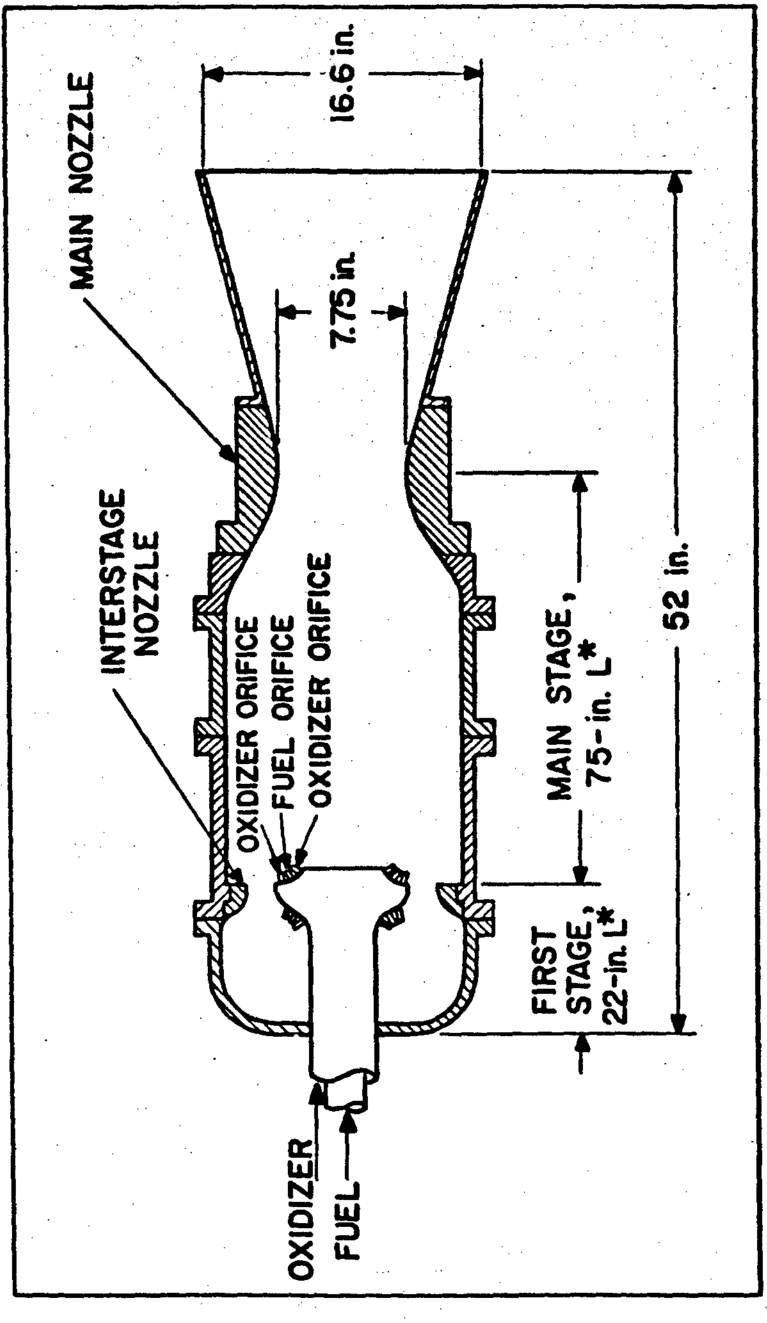
MAIN NOZZLE
16.6 in.
7.75 in.
INTERSTAGE NOZZLE
OXIDIZER ORIFICE
FUEL ORIFICE
OXIDIZER ORIFICE
MAIN STAGE, 75-in. L*
52 in.
FIRST STAGE, 22-in. L*
OXIDIZER
FUEL

Figure 4. Configuration of Uncooled Two-Stage 20,000-lb-thrust Rocket Engine

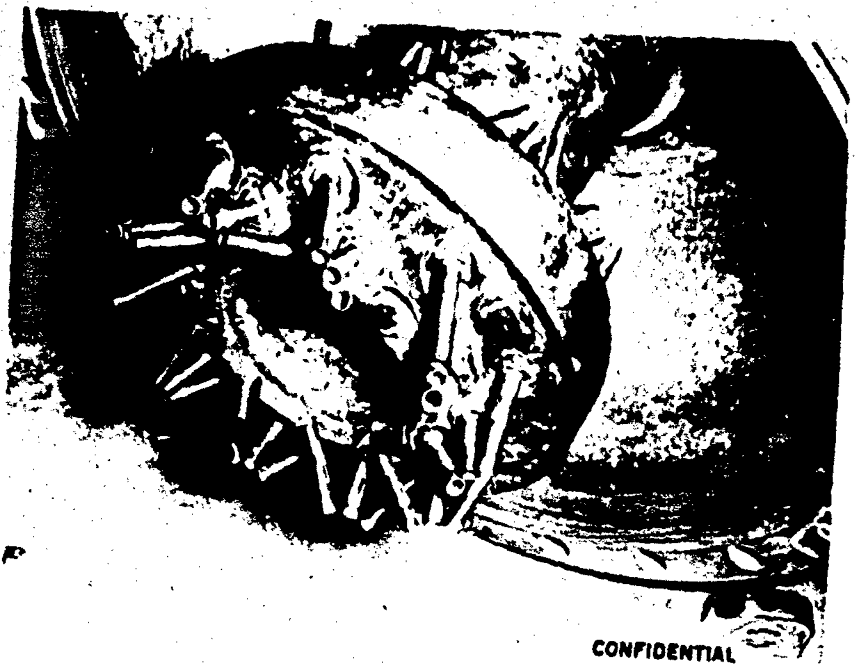
CONFIDENTIAL

Figure 5. Injector Body of Two-Stage 20,000-lb-thrust Engine Shown in Figure 4

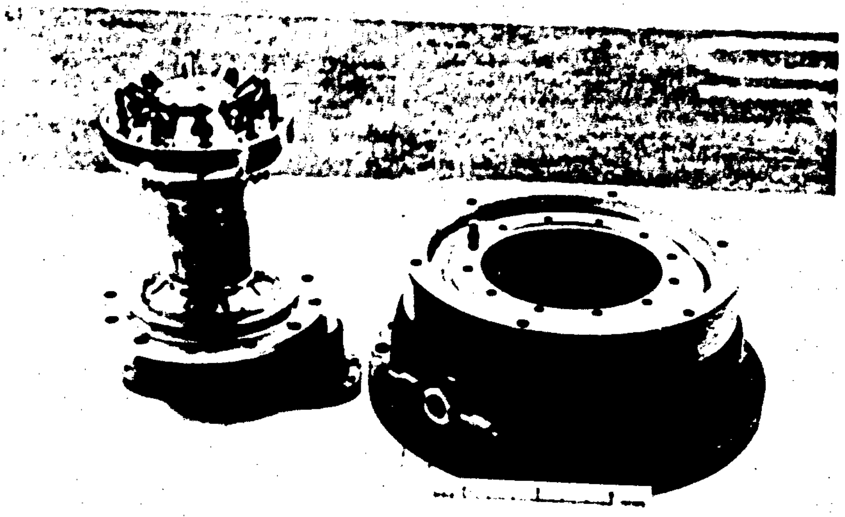

CONFIDENTIAL

Figure 6. Alternative Injector Body of Two-Stage 20,000-lb-thrust Engine Shown in Figure 4

[redacted]

[redacted]

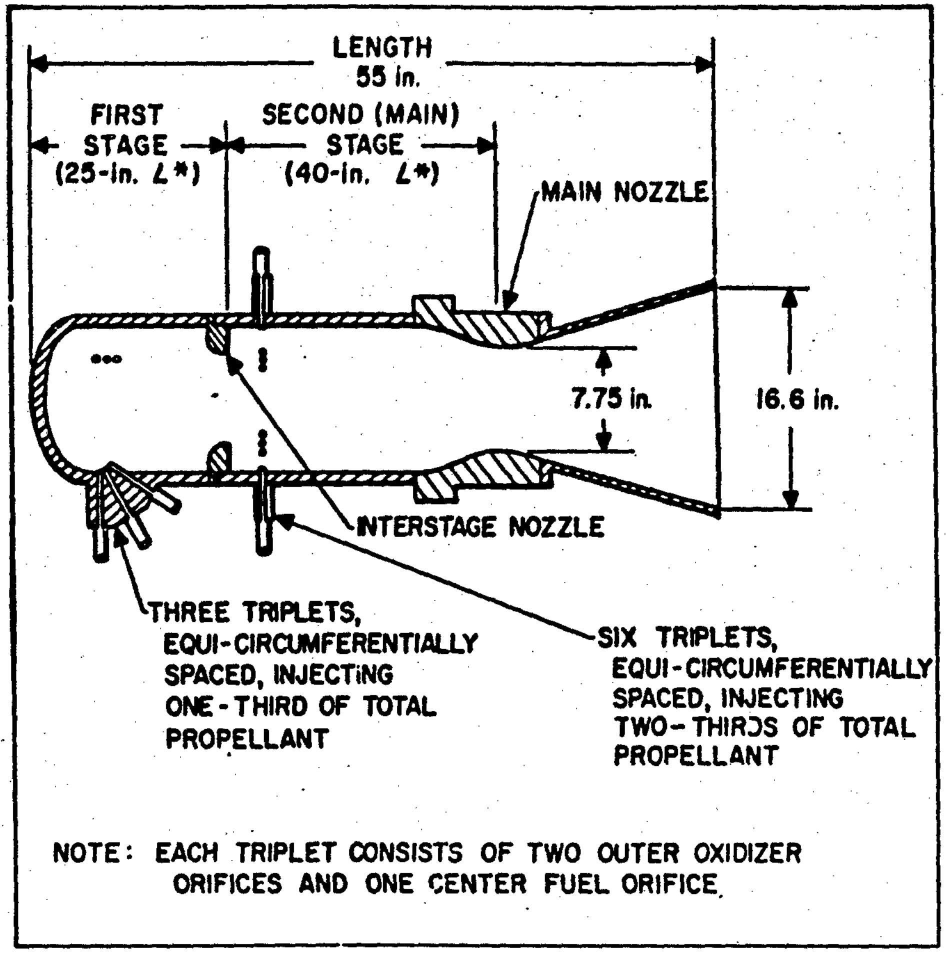
LENGTH
55 in.
FIRST
STAGE
(25-in. L*)
SECOND (MAIN)
STAGE
(40-in. L*)
MAIN NOZZLE
7.75 in.
16.6 in.
INTERSTAGE NOZZLE
THREE TRIPLETS, EQUI-CIRCUMFERENTIALLY SPACED, INJECTING ONE-THIRD OF TOTAL PROPELLANT
SIX TRIPLETS, EQUI-CIRCUMFERENTIALLY SPACED, INJECTING TWO-THIRDS OF TOTAL PROPELLANT
NOTE: EACH TRIPLET CONSISTS OF TWO OUTER OXIDIZER ORIFICES AND ONE CENTER FUEL ORIFICE.

Figure 7. Configuration of Another Uncooled Two-Stage 20,000-lb-thrust Rocket Engine

[redacted]

[redacted]

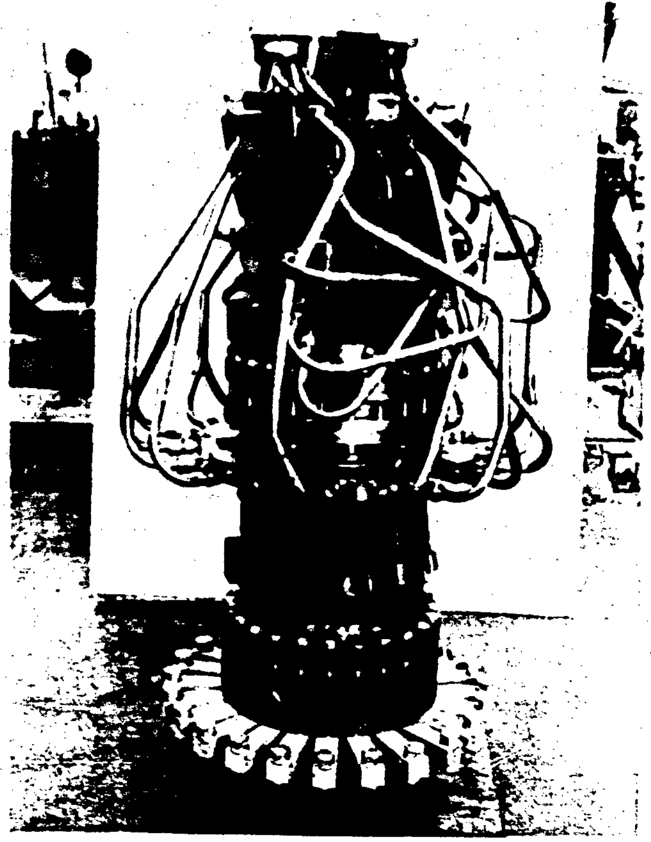

Figure 8. Two-Stage Engine of Figure 7, Showing Manifolding of Orifices

[redacted]

U. S. GOVERNMENT PRINTING OFFICE : 1957 O - 416612

[redacted]

128783

rmed Services Technical Information Agency

Reproduced by

DOCUMENT SERVICE CENTER

KNOTT BUILDING, DAYTON, 2, OHIO

This document is the property of the United States Government. It is furnished for the duration of the contract and shall be returned when no longer required, or upon recall by ASTIA to the following address: Armed Services Technical Information Agency, Document Service Center, Knott Building, Dayton 2, Ohio.

OTICE: WHEN GOVERNMENT OR OTHER DRAWINGS, SPECIFICATIONS OR OTHER DATA RE USED FOR ANY PURPOSE OTHER THAN IN CONNECTION WITH A DEFINITELY RELATED OVERNMENT PROCUREMENT OPERATION, THE U. S. GOVERNMENT THEREBY INCURS O RESPONSIBILITY, NOR ANY OBLIGATION WHATSOEVER; AND THE FACT THAT THE OVERNMENT MAY HAVE FORMULATED, FURNISHED, OR IN ANY WAY SUPPLIED THE AID DRAWINGS, SPECIFICATIONS, OR OTHER DATA IS NOT TO BE REGARDED BY MPLICATION OR OTHERWISE AS IN ANY MANNER LICENSING THE HOLDER OR ANY OTHER ERSON OR CORPORATION, OR CONVEYING ANY RIGHTS OR PERMISSION TO MANUFACTURE, SE OR SELL ANY PATENTED INVENTION THAT MAY IN ANY WAY BE RELATED THERETO.

[redacted]